

# THE JOURNAL OF PHYSICAL CHEMISTRY

(Registered in U. S. Patent Office)

## CONTENTS

Ralph G. Pearson and Ronald A. Munson: The Determination of Ionic Mobilities Directly from Resistance Measurements.		
C. E. O'Neill and D. J. C. Yates: The Effect of the Support on the Infrared Spectra of Carbon Monoxide Adsorbed on Nickel.	897	
Per S. Stensby and Jerome L. Rosenberg: Fluorescence and Absorption Studies of Reversible Aggregation in Chlorophyll.	901	
Robert W. Johnson and A. H. Daane: The Lanthanum-Boron System.	906	
Daniel W. Brown and Leo A. Wall: Gamma Irradiation of Liquid and Solid Oxygen.	909	
J. Lamborn and A. J. Swallow: The Protection Effect in the $\gamma$ -Radiolysis of Benzene-Cyclohexane Mixtures and its Explanation in Terms of Selectivity of the Primary Radiation Act.	915	
F. P. Del Greco and J. W. Gryder: Infrared and Raman Spectral Study of Nitrate Solutions in Liquid Hydrogen Fluoride.	920	
F. J. C. Rossotti and Hazel Rossotti: Graphical Methods of Determining Self-association Constants. I. Systems Containing Few Species.	922	
F. J. C. Rossotti and Hazel Rossotti: Graphical Methods of Determining Self-association Constants. II. Systems Containing Many Species.	926	
R. R. Irani and C. F. Callis: Metal Complexing by Phosphorus Compounds. IV. Acidity Constants.	930	
R. L. Every, W. H. Wade and Norman Hackerman: Free Energy of Adsorption. II. The Influence of Substrate Substance in the Systems $Al_2O_3$ and $TiO_2$ with $n$ -Hexane, $CH_3OH$ and $H_2O$ .	934	
Joseph L. Weininger: The Reactions of Active Nitrogen with Polyolefins.	937	
Edward P. Rack and Adon A. Gordus: Effect of Moderators on the ( $n, \gamma$ ) Activated Reaction of $Br^{80}$ with Methane.	941	
Bruno Reitzner: The Influence of Water on the Thermal Decomposition of $\alpha$ -Lead Azide.	944	
P. J. Horner and A. J. Swallow: The $\gamma$ -Radiolysis of Solutions of Hydrogen Chloride in Cyclohexane.	948	
Gideon Czapski, Joshua Jortner and Gabriel Stein: The Mechanism of Oxidation by Hydrogen Atoms in Aqueous Solution. I. Mass Transfer and Velocity Constants.	953	
Gideon Czapski, Joshua Jortner and Gabriel Stein: The Mechanism of Oxidation by Hydrogen Atoms in Aqueous Solution. II. Reaction Mechanisms with Different Scavengers.	956	
Gideon Czapski, Joshua Jortner and Gabriel Stein: The Role of Hydrogen Atoms in the Decomposition of $H_2O_2$ and in the Radiation Chemistry of Water.	960	
Allan R. Shultz: Degradation of Polymethylmethacrylate by Ultraviolet Light.	964	
Antonio Indelli: Kinetic Salt Effects by the Tetraalkylammonium Ions.	967	
Jehuda Feitelson: Interactions of Dipolar Ions with Ionized Polymers. Electrostatic and Specific Effects.	972	
J. H. Sinfelt and J. C. Rohrer: Kinetics of the Catalytic Isomerization-Dehydroisomerization of Methylcyclopentane.	975	
O. D. Bonner and O. C. Rogers: The Osmotic and Activity Coefficients of some Bolaform Sulfonates.	978	
Lyle E. Dawson, Jerry E. Berger and Hartley C. Eckstrom: Solvents having High Dielectric Constants.	981	
XII. Reaction of Sodium Phenoxide with Alkyl Iodides in these Media.		986
Philip W. Brewster, Frederick C. Schmidt and Ward B. Schaap: The Conductances of a Number of Acids and Divalent Metal Salts in Anhydrous Ethanolamine.	991	
C. P. Fenimore and G. W. Jones: Rate of Reaction $O + H_2 \rightarrow OH + H$ in Flames.	993	
Arnold Reisman and Joan Mineo: Compound Repetition in Oxide-Oxide Interactions. The System $Cs_2O-Nb_2O_5$ .	996	
John E. Lind, Jr., and Raymond M. Fuoss: Conductance of the Alkali Halides. I. Potassium Chloride in Dioxane-Water Mixtures.	999	
H. Bradford Thompson and Stephen L. Hanson: Interpretation of the Electric Moments of Polymethylene Dihalides and Dicyanides.	1005	
G. H. Cartledge: The Comparative Roles of Oxygen and Inhibitors in the Passivation of Iron. III. The Chromate Ion.	1009	
J. G. Aston and H. Chon: Lateral Interaction on a Smooth Surface.	1015	
D. W. Rudd, D. W. Vose and S. Johnson: The Permeability of Copper to Hydrogen.	1018	
I. M. Kolthoff and S. Ikeda: Polarographic and Acid Properties of Thorium Perchlorate in Acetonitrile.	1020	
J. L. Lacina, W. D. Good and J. P. McCullough: The Heats of Combustion and Formation of Thiaadamantane.	1026	
Emile Rutner: The Reflectance Spectra of Chlorocobaltous and Chloroferri Complex Ions on Dowex-1 Anion-Exchange Resin.	1027	
John H. Kennedy: Distribution Experiments in Fused Salts. I. The Distribution of Thallium Chloride between $KNO_3$ and $AgCl$ , and between $K_2S_2O_7$ and $AgCl$ .	1030	
Ralph Gorden, Jr., and P. Ausloos: Vapor-Phase Photolysis of Formic Acid.	1033	
J. K. Nickerson, K. A. Kobe and John H. McKetta: The Thermodynamic Properties of the Methyl Ketone Series.	1037	
NOTES		
R. S. Slysh and C. R. Kinney: Some Kinetics of the Carbonization of Benzene, Acetylene and Diacetylene at $1200^\circ$ .	1044	
D. C. Fox and M. J. Katz: Stepwise Adsorption of Krypton on Nickel.	1045	
W. Channing Nicholas and W. Conard Fernelius: A Thermodynamic Study of Some Coordination Complexes of Bivalent Metal Ions with Histamine.	1047	
Sherril D. Christian, Edward Neparko, Harold E. Affsprung and Frank Gibbard: The Calculation of Liquid Mole Fractions and Activity Coefficients from Activity Data.	1048	
Aleksander Kreglewski and Bruno J. Zwolinski: A New Relation for Physical Properties of $n$ -Alkanes and $n$ -Alkyl Compounds.	1050	
Jehanoux F. Bagli: Evidence of the Intramolecular Vibrational Effect in $p$ -Benzoquinone.	1052	
W. J. McManamey: Hydration Studies for the Extraction of Inorganic Nitrates by Alcohols.	1053	
Maurice M. Kreevoy and Richard L. Hansen: The Reaction of Alkylmercuric Iodides with Acid in the Presence of Oxygen.	1055	
R. Benz and J. A. Leary: Some Thermodynamic Prop-		

# THE JOURNAL OF PHYSICAL CHEMISTRY

(Registered in U. S. Patent Office)

W. ALBERT NOYES, JR., EDITOR

ALLEN D. BLISS

ASSISTANT EDITORS

A. B. F. DUNCAN

EDITORIAL BOARD

A. O. ALLEN  
C. E. H. BAWN  
J. BIGEISEN  
D. D. ELEY

D. H. EVERETT  
S. C. LIND  
F. A. LONG  
K. J. MYSELS

J. E. RICCI  
R. E. RUNDLE  
W. H. STOCKMAYER  
A. R. UBBELOHDE

E. R. VAN ARTSDALEN  
M. B. WALLENSTEIN  
W. WEST  
EDGAR F. WESTRUM, JR.

Published monthly by the American Chemical Society at 20th and Northampton Sts., Easton, Pa.

Second-class mail privileges authorized at Easton, Pa. This publication is authorized to be mailed at the special rates of postage prescribed by Section 131.122.

The *Journal of Physical Chemistry* is devoted to the publication of selected symposia in the broad field of physical chemistry and to other contributed papers.

Manuscripts originating in the British Isles, Europe and Africa should be sent to F. C. Tompkins, The Faraday Society, 6 Gray's Inn Square, London W. C. 1, England.

Manuscripts originating elsewhere should be sent to W. Albert Noyes, Jr., Department of Chemistry, University of Rochester, Rochester 20, N. Y.

Correspondence regarding accepted copy, proofs and reprints should be directed to Assistant Editor, Allen D. Bliss, Department of Chemistry, Simmons College, 300 The Fenway, Boston 15, Mass.

Business Office: Alden H. Emery, Executive Secretary, American Chemical Society, 1155 Sixteenth St., N. W., Washington 6, D. C.

Advertising Office: Reinhold Publishing Corporation, 430 Park Avenue, New York 22, N. Y.

Articles must be submitted in duplicate, typed and double spaced. They should have at the beginning a brief abstract, in no case exceeding 300 words. Original drawings should accompany the manuscript. Lettering at the sides of graphs (black on white or blue) may be pencilled in and will be typeset. Figures and tables should be held to a minimum consistent with adequate presentation of information. Photographs will not be printed on glossy paper except by special arrangement. All footnotes and references to the literature should be numbered consecutively and placed in the manuscript at the proper places. Initials of authors referred to in citations should be given. Nomenclature should conform to that used in *Chemical Abstracts*, mathematical characters be marked for italic, Greek letters carefully made or annotated, and subscripts and superscripts clearly shown. Articles should be written as briefly as possible consistent with clarity and should avoid historical background unnecessary for specialists.

Remittances and orders for subscriptions and for single copies, notices of changes of address and new professional connections, and claims for missing numbers should be sent to the American Chemical Society, 1155 Sixteenth St., N. W., Washington 6, D. C. Changes of address for the *Journal of Physical Chemistry* must be received on or before the 30th of the preceding month.

Claims for missing numbers will not be allowed (1) if received more than sixty days from date of issue (because of delivery hazards, no claims can be honored from subscribers in Central Europe, Asia, or Pacific Islands other than Hawaii), (2) if loss was due to failure of notice of change of address to be received before the date specified in the preceding paragraph, or (3) if the reason for the claim is "missing from files."

Subscription rates (1961): members of American Chemical Society, \$12.00 for 1 year; to non-members, \$24.00 for 1 year. Postage to countries in the Pan-American Union \$0.80; Canada, \$0.40; all other countries, \$1.20. Single copies, current volume, \$2.50; foreign postage, \$0.15; Canadian postage \$0.10; Pan-American Union, \$0.10. Back volumes (Vol. 56-64) \$30.00 per volume; foreign postage, per volume \$1.20, Canadian, \$0.40; Pan-American Union, \$0.80. Single copies: back issues, \$3.00; for current year, \$2.50; postage, single copies: foreign, \$0.15; Canadian, \$0.10; Pan-American Union, \$0.10.

The American Chemical Society and the Editors of the *Journal of Physical Chemistry* assume no responsibility for the statements and opinions advanced by contributors to THIS JOURNAL.

The American Chemical Society also publishes *Journal of the American Chemical Society*, *Chemical Abstracts*, *Industrial and Engineering Chemistry*, International Edition of *Industrial and Engineering Chemistry*, *Chemical and Engineering News*, *Analytical Chemistry*, *Journal of Agricultural and Food Chemistry*, *Journal of Organic Chemistry*, *Journal of Chemical and Engineering Data*, *Chemical Reviews*, *Chemical Titles* and *Journal of Chemical Documentation*. Rates on request.

erties of the System PuCl <sub>3</sub> -NaCl from Electromotive Force Data.....	1056	W. H. Stockmayer, Roy R. Miller and Robert J. Zeto: Kinetics of Borohydride Hydrolysis.....	1076
Daniel Cubicciotti: Energies of the Gaseous Alkaline Earth Halides.....	1058	Theodore L. Brown: The Electronic Properties of Alkyl Groups. III. The Intensity of the Infrared Nitrile Absorption in <i>para</i> -Alkylbenzonitriles.....	1077
G. A. Somorjai: Vapor Pressure and Solid-Vapor Equilibrium of Cadmium Selenide.....	1059	B. L. Baker and G. W. Hodgson: Rate of Formation of the Nickel Complex of Pheophytin <i>a</i> .....	1078
I. Shapiro, Robert E. Williams and Sidney G. Gibbins: 2,4-Dimethylenetetra borane: Structure from N.m.r. Spectra.....	1061	Thomas H. Fife and Thomas C. Bruce: The Temperature Dependence of the $\Delta\rho D$ Correction for the Use of the Glass Electrode in D <sub>2</sub> O.....	1079
Joseph M. Pagano, David E. Goldberg, and W. Conrad Fernelius: A Thermodynamic Study of Homopiperazine, Piperazine, and N-(2-Aminoethyl)-piperazine and their Complexes with Copper(II) Ion.....	1062	William Ves Childs and Edward S. Amis: Polarography in Water and Water-Ethanol. I. Uranium(VI) in Chloride and Perchlorate Media in one Molar Acid.....	1080
William N. Lipscomb: Topologies of B <sub>4</sub> and B <sub>7</sub> Hydrides.....	1064	Karol J. Mysels: Improvements in the Design of Conductivity Cells.....	1081
Russell S. Drago and Donald Bafus: The N.m.r. Spectra of Dimethylpropionamide-Iodine Solutions.....	1066	David H. Kirkwood and John Chipman: The Free Energy of Silicon Carbide from its Solubility in Molten Lead.....	1082
E. J. Slowinski, Jr., and W. L. Masterton: A Simple Absolute Method for the Measurement of Surface Tension.....	1067	Lester P. Kuhn and Chester Butkiewicz: The Isotope Exchange Reaction between Labelled Nitric Oxide, <sup>14</sup> NO and Nitrosyl <sup>14</sup> NOCl.....	1084
Aaron Wold, Ronald J. Arnott and Norman Menyuk: Hexagonal Iron Nitrides.....	1068	R. A. Robinson and R. W. Green: Some Physical Properties of Aqueous Picolinic Acid Solutions.....	1084
John E. Hearst and Jerome Vinograd: Sedimentation Equilibrium in a Density Gradient: An Evaluation of the Errors Caused by Refractor, of Light in the Photometric Determination of Molecular Weight and Buoyant Density.....	1099	W.-Y. Wen and I. M. Klotz: Acidity Constant of a Protein Conjugate in D <sub>2</sub> O.....	1085
Harold A. Scheraga: Effect of Hydrophobic Bonding on Protein Reactions.....	1071	COMMUNICATIONS TO THE EDITOR	
R. E. Rathbun and A. L. Babb: Self-Diffusion in Liquids. III. Temperature Dependence in Pure Liquids.....	1072	Max Matheson: Some Aspects of the Rotating Sector Determination of the Absolute Rate Constants in Radical Polymerization Reactions: a Correction.....	1087
Norman C. Li, Philomena Tang and Raj Mathur: Deuterium Isotope Effects on Dissociation Constants and Formation Constants.....	1074	G. E. Ryschkewitsch and E. R. Birnbaum: Amine Boranes. II. Pyridine Borane-Propanol Reaction Kinetics.....	1087
		A. E. Shilov: On the Paper "Pyrolysis of Allyl Chloride" by L. J. Hughes and W. F. Yates.....	1088

# THE JOURNAL OF PHYSICAL CHEMISTRY

(Registered in U. S. Patent Office) (© Copyright, 1961, by the American Chemical Society)

VOLUME 65

JUNE 26, 1961

NUMBER 6

## THE DETERMINATION OF IONIC MOBILITIES DIRECTLY FROM RESISTANCE MEASUREMENTS<sup>1</sup>

BY RALPH G. PEARSON AND RONALD A. MUNSON

*Chemistry Department, Northwestern University, Evanston, Ill.*

*Received May 28, 1960*

The theory for the changes in conductivity of electrolyte solutions due to the replacement of one ionic species by another is developed and applied to electrodes of several geometries. The relative change of resistance measured between concentric cylindrical platinum electrodes in aqueous solutions of potassium chloride and magnesium sulfate during voltage pulses of 100 to 550 volts of a duration of 2 to 1000 microseconds is used to calculate the mobility of the cations and hydrogen ion. The results indicate that similar measurements may possibly be used to determine mobilities directly from resistance measurements without the need of transference number data.

The flow of electric charge across a boundary between two simple electrolyte solutions which have an anion (or cation) in common causes the replacement of the cation (anion) of the first solution by the cation (anion) from the second. This replacement may take the form of the movement of the boundary between the layers, if the slower ion follows the faster, or may result in the creation and movement of a mixed region, if the faster ion follows the slower. The general theory of concentration changes during electrolysis has been developed by Kohlrausch<sup>2</sup> and Weber.<sup>3</sup> As one ion replaces another the conductivity of the involved region of the solution changes in a manner dependent upon the mobilities of the leading and following ions, but independent of that of the common ion. The measurement of the resistance change during the passage of current in cells containing such a boundary allows the calculation of the mobilities of the leading and following ions.

**General Theory.**—The equation of continuity for a cation present in a concentration (expressed in charge per unit volume)  $\alpha$ , having a mobility  $a$ , and moving under an electric field  $\vec{E}$  is given by

$$\frac{\partial \alpha}{\partial t} = -\nabla \cdot (\alpha a \vec{E}) \quad (1)$$

The equation of continuity for an anion is similar but has an inverted sign. The conductivity  $\sigma$  is defined by

$$\vec{i} = \sigma \vec{E} \quad (2)$$

in terms of the electric field and the current density  $\vec{i}$ . Elimination of the electric field between equations 1 and 2 yields

$$\frac{\partial \alpha}{\partial t} = - \left[ \vec{i} \cdot \nabla \frac{2\alpha}{\sigma} + \frac{2\alpha}{\sigma} \nabla \cdot \vec{i} \right] \quad (3)$$

the second term of which is zero since the current density must be divergenceless in order to maintain electroneutrality.

$$\nabla \cdot \vec{i} = 0 \quad (4)$$

Under the assumptions that the mobility of the ion is independent of the electrolyte concentration and the electric field, we find

$$\frac{\partial \alpha}{\partial t} = -a \vec{i} \cdot \nabla \left( \frac{\alpha}{\sigma} \right) \quad (5)$$

Each ionic species present in solution obeys an equation similar to equation 5. Dividing each of the equations for each ionic species by the mobility of that species and adding all of the equations together, we obtain

$$\frac{1}{a} \frac{\partial \alpha}{\partial t} + \frac{1}{b} \frac{\partial \beta}{\partial t} + \dots + \frac{1}{c} \frac{\partial \rho}{\partial t} + \dots = -\vec{i} \cdot \nabla \left( \frac{1}{\sigma} \right) (\alpha + \beta + \dots + \rho + \dots) \quad (6)$$

The right-hand side of equation 6 is zero due to electroneutrality. Integration of equation 6 produces the regulating function which governs the concentrations of the ions during electrolysis throughout the solution in terms of the mobilities

(1) Taken in part from the Ph.D. thesis of R. A. Munson, National Science Foundation Predoctoral Fellow (1955–1958).

(2) F. Kohlrausch, *Wied. Ann.*, **62**, 209 (1897).

(3) H. Weber, *Sitz. Preuss. Akad. Wiss.*, 936 (1897).

of the ions involved and the concentrations present at the start of the current passage.

For the particular case of two cations (of concentrations  $\alpha$  and  $\beta$  and mobilities  $a$  and  $b$ , respectively) and a common anion (of mobility  $c$ ), the regulating function, which is a function of position, is

$$\alpha \left( \frac{a+c}{a} \right) + \beta \left( \frac{b+c}{b} \right) = H(x,y,z) \quad (7)$$

The conductivity is the sum of the conductivity contributions of each of the ions present.

$$\sigma = (a+c)\alpha + (b+c)\beta \quad (8)$$

Elimination of  $\alpha$  and  $\beta$  from equations 5, 7 and 8 gives

$$\frac{\partial M}{\partial t} = -M^2 \vec{i} \cdot \nabla M \quad M = \frac{\sqrt{abH}}{\sigma} \quad (9)$$

in terms of the resistivity parameter  $M$ . The significance of the dot product of equation 9 is that only that current which is parallel to a concentration gradient contributes to the movement of this gradient. The complete solution of equation 9 depends upon the geometry of the electrodes, the initial condition, and the time and spatial dependence of the current density. The spatial dependence of the current density must be determined from the geometry of the cell in such a manner that equation 4 is satisfied. The solution of equation 9 gives the conductivity as a function of position and time. The resistance as a function of time is then determined by the integral

$$R = \int \frac{ds}{\sigma A} \quad (10)$$

where  $A$  is the area of a lamina of solution between the measuring electrodes which has a thickness  $ds$  and a conductivity  $\sigma$ .

In the following specific cases it is assumed that the solution is made up of one cation and one anion, of mobilities  $b$  and  $c$ , with the same concentration throughout the solution. The second ion, of mobility  $a$ , then is introduced at one of the electrodes. A constant current is assumed.

**Plane Electrodes.**—The relative change in resistance due to the process at one electrode where  $q$  is the separation between the plane electrodes is given by

$$\frac{\Delta R_{vt}}{R_{vt=0}} = \frac{bVt}{q^2} \left[ \frac{b}{a} - 1 \right] \quad a < b \quad (11)$$

$$\frac{\Delta R_{vt}}{R_{vt=0}} = \frac{aVt}{q^2} \left[ \frac{b^3}{a^3} - 1 \right] \quad a > b \quad (12)$$

$V$  is the applied voltage corrected for the potential drop at the electrode surfaces. If  $b$  should be zero, equation 12 remains valid although the regulating function is no longer obeyed. Measurements with plane electrodes are complicated by the replacement of ions at both electrodes leading to simultaneous resistivity changes at each electrode.

This difficulty may be avoided by the use of concentric spherical or cylindrical electrodes having sufficiently large ratios of outer to inner radii. The advantages of such electrodes come from two sources. First, the laminae of the solution in the vicinity of the large outer electrode make a small contribution to the total resistance as compared to

those laminae in the vicinity of the inner electrode. Second, the greater surface area of the outer electrode means that significant changes in the conductivity of the laminae close to the fine central electrode may occur before the double layer can be charged and the replacement of ions starts at the outer electrode.

**Concentric Cylindrical Electrodes.**—The solution of equation 9 for cylindrical geometry is

$$r^2 = p^2 + 2i_0 M^2 t \quad (13)$$

where  $i_0 = ir$  is a constant proportional to the current. The evaluation of the integration constant,  $p^2$ , has been made by use of the initial condition that the boundaries must start out from the surface of the central electrode which has a radius of  $p$ .

If the following ion has a mobility less than that of the leading ion, the boundary between the leading and following ion regions remains sharp. The conductivity of the following ion region may be obtained from equation 7. The position of the boundary is given by equation 13 with the use of a resistivity parameter which is the geometric mean of that of the leading and following regions. The position of the boundary,  $l$ , is given by

$$l^2 = p^2 + \frac{2bVt}{\ln q/p} \quad (14)$$

where  $q$  is the radius of the outer electrode. Integration of equation 10 for this case gives the relative change in resistance

$$\frac{\Delta R_{vt}}{R_{vt=0}} = \left( \frac{b}{a} - 1 \right) \frac{\log l^2/p^2}{\log q^2/p^2} \quad (15)$$

As  $Vt$  becomes large a plot of the relative change in resistance versus logarithm  $Vt$  approaches a straight line. From the slope of this limiting straight line and a knowledge of the radial dimensions of the electrodes, the ratio  $b/a$  may be determined. Extrapolation of this limiting slope back to zero relative change in resistance gives the value of  $Vt$  when

$$2bVt = p^2 \ln q/p$$

and thus both  $a$  and  $b$  may be determined from the data.

If the following ion has a mobility greater than that of the leading ion a mixed region is also produced. The conductivity of the following ion region is found through the regulating function; the conductivity of the mixed region is determined from equation 13. The position of the boundary between the leading ion and the mixed region ( $n$ ) and the position of the boundary between the mixed and the following ion region ( $m$ ) are found by substitution of the value of the resistivity parameter for the leading and following region, respectively, into equation 13.

$$m^2 = p^2 + \frac{2b^2Vt}{a \ln q/p} \quad n^2 = p^2 + \frac{2aVt}{\ln q/p} \quad (16)$$

The result of the integration of equation 10 is

$$\frac{\Delta R_{vt}}{R_{vt=0}} = \left( \frac{b}{a} - 1 \right) \frac{\log m^2/p^2}{\log q^2/p^2} - \frac{\log n^2/m^2}{\log q^2/p^2} + \left( \frac{1-b}{a} \right) \frac{p}{\ln q/p} - \frac{p}{\sqrt{aVt \ln q^2/p^2}} \left( \cos^{-1} \frac{p}{n} - \cos^{-1} \frac{p}{m} \right) \quad (17)$$

The first term on the right-hand side is the contribution of the pure following ion region to the relative change in resistance; the last three terms are the contribution of the mixed region. From the limiting slope of a plot of the relative change in resistance *vs.* logarithm  $Vt$  the ratio of the mobilities is again obtainable. For large values of  $Vt$  the contribution of the mixed region to the relative change in resistance becomes constant

$$\lim_{Vt \rightarrow \infty} \frac{\Delta R_{\text{mixed region}}}{R_{v=0}} = -\frac{\log a^2/b^2}{\log q^2/p^2} + \left(1 - \frac{b}{a}\right) \left(\frac{1}{\ln q/p}\right) \quad (18)$$

Extrapolation of the limiting slope and the limiting mixed region contribution back to their intersection gives the value of  $Vt$  when

$$\frac{b^2}{a} = \frac{p^2 \ln q/p}{2Vt}$$

Thus the calculation of the mobilities of both the leading and following ions is possible.

**Concentric Spherical Electrodes.**—Spherical geometry also allows the determination of the mobilities of the leading and following ions. The solution of equation 9 is

$$r^3 = p^3 + 3i_0 M^2 t \quad (19)$$

where  $i_0 = ir^2$  is a constant proportional to the current. The other symbols have the corresponding definition to that of concentric cylindrical geometry. For the case of a slower following ion no mixed region is formed and the relative change in resistance is found to be

$$\frac{\Delta R_{vt}}{R_{v=0}} = \left(\frac{b}{a} - 1\right) \left[1 - \frac{p}{\left(p^3 + \frac{3bVt}{p} - \frac{1}{q}\right)^{1/3}}\right] \quad (20)$$

Again a slope intercept method may be employed to determine the values of  $a$  and  $b$ .

**Additional Considerations.**—It has been assumed in the foregoing examples that the current was constant. Experimentally it may be convenient to employ a constant voltage, in which case the factor  $Vt$  must be multiplied by the normalized time integral of the relative conductance. This integral may be calculated directly from the experimental data.

In the cases in which the time necessary for the charging of the double layer is significant, the quantity  $Vt$  must be corrected by subtracting a constant term. The magnitude of this correction allows the estimation of the double layer capacity.

The determination of the mobilities as presented here involves the knowledge of the relative positions of the electrodes. Similarly, the calculation of mobilities by the usual methods involves the uncertainty of the geometric cell constant.

### Experimental

The central electrode was made of a fine platinum wire (#1 wire,  $1.27 \times 10^{-3}$  cm. radius) which was surrounded concentrically and supported by a conventional platinum gauze electrode 2.9 cm. in height and 0.7 cm. in radius. The cell was used as one of the upper arms of a Wheatstone type bridge which had variable capacitors in parallel with each of the upper arms. The bridge connections to the cell were such that the outer electrode was kept closest to ground potential. The resistances which served as the

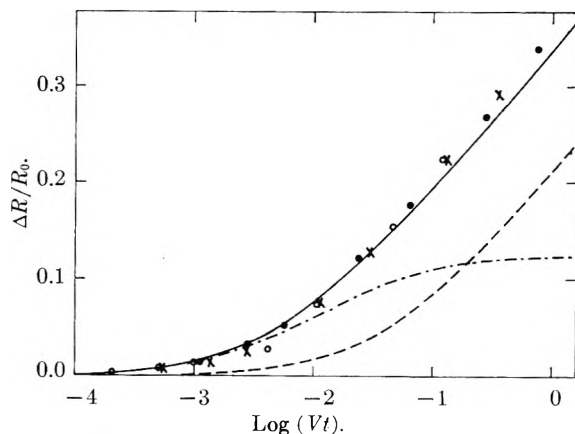


Fig. 1.—Potassium chloride, relative decrease in resistance as a function of  $\log(Vt)$ : ●, 550 volt pulse; ×, 270 volt pulse; ○, 100 volt pulse; —, theoretical decrease in resistance; —, contribution of hydrogen ion region; —·—, contribution of mixed region.

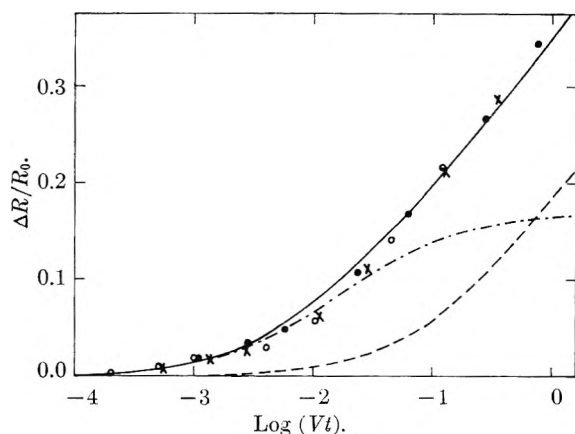


Fig. 2.—Magnesium sulfate relative decrease in resistance as a function of  $\log(Vt)$ : ●, 550 volt pulse; ×, 270 volt pulse; ○, 100 volt pulse; —, theoretical decrease in resistance; —, contribution of hydrogen ion region; —·—, contribution of mixed region.

lower arms of the bridge were always equal (within 0.1%) and one hundredth or less of the resistance of the upper arms. The balance of the bridge was obtained by adjusting the variable capacitors and the resistance of the remaining upper arm of the bridge. The balance of the bridge was observed with a Tektronix 535 oscilloscope and its high-gain differential preamplifier (53D/54D). A square pulse was produced by the discharge of a 15 microfarad capacitor. The 100 to 550 volt pulse was cut off after three milliseconds by a mechanical relay.

Bridge balance was obtained in the following manner: The bridge was pulsed with the 550 volt pulse and the resistance and capacitance were balanced so that at resistive balance at two microseconds, the initial transients were as symmetrical as possible. The same capacitor setting was then used throughout a run and the trace on the oscilloscope screen at a given time brought to zero by adjusting the bridge resistance. This method of balancing the bridge, although somewhat arbitrary, was selected for its convenience and reproducibility of results.

Calculations based upon the geometrical cell constant and the known equivalent conductivities of the solutions employed indicate that the experimental resistances obtained from the measurements with the 100 volt pulse at two microseconds are quite close to the absolute values of the resistances.

The reproducibility of the results depends to a large extent on the construction of the electrodes. With the central wire electrode stretched as tightly as possible so as to prevent gross movement, a maximum irreproducibility of about  $\pm 1\%$  was obtained.

The solution had to be stirred so as to remove electrolysis products from the vicinity of the central wire which otherwise greatly affected the result of a following pulse. The measured resistance was independent of the rate of stirring, even for one millisecond pulses, so long as the stirring was not so violent as to vary the level of the solution on the electrode or the position of the fine central electrode.

The voltage pulses had a rise time of about one microsecond and the decay of the pulse voltage at one millisecond amounted to 6.6 to 0.4%, depending upon the bridge resistance.

The water used in the preparation of the solutions was prepared by passing distilled water through a mixed bed ion exchange resin and had a specific conductivity at 20° of less than  $9 \times 10^{-7}$  ohm<sup>-1</sup> cm.<sup>-1</sup>. The concentration ranges employed were  $0.48 \times 10^{-4}$  M to  $9.3 \times 10^{-4}$  M for KCl and  $0.24 \times 10^{-4}$  to  $4.8 \times 10^{-4}$  M for MgSO<sub>4</sub>. The electrolytes were of reagent grade.

### Results and Discussion

As no observable trend in the relative decrease of resistance was found in the concentration range employed, the results at the different concentrations have been averaged together. The agreement of the results with theory over the various concentrations and voltages indicates that a possible heat effect is negligible. Figures 1 and 2 exhibit the experimental relative decrease in resistance as well as the theoretical curve. The values of  $Vt$  used are corrected (increased) for the time integral of the relative conductance. The largest correction is 0.14 logarithm unit. The agreement between theory and experiment for all concentrations indicates that the double layer capacity of the central electrode is smaller than a microfarad per square centimeter.

The electrode reactions producing the protons at the central wire are most likely the oxidation of water and the oxidation of the electrode surface. In the potassium chloride solutions some oxidation of chloride ion probably will occur also.

Solution of the problem of diffusion from a cylindrical source<sup>5</sup> indicates that diffusion of a layer of acid built up on the central electrode due to the non-discharge of the anion should not appreciably affect the measured resistance. The acid penetrates only part of the way into the hydrogen ion region. Since the conductivity of this region already has increased seven times, as expected from the regulating function, the additional increase has little effect on the total resistance.

(5) R. A. Munson, "Dissertation," Northwestern University, 1959, pp. 59 ff.

Calculations treating the effect of space charge (equation 4 is an approximation) and concentration forces on the conductivity indicate that space charge forces tend to decrease the conductivity and concentration forces tend to increase the conductivity. If the region of solution closer to the electrode than  $10^{-5}$  cm. is neglected, the changes in overall resistance are of the order of parts per million for the concentration forces and several parts per thousand for the space charge forces. Both effects are far smaller than the error of the measurements reported. In the lamina of solution adjacent to the central electrode and  $10^{-5}$  cm. thick, concentration and especially space charge forces are very important and the treatment presented in this paper is no longer valid. However, the resistivity of this region is already swamped out at two microseconds by the diffusion of the acid layer built up on the central electrode. This region of solution should make no contribution to the resistance in the measurements reported.

The influence of the Wien effect upon the over-all resistance is of no importance with the electric fields employed in these experiments.

Table I compares the mobilities as calculated from the experimental data with literature values.<sup>6</sup> The order of magnitude agreement is what may be expected from the crudeness of the experimental data. However, it should be mentioned that the apparatus used was designed with a different purpose in mind and was only incidentally applicable to the present work.

TABLE I

MOBILITIES OF CATIONS (CM.<sup>2</sup> VOLT<sup>-1</sup> SEC.<sup>-1</sup>)  $\times 10^4$  AT 20°

KCl soln.	Expt.	Lit. <sup>a</sup>
K <sup>+</sup>	5.8	6.9
H <sup>+</sup>	40.	33.7
Mg <sup>2+</sup>	2.8	4.9
H <sup>+</sup>	37.	33.7

<sup>a</sup> At infinite dilution.

**Acknowledgment.**—The authors thank Dr. D. D. DeFord for the design of and his advice concerning the electronic equipment employed as well as for helpful discussions.

(6) See for example R. A. Robinson and R. H. Stokes, "Electrolyte Solutions," Butterworth Scientific Publications, 1959, Appendix 6.2.

# THE EFFECT OF THE SUPPORT ON THE INFRARED SPECTRA OF CARBON MONOXIDE ADSORBED ON NICKEL

By C. E. O'NEILL AND D. J. C. YATES

*Stanley-Thompson Laboratories, School of Mines, Columbia University, New York 27, New York*

*Received July 5, 1960*

An experimental study has been made of the effect of the support in changing the adsorption characteristics of carbon monoxide on nickel supported on alumina, silica and titania. These changes have been determined by the effects which they produce on the infrared spectra of chemisorbed carbon monoxide. A new cell has been developed with sealed-on magnesium oxide windows, usable to at least  $8\ \mu$ , and has a small volume. The whole cell can be heated to  $400^\circ$  while evacuating the sample. The sample can be moved out of the optical path without affecting the sample conditions. Carbon monoxide adsorbs on nickel surfaces in two forms.<sup>1</sup> In one species, CO is attached to one nickel atom (linear), while in the other the molecule is attached to two nickel atoms (bridged). A marked variation was found, as the support was changed, both in the strength of adsorption, and in the relative numbers of the two species. In general, alumina and titania have marked effects on the adsorption of CO on supported nickel. Silica seems to have little, or no, effect.

## Introduction

Evaporated films of metals, first used by Beeck, Smith and Wheeler,<sup>2</sup> have been accepted as the best method of obtaining metal surfaces in a clean and reproducible state. Nevertheless, for many catalytic reactions supported metals have to be used. By this means, metals can be studied in a state of high dispersion up to relatively high temperatures. Refractory oxides<sup>3,4</sup> are most often used as supports.

The influence of the support in producing differences between the surface properties of unsupported and supported metals has been a source of controversy. For nickel on silica, Schuit and van Reijen<sup>5</sup> concluded that when the supported and unsupported systems are compared per unit area of metal surface, they are similar. Bond,<sup>6</sup> studying the reaction between ethylene and deuterium on platinum, concluded that the supports used (silica, silica-alumina, alumina) influenced the reaction in a subtle way. He also considered that the problem can only be approached by the application of the most sensitive techniques.

The infrared spectra of adsorbed molecules provides this sensitive technique. The first observation by this method is that of Eischens and Pliskin,<sup>7</sup> using platinum. When CO is adsorbed on metals, two types of absorption bands usually occur. One is due to the stretching vibrations of a CO molecule held by its carbon end to one surface metal atom (a linear species) and the other is due to a CO molecule held to two metal atoms (a bridged species). The spectra of CO on platinum show differences when the support is changed from silica to alumina; more of the bridged species was present when the alumina was used. Preliminary results obtained in this investigation using nickel supported on alumina showed that the ratio of linear to bridged species varied considerably when the CO pressure varied.

Three supports were used in this investigation: alumina, silica and titania. Drastic effects of the support have been found on adsorbing CO. In addition to large, pressure-dependent variations in the ratio of linear to bridged species, large changes in the strength of binding of both species to the surface have been observed. When silica is used as the support, only about 25% of the adsorbed CO could be removed by evacuation for 30 minutes at room temperature. Under the same conditions, 90% of the adsorbed gas could be removed from nickel supported on titania.

## Experimental

**Materials and Sample Preparation.**—Alumina (Alon C) and silica (Cabosil HS5) were gifts from the G. L. Cabot Co. of Boston. The surface areas (given by the supplier) are  $100\ \text{m}^2/\text{g}$ . for alumina and  $300\text{--}350\ \text{m}^2/\text{g}$ . for silica. Titania (anatase, code No: MP-1579) of surface area  $290\ \text{m}^2/\text{g}$ . was the gift of the National Lead Co., Titanium Division, South Amboy, N. J.

All the supports were covered with 9% nickel in this way. An aqueous solution of nickel nitrate (C. R., Fisher Scientific Co.) containing 0.9 g. of nickel was prepared. The volume of water used varied from support to support, being just sufficient in all cases to form a creamy paste when added to 10 g. of the oxide. The nitrate solution was added to the powder and stirred until a homogeneous mixture was obtained, and which was dried at  $110^\circ$ .

The nickel nitrate coated supports were pressed into self-supporting<sup>8</sup> discs in a 2.5 cm. die, using a pressure of  $4000\ \text{lb.}/\text{in}^2$ . The pressure was kept low to keep the permeability of the disc high, and to avoid other effects such as those reported<sup>8</sup> at pressures of  $100,000\ \text{lb.}/\text{in}^2$ . For alumina and titania 0.125 g. of powder was used, giving "optical thicknesses" of  $25\ \text{mg.}/\text{cm}^2$ . Thinner samples ( $20\ \text{mg.}/\text{cm}^2$ ) were used with silica. The weights of the samples used in the cell varied from 30 to 50 mg.

Carbon monoxide (C. P. grade) and pre-purified hydrogen (99.9%) grade were obtained from the Matheson Co., Inc. Oxygen was removed from hydrogen by a Baker Deoxo catalytic purifier. Both of these gases were dried by passage through traps cooled to  $77^\circ\text{K}$ . Carbon dioxide was obtained as the commercial solid and purified by vacuum distillation.

**Apparatus.**—Cells used previously for infrared studies on supported metals,<sup>9,10</sup> have been subject to three main disadvantages. A vertical light beam had to be used instead of the normal horizontal beam, the cell had a large dead space, and the sample is fixed in a rather long optical path (about 20 cm.). These first two points have been discussed elsewhere.<sup>9,10</sup> The fixed sample has the consequence that it is difficult, in some cases, to differentiate between the spectra of adsorbed gases and the same gas in the vapor phase.

(1) R. P. Eischens, W. A. Pliskin and S. A. Francis, *J. Chem. Phys.*, **22**, 1786 (1954).

(2) O. Beeck, A. E. Smith and A. Wheeler, *Proc. Roy. Soc. (London)* **A177**, 62 (1940).

(3) D. A. Dowden, *Ind. Eng. Chem.*, **44**, 977 (1952).

(4) W. B. Innes, in "Catalysis" (ed. P. H. Emmett), Vol. I, Reinhold Publ. Corp., New York, N. Y., 1954, p. 245.

(5) G. C. A. Schuit and I. L. van Reijen, *Advances in Catalysis*, **10**, 242 (1958).

(6) G. C. Bond, *Trans. Faraday Soc.*, **52**, 1235 (1956).

(7) R. P. Eischens and W. A. Pliskin, *Advances in Catalysis*, **10**, 2 (1958).

(8) R. S. McDonald, *J. Phys. Chem.*, **62**, 1168 (1958).

(9) R. P. Eischens, S. A. Francis and W. A. Pliskin, *ibid.*, **60**, 194 (1956).

(10) A. C. Yang and C. W. Garland, *ibid.*, **61**, 1504 (1957).

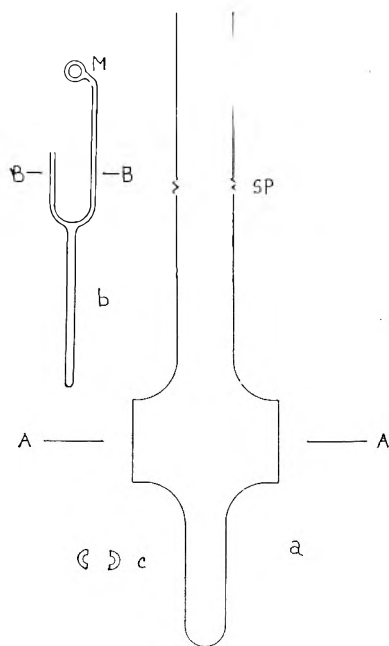


Fig. 1.—Adsorption cell with magnesium oxide windows; a, side view showing soda to Pyrex seal (SP); b, Pyrex glass sample holder; c, cross section of sample holder along BB.

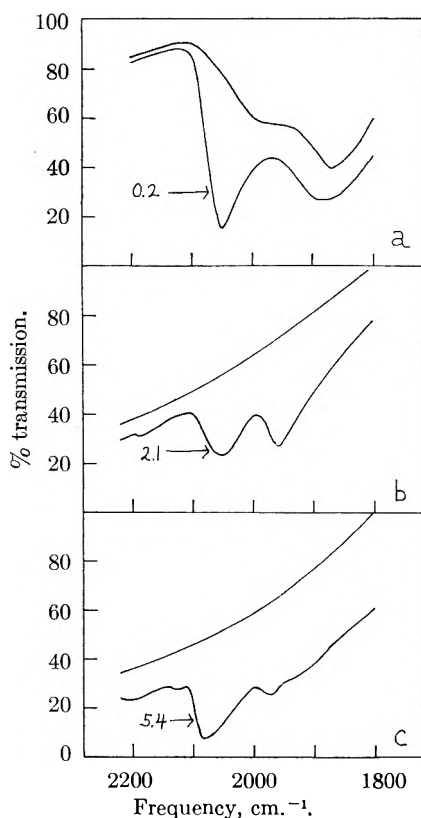


Fig. 2.—Typical transmission spectra as recorded by the spectrometer for nickel supported on (a) silica, (b) alumina and (c) titania. The upper curves in each case are the spectra of the reduced samples. The lower spectra were recorded after carbon monoxide addition. The pressures used (in mm.) are given as figures on the diagram.

The self-supporting discs were mounted vertically in a cell (volume 48 cm.<sup>3</sup>) with magnesium oxide windows, shown in Fig. 1. The windows are directly glass-blown to soda glass,<sup>11</sup> permitting the whole cell to be evacuated up to 400°

while heating with an external furnace. The 2 cm. diameter windows were 0.1 cm. thick, and spaced 3.6 cm. apart along the optical axis AA. The samples were held in a Pyrex glass U shaped holder, shown at b in Fig. 1. The glass rod on the bottom kept the holder in the optical path. A glass-enclosed magnet M enabled the sample to be lifted out of the beam for separate spectral analysis of the gas phase.

An all-glass vacuum system was used, with a mercury diffusion pump and rotary backing pump. The ultimate kinetic vacuum of the system was  $5 \times 10^{-6}$  mm.; all values given were recorded while pumping. A Perkin-Elmer model 21 double-beam spectrometer was used, with a calcium fluoride prism. For highly scattering samples, it is desirable that the sample be placed at a focus. The model 21 does not have an accessible focus, so one was provided by an external mirror system. Wire meshes were placed in the reference beam to balance out energy losses caused by the mirrors, cell and sample. The reduced samples had these approximate percentage transmissions at 2000 cm.<sup>-1</sup>: alumina 1.5, silica 8.0 and titania 2.0. To minimize heating effects, the source was run at 0.3 ampere.

The spectrometer slits were widened to compensate for the energy losses. At 2000 cm.<sup>-1</sup>, these slit widths (in mm.) were used: for alumina 0.360, for silica 0.136 and for titania 0.320. The corresponding spectral slit widths are 6.8, 3.0 and 6.0 cm.<sup>-1</sup>. The standard slit program gives a width of 0.068 mm. at 2000 cm.<sup>-1</sup>, corresponding to a spectral slit width of 1.8 cm.<sup>-1</sup>.

**Procedure.**—The sample was inserted in the cell and evacuated. The cell was heated to 120–150°, and the sample kept at this temperature until vacua of about  $10^{-4}$  mm. were obtained. Hydrogen, at a pressure of 40 cm. was let in, and the temperature increased uniformly to 350° in an hour. The hydrogen was changed about ten times during this period. The sample was kept at 350° for one hour, and then evacuated at 350° for 30 minutes. The final vacuum obtained after this was about  $10^{-5}$  mm. The cell tap was closed and the sample cooled to room temperature under vacuum.

The background spectrum was recorded from 4000 to 1200 cm.<sup>-1</sup>. A measured dose of CO was adsorbed and the spectrometer started. The region from 2300 to 1200 cm.<sup>-1</sup> usually was scanned, and spectra were taken for each dose until equilibrium was obtained. The CO pressure then was measured, and other doses added in the same way.

After the equilibrium spectrum of the last dose was recorded, the sample was evacuated for times from 30 seconds to 30 minutes. The vacuum obtained just before isolating the cell was measured for each of these evacuations.

All reductions after the initial one were done in the same fashion, except that the heating time to 350° was reduced to 20 minutes. The samples were kept in hydrogen at 350° for 20 minutes and evacuated for 10 minutes at 350°.

## Results

**Spectra Obtained by Adsorption.**—All spectra were obtained at room temperature. Figure 2 show typical spectra for each system; the alumina (b) and titania (c) samples have uniform backgrounds. The slope is caused by the scattering characteristics of the metal and the support.

Alumina and titania have no absorption bands themselves in this region. Silica (2a), however, has broad bands at 1970 and 1870 cm.<sup>-1</sup>, superimposed on a sloping background, and a steep drop in transmission between 2100 and 2000 cm.<sup>-1</sup>. From the recorded spectra, transmission curves have been calculated, and are given in Figs. 3, 4 and 5.

The maximum pressure of CO was used for each support. Two factors limited this. First, the pressure had to be kept below that at which nickel carbonyl began to form. Secondly, the photometric accuracy of the spectrometer falls off at transmissions less than about 5%.

Apparent peak optical densities ( $d$ ) of all bands



are given in Table I. These are defined by  $d = \log (T_0/T)\nu$ , where  $T_0$  is the transmission of the reduced sample and  $T$  that with the adsorbed gas, at frequency  $\nu$ .

TABLE Ia

PRESSURE OF CARBON MONOXIDE ABOVE SUPPORTED NICKEL, ON ADSORPTION, AND OPTICAL DENSITIES OF RESULTING BANDS

Pressure, mm.	Ratio of peak optical densities, $d_L/d_B$	Linear species peak optical density, $d_L$	Bridged species peak optical density, $d_B$
Silica support			
<0.05	1.62	0.11	0.07
0.2	3.10	0.81	.26
1.3	2.50	1.40	.59
Alumina support			
<0.05	1.10	0.25	0.23
0.75	0.86	.31	.36
2.1	0.86	.37	.43
4.5	1.40	.63	.45
10.6	1.47	.70	.47
Titania support			
0.50	6.2	0.68	0.11
2.7	4.9	.78	.16
5.4	2.2	.87	.38
9.1	1.1	.92	.81

TABLE Ib

EVACUATION OF CARBON MONOXIDE FROM SUPPORTED NICKEL, AND OPTICAL DENSITIES OF RESULTING BANDS

Evacuation, time, min.	Ratio of peak optical densities, $d_L/d_B$	Linear species peak optical density, $d_L$	Bridged species peak optical density, $d_B$
Silica support			
0.5	1.98	1.12	0.57
1.75	1.81	0.98	.54
4.75	1.89	.98	.52
31.5	1.85	.90	.49
Alumina support			
0.5	1.13	0.47	0.41
1.5	1.07	.41	.38
4.5	1.04	.39	.37
28.5	1.04	.37	.36
Titania support			
0.5	1.7	0.46	0.14
1.5	1.2	.20	.12
7.5	0.97	.10	.11
25.5	0.94	.06	.08

Figures 2 to 5 show a general lowering of transmission when the CO is adsorbed. Some of this lowering is removed when the gas is desorbed, using silica and alumina, but much less so with titania. The lowering may be caused by electronic changes in the supported nickel. It is unlikely to be entirely the result of a refractive index change from adsorption, as smaller transmission changes were observed with nickel oxide.

In all cases after the adsorption experiments the samples were evacuated and re-reduced. The same sequence, and size, of CO doses as adsorbed before were again adsorbed. The peak optical densities showed that some nickel surface area loss (relative to the initial reduction) occurred with

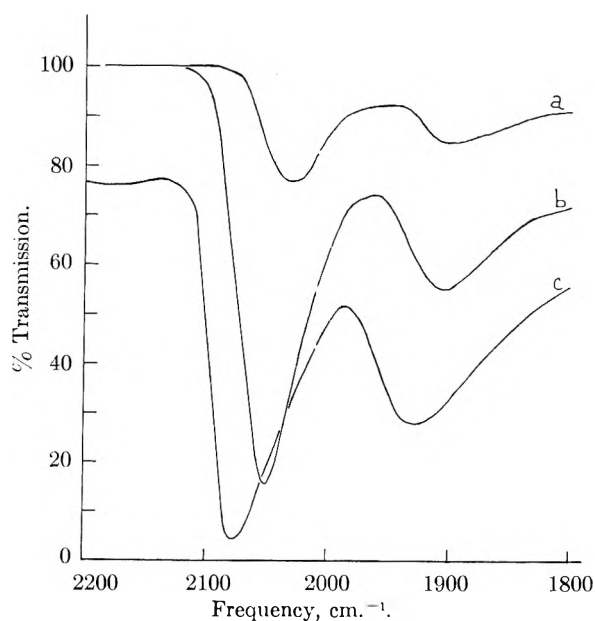


Fig. 3.—The spectra of carbon monoxide adsorbed on silica supported nickel. Pressures of carbon monoxide in mm.: a, less than 0.1; b, 0.2; c, 1.3.

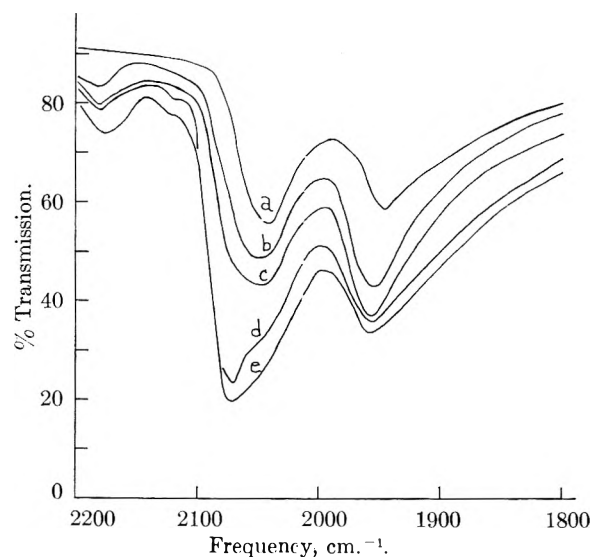


Fig. 4.—The spectra of carbon monoxide adsorbed on alumina supported nickel. Pressures of carbon monoxide in mm.: a, less than 0.1; b, 0.75; c, 2.1; d, 4.5 and e, 10.6.

silica, but very little change took place with alumina and titania. All the frequencies of the linear and bridged species were the same, within experimental error, for each particular combination of support and CO pressure. This also applied when other samples were made from the same batch of oxides, and the effects found here seem independent of the history of the reduction cycles of the samples.

**Spectra Obtained on Evacuation.**—After the sample was evacuated, its spectrum was recorded. Spectra were obtained for each time of evacuation. Wide differences were found to exist between the various supports and to clarify these, the percentage of each species removed as a function of time is shown in Fig. 6. These percentages have been derived from the optical densities of the peaks obtained after evacuation, relative to the densities

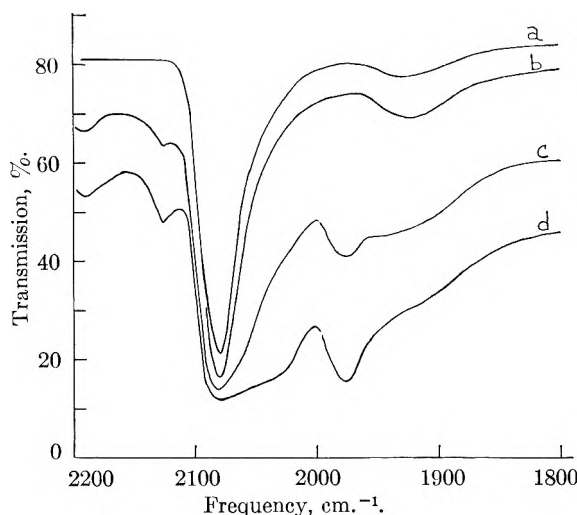


Fig. 5.—The spectra of carbon monoxide adsorbed on titania supported nickel. Pressures of carbon monoxide in mm.: a, 0.5; b, 2.7; c, 5.4 and d, 9.1.

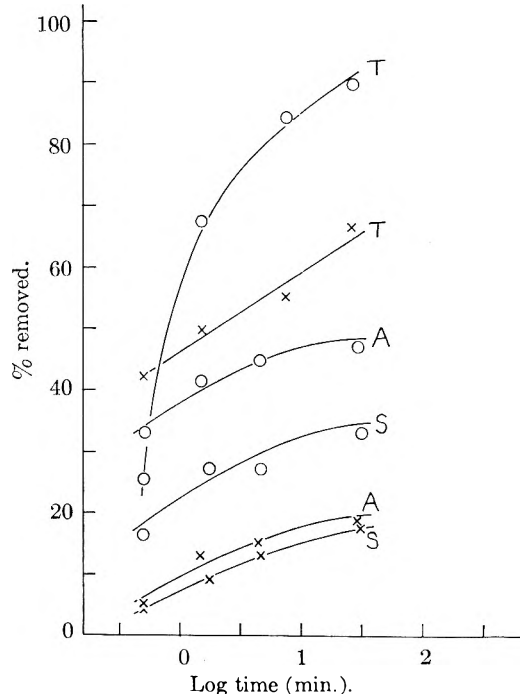


Fig. 6.—Removal of the linear (O) and bridged (X) species of carbon monoxide as a function of time of evacuation. Supports used: A, anatase; S, silica; T, titania.

obtained at the end of the adsorption experiments.

A very large general lowering of transmission occurred using anatase and was not reversible on evacuation. Hence, the peak optical densities both for the last dose adsorbed and for the evacuations have been calculated as differences between the densities of the peak to the optical density of the particular spectrum concerned at 2130  $\text{cm}^{-1}$ .

**Surface Species Observed.**—In general, the strongest bands found in the spectra are caused by two species that have been assigned by Eischens, *et al.*<sup>9</sup> by analogy with structure of metal carbonyls.<sup>12</sup> One is the stretching frequency of a CO molecule held to one nickel atom (linear CO) and

the other is the stretching frequency of a molecule held to two nickel atoms (bridged CO). In this work, the linear CO has bands in the region 2080 to 2030  $\text{cm}^{-1}$ , while the bridged molecules absorb at 1975 to 1900  $\text{cm}^{-1}$ .

At fairly high CO pressures a species absorbing at 2170 to 2190  $\text{cm}^{-1}$  has been observed. It is best described as a CO molecule held *via* the carbon atom to an oxygen atom.<sup>13</sup> This oxygen atom is held to a nickel atom. Except for titanium dioxide where a weak band appeared, this band did not appear when CO was added at similar pressures to the pure supports. To ensure comparable conditions, the pure supports were "reduced" in hydrogen before this experiment.

## Discussion

**Spectra Obtained with the Silica Support.**—It has been considered for many years<sup>2</sup> that a chemisorbed monolayer is formed on evaporated films at a pressure of 0.1 mm. This idea recently has been criticised,<sup>14,15</sup> and seems incorrect. With supported nickel Schuit and van Reijen<sup>5</sup> suggested using pressures of 100 mm. to form a monolayer. There remains some doubt as to the pressure at which a monolayer is formed for supported metals, if indeed a unique pressure exists, so the widest possible pressure range has been used in this work.

Data on the Cabosil-nickel system have been given by Eischens, *et al.*,<sup>9</sup> who presented a spectrum taken with 0.1 mm. pressure of CO. The linear species was found to be at a wave length of 4.82  $\mu$  (2074  $\text{cm}^{-1}$ ) and bridged species at 5.19  $\mu$  (1926  $\text{cm}^{-1}$ ). These values and frequencies are close to those found here at 1.3 mm. pressure (2075 and 1925  $\text{cm}^{-1}$ ).

Figure 3 shows that the linear band formed after dose 2, centered at 2050  $\text{cm}^{-1}$ , cuts through the low frequency side of the linear band at 2075  $\text{cm}^{-1}$ , found on adding dose 3. Hence, as the species absorbing at 2075  $\text{cm}^{-1}$  are formed, some of those species previously absorbing at 2050  $\text{cm}^{-1}$  are removed by one means or another. This phenomenon occurs over quite a range of coverage.

The 2050  $\text{cm}^{-1}$  band is caused by strongly held linear CO and the 2075  $\text{cm}^{-1}$  band is due to weakly held linear CO. Two explanations of these results are possible. The first,<sup>9</sup> is that the 2075  $\text{cm}^{-1}$  band is due to the presence of two linearly attached CO molecules on one nickel atom. This configuration seems probable only on those nickel atoms which occupy corners and edges. Secondly, there may be a change in lateral interaction between adsorbed molecules. The mutual repulsion of the closely packed system formed at higher coverages may be such as to weaken the over-all strength of adsorption of those molecules adsorbed at low coverage. The second model is only a tentative one, and the two molecules on one site model cannot be ruled out. The above process did not occur with the other supports, for either CO species.

(13) R. P. Eischens and W. A. Pliskin, *Advances in Catalysis*, **9**, 662 (1957).

(14) A. S. Porter and F. C. Tompkins, *Proc. Roy. Soc. (London)*, **A217**, 544 (1953).

(15) D. F. Klemperer and F. S. Stone, *ibid.*, **A243**, 375 (1957).

(12) J. W. Cable and R. K. Sheline, *Chem. Revs.*, **56**, 1 (1956).

The above data do not give any information about the difference, if any, between unsupported nickel and silica supported nickel. The work of Pickering and Eckstrom,<sup>16</sup> using evaporated nickel, would seem to provide the nearest comparison by spectroscopic means. The spectra show only the linear type of CO at 2058  $\text{cm}^{-1}$ . However, the 2058  $\text{cm}^{-1}$  band is ascribed to nickel carbonyl in the summary. This, together with the non-observation of a band due to bridged CO, makes the significance of these results difficult to assess. The evacuation characteristics of the systems give a non-spectroscopic method of ascertaining the effect of the silica support. Isotherms on reduced nickel powders at room temperatures obtained by us show that about 28% of the adsorbed CO was removed by 30 minutes evacuation. For silica supported nickel, Fig. 6 shows that about 25% of the CO was removed in 31.5 minutes.

For the reduced nickel system the particular silica support used here seems to have little, if any, effect on the adsorption of carbon monoxide.

**Spectra Obtained Using Alumina.**—Figure 3 shows that the linear CO absorbs at 2040  $\text{cm}^{-1}$  at low pressure, and at 2070  $\text{cm}^{-1}$  at the highest pressure used. Over the same pressure range, the bridged species moved from 1945 to 1958  $\text{cm}^{-1}$ . No estimate can be given of the coverage at a pressure of 10.6 mm., as higher pressures could not be used.

Infrared spectra of CO adsorbed on nickel on alumina were reported by Garland.<sup>17</sup> At low coverage bands were found at 2045 and 1910  $\text{cm}^{-1}$ , and at higher coverages bands at 2075 and 1960  $\text{cm}^{-1}$  appeared. The effect of evacuation was discussed, and appears about the same as that found here. The shortest time of evacuation was 30 minutes. These results are in general agreement with those found in this work. Unfortunately, a more detailed comparison is not possible as, although the amount of CO in the cell was given, pressures after adsorption were not measured.<sup>17</sup> Quantitative comparison of the spectra is further complicated by the absence of a numerical scale on the transmission axes.

The effect of the support was not explicitly considered by Garland. He attributed the differences between his results using alumina (Alon C) and earlier<sup>9</sup> results on silica (Cabosil) to differences in sample preparation.

**Spectra Obtained Using Titania.**—Figure 5 shows that at low pressures, a strong linear band appears at 2080  $\text{cm}^{-1}$ , but only a weak bridged band is present at 1925  $\text{cm}^{-1}$ . At 5.4 mm., the linear band is more intense at much the same frequency as before, but the growth of the band at 1925  $\text{cm}^{-1}$  is masked by the occurrence of a strong band at 1975  $\text{cm}^{-1}$ . The pressure at which this latter band occurs is not known accurately. A series of experiments on the same sample showed that, despite two series of oxidation experiments in between, in three separate adsorption experiments, the 1975  $\text{cm}^{-1}$  band always appeared between 2.1 and 6.1 mm. At pressures up to 9.1 mm., the

1975  $\text{cm}^{-1}$  band grows rapidly, becoming nearly as intense as the linear band.

On evacuation the linear band shifts to lower frequencies, although little frequency change in this band occurred on adsorption. This is partly due to the presence of a more strongly held band at about 2040  $\text{cm}^{-1}$  which forms a distinct shoulder on the 2080  $\text{cm}^{-1}$  peak for the first two evacuations (0.5 and 1.5 minutes). These two bands merge on further evacuation. The 2040  $\text{cm}^{-1}$  band is present on adsorption at 9.1 mm., and possibly at 5.4 mm. The 1975  $\text{cm}^{-1}$  band is nearly all removed by evacuation for 30 seconds, while the 1925  $\text{cm}^{-1}$  band is described more slowly.

These results are in sharp contrast with those found on silica and alumina. First, the strength of attachment of both species (linear 2080  $\text{cm}^{-1}$ , bridged 1925  $\text{cm}^{-1}$ ) is much weaker than for the same species on the other supports. Figure 6 shows that 90% of the linear species is removed in 25.5 minutes, and 64% of the bridged species in the same time.

The second unusual aspect of the titania results is the occurrence of the bridged band at 1975  $\text{cm}^{-1}$ , which must be extremely weakly held as it is virtually removed by 30 seconds evacuation. The bridged species, on the other supports used here, is more strongly held than the linear species. This 1975  $\text{cm}^{-1}$  band is a good example of a weakly chemisorbed molecule. Its spectral characteristics show that it is chemisorbed, while its extreme ease of removal indicates its weak interaction with the adsorbent.

**Ratio of Linear to Bridged Forms of Carbon Monoxide.**—With the silica support the linear band seems about twice as intense as the bridged band, as judged by the peak optical densities. Table Ia shows that  $d_L/d_B$  varies from 1.6 to 3.1 (on adsorption) in an irregular fashion. Other adsorption measurements on the same sample which had been re-reduced after some nickel oxide experiments gave a more constant value varying from 2.1 to 2.4. Table Ib shows that a ratio independent of variations due to pressure of adsorption can be found from evacuation experiments. The ratio is fairly constant (1.85) for times greater than 0.5 minute. With alumina, while more of the molecules are adsorbed in the bridged fashion, the  $d_L/d_B$  still varies on adsorption. On evacuation, the ratio decreases and becomes 1.04. On anatase, the  $d_L/d_B$  ratio is much higher (6.2) at low coverages, and drops to 1.1 at higher coverages. On evacuation it drops to 0.94. It is not known whether this is a constant value, or whether it would decrease at longer times of evacuation.

When the influence of the weakly adsorbed species is removed by evacuation, in all cases more constant values of  $d_L/d_B$  are obtained. Silica has a ratio of 1.85 and alumina 1.04, and these values probably are characteristic of the strongly held species on each metal-support combination. On titania such large variations are found, both on adsorption and desorption, that no characteristic value for  $d_L/d_B$  can be given for this system.

The occurrence of the linear and bridged modes<sup>1</sup> of attachment of CO on nickel, is of importance in

(16) H. L. Pickering and H. C. Eckstrom, *J. Phys. Chem.*, **63**, 512 (1959).

(17) C. W. Garland, *ibid.*, **63**, 1423 (1959).

clarifying observations made by classical methods. Beeck<sup>18</sup> found the monolayer capacity for carbon monoxide to be twice that for hydrogen, the  $V_{CO}/V_{H_2}$  ratio being 2.0. More recent data<sup>19</sup> on evaporated films give a value of about 1.5. This non-integer value finds ready explanation in terms of the infrared data, and it would be of importance if the relative numbers of the two species could be found spectroscopically.

To do this, the relative extinction coefficients of the species must be known. The best method of estimating these coefficients is to compare the relative strengths of the bands due to bridged and linearly held CO in various metal carbonyls. Infrared data are available for iron enneacarbonyl,<sup>20</sup> iron tetracarbonyl<sup>21</sup> and dicobalt octacarbonyl.<sup>22</sup> The spectra in the above papers are not suitable for quantitative calculations of relative optical density. Iron enneacarbonyl was examined in the solid state and a strong Christiansen filter effect<sup>23</sup> distorted the intensities considerably. In the iron tetracarbonyl spectra, the bridged band overlapped the linear band. For cobalt carbonyl well-resolved spectra are given, but the linear band is split into three components, and comparison with the narrow bridged band could not easily be made from peak optical densities.

Until some method is devised for determining relative extinction coefficients, infrared data cannot give the relative numbers of these two species. Hence, the "normality" of a  $V_{CO}/V_{H_2}$  ratio of 1.3 as inferred by Schuit and van Reijen<sup>5</sup> from infrared data on nickel, must be regarded as provisional.

(18) O. Beeck, *Advances in Catalysis*, **2**, 151 (1950).

(19) P. M. Gundry and F. C. Tompkins, *Trans. Faraday Soc.*, **53**, 218 (1957).

(20) R. K. Sheline and K. S. Pitzer, *J. Am. Chem. Soc.*, **72**, 1107 (1950).

(21) R. K. Sheline, *ibid.*, **73**, 1615 (1951).

(22) J. W. Cable, R. S. Nyholm and R. K. Sheline, *ibid.*, **76**, 3373 (1954).

(23) W. C. Price and K. S. Tetlow, *J. Chem. Phys.*, **16**, 1157 (1948).

**General Remarks.**—The effect of the support in changing the ratio of linear to bridged species of CO is probably a function of the electrical properties of the junction formed at the points where the metal is in intimate contact with the substrate. The properties of these metal-support junctions will vary considerably from oxide to oxide. They are expected to be related to both the semi-conductivity of the particular oxide used and to the nature of the interstitial compounds formed at the junction. Little reliable information seems available on the semi-conductive properties of finely divided oxides. The oxides used here, although fairly pure by normal standards, are impure by the standards needed to obtain interpretable conductivity data of the type obtained, for example, on germanium. Until the electrical characteristics of high area oxides are much more clearly understood, it seems that little is to be gained by theoretical speculations about their electrical characteristics, and of those of the metal-oxide junctions. Evidence is accumulating, especially for alumina and titania, that wide variations in surface properties of these oxides can occur when their method of preparation is changed. Hence, it is unlikely that the results reported here can be extrapolated to other silicas, aluminas and titanias, and such comparisons should not be made.

**Acknowledgments.**—We wish to thank the International Nickel Company for generous financial help for equipment and grants which supported this work. Thanks are also due to Professor Jack H. Schulman for his interest and encouragement during this work, and to Professor R. S. Halford, of the Chemistry Department, for helpful discussions on spectroscopic aspects of this work.

We also wish to thank Dr. N. Sheppard (of the University Chemical Laboratories, Cambridge) for helpful discussions on the original idea of using a cell with magnesium oxide windows for adsorption studies.

## FLUORESCENCE AND ABSORPTION STUDIES OF REVERSIBLE AGGREGATION IN CHLOROPHYLL<sup>1</sup>

BY PER S. STENSBY AND JEROME L. ROSENBERG

Contribution No. 1082 from the Department of Chemistry, University of Pittsburgh, Pittsburgh 13, Pennsylvania

Received August 4, 1960

Changes in the fluorescence spectrum of chlorophyll *a* and *b* have been used to observe reversible changes that these substances undergo at high concentration and low temperature. In both cases the change is reflected in the appearance of an intense fluorescence band above 700  $\mu$ . Absorption spectroscopy confirms the formation of reversibly aggregated species at temperatures below  $-100^\circ$ .

One of the accepted mechanisms for the concentration quenching of dye fluorescence in solution is the formation of non-fluorescent dimers.<sup>2</sup> The

stability of such dimers has been confirmed in a number of cases by observations of concentration-dependent changes in the absorption spectrum and in the action spectrum for fluorescence.<sup>3-6</sup> A more

(1) Presented at the Symposium on Molecular Fluorescence, Pittsburgh Conference on Analytical Chemistry and Applied Spectroscopy, March, 1960. These studies were aided by a contract between the Office of Naval Research, Department of the Navy, and the University of Pittsburgh, NR304-416.

(2) T. Förster, "Fluoreszenz Organischer Verbindungen," Vandenhoeck und Ruprecht, Göttingen, 1951, p. 2f2 ff.

(3) E. Rabinowitch and L. F. Epstein, *J. Am. Chem. Soc.*, **63**, 69 (1941).

(4) J. Lavorel, *J. Phys. Chem.*, **61**, 1600 (1957).

(5) T. Förster and E. König, *Z. Elektrochem.*, **61**, 344 (1957).

(6) G. Weber and F. W. J. Teale, *Trans. Faraday Soc.*, **54**, 640 (1958).

recent theoretical treatment indicates that dimers need not always be non-fluorescent.<sup>7</sup> In fact, Brody found experimentally that chlorophyll in alcoholic solutions shows an increased fluorescence under conditions where dimerization might be expected to occur, and that the fluorescence spectrum of the dimer is decidedly different from that of the monomer.<sup>8</sup> The following investigation was undertaken to confirm this finding of Brody, to improve the experimental discrimination of the fluorescence spectra in the near infrared, to look for long-lived emission, and to study changes in the absorption spectrum that might be correlated with the fluorescence.

### Experimental

Chlorophylls *a* and *b* were extracted from spinach, separated, purified, and analyzed by a modification of the procedure of Zscheile and Comar,<sup>9</sup> and stored in cold ether solution. Allomerized chlorophyll was prepared by air oxidation of an alcoholic solution of chlorophyll at room temperature.

Ethanolic solutions for absorption or emission spectroscopy were thoroughly degassed by the Thunberg technique. At low temperatures the solutions were clear glasses. Concentrations were determined spectrophotometrically by comparing absorbances at the red peaks in ether solution with the extinction values of Zscheile and Comar.<sup>9</sup> Fluorescence was observed from the illuminated surface of the cell at a direction perpendicular to the exciting light. The observed fluorescence spectra were badly distorted by almost complete reabsorption of the principal fluorescence peak. Since the main interest in this work lay in the fluorescence at longer wave lengths than the principal peak, this was not serious. The fluorescence data are reported as observed meter readings corrected for detector sensitivity but not for reabsorption. Absorption spectra were measured in a Cary-14 recording spectrophotometer. Optical paths as low as  $4 \times 10^{-3}$  cm. were obtained by inserting flat strips of glass as spacers into a rectangular cross-section cell. The absorption cell was mounted in an aluminum block which was immersed in a Dewar containing an amylene-bath cooled by circulating liquid nitrogen through copper coils. Smaller paths were achieved for room temperature experiments without deoxygenation by the optical flat sandwich technique.

For measurements of fluorescence spectra the emission was passed through a Bausch and Lomb 250 mm. grating monochromator blazed for a maximum first-order intensity of 750 m $\mu$ . Corning filters were used, when necessary, to exclude second-order transmission. The monochromator slits were set for a band width of 20 m $\mu$ . The detector was a DuMont 6911 red-sensitive photomultiplier. The monochromator-detector combination varied in sensitivity by less than 10% over the region of maximum response, 630 to 790 m $\mu$ . The sensitivity was 50% of maximum at 630 and 880 m $\mu$ , 37% at 900, and 2% at 1000.

### Results

**Chlorophyll *a*.**—The fluorescence spectrum of a  $5 \times 10^{-5}$  *M* ethanolic solution had its principal peak at 676 m $\mu$  and a secondary peak at 728 m $\mu$  at room temperature, the ratio of the peak heights being 3.7. At  $-196^\circ$  the peaks shifted to 682 and 740 m $\mu$ , the peak ratio to 3.1, and both peaks were sharper. These shifts are normal for simple temperature effects.

For an  $8.2 \times 10^{-3}$  *M* solution the peaks were at 680 and 734 m $\mu$  at room temperature and at 695 and 734 m $\mu$  at  $-196^\circ$  (Fig. 1). The peak height ratio decreased from 1.4 to 0.4 at  $-196^\circ$ . The differences between dilute and concentrated solutions at room temperature with respect to both

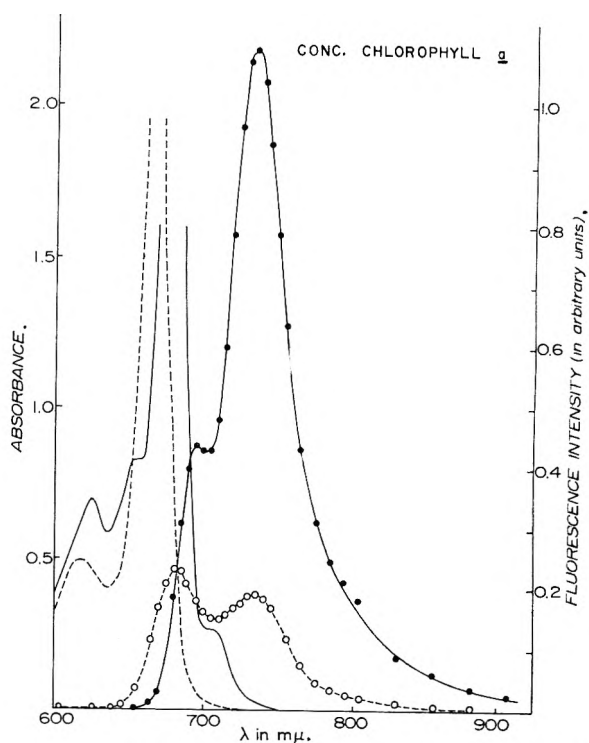


Fig. 1.—Concentrated chlorophyll *a*; solution,  $8 \times 10^{-3}$  *M* in ethanol; --- (no points), absorbance at  $25^\circ$ ; — (no points), absorbance at  $-196^\circ$ ; --○--○--, fluorescence at  $25^\circ$ ; —●—●—, fluorescence at  $-196^\circ$ .

peak location and peak height ratio are presumably due to differences in reabsorption. The anomalous increase in the secondary peak in the concentrated solutions at  $-196^\circ$  and the occurrence of this peak at a shorter wave length than the secondary peak for the dilute solution both indicate a new molecular species in cold concentrated solution. The data suggest that a small amount of dimer might exist at room temperature in the concentrated solution. These results confirm those of Brody in general, except that our new peak is located at a somewhat longer wave length than his. We believe that the discrepancy is due to Brody's use of a detector with a strongly wave length dependent response. The emission was followed to 1000 m $\mu$  but no additional peak was found in either dilute or concentrated solutions. Also, no delayed emission lasting more than a milli-second was detected at any wave length below 1000 m $\mu$ , within the limited sensitivity of the detector.

The absorption spectrum of a concentrated solution was studied as a continuous function of temperature between  $+25$  and  $-196^\circ$ . During the cooling of an  $8.2 \times 10^{-3}$  *M* ethanolic solution, new shoulders developed at about  $-100^\circ$  on both the short and long wave length sides of the peak. At  $-196^\circ$  these shoulders had developed into definite peaks at 654 and 705 m $\mu$ , the main peak being at 676 m $\mu$  (Fig. 1). A similar experiment with a  $3.5 \times 10^{-5}$  *M* solution showed a similar shift of the main peak and a similar new peak at 654 m $\mu$  but no new features on the long wave length side of the main peak. The 705 m $\mu$  peak in the concentrated solution is thus definitely associated with a

(7) E. G. McRae and M. Kasha, *J. Chem. Phys.*, **28**, 721 (1958).

(8) S. S. Brody, *Science*, **128**, 838 (1958).

(9) F. P. Zscheile and C. L. Comar, *Botan. Gaz.*, **102**, 463 (1941).

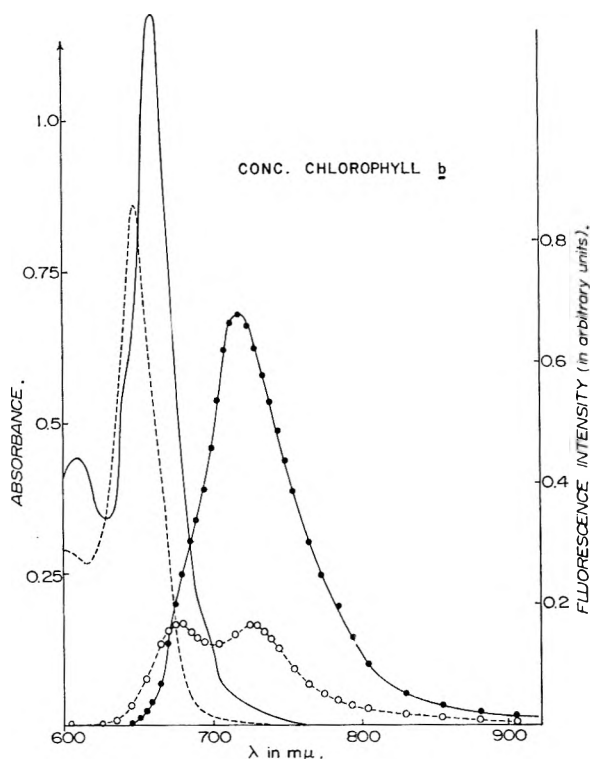


Fig. 2.—Concentrated chlorophyll *b*; solutions: for absorbance,  $5 \times 10^{-3} M$  in ethanol; for fluorescence,  $7 \times 10^{-3} M$  in ethanol; --- (no points), absorbance at  $25^\circ$ ; — (no points), absorbance at  $-196^\circ$ ; --○--○--, fluorescence at  $25^\circ$ ; —●—●—, fluorescence at  $-196^\circ$ .

new component that is not formed in dilute solutions. In a separate experiment with a concentrated solution the main blue absorption peak shifted from  $431 m\mu$  at  $25^\circ$  to  $441 m\mu$  at  $-196^\circ$ . The minor bands in the  $500\text{--}600 m\mu$  region lost some of their sharpness at  $-196^\circ$ .

Because of a recent report of Brody<sup>10</sup> that evidence for dimerization in concentrated solution can be observed in the absorption spectrum even without cooling, we made repeated efforts to observe the effect at room temperature. Even with a differential procedure the absorption spectrum of solutions up to  $8 \times 10^{-3} M$  was found to be identical at  $25^\circ$  with that of a dilute solution. Solutions containing more chlorophyll than this showed a broadening of the absorption spectrum on both sides of the red band, but all such preparations contained undissolved pigment. The broadened spectrum was also observed with purposely dried preparations, made by allowing solutions to evaporate to air-dryness in the cell.

**Chlorophyll *b*.**—Similar phenomena were found with ethanolic solutions of chlorophyll *b*. In dilute solutions the fluorescence peaks were at  $667$  and  $715 m\mu$  at  $25^\circ$  and at  $665$  and  $727 m\mu$  at  $-196^\circ$ . The reason for the unexpected slight decrease in the wave length of the first peak was not clear, but we did not attach as much significance to any of the positions of the peaks below  $700$

as to those above  $700$  because of reabsorption. The ratios of the two peak intensities were  $3.0$  at room temperature and  $3.3$  at  $-196^\circ$ . In concentrated solutions, however, a new intense peak occurred at  $718 m\mu$  at  $-196^\circ$  (Fig. 2), masking the  $725$  secondary peak observed at room temperature. At a concentration of  $7 \times 10^{-3} M$  the original main peak,  $675 m\mu$  at room temperature, appeared at  $-196^\circ$  only as a shoulder at  $680 m\mu$ . At intermediate concentrations the two peaks were resolved, the new one moving  $15 m\mu$  toward the infrared. The  $718 m\mu$  probably corresponds to the same species as Brody's  $695 m\mu$  shoulder; in fact, our sample showed an apparent shift in the new peak to  $695 m\mu$ , uncorrected for detector response, if a 1P21 blue-sensitive photomultiplier tube was used. With neither detector, however, could we confirm a new shoulder or peak shifted to the shorter wave length side, as Brody had reported. No additional fluorescence peaks were found in the range extending to  $1000 m\mu$ . As with chlorophyll *a*, none of the observed emission had a half-life greater than a millisecond.

In absorption new inflections were observed on both sides of the principal band in concentrated solutions at  $-196^\circ$  (Fig. 2). Under these conditions the main peak was at  $661 m\mu$  and the new shoulders were at  $642$  and  $695 m\mu$  for  $5 \times 10^{-3} M$  solutions.

**Allomerized Chlorophyll *a*.**—The fluorescence spectrum of concentrated solutions in ethanol was found not to be temperature dependent, although the fluorescence yield increased about threefold on cooling from  $25$  to  $-196^\circ$ .

### Discussion

Our fluorescence data support Brody's conclusion that a reversible aggregation of chlorophylls *a* and *b* occurs in concentrated alcoholic solution. Our absorption data support this interpretation and also indicate that the aggregate forms in appreciable amounts only below  $-100^\circ$ . The absence of considerable dimerization at room temperature confirms the findings of Watson and Livingston, based on absorption spectra and on the concentration and temperature dependence of self-quenching of fluorescence.<sup>11</sup> The experiments of Weber and Teale<sup>6</sup> and of Forster and Livingston<sup>12</sup> on the wave length dependence of fluorescence yield in concentrated solutions, might be interpreted by assuming a few per cent. of a non-fluorescent dimer at room temperature, which would escape detection in absorption spectroscopy.<sup>13</sup> Even this view entails some difficulties. According to McRae and Kasha,<sup>7</sup> the fluorescence of a dimer should depend in the first instance on the relative orientation of the two halves of the molecule. An arrangement compatible with the observed strong fluorescence at low temperature, such as a non-parallel arrangement of the conjugated planes of the two monomeric moieties or a parallel arrangement with some parallel displacement, would have the same high transmission

(10) S. S. Brody, Paper presented at the Symposium on Molecular Fluorescence, Pittsburgh Conference on Analytical Chemistry and Applied Spectroscopy, March, 1960. S. S. Brody and M. Brody, *Nature*, **189**, 547 (1960).

(11) W. F. Watson and R. Livingston, *J. Chem. Phys.*, **18**, 802 (1950).

(12) L. S. Forster and R. Livingston, *ibid.*, **20**, 1315 (1952).

(13) E. Rabinowitch, *Plant Physiol.*, **35**, 477 (1960).

probability at room temperature. Then the invocation of dimers to account for room temperature fluorescence quenching would either require differently structured dimers at high and low temperatures or a single form of dimer to which the *ad hoc* hypothesis of a strongly temperature-dependent collisional or internal conversional quenching is applied. The indications of absorption spectrum broadening at room temperature,<sup>10</sup> we believe, are due to scattering by suspended particles in saturated solutions. For these reasons we feel that the dimer stable at low temperature is probably not the prevalent form of chlorophyll important for *in vivo* photosynthesis. We do not mean to exclude the role of reversible changes in the small fraction of chlorophyll molecules participating chemically in the photosynthetic process.

The low stability of the chlorophyll dimer is not surprising. Practically all the authenticated cases of reversible room temperature-stable dye dimers have occurred with ionic dyes, such as thionin, acridine and crystal violet cations and fluorescein and eosin anions. Levinson, *et al.*,

attribute the stability of such dimers to the coulombic forces of ion pairing as influenced by charge delocalization.<sup>13</sup> Non-ionic dimers would then be restricted to those formed only in the excited states by electronic excitation delocalization, such as pyrene,<sup>14</sup> or to those whose ground-state stabilization is of the much weaker van der Waals type. This latter category, including chlorophyll, would be expected only at low temperatures.

The relative inability of allomerized chlorophyll to dimerize at low temperature may be due to steric barriers of the bulky alkoxy substituent at carbon-10.

The changes reported here differ by their concentration dependence from the temperature- and solvent-dependent changes reported by Freed and co-workers and ascribed to reversible solvation.<sup>15,16</sup> Freed's measurements were all made with dilute chlorophyll solutions.

(13) G. S. Levinson, W. T. Simpson and W. Curtis, *J. Am. Chem. Soc.*, **79**, 4314 (1957).

(14) T. Förster, *Z. Elektrochem.*, **59**, 976 (1955).

(15) S. Freed and K. M. Sancier, *J. Am. Chem. Soc.*, **76**, 198 (1954).

(16) S. Freed, *Science*, **125**, 1248 (1957).

## THE LANTHANUM-BORON SYSTEM<sup>1</sup>

BY ROBERT W. JOHNSON AND A. H. DAANE

*Institute for Atomic Research and Department of Chemistry, Iowa State University, Ames, Iowa*

*Received August 11, 1960*

From thermal, metallographic, X-ray and electrical resistance data a phase diagram is proposed for the lanthanum-boron system. Two compounds are formed, LaB<sub>4</sub> and LaB<sub>6</sub>. The former has a very narrow range of homogeneity and decomposes peritectically at 1800 ± 15°. The crystal system is tetragonal, and the compound is a metallic type conductor. LaB<sub>6</sub> exists in the range 85.8 to 88% boron, melts above 2500°, and has a simple cubic lattice. The color of this compound changes with composition, going from purple to a bright blue with increasing boron content. The addition of boron to lanthanum has no measurable effect on the melting point or transition points of the metal. The addition of lanthanum to boron appears to have very little effect on the melting point of boron. There is metallographic evidence for an allotropic transformation in boron above 2100°. Evidence also is given for a new compound CaB<sub>4</sub>, which appears to be isomorphous with LaB<sub>4</sub>.

### Introduction

The past decade has seen an increasing interest in compounds between transition metals and boron, carbon, nitrogen and silicon. This group of refractory compounds is under study not only because they possess useful properties, but also because knowledge about the nature of their bonding is expected to contribute to the understanding of metallic bonds. Work on metal-boron systems has been hampered until recent years because elemental boron was not available in sufficient purity to permit reliable experimental results to be obtained, and as a result the state of knowledge of borides is less developed than that of carbides, nitrides and silicides. There is additional incentive for study of borides rather than the other refractory compounds because "electron deficient" bonding found in the boron hydrides and their derivatives is present in the boron "frameworks" of some borides. It would be desirable to seek a common basis for understanding the boron bonding in both sets of compounds.

The employment of the lanthanides (and scandium and yttrium) in the study of a set of compounds such as borides can be very useful because the size of the metal atom can be varied while other factors are nearly constant, thus helping the investigator to distinguish between size effects and effects due to other factors. The study of the lanthanum-boron system was undertaken for the above reasons, and also as a part of a program of investigation of the effects of interstitial type elements on the properties of the rare-earth metals.

Kiessling,<sup>2</sup> Kieffer and Benesovsky,<sup>3</sup> and Robins<sup>4</sup> have reviewed borides and other refractory compounds, and references 5-17 include most of the recent work on rare-earth borides.

(2) (a) R. Kiessling, *Acta Chim. Scand.*, **4**, 209 (1950); (b) *Powder Metallurgy*, No. 3 (1959).

(3) Kieffer and Benesovsky, *ibid.*, No. 1/2 (1958).

(4) D. A. Robins, *ibid.*, No. 1/2 (1958).

(5) L. Brewer, D. L. Sawyer, D. H. Templeton and C. H. Dauben, *J. Am. Ceram. Soc.*, **34**, 173 (1951).

(6) J. M. Lafferty, *J. Appl. Phys.*, **22**, 299 (1951).

(7) F. Bertaut and P. Blum, *Compt. rend.*, **234**, 2621 (1952).

(8) A. Zalkin and D. H. Templeton, *Acta Cryst.*, **6**, 269 (1953).

(9) H. C. Longuet-Higgins and M. De V. Roberts, *Proc. Roy. Soc. (London)*, **A224**, 336 (1954).

(1) Contribution No. 908. Work was performed in the Ames Laboratory of the U. S. Atomic Energy Commission.

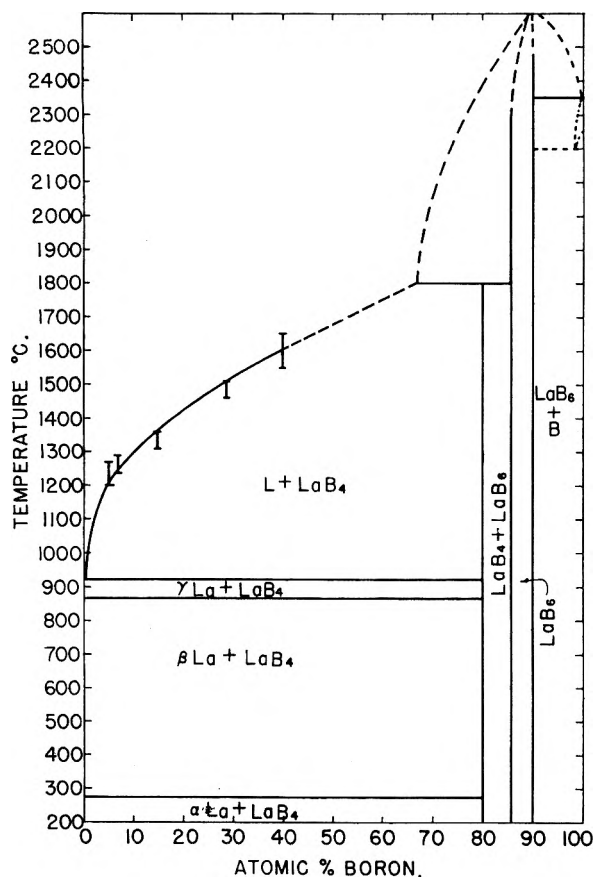


Fig. 1.—Phase diagram proposed for the lanthanum-boron system.

### Experimental

**Materials.**—The lanthanum was prepared at this Laboratory by reduction of sintered  $\text{LaF}_3$  with distilled calcium metal that was vacuum melted just prior to the reduction. The reactants were contained in a tantalum crucible, and the reduction carried out under an atmosphere of purified argon. Spectrographic analysis of the lanthanum used for investigating the effect of boron on the melting point and the upper transition point revealed traces of Al, Ca, Cu, Fe, Mg, Mn, Ni and Si. Most of these were barely detectable, meaning that the probable amount of each was less than 0.01%. The oxygen content was estimated by a spectrographic method to be less than 1450 p.p.m. Chemical analysis showed 52 p.p.m. carbon and 19 p.p.m. nitrogen. The lanthanum used for investigating the liquidus curve and for preparing  $\text{LaB}_4$  averaged 500 p.p.m. carbon, 200 p.p.m. nitrogen and greater than 2000 p.p.m. oxygen, the metallic impurities being about the same as in the other sample.

Spectrographic analysis of the  $\text{LaB}_4$  that was prepared revealed barely detectable amounts of Al, Ca, Cr, Cu, Fe, Mg, Mn, Si and Ta. Chemical analysis did not detect the presence of carbon or nitrogen in the  $\text{LaB}_4$ . No carbon was detected in the  $\text{LaB}_6$ , but the nitrogen content is unknown, due to analytical difficulties.

- (10) F. Bertaut and P. Blum, *Acta Cryst.*, **7**, 81 (1954).
- (11) F. Gaume-Mahn, *Bull. soc. chim. France*, 1862 (1956).
- (12) B. Post, D. Moskowitz and F. W. Glaser, *J. Am. Chem. Soc.*, **78**, 1800 (1956).
- (13) I. Binder, *Powder Met. Bull.*, **7**, 74 (1956).
- (14) E. J. Felten, I. Binder and B. Post, *J. Am. Chem. Soc.*, **80**, 3479 (1958).
- (15) H. Eick and P. Gillis, Abst. of Papers of 133rd meeting of the ACS, 57Q, 1958.
- (16) H. Eick and P. Gillis, Abst. of Papers of 134th meeting of the ACS, 1A, 1958.
- (17) A. U. Seybolt, Gen. Elec. Co. Research Report No. 59-RL-2180, 959.

The boron was obtained from Fairmont Chemical Co., and a vacuum fusion analysis showed 2.09% oxygen before arc melting and 0.26% oxygen after arc melting.

**Preparation of Samples.**—The samples of composition between pure lanthanum and  $\text{LaB}_4$  were prepared by heating weighed amounts of lanthanum and  $\text{LaB}_4$  in a tantalum crucible under a vacuum to 1500° for 15 min. in an induction furnace.

The  $\text{LaB}_4$  was made by arc melting pressed boron powder with a two to threefold excess of lanthanum metal. Impurities such as carbon, nitrogen and oxygen tended to stay in the lanthanum phase while pure  $\text{LaB}_4$  crystallized in the melt on cooling. The lanthanum and impurities were dissolved in dilute hydrochloric acid, leaving black  $\text{LaB}_4$  crystals having smooth shiny faces and sharp edges.

Lanthanum hexaboride was prepared by heating the required amounts of  $\text{LaB}_3$  and boron *in vacuo* at 1600 for 15 min. Alloys of higher boron content than  $\text{LaB}_6$  were prepared by arc melting the required amount of  $\text{LaB}_6$  with previously arc melted boron.

**Analysis.**—The composition of alloys between lanthanum and  $\text{LaB}_4$  was known from the exact weights of the lanthanum and  $\text{LaB}_4$  used to make up the alloy. Melting of the components in a tantalum crucible did not alter the composition since neither lanthanum nor the boron in it seriously attacked the crucible, unless the carbon content of the lanthanum was abnormally high. The composition of  $\text{LaB}_4$  and  $\text{LaB}_6$  was obtained from the measured density and lattice constants as described below, the densities being measured by pycnometric methods.

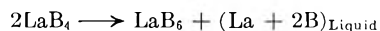
The composition of arc-melted high boron samples was known from the weights of the  $\text{LaB}_6$  and boron used to make up the sample.

**Thermal Analysis.**—Heating and cooling curves of pure lanthanum and lanthanum-rich alloys were carried out in a vacuum resistance furnace with a tantalum wire heating element which was not in direct contact with ceramics. A pressure of  $1 \times 10^{-4}$  mm. or less was maintained during runs made with this furnace. The e.m.f. of the Pt-Pt, 13% Rh thermocouple was read on a portable precision potentiometer at one minute intervals. The cooling rate was about one degree per minute. A cooling curve was first obtained for the pure metal before adding  $\text{LaB}_4$  to it, so that any change due to the addition could be detected to within about one degree.

Since the liquidus curve (see Fig. 1) could not be found by the usual cooling curve method, a different method was used for its estimation. An alloy of known composition was heated slowly until the  $\text{LaB}_4$  crystals floating on the liquid surface just disappeared, and this temperature recorded. The temperature of reappearance of the crystals on cooling was also recorded, and the liquidus temperature chosen between these two temperatures for the alloy observed.

The decomposition temperature of  $\text{LaB}_4$  was apparent as a sudden change of resistance that occurred in the compound on heating. This method of measurement had been calibrated at the melting point of platinum, which was taken as 1773°.

The composition of the liquid formed by the peritectic reaction of  $\text{LaB}_4$  was chosen by making the assumption that the  $\text{B}_6$  octahedral groups present in the  $\text{LaB}_4$  structure do not decompose into atoms but rearrange to form the  $\text{LaB}_6$  structure. Three-fourths of the boron atoms in  $\text{LaB}_4$  are present in octahedral groups; and if *only* those groups formed  $\text{LaB}_6$ , then this equation would apply



Therefore, the above assumption places an upper limit of 66.7% B on the composition of the liquid. The curve through the experimentally determined liquidus points extrapolates smoothly to 66.7% B at 1800°, so this point was taken as the best choice of the composition.

For the estimation of melting points of samples having a composition 85.8% B and higher, a graphite susceptor and granulated graphite insulation contained in an MgO crucible made up the "core" of the induction furnace. Runs made with the latter "core" were carried out under an argon atmosphere, and temperatures near 2500° could be attained.

To examine the electrical properties of the compounds, a crystal 0.5 mm. or larger was put into a device which held the sample between spring-loaded contacts through which a current was passed. Two 5-mil tantalum wires could be



made to contact the crystal at the desired points, and were connected to a potentiometer. This arrangement could yield only crude values of resistivity, but was quite satisfactory for determining whether the resistivity increased or decreased with temperature.

**X-Ray Diffraction.**—X-Ray powder patterns were obtained of  $\text{LaB}_4$  and of the  $\text{LaB}_6$  phase at the extremes of composition. A 114 mm. Debye-Scherrer camera and  $\text{Cu K}\alpha$  radiation were employed. The precise lattice constants for the (cubic) hexaboride samples were calculated by extrapolating a plot of lattice constant *vs.*  $\sin^2\theta$  to  $\theta = 90^\circ$ . For the (tetragonal) tetraboride, the  $a_0$  constant was obtained by extrapolating on a similar plot  $a_0$  values calculated from  $hk0$  and  $hkl$  reflections. The  $a_0$  value thereby obtained then was used in constructing a similar plot for  $c_0$ , choosing  $hkl$  reflections for which  $h^2 + k^2$  is smaller than  $l^2$ .

The effect of boron additions on the  $\alpha \rightarrow \beta$  transition of lanthanum was studied with the aid of a high temperature X-ray diffractometer designed by Chiotti.<sup>18</sup> The Geiger counter was set to receive diffracted radiation from a  $\{101\}$  or  $\{102\}$  reflection of the hexagonal modification of lanthanum. The sets of atomic planes which give rise to these reflections are not present in the  $\beta$ (fcc) form, so that when the sample transformed on heating, the recorded radiation intensity dropped to the level of the background radiation. The temperature of the sample was obtained from a measurement of the e.m.f. of a chromel-alumel thermocouple in the sample holder next to the sample.

**Metallography.**—Metallographic preparation of alloys consisted of preliminary grinding of the bakelite-mounted samples of SiC paper down to 600 grit. Arc-melted samples richer in boron than  $\text{LaB}_4$  were then polished on a lap wheel with diamond dust, and required no etching before microscopic examination. After grinding the lanthanum-rich alloys could be directly etched in 2% aqueous  $\text{HNO}_3$ , producing a chemical polishing effect on the lanthanum matrix and leaving the  $\text{LaB}_4$  unaffected. This procedure, although producing a clean, undistorted surface on the lanthanum, tends to exaggerate the impurity phases present, and etches the surface in relief to some extent. The microstructure of the alloys was interpreted by making a comparison with the microstructure observed for the particular pure metal sample.

## Results

**Phase Relationships.**—The solubility of boron in  $\beta$ - or  $\alpha$ -lanthanum is very low, as concluded from the following evidence: Alloys containing greater than 0.1 at. % boron and which were slowly cooled from the liquid state contain  $\text{LaB}_4$  crystals which appear to have formed while the lanthanum was molten. In addition, such alloys have the same melting point and transition point as pure lanthanum. Microstructures of alloys up to 25% boron were examined, and found to contain  $\text{LaB}_4$  crystals in a matrix of lanthanum, the identity of the crystals being verified by an X-ray diffraction pattern of some of them that were mechanically removed from the polished metal surface. An examination was made for a compound between lanthanum and  $\text{LaB}_4$  which might be stable only at high or low temperatures. No evidence of such a compound was found.

The addition of boron to lanthanum was found to have no measurable effect on the  $\alpha \rightarrow \beta$  transformation of lanthanum. A sample of pure lanthanum and a 5% boron alloy made from the same batch of metal both showed the transition (on heating) over a 15° temperature range averaging 275°.

The liquidus curve rises sharply from the melting temperature of pure lanthanum and smoothly curves over to the peritectic horizontal of  $\text{LaB}_4$ . The first compound,  $\text{LaB}_4$ , has a very narrow range

of homogeneity, the evidence being: (1) no variation in the lattice constants of  $\text{LaB}_4$  was found; (2) the manner of preparation of the  $\text{LaB}_4$  was such that it should contain the maximum possible per cent. of La. A weighed amount of  $\text{LaB}_4$  was heated *in vacuo* at 1500° for 15 min. in a tantalum crucible. This caused the crystals to appear somewhat pink because of a layer of  $\text{LaB}_6$  on the surface, which in turn was caused by volatilization of La from the crystals. The measured loss in weight after this treatment was about one milligram per gram  $\text{LaB}_4$ . If it is assumed that La diffusion within the crystals was sufficient to maintain a nearly uniform composition throughout, then it must be concluded that the crystals were then as depleted in La as possible.

That the pink color was actually  $\text{LaB}_6$  was verified by an X-ray diffraction pattern. The assumption of a rapid diffusion rate for La in  $\text{LaB}_4$  is supported by the fact that a pressed mixture of  $\text{LaB}_4$  crystals and boron can be completely converted to  $\text{LaB}_6$  crystals by heating *in vacuo* at 1500° for 15 min. If the diffusion rate were not rapid the crystals would contain some unreacted  $\text{LaB}_4$ .

The composition of  $\text{LaB}_4$  was calculated from the pycnometric density and the lattice constants by using the formula

$$\text{Formula weight} = \frac{(\text{volume of unit cell in } \text{\AA}^3) (\text{density})}{\text{per unit cell} \quad 1.6602}$$

and making the assumption that the difference between the observed formula weight and the formula weight corresponding exactly to the formula  $\text{LaB}_4$  was due to a deficiency of boron in the structure. The empirical formula calculated was  $\text{LaB}_{3.53 \pm 0.1}$ .

Lanthanum tetraboride decomposes at 1800  $\pm$  15° to  $\text{LaB}_6$  plus a liquid. Evidence of the decomposition was seen in the microstructure of an  $\text{LaB}_4$  sample after heating above 1800°, which showed crystals of  $\text{LaB}_6$  surrounded by  $\text{LaB}_4$ , which in turn contained small pockets of lanthanum metal.

The compound  $\overline{\text{LaB}_6}$  exists over a range of composition, extending from 85.8% boron ( $\text{LaB}_6$ ) to about 88% boron ( $\text{LaB}_{7.8}$ ). The melting point lies above 2500°, which is the highest temperature reached in the induction furnace. The compound was fused in an arc-melting furnace, but under those conditions the melting point was difficult to estimate. That 85.8% boron ( $\text{LaB}_6$ ) is very close to one side of the composition range was seen by the fact that when stoichiometric quantities of  $\text{LaB}_4$  and boron were mixed intimately and heated *in vacuo* at 1500–1600° to prepare  $\text{LaB}_6$ , the product contained small amounts of  $\text{LaB}_4$  due to a slight inhomogeneity of the specimen. The composition of the boron-rich side was calculated from a density measurement of the crystals, assuming that the structure remains intact except for being depleted of part of its La content, resulting in a defect lattice. From the measured density, 3.98 g./cc., it can be concluded that lanthanum atoms have been removed, since the structure and lattice constants remain the same while the boron content increases from 85.8 to 88%. The theoretical density at 85.8% is 4.714

(18) P. Chiotti, *Rev. Sci. Instr.*, **25**, No. 7, 683 (1954).

g./cc. Observation of the boron-rich  $\text{LaB}_6$  crystals under a microscope showed that less than 5% free boron was present. Unless boron atoms have replaced lanthanum atoms (which seems unlikely), a defect lattice has been formed.

The microstructure of arc melted alloys of composition between 89 and 99.5% boron shows primary crystals of the  $\overline{\text{LaB}}_6$  phase in a matrix of boron, which has a silvery metallic luster. The matrix shows evidence of having rejected more  $\overline{\text{LaB}}_6$  in a eutectoid reaction. The composition of the decomposed phase must lie very close to about 99% boron, judging by the relative amounts of  $\overline{\text{LaB}}_6$  and boron in the eutectoid-appearing areas. This high boron content of the phase in question suggests that it is a solid solution of La in a modification of boron stable only at very high temperatures, rather than being a new La-B compound. The supposed transition would have to be quite close to the melting point of boron (within a few hundred degrees), since diffusion must be very rapid in order to allow a eutectoid structure to be formed in spite of the very rapid cooling of the arc-melted sample. The above evidence is the basis for the suggestion of a transformation in boron in the range  $2250 \pm 100^\circ$ . The matrix phase was found by an X-ray powder pattern to be the  $\beta$ -rhombohedral form of boron identified by Sands and Hoard.<sup>19</sup> The same powder pattern was obtained for the arc-melted boron.

The melting point of boron was obtained by heating the upper part of a  $1/2$ -inch diameter cylinder of pressed boron under argon in a high temperature induction furnace, and observing with an optical pyrometer the temperature at which the top of the cylinder started to sag under its own weight. Examination of the cooled sample produced evidence of incipient melting at the top of the sintered cylinder.

It should be mentioned that the presence of carbon, nitrogen or oxygen in the boron used for investigation of the boron-rich end of the system causes different behavior than that observed for the highest purity arc-melted boron. Only oxygen was present in a significant amount in the starting material used in this study, and for that reason the boron was arc melted previous to La addition. This procedure removed most of the oxygen as volatile boron oxides.

**Physical Properties of the Compounds.**—A measurement of the resistivity of a single crystal of  $\text{LaB}_4$  that was approximately a cube one millimeter on an edge showed that the resistivity behaves like that of a metal, *i.e.*, decreases with decreasing temperature. The resistivity is about  $24 \pm 12 \times 10^{-6}$  ohm-cm. at room temperature and decreases to about half of that value at  $-190^\circ$ . The contact resistance is about 1000 times greater than the "true" resistance of this crystal, and this contact resistance increases as the temperature is lowered.  $\text{LaB}_4$  has been reported to be tetragonal.<sup>12</sup> The close similarity of its X-ray powder pattern with that of  $\text{CeB}_4$  suggests that  $\text{LaB}_4$  is isomorphous with  $\text{CeB}_4$ , the structure of which was determined by Zalkin and Templeton.<sup>8</sup> Pre-

cise lattice constants were obtained by successive extrapolations of lattice constant *vs.*  $\sin^2\theta$  to  $\sin^2\theta = 1$ . The resulting constants are:  $\alpha_0 = 7.3240 \pm 0.0005 \text{ \AA.}$ ,  $c_0 = 4.1811 \pm 0.0006 \text{ \AA.}$

The compound  $\overline{\text{LaB}}_6$  has a pink-purple color at the composition of maximum La content, 85.8% boron. As the compound becomes more deficient in La, a fairly exact composition is reached where the color changes to blue. It has been reported that  $\overline{\text{LaB}}_6$  is a metallic-type conductor. At the composition of minimum La content it is still a metallic-type conductor, but the contact resistance behaves like that of  $\text{LaB}_4$ . Throughout the composition range the crystal structure remains simple cubic. What is somewhat unexpected is that the lattice constant remains unchanged, within experimental error. The lattice constant found by extrapolating a plot of  $a_0$  *vs.*  $\sin^2\theta$  to  $\sin^2\theta = 1$ , is  $4.1561 \pm 0.0003 \text{ \AA.}$

### Discussion

#### The Region between Lanthanum and $\text{LaB}_4$ .

It is interesting to compare the metal-rich side of the La-B system with that of the La-C system.<sup>20</sup> The solubility of carbon in liquid and in solid lanthanum is much greater than that of boron. There is a eutectic at 20.7 at. % carbon and a solubility of about 3 at. % carbon in lanthanum near the transition temperature ( $868^\circ$ ). Since the dilute solutions of each element in lanthanum should be similar, the difference in the solubilities probably is due mainly to the relative stability of the compounds in equilibrium with the solutions.

It should be mentioned here that if carbon is present in significant amounts in La-B alloys, the melting point of lanthanum is lowered, and a eutectic reaction occurs at  $850^\circ$ . A ternary compound is formed, the formula of which is estimated to be  $\text{LaBC}$ . X-Ray powder patterns of the compound were obtained, but not indexed.

Post, Moskowitz and Glaser<sup>12</sup> reported lattice constants for a compound  $\text{LaB}_x$ , where  $x$  was believed to be 3 or 4. Attempts were made to prepare this compound but without success. As far as the La-B phase diagram is concerned, lanthanum-rich alloys indicate that the lanthanum phase is in equilibrium with  $\text{LaB}_4$  from room temperature to  $1800^\circ$ . A pressed mixture of fine  $\text{LaB}_4$  powder and powdered boron having an overall composition between that of  $\text{LaB}_4$  and  $\text{LaB}_6$  was heated in a helium atmosphere for two days at  $850^\circ$ , and an X-ray powder pattern then obtained. No lines were observed which could not be attributed to  $\text{LaB}_4$  or to  $\text{LaB}_6$ . Also, the microstructure of the slowly cooled alloy, which shows  $\text{LaB}_6$  in contact with  $\text{LaB}_4$ , does not show evidence of a reaction product at the boundary of the two phases.

**The Compounds  $\text{LaB}_4$  and  $\text{LaB}_6$ .**—The  $\text{MB}_6$  type boride is found for the elements Ca, Sr, Ba, Th and the rare earths, but not for the alkali metals. The alkaline earth hexaborides are not strongly colored as are the hexaborides of thorium and the rare earths. Lafferty<sup>6</sup> has measured the

(19) D. Sands and J. L. Hoard, *J. Am. Chem. Soc.*, **79**, 5582 (1957).

(20) K. Gschneidner and A. H. Daane, *Trans. AIME*, **215**, 192 (1959).

Hall coefficient of  $\overline{\text{LaB}_6}$ , and reports that it corresponds to about one negative carrier per lanthanum atom. This experimental evidence indicates that the boron framework of the structure (see Fig. 2) requires two electrons from each metal atom present, or two for each  $\text{B}_6$  group, and that when extra electrons are present as in the case of  $\overline{\text{LaB}_6}$ , they behave as "free" electrons, and give metallic-type electrical properties to the lattice. Theoretical treatment by the method of linear combination of atomic orbitals (LCAO)<sup>9</sup> has given the same result; each  $\text{B}_6$  octahedral group requires 20 electrons, 6 for the external bonds between octahedra, and 14 for the molecular orbitals within the octahedron. It is possible to attribute the range of homogeneity of  $\overline{\text{LaB}_6}$  to this electron requirement as follows: The stability of the compound seems to be dictated more by the covalently bonded boron framework than by the characteristics of the metal atom, since the high melting point and high hardness are more akin to pure boron, diamond, and similarly covalently bonded lattices. It is therefore expected that as long as the boron framework has its electronic requirements satisfied, the stability will not be greatly affected by other changes such as the removal of metal atoms to form vacancies. However, the formation of vacancies apparently cannot continue indefinitely without causing instability, for otherwise the phase should exist at 90% boron, for at that composition the electronic requirements of the boron framework are still met.

It would be of interest to know the effect of any "extra" electrons on the stability of the hexaboride structure. If it were possible to change the number of electrons present while holding all other things constant, the effect of this might be measured by noting a change in the lattice constant, with the assumption made that a contraction means enhanced stability and that an expansion means lessened stability, since boron-boron bonds would be stretched. Another assumption to be made is that there is no interaction between the "extra" electrons and electrons of the boron framework. One approach would be to look at a plot of lattice constant of  $\text{MB}_6$  compounds vs. the ionic radius of the metal. If the ionic radius were the only property of the metal that affected the lattice constant, then a smooth curve would be obtained. If then the valence of the metal exercised an influence, one would expect a smooth curve for the rare earths (when triply ionized) and a separate smooth curve for alkaline earth elements. (The points corresponding to the rare-earth elements which sometimes exhibit divalency may not fall on either curve regardless of whether the divalent or trivalent radius is used, since there is no need to assume a uniform valence for all of the ions in the lattice. As will be shown later, it is not likely that any rare earths are tetravalent in the hexaborides.) The point for  $\text{ThB}_6$  might be separate from both curves. If the lattice constants used in the above plot are not measured at  $0^\circ\text{K}$ ., then deviations may occur due to differences of thermal expansion between  $0^\circ\text{K}$ . and room temperature. Although the available values of ionic radii (and to a lesser extent, the

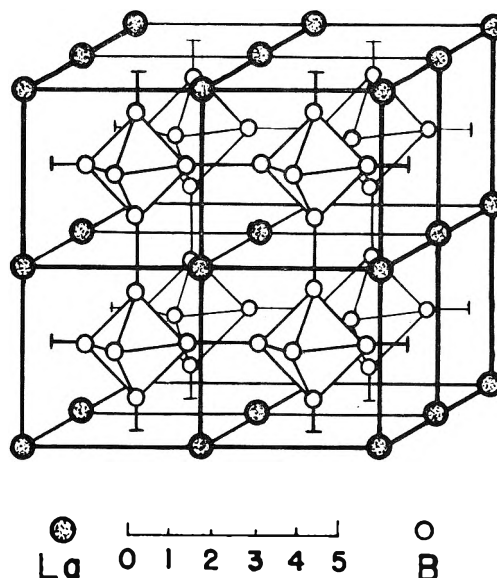


Fig. 2.—The lattice of  $\text{LaB}_6$ .

lattice constants) are in poor agreement (see Fig. 3), it is worth noting that the minimum values of the ionic radii of the rare earths are not low enough to allow the point (or region) representing  $\text{CaB}_6$  to fall within it. (The lattice constant of  $\text{CaB}_6$  chosen for the plot is a value determined at this Laboratory using  $\text{CaB}_6$  of good purity, the  $a_0$  being  $4.1522 \pm .0006 \text{ \AA}$ .) The coefficients of expansion of  $\text{LaB}_6$  and  $\text{CaB}_6$  are  $6.4 \times 10^{-6}$  and  $6.5 \times 10^{-6}$ , respectively,<sup>23</sup> so the separation on the graph is not likely to disappear if lattice constants are all corrected to  $0^\circ\text{K}$ . It might reasonably be concluded from this evidence that the extra "free" electron present in  $\overline{\text{LaB}_6}$  and most other rare-earth hexaborides causes a contraction of the lattice. The supposed contraction can be used to explain the lack of the expected contraction of  $\overline{\text{LaB}_6}$  as lanthanum is removed to form a defect lattice. The removal of lanthanum atoms results in a lowering of the concentration of the "free" electrons, which in turn should tend to expand the lattice. Thus the lack of variation of the lattice constant might be regarded as the result of a near balance between tendencies of expansion and contraction. The deviations of  $\text{EuB}_6$  and  $\text{YbB}_6$  from the rare-earth curve can be attributed mainly to the presence of divalent ions in the lattice.

Felten, Binder and Post<sup>14</sup> prepared samples of  $\text{EuB}_6$  of varying (and unspecified) composition, and observed that the lattice constant varied between 4.184 and 4.170  $\text{\AA}$ . Although they did not suggest a reason for the variation, this effect can be explained as follows: At the maximum europium content most (or all) europium ions are divalent. As the lattice becomes depleted of europium some of the remaining ions lose an electron and become trivalent in order to satisfy the electronic requirements of the boron framework. Since the trivalent ion is significantly smaller than the divalent ion, the lattice tends to contract as this change occurs.

In the tetraboride structure determination by

(23) G. S. Zhdanov and N. N. Zhuravlev, A. A. Stepanova and M. M. Umanskii, *Soviet Physics, Crystallography*, **2**, 284 (1957).

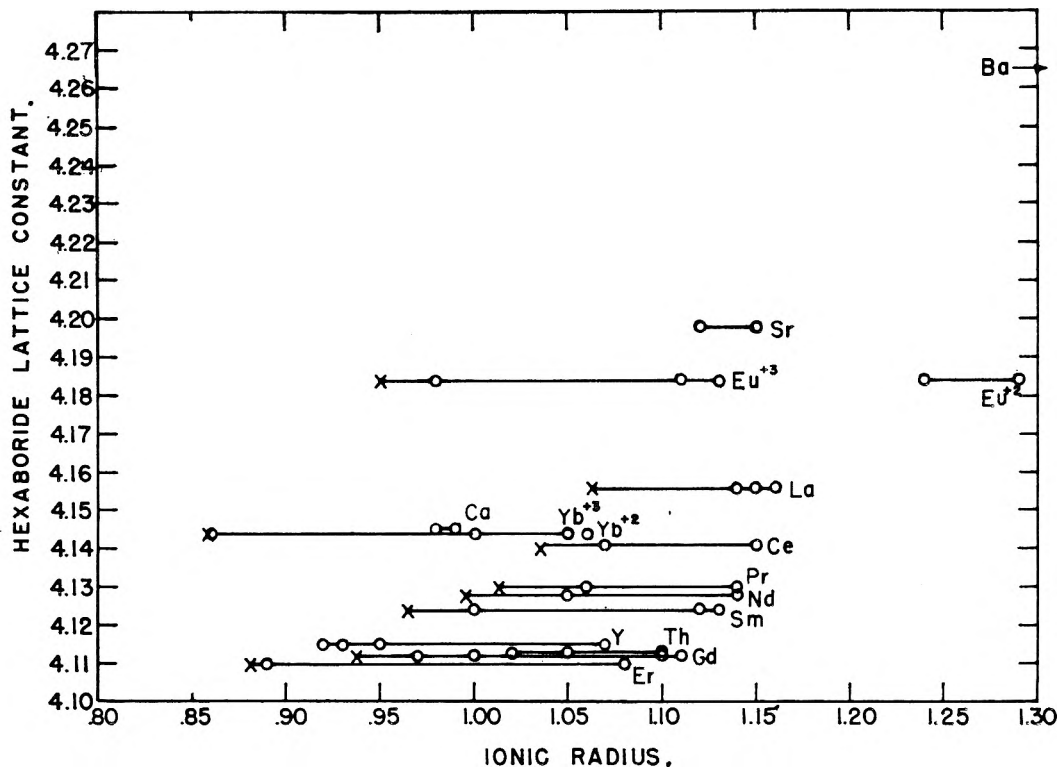


Fig. 3.—Plot of chosen values of hexaboride lattice constant vs. various values of the radius of the metal ion. The radius values represented by circles were taken from Landolt-Börnstein.<sup>22</sup> The values marked with an "x" are from Templeton and Dauben.<sup>23</sup>

Zalkin and Templeton<sup>8</sup> only the metal atom positions could be determined. They estimated the locations of the boron atoms by geometrical considerations and adjusted the parameters to make the boron atoms as nearly equidistant as possible and as far from the Th atoms as possible. This is mentioned in order to make clear the fact that any given bond distance should not be regarded as a precisely measured value. Double bonds as well as single bonds may be present, and these would have different bond lengths. Of the 16 atoms per unit cell, 12 are present in octahedral groups, and the other four bond these together in the basal plane. In the *c* direction, the octahedra are bonded to one another in the same manner as in  $\text{LaB}_6$ .

Lipscomb and Britton<sup>24</sup> have suggested a model for the electronic structure of tetraborides. As applied to  $\text{LaB}_4$ , the following assumptions are necessary: (1) Each boron octahedral unit requires twenty electrons as in the case of  $\text{LaB}_6$ ; (2) All four orbitals of the other boron atoms are used; and (3) The lanthanum atoms are triply ionized, and there are no La-B covalent bonds. The second condition is met if the non-octahedral boron atoms are bonded to the octahedra with single bonds, and bonded to one another with a double bond. The number of electrons required per unit cell is then  $2(20) + 4(4) = 56$ . The 16 boron atoms contribute 48 electrons, so the four metal

atoms must supply two electrons apiece. The compound  $\text{LaB}_4$  should then have four "extra" electrons per unit cell. If the tetraboride electron requirements are as described then the compound would likely be a metallic-type conductor, as has been found to be the case. Another possibility that arises is that the compound  $\text{CaB}_4$  may exist, which should be a semiconductor or an insulator. As a further check on the above hypothesis, calcium and boron were heated together under argon, and an X-ray powder pattern obtained of the reaction product. Eleven lines were indexed on a tetragonal cell having  $a_0 = 7.11 \text{ \AA}$ ,  $c_0 = 4.11$ . The indices of the eleven lines are in the same sequence as the corresponding lines of the  $\text{LaB}_4$  pattern, and the lattice constants are very close to what would be expected. It was not possible to make other measurements on the material obtained.

It might be asked why  $\text{LaB}_4$  does not show a wide range of homogeneity as does  $\text{LaB}_6$ , since removal of some lanthanum atoms would presumably not disturb the electron requirements of the boron framework. It is suggested as a possible answer that the vacancy left by removal of a lanthanum atom is mechanically unstable with respect to the configuration of boron atoms in  $\text{LaB}_6$ . The statement should become more valid as  $1800^\circ$  is approached since at that temperature the whole structure is unstable with respect to  $\text{LaB}_6$ .

**Boron-rich Phases.**—Two types of dodecaborides have been reported, the  $\text{AlB}_{12}$  type, which is found only for aluminum,<sup>25</sup> and the  $\text{UB}_{12}$  type, which is also formed by zirconium,<sup>26</sup> yttrium, dysprosium,

(22) Landolt-Börnstein "Zahlenwerte und Funktionen," 6th Ed. Vol. I, Part 4, J. Springer, Berlin, 1955.

(23) D. H. Templeton and C. H. Dauben, *J. Am. Chem. Soc.*, **76**, 5237 (1954).

(24) W. N. Lipscomb and D. Britton, *J. Chem. Phys.*, **33**, 275 (1960).

holmium, erbium, thulium and lutetium.<sup>27</sup> The boron frameworks in the modifications of  $\text{AlB}_{12}$  are probably based on icosahedral groups. The most likely reason that lanthanum does not form a boride of the  $\text{AlB}_{12}$  type is that the size factor is unfavorable. The face-centered-cubic lattice of  $\text{UB}_{12}$  has a structure<sup>28</sup> in which each uranium atom

(25) R. W. G. Wyckoff, "Crystal Structures," Interscience Publishers, Inc., New York, N. Y., 1948.

(26) M. Hansen, "Constitution of Binary Alloys," 2nd Ed., McGraw-Hill Book Co., Inc., New York, N. Y., 1958.

(27) I. Binder, S. LaPlaca and B. Post, Conference on Boron sponsored by U. S. Army Signal Research and Development Laboratory at Asbury Park, N. J., Sept. 18, 19, 1959.

is surrounded by 24 boron atoms and each boron atom has five boron neighbors. In this case also, the size factor evidently prevents the formation of an  $\text{LaB}_{12}$  phase.

**Acknowledgments.**—The authors wish to thank Messrs. Clarence Habermann and Gene Wakefield for the preparation of some of the metal used, and the spectrographic and analytical chemistry groups for the analyses performed. Thanks are also owed to Dr. K. Ruedenberg for a helpful discussion of some of the theoretical aspects of bonding.

(28) F. Bertaut and P. Blum, *Compt. rend.*, **229**, 666 (1949).

## $\gamma$ -IRRADIATION OF LIQUID AND SOLID OXYGEN<sup>2</sup>

BY DANIEL W. BROWN AND LEO A. WALL

National Bureau of Standards, Washington 25, D. C.

Received August 16, 1960

แผนกห้องสมุด กรมวิทยาศาสตร์  
กระทรวงอุตสาหกรรม

Experiments were performed to determine the  $G$ -values for ozone formation and also the variation in ozone concentration in  $\gamma$ -irradiated liquid and solid oxygen as a function of radiation dosage, both when in the undiluted state and when mixed with argon, nitrogen or krypton. In undiluted oxygen both at 77 and at 90°K. the average  $G$ -value observed was  $6.0 \pm 0.3$  molecule/100 e.v. absorbed; at 4.2°K., it was about 4.6. From the  $G$ -values in mixtures it is inferred that significant energy transfer from diluents to oxygen occurs, but that the effect is obscured by kinetic complications when the diluent is argon or krypton. The slope of the curve when ozone content is plotted as a function of radiation dose decreases by 35% in undiluted oxygen and by 45% in a 1:1 mixture of argon and oxygen between doses of 0 and  $2.0 \times 10^{22}$  e.v./g. at 77°K. The  $G$ -values for  $\text{NO}_2$  formation in the mixtures containing nitrogen varied between 0.4 and 0.9 molecule/100 e.v. absorbed.

### Introduction

Although a considerable amount of published work is available on the gas-phase irradiation of oxygen,<sup>3-6</sup> the only readily available references to irradiations in the liquid phase are in the paper by Kercher and co-workers and in English translations of papers presented in 1955 by Pshezhetsky and co-workers.<sup>7,8</sup>

The latter investigators used an electron beam to irradiate liquid oxygen both in bulk and also when diluted 1:1 with nitrogen. In brief, they concluded that: (1) the initial  $G$ -value for ozone production in bulk oxygen was between 12 and 15 molecules per 100 e.v. absorbed; (2) about as much ozone was formed in a 1:1 mixture of oxygen and nitrogen as in bulk oxygen for equivalent doses of irradiation; (3) in bulk oxygen, a steady-state concentration of ozone was achieved which was equivalent to about 4.5%  $\text{O}_3$ ; (4) the  $G$ -value for formation of nitrogen dioxide in the diluted sample was only about 1.5. Kercher, *et al.*, used

$\gamma$ -radiation from cobalt-60 and obtained a  $G$ -value of 6 in liquid oxygen.

The initial purpose of our work was to measure the yields of ozone in several liquid and solid mixtures of argon and oxygen as a function of irradiation dose. Since argon cannot form stable compounds, the only observed product in the mixture must be ozone, as in the irradiation of bulk oxygen. The yield in the mixture, however, can be affected by energy transfer and by the dilution. Experiments were also performed mixing the oxygen with krypton and xenon to determine whether the ozone yield varied with the ionization potential of the additive. Some irradiations were performed with ultraviolet light in order to observe the behavior upon dilution in the absence of energy transfer to the oxygen. Since the  $G$ -value obtained with bulk oxygen differed substantially from that given by Pshezhetsky, a few mixtures of oxygen and nitrogen were irradiated to make additional comparisons possible.

### Experimental

The irradiations were performed in a cobalt-60 source shielded by water. The dose rate was about  $0.3 \times 10^{20}$  e.v./g. hr. It was assumed that absorbed energy varied as the electron density (electrons/g.) of the irradiated material.

Each sample contained about 0.3 mole. The manufacturers' standards of purity were: oxygen > 99.5%; argon > 99.9%; krypton > 99.95%; xenon > 99.92%; and nitrogen > 99.996%. Several samples of oxygen were generated from  $\text{KClO}_3$ . The samples were irradiated in glass tubes held in dewars containing liquid  $\text{N}_2$ ,  $\text{O}_2$  or He.

The ozone content after irradiation was determined dilatometrically or by titrating iodine released in passing the gases through unbuffered potassium iodide solutions. When the former method was used the data of the Armour

(1) Supported by the Department of the Army under the National Bureau of Standards Free Radical Research Program.

(2) Presented at the 136th meeting of the Am. Chem. Soc., Atlantic City, N. J., September 1959.

(3) W. F. Busse and F. Daniels, *J. Am. Chem. Soc.*, **50**, 3271 (1928).

(4) S. C. Lind, "The Chemical Effects of Alpha Particles and Electrons," Chemical Catalog Co., 2nd Ed., New York, N. Y., 1929, p. 91.

(5) L. A. M. Henry, *Bull. soc. chim. Belg.*, **40**, 371 (1931).

(6) J. F. Kercher, J. S. McNulty, J. L. McFarling and A. Levy, *Radiation Research*, **13**, 452 (1960).

(7) S. Ya. Pshezhetsky, Conference of the Academy of Sciences of the U. S. S. R. on the Peaceful Uses of Atomic Energy (1955), p. 45 of Consultants Bureau's English Translation.

(8) S. Ya. Pshezhetsky, I. Ya. Myasnikov and N. A. Buneev, Academy of Sciences of the U. S. S. R. Symposium on Radiation Chemistry (1955), p. 111 of Consultants Bureau's English Translation.

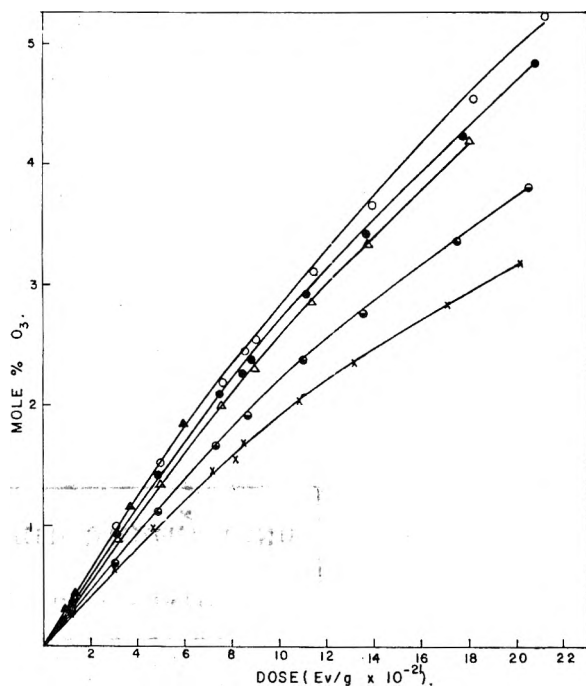


Fig. 1.—Ozone yields at 77°K. from  $\gamma$ -irradiation (from dilatometer measurements). Bulk oxygen:  $\circ$ ,  $e_{o_2} = 1.00$ .  $O_2$ -Ar system:  $\Delta$ ,  $e_{o_2} = 0.92$ ;  $\bullet$ ,  $e_{o_2} = 0.86$ ;  $\odot$ ,  $e_{o_2} = 0.64$ ;  $\times$ ,  $e_{o_2} = 0.47$ .  $O_2$ -Kr system:  $\blacktriangle$ ,  $e_{o_2} = 0.63$ .

Research Foundation<sup>7</sup> were used to calculate the ozone content from the observed decrease in volume. The titration method gave significantly lower results than the dilatometric method if the initial ozone content was much greater than 0.5 mole %. The ozone was greatly concentrated during the evaporation and some probably decomposed in the gas phase before it contacted the solution. For this reason the dilatometric method was used if more than 0.5%  $O_3$  was to be formed.

In mixtures containing  $N_2$  some  $NO_2$  is formed. This was determined gravimetrically. The ozone in these mixtures was determined dilatometrically. A correction was applied to take into account the small amount of  $NO_2$  that formed.

The ultraviolet irradiations were performed with a mercury lamp (Hanovia, Type L). During irradiations, a quartz tube containing the samples was positioned at the bottom of a quartz-tipped dewar filled with liquid nitrogen. The same apparatus and experimental conditions (dewar, sample tube, geometry and exposure time) were used for all ultraviolet irradiations.

### Results

The variation of ozone content with dose is shown in Fig. 1. The original solution compositions are given in oxygen electron fraction,  $e_{o_2}$ . Included are mixtures of argon and oxygen and one mixture of krypton and oxygen, all irradiated at 77°K. It appears from these data that the stationary ozone content in liquid oxygen is higher than the value of 4.5% estimated by Pshezhetsky, *et al.*<sup>8</sup> The lines are only slightly curved. For example, between 0 and  $20 \times 10^{21}$  e.v./g. the slopes decrease by 35 and 45%, respectively, for oxygen electron fractions of 1.0 and 0.47. If changes in slope are compared between ozone contents of 0 and 3.0% instead of in the range of irradiation previously mentioned, the respective decreases are about 30 and 50%. The slopes of the curves for the other argon-containing samples decrease by percentages

more nearly equal to that of the slope for bulk oxygen. Only the decrease in slope for the sample with the highest argon content seems significantly greater than that calculated from the data with bulk oxygen.

At ozone concentrations around 0.5% the titration method appeared to give reasonably accurate results. This is shown in Fig. 2 in which  $G$ -values for ozone production, determined by titrations at low doses and from the initial slopes of the curves in Fig. 1, are plotted as a function of the electron fraction of oxygen (the mole fraction of oxygen is slightly greater than the electron fraction in oxygen-argon mixtures). The  $G$ -values are based on the total energy absorbed by the solutions. In undiluted oxygen the value found agreed with that of Kercher, *et al.*<sup>6</sup> Most values depart slightly from the diagonal in the all-liquid region in a direction indicating energy transfer from argon to oxygen, although the effect is more marked with the titration data. The  $G$ -values determined by the titration method for low doses of irradiation are in most cases somewhat greater than those calculated from the dilatometer measurements, thus indicating that at low doses the iodine determinations do not give seriously low results.

At 77°K., the solubility of argon in liquid oxygen is limited. The phase boundaries indicated on Fig. 2 refer to the visual appearance or disappearance of phases in oxygen-argon mixtures. The dip of the  $G$ -values toward and eventually below the diagonal seems to be associated with the solid phase. To test this hypothesis, a few runs were made at 90°K., at which temperature all oxygen-argon mixtures are liquid. The resulting  $G$ -values are plotted in Fig. 3. It is seen that all points lie above the diagonal.

A single solution of krypton and oxygen was irradiated at each temperature, and the resulting  $G$ -values are also inserted in Figs. 2 and 3. Krypton is apparently at least as effective as argon in promoting ozone formation when present at the same electron fraction. It may even be better since the value in Fig. 2 should probably be compared with the other dilatometer results, and the result at 90°K. definitely seems higher than that found with argon solutions. It should be realized that the mole fraction of oxygen is considerably larger than the electron fraction in krypton-oxygen mixtures, whereas it is only slightly larger in argon-oxygen mixtures. The mixture used to obtain the result with xenon (Fig. 2) was heterogeneous. Therefore the  $G$ -value obtained only indicates that the small amount of xenon in solution did not grossly affect the yield.

In Table I are given conditions of sample preparation, source and exposure, along with the attained ozone concentrations and  $G$ -values. The ozone content usually was determined by the titration method. It is concluded that: (1) minor variations in preparation procedures do not grossly affect the yield; (2) samples of the oxygen ordinarily used (99.5%) give the same results as samples prepared chemically which presumably are of higher purity; (3) contamination by traces of water has no effect; (4) yields obtained by irradiation

(9) "Handbook of Chemistry and Physics," 38th edition, Chemical Rubber Publishing Co., 1956, p. 2046.

tion at 4.2°K. are slightly lower than those at 77°K. Since the  $G$ -value for ozone formation is not extremely dependent on the purity of the oxygen or the temperature of formation, such variations cannot account for the discrepancy between Pshezhetsky's  $G$ -value in bulk oxygen and our own.

In Fig. 4 are plotted the ozone contents found in samples of oxygen exposed to ultraviolet radiation at 77°K. as a function of the electron fraction of oxygen. These data will be discussed later and compared with those of the  $\gamma$ -ray work.

The  $G$ -values for  $O_3$  and  $NO_2$  formation in mixtures of oxygen and nitrogen are plotted as a function of the electron fraction of oxygen in Fig. 5. It is obvious that nitrogen is much more effective in promoting ozone formation than was argon. Unfortunately, the volume contractions for the sample having an  $e_{O_2}$  of 0.53 scatter badly, and the  $G$ -value calculated for this sample would be anything between 6 and 8, but values much greater than that in bulk oxygen are not very plausible. The  $G$ -values for  $NO_2$  formation appear to level off as the oxygen is diluted. The values are much lower than those for ozone formation.

### Discussion

In condensed systems exposure to  $\gamma$ -radiation causes formation of ions and excited species distributed in relatively small regions of high local concentration called spurs. Since molecular oxygen has an electron affinity one wonders if there is much tendency for it to capture electrons before neutralization can occur. In this regard we repeated for liquid oxygen some features of the calculation performed for water by Samuel and Magee.<sup>10</sup> Their results indicated that electrons return so quickly that capture is not appreciable. In oxygen the mean free path of the electron is greater than in water and energy losses in collisions between electrons and molecules are smaller than in water.<sup>11</sup> In accord with these differences rather longer time intervals between ionization and neutralization are obtained than found for water. Reported values of the probability of attachment of an electron to molecular oxygen<sup>11</sup> are such that we feel the over-all capture probability may be significant but that most of the electrons will still escape. The distribution of secondary electrons and assumptions regarding the retention of energy by the electron during its return affect the result. The effect of capture is speculative but if the ultimate neutralization involves the negative molecule ion one would expect the time interval between ionization and neutralization to be increased because an ion moves much less rapidly than an electron of the same energy.

After neutralization and perhaps along with it, if electron capture is significant, various reactions occur as the species in the spur separate by diffusion. These include dissociation to form oxygen atoms, combination of these atoms, reaction of

(10) A. H. Samuel and J. L. Magee, *J. Chem. Phys.*, **21**, 1080 (1953).

(11) H. S. W. Massey and E. H. S. Burhop, "Electronic and Ionic Impact Phenomena," Clarendon Press, New York, N. Y., 1952, Chapter IV.

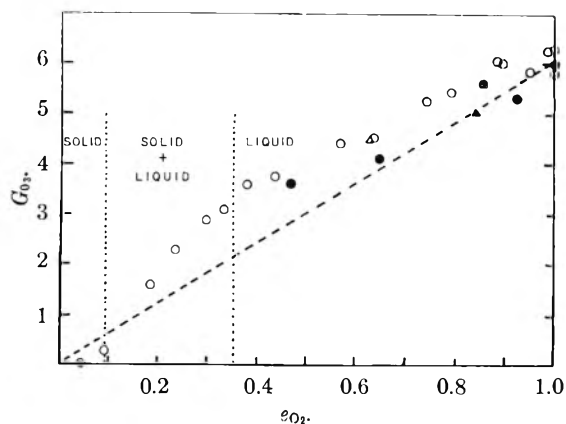


Fig. 2.— $G$ -values for ozone formation at 77°K. (after  $\gamma$ -irradiation of  $1.6 \times 10^{21}$  e.v./g.)  $O_2$ -Ar system:  $\circ$ , by titration method;  $\bullet$ , by dilatometer method.  $O_2$ -Kr system:  $\Delta$ , by dilatometer method.  $O_2$ -Xe system:  $\blacktriangle$ , by dilatometer method.

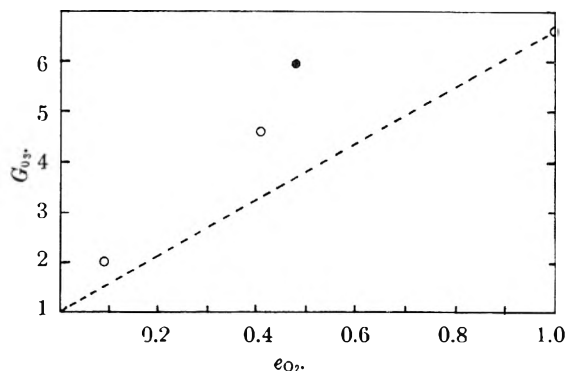


Fig. 3.— $G$ -values for ozone formation at 90°K. (after  $\gamma$ -irradiation of  $1.3 \times 10^{21}$  e.v./g.)  $O_2$ -Ar system:  $\circ$ , by titration method.  $O_2$ -Kr system:  $\bullet$ , by titration method.

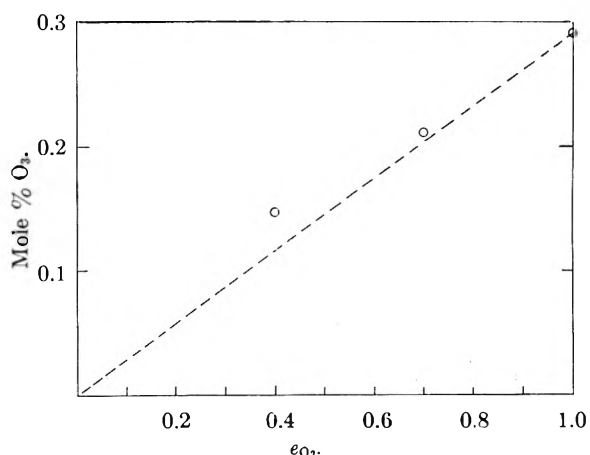


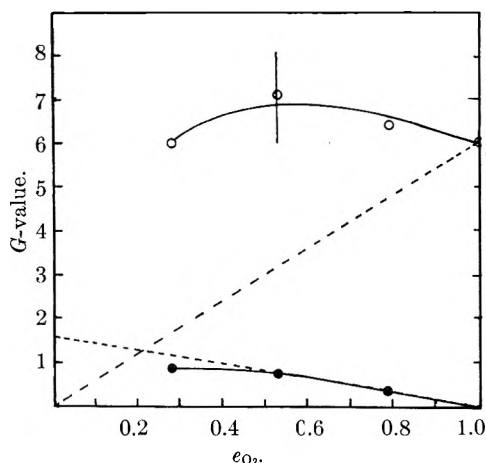
Fig. 4.—Ozone yield from ultraviolet irradiations at 77°K. in  $O_2$ -Ar system.

atomic oxygen with molecular oxygen or ozone, deactivation or reaction of excited species. These can only be discussed in general terms.

With regard to reaction of excited molecules to form ozone, we point out that the reaction  $2O_2 \rightarrow O_3 + O$  is endothermic by about 4 e.v. Considerable excitation energy will be required to make this reaction rapid at 77°K. Reactions not involving atom formation are less endothermic,  $3O_2 \rightarrow 2O_3$  for example requires about 3 e.v. Deactivation com-

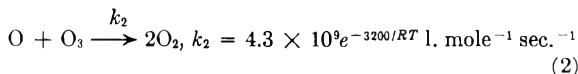
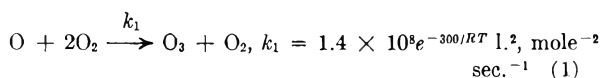
TABLE I  
 FORMATION OF OZONE BY  $\gamma$ -RAYS

O <sub>2</sub> source	Treatment before irradiation	Irradn. temp., °K.	Dose, e.v./g. $\times 10^{21}$	O <sub>3</sub> content, mole %	Method	G-value
Usual (99.5%)	None	77	1.36	0.43	Titration	6.0
Usual (99.5%)	Silica gel, 193°K.	77	1.36	.46	Titration	6.3
From KClO <sub>3</sub>	Silica gel, 90°K.	77	1.36	.44	Titration	6.1
Usual (99.5%)	Silica gel, 193°K., H <sub>2</sub> O added	77	3.1	.98	Dilatometer	5.9
Usual (99.5%)	Silica gel, 193°K.	4.2	0.67	.16	Titration	4.6
Usual (99.5%); argon added ( $e_{O_2} = 0.46$ )	Silica gel, 193°K.	4.2	2.1	.29	Titration	2.3


 Fig. 5.—G-values in O<sub>2</sub>-N<sub>2</sub> system at 77°K. from  $\gamma$ -irradiation: O, G<sub>O<sub>3</sub></sub>; ●, G<sub>NO<sub>2</sub></sub>.

petes with reaction of excited species and the resultant importance of ozone formation from reactions involving excited species is unknown. In gas phase at an average temperature of 147°K. studies with slow electrons may indicate that ozone formation starts at 3 e.v.<sup>12</sup> This is less than the bond strength of O<sub>2</sub> (about 5 e.v.).

Some values from gas phase data relevant to reaction of oxygen atoms are<sup>13</sup>



Other workers<sup>14</sup> give somewhat different values, but the activation energy for reaction 2 is always considerably larger than that for reaction 1. In liquid the activation energy for diffusion might be observed, particularly for reaction 1. Excess kinetic energy possessed by the atom would lower these values. If the above rate constants are indicative of the relative reaction rates reaction 2 can be ignored in considering our results.

Combination of oxygen atoms competes with reaction 1. It too requires a third body and except for diffusion would be expected to have negligible activation energy. We have not found a

(12) G. Glockler and J. L. Wilson, *J. Am. Chem. Soc.*, **54**, 4544 (1932).

(13) H. B. Urbach, R. J. Wnuk, J. A. Wojtowicz and J. A. Zaslowsky, 136th Meeting of Am. Chem. Soc., Abstracts, p. 47S.

(14) A. E. Axworthy and S. W. Benson, "Ozone Chemistry and Technology," Advances in Chemistry Series No. 21, Am. Chem. Soc., 1959, pp. 388-397.

value for its rate constant in the literature. As a spur grows old diffusive separation of the atoms increasingly favors reaction 1 over combination. We have used Dyne and Kennedy's<sup>15</sup> theoretical calculation on the efficiency of scavengers in liquid water to estimate the fraction of atoms forming ozone. We assumed the rate and diffusion constants applied to hydroxyl radicals were valid for oxygen atoms in liquid oxygen and that the rate constant for combination of atoms equals  $10 k_1$ . The oxygen concentrations we studied are much higher than the range of scavenger concentrations they assumed so that the product  $k_1 O_2$  is in the range they used for the product [(scavenger concentration) (rate constant for scavenging)]. When 4 atoms are formed per spur we estimate about 80% of these form ozone at an oxygen fraction of 0.1 and greater than 90% form ozone in undiluted oxygen. More atoms formed per spur decrease these values somewhat but ozone formation seems definitely favored.

The G-value for ion pair formation in oxygen in phase is 3.2 molecules per 100 e.v.<sup>16</sup> In liquid a higher value is expected because the dielectric constant is greater than in gas. A G-value of 6 in undiluted liquid oxygen from reaction 1 alone could thus be obtained if 2 atoms are formed per ion pair and if combination of atoms is unimportant. In gas phase combination of atoms is even less likely and G-values for ozone formation range from 6-9.<sup>3,5,6</sup> Since values greater than twice that for ion pair formation sometimes are obtained it is reasonable to assume reactions of excited species contribute to these ozone yields. The somewhat lower value in liquid may mean such reactions are less important in condensed phase or that our estimate of the fraction of atoms that form ozone is high. Also, in gas phase neutralization may always involve negative ions<sup>17</sup> and the difference between gas and liquid may be connected with the neutralization reactions.

At 4.2°K. any difference in activation energy between reaction 1 and atom combination will greatly increase the importance of the latter. Slower diffusion in the solid will also favor combination and presumably accounts for differences between results at 77 and 90°K. at low oxygen fractions. Since the G-value for ozone formation is only 30% lower at 4.2°K. than at 77°K. (Table I)

(15) P. J. Dyne and J. W. Kennedy, *Can. J. Chem.*, **36**, 1518 (1958).

(16) J. Weiss and W. Bernstein, *J. Chem. Phys.*, **22**, 1593 (1954).

(17) J. L. Magee and M. Burton, *J. Am. Chem. Soc.*, **73**, 523 (1951).



participation of excited atoms or molecules as reactants with oxygen or as diffusing species seems indicated.

In discussing the radiation chemistry of mixtures it is usually assumed that energy is absorbed by the components in proportion to their electron fractions. At electron energies in the vicinity of the highest ionization potential and below, this is not valid but much of the absorbed energy will come from more energetic electrons. Large atoms absorb disproportionately little energy and so their presence detracts from the validity of the assumption. If it is valid the  $G$ -value for ozone formation is proportional to the oxygen fraction in the absence of energy transfer or kinetic complications. Points above the diagonal thus can imply energy has been transferred to the oxygen.

Before considering the effects in the presence of diluants we discuss the curvature shown by the lines in Fig. 1. We do not think this results from an increasing importance of reaction 2 because its activation energy is too high for it to be rapid at 77°K. However, even equality of the rate constants for reactions 1 and 2 would only account for a maximum change of 5% in the slope whereas changes approaching 50% are observed. Presumably the decreases result from radiolysis of the ozone. If this is so and the foregoing assumption about energy distribution is valid the  $G$ -value for ozone decomposition can be estimated from the initial  $G$ -value for its formation and the curvature of the lines. In undiluted oxygen  $G$ -values of 26 for decomposition and 6 for formation give a reasonable fit over the experimental range. The stationary concentration of ozone calculated with these  $G$ -values equals 14 mole % but phase separation would occur before this figure was reached and a lower value would be observed.

Since the curvature is more marked at the lowest oxygen fraction a higher  $G$ -value for decomposition would be obtained. The increase may result from energy transfer from argon to ozone or some chain character may come into the decomposition at low oxygen fractions.<sup>18</sup>

The effects of argon, krypton and nitrogen on the initial  $G$ -values for ozone formation (Figs. 2, 3 and 5) may be complicated by kinetic factors. In discussing the relative importance of reaction 1 and combination of atoms we estimated that decreasing the oxygen fraction from 1 to 0.1 did not greatly affect the efficiency of forming ozone. In any event the decrease would depress the ozone yield below the diagonal. Since the medium is changed by dilution the relative ability of oxygen and diluant to remove reaction energy also becomes important. Effects from this cause are not considered in the above estimate and their magnitude and direction are not predictable.

The results obtained in the ultraviolet experi-

ments (Fig. 4) may have some bearing on this question. The essential point is the path length and extinction coefficients calculated for the optically active region (below 2100 Å.<sup>19</sup>) are such that nearly all the light should have been absorbed by the solutions; despite this the ozone yield falls off markedly. These yields are plotted *versus* the electron fraction to facilitate comparison of the oxygen fractions with those in the  $\gamma$ -ray work. It is thought the decrease in yield may result from the complication suggested above.

There are objections to this suggestion. The extinction coefficients referred to above were calculated from published values<sup>20</sup> for the gas phase by correction for the difference in density between gas and liquid. They may be in error. The effect of the decreased oxygen fraction on the competition between reactions 1 and atom combination may be greater than estimated. In support of the suggestion nitrogen is observed to behave as if energy absorbed by it brings about as much ozone formation as if it were all absorbed by the oxygen. In the same concentration range argon is apparently less effective despite having similar ionization potentials and cross sections for ionization and excitation. It has been suggested that N<sub>2</sub> is considerably more effective than O<sub>2</sub> as a third body in reaction 1<sup>21</sup> although another group of workers finds little difference.<sup>14</sup> In addition the somewhat greater effect found with krypton relative to argon suggests a kinetic explanation, since at the same electron fraction the mole fraction of oxygen is much greater in the solutions containing krypton. It is felt that energy transfer probably occurs in all these solutions but that the results are occluded with argon and to a lesser extent with krypton.

Mechanisms of energy transfer are speculative. Oxygen is known to assist forbidden transitions of excited molecules. There may be enough time between ionization and neutralization for charge transfer to occur if a significant fraction of electrons are captured. If transfer mechanisms are very specific there is no need of kinetic argument to account for different behavior with different diluents.

If the  $G$ -values for NO<sub>2</sub> formation in Fig. 5 are extrapolated linearly back to  $e_{0_2} = 0$  an intercept of about 1.5 is obtained. This might be regarded as the  $G$ -value for formation of N atoms in nitrogen.  $G$ -values of 0.4 to 0.8 have been reported for stabilization of N atoms at 4.2°K.<sup>22</sup> A higher value in liquid phase is consistent with more rapid diffusion in the liquid.

(19) E. Briner, ref. 14, pp. 1-6.

(20) K. Watanabee, E. C. Y. Inn and M. Zelikoff, *J. Chem. Phys.*, **21**, 1026 (1953)

(21) W. D. McGrath and R. G. W. Norrish, *Proc. Roy. Soc. (London)*, **A242**, 265 (1957).

(22) L. A. Wall, D. W. Brown and R. E. Florin, *J. Phys. Chem.* **63**, 1762 (1959).

(18) S. Ya. Pshchetskiy, *et al.*, *Zhiv. Fiz. Khim.*, **32**, 1605 (1958).

# THE PROTECTION EFFECT IN THE $\gamma$ -RADIOLYSIS OF BENZENE-CYCLOHEXANE MIXTURES AND ITS EXPLANATION IN TERMS OF SELECTIVITY OF THE PRIMARY RADIATION ACT

BY J. LAMBORN AND A. J. SWALLOW

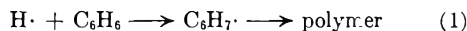
*Nuclear Technology Laboratory, Department of Chemical Engineering and Chemical Technology, Imperial College, London, S.W. 7, England*

Received September 7, 1960

Polymer yields in  $\gamma$ -irradiated benzene-cyclohexane mixtures are lower than would be obtained if the radiolysis of the two components proceeded independently, this being in agreement with previous measurements of hydrogen yields. The results are explained in terms of preferential excitation of the  $\pi$  electrons of benzene by the fast electrons produced in the system.

## Introduction

The yield of hydrogen in irradiated cyclohexane-benzene mixtures is very much less than would be obtained if the radiolysis of the two components proceeded independently.<sup>1</sup> The decrease in yield is partly due to the removal of hydrogen atoms produced from cyclohexane, by the reaction<sup>2</sup>



but the major part of the decrease appears to be due to "protection" of cyclohexane by benzene, possibly by some form of energy transfer. Although hydrogen is the major irradiation product of cyclohexane, polymer is almost equally important. In the case of benzene, polymer is by far the major product.<sup>3</sup> It therefore seemed desirable to seek confirmation of the protection effect by examining the irradiated mixture for polymer.

## Experimental

The irradiation vessel was a glass tube sealed by two mercury traps (Fig. 1). The vessel was cleaned, dried and weighed, and filled with the mixture to be irradiated. "Spectrosol" cyclohexane and "Analar" benzene from Hopkin and Williams Ltd. were used. Mercury was added and the system was deaerated by the passage of nitrogen (oxygen-free) which had been saturated by the organic mixture's vapor by passage through a gas washing bottle. The system was irradiated with  $\gamma$ -rays from a kilocurie cobalt-60 source.<sup>4</sup> The dose rate was determined with the Fricke dosimeter (in 0.1 N  $\text{H}_2\text{SO}_4$ ),  $G$  being taken as 15.5.<sup>5</sup> The dose rate in the dosimeter was  $0.72 \times 10^6$  rad./hr. The dose rate in the mixture was obtained by multiplying the dose rate in the Fricke dosimeter by the ratio of the electron densities of the mixture and water. Mixtures were given a total dose of  $40\text{--}70 \times 10^6$  rad. and after irradiation the vessel and contents were weighed. Volatile substances were evaporated off by the passage of nitrogen while the system was heated in a boiling water-bath. The vessel and contents, (mercury + polymer), were then weighed to constant weight. This procedure gave an accurate result since neither cyclohexane<sup>6</sup> nor benzene,<sup>7</sup> nor presumably a mixture of the two, gives a significant amount of material of molecular weight intermediate between the original and about twice the original molecular weight. After weighing, the mercury was separated from the polymer and weighed. Thus by difference the amount of high boiling product was determined. Knowing the weight and composition of the

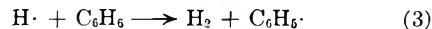
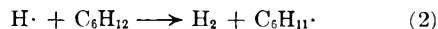
mixture before irradiation, and the total dose given, the  $G$ -value for conversion to polymer was obtained.

## Results and Discussion

The results of our work are shown in Fig. 2. In the case of pure cyclohexane the yield for cyclohexane converted to polymer ( $G = 4.03$ ) is in excellent agreement with other determinations of the same quantity,<sup>8,9</sup> and with the value of  $G = 2.0$  for dicyclohexyl (*i.e.*,  $G = 4.0$  for cyclohexane converted) in the fast-electron irradiation of cyclohexane.<sup>6,10</sup> It should be noted that although the nature of the polymer depends on dose rate, dicyclohexyl being the only product at high dose rates<sup>6</sup> whereas cyclohexylcyclohexene appears at lower dose rates,<sup>9</sup> the yield of total polymer would not be expected to depend appreciably on dose rate. This is confirmed by the present work.

In the case of benzene our yield of  $G = 0.98$  is in good agreement with  $G = 0.93$  as determined for  $\gamma$ -rays by Gordon, *et al.*,<sup>8</sup> and does not differ appreciably from  $G = 0.75$  as determined for fast electrons by Patrick and Burton.<sup>3</sup>

We have compared our polymer yields with yields calculated from Burton and Patrick's determinations of hydrogen yield.<sup>2</sup> To do the calculation we have assumed that the hydrogen in the mixture is formed partly by unimolecular decomposition of the two constituents and partly by reactions of hydrogen atoms such as



The hydrogen yield in the mixture is then given by

$$G_{\text{H}_{2m}} = aG_{\text{H}_{2b}} + (1 - a)G_{\text{H}_{2c}} \quad (4)$$

where  $G_{\text{H}_{2m}}$  is the yield of hydrogen as corrected for reaction 1 by Burton and Patrick,<sup>2</sup>  $G_{\text{H}_{2b}}$  and  $G_{\text{H}_{2c}}$  are the yields of hydrogen from pure benzene and pure cyclohexane, respectively, and "a" is the fraction of energy absorbed by the benzene. Other mechanisms may contribute to the formation of hydrogen, but would not be likely to make an appreciable difference to equation 4.

Similarly we have assumed that polymer is formed exclusively by combination of the radiation-produced organic free radicals with each other, and that no organic radicals react in any other way.

(8) P. J. Horner and A. J. Swallow, *ibid.*, **65**, 953 (1961).

(9) E. S. Waight and P. Walker, *J. Chem. Soc.*, 2225 (1960).

(10) T. D. Nevitt and L. P. Remsberg, *J. Phys. Chem.*, **64**, 969 (1960).

(1) J. P. Manion and M. Burton, *J. Phys. Chem.*, **56**, 560 (1952).

(2) M. Burton and W. N. Patrick, *ibid.*, **58**, 421 (1954).

(3) W. N. Patrick and M. Burton, *J. Am. Chem. Soc.*, **76**, 2626 (1954).

(4) G. R. Hall and M. Streat, to be published.

(5) J. L. Haybittle, R. D. Saunders and A. J. Swallow, *J. Chem. Phys.*, **25**, 1213 (1956).

(6) H. A. Dewhurst, *J. Phys. Chem.*, **63**, 813 (1959).

(7) S. Gordon, A. R. Van Dyken and T. F. Doumani, *ibid.*, **62**, 20 (1958).

The yield for monomer converted to polymer in the mixture,  $G_{pm}$ , is then given by

$$G_{pm} = aG_{pb} + (1 - a)G_{pc} \quad (5)$$

where  $G_{pb}$  and  $G_{pc}$  are the yields of monomer converted to polymer for pure benzene and pure cyclohexane, respectively. If disproportionation is an important reaction of free radicals or if polymer is formed by any other mechanism, then it is possible (but not certain) that equation 5 may need to be modified to some extent.

From equations 4 and 5 we obtain

$$G_{pm} = \left( \frac{G_{pc} - G_{pb}}{G_{H2c} - G_{H2b}} \right) G_{H2m} + G_{pc} - \left( \frac{G_{pc} - G_{pb}}{G_{H2c} - G_{H2b}} \right) G_{H2c} \quad (6)$$

Values of  $G_{pb}$  and  $G_{pc}$  may be taken from our work to be 0.98 and 4.03, respectively. There is no general agreement as to the value of  $G_{H2c}$ , but if we are to make use of Burton and Patrick's other data it seems best to adopt their value of 4.3.<sup>2</sup>  $G_{H2b}$  may be taken to be 0.036.<sup>1</sup> Substituting these values in equation 6 we obtain

$$G_{pm} = 0.715G_{H2m} + 0.96 \quad (7)$$

Polymer yields calculated from this equation are shown in Fig. 2 and are seen to be in reasonable agreement with our experimentally determined values. It may be that Burton and Patrick's relatively low value of  $G_{H2c} = 4.3$  is due to the presence of impurities in the cyclohexane used. These would have little effect on  $G_{H2m}$ . If this is the case and we adopt the more generally assumed value of 5.3 for  $G_{H2c}$ , then for 5% electron fraction benzene (4.7% volume fraction) the calculated polymer yield will be 15% less than shown in Fig. 2. Other calculated points will be in error to a smaller extent.

It is clear both from our results and from Burton and Patrick's that benzene "protects" cyclohexane. To explain this phenomenon we must examine the manner in which the radiation energy is distributed between the two components. The fast electrons produced by Compton scattering cause by far the greatest part of the chemical effect and are often considered to impart energy to the two components approximately in the ratio of their electron fraction in the mixture, irrespective of molecular structure.<sup>11</sup> An impression of the irrelevance of molecular structure is also given by stopping power measurements, which show that the stopping power of molecules to fast charged particles is very nearly an additive function of the numbers of atoms present.<sup>12</sup> Stopping power however does not provide a sensitive indication of the influence of molecular structure on the transfer of the energy of the fast electrons to molecules,<sup>13</sup> and existing measurements leave it possible that molecular structure may have an important effect. That molecular structure is in fact important is shown by previous work,<sup>14-16</sup> which shows that

(11) M. Burton, W. H. Hamill and J. L. Magee, *Geneva Conf.*, **29**, 391 (1958).

(12) L. H. Gray, *Proc. Camb. Phil. Soc.*, **40**, 72 (1944).

(13) Cf. R. H. Platzman, "Symposium on Radiobiology," Ed. Nickson, John Wiley and Sons, New York, N. Y., 1952, p. 139.

(14) E. Fermi, *Z. Physik*, **29**, 315 (1924).

(15) H. A. Bethe, *Ann. Physik*, **5**, 325 (1930).

(16) E. N. Lassettre, *Radiation Research, Suppl.* **1**, 530 (1959).

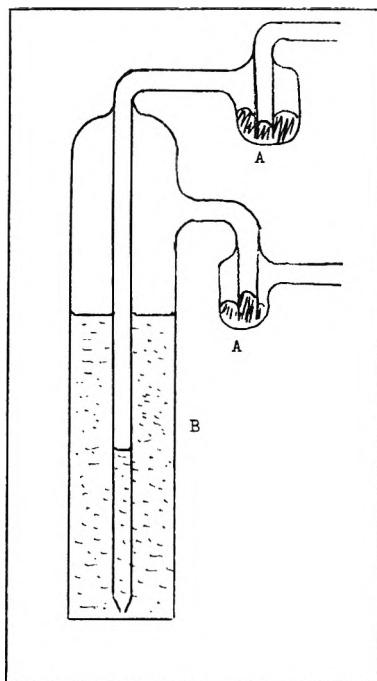


Fig. 1.—Irradiation vessel; A, mercury seal pots; B, mixture to be irradiated.

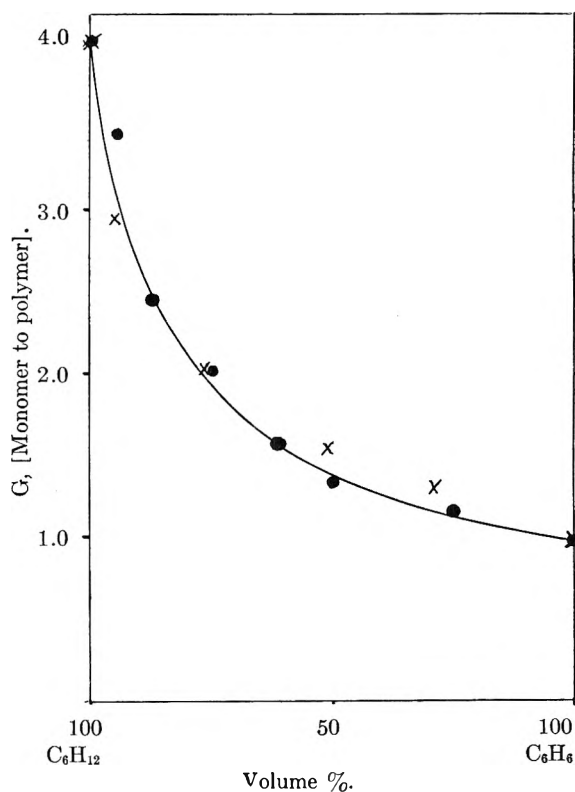


Fig. 2.—Number of molecules of mixture converted to polymer per 100 e.v. as a function of composition by volume: ●, results of this work; X, results calculated from Burton and Patrick's work. The line is theoretical, calculated according to equations 8 and 5.

the probability of excitation or ionization by fast electrons is related to the probability of excitation or ionization by electromagnetic radiation. For the present system, the extinction co-

efficient of benzene is greater than that of cyclohexane throughout the entire range down to 1500 Å.,<sup>17</sup> so that benzene will receive more energy than indicated by its electron fraction.

An estimate of the energy distribution may be made if we accept the conclusions of Inokuti.<sup>18</sup> Inokuti has shown that for the action of fast electrons on benzene the cross section for excitation of  $\pi$ -electrons to low levels is very large, and is about ten times as great as the total inelastic cross-section for  $\sigma$ -electrons. Assuming that the cross section per molecule for  $\sigma$ -electrons is in the ratio of 24 to 36 for benzene and cyclohexane, and that the picture is not very different for slow electrons, we obtain for the fraction of the total energy taken up by the benzene

$$a = \frac{2n(10E_{\pi} + E_{\sigma})}{3E_{\sigma} + n(20E_{\pi} - E_{\sigma})} \quad (8)$$

where  $n$  = mole fraction of benzene in the mixture,  $E_{\pi}$  = mean energy given to a benzene molecule when it is excited to one of its lowest strongly allowed excited states and  $E_{\sigma}$  = mean energy given to a molecule of benzene or cyclohexane when the  $\sigma$ -electrons are activated by radiation. We take  $E_{\pi}$  as 7 e.v. since this is between the energy of the first strongly allowed excited state of benzene (6.74 e.v.) and the ionization potential (9.2 e.v.). We take  $E_{\sigma}$  as 10 e.v. (the final conclusion is not highly sensitive to the values taken).

(17) L. W. Pickett, M. Muntz and E. M. McPherson, *J. Am. Chem. Soc.*, **73**, 4862 (1951).

(18) M. Inokuti, *Isotopes and Radiation (Tokyo)*, **1**, 82 (1958).

The fraction "a" can then be determined for various volume percentages, and knowing this, in conjunction with equation 5, the polymer yield may be calculated. A line calculated on this basis is shown in Fig. 2. Considering the various assumptions made, the agreement with experiment is remarkably good. We may therefore conclude that the protective action of benzene is due to its preferentially taking up the energy of the fast electrons rather than to an initially random absorption of energy followed by some form of "energy transfer" from cyclohexane to benzene. Although the selective action of sub-excitation electrons has previously been recognized,<sup>19,20</sup> the implications of the selectivity of the action of fast electrons do not appear to have been fully discussed and it seems likely that many other cases of "protection" or "energy transfer,"<sup>21,22</sup> may be largely explicable in such terms. It should also be noted that selectivity should be particularly important in biological systems, since aromatic groups form a large part of cell constituents such as nucleic acids and proteins.

**Acknowledgments.**—The authors wish to thank Dr. J. Murrell for helpful comments and the Department of Scientific and Industrial Research for a Studentship granted to one of them (J.L.).

(19) R. H. Platzman, *Radiation Research*, **2**, 1 (1955).

(20) J. Weiss, *Nature*, **174**, 78 (1954).

(21) M. Magat, L. Bouby, A. Chapiro and N. Gilon, *Z. Elektrochem.*, **62**, 307 (1958).

(22) D. R. Kalkwarf, *Nucleonics*, **18**, No. 5, 76 (1960).

## INFRARED AND RAMAN SPECTRAL STUDY OF NITRATE SOLUTIONS IN LIQUID HYDROGEN FLUORIDE<sup>1</sup>

By F. P. DEL GRECO AND J. W. GRyder

*Department of Chemistry, The Johns Hopkins University, Baltimore, Md.*

*Received September 21, 1960*

Infrared and Raman spectra are reported for HF solutions of HNO<sub>3</sub>, N<sub>2</sub>O<sub>5</sub>, KNO<sub>3</sub>, KF and H<sub>2</sub>O. Comparison of these spectra with those for other systems indicates that nitrates react with anhydrous HF to form the species NO<sub>2</sub><sup>+</sup>, HNO<sub>3</sub>, H<sub>3</sub>O<sup>+</sup> and solvated F<sup>-</sup>. No evidence was found for the species H<sub>2</sub>NO<sub>3</sub><sup>+</sup> which had been postulated to explain the results of cryoscopic and electrical conductivity measurements.

Fredenhagen interpreted electrical conductivity and boiling point elevation data by postulating that KNO<sub>3</sub> reacts with liquid anhydrous hydrogen fluoride in accord with the equation<sup>2</sup>



Since in this reaction HNO<sub>3</sub> assumes the unlikely role of an acid substantially weaker than HF, the present investigation was undertaken to see if spectroscopic evidence could be found for the existence of H<sub>2</sub>NO<sub>3</sub><sup>+</sup> in liquid hydrogen fluoride solutions of KNO<sub>3</sub> and other nitrates.

(1) Based on a dissertation to be submitted by F. P. Del Greco to the Faculty of Philosophy of The Johns Hopkins University in partial fulfillment of the requirements for the degree of Doctor of Philosophy.

(2) K. Fredenhagen, *Z. Elektrochem.*, **37**, 684 (1931), and references cited therein.

### Experimental

**Chemicals.**—Liquid hydrogen fluoride was distilled from tanks of General Chemical "high purity" anhydrous HF and used without further purification. Electrical conductivity measurements on this material showed it to have a specific conductance of about  $10 \times 10^{-4}$  ohm<sup>-1</sup> cm.<sup>-1</sup>, and its infrared spectrum was not noticeably different from that obtained for carefully purified HF by Maybury, Gordon and Katz.<sup>3</sup> Potassium nitrate was twice recrystallized, vacuum oven dried, and stored and dispensed in a drybox. Anhydrous nitric acid was obtained by low pressure room temperature distillation from a solution of NaNO<sub>3</sub> in a fourfold excess of H<sub>2</sub>SO<sub>4</sub> and collected at Dry Ice temperature. Dinitrogen pentoxide was prepared by dehydration of 100% nitric acid with P<sub>4</sub>O<sub>10</sub> followed by low pressure room temperature distillation of the product from the mixture and collected at Dry Ice temperature. Anhy-

(3) R. H. Maybury, S. Gordon and J. J. Katz, *J. Chem. Phys.*, **23** 1277 (1955).

drous sulfuric acid was prepared by mixing together appropriate amounts of analyzed fuming and 95% sulfuric acids. Potassium fluoride was prepared by dissolving KOH in a large excess of liquid HF in a platinum dish. The mixture was heated to molten  $\text{KHF}_2$ , briefly electrolyzed, then heated strongly until no further HF was given off, and stored and dispensed in a drybox. Reagent grade methanol and potassium sulfate were used without further purification.

**Apparatus and Procedure.**—Solutions were made up in an apparatus constructed entirely of polyethylene tubing which was largely welded together. The necessary demountable joints were slip-fit and wired together. While polyethylene vessels are not suitable for long term storage of liquid HF, we have found it possible to use the same apparatus for making up solutions repeatedly, provided that contact is limited to an hour or two. Polyethylene which, of necessity, came in contact with HF for more than a few hours at a time was normally replaced after each use. Solutes were transferred to a chamber of known volume in the apparatus in an atmosphere of Seaford nitrogen, and HF from the tank was condensed in on top of the solute at 0° or lower. Normally about 20 minutes were required to make up a 20 ml. solution. After thorough mixing, the solutions were transferred directly to one of the cells for examination.

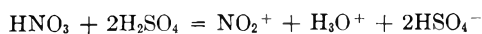
Raman spectra were obtained with 4358 Å. exciting light filtered through a one cm. thickness of saturated  $\text{NaNO}_2$  and 2 cm. of 0.035 g./l. rhodamine b solution in water. Both filter solutions were refrigerated to keep the temperature of the samples below 10° at all times. The source consisted of six General Electric A-H2 mercury lamps surrounded by magnesium oxide coated reflectors, the spectrograph was a fast grating instrument with 8 Å./mm. dispersion in the region of interest, and the spectra were photographed on Eastman 103a-O plates. The Raman cell and its exit window were constructed of Kel-F (Minnesota Mining and Manufacturing Co. brand of polychlorotrifluoroethylene) which had been specially heat treated and polished to make it more transparent to visible light. The illuminated portion of the cell was 4.5 in. long and had a capacity of 20 ml. The "black" end of the Raman cell was made of Teflon (E. I. du Pont de Nemours Co. brand of polytetrafluoroethylene) covered on the outside with black masking tape and had Kel-F side arms connecting with bulged polyethylene tubing to provide for mixing, and through which the samples were introduced. Exposures of 3–6 hours were generally necessary and the spectra obtained were acceptable but not of outstanding quality.

Infrared spectra were obtained on a Perkin-Elmer Model 21 double beam spectrophotometer equipped with NaCl optics. The cell was patterned after that described by Maybury, Katz and Gordon<sup>4</sup> with the exception that the silver chloride windows were set into place in cell halves constructed of 1/2 in. thick pieces of 2 in. diameter Kel-F rather than nickel and the two cell halves, sealed with polyethylene gaskets rather than Teflon, were held together with a frame made of 1/2 in. aluminum plates. By comparison with other spectra it is apparent that the cell thickness was of the order of 10  $\mu$  or less in most cases. To allow for entrance and mixing, bulged polyethylene tubing was provided for this cell also; the connection to the cell was made with 1/4 in. o.d., 1/16 in. i.d., Teflon tubing.

At times, when it was desired to add additional chemicals to the contents of one of the cells, the sample being added was isolated in a section of the polyethylene tubing with clamps and then allowed to trickle into one of the bulged regions of the tubing where mixing took place at 0°.

### Results and Discussion

It has been shown from the results of a cryoscopic and Raman spectroscopic study of dilute solutions of  $\text{HNO}_3$  in  $\text{H}_2\text{SO}_4$  that in those solutions the equilibrium



is operative. Of particular interest to us are the results of the Raman investigation<sup>5</sup> in which

(4) R. H. Maybury, J. J. Katz and S. Gordon, *Rev. Sci. Instr.*, **25**, 1133 (1954).

the spectral features of  $\text{NO}_2^+$  and  $\text{HNO}_3$  (and  $\text{H}_2\text{SO}_4$  and  $\text{HSO}_4^-$ ) were clearly identified. Subsequently, one of the infrared bands of  $\text{NO}_2^+$  was observed in the spectrum of dilute solutions of  $\text{HNO}_3$  in  $\text{H}_2\text{SO}_4$ .<sup>6</sup> Table I lists some of the fundamentals of the vibrational spectra of  $\text{HNO}_3$  and  $\text{NO}_2^+$ .

**1. Identification of  $\text{NO}_2^+$  and  $\text{HNO}_3$ .**—A single, strong and sharp Raman line at 1400  $\text{cm}^{-1}$  comprises the observed Raman spectrum of a 1.3 *f* solution of  $\text{N}_2\text{O}_5$  in liquid HF, and it is also the only Raman line observed in the Raman spectra of 2.5 *f* solutions  $\text{HNO}_3$  or  $\text{KNO}_3$  in liquid HF. However, in the Raman spectrum of a 5 *f* solution of  $\text{KNO}_3$  in liquid HF the strong line at 1400  $\text{cm}^{-1}$  is accompanied by a weak and rather broad Raman line at 1300  $\text{cm}^{-1}$ . Similarly, in the Raman spectrum of a liquid HF solution 2.5 *f* in  $\text{KNO}_3$  and KF, again both the 1400  $\text{cm}^{-1}$  line (medium) and the 1300  $\text{cm}^{-1}$  (weak) appear. During the course of the addition of water to a 2.5 *f* solution of  $\text{HNO}_3$  in liquid HF the originally strong and solitary 1400  $\text{cm}^{-1}$  line in the Raman spectrum of the solution decreases in intensity, and as it does so the previously mentioned broad 1300  $\text{cm}^{-1}$  line appears and gradually increases in intensity; in the spectrum of the solution to which 7 moles of water have been added per mole of  $\text{HNO}_3$  the 1400  $\text{cm}^{-1}$  line can no longer be detected, and the broad 1300  $\text{cm}^{-1}$  line is strong.

Comparison of these results with those obtained in the study of the Raman spectra of solutions of  $\text{HNO}_3$  in other strong acids<sup>5</sup> (see Table I) suggests strongly that  $\text{NO}_2^+$  and  $\text{HNO}_3$ , respectively, are responsible for the 1400 and 1300  $\text{cm}^{-1}$  lines observed in the Raman spectra of solutions of nitrates in liquid HF.

Figure 1 shows a series of infrared spectra of a 2.5 *f* solution of  $\text{KNO}_3$  in liquid HF to which has been added progressively larger amounts of water. Similar results have been obtained for a solution of  $\text{N}_2\text{O}_5$  in liquid HF. The features of the spectra in Fig. 1 pertinent to the present discussion are (1) the sharp absorption peak at 2360  $\text{cm}^{-1}$ , which decreases in intensity as water is added to the solution, and (2) the peaks at 1680 and 1310  $\text{cm}^{-1}$  and also a broad peak, partially obscured by background absorption, centered at 930  $\text{cm}^{-1}$ . Again referring to Table I, it is evident that the 2360  $\text{cm}^{-1}$  peak in the spectra in Fig. 1 may be attributed to the spectrum of  $\text{NO}_2^-$ , and that the 1680, 1310 and 930  $\text{cm}^{-1}$  peaks are likely to be part of the infrared spectrum of nitric acid.

Clearly, the spectroscopic evidence establishes the existence of  $\text{NO}_2^+$  in the dilute solutions of nitrates in liquid HF, and that evidence seems also to rule out  $\text{H}_2\text{NO}_3^+$  as the nitrogen containing species with which  $\text{NO}_2^+$  is in equilibrium in liquid HF solutions of nitrates. It appears unlikely that any acceptable structure can be devised for the ion  $\text{H}_2\text{NO}_3^+$  which would allow it to imitate  $\text{HNO}_3$  so well. For an  $\text{H}_2\text{NO}_3^+$  ion with the two hydrogen atoms on different oxygen atoms, as would be the

(5) C. K. Ingold, D. J. Millen and H. G. Poole, *J. Chem. Soc.*, 2576 (1950). The series covers pp. 2473–2627.

(6) R. A. Marcus and J. M. Fresco, *J. Chem. Phys.*, **27**, 564 (1957).

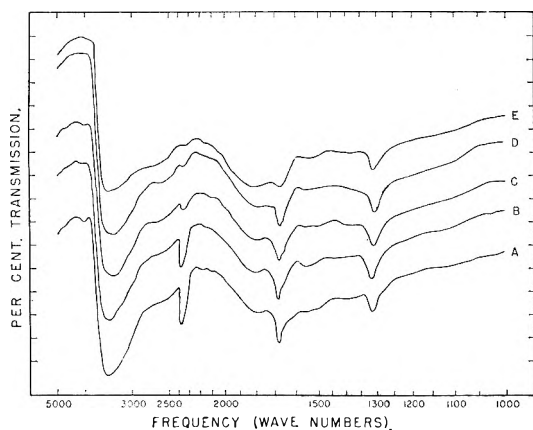


Fig. 1.—Infrared spectra of  $\text{H}_2\text{O}$  and 0.05 mole of  $\text{KNO}_3$  in 1 mole of  $\text{HF}$ : A, 0.0 mole of  $\text{H}_2\text{O}$ ; B, 0.05 mole of  $\text{H}_2\text{O}$ ; C, 0.10 mole of  $\text{H}_2\text{O}$ ; D, 0.15 mole of  $\text{H}_2\text{O}$ ; E, 0.40 mole of  $\text{H}_2\text{O}$ .

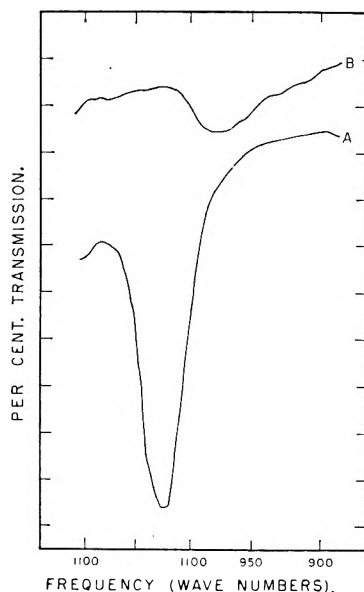


Fig. 2.—Infrared spectra of methanol and liquid  $\text{HF}$ : A, pure liquid methanol; B, 2.5  $f$  methanol in liquid  $\text{HF}$ .

TABLE I

OBSERVED VIBRATIONAL FUNDAMENTALS FOR  $\text{HNO}_3$  AND  $\text{NO}_2^+$

Symmetry and assignment	Raman, <sup>a</sup> $\text{cm}^{-1}$	Infrared, <sup>b</sup> $\text{cm}^{-1}$
Liquid $\text{HNO}_3$		
$\nu_1$ ; $A_1$ $\text{NO}_2$ stretch	1300	1308
$\nu_4$ ; $B_2$ $\text{NO}_2$ stretch	1675	1680
$\nu_2$ ; $A_1$ N-OH stretch	925	924
$\text{NO}_2^+$ in $\text{H}_2\text{SO}_4$ solution		
$\nu_1$ ; symmetric stretch	1403	
$\nu_3$ ; antisymmetric stretch		2360

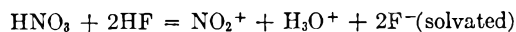
<sup>a</sup> C. K. Ingold and D. J. Millen, *J. Chem. Soc.*, 2612 (1950) and references cited therein. <sup>b</sup> Reference 6.

most reasonable structure, one expects that the absorption peaks found at  $1308 \text{ cm}^{-1}$  ( $A_1$   $\text{NO}_2$  stretch) and  $1680 \text{ cm}^{-1}$  ( $B_2$   $\text{NO}_2$  stretch) in the infrared spectrum of liquid nitric acid would be substantially shifted to lower frequencies, both as the result of an increased apparent mass for the oxygen atoms, and also because of the improved oppor-

tunity for hydrogen bonding provided by the hydrogen atoms.

On the other hand, if  $\text{H}_2\text{NO}_3^+$  were to have the same general configuration as nitric acid, but with two hydrogen atoms on the hydroxyl oxygen rather than one, then from the same considerations as above one would expect the absorption peak found at  $925 \text{ cm}^{-1}$  ( $A_1$  N-OH stretch) in the infrared spectrum of nitric acid to be shifted to lower frequency. In the case of methanol, a compound which certainly becomes protonated in liquid  $\text{HF}$  solution,<sup>2,7</sup> the expected shift was indeed found. The infrared absorption spectrum of liquid methanol includes a strong peak at  $1025 \text{ cm}^{-1}$  assigned to the  $A_1$  C-OH stretch.<sup>8</sup> As shown in Fig. 2, in the infrared spectrum of a 2.5  $f$  solution of methanol in liquid  $\text{HF}$  the  $1025 \text{ cm}^{-1}$  peak is shifted to ca.  $975 \text{ cm}^{-1}$ .

2. Evidence Concerning  $\text{H}_3\text{O}^+$  and Solvated  $\text{F}^-$ .—While it is clear that some equilibrium of the sort



is operative in the solutions of nitrates in liquid  $\text{HF}$ , just as analogous equilibria have been found to be the case for solutions of nitric acid in other strong acids,<sup>5</sup> the identification of features attributable to  $\text{H}_3\text{O}^+$  and solvated  $\text{F}^-$  in the spectra shown in Fig. 1 is complicated by the fact that the infrared absorption peaks reported for those ions tend to be rather broad and in general would be overlapped if not obscured by other peaks in the spectra. Furthermore, there is much uncertainty as to the location and assignment of the infrared spectral peaks attributable to  $\text{H}_3\text{O}^+$ , and, especially, solvated  $\text{F}^-$ ; Tables II and III list some of the reports which have been made for those ions.

TABLE II

INFRARED ABSORPTION MAXIMA OBSERVED FOR  $\text{H}_3\text{O}^+$  (PYRAMIDAL)

Location and assignment			Obsd. in	Ref.
$\nu_2$ , $\text{cm}^{-1}$	$\nu_4$ , $\text{cm}^{-1}$	$\nu_1$ and $\nu_3$ , $\text{cm}^{-1}$		
1134	1670	3000	Cryst. $\text{H}_3\text{O}^+\text{NO}_3^-$	<sup>a</sup>
1060	1705	2650-3380	Cryst. $\text{H}_3\text{O}^+\text{I}^-$	<sup>b</sup>
1205	1750	2900	Aq. acid soln.	<sup>c</sup>

<sup>a</sup> D. E. Bethell and N. J. Sheppard, *J. Chem. Phys.*, 21, 1421 (1953). <sup>b</sup> C. C. Ferriso and D. F. Hornig, *ibid.*, 23, 1464 (1955). <sup>c</sup> M. Falk and P. A. Giguere, *Can. J. Chem.*, 35, 1195 (1957).

In Fig. 3 there is clear evidence of peaks at  $2500$ ,  $1570$  and  $1820 \text{ cm}^{-1}$  in the infrared spectrum of 2.5  $f$   $\text{KF}$  in liquid  $\text{HF}$ . The peak at  $1820 \text{ cm}^{-1}$  is evident in the spectrum of liquid  $\text{HF}$  shown in Fig. 3, and also in the spectrum of liquid  $\text{HF}$  published by Maybury, Gordon and Katz<sup>3</sup> but not in the spectrum of liquid  $\text{HF}$  published by Adams and Katz.<sup>9</sup> In the spectra in Fig. 1, the peak at  $2500 \text{ cm}^{-1}$  is the only feature which can be confidently associated with the presence of (solvated) fluoride ion in the solution.

In the infrared spectrum of a 5  $f$  solution of water in liquid  $\text{HF}$  shown in Fig. 3, the  $2500$  and  $1820 \text{ cm}^{-1}$  absorptions found in the  $\text{KF}$  solution

(7) R. M. Adams and J. J. Katz, *J. Mol. Spec.*, 1, 306 (1957).

(8) A. Borden and E. F. Barker, *J. Chem. Phys.*, 6, 553 (1938).

(9) R. M. Adams and J. J. Katz, *J. Opt. Soc. Am.*, 46, 895 (1956).

TABLE III

INFRARED ABSORPTION MAXIMA OBSERVED FOR SOLVATED F <sup>-</sup>		Obsd. in	Ref.
Location and assignment $\nu_2$ , cm. <sup>-1</sup>	$\nu_3$ , cm. <sup>-1</sup>		
1233	1473	Solid KHF <sub>2</sub>	b
1206	1536	Aq. KHF <sub>2</sub> soln.	c
Absent	1535(weak)	27 f aq. HF	c
	1820 <sup>a</sup>	Organic 'bases' in liq. HF	7
Additional peaks			
1105 and 1015 cm. <sup>-1</sup>		Aq. KHF <sub>2</sub> , and KHF <sub>2</sub>	
For H <sub>3</sub> F <sub>2</sub> <sup>-</sup> , higher polymers		In dil. aq. HF only	c
2500 cm. <sup>-1</sup> "solvated HF <sub>2</sub> <sup>-</sup> "		2 f NaF in liq. HF	3
810 cm. <sup>-1</sup> H bend in molecular complexes of HF + organic bases <sup>d</sup>			7

<sup>a</sup> J. and P.<sup>c</sup> observed this peak in aq. HF spectra when > 9 f. <sup>b</sup> R. Newman and R. M. Badger, *J. Chem. Phys.*, 19, 1207 (1951). <sup>c</sup> L. H. Jones and R. A. Penneman, *ibid.*, 22, 781 (1953).

spectrum are observed, and there also clearly appear a peak at 1660 cm.<sup>-1</sup> and a very broad absorption centered at ca. 1200 cm.<sup>-1</sup>. It is likely that the latter two peaks, since they appear together, represent part of the infrared spectrum of H<sub>3</sub>O<sup>+</sup> (Table II). Marcus and Fresco attributed a peak they observed at 1680 cm.<sup>-1</sup> in the infrared spectrum of 11.8 weight % HNO<sub>3</sub> in H<sub>2</sub>SO<sub>4</sub> to H<sub>3</sub>O<sup>+</sup>.<sup>6</sup> However, in a solution of that concentration HNO<sub>3</sub> should be detectable,<sup>6</sup> and the 1680 cm.<sup>-1</sup> peak of its infrared spectrum would certainly overlap the peaks of other species whose spectra include absorption in that region. We have found that in the infrared spectrum of 96% sulfuric acid a peak appears at 1650 cm.<sup>-1</sup> which is not present in the infrared spectrum of 100% H<sub>2</sub>SO<sub>4</sub> nor in the spectrum of 100% H<sub>2</sub>SO<sub>4</sub> to which Na<sub>2</sub>SO<sub>4</sub> has been added (Fig. 4). It has been shown that, up to a concentration of ca. 40 moles %, water is a strong electrolyte in H<sub>2</sub>SO<sub>4</sub>.<sup>10</sup> While it is uncertain how strongly solvated the resulting H<sub>3</sub>O<sup>+</sup> ion is, the 1650 cm.<sup>-1</sup> peak in the infrared spectrum of 96% H<sub>2</sub>SO<sub>4</sub> (12 moles % water) is evidently related to a vibration of the hydronium ion, whatever the detailed condition of that species is. In the infrared spectrum of a 21 weight % KNO<sub>3</sub> solution in 100% H<sub>2</sub>SO<sub>4</sub> (13 weight % HNO<sub>3</sub>) there is a broad peak at 1680 cm.<sup>-1</sup> (Fig. 4), which indicates that the nitric acid peak at 1680 cm.<sup>-1</sup> can obscure the peak expected at 1650 cm.<sup>-1</sup> for H<sub>3</sub>O<sup>+</sup>.

Comparing the spectra in Fig. 1 with those in Fig. 3 it is seen that the 2500 cm.<sup>-1</sup> peak of solvated F<sup>-</sup> is the only one appearing in a sufficiently isolated region of the spectrum to be readily identifiable as such, but the broadening experienced by the 1680 cm.<sup>-1</sup> peak of nitric acid in Fig. 1 is not an unreasonable occurrence in view of the extensive absorption that the spectra of solutions of KF and H<sub>2</sub>O in liquid HF exhibit in that region.

An additional feature of the infrared spectrum of

(10) T. F. Young, L. F. Maranville and H. M. Smith, "The Structure of Electrolytic Solutions," W. J. Hamer, editor, John Wiley and Sons, Inc., New York, N. Y., 1959, pp. 35-63.

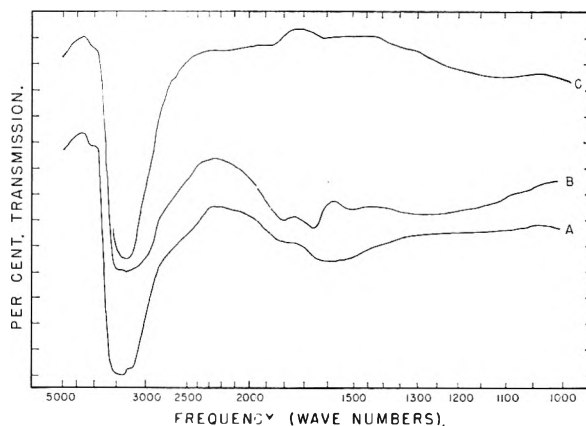


Fig. 3.—Infrared spectra of liquid HF, and KF and H<sub>2</sub>O in HF solution. A, 2.5 f KF in HF; B, 5.0 f H<sub>2</sub>O in HF; C, liquid HF.

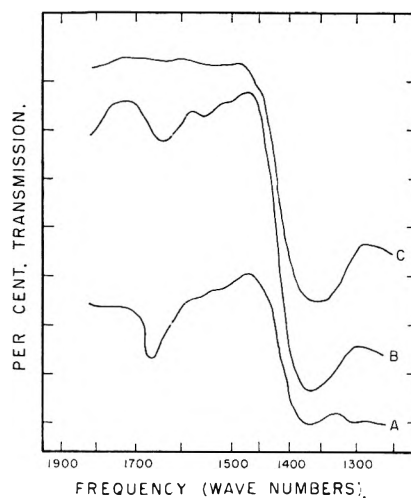


Fig. 4.—Infrared spectra of KNO<sub>3</sub>, Na<sub>2</sub>SO<sub>4</sub> and H<sub>2</sub>O in sulfuric acid: A, 21 wt. % KNO<sub>3</sub> in 100% H<sub>2</sub>SO<sub>4</sub>; B, 4 wt. % H<sub>2</sub>O in H<sub>2</sub>SO<sub>4</sub> (ordinary concn. acid); C, 11.5 wt. % Na<sub>2</sub>SO<sub>4</sub> in 100% H<sub>2</sub>SO<sub>4</sub>.

water in HF is a wide peak at about 800 cm.<sup>-1</sup>, and it also appears in the infrared spectrum of nitrates in liquid HF. Adams and Katz<sup>7</sup> have attributed absorption peaks they observed at ca. 800 cm.<sup>-1</sup> in the infrared spectra of HF in organic bases (ethers, ketones) to a hydrogen bending motion in a molecular complex formed by the organic base and HF.

Fredenhagen's statement that boiling point elevation data imply the presence of four particles in solutions of KNO<sub>3</sub> in liquid HF<sup>2</sup> can be reconciled with the new evidence if one assumes that the reaction



has an equilibrium constant such that under Fredenhagen's conditions the concentration of HNO<sub>3</sub> is about twice that of NO<sub>2</sub><sup>+</sup>.

**Acknowledgments.**—Expenses incurred during the course of this work have been met in part by funds from National Science Foundation Grant G 2745. One of us (F. P. D.) acknowledges grants-in-aid from the Hynson, Westcott and Dunning Fund during the years 1956-1960.

# GRAPHICAL METHODS OF DETERMINING SELF-ASSOCIATION CONSTANTS. I. SYSTEMS CONTAINING FEW SPECIES

BY F. J. C. ROSSOTTI AND HAZEL ROSSOTTI

*Department of Chemistry, The University of Edinburgh, Scotland*

*Received September 23, 1960*

New graphical methods of calculating self-association constants for systems containing a monomer and up to three oligomers are proposed and compared with existing methods.

Methods<sup>1-8</sup> for determining equilibrium constants of self-association reactions



have lagged far behind those for treating binary complex formation. This paper and its sequel describe a more comprehensive treatment of the computation of stoichiometric self-association constants defined by

$$\beta_q = \frac{[B_q]}{b^q} \quad (2)$$

where  $b$  is the concentration of free monomer. Emphasis is placed on making the fullest use of the experimental data, and on obtaining realistic limits of error for the constants.

### Concentration Variables.

The total analytical concentration of  $B$  is given by

$$B = \sum_1^Q q[B_q] = \sum_1^Q q\beta_q b^q \quad (3)$$

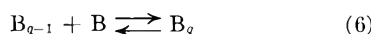
where  $B_q$  is the highest oligomer formed in the concentration range studied. The sum of the concentrations of each species is given by

$$S = \sum_1^Q [B_q] = \sum_1^Q \beta_q b^q \quad (4)$$

If one or both of the functions  $B(b)$  or  $S(b)$  can be determined, the power series 3 or 4 may in principle be solved for the  $(Q - 1)$  unknown parameters  $\beta_q$  provided that the activity coefficients of all species remain effectively constant over the concentration range studied. Stepwise association constants

$$K_q = \frac{[B_q]}{[B_{q-1}]b} = \frac{\beta_q}{\beta_{q-1}} \quad (q \geq 2) \quad (5)$$

for the reactions



may then be calculated. Experimental methods for determining values of  $b$  and  $S$  in solution have been described elsewhere.<sup>5</sup> The value of  $S$  in gaseous systems may be calculated using the ideal gas law. Although it is usually possible to measure

only one of the variables  $b$  or  $S$  as a function of  $B$ , the relationship<sup>1,4</sup>

$$\frac{dS}{db} = \frac{B}{b} \quad (7)$$

follows from equations 3 and 4, regardless of the nature of the species present.

**Calculation of  $b$  from  $S(B)$ .**—The value of  $b$  may be obtained from measurements of  $B$  and  $S$  using Bjerrum's integrated form<sup>1</sup> of equation 7

$$\log \frac{b}{b_1} = \frac{1}{2.303} \int_{S_1}^S \frac{1}{B} dS = \int_{S_1}^S \frac{S}{B} d \log S \quad (8)$$

where  $S_1$  is the value of  $S$  corresponding to a known value,  $b_1$ , of the monomer concentration. It is often difficult to determine a suitable point,  $S_1$ ,  $b_1$ , for systems in which appreciable association occurs at the lowest concentrations studied. We recommend two different types of method: (i) In sufficiently dilute solutions, it is likely that the dimer will be the only complex formed. Then from equations 2, 3 and 4

$$b = 2S - B \quad (9)$$

and

$$\log (B - S) = \log \beta_2 + 2 \log (2S - B) \quad (10)$$

Thus if the plot of  $\log (B - S)$  against  $\log (2S - B)$  is a straight line of slope 2, the value of  $b$  at any point on the line is given by equation 9. Alternatively, if equation 9 is valid

$$\frac{B}{S} = \frac{1 + 2b}{1 + b} \quad (11)$$

where  $b = \beta_2(2S - B)$ . A smooth curve may then be drawn through the experimental points  $BS^{-1}$ ,  $\log (2S - B)$ , using the template  $BS^{-1}(\log b)$ , calculated by means of equation 11. The value of  $b$  for any point lying on the curve may then be obtained using equation 9. (ii) If complexes higher than the dimer are present in the most dilute solutions studied, the curves  $B(B/S)$  and  $S(B/S)$  may be extrapolated until they meet at the point where  $B/S = 1$  and  $B = S = b$ .

If neither procedure (i) nor (ii) gives a satisfactory value of  $b_1$ , an approximate value may be used to calculate preliminary association constants, which are then used to refine the value of  $b_1$ .

**Calculation of  $S$  from  $b(B)$ .**—The value of  $S$  may be similarly obtained from measurements of  $B$  and  $b$ , using Kreuzer's integrated form<sup>4</sup> of equation 7

$$S - S_1 = \int_{b_1}^b \frac{B}{b} db = 2.303 \int_{b_1}^b B d \log b \quad (12)$$

A convenient point,  $S_1$ ,  $b_1$ , at which  $S_1$  is known may be found by methods analogous to those described above. Thus in the region where the dimer is the only complex formed

- (1) J. Bjerrum, *Kem. Maanedstidblad*, **24**, 21 (1943).
- (2) M. Davies and H. E. Hallam, *J. Chem. Educ.*, **33**, 322 (1956).
- (3) H. Dunken, *Z. physik. Chem.*, **45B**, 201 (1940).
- (4) J. Kreuzer, *ibid.*, **53B**, 213 (1943).
- (5) F. J. C. Rossotti and H. Rossotti, "The Determination of Stability Constants," McGraw-Hill Book Co., New York, N. Y., in press, Chap. 16.
- (6) N. E. White and M. Kilpatrick, *J. Phys. Chem.*, **59**, 1044 (1955).
- (7) K. L. Wolf, H. Dunken and K. Merkel, *Z. physik. Chem.*, **46B**, 287 (1940).
- (8) K. L. Wolf and R. Wolff, *Angew. Chem.*, **61**, 191 (1949).



$$2S = B + b \quad (13)$$

The validity of equation 13 may be tested by means of the linear relationship.

$$\log(B - b) = \log 2\beta_2 + 2 \log b$$

or by ascertaining that the experimental points  $Bb^{-1}$ ,  $\log b$  may be fitted by a template  $Bb^{-1}(\log b)$  calculated using the relationship

$$\frac{B}{b} = 1 + 2b \quad (14)$$

If equation 13 is not valid, plots of  $B$  and  $b$  against  $B/b$  may be extrapolated until they meet at the point where  $B/b = 1$  and  $B = b = S$ . The method of successive approximations may again be used if these procedures fail to give a reliable value of  $S_1$ .

#### Computation of Association Constants from Data of High Precision

**Direct Calculation.**—The association constants  $\beta_q$  may be obtained in principle<sup>9</sup> from either of the functions  $B(b)$  or  $S(b)$  by the solution of  $(Q - 1)$  simultaneous equations 3 or 4. However, if  $m > (Q - 1)$  sets of values  $B$ ,  $b$  or  $S$ ,  $b$  are available,  $m!/(Q - 1)!(m - Q + 1)!$  equations would have to be solved in order to use all the data. Calculations of this type may readily be performed by a high-speed electronic computer, but are very tedious to carry out with a desk calculator. Moreover, since the equations will probably be ill-conditioned on account of small experimental errors, it may be difficult to choose the "best" set of constants, and to estimate realistic limits of error.

**Successive Extrapolation.**—In the absence of an electronic computer, self-association constants are most conveniently obtained by graphical methods. For example, data  $B$ ,  $b$  may be analyzed by plotting the function

$$F_2 = \frac{B - b}{b^2} = 2\beta_2 + 3\beta_3b + \sum_4^Q q\beta_q b^{q-2} \quad (15)$$

against  $b$ . The value of  $2\beta_2$  is given by the intercept and that of  $3\beta_3$  as the limiting slope as  $b$  tends to zero. Higher values of  $\beta_q$  may be similarly obtained by the successive extrapolation method, which is analogous to that introduced by Leden<sup>10</sup> for determining stability constants of binary mononuclear complexes. In general, values of  $t\beta_t$  and  $(t + 1)\beta_{t+1}$  may be obtained as the intercept and limiting slope of the plot of

$$F_t = Bb^{-t} - \sum_1^{t-1} q\beta_q b^{q-t} = t\beta_t + (t + 1)\beta_{t+1}b + \sum_{t+2}^Q q\beta_q b^{q-t} \quad (16)$$

against  $b$ . Steiner<sup>11</sup> used the limiting slopes of functions  $F_t(b)$  to obtain association constants from data  $B$ ,  $b$ . White and Kilpatrick<sup>6</sup> have used a similar procedure, based on equation 4, to obtain values of  $\beta_t$  from data  $S$ ,  $b$ .

Small errors in the computation of the lower constants by these methods will accumulate, and

(9) G. Preuner and W. Schupp, *Z. physik. Chem.*, **68**, 129 (1909).

(10) I. Leden, *ibid.*, **188A**, 160 (1941); "Potentiometrisk Undersökning av några Kadmiumsalters Komplexitet," Lund, 1943.

(11) R. F. Steiner, *Arch. Biochem. Biophys.*, **39**, 333 (1952); **44**, 120 (1953); **49**, 400 (1954).

may result in gross errors in the higher constants. However, if measurements have been made at high concentrations, and the formula of the highest complex is known, functions of the type

$$\frac{B - b}{b^Q} = Q\beta_Q + (Q - 1)\beta_{Q-1}b^{-1} + \sum_2^{Q-1} q\beta_q b^{q-Q} \quad (17)$$

may be plotted against  $b^{-1}$ . The value of  $\beta_Q$  is obtained from the intercept, and that of  $\beta_{Q-1}$  from the limiting slope as  $b^{-1}$  tends to zero. Values of the lower constants may also be obtained by successive extrapolation of polynomials in  $b^{-1}$ . The two sets of constants obtained from polynomials in  $b$  and  $b^{-1}$  may be refined by successive approximations to ensure that the functions  $B(b)$  and  $S(b)$ , calculated by substitution of the stability constants into equations 3 and 4, give an adequate description of the experimental data.

The main advantage of successive extrapolation methods is their independence of any assumption about the nature of the complexes. However, they can only be used successfully for experimental data of high precision. Moreover, if  $Q > 3$ , the whole range of experimental data cannot be considered simultaneously, nor can limits of error in the constants readily be obtained.

#### Curve-fitting Methods.

The precision of the measurements as carried out often is insufficient to justify the calculation of more than three independent parameters. Association constants may therefore be conveniently obtained by curve-fitting methods of the type introduced by Sillén.<sup>12</sup> The procedures recommended below mainly use logarithmic plots which allow the functions  $B(b)$  and  $S(b)$  to be considered simultaneously over the whole concentration range studied. They give realistic estimates of the limits of error in the constants obtained, and an automatic check on the agreement between the calculated functions, and the experimental lots. Computational errors may be introduced by (i) the smoothing of experimental data and choice of residual integral in calculating  $b$  or  $S$ , and (ii) the use of log-log plots which appear to reduce small discrepancies between experimental and calculated functions. The validity of the association constants should therefore always be checked by substituting them into equations 3 and 4 to ensure that good agreement between the observed and calculated functions  $B(S)$  is obtained over the whole concentration range studied.

**The Degree of Association of the Complexes.**—Some indication of the type of species present may be obtained by calculating the degree of association

$$\bar{\nu} = \frac{B - b}{S - b} = \frac{\sum_2^Q q[B_q]}{\sum_2^Q [B_q]} \quad (18)$$

of the complexes. An integral value of  $\bar{\nu} = Q$  over the whole concentration range shows that there is a unique oligomer,  $B_Q$ . If  $\bar{\nu}$  varies with concentration, a number of complexes are formed, and  $Q \geq \bar{\nu}_{\max}$ . For example, if  $\bar{\nu}_{\max} = 3.2$  and  $(d\bar{\nu}/$

(12) L. G. Sillén, *Acta Chem. Scand.*, **10**, 186 (1956).

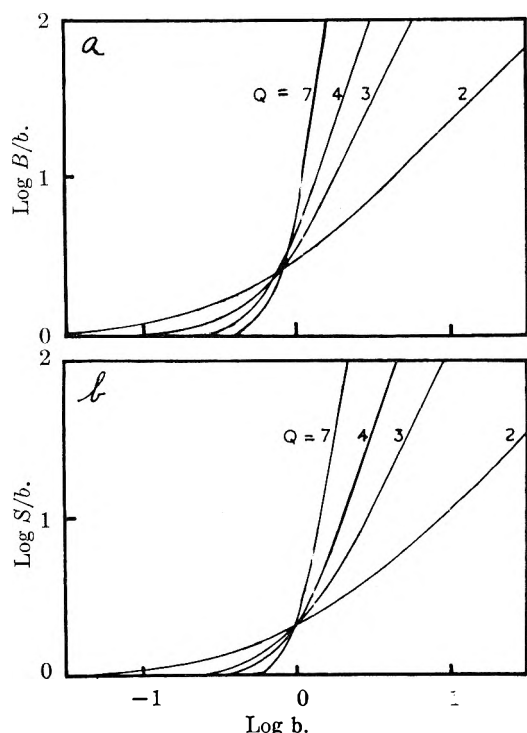


Fig. 1.—(a)  $\log B/b$  and (b)  $\log S/b$  as functions of  $\log b$  for several values of  $Q$  (equations 21 and 22).

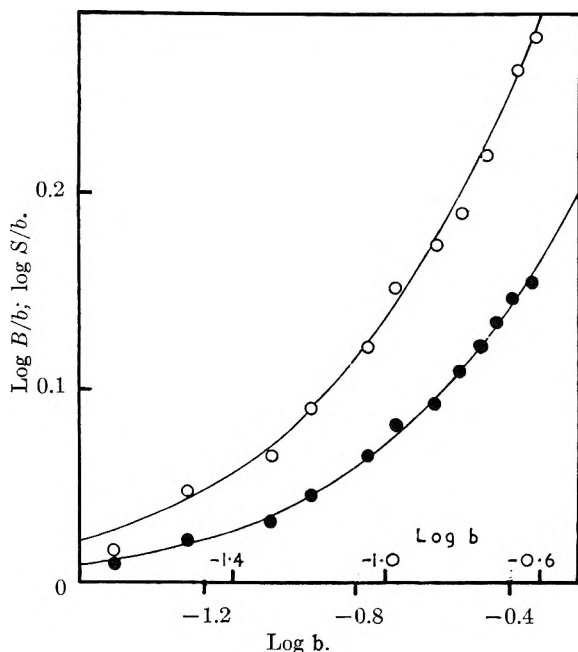


Fig. 2.—Benzenesulfonanilide in naphthalene<sup>15</sup> at 80°. Normalized curves  $\log Bb^{-1}(\log b)_Q$  and  $\log Sb^{-1}(\log b)_Q$  for  $Q = 2$  superimposed on the experimental data  $\log Bb^{-1}(\log b)$  (open circles) and  $\log Sb^{-1}(\log b)$  (full circles) in the position corresponding to  $\log \beta_2 = 0.28$ .

$dB)_{\bar{v}_{\max}}$  is low, it is likely that  $Q = 4$  or  $5$ . If  $\bar{v}$  rises sharply with concentration to give high values of  $\bar{v}_{\max}$ , an extended series of "multimers"<sup>13</sup> may be formed.<sup>14</sup>

(13) M. Davies in "Hydrogen Bonding," ed. D. Hadzi and H. W. Thompson, Pergamon Press, London, 1959, p. 560.

(14) F. J. C. Rossotti and H. Rossotti, *J. Phys. Chem.*, **65**, 930 (1961); D. M. W. Anderson, J. L. Duncan and F. J. C. Rossotti, *J. Chem. Soc.*, in press (1961).

**Treatment of a Single Complex,  $B_Q$ .**—Several graphical methods may be used to obtain the association constant of a single oligomer,  $B_Q$ . (i) If the functions  $B(b)$  or  $S(b)$  are used, no previous knowledge of  $Q$  is required. From equations 3 and 4

$$\log(B - b) = \log Q\beta_Q + Q \log b \quad (19)$$

and

$$\log(S - b) = \log \beta_Q + Q \log b \quad (20)$$

The plots of  $\log(B - b)$  and  $\log(S - b)$  against  $\log b$  are therefore straight lines of slope  $Q$  and of intercept  $\log Q\beta_Q$  and  $\log \beta_Q$ , respectively. (ii) Alternative rearrangement of equations 3 and 4 gives

$$\log \frac{B}{b} = \log(1 + Q\beta_Q b^{Q-1}) = \log(1 + Qb^{Q-1}) \quad (21)$$

and

$$\log \frac{S}{b} = \log(1 + \beta_Q b^{Q-1}) = \log(1 + b^{Q-1}) \quad (22)$$

where the normalized (dimensionless) variable  $b$  is given by

$$\log b = \log b + \frac{1}{Q-1} \log \beta_Q \quad (23)$$

The experimental values of  $\log Bb^{-1}$  and  $\log Sb^{-1}$  are best plotted on the same diagram as functions of  $\log b$ . Sets of normalized curves  $\log Bb^{-1}(\log b)_Q$  and  $\log Sb^{-1}(\log b)_Q$  may be calculated for different values of  $Q$  using equations 21 and 22, (see Fig. 1). Pairs of theoretical curves for the same value of  $Q$  are plotted on the same scale as the experimental curves, and superimposed on them so that the ordinates of the two graphs are coincident (see Fig. 2). The correct value of  $Q$  is that which gives normalized curves of the same shape and separation as the experimental plots. The association constant may be obtained by solving equation 23, using corresponding values of  $b$  and  $b$  in the position of best fit. The limits of error in  $\beta_Q$  are obtained from the permissible displacement of the normalized curves along the  $\log b$  axis.

Values of  $Q$  and  $\beta_Q$  may be obtained similarly from plots of  $B/b$  or  $S/b$  against  $\log b$ . (iii) Combination of equations 3 and 4 gives the linear relationship

$$\log(B - S) = Q \log(QS - B) + \log \beta_Q - (Q - 1) \log(Q - 1) \quad (24)$$

The non-logarithmic form of equation 24 has been used by Dunker<sup>3,7</sup> and others to obtain values of  $\beta_Q$  by one-point calculation. The value of  $Q$  must be found from equation 18, or by trial and error.

**Treatment of the System  $B + B_2 + B_Q$ .**—The data  $B, S, b$  can often be described in terms of the formation of a dimer, and of one other oligomer  $B_Q$  usually a trimer. For systems of this type, equations 3 and 4 may be written

$$B = \frac{B - b}{b^2} = 2\beta_2 + Q\beta_Q b^{Q-2} \quad (25)$$

and

$$S = \frac{S - b}{b^2} = \beta_2 + \beta_Q b^{Q-2} \quad (26)$$

(15) W. Sheele and A. Hartman, *Kolloid-Z.*, **131**, 126 (1953).

Substitution of the normalized variables

$$\log F = \log F - \log \beta_2 \quad (27)$$

$$\log \Phi = \log \Phi - \log \beta_2 \quad (28)$$

and

$$\log b = \log b + \frac{1}{Q-2} \log \frac{\beta_Q}{\beta_2} \quad (29)$$

into equations 25 and 26 gives

$$\log F = \log (2 + Qb^{Q-2}) \quad (30)$$

and

$$\log \Phi = \log (1 + b^{Q-2}) \quad (31)$$

The experimental values of  $\log F$  and  $\log \Phi$  are plotted on the same diagram as functions of  $\log b$ . Pairs of theoretical curves  $\log F (\log b)_Q$  and  $\log \Phi (\log b)_Q$  are calculated for a number of likely values of  $Q$ . These are superimposed on the experimental plot in the position of best fit with the axes of the two graphs parallel (see Fig. 3). The correct value of  $Q$  is that used to calculate the pair of normalized curves of the same shape and separation as the experimental functions. The values of  $\beta_2$  and  $\beta_Q$  may be obtained by solving equations 27 and 29, or 28 and 29, using corresponding values of the logarithms of  $b$  and  $b$ , and of either  $F$  and  $F$  or  $\Phi$  and  $\Phi$ , in the position of best fit. The limits of error in  $\log \beta_2$ , may be obtained from the permissible vertical movement of the normalized curves across the experiment data and those in  $\log \beta_Q/\beta_2$  from the permissible horizontal movement. Analogous curve-fitting methods may be developed for analysing systems containing monomer and any two complexes of unknown stability, provided that the formula of one of them is known.

**Treatment of the System  $B + B_2 + B_3 + B_4$ .**—If monomer, dimer, trimer and tetramer are present, equations 3 and 4 may be written as

$$F = \frac{B - b}{b^2} = 2\beta_2 + 3\beta_3b + 4\beta_4b^2 \quad (32)$$

$$\Phi = \frac{S - b}{b^2} = \beta_2 + \beta_3b + \beta_4b^2 \quad (33)$$

whence

$$\log F = \log F - \log \beta_2 = \log (2 + 3Rb + 4b^2) \quad (34)$$

$$\log \Phi = \log \Phi - \log \beta_2 = \log (1 + Rb + b^2) \quad (35)$$

where

$$\log b = \log b + \frac{1}{2} \log \frac{\beta_4}{\beta_2} \quad (36)$$

and

$$R = \frac{\beta_3}{(\beta_2\beta_4)^{1/2}} \quad (37)$$

Thus the shapes of the functions  $\log F (\log b)$  and  $\log \Phi (\log b)$  are determined by the parameter  $R$ , and their positions on the ordinate and abscissa depend on the values of  $\beta_2$ , and on the ratio  $\beta_4/\beta_2$ , respectively. The experimental functions  $\log F (\log b)$  and  $\log \Phi (\log b)$  are plotted on the same graph, and compared with pairs of normalized curves  $\log F (\log b)_R$  and  $\log \Phi (\log b)_R$ , calculated for a number of values of  $R$ , using equations 34 and 35 (see Fig. 4). The correct value of  $R$  is that used to calculate normalized curves of the same shape and separation as the experimental

(16) D. M. W. Anderson, J. L. Duncan and F. J. C. Rossotti, *J. Chem. Soc.*, 140 (1961).

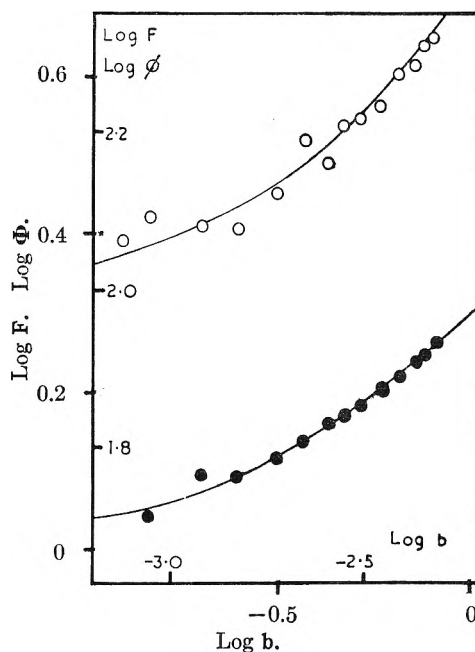


Fig. 3.—Pyrazole in carbon tetrachloride<sup>16</sup> at 18°. Normalized curves  $\log F (\log b)_Q$  and  $\log \Phi (\log b)_Q$  for  $Q = 3$  superimposed on the experimental data  $\log F (\log b)$  (open circles) and  $\log \Phi (\log b)$  (full circles) in the position corresponding to  $\log \beta_2 = 1.67$  and  $\log \beta_3 = 3.89$ .

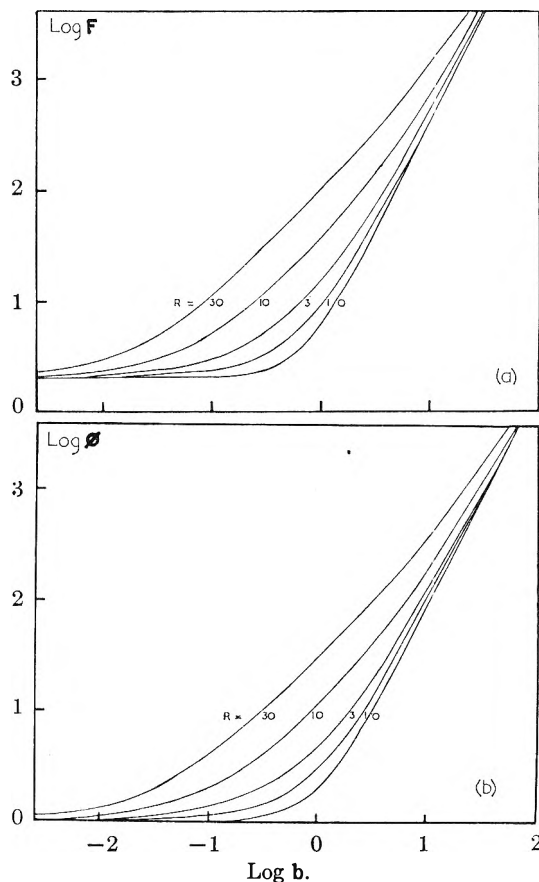


Fig. 4.—(a)  $\log F$  and (b)  $\log \Phi$  as functions of  $\log b$  for several values of  $R$  (equations 34 and 35).

functions. The values of  $\beta_2$  and  $\beta_4$  may be obtained by solving equations 34 and 36, or 35 and 36 using corresponding values of the logarithms of  $b$  and

$b$ , and of  $F$  and  $\mathbf{F}$  or  $\Phi$  and  $\Phi$  in the position of best fit. The value of  $\beta_3$  may then be calculated from the appropriate value of  $R$  by means of equation 37. The limits of error in the association constants may be obtained from the permissible variations in  $R$ , and in the position of acceptable fit. A similar treatment may be devised for any system containing three complexes of known formula but of unknown stability.

#### Analysis of Weight Average Molecular Weights.

—The weight average molecular weights,  $\bar{M}_w$ , of solutions of high polymers may sometimes be obtained from measurements of turbidity or of sedimentation velocity. Steiner<sup>11</sup> has shown that, since

$$\bar{M}_w = \frac{M_1 \sum_1^Q q^2 [B_q]}{\sum_1^Q q [B_q]} = \frac{M_1 \sum_1^Q q^2 \beta_q b^q}{B} \quad (38)$$

the value of  $b$  may be obtained using the expression

$$\log \frac{b}{B} - \log \frac{b_1}{B_1} = \int_{B_1}^B \left( \frac{M_1}{\bar{M}_w} - 1 \right) d \log B \quad (39)$$

where  $M_1$  is the molecular weight of the monomer. The free monomer concentration must have a known value,  $b_1$ , at one total concentration,  $B_1$ . The function  $B(b)$  may then be treated as described above. If required, the function  $S(b)$  may be obtained by a second integration, using equation 12. Alternatively, equation 38 may be rearranged to

$$W = \frac{\bar{M}_w B}{M_1 b} = \sum_1^Q q^2 \beta_q b^{q-1} \quad (40)$$

and curve-fitting methods may be applied to the power series  $W(b)$ . For example, if  $Q = 3$

$$\frac{W - 1}{b} = 4\beta_2 + 9\beta_3 b \quad (41)$$

The values of  $\beta_2$  and  $\beta_3$  may be obtained by a procedure analogous to that described for the functions  $F(b)$  and  $\Phi(b)$ , using equations 25 and 26. The three sets of data  $(\bar{M}_w, b)$ ,  $(B, b)$  and  $(S, b)$  may therefore be treated simultaneously.

## GRAPHICAL METHODS OF DETERMINING SELF-ASSOCIATION CONSTANTS. II. SYSTEMS CONTAINING MANY SPECIES

By F. J. C. ROSSOTTI AND HAZEL ROSSOTTI

*Department of Chemistry, The University of Edinburgh, Scotland*

*Received September 28, 1960*

The number of independent self-association constants which may be determined for systems containing a large number of multimers is limited by the precision of the experimental data. New graphical methods are proposed for determining approximate association constants on the assumptions that the constants are related to one, two or three determinable parameters. The methods are illustrated with reference to 2-*n*-butylbenzimidazole, *N*-methylformamide, *N*-propylacetamide and *N*-methyltrichloroacetamide in benzene, and to aqueous butyric acid.

In spite of numerous treatments<sup>1-6</sup> of equilibria in systems which are extensively associated, few attempts have been made to obtain a large number of independent association constants. Although values<sup>7</sup> of  $\beta_q$  have been obtained by successive extrapolation<sup>4</sup> and successive approximations,<sup>8</sup> the precision of the data rarely permits the determination of more than two or three independent association constants. Now, if several constants were inter-related, the number of independent parameters to be determined would be reduced. Many authors have assumed that all the stepwise association constants  $K_q$  are identical<sup>2,8-17</sup> or that

the first one or two stepwise association constants differ from the rest.<sup>12,18-21</sup> Other one-parameter relationships between stepwise association constants have been given by Connick and Reas,<sup>3</sup> and a two-parameter relationship was suggested by Lassettre<sup>1</sup> in 1937.

The treatment of simple systems by curve-fitting<sup>7</sup> is now extended to show how experimental data for more highly associated systems may be described in terms of one, two, or three independent parameters. If  $\bar{v}$  (equation I-18) tends to high values and  $d\bar{v}/db$  increases sharply, we assume that a very large series of multimers is formed and test various simple hypotheses concerning the inter-relationship of the association constants.

(1) E. N. Lassettre *J. Am. Chem. Soc.*, **59**, 1383 (1937); *Chem. Revs.*, **20**, 259 (1937).

(2) K. L. Wolf and R. Wolff, *Angew. Chem.*, **61**, 191 (1949).

(3) R. E. Connick and W. H. Reas, *J. Am. Chem. Soc.*, **73**, 1171 (1951).

(4) N. E. White and M. Kilpatrick, *J. Phys. Chem.*, **59**, 1044 (1955).

(5) M. Davies and H. E. Hallam, *J. Chem. Educ.*, **33**, 322 (1956).

(6) F. J. C. Rossotti and H. Rossotti, "The Determination of Stability Constants," McGraw-Hill Book Co., New York, N. Y., in press, Chap. 16.

(7) F. J. C. Rossotti and H. Rossotti, *J. Phys. Chem.*, **65**, 926 (1961), where symbols are defined and equations with numbers preceded by Roman I will be found.

(8) K. L. Wolf, H. Dunken and K. Merkel, *Z. physik. Chem.*, **46B**, 287 (1950).

(9) H. Kempfer and R. Mecke, *ibid.*, **49B**, 229 (1940).

(10) J. Kreuzer and R. Mecke, *ibid.*, **49B**, 309 (1941).

(11) J. Kreuzer, *ibid.*, **53B**, 213 (1943).

(12) J. Bjerrum, *Kem. Maanedssblad*, **24**, 21 (1943).

(13) R. Ginell, *J. Coll. Sci.*, **3**, 1 (1948); **5**, 99 (1950).

(14) K. L. Wolf and G. Metzger, *Ann.*, **563**, 157 (1949).

(15) Y. Doucet and S. Bugnon, *J. chim. phys.*, **54**, 155 (1957).

(16) E. Thilo and G. Kruger, *Z. Elektrochem.*, **61**, 24 (1957).

(17) P. J. Flory, *J. Chem. Phys.*, **12**, 425 (1944); **14**, 49 (1946).

(18) G. Briegleb, *Z. physik. Chem.*, **51B**, 9 (1941); G. Briegleb and W. Strohmeier, *Z. Elektrochem.*, **57**, 668 (1953).

(19) E. G. Hoffmann, *ibid.*, **53B**, 179 (1943).

(20) N. D. Coggeshall and E. L. Saier, *J. Am. Chem. Soc.*, **73**, 5414 (1951).

(21) M. Davies and D. K. Thomas, *J. Phys. Chem.*, **60**, 763 (1956).

### One Parameter Series.

The simplest type of extensive self-association is where the stepwise association constants,  $K_q$ , for the successive reactions I-6 are all identical. We set

$$K_q = K \quad (q \geq 2) \quad (1)$$

$$\beta_q = K^{q-1} \quad (q \geq 1) \quad (2)$$

and

$$b = Kb \quad (3)$$

Substituting into equations I-3 and I-4, we obtain

$$Bb^{-1} = \sum_1^{\infty} qb^{q-1} = (1-b)^{-2} \quad \text{for } b < 1 \quad (4)$$

$$Sb^{-1} = \sum_1^{\infty} b^{q-1} = (1-b)^{-1} \quad \text{for } b < 1 \quad (5)$$

Normalized curves  $Bb^{-1}(\log b)$  and  $Sb^{-1}(\log b)$  may be calculated using equations 4 and 5 and plotted using a single pair of coordinate axes. The experimental data  $Bb^{-1}(\log b)$  and  $Sb^{-1}(\log b)$  are plotted together on a second sheet of graph paper using the same coordinate scales. If equation 1 is indeed valid, then the experimental plots will be of the same shape as the normalized curves, but displaced along the abscissa. In the position of best fit, the single parameter  $K$  is found by solving equation 3. The limits of error are given by the permissible displacement of the normalized curves. The over-all association constants are found by substitution into equation 2.

The above approach may be extended readily to systems in which the stepwise association constants,  $K_q$ , are functions of both  $q$  and a single parameter,  $K$ . However, as one parameter systems are merely special cases of two parameter systems with identical parameters, this approach is not pursued. Connick and Reas<sup>3</sup> have previously suggested a similar curve-fitting procedure, using only one normalized curve. However, our recommended procedure of simultaneously fitting a pair of experimental functions restricts the range of possible fits to a marked extent.

### Two Parameter Series.

Although experimental data sometimes may be described by a unique parameter, successive stepwise association constants might be expected<sup>22,23</sup> to increase with  $q$  toward some constant value. Hence, we now examine a number of two-parameter models, calculated on simple hypotheses.

**Hypothesis I.**—If the stepwise association constants are only identical for  $q \geq 3$ , equation 2 is replaced by

$$\beta_q = \beta_2 K^{q-2} \quad (q \geq 2) \quad (6)$$

Combining equations I-3 and 6

$$T = \frac{B-b}{b} = \sum_2^{\infty} q\beta_2 K^{q-2} b^{q-1} \quad (7)$$

We define a normalized variable by

$$T = \frac{TK}{\beta_2} \quad (8)$$

and combine equations 3, 7 and 8 to give

(22) L. Saroléa-Mathot, *Trans. Faraday Soc.*, **49**, 8 (1953).

(23) N. D. Coggeshall, *J. Chem. Phys.*, **18**, 978 (1950).

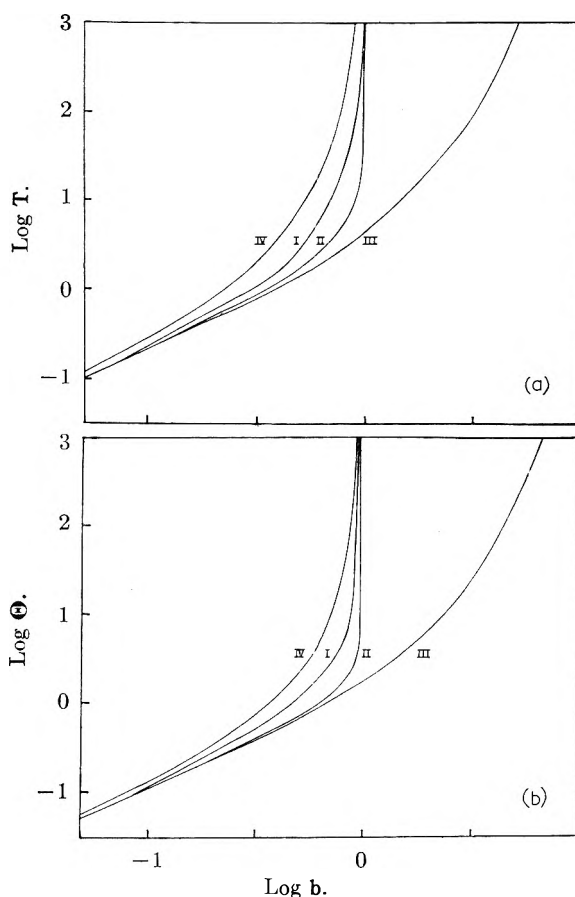


Fig. 1.—(a)  $\log T$  and (b)  $\log \Theta$  as functions of  $\log b$  for extensive self-association according to Hypotheses I, II, III and IV.

$$T = \frac{b(2-b)}{(1-b)^2} \quad \text{for } b < 1 \quad (9)$$

Similarly equations I-4, and 6 give

$$\Theta = \frac{S-b}{b} = \sum_2^{\infty} \beta_2 K^{q-2} b^{q-1} \quad (10)$$

We define a further normalized variable by

$$\Theta = \frac{\Theta K}{\beta_2} \quad (11)$$

and combine equations 3, 10 and 11 to give

$$\Theta = \frac{b}{1-b} \quad \text{for } b < 1 \quad (12)$$

Systems where  $\beta_2 = K$  are included as a special case of the present model.

**Hypothesis II.**—If the first few stepwise associations occur less readily than the rest, we may set

$$K_q = \frac{q-2}{q-1} K \quad (q \geq 3) \quad (13)$$

Hence,  $K_3 = K/2$ ,  $K_q \rightarrow K$  as  $q \rightarrow \infty$  and

$$\beta_q = \frac{\beta_2 K^{q-2}}{q-1} \quad (q \geq 2) \quad (14)$$

Combining equations I-3, 3, 8 and 14

$$T = \sum_2^{\infty} \frac{qb^{q-1}}{q-1} = \frac{b}{1-b} - \ln(1-b) \quad \text{for } b < 1 \quad (15)$$

Similarly, combining equations I-4, 3, 11 and 14

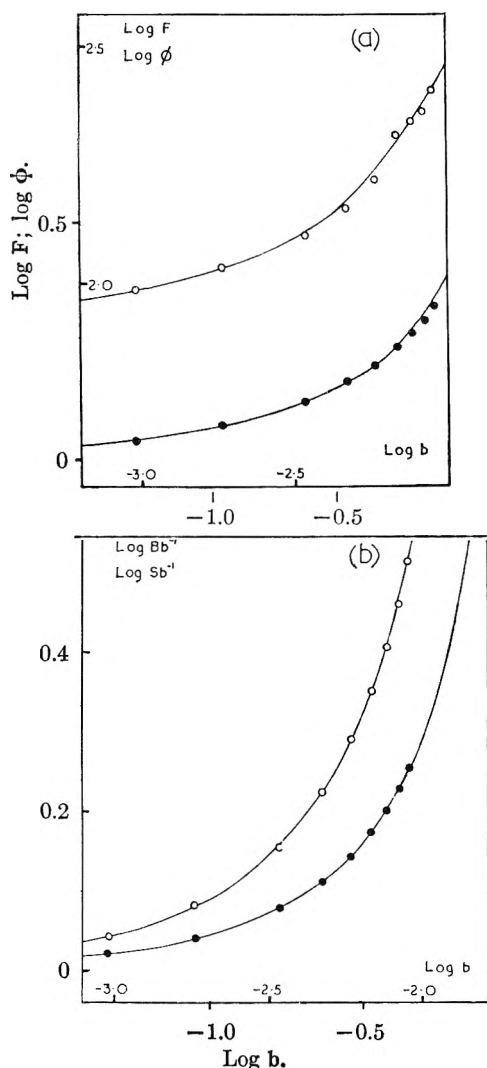


Fig. 2.—N-Propylacetamide in benzene at 21.80°. (a) Normalized curves  $\log F(\log b)_R$  and  $\log \phi(\log b)_R$  for  $R = 1$  (equations I-34 and I-35) superimposed on the experimental data  $\log F(\log b)$  (open circles) and  $\log \phi(\log b)$  (full circles) in the position corresponding to values of  $\beta_2$ ,  $\beta_3$  and  $\beta_4$  given in Table I. (b) Normalized one-parameter curves  $\log Bb^{-1}(\log b)$  and  $\log Sb^{-1}(\log b)$  superimposed on the experimental data  $\log Bb^{-1}(\log b)$  and  $\log Sb^{-1}(\log b)$  in the position corresponding to  $\log K = 1.69$ .

$$\Theta = \sum_2^{\infty} \frac{b^{q-1}}{q-1} = -\ln(1-b) \quad \text{for } b < 1 \quad (16)$$

**Hypothesis III.**—As a check on the sensitivity of the normalized functions  $\log T(\log b)$  and  $\log \Theta(\log b)$  to the particular model adopted we now suppose that each addition to the growing multi-chain becomes progressively more difficult and set

$$K_q = \frac{K}{q-1} \quad (q \geq 3) \quad (17)$$

Hence,  $K_3 = K/2$ ,  $K_q \rightarrow 0$  as  $q \rightarrow \infty$  and

$$\beta_q = \frac{\beta_2 K^{q-2}}{(q-1)!} \quad (q \geq 2) \quad (18)$$

The analogs of equations 9 and 12 are now

$$T = \sum_2^{\infty} \frac{qb^{q-1}}{(q-1)!} = eb(1+b) - 1 \quad (19)$$

and

$$\Theta = \sum_2^{\infty} \frac{b^{q-1}}{(q-1)!} = e^b - 1 \quad (20)$$

**Hypothesis IV.**—Finally, it may be supposed that the first few stepwise associations occur more readily than the rest. If we set

$$K_q = \frac{q-1}{q-\frac{1}{2}} K \quad (q \geq 3) \quad (21)$$

then  $K_3 = 2K$ ,  $K_q \rightarrow K$  as  $q \rightarrow \infty$  and

$$\beta_q = \beta_2(q-1)K^{q-2} \quad (q \geq 2) \quad (22)$$

The analogs of equations 9 and 12 become

$$T = \sum_2^{\infty} q(q-1)b^{q-1} = \frac{2b}{(1-b)^3} \quad (23)$$

and

$$\Theta = \sum_2^{\infty} (q-1)b^{q-1} = \frac{b}{(1-b)^2} \quad (24)$$

**Other Two-parameter Series.**—The four hypotheses detailed above do not exhaust the possibilities of this approach. If the experimental data conform to none of the above models, some indication will be obtained of how the dependence of  $K_q$  upon  $q$  differs from the forms already chosen, and an appropriate new hypothesis may be set up.

**Determination of the Parameters.**—A unique pair of normalized curves  $\log T(\log b)$  and  $\log \Theta(\log b)$  may be calculated for each hypothesis, using equations 9 and 12 and their analogs, see Figs. 1a and 1b. It is convenient to plot the curves for each hypothesis on a separate sheet of graph paper, using common coordinate axes. The experimental data  $\log T(\log b)$  and  $\log \Theta(\log b)$  are plotted similarly on a further sheet of graph paper. If these are of the same shape as a normalized pair of curves, and may be superimposed on them by movements parallel to the coordinate axes, then the appropriate model is a valid representation of the system, within the limits of experimental error. In the position of best fit, values of the parameters  $K$  and  $\beta_2$  may be found by solving equations 3 and 8 or 11. Limits of error are found from the tolerable displacement of the experimental functions over the normalized curves, parallel to the coordinate axes. Values of the required stepwise and over-all association constants are found by substitution into equations 1 and 6, or the appropriate analogs.

As the experimental data are usually only available over a restricted concentration range, it is sometimes possible for the experimental functions  $\log T(\log b)$  and  $\log \Theta(\log b)$  to fit normalized curves calculated according to more than one hypothesis. In such cases, the several hypotheses are equally valid representations of the data over the concentration range available. However, values of the over-all association constants obtained will usually be found to be approximately equal, irrespective of the particular hypotheses. Subject to the assumptions of each model, values of  $\beta_q$  will be significant, provided that  $q\beta_q b^q/B$  and  $\beta_q b^q/S$  are significantly greater than zero. Clearly, the maximum value of  $q$  in the system will be greater than or equal to the maximum value of  $v$ .

In some cases, experimental data over a restricted concentration range may be equally consistent with the formation of a few oligomers and with the formation of a large series of multimers. It is therefore essential to apply systematically the methods outlined in Part I and in the present paper.

### Three-parameter Series.

A unique normalized curve calculated on a particular two-parameter hypothesis may just fail to represent an experimental system adequately. Moreover the systematic deviation may suggest that, although the model is basically valid, one of the association constants differs from the hypothetical sequence. The shape of the normalized curve may be varied systematically by introducing a third (shape) parameter  $R$ . In this way, a family of normalized curves  $\log T(\log b)_R$  and  $\log \Theta(\log b)_R$  may be calculated for comparison with the analogous experimental functions.

The procedure is illustrated by modifying the two parameter hypothesis I, on the assumption that the trimerization constant falls out of the regular sequence. Hence, our modified hypothesis is that the stepwise association constants are only identical for  $q \geq 4$ , and that the over-all association constants are only represented by equation 6 for  $q \geq 4$ . The shape parameter is defined by

$$R = \beta_3/\beta_2K \quad (25)$$

and equations 9 and 12 are extended to

$$T = \frac{b(2-b)}{(1-b)^2} + 3(R-1)b^2 \quad (26)$$

and

$$\theta = \frac{b}{1-b} + (R-1)b^2 \quad (27)$$

Clearly equations 9 and 12 are special cases of 26 and 27 for  $R = 1$ .

Pairs of normalized curves  $\log T(\log b)_R$  and  $\log \Theta(\log b)_R$  may be calculated for a number of values of  $R$ . If the shape of the experimental functions lies between those of normalized functions for two particular values of  $R$ , the best value of this parameter, and its limits of error may be determined readily. The values of the two parameters  $K$  and  $\beta_2$  are found precisely as before, and values of the over-all association constants calculated using equations 6 ( $q \geq 4$ ), 27 and the analog of equation 10.

### Applications

The methods described above have been applied to data  $B(S)$  for numerous systems.<sup>24</sup>

The values of  $\beta_q$  obtained for N-methylformamide<sup>25</sup> in benzene at 35.07° and for 2-n-butylbenzimidazole<sup>4</sup> in benzene at 5.5° are in excellent agreement with those of the original authors. However, earlier interpretations of data for some systems have now been found to be incorrect or incomplete.

**N-Propylacetamide in Benzene at 21.80°.**—The data<sup>25</sup> are consistent with the formation of an ex-

(24) D. M. W. Anderson, J. L. Duncan and F. J. C. Rossotti, *J. Chem. Soc.*, May (1961); F. J. C. Rossotti and H. Rossotti, unpublished work.

(25) M. Davies and D. K. Thomas, *J. Phys. Chem.*, 60, 767 (1956).

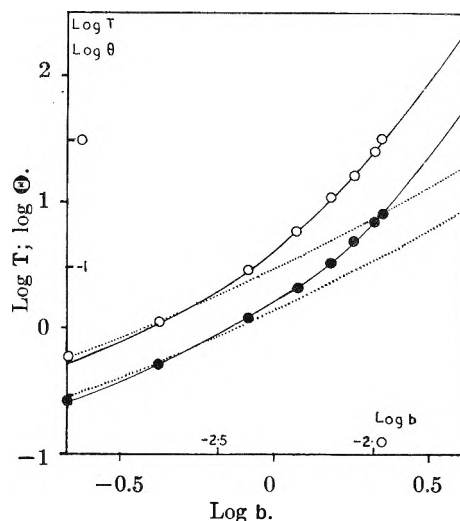


Fig. 3.—N-Methyltrichloroacetamide in benzene at 24.57°. Normalized curves  $\log T(\log b)$  and  $\log \Theta(\log b)$  (full lines) for Hypothesis III superimposed on the experimental data  $\log T(\log b)$  (open circles) and  $\log \Theta(\log b)$  (full circles) in the position corresponding to  $\log \beta_2 = 0.80$  and  $\log K = 2.31_5$ . The dotted functions  $\log T(\log b)$  and  $\log \Theta(\log b)$  are calculated from the association constants given by the original authors.<sup>25</sup>

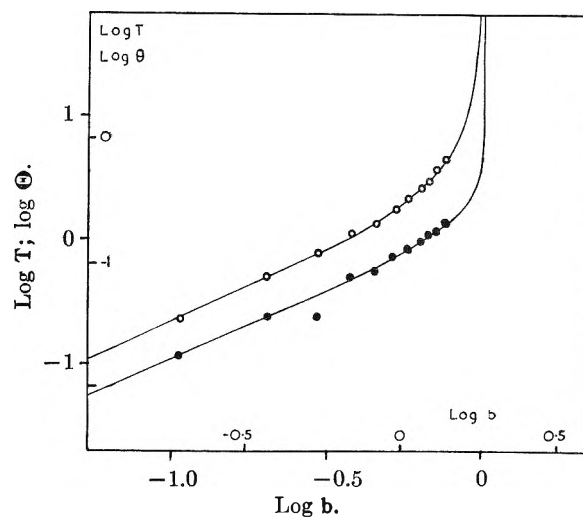


Fig. 4.—Aqueous butyric acid at 0°. Normalized curves  $\log T(\log b)$  and  $\log \Theta(\log b)$  for Hypothesis II superimposed on the experimental data  $\log T(\log b)$  (open circles) and  $\log \Theta(\log b)$  (closed circles) in the position corresponding to  $\log \beta_2 = -1.09$  and  $\log K = -0.26$ .

tended series of multimers. The association constants are in substantial agreement with those of the original authors, regardless of which of the several acceptable hypotheses is used (see Table I). However, application of methods suggested in Part I shows that the data can be described equally well in terms of the formation of only dimer, trimer and tetramer (see Fig. 2). Thus there is no definite evidence for the existence of species higher than  $B_4$  in the mole fraction concentration range  $B \geq 0.03$ .

**N-Methyltrichloroacetamide in Benzene at 24.57°.**—The data<sup>25</sup> are consistent with the formation of an extended series of multimers for which  $\log \beta_2 = 0.80 \pm 0.01$  and  $\log K_q = 2.31_5 \pm 0.015 - \log(q-1)$  (Hypothesis III), but are incompatible with the

TABLE I  
 ASSOCIATION CONSTANTS (MOLE FRACTION SCALE) FOR N-PROPYLACETAMIDE IN BENZENE AT 21.80°

	B + B <sub>2</sub> + B <sub>3</sub> + B <sub>4</sub>	1 Parameter series	Hypothesis I	Hypothesis III	Lassette series	Davies and Thomas <sup>26</sup>
log β <sub>2</sub>	1.63 ± 0.02	1.69 ± 0.01	1.68 ± 0.02	1.63 ± 0.02	1.73 ± 0.04	1.70 ± 0.02
log β <sub>3</sub>	3.49 ± 0.02	3.38	3.41	3.49	3.46	3.42
log β <sub>4</sub>	5.35 ± 0.04	5.07	5.14	5.17	5.19	5.14
log β <sub>5</sub>	— ∞	6.76	6.87	6.73	6.92	6.86
log K <sub>q</sub>	.....	1.69 ± 0.01	1.73 ± 0.03	2.16 ± 0.03 - log(q - 1)	1.73 ± 0.04	1.72 ± 0.02

formation of only dimer and trimer, as suggested by the original authors (see Fig. 3).

**Aqueous Butyric Acid at 0°.**—Values of *b* have been calculated from measurements<sup>26</sup> of *B(S)* by Davies and Griffiths<sup>27</sup> who assumed that all oligomers have identical acid dissociation constants. This assumption has been partially substantiated by potentiometric measurements of the acid dissociation constants of the monomer, dimer and trimer.<sup>28</sup>

The data for *B* ≤ 2.5 molal were originally interpreted<sup>27</sup> in terms of the formation of only the dimer, tetramer and dodecamer, but it is now found that they are equally compatible with the formation of an extended series of multimers. Hypotheses I and II are acceptable and give similar values of the association constants (see Table II). The presence of an extended series of multimers is also indicated by application of the Lassette treatment<sup>1</sup> in the concentration range *B* ≤ 2.0 molal. In the con-

centration range 2.5 ≤ *B* ≤ 17.0,  $\bar{v}$  rises sharply from 3.8 to 27.2. Higher estimates<sup>27</sup> of the degree of association of the multimers are based on the misapplication of a Kreuzer relationship, which is only valid for a system containing a unique oligomer.<sup>11</sup>

 TABLE II  
 ASSOCIATION CONSTANTS (MOLAL SCALE) FOR AQUEOUS BUTYRIC ACID AT 0°

	Hypothesis I	Hypothesis II	Davies and Griffiths <sup>27</sup>
log β <sub>2</sub>	-1.13 ± 0.01	-1.09 ± 0.02	-1.02
log β <sub>3</sub>	-1.56	-1.65	-∞
log β <sub>4</sub>	-1.99	-2.08	-1.64
log β <sub>5</sub>	-2.42	-2.47	-∞
log K <sub>q</sub>	-0.43 ± 0.02	log $\left(\frac{2-q}{1-q}\right)$ - 0.26 ± 0.03	.....
log β <sub>12</sub>	.....	.....	-3.5

**Acknowledgments.**—We are grateful to the Earl of Moray Endowment, and to the Imperial Chemical Industries Limited, for the purchase of calculating machines.

(26) E. R. Jones and C. R. Bury, *Phil. Mag.*, 4, 841 (1927).

(27) M. Davies and D. M. L. Griffiths, *Z. physik. Chem. (Frankfurt)*, 6, 143 (1956).

(28) D. L. Martin and F. J. C. Rossotti, *Proc. Chem. Soc.*, 60 (1959); and unpublished work.

## METAL COMPLEXING BY PHOSPHORUS COMPOUNDS. IV. ACIDITY CONSTANTS

BY R. R. IRANI AND C. F. CALLIS

*Monsanto Chemical Company, Research Department, Inorganic Chemicals Division, St. Louis 66, Mo.*

Received October 17, 1960

Using high speed computers together with *pH*-titration, the successive acidity constants of linear phosphoric acids with 1, 2, 3, 6 and 60 phosphorus atoms per chain have been evaluated at 25° and unit ionic strength. It was found that the end hydrogen becomes more acidic, and the last two acidity constants both approach a value of ca. 10<sup>-8</sup> as the chain length increases. Imidodiphosphoric and diimidotriphosphoric acids were found to be weaker acids than pyrophosphoric and triphosphoric acid, respectively. The difference is discussed on the basis of electronegativities.

### Introduction

In a general study of metal complexing by phosphorus compounds, the determination and interpretation of acidity constants is an integral part. The hydrogen ion is a cation itself, and the strength with which it is associated with anions must be somewhat similar to that for other cations. Because of competition between the hydrogen and other metal ions, acidity constants are necessary in interpreting *pH* dependence of metal complexes, and, therefore, the effects of structural changes in the molecules.

### Experimental

**Chemicals.**—Sodium salts or the acids were used as the source of the phosphorus-containing anions. When the

salts were used, they were converted into the tetramethylammonium salt using the tetramethylammonium form of 100–200 mesh Dowex 50W-xZ ion-exchange resin. When the acids were the starting materials, they were neutralized with the proper amount of Eastman Kodak's tetramethylammonium hydroxide to produce the tetramethylammonium salt.

The 99.5+% tetrasodium pyrophosphate and pentasodium tripolyphosphate hexahydrate were obtained as previously described.<sup>1</sup> Phosphoramidic acid monohydrate and the hexahydrates of tetrasodium imidodiphosphate and pentasodium diimidotriphosphate were kindly supplied by Dr. M. L. Nielsen of Monsanto's Research and Engineering Division; nuclear magnetic resonance, infrared, as well as chemical analyses showed these samples to be better than 97% pure<sup>2</sup> with the balance being a mixture of similar

(1) R. R. Irani and C. F. Callis, *J. Phys. Chem.*, 64, 1398 (1960).  
 (2) M. L. Nielsen, private communication.



species. Merck's reagent grade 85% phosphoric acid was used as the source of orthophosphate ions. The long chain linear phosphates were characterized by their  $\text{Na}_2\text{O}/\text{P}_2\text{O}_5$  ratio.<sup>1</sup>

Boiled distilled water was used for solution make-up. All other chemicals were reagent grade.

**Procedure.**—All solutions were used within 15 minutes after make-up, so that no hydrolytic degradation is expected. In the case of phosphoramidate, which hydrolyzes very rapidly,<sup>3</sup> a special procedure to be described later was adopted. All runs were at  $25 \pm 0.1^\circ$ .

Excepting phosphoramidic acid, the acidity constant determinations were as follows. Using stock standard solutions of HCl and the appropriate anions, two solutions having the same total ionic strength were prepared with tetramethylammonium bromide as the supporting electrolyte. One solution had a total volume of 100 ml. and was 0.01 M in tetramethylammonium salt of the anion whose acidity constants are to be determined. The other solution, the titrant, was also 0.01 M in the tetramethylammonium salt and generally 0.1 M HCl. To 100 ml. of the first solution, stirred with a magnetic stirrer under a nitrogen atmosphere, some forty aliquots of the titrant were added successively and the equilibrium pH noted.

In the case of the phosphoramidic acid, several solutions containing HCl and tetramethylammonium bromide to give a final ionic strength of 1.0 were prepared. Weighed amounts of phosphoramidic acid were then put into each solution such that the ratio of the number of equivalents of  $\text{H}^+$  to the number of moles of phosphoramidate in the final solution was 0.5, 1.0, 1.5 and 2.0.

### Interpretation of Data

**General Equations.**—At any specific pH and temperature if  $\text{X}^{(-a)}$ ,  $\text{HX}^{(-a+1)}$ , ...,  $\text{HiX}^{(-a+i)}$ , ...,  $\text{HaX}$  are the free phosphorus-containing anion, monohydrogen anion,  $i$ -th hydrogen anion, and neutral species, respectively, then

$$\bar{a} = \frac{\sum_{i=0}^{i=a} i[\text{HiX}^{(-a+i)}]}{\sum_{i=0}^{i=a} [\text{HiX}^{(-a+i)}]} = \frac{\sum_{i=1}^{i=a} (i - \bar{a})[\text{HiX}^{(-a+i)}]}{[\text{X}^{-a}]} \quad (1)$$

where brackets indicate concentration and  $\bar{a}$  is the average number of hydrogens associated with the anion. The successive apparent acidity constants are

$$K_i = \frac{[\text{H}^+][\text{H}_{(i-1)}\text{X}^{(-a+i-1)}]}{[\text{H}_i\text{X}^{(-a+i)}]} \quad (2)$$

From equations 1 and 2

$$\bar{a} = \frac{\sum_{i=1}^{i=a} \frac{i[\text{H}^+]^i}{K_1 \cdots K_i - K_a}}{1 + \sum_{i=1}^{i=a} \frac{[\text{H}^+]^i}{K_1 \cdots K_i - K_a}} \quad (3)$$

**Evaluation of  $\bar{a}$ .**—When  $y$  ml. of a solution that is  $C_1$  molar in  $[(\text{CH}_3)_4\text{N}]_a\text{X}$  and  $C_2$  molar in HCl are added to  $b$  ml. of a solution with a molarity of  $C_1$  in  $[(\text{CH}_3)_4\text{N}]_a\text{X}$ , both solutions being at the same temperature and ionic strength, then

$$C_1 = \sum_{i=0}^{i=a} [\text{HiX}^{(-a+i)}] \quad (4)$$

assuming that tetramethylammonium does not form any complexes with the phosphate anions. This assumption is very reasonable in view of work by Van Wazer and Campanella<sup>4</sup> and others. Also

(3) O. T. Quimby, A. Narath and F. H. Lohman, *J. Am. Chem. Soc.*, **82**, 1099 (1960).

(4) J. R. Van Wazer and D. Campanella, *ibid.*, **72**, 655 (1950).

$$\frac{yC_2}{b+y} = [\text{H}^+] + \sum_{i=1}^{i=a} i[\text{HiX}^{(-a+i)}] \quad (5)$$

so that from equations 1, 4 and 5

$$\bar{a} = \frac{yC_2}{C_1(b-y)} - \frac{[\text{H}^+]}{C_1} \quad (6)$$

### Results and Discussion

The raw data which are averages of two runs for the titration of the phosphorus-containing anions with hydroxide are voluminous and are deposited with the American Documentation Institute.<sup>5</sup> The hydrogen ion concentration,  $[\text{H}^+]$ , was obtained from pH readings using the activity coefficient corrections<sup>6</sup> for HBr<sup>7</sup> at  $25^\circ$  and the appropriate ionic strength.

From equations 3 and 6, the complete pH-titration curves, except for phosphoramidic acid, were then fit to a modified least squares non-linear program of an IBM 704 computer to yield the best values of the various acid dissociation constants that are consistent with the experimental data. Using these acidity constants, the values of  $\bar{a}$  were back-calculated on the computer. It was found that in all cases the standard deviation between the measured and calculated  $\bar{a}$  values varied between 0.04 and 0.08 for the various acids, and the total correlation coefficients were all larger than 0.996, indicating excellent fit.<sup>8</sup> A typical comparison of calculated and measured  $\bar{a}$  values is given in Table I for diimidotriphosphoric acid.

The various apparent acid dissociation constants that were evaluated at several ionic strengths are summarized in Table II. The errors shown as  $\pm$  are the statistical 95% confidence limits. The accurate evaluation of dissociation constants of the strong hydrogens of the acids require that the hydrogen ion concentration be established with greater accuracy than is attainable with conventional pH meters, so that these strong-hydrogen constants are only rough estimates.

The acid dissociation constants obtained for pyrophosphoric and triphosphoric acids at unit ionic strength and  $25^\circ$  are in good agreement with previous measurements,<sup>6,9</sup> particularly since the complete titration curve was used to evaluate them. Also, Watters, *et al.*,<sup>6,9</sup> inserted the hydrogen ion activity into their acid dissociation constants, whereas the constants reported here were calculated using molar concentrations for all the species. Had the exact procedure of Watters, *et al.*,<sup>6,9</sup> for evaluating the acidity constants been adopted, much better agreement would have resulted.

(5) Material supplementary to this article has been deposited as Document Number 6547 with the ADI Auxiliary Publication Project, Photoduplication Service, Library of Congress, Washington 25, D. C. A copy may be secured by citing the Document Number and by remitting \$2.50 for photoprints, or \$1.75 for 35 mm. microfilm in advance by check or money order payable to: Chief, Photoduplication Service, Library of Congress.

(6) J. I. Watters, E. D. Loughran and S. M. Lambert, *J. Am. Chem. Soc.*, **78**, 4855 (1956).

(7) H. S. Harned, A. S. Keston and J. G. Donelson, *ibid.*, **58**, 989 (1936).

(8) W. J. Youden, "Statistical Methods for Chemists," John Wiley and Sons, Inc., New York, N. Y., 1955.

(9) S. M. Lambert and J. I. Watters, *J. Am. Chem. Soc.*, **79**, 4262 (1957).

TABLE I

TITRATION OF 100 ML. OF A SOLUTION OF 0.0100 M $[(\text{CH}_3)_4\text{N}]_5\text{P}_3\text{O}_8(\text{NH})_2$ WITH A SOLUTION 0.09865 M IN HCl AND 0.0100 M IN $[(\text{CH}_3)_4\text{N}]_5\text{P}_2\text{O}_8(\text{NH})_2$ AT 25°				18	6.74	1.49	1.50
Both solutions contained sufficient $(\text{CH}_3)_4\text{NBr}$ to produce a total ionic strength of 0.1				19	6.59	1.57	1.57
				20	6.38	1.68	1.64
				21	6.18	1.78	1.71
				22	5.86	1.88	1.78
				23	5.44	1.95	1.84
				24	4.98	2.00	1.91
				25	4.62	2.02	1.97
				26	4.40	2.05	2.03
				28	4.10	2.10	2.14
				30	3.84	2.17	2.25
				35	3.38	2.39	2.50
				40	3.04	2.64	2.70
				45	2.77	2.87	2.84
				50	2.60	3.03	2.96
				55	2.46	3.16	3.05
				60	2.37	3.24	3.15
				65	2.30	3.31	3.24
				70	2.23	3.38	3.30
				75	2.20	3.41	3.41
				80	2.14	3.47	3.45
				85	2.10	3.51	3.51
				90	2.08	3.52	3.61
				95	2.02	3.58	3.58
				100	2.00	3.60	3.67
				110	1.94	3.66	3.69
				120	1.90	3.70	3.76

TABLE II

## APPARENT ACID DISSOCIATION CONSTANTS FOR PHOSPHORUS COMPOUNDS

Acid	$pK_1$	$pK_2$	$pK_3$	$pK_4$	$pK_5$
— At ionic strength of 0.1 —					
Imidodiphosphoric	$10.22 \pm 0.09$	$7.32 \pm 0.12$	$2.66 \pm 0.09$	(1.5) <sup>a</sup>	...
Diimidotriphosphoric	$9.84 \pm .08$	$6.61 \pm .09$	$3.03 \pm .10$	(2) <sup>a</sup>	(1) <sup>a</sup>
— At ionic strength of 0.2 —					
Imidodiphosphoric	$9.72 \pm 0.10$	$7.08 \pm 0.09$	$2.85 \pm 0.08$	(2) <sup>a</sup>	...
Diimidotriphosphoric	$9.92 \pm .03$	$7.02 \pm .03$	$3.83 \pm .03$	(2) <sup>a</sup>	(0) <sup>a</sup>
— At ionic strength of 0.3 —					
Imidodiphosphoric	$9.77 \pm 0.12$	$7.05 \pm 0.12$	$2.81 \pm 0.06$	(2) <sup>a</sup>	...
Diimidotriphosphoric	$9.95 \pm .03$	$7.74 \pm .17$	$3.94 \pm .05$	(2) <sup>a</sup>	(0) <sup>a</sup>
— At ionic strength of 1.0 —					
Orthophosphoric	$11.1 \pm 0.09$	$6.61 \pm 0.11$	$2.36 \pm 0.11$	...	...
Pyrophosphoric	$8.74 \pm .07$	$5.98 \pm .07$	$1.75 \pm .04$	(1.7) <sup>a</sup>	...
Triphosphoric	$8.56 \pm .10$	$5.69 \pm .11$	$2.04 \pm .09$	$1.15 \pm 0.15$	(0.5) <sup>a</sup>
$(\text{HO})_2\text{P} \begin{array}{l} \text{O} \\ \text{O} \\ \text{OH} \end{array} \begin{array}{l} \text{O} \\ \text{O} \\ \text{OH} \end{array} \text{P} \begin{array}{l} \text{O} \\ \text{O} \\ \text{OH} \end{array} \text{P}(\text{OH})_2$ with $n = 4$	$8.13 \pm 0.14$	$5.98 \pm 0.18$	$2.19 \pm 0.10$	(2.1) <sup>a</sup>	...
with $n = 58$	$8.17 \pm .04$	$7.22 \pm .04$	?	?	...
Phosphoramidic	$8.28 \pm .1$	$3.3 \pm .1$	...	...	...
Imidodiphosphoric	$10.36 \pm .10$	$7.62 \pm .13$	$3.05 \pm 0.18$	(1.5) <sup>a</sup>	...
Diimidotriphosphoric	$10.00 \pm .10$	$6.86 \pm .10$	$3.36 \pm .10$	(2.0) <sup>a</sup>	(1.0) <sup>a</sup>

<sup>a</sup> Rough estimate—large errors may exist so that these constants are indeterminate.

Even though the acidity constants for imidodiphosphoric and diimidotriphosphoric acid were evaluated at several ionic strengths, no extrapolation to infinite dilution was attempted, since complications due to solvolysis have been reported to take place.<sup>9</sup> However, comparison between various species can be made at a unit ionic strength.

The present work shows that substitution of an -NH- group to link the phosphorus atoms rather than an oxygen has caused the imidodiphosphoric and diimidotriphosphoric to become weaker acids

than pyrophosphoric and triphosphoric acids, respectively. Schwarzenbach and Zurc,<sup>10</sup> making measurements in the presence of sodium ions, reported data showing methylene diphosphonic acid to be a weaker acid than pyrophosphoric. On the other hand, Crutchfield and Edwards<sup>11</sup> have found peroxydiphosphoric acid to be a stronger acid than pyrophosphoric acid. All of the above

(10) G. Schwarzenbach and J. Zurc, *Monatsh.*, **81**, 202 (1950).

(11) M. M. Crutchfield and J. O. Edwards, *J. Am. Chem. Soc.*, **82**, 3533 (1960).

listed findings can be qualitatively explained on the basis of electronegativities.

Since the electronegativity increases in going from  $-CH_2-$  to  $-NH-$  to  $-O-$  to  $-O-O-$ , one would expect that the presence of these groups between end phosphorus atoms would facilitate removal of hydrogen ions in the order shown. And this is precisely what has been found. However, approximate data<sup>12</sup> indicate hypophosphoric acid to be a stronger acid than imidodiphosphoric acid, but weaker than pyrophosphoric acid. According to the qualitative explanation given here, this leads to assuming that the absence of a linking group between phosphorus atoms is equivalent to placing a group having an electronegativity between 3.0 and 3.5.<sup>13</sup>

For the linear phosphoric acids, the results in

(12) W. D. Treadwell and G. Schwarzenbach, *Helv. Chim. Acta*, **11**, 405 (1928).

(13) E. J. Little and M. M. Jones, *J. Chem. Educ.*, **37**, 231 (1960).

Table II show that the end hydrogen becomes more acidic, and the difference between the last two acidity constants decreases as the chain length increases. Van Wazer and Holst<sup>14</sup> attributed the difference between the last two ionization constants of pyrophosphoric acid to a combination of resonance coupling between adjacent  $PO_4$  groups and to the electrostatic effect of successive ionizations. They also predicted that the last two acidity constants of polyphosphoric acids should both approach a value of  $10^{-8}$  as the polyphosphate chain is lengthened. Our data, particularly those obtained on the phosphate with a chain length of 60 confirms their prediction.

**Acknowledgments.**—The authors thank Mr. A. W. Dickinson for programming the data on the IBM 704 computer and Mr. W. W. Morgenthaler for making some of the measurements.

(14) J. R. Van Wazer and K. A. Holst, *J. Am. Chem. Soc.*, **72**, 639 (1950).

## FREE ENERGY OF ADSORPTION. II. THE INFLUENCE OF SUBSTRATE STRUCTURE IN THE SYSTEMS $Al_2O_3$ AND $TiO_2$ WITH *n*-HEXANE, $CH_3OH$ AND $H_2O$

By R. L. EVERY, W. H. WADE AND NORMAN HACKERMAN

*Department of Chemistry, The University of Texas, Austin, Texas*

*Received October 17, 1960*

The free energies of adsorption for these systems were calculated from adsorption isotherms at 25° using the Gibbs adsorption equation and were found to vary significantly as a function of specific surface area. The integral entropies of water adsorption on alumina and titania were found to decrease monotonically with decrease in particle size for each adsorbent.

### Introduction

It is hardly conceivable that the lattice structure of a solid can terminate so abruptly as to leave unsatisfied chemical forces at the surface. Moreover, it is unlikely that for metal oxide surfaces the less polarizable metal ions are present in the surface in any quantity. Instead, the major portion of the surface is composed of relatively polarizable oxide ions with hydrogen or some other attached chemical species to satisfy chemical valences. This is a rather elementary picture of the surface of an oxide; a region differing in properties and structure from that of the bulk, predominantly covered with hydroxyl groups (when exposed to usual atmospheres) interspersed with oxygen ions bridged to the metal ions, and arranged in such a manner so as to represent the lowest surface free energy.

The present work is an extension of that reported earlier<sup>1</sup> on the influence of  $SiO_2$  particle size on the adsorption behavior of water, *n*-hexane and methanol. In that study maxima in free energies of adsorption of all three adsorbates were found in the middle range of particle sizes studied. For water adsorption, both the integral enthalpy and entropy of adsorption decreased with decreasing particle size. To determine whether or not this is

specific to  $SiO_2$  substrates, it was decided to use  $Al_2O_3$  and  $TiO_2$  samples of varying specific area as adsorbents with the three adsorbates previously used.

### Experimental

**Material.**—The five  $Al_2O_3$  and three  $TiO_2$  sample used are listed in Table I along with the manufacturer's analysis as to purity and crystal structure. The samples were vacuum outgassed, usually at 160° and  $10^{-5}$  mm., for at least 24 hours. This temperature was selected as the best compromise in obtaining maximum removal of physically adsorbed water with minimum loss of surface hydroxyl groups.

The water used was double distilled. After being put in the vacuum system, it was repeatedly frozen with Dry Ice and degassed under a vacuum of about  $10^{-6}$  mm. until free of dissolved gases. The *n*-hexane was obtained from Phillips Petroleum Company and analyzed by them to be 99.98% pure. The methanol was obtained from Baker Chemical Company and analyzed by them to be 99.94% pure. The *n*-hexane and methanol were each refluxed under vacuum with  $CaH_2$  for a period of two hours to reduce the water content to a minimum, and then distilled into receiver bulbs with standard break-off seals. These bulbs were sealed, removed from the condenser while under vacuum, and attached to the adsorption apparatus. They were repeatedly frozen with liquid nitrogen and degassed under a vacuum of about  $5 \times 10^{-6}$  mm. until free of residual dissolved gases.

**Apparatus.**—The volumetric adsorption apparatus for water has been described previously.<sup>2</sup> The same general design was used in the construction of two other volumetric

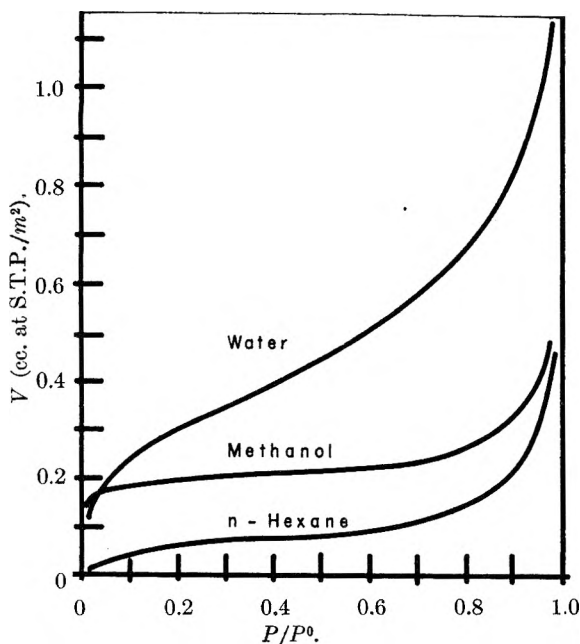
(1) R. L. Every, W. H. Wade and N. Hackerman, *J. Phys. Chem.*, **65**, 25 (1961).

(2) N. Hackerman and A. C. Hall, *ibid.*, **62**, 1212 (1958).

TABLE I

Sample	Surface area, m. <sup>2</sup> /g.	Designation of manufacturer	Crystalline modification	Composition %				Ign. loss	Others
				Al <sub>2</sub> O <sub>3</sub>	TiO <sub>2</sub>	SiO <sub>2</sub>	Fe <sub>2</sub> O <sub>3</sub>		
A <sup>a</sup>	0.222	T-60	α-Al <sub>2</sub> O <sub>3</sub>	99.8		0.04	0.06		0.12 Na <sub>2</sub> O
B <sup>b</sup>	2.72	Alucer MC	α-Al <sub>2</sub> O <sub>3</sub>	99.97	0.001	.01	.003		0.01 Na <sub>2</sub> O Trace CaO
C <sup>c</sup>	65.2	Alon C	γ-Al <sub>2</sub> O <sub>3</sub>	99.9					
D <sup>b</sup>	109	Alucer MA	γ-Al <sub>2</sub> O <sub>3</sub>	99.96	0.001	.009	.004		0.01 Na <sub>2</sub> O Trace CaO
E <sup>a</sup>	221	F-20	Amorph.	92.0		.09	.12	6.8	0.80 Na <sub>2</sub> O
F <sup>d</sup>	7.65	MP-1363-4	Anatase	0.51	98.5	.05	.006		
G <sup>d</sup>	10.5	MP-1363-2	Anatase	0.007	99.6	.20	.005		
H <sup>d</sup>	188	MP-1363-1	Rutile	0.001	89.6	.20	.01	10.3	0.03 Chloride

<sup>a</sup> Supplied by the Aluminum Company of America. <sup>b</sup> Supplied by the Gulton Industries, Inc. <sup>c</sup> Supplied by the Mr. Gregor Berstein of Godfrey L. Cabot, Inc. <sup>d</sup> Supplied by the National Lead Company.

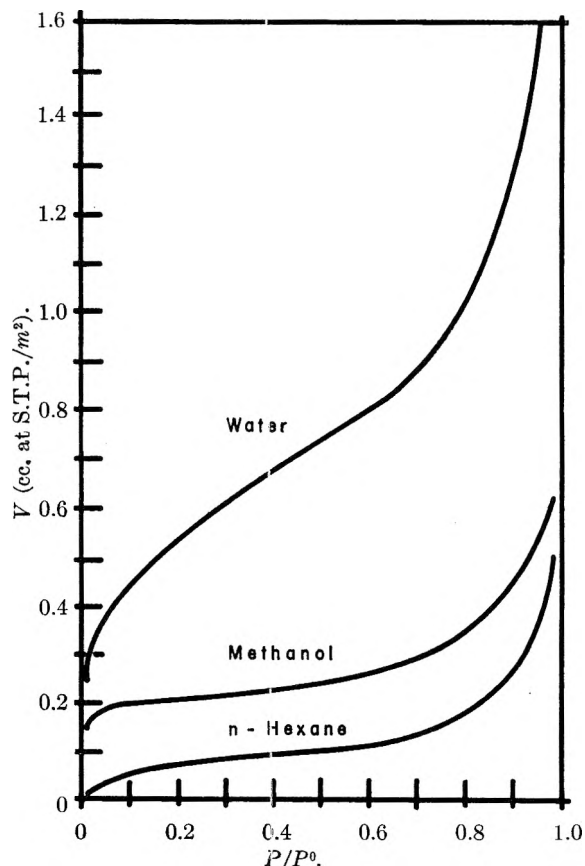
Fig. 1.—Typical adsorption isotherms for Al<sub>2</sub>O<sub>3</sub>.

adsorption systems for hydrocarbon studies. These were equipped with mercury cutoffs to prevent losses to stopcock lubricants. The sample bulb temperatures were controlled by water-baths to  $\pm 0.01^\circ$ . Room temperature was maintained approximately  $2^\circ$  above sample temperature to avoid unwanted condensation. Pressures were read on large bore Hg manometers with traveling telescopes of 0.01 mm. readability.

**Calculations.**—The free energies of adsorption for the systems indicated were determined from application of the Gibbs equation<sup>3</sup> to adsorption isotherms measured at  $25^\circ$ . The application of this equation to adsorption studies has been discussed by several workers.<sup>1-7</sup> The equation in its original form is given as

$$\pi = RT \int_{P=0}^{P=P^0} \Gamma d \ln P$$

Here  $\pi$  is regarded as the free energy of adsorption per unit surface area. Assuming ideality in the gas phase,  $\Gamma$  is equal to the volume,  $V$ , of gas adsorbed per cm.<sup>2</sup> at S.T.P.  $\pi$  was evaluated graphically from plots of  $V/P$  vs.  $P/P^0$  to provide the numerical solution to the integral. As found previously<sup>1</sup> the isotherms were difficult to reproduce near saturation vapor pressure so that the isotherms and derived

Fig. 2.—Typical adsorption isotherms for TiO<sub>2</sub>.

quantities carry some uncertainty ( $\pm 5\%$  for  $\pi$ -values) in the extrapolation to  $P^0$ .

The isotherms were satisfactory up to about  $0.9P^0$ , and these values of the integral from zero pressure to 90% saturation are also listed in Table III. Some samples exhibited hysteresis loops, and for these the ascending branches were used in the integration. Net integral heats of adsorption  $\Delta H_a$  for the water-Al<sub>2</sub>O<sub>3</sub> and water-TiO<sub>2</sub>, as listed in Table III, were calculated from as yet unpublished immersional heats data.<sup>8</sup> The difference between the heat of immersion and the net integral heat of adsorption with liquid water as the reference state is just the surface enthalpy of water, 118.5 erg/cm.<sup>2</sup>.<sup>9</sup> From the experimentally determined quantities  $\pi$  and  $\Delta H_a$ , the integral entropies of adsorption (Table III) were calculated for these systems using the two dimensional thermodynamic analog

$$\pi = \Delta H_a - T \Delta S_a$$

It should be noted that for a more exact treatment, the

(3) J. W. Gibbs, "Collected Works," Longmans, Green and Co., New York, N. Y., 1928, p. 314.

(4) D. H. Bangham, *Trans. Faraday Soc.*, **33**, 805 (1937).

(5) D. H. Bangham and R. I. Razouk, *ibid.*, **33**, 1462 (1937).

(6) H. H. Rowley and W. B. Innes, *J. Phys. Chem.*, **46**, 537 (1942).

(7) G. E. Boyd and H. K. Livingston, *J. Am. Chem. Soc.*, **64**, 2383 (1942).

(8) W. H. Wade, R. L. Every and N. Hackerman, to be published.

(9) G. Jura and W. D. Harkins, *J. Am. Chem. Soc.*, **66**, 1362 (1944).

TABLE IIa

Water									
$P/P^0$	Sample A <sup>a</sup> OG—160° V/P <sup>c</sup>	Sample B OG—160° V/P	Sample B OG—450° V/P	Sample C OG—160° V/P	Sample D OG—160° V/P	Sample E OG—160° V/P	Sample F OG—160° ←260° V/P	Sample G OG—160° V/P	Sample H OG—160° ←260°
0.01	6.398	6.496	24.41	5.157	5.354	2.264	9.961	6.772	5.945
.025	5.079	3.976	17.72	2.778	3.386	1.870	5.787	4.173	4.488
.05	2.673	1.886	5.906	1.555	1.575	1.362	3.256	2.224	1.429
.10	1.401	1.157	1.870	0.949	1.047	0.925	1.791	1.500	0.898
.20	0.858	0.724	1.020	.626	0.701	.598	1.110	0.909	.520
.30	.646	.551	0.744	.469	.551	.461	0.866	.669	.409
.40	.547	.472	.602	.409	.461	.394	.717	.551	.391
.50	.472	.413	.528	.374	.406	.382	.626	.496	.390
.60	.437	.390	.394	.354	.370	.382	.567	.457	.390
.70	.465	.394	.472	.354	.362	.394	.531	.441	.391
.80	.535	.409	.472	.354	.378	.413	.551	.476	.398
.90	.701	.469	.512	.394	.512	.445	.618	.598	.476
.95	.839	.531	.583	.433	.646	.469	.709	.728	.551
.98	.945	.665	.689	.496	.760	.484	.789	.831	.614

<sup>a</sup> See Table III for specific surface areas. <sup>b</sup> Outgassing temperatures. <sup>c</sup> Units—cc. at S.T.P. per m.<sup>2</sup> per cm.

TABLE IIb

Methanol									
$P/P^0$	Sample A <sup>a</sup> OG—160° V/P <sup>c</sup>	Sample B OG—160° V/P	Sample C OG—160° V/P	Sample D OG—160° V/P	Sample D OG—160° V/P	Sample E OG—160° ←300° V/P	Sample F OG—160° OG—260° V/P	Sample G OG—160° V/P	Sample H OG—160° V/P
0.01	0.625	1.050	0.825	1.120	0.605	1.000	1.225	0.910	0.480
.025	.460	0.625	.515	0.700	.395	0.655	0.575	.645	.320
.05	.225	.267	.268	.225	.209	.195	.309	.278	.157
.10	.128	.155	.143	.185	.123	.115	.160	.160	.084
.20	.075	.084	.076	.074	.068	.055	.085	.083	.047
.30	.056	.056	.052	.049	.047	.038	.058	.057	.031
.40	.046	.045	.042	.038	.035	.030	.047	.043	.026
.50	.041	.037	.034	.032	.028	.028	.041	.038	.025
.60	.037	.030	.030	.028	.026	.028	.037	.035	.024
.70	.035	.028	.027	.025	.025	.029	.035	.033	.024
.80	.037	.027	.027	.026	.025	.031	.036	.037	.026
.90	.042	.030	.029	.032	.026	.035	.042	.049	.032
.95	.052	.037	.036	.037	.032	.038	.048	.057	.041
.98	.060	.045	.041	.046	.035	.040	.052	.064	.047

<sup>a</sup> See Table III for specific surface areas. <sup>b</sup> Outgassing temperatures. <sup>c</sup> Units—cc. at S.T.P., per m.<sup>2</sup> per cm.

entropies of adsorption should be normalized to constant surface coverage. The entropies as tabulated here were obtained at constant relative pressure and vary from that at constant coverage by not more than 10%.

The effective area of the substrate occupied by the various adsorbate molecules,  $\omega$  (Table III), was calculated relative to the B.E.T. areas using Kr. Experimental points used in these calculations were taken in the pressure range  $0.05P^0$  to  $0.30P^0$ .

### Results and Discussion

Since all the measured isotherms were of similar structure only typical curves for the three adsorbates on a particular sample of each of the adsorbents were given in Figs. 1 and 2 for alumina and titania, respectively. All isotherms used in the integrations were constructed from between fifteen and fifty experimental values, with the values having an average deviation of less than 2% from the smoothed isotherms. The remaining isotherms may be reconstructed by reference to Table II. In this table, points from the adsorption branch at arbitrarily selected intervals of  $P/P^0$  were chosen from the smoothed  $V/P$  vs.  $P/P^0$  plots.

The relatively non-porous character of the eight adsorbent samples was confirmed by the reversibility of most of the adsorption isotherms at high relative pressure with all three adsorbates. The hexane, methanol and water desorption branches

followed the adsorption branches at all relative pressures, with the exception of water on samples C, E, and F, and the methanol on sample E. Samples C and F showed small hysteresis loops persisting at low relative pressures, which are probably due to irreversible hydration-rehydration phenomena involving surface hydroxyl groups. Sample E, a gel, showed rather prominent hysteresis loops with both water and methanol at higher relative pressures due to irreversible pore filling.

From Fig. 1, one observes that at low relative pressures the volume of methanol adsorbed on  $Al_2O_3$  is greater than that for water which indicates greater bonding for methanol than water at low surface coverage. The methanol isotherm crosses the water isotherm at higher relative pressure. This same type of behavior was reported for similar systems.<sup>10,11</sup>

**Effect of Outgassing Temperatures.**—The effect of increased outgassing temperature on the adsorption isotherm of water on 2.72 m.<sup>2</sup>/g. crystalline  $Al_2O_3$  is the same as that found with water on the crystalline  $SiO_2$  samples<sup>1</sup>; *i.e.*, the volume

(10) B. R. Puri, R. Datt and L. R. Sharma, *J. Indian Chem. Soc.*, 33, 237 (1956).

(11) E. H. Loeser, W. D. Harkins and S. B. Twiss, *J. Phys. Chem.*, 57, 251 (1953).

TABLE IIc

P/P <sup>0</sup>	n-Hexane						
	Sample A <sup>a</sup> OG—160° V/P <sup>c</sup>	Sample B OG—160° V/P	Sample C CG—160° V/P	Sample D OG—160° V/P	Sample F OG—260° V/P	Sample G OG—160° V/P	Sample H OG—160° V/P
0.01	0.0583	0.0600	0.0605	0.0605	0.0912	0.1755	0.1505
.025	.0475	.0535	.0495	.0505	.0759	.1305	.1090
.05	.0326	.0430	.0385	.0427	.0495	.0840	.0583
.10	.0227	.0313	.0285	.0308	.0333	.0488	.0323
.20	.0151	.0217	.0195	.0214	.0228	.0271	.0210
.30	.0123	.0174	.0150	.0168	.0180	.0211	.0166
.40	.0109	.0148	.0125	.0142	.0153	.0177	.0143
.50	.0104	.0135	.0116	.0130	.0139	.0158	.0129
.60	.0102	.0130	.0111	.0125	.0134	.0153	.0124
.70	.0105	.0131	.0113	.0135	.0136	.0158	.0125
.80	.0117	.0139	.0124	.0186	.0151	.0175	.0130
.90	.0140	.0194	.0161	.0495	.0197	.0220	.0151
.95	.0212	.0258	.0234	.0812	.0272	.0231	.0180
.98	.0316	.0334	.0310	.0975	.0350	.0450	.0206

<sup>a</sup> See Table III for specific surface areas. <sup>b</sup> Outgassing temperatures. <sup>c</sup> Units—cc. at S.T.P., per m.<sup>2</sup> per cm.

TABLE III

Sample	Water						Methanol			n-Hexane				
	OG temp., °C.	O-0.9P <sup>0</sup>	O-P <sup>0</sup>	$\pi^a$ $\Delta H_{a^a}$	$\Delta S_a$	$\omega^c$	OG temp., °C.	O-0.9P <sup>0</sup>	O-P <sup>0</sup>	$\omega^c$	OG temp., °C.	O-0.9P <sup>0</sup>	O-P <sup>0</sup>	$\omega^c$
A	160	218	241	623	1.28	11.6	160	102	110	21.7	160	22.3	26.2	88.5
B	160	187	202	575	1.25	12.8	160	116	122	21.3	160	29.0	33.4	61.5
	450	398	413	1017	2.02	10.1								
C	160	159	171	326	0.52	13.4	160	100	105	21.2	160	25.9	29.9	64.7
D	160	187	206	322	.39	12.6	160	120	125	21.9	130	30.6	44.2	60.7
							300	87	91	24.8				
E	160	137	149	236	.29	14.6	160	103	108	29.3				
							300	102	108	29.3				
F	160	280	298	608	1.04	10.2	160 and 260	144	150	19.5	130 and 260	32.1	36.6	63.3
	260	280	298	743	1.40	10.2								
G	160	230	248	469	0.71	10.4	160	117	125	19.8	130	40.4	46.4	53.9
H	160	164	179	231	0.174	16.5	160	62.7	68.7	36.4	130	31.7	34.8	69.7
	260	164	179	287	0.362	15.5								

<sup>a</sup> Units of ergs./cm.<sup>2</sup>. <sup>b</sup> Units of ergs./cm.<sup>2</sup>/°. <sup>c</sup> Units of Å.<sup>2</sup>

of water adsorbed is increased. Similarly, the methanol adsorption behavior at a higher outgassing temperature on the 109 m.<sup>2</sup>/g. Al<sub>2</sub>O<sub>3</sub> parallels the effect of outgassing temperature for the methanol-SiO<sub>2</sub> system,<sup>1</sup> *i.e.*, less methanol is adsorbed. The same explanation given for the effect of outgassing temperature on crystalline SiO<sub>2</sub> is offered here. The hydroxyl groups and the physically adsorbed water which are removed at the higher outgassing temperature are rehydrated during water adsorption, but are, in general, not subject to methylation during methanol adsorption. Since depopulation of surface hydroxyl groups affords less opportunity for hydrogen bonding with hydroxyl groups in methanol, a decrease in volume adsorbed, *i.e.*,  $\pi$ , is to be expected. No change in the free energy of adsorption due to outgassing temperature was noted for any of the three adsorbates on TiO<sub>2</sub>. Either there is little physically adsorbed water on the titania surface following the 160° outgassing pretreatment, or, as suggested by Laporte,<sup>12</sup> the outgassing temperatures, etc., used were too low to eliminate the residual water and to dehydrate the hydroxyl groups which must be present.<sup>12</sup> The former seems more likely from a

consideration of the variation of unpublished immersionsal heats with sample outgassing temperature.<sup>8</sup>

**Particle Size Effect.**—In previous adsorption studies on SiO<sub>2</sub><sup>1</sup> it was noted that the integral free energies of adsorption increased, passed through a maximum, and then decreased with increasing specific surface area of the substrate. When the free energy was separated into the enthalpy and entropy contributions for H<sub>2</sub>O adsorption, it was seen that both decreased uniformly with decreasing adsorbate particle size. This was explained by a direct correlation between surface amorphicity and particle size.

In the present study, even confining attention to the 160° isotherms, there is not the same variation of  $\pi$  with specific area as before for all adsorbates.

For water adsorption on both substrates the enthalpies and entropies unfolded from the  $\pi$ -values both decrease with decreasing particle size as do the  $\pi$ 's themselves. This demonstrates how general this adsorption phenomenon is, at least with respect to water adsorption—the explanation once again being that low specific area samples have a more crystalline surface than do high specific area samples. This would almost seem to be a funda-

(12) F. Laporte, *Publ. sci. et tech. ministere air*, Notes tech. No. 39, 1 (1950).

mental property of a surface since the present samples were not subjected to any distortional forces (*e.g.*, grinding) subsequent to crystallization at elevated temperatures.

With methanol and *n*-hexane as adsorbates, there is no clear variation of  $\pi$  with specific area and in the absence of any adsorption heats for these samples, it is not possible to calculate entropies of adsorption. It would be expected that in proceeding from polar to non-polar adsorbates, physical adsorption phenomena become less sensitive to ionic structure and more dependent solely on the substrate density. On this basis, the integral en-

thalpies and entropies of adsorption would be decreasingly independent of particle size in proceeding from water to methanol to *n*-hexane. The heats of these samples are being measured at present to verify this.

Lastly, it is observed that the molecular areas,  $\omega$ , are found to be more uniform than on SiO<sub>2</sub>. On both Al<sub>2</sub>O<sub>3</sub> and TiO<sub>2</sub> the areas were approximately:  $\omega_{\text{H}_2\text{O}} \cong 11 \text{ \AA}^2$ ,  $\omega_{\text{CH}_3\text{OH}} \cong 21 \text{ \AA}^2$  and  $\omega_{\text{C}_6\text{H}_{14}} \cong 60 \text{ \AA}^2$ .

**Acknowledgment.**—The authors express appreciation to the American Petroleum Institute (Project 47D) for their continued interest and support.

## THE REACTIONS OF ACTIVE NITROGEN WITH POLYOLEFINS

By JOSEPH L. WEININGER

*Research Laboratory, General Electric Company, Schenectady, N. Y.*

*Received October 21, 1960*

The reactions of active nitrogen with linear crystalline polyethylene, polypropylene and polyisobutylene were studied from 39 to 146°. They have the same condensable gas products, hydrogen cyanide and cyanogen, but when methyl groups are present on the polymer chain, ammonia is also formed. Crosslinking of the polymers occurs, except for polyisobutylene and reactions with amorphous polymer are more vigorous than with crystalline ones. Activation energies for these processes are estimated and the course of the reaction is discussed.

### Introduction

The nature of active nitrogen, the mechanism of its afterglow,<sup>1</sup> and its gas phase reactions with organic molecules<sup>2</sup> have been reviewed. The purpose of the present study, of which a part has been briefly summarized,<sup>3</sup> was the investigation of the reactions of active nitrogen at polymer surfaces. Polyethylene and polypropylene are chemically simple polymers, closely related to the hydrocarbons, whose active nitrogen reactions were studied by others. Zinman<sup>4</sup> studied the reaction of active nitrogen with carbon, but most of the previous investigations were concerned with homogeneous gas reactions so that the present study is the first of the interaction of active nitrogen and a polymer.

### Experimental

**Apparatus and Reactants.**—Figure 1 shows the discharge, reaction and electrical systems of the apparatus. The water-cooled discharge tube (DT) was made of wide Pyrex tubing in the form of an open V with aluminum electrodes. The distance between electrodes was 54 cm., and that from the center of discharge to the reaction vessel (RV) was 16 cm. Two 931A photomultiplier tubes (Ph) were located in front of the reaction vessel, the lower tube being opposite to the inlet of an ancillary manifold used for gas reactions, as for example, for titration reactions of nitrogen atoms with nitric oxide.

The electrical circuit was a simple r-c network. The average sparking voltage of the condenser discharge was about 2.5 kv., and the running voltage 1.0 kv. The vacuum system consisted of the conventional components, except that for faster flow rates a pump with very large capacity was used.

The reaction vessel was a tube, 2 inches in diameter and 12 inches long, terminating in a tapered seal. The sample was introduced in a small beaker, perforated on all sides,

and located at the end of a thermocouple well (see Fig. 1). The temperature at that point was taken as the temperature of the sample. The error due to this assumption should not have been more than  $\pm 5^\circ$ .

Linde (H.P. Dry) molecular nitrogen was used. It was free of oxygen but was passed through a liquid nitrogen trap to eliminate traces of moisture. Nitric oxide was distilled several times before use.

Marlex-50 (Phillips Petroleum Co.) was chosen for this study because it has a simple and well-defined structure. It is a high-density (0.96), highly crystalline polymer, unbranched, with each chain terminating in one methyl and one vinyl group. Its viscosity molecular weight of 35,000 was determined by Lawton, Balwit and Powell.<sup>5</sup> Two types of mainly isotactic polypropylene, Profax (Hercules Powder Co.) and Avisun (Avisun Corp.), were used interchangeably because their reactions with active nitrogen were identical. Finally, polyisobutylene (Enjay Co.) was examined in a single experiment. Its lack of crystallinity made it difficult to prepare films suitable for the present investigation.

**Reaction Procedure and Analyses.**—After a vacuum treatment and exposure of the polymer films to molecular nitrogen the reactions proceeded for 30 to 120 minutes until 20 to 80  $\mu$ -l. of gaseous products were obtained for analysis.

Condensable products were identified and analyzed by three techniques: gas chromatography, infrared and mass spectrometry. A Beckman model 7 double-beam infrared spectrophotometer was calibrated for quantitative analyses of HCN at 714 cm.<sup>-1</sup>, and for NH<sub>3</sub> at various wave numbers, including the doublet at 927 and 962 cm.<sup>-1</sup>. This was followed by chromatographic analysis in a Perkin-Elmer Vapor Fractometer (Model 154) equipped with a 4-meter column of di-2-ethylhexyl sebacate [(CH<sub>2</sub>)<sub>6</sub>(COOC<sub>2</sub>H<sub>5</sub>)<sub>2</sub>] as the stationary liquid phase, which had been calibrated for quantitative analyses of cyanogen and hydrogen cyanide. For HCN, gas chromatography was suitable above 40  $\mu$ -l. when tailing of peaks was not a serious problem. With smaller samples of HCN, infrared determination was preferred.

After an initial decrease in the intensity of the nitrogen afterglow, which is a measure of the active nitrogen concentration, the intensity remained constant. It was measured with a photomultiplier tube, which was calibrated by means of the titration reaction of active nitrogen with nitric oxide.<sup>6</sup> This reaction proceeds quantitatively.

(1) K. R. Jennings and J. W. Linnett, *Quart. Rev.*, **12**, 116 (1958).

(2) H. G. V. Evans, G. R. Freeman and C. A. Winkler, *Can. J. Chem.*, **34**, 1271 (1956).

(3) J. L. Weininger, *Nature*, **186**, 546 (1960). In this publication the conversion factor for N<sub>3</sub> → 2N, should read 51%.

(4) W. A. Zinman, *J. Am. Chem. Soc.*, **82**, 1262 (1960).

(5) E. J. Lawton, J. S. Balwit and R. S. Powell, *J. Polymer Sci.*, **32**, 257 (1958).

TABLE I  
PRODUCTION OF ACTIVE NITROGEN AND ITS REACTION WITH POLYOLEFINS

Temp., °C.	Duration, min.	Active N flow rate, μ-l./min.	Molec. conversion N <sub>2</sub> → 2N, %	Condensable products			NH <sub>3</sub> / HCN	Total nitrogen equiv., μ-l.	Conver- sion N → N equiv., %	Gel formation, %	Vinyl decrease, %
				HCN	C <sub>2</sub> N <sub>2</sub> Per cent.	NH <sub>3</sub>					
Polyethylene											
39	120.2	608	37	69.5	31.5	0	0	24.9	0.034	1.0	7.5
51	93.1	344	27	86.2	13.8	0	0	32.1	.10	2.6	8.5
57	59.6	608	37	84.5	15.5	0	0	29.0	.08	..	..
68	74.8	608	37	76.1	23.9	0	0	55.3	.12	1.7	6.5
73	60.0	1245	52	85.5	14.5	0	0	49.4	.066	3.9	..
89	60.0	1205	51	84.2	15.8	0	0	60.0	.083	7.1	24
100	60.0	1075	48	85.8	14.3	0	0	77.3	.11	..	..
107	60.3	1100	49	80.0	16.9	3.1	0.04	85.6	.13	10.7	17
120	60.1	1025	47	81.1	18.9	0	0	68.6	.11	11.7	21.5
141 <sup>a</sup>	40.0	210	21	84.4	14.4	1.1	0.01	110.1	1.32	20.3	48
Polypropylene											
59	30.0	224	26	79.6	0.4	20.0	0.25	71.4	1.0	..	..
86	60.0	316	26	80.4	19.6	0	0	95.9	0.51	2.7	..
97	59.3	169	14	82.7	2.0	15.4	0.19	41.7	0.77	8.2	..
102	20.0	238	19	93.7	6.5	0	0	45.9	1.3	2.2	..
108	60.0	245	20	81.7	14.0	4.4	0.05	49.6	0.45	6.5	..
121	30.0	244	28	67.1	1.8	31.0	0.46	139.0	1.5	2.6	..
146	39.9	293	24	68.8	4.4	26.7	0.39	169.2	1.6	..	..
Polyisobutylene											
100	60.0	257	21	76.2	8.0	15.8	0.21	135.8	1.3	0	..

<sup>a</sup> Above crystal melting point.

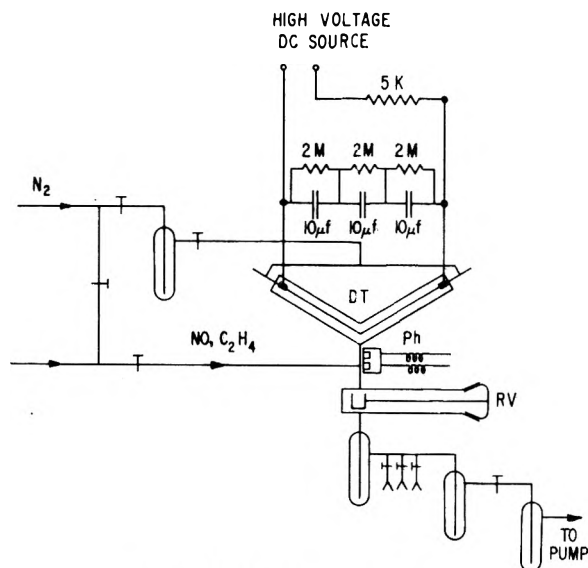


Fig. 1.—Active nitrogen apparatus.

The disappearance of vinyl groups in the linear Marlex polyethylene was observed by monitoring the infrared absorption peaks at 909 and 990  $\text{cm}^{-1}$  of the transparent polymer samples before and after the reactions. Finally, solubility measurements<sup>6</sup> were used to determine the gel in the samples after the reaction with active nitrogen.

### Results

The results of this study are shown in Table I and Fig. 2. The latter shows the extent of the reaction with active nitrogen in terms of the product obtained for a given concentration of nitrogen atoms per unit time. It can also be seen from the

(6) G. B. Kistiakowsky and G. G. Volpi, *J. Chem. Phys.*, **27**, 1141 (1957).

numerical data that polypropylene is more reactive than the linear polyethylene, and that polyethylene is more reactive above than below its crystal melting point. Both crosslink, and polypropylene also produces ammonia. Polyisobutylene does not crosslink, but forms ammonia as one of the main products of the reaction.

In Table I the flow rate of active nitrogen is based on the intensity of the nitrogen afterglow since the intensity is proportional to the square of the atom concentration. The molecular nitrogen was maintained in the reaction system at about 2 mm. pressure, and the conversion of nitrogen atoms to nitrogen-containing species (*i.e.*, nitrogen-equivalent) was calculated from the total pressure in the system, including the partial pressure of nitrogen atoms. The "total nitrogen-equivalent" refers to the sum of nitrogen-containing products. Its concentration is given in one column, its composition in terms of per cent. in others. The ratio of NH<sub>3</sub> to HCN is significant and will be discussed below.

Table II contains the activation energies of the least-square plots of Fig. 2, as well as those for HCN and C<sub>2</sub>N<sub>2</sub> formation, and their probable errors. These errors stem from the experimental difficulties, which involve small changes in the polymer and small concentrations of products. A value of about 1 to 2 kcal./mole for the activation energy of formation of condensable products (for both polyethylene and polypropylene), and for vinyl decrease, is clearly distinguishable from one of about 5 kcal./mole for gel formation.

### Discussion

Polyolefins give the same gaseous reaction products with active nitrogen as their monomers, or

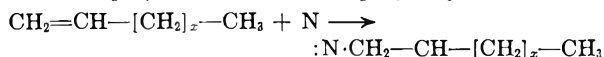


TABLE II  
ACTIVATION ENERGIES (KCAL./MOLE)

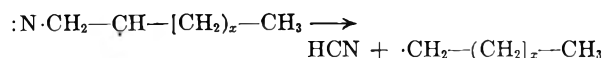
Polyethylene	
HCN formation	1.7 ± 0.7
C <sub>2</sub> N <sub>2</sub> formation	0.9 ± .7
Formation of total N equivalent	1.4 ± .5
Vinyl decrease	1.3 ± .7
Crosslinking (gel formation)	5.0 ± .9
Polypropylene	
Formation of total N equivalent	2.1 ± .9

other simple hydrocarbons, in gas-phase reactions. Even the major constituent, hydrogen cyanide, is present to about the same extent (80%) but there remains a significant difference in the remaining products, cyanogen and ammonia. Nearly 20% of the condensable gas from polyethylene was cyanogen as compared with a maximum of about 2% in previous hydrocarbon reactions; with polypropylene and polyisobutylene a considerable amount of ammonia was formed.

The significant changes in the polymer were the abrupt increase in reactivity of polyethylene at the crystal melting point, the occurrence of crosslinking in both polyethylene and polypropylene, and the simultaneous degradation of the polymer chain as shown by the disappearance of vinyl bonds in polyethylene. These observations establish a parallelism between polymer reactions due to active nitrogen and reactions induced by radiation, which have been investigated thoroughly.<sup>7,8</sup> To explain the reaction between active nitrogen and polymers it is therefore possible to combine the mechanisms which have been established for radiation-induced changes with the unified mechanism of active nitrogen reactions.<sup>2</sup> As the primary process, a number of reaction complexes can be formed, for example, a biradical from polyethylene



Thus, nitrogen-containing molecules or radicals are formed by the attack of the nitrogen atom on the carbon-carbon bond.



Hydrogen atoms liberated in the free radical formation reactions will abstract more hydrogen in the interior of the polymer. This leads to free radical chains with free electrons on secondary C atoms, which in turn, will crosslink and couple. The evidence of crosslinking in depth, as shown by gel tests, together with the larger activation energy of crosslinking, points to diffusion of H (and N) atoms into the polymer. The effect of

(7) F. A. Bovey, "Effects of Ionizing Radiation on Natural and Synthetic High Polymers," Interscience Publ., New York, N. Y., 1958, pp. 53, 90.

(8) A. A. Miller, E. J. Lawton and J. S. Balwit, *J. Phys. Chem.*, **60**, 599 (1956).

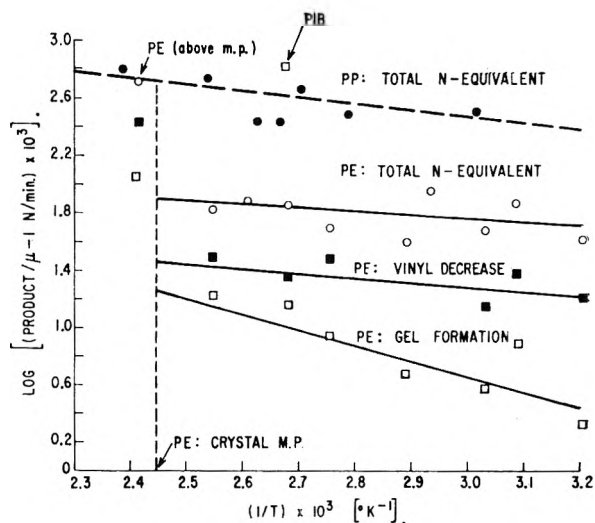


Fig. 2.—Reaction of active nitrogen with polyolefins as a function of temperature: PE = polyethylene; PP = polypropylene; PIB = polyisobutylene. Product given as  $\mu$ -l. for total N-equivalent, and as per cent. changes for gel formation and vinyl decrease.

temperature on diffusion may also be important because the increased mobility of polymer chains, with increased temperature, might affect diffusion.

The formation of ammonia in the reaction with polypropylene and polyisobutylene is of particular interest because of the previous observation of Dewhurst and Cooper<sup>9</sup> of a connection between ammonia formation and methyl substitution in gaseous methylsilanes. This correlation which also appears for the polymers is shown in Table I. Thus, the formation of ammonia in the polymer reaction supports the conclusion of Dewhurst and Cooper that ammonia is formed directly by a molecular process in which the nitrogen atom removes either two or three hydrogen atoms from the methyl group in one step, either through the formation of the amine radical, NH<sub>2</sub>, suggested by them, or by a displacement reaction, similar to that recently reported for high energy atomic hydrogen reactions by Henschman, *et al.*<sup>10</sup>

Further evidence for the formation of ammonia from substituted methyl groups is also being obtained from a study, currently under way, of the reaction of active nitrogen with liquid cyclic dimethylsiloxanes, [(CH<sub>3</sub>)<sub>2</sub>SiO]<sub>4</sub> and [(CH<sub>3</sub>)<sub>2</sub>SiO]<sub>7</sub>. In these liquid-phase reactions the ratio NH<sub>3</sub>/HCN reaches a value of about 0.5 at elevated temperatures.

I am indebted to many colleagues at the General Electric Research Laboratory, particularly Dr. H. A. Dewhurst, for advice and assistance.

(9) H. A. Dewhurst and G. D. Cooper, *J. Am. Chem. Soc.*, **82**, 4220 (1960).

(10) M. Henschman, D. Urech and R. Wolfgang, *Can. J. Chem.*, **38**, 1722 (1960).

# EFFECT OF MODERATORS ON THE $(n, \gamma)$ ACTIVATED REACTION OF $\text{Br}^{80}$ WITH $\text{CH}_4$ <sup>1</sup>

BY EDWARD P. RACK<sup>2</sup> AND ADON A. GORDUS

*Department of Chemistry, The University of Michigan, Ann Arbor, Michigan*

*Received October 21, 1960*

In an excess of gaseous methane,  $13.3 \pm 0.5\%$  of  $\text{Br}^{80}$  produced by the  $\text{Br}^{79}(n, \gamma)\text{Br}^{80}$  process was found to become stabilized as organic activity. Varying amounts of inert gases,  $\text{Br}_2$ ,  $\text{C}_2\text{H}_5\text{Br}$ ,  $\text{CF}_4$  and  $\text{C}_2\text{F}_6$  were added to determine the manner in which these additives moderate the reaction of  $\text{Br}^{80}$  with  $\text{CH}_4$ . These data suggest that the reaction with methane occurs principally, if not completely, as a result of the recoil kinetic energy acquired by the  $\text{Br}^{80}$  in the  $(n, \gamma)$  activation process.

## Introduction

Willard, *et al.*,<sup>3</sup> have shown that  $\text{I}^{128}$  produced by the  $\text{I}^{127}(n, \gamma)\text{I}^{128}$  process is able to displace hydrogen from gaseous methane to form  $\text{CH}_3\text{I}^{128}$ . In a later study, Levey and Willard<sup>4</sup> observed that molecules with ionization potentials lower than that of an iodine atom are more effective than inert gases as moderators for the  $\text{I}^{128} + \text{CH}_4$  reaction. They interpreted these data as indicating that the positive charge<sup>5</sup> associated with at least 50% of the  $\text{I}^{128}$  atoms is an important factor in the reaction with methane.

Tritons produced by  $\text{He}^3(n, p)\text{H}^3$  activation have been found<sup>6,7</sup> to displace hydrogen from gaseous methane. This reaction has been shown to occur as a result of the 192,000 e.v. recoil kinetic energy acquired by the tritons in the  $(n, p)$  activation process.<sup>8</sup>

Bromine-80 formed by the isomeric transition of  $\text{Br}^{80m}$  was found to react with gaseous methane.<sup>9</sup> Due to internal conversion, this activation process results in a highly charged  $\text{Br}^{80}$ . It was suggested<sup>9</sup> that, following the isomeric transition in  $\text{Br}^{80m}$  containing molecules, charge transfer occurred and, due to coulomb repulsion, kinetic energy was acquired by the  $\text{Br}^{80}$ . The data appeared to indicate that the excess kinetic energy of the  $\text{Br}^{80}$  was of greater importance than positive charge.

Bromine-80 produced by the  $\text{Br}^{79}(n, \gamma)\text{Br}^{80}$  process was also found to react with gaseous methane,<sup>9</sup> >95% of the organic activity being due to  $\text{CH}_3\text{Br}^{80}$ . Of the order of 18% of the  $\text{Br}^{80}$  was found in organic combination. For this species, Wexler determined<sup>5</sup> that approximately 18% of the neutron activation processes resulted in a positively charged  $\text{Br}^{80}$ .

(1) Presented in part at the Symposium on the Chemical Effects of Nuclear Transformations at Prague, Oct., 1960, sponsored by the International Atomic Energy Agency. This work was supported in part by a grant from The University of Michigan-Memorial Phoenix Project and by the U. S. Atomic Energy Commission, Division of Research, Contract No. AT(11-1)-912.

(2) Based on work performed in partial fulfillment of the requirements of the Ph.D. degree of E. P. R. Receipt of Procter and Gamble fellowship is gratefully acknowledged.

(3) J. F. Hornig, G. Levey and J. E. Willard, *J. Chem. Phys.*, **20**, 1556 (1952).

(4) G. Levey and J. E. Willard, *ibid.*, **25**, 904 (1956).

(5) S. Wexler and H. Davies, *ibid.*, **20**, 1688 (1952).

(6) (a) A. A. Gordus, M. C. Sauer, Jr., and J. E. Willard, *J. Am. Chem. Soc.*, **79**, 3284 (1957); (b) M. Amr. El Sayed and R. Wolfgang, *ibid.*, **79**, 3286 (1957).

(7) (a) M. Amr. El Sayed, P. J. Estrup and R. Wolfgang, *J. Phys. Chem.*, **62**, 1356 (1958); (b) P. J. Estrup and R. Wolfgang, *J. Am. Chem. Soc.*, **82**, 2661 (1960).

(8) P. J. Estrup and R. Wolfgang, *ibid.*, **82**, 2665 (1960).

(9) A. A. Gordus and J. E. Willard, *ibid.*, **79**, 4609 (1957).

We have investigated the reaction of  $\text{Br}^{80}$ , formed by  $(n, \gamma)$  activation, with gaseous methane in an attempt to determine whether the reaction occurs principally because of the positive charge or because of the  $\gamma$ -recoil kinetic energy acquired by the  $\text{Br}^{80}$ .

If the positive charge is responsible for the reactivity of the  $\text{Br}^{80}$ , then different extents of reaction with  $\text{CH}_4$  would be expected for  $(n, \gamma)$  activated  $\text{Br}^{80m}$  and  $\text{Br}^{82}$  since 12 and 25%, respectively, of these isotopes are positively charged.<sup>5</sup> A single experiment<sup>9</sup> indicated that both  $\text{Br}^{80}$  and  $\text{Br}^{80m}$  react with  $\text{CH}_4$  to produce the same per cent. of organic activity. In gaseous mixtures of  $\text{Br}_2$  and  $\text{C}_2\text{H}_5\text{Br}$ ,  $\text{C}_6\text{H}_6$  or  $n\text{-C}_3\text{H}_7\text{Br}$ , the per cent. organic activity was also found to be the same for the three isotopes.<sup>10</sup> The lack of an isotope effect in these latter experiments could be due, however, to the fact that the ionization potential of the main component of each system is less than that of Br.

## Experimental

Quartz bullets, 4–5 ml. in size, were filled with additive,  $\text{CH}_4$ , and 2 mm. of  $\text{Br}_2$ , so that the total pressure was (generally) about 1 atm.

The samples were irradiated in the University of Michigan megawatt reactor for approximately 2 sec. at a thermal neutron flux of  $1.5 \times 10^{14}$  n/cm.<sup>2</sup>-sec. and an accompanying  $\gamma$ -radiation flux of 8000 r./min. Because of the presence of scavenger  $\text{Br}_2$ , there occurred negligible radiation-induced effects.

The samples were broken in a separatory funnel beneath a two-phase mixture of  $\text{CHCl}_3$  and  $\text{I}_2$  and aqueous  $\text{Na}_2\text{SO}_4$ . The two portions were counted to determine the activity in each phase and, after correcting for  $\text{Br}^{80m}$  content and counting coincidence and density effects, the per cent. of the total activity present in the organic phase was determined.

## Results

The per cent. of the  $\text{Br}^{80}$  present as organic activity for the various systems are listed in Table I.

To interpret correctly the data where the bromine was present as  $\text{C}_2\text{H}_5\text{Br}$ , it is necessary to realize that a small fraction of the  $\text{Br}^{80}$  will not split from the  $\text{C}_2\text{H}_5\text{Br}^{80}$  molecule and thus will be recorded as organic activity. This failure to bond rupture, which amounts to 0.33%,<sup>11</sup> must be subtracted from these data of Table I. In addition, the  $\text{Br}^{80}$  could react with the molecular additives and contribute to the observed organic activity. Thus, it is necessary to correct further these data of Table I for the fractional reactivity with the molecular additives. To do this, we subtracted from the observed values the product of the mole fraction of the additive, multiplied by the extent

(10) J. B. Evans, J. E. Quinlan, M. C. Sauer, Jr., and J. E. Willard, *J. Phys. Chem.*, **62**, 1351 (1958).

(11) A. A. Gordus, unpublished data.

TABLE I

PER CENT. Br<sup>80</sup> STABILIZED IN ORGANIC COMBINATION IN VARIOUS GASEOUS MIXTURES<sup>a</sup>

Additive	Pressure CH <sub>4</sub> , mm.	Mole fraction additive <sup>b, c</sup>	% Br <sup>80</sup> as organic <sup>d</sup>	
He	654	0.040(7)	13.5(2)	13.6(4)
	549	.131(2)	12.6(1)	12.6(2)
	440	.165(5)	12.0(2)	12.0(2)
	127	.703(123)	8.5(4)	9.2(4)
Ne	416	.111(12)	11.2(4)	12.5(3)
	454	.221(17)	10.8(3)	
	239	.476(52)	9.6(2)	
	239	.478(52)	8.6(4)	
Ar	501	.202(26)	12.1(5)	12.2(5)
	238	.427(35)	5.5(6)	6.7(4)
	148	.653(40)	4.8(6)	
Kr	649	.059(1)	11.5(3)	11.5(4)
	589	.141(2)	8.7(4)	8.9(3)
	283	.342(3)	5.3(2)	5.6(2)
	106	.462(7)	3.6(3)	3.6(1)
Xe <sup>e</sup>	663	.029(2)	11.8(3)	14.2(2)
	662	.061(1)	11.3(4)	13.8(4)
	568	.096(1)	9.8(3)	10.0(4)
	335	.156(2)	6.9(3)	8.0(4)
	150	.302(4)	5.1(5)	4.7(5)
CF <sub>4</sub>	557	.139(2)	8.0(2)	8.4(3)
	437	.356(3)	4.7(2)	5.0(3)
	262	.626(5)	2.8(1)	3.4(1)
C <sub>2</sub> F <sub>6</sub>	498	.223(2)	6.3(3)	
	368	.428(3)	5.2(2)	6.6(2)
Br <sub>2</sub>	714	.003(1)	13.1(7)	14.3(6)
	658	.005(1)	13.4(4)	
	656	.034(7)	11.3(3)	13.0(2)
	629	.096(7)	10.4(1)	10.9(2)
	268	.195(15)	6.6(1)	7.2(1)
C <sub>2</sub> H <sub>5</sub> Br <sup>f</sup>	112	.360(29)	3.2(1)	4.4(1)
	699	.015(4)	12.8(4)	13.1(4)
	657	.029(1)	12.4(4)	13.4(3)
	467	.045(2)	11.1(3)	11.6(3)
	323	.067(3)	10.5(2)	12.1(3)
	213	.109(4)	9.0(7)	9.1(2)
	360	.205(2)	7.2(1)	7.5(1)
183	.356(5)	5.8(1)		
179	.454(5)	5.4(1)	5.5(1)	

<sup>a</sup> All samples, except where noted, contained 2 mm. Br<sub>2</sub>. Calculated assuming additive pressures. <sup>b</sup> Uncertainty in last figure or figures (given in parenthesis) is based on estimates of determining individual pressures. <sup>c</sup> Uncertainties (given in parenthesis) based on estimates of uncertainty in positioning 18.0 min. slope through decay data for inorganic and organic fractions for each run. <sup>d</sup> Samples contained 2 mm. C<sub>2</sub>H<sub>5</sub>Br and 0.2 mm. Br<sub>2</sub>. <sup>e</sup> 0.2 mm. Br<sub>2</sub> scavenger present.

of reaction with essentially pure additive to produce organically bound Br<sup>80</sup>. These maximum extents of reaction to produce organic Br<sup>80</sup> are, correcting for any failure to bond rupture: CF<sub>4</sub>—0.7, C<sub>2</sub>F<sub>6</sub>—3.0, and C<sub>2</sub>H<sub>5</sub>Br—2.2%.

These corrected data of Table I are depicted graphically in Figs. 1 and 2. The solid curves are calculated according to the Estrup-Wolfgang (E-W) theory,<sup>8</sup> the method being described below. In order to avoid confusion, the uncertainties have been omitted from these figures.

Extrapolating the data for the systems where

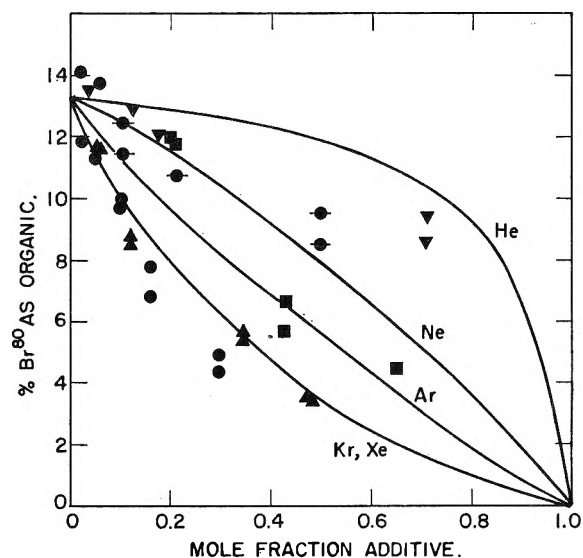


Fig. 1.—Effect of inert-gas moderators on the reaction of gaseous CH<sub>4</sub> with Br<sup>80</sup> activated by the (n, $\gamma$ ) process. Moderators: helium,  $\nabla$ ; neon,  $\circ$ ; argon,  $\blacksquare$ ; krypton,  $\blacktriangle$ ; xenon,  $\bullet$ .

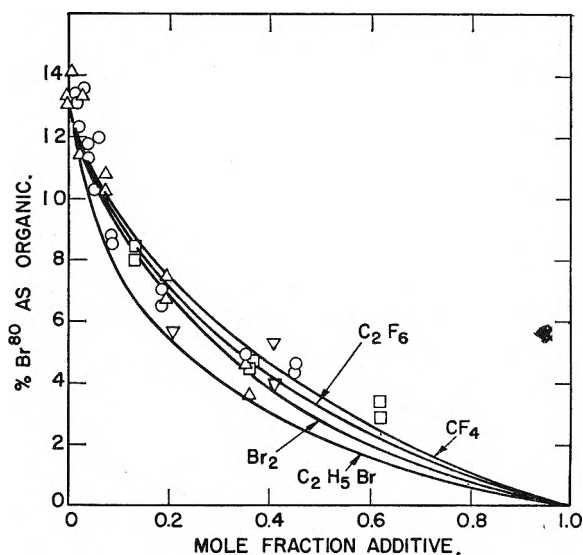


Fig. 2.—Effect of molecular moderators on the reaction of gaseous CH<sub>4</sub> with Br<sup>80</sup> activated by the (n, $\gamma$ ) process. Moderators: CF<sub>4</sub>,  $\square$ ; C<sub>2</sub>F<sub>6</sub>,  $\nabla$ ; Br<sub>2</sub>,  $\triangle$ ; C<sub>2</sub>H<sub>5</sub>Br,  $\circ$ .

the mole fraction of the additive was less than 0.1, it was found that at zero mole fraction additive  $13.3 \pm 0.5\%$  of the Br<sup>80</sup> reacts with CH<sub>4</sub> to become stabilized in organic combination. The only other determination of this quantity was made by Gordus and Willard<sup>9</sup> and indicated 18% Br<sup>80</sup> as organic. The reason for this difference is probably due to the presence of radiation-induced reactions in their experiments. The  $\gamma$ -dose received by their samples was almost 100 times that received by our samples.

### Discussion

It should be possible to interpret qualitatively the effects of the different moderators. There are various ways in which the Br<sup>80</sup> + CH<sub>4</sub> reaction can be moderated, depending upon the nature of the Br<sup>80</sup> and the moderator: (1) removal of the Br<sup>80</sup> kinetic-energy; (2) neutralization of Br<sup>80</sup>

ions; (3) inelastic collisions resulting in the quenching of excited  $\text{Br}^{80}$  ions or atoms; (4) reaction of  $\text{Br}^{80}$  with the additive, the  $\text{Br}^{80}$  becoming stabilized in chemical combination.

Excess kinetic energy may be removed as a result of collisions of  $\text{Br}^{80}$  with other atoms or molecules. Charge transfer between  $\text{Br}^+$  and an additive is highly probable if the ionization potential of the additive is less than that of  $\text{Br}$  (11.84 e.v.). If the ionization potential of the additive is greater than that of  $\text{Br}$ , charge transfer would be of importance only if the relative velocities of the  $\text{Br}^+$  ion and the additive were large.<sup>12</sup>

A maximum  $\text{Br}^{80}$  velocity of  $2.5 \times 10^6$  cm./sec. results from the  $(n, \gamma)$  activation. For a relative velocity of this magnitude, Gurnee and Magee<sup>12</sup> calculate that charge-transfer processes possessing an energy defect greater than about 0.15–0.20 e.v. have only a small probability of occurrence.

Inert gases cannot moderate *via* process 4. In addition, inert gases are found to be inefficient in quenching excited species<sup>13</sup> and, because of their high ionization potentials, are very inefficient in undergoing charge-transfer with  $\text{Br}^+$  ions. Therefore, if moderation of the reaction by the inert gases occurs, it must be due mainly to process 1.

We may next examine the experimental data for the samples containing inert gases. Referring to Fig. 1 and ignoring the solid curves, it is seen that each inert gas is capable of suppressing the extent of formation of organic  $\text{Br}^{80}$ . If the inert gases moderate the reaction principally *via* process 1, then the relative effectiveness of the additives would depend on the size of the inert-gas atoms and on the fractional energy transfer per  $\text{Br}^{80}$ -inert gas collision. Thus, a plot such as Fig. 1 should indicate that the moderating efficiencies increase in the order: He, Ne, Ar, Kr–Xe. As seen, the data of Fig. 1 are in accord with that expected for kinetic energy moderation.

We may also attempt to determine qualitatively whether the formation of organic  $\text{Br}^{80}$  is due totally to processes requiring excess kinetic energy. This may be accomplished by extrapolating the data of Fig. 1 to zero mole fraction  $\text{CH}_4$ . If, for example, the data extrapolated to 6%, such data would suggest that 6% of the organic  $\text{Br}^{80}$  is formed *via* thermal processes and  $13.3 - 6 = 7.3\%$  *via* excess kinetic-energy processes. The data for Ar, Kr and Xe, however, extrapolate to about  $0 \pm 2\%$ , and there is no reason to expect the helium and neon data to extrapolate to a value which differs from that of the other inert-gases. Therefore, it would appear that the organic  $\text{Br}^{80}$  is formed principally *via* reactions requiring excess kinetic energy.

The molecular additives are capable of moderating according to all four processes. However, as with the inert-gases, we may eliminate certain processes from consideration.

Molecular  $\text{Br}_2$  and  $\text{C}_2\text{H}_5\text{Br}$  should be able to moderate efficiently *via* all four processes.

For  $\text{CF}_4$  we would expect charge-transfer to be a very inefficient process since the ionization potential

of  $\text{CF}_4$  (probably about 13 e.v.) is greater than that of  $\text{Br}$ . This compound has been found to be highly inefficient in quenching excited  $\text{I}^{128}$  ions.<sup>14</sup> Therefore, it might also be expected that  $\text{CF}_4$  should be inefficient in quenching excited  $\text{Br}^{80}$  atoms or ions. Reactions of  $\text{Br}^{80}$  atoms or ions with  $\text{CF}_4$  to yield inorganic or organic  $\text{Br}^{80}$  are more endothermic than similar reactions of  $\text{Br}^{80}$  with  $\text{CH}_4$ . Therefore, it is possible that the  $\text{Br}^{80}$  would react preferentially with  $\text{CH}_4$ . This conclusion is substantiated by the fact that the reaction of  $\text{Br}^{80}$  with excess  $\text{CF}_4$  results in only 0.7%  $\text{Br}^{80}$  as organic, whereas 13.3%  $\text{Br}^{80}$  as organic is found in the  $\text{Br}^{80} + \text{CH}_4$  reaction. In addition, the endothermicities for the reaction with  $\text{CF}_4$  to form inorganic and organic  $\text{Br}^{80}$  are of the same order magnitude (80–90 kcal.). As an approximation, it is possible that only about 0.7%  $\text{Br}^{80}$  as inorganic would result in the reaction with  $\text{CF}_4$ . Since processes 2, 3 and 4 are probably of minor importance, we would expect  $\text{CF}_4$  to moderate principally *via* process 1.

Similar arguments may be presented for  $\text{C}_2\text{F}_6$  moderation. On the basis of experiments<sup>14</sup> with  $\text{I}^{128}$ , quenching should be unimportant. Because of the high endothermicities and the low extent of production of organic  $\text{Br}^{80}$  (3%), reaction of  $\text{Br}^{80}$  with  $\text{C}_2\text{F}_6$  to yield inorganic  $\text{Br}^{80}$  may also be of minor importance. The ionization potential of  $\text{C}_2\text{F}_6$  is not available in the literature; however, it is probably of the order of 11.7–12 e.v. Since the ionization potential of  $\text{Br}$  is 11.84 e.v., charge-exchange could be possible. Removal of kinetic energy, process 1, could also occur.

Experimentally, it is observed that the moderation exhibited by all the molecular additives is quite similar to that exhibited by krypton and xenon. It was seen from the inert-gas data that thermal processes are of little importance. The ionization potentials, quenching abilities, etc., and the chemical reactivities toward bromine atoms or ions vary greatly among the molecular additives. Since similar moderation efficiencies result from substances of similar molecular or atomic weights (xenon, krypton and the molecular additives), these data would suggest that, for the molecular additives, processes 2, 3 and 4 are not as important as kinetic-energy transfer. Thus, it would appear that the reaction of  $\text{Br}^{80}$  with  $\text{CH}_4$  proceeds mainly *via* a mechanism involving hot  $\text{Br}^{80}$  atoms.

### Kinetic Theory

Estrup and Wolfgang<sup>8</sup> (E-W) have developed a kinetic theory of hot atom reactions based partially on the mathematics of neutron-cooling processes. It is of interest to determine if our data can be described by this theory.

One of the assumptions made by E-W is that the activated atoms are formed with an initial kinetic energy which is greatly in excess of that required for reaction. Therefore, on the average, the hot atoms undergo a number of collisions and assume a statistically-defined distribution of energies prior to reaction. Thus, to utilize this theory,

(12) E. F. Gurnee and J. L. Magee, *J. Chem. Phys.*, **26**, 1237 (1957).

(13) K. J. Laidler, "The Chemical Kinetics of Excited States," Oxford University Press, Oxford, 1955, p. 103.

(14) E. P. Rack and A. A. Gordus, unpublished data.

it is necessary that the  $\text{Br}^{80}$  atoms (or ions) also form a similar statistical distribution.

In the  $\text{Br}^{79}(n,\gamma)\text{Br}^{80}$  reaction, the neutron binding energy is released frequently as a  $\gamma$ -ray cascade. Data of Muehlhause<sup>15</sup> indicate that an average of 3.4  $\gamma$ -quanta are emitted per neutron capture. That cascade  $\gamma$ -emission occurs is further supported by the failure to bond rupture observations.<sup>11</sup> Because of the resulting partial cancellation of  $\gamma$ -recoil momenta in cascade  $\gamma$ -emission, the  $\text{Br}^{80}$  atoms will be formed with a distribution of energies ranging from some low value to a maximum of about 357 e.v.<sup>16</sup>

Since the complete neutron capture  $\gamma$ -ray cascade spectrum is not known, it is not possible to calculate the distribution of recoil energies of the  $\text{Br}^{80}$ . Such a calculation has been performed, however, for the  $\text{Cl}^{35}(n,\gamma)\text{Cl}^{36}$  activation process,<sup>17</sup> and, although the energy was not distributed statistically, it could serve as a reasonable approximation.

To utilize the E-W kinetic treatment for the  $\text{Br}^{80}$  reaction we must assume that there results an approximate statistical distribution of energies. In addition, two remaining assumptions stated by E-W must apply. They are: (1) that energy loss occurs as a result of elastic-sphere collisions; (2) that the minimum energy required for reaction is large compared with thermal energies.

This last assumption is plausible. The reaction with methane could not occur *via* the usual photochemical mechanism:  $\text{Br}^{80} + \text{CH}_4 \rightarrow \text{CH}_3 + \text{HBr}^{80}$  followed by  $\text{CH}_3 + \text{Br}_2 \rightarrow \text{CH}_3\text{Br} + \text{Br}$ , since the  $\text{Br}^{80}$  content of  $\text{Br}_2$  is extremely small. It would appear that the reaction must be a one-step process:  $\text{Br}^{80} + \text{CH}_4 \rightarrow \text{CH}_3\text{Br}^{80} + \text{H}$ . For ground-state Br atoms, this reaction is endothermic by 1.51 e.v. However, if this energy is to be supplied by the  $\text{Br}^{80}$ , then only a fraction of the kinetic energy of the  $\text{Br}^{80}$  could be available for the internal energy of the activated complex. According to the usual calculations,<sup>18</sup> for reaction to occur, the  $\text{Br}^{80}$  must possess at least  $(1.51)(96/16) = 9.0$  e.v. of recoil energy. If the reaction is a result of ground state bromine ions, then possible processes are:  $\text{Br}^+ + \text{CH}_4 \rightarrow \text{CH}_3\text{Br}^+ + \text{H}$  (0.20 e.v. endothermic) or  $\text{Br}^+ + \text{CH}_4 \rightarrow \text{CH}_3\text{Br} + \text{H}^+$  (2.35 e.v. endothermic). For these reactions to occur, the  $\text{Br}^+$  must possess at least 1.2 and 14.1 e.v. of recoil energy, respectively.

A reaction analogous to that observed in mass-spectrometric studies by Henglein and Muccini<sup>19</sup> [ $\text{I}_2^+ + \text{CH}_4 \rightarrow \text{CH}_4\text{I}^+ + \text{I}$ ] cannot be of importance in the formation of the  $\text{CH}_3\text{Br}^{80}$ . Our data indicate that  $\text{Br}^{80}$  excess kinetic energy is required in all systems, and except where  $\text{Br}_2$  was the "additive," any  $\text{Br}^{80}$  ions would, on the average, be cooled

(15) C. O. Muehlhause, *Phys. Rev.*, **79**, 277 (1950).

(16) If the neutron binding energy (7.3 mev.) is released as a single  $\gamma$  quantum, and if one considers the recoil momentum as being transferred entirely to the  $\text{Br}^{80}$ , then its energy is  $= 537 E^2/M = (537)(7.3)^2/80 = 357$  e.v.

(17) C. Hsiung, H. Hsiung and A. A. Gordus, *J. Chem. Phys.*, **34**, 535 (1961).

(18) J. E. Willard, *Ann. Rev. Phys. Chem.*, **6**, 141 (1955).

(19) A. Henglein and G. A. Muccini, *Z. Naturforsch.*, **15a**, 584 (1960).

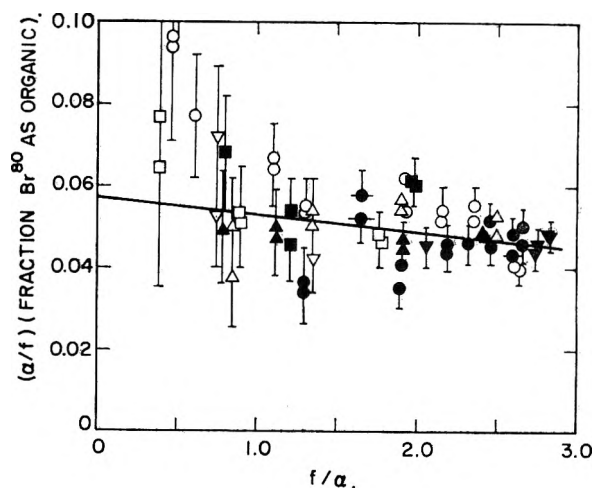


Fig. 3.—Plot corresponding to equation 1 for the  $\text{Br}^{80}$  in organic combination. Moderator symbols are listed in captions for Figs. 1 and 2.

to almost thermal energies before encountering a  $\text{Br}_2$  molecule, and thus forming  $\text{Br}^{80}\text{Br}^+$ .

#### Kinetic Theory Evaluation

The E-W theory involves two variables,  $\alpha$  and  $f$ . The quantity  $\alpha$  is the average logarithmic energy loss per collision and is a function of the mass of hot atoms and the mass of the molecule or atom with which the hot atom collides. The quantity  $f$  is the probability that the collision be with  $\text{CH}_4$ , and is a function of the mole fractions of the components and the cross-sections for the various collisions. To calculate these cross sections we used the diameters<sup>20</sup>: He, 2.2; Ne, 2.6; Ar, 3.6; Kr, 4.3; Xe, 4.9;  $\text{Br}_2$ , 8.4;  $\text{CF}_4$ , 5.5;  $\text{C}_2\text{F}_6$ , 6.8;  $\text{C}_2\text{H}_5\text{Br}$ , 9.0; Br, 4.2;  $\text{CH}_4$ , 4.2 Å.

The derivation of E-W indicate that for a system composed of a single reactant

$$(\alpha/f)(\text{fraction of the activity in a given form}) = I - (f/\alpha)K \quad (1)$$

For the  $\text{Br}^{80} + \text{CH}_4$  system, the methane is the reactant. The systems containing the molecular additives, to be precise, should not follow this equation. However, as stated above, because of the observed low extents of reaction of  $\text{Br}^{80}$  with the additives to produce organic  $\text{Br}^{80}$ , we have assumed that all these additives are non-reactive. The fraction of the activity in a given form can be chosen as the fraction of  $\text{Br}^{80}$  found as organic. Gas chromatographic analysis<sup>9</sup> indicated that the organic  $\text{Br}^{80}$  was mainly  $\text{CH}_3\text{Br}^{80}$ .

According to the above equation, a plot of  $(\alpha/f)$  (fraction  $\text{Br}^{80}$  as organic) vs.  $f/\alpha$  should approximate a straight line, and equally important, all points should fall on the same line, regardless of the moderator used.<sup>8</sup>

Figure 3 is a plot of the experimental data corresponding to this equation. In addition, for essentially pure methane,  $f/\alpha = 2.84$  and  $(\alpha/f)$  (fraction of  $\text{Br}^{80}$  as organic) = 0.0470. The best straight line drawn through the data and ending at

(20) (a) S. Chapman and T. J. Cowling, "The Mathematical Theory of Non-uniform Gases," Cambridge, 1953, p. 229; (b) The diameters for  $\text{Br}_2$ ,  $\text{CF}_4$ ,  $\text{C}_2\text{F}_6$  and  $\text{C}_2\text{H}_5\text{Br}$  were estimated.

the point (2.84, 0.0470) has an intercept  $I = 0.057 \pm 0.005$  and a slope  $-K = -(0.0035 \pm 0.0020)$ . It should be emphasized that the points for all moderators, with the possible exception of  $C_2H_5Br$ , appear to approximate the same line. The upward trend exhibited by the  $C_2H_5Br$  data could be due, in part, to an incorrect choice of the value of the apparent diameter of the compound.

The solid curves of Figs. 1 and 2 were calculated using eq. 1 and the above values of  $K$  and  $I$ . It is seen that the curves for Xe and Kr moderation are identical. This is due to the fact that, whereas the Xe-Br cross-section is larger than that of the Kr-Br, per collision, because of the similarity in atomic weights, krypton is capable of removing, on the average, more energy from  $Br^{80}$  than is xenon. It

should also be noted that this kinetic theory results in curves for the molecular additives (Fig. 2) which are in reasonable agreement with the data. This suggests, as do the data of Fig. 3, that the molecular additives serve mainly to remove  $Br^{80}$  excess kinetic energy. If moderation by the molecular additives were *via* a process other than kinetic-energy removal, it would only be under the most fortuitous circumstances that their moderation data would be described by the kinetic-theory curves.

In summary, the data of Fig. 3 would tend to support the conclusion stated earlier that the reaction of  $Br^{80}$  with methane occurs principally, if not completely, as a result of the  $\gamma$ -recoil kinetic energy acquired by  $Br^{80}$ .

## THE INFLUENCE OF WATER ON THE THERMAL DECOMPOSITION OF $\alpha$ -LEAD AZIDE

BY BRUNO REITZNER

*Explosives Research Section, Picatinny Arsenal, Dover, New Jersey*

*Received October 21, 1960*

The thermal decomposition of  $\alpha$ - $Pb(N_3)_2$  is considerably affected by water vapor. At water vapor pressure below 8.9 mm. ( $t = 240^\circ$ ) the induction period of the autocatalytic reaction  $Pb(N_3)_2 \rightarrow Pb + 3N_2$  increases with increasing water vapor pressure. Above 8.9 mm. the autocatalytic reaction is completely suppressed, and a hydrolysis reaction takes place which yields a basic lead azide and  $HN_3$ . Hydrazoic acid is partially decomposed to give  $N_2$  and  $NH_3$  which reacts with undecomposed  $HN_3$  to give  $NH_4N_3$ . The increase in the induction period and the suppression of the autocatalytic reaction are explained as being due to the poisoning action of the water vapor on the autocatalytic lead nuclei. An explanation for the long induction periods found with alkali and alkaline earth azides is proposed.

### Introduction

The thermal decomposition of  $\alpha$ -lead azide under vacuum was intensively studied during the past 30 years by Garner and his school,<sup>1-4</sup> and more recently by Griffiths and Groocock.<sup>5</sup> The decomposition curves (fractional decomposition,  $\alpha$ , vs. time) obtained by these authors were sigmoid indicating an autocatalytic reaction. The induction times derived from these curves were relatively short compared with the duration of the main reaction. The final solid decomposition product was lead. Recently, Todd<sup>6</sup> described the thermal decomposition of  $\alpha$ -lead azide in air at  $240^\circ$ . He found tetragonal lead oxide as the final solid decomposition product and two intermediates which he identified as basic lead azides. Stammler, Abel and Kaufman<sup>7</sup> studied the decomposition in air by a thermogravimetric method. The decomposition curves were characterized by steps at about 11.8-12.4 and 16.0-16.8% loss in weight. Decomposition beyond the last step was practically negligible at temperatures of  $200^\circ$  and below.

The object of the present work is to find a link

between the different reaction mechanisms under vacuum and in air.

### Experimental Procedures

Thermal decompositions were carried out under nitrogen in the apparatus shown in Fig. 1, in which the volume of nitrogen released during decomposition was measured. The reaction vessels were charged with 50 mg. of pure  $\alpha$ -lead azide (cationic impurities less than 0.1%; particle size approximately  $7\mu$ ), flushed with pure nitrogen while the outlet tubes were immersed in the displacement liquid and sealed. The total volume of the sealed reaction vessels and the outlet tubes was approximately 0.4 cc. The vessels were completely immersed in the metal bath. Thermal equilibrium was reached after 3 minutes. The measured volume of nitrogen was corrected to standard conditions. The water vapor pressure over the lead azide samples was controlled by the displacement liquids ( $H_2SO_4$  and  $H_3PO_4$  of various concentrations, dioctyl phthalate, and dilute NaOH and  $AgNO_3$  solutions). The reaction temperatures were 200, 240 and  $250^\circ$  (deviation  $\pm 0.5^\circ$ ).

### Results

Tests at  $200^\circ$  with 0.01  $N$   $AgNO_3$  solution and concd.  $H_2SO_4$  as displacement liquids showed a fractional decomposition ( $\alpha$ ) of only about 0.003 after 96 hours. In both cases X-ray diffractograms of the decomposition products were still those of  $\alpha$ -lead azide. Silver azide was found in the  $AgNO_3$  solution. Decomposition at  $250^\circ$  with concentrated  $H_2SO_4$  as the displacement liquid yielded a curve similar to those shown in Fig. 2. The induction period was 1 hour 10 minutes, followed by an acceleratory period. The sample exploded after 1 hour 26 minutes, when  $\alpha$  had reached a value

- (1) W. E. Garner and A. S. Gomm, *J. Chem. Soc.*, 2123 (1931).
- (2) W. E. Garner, A. S. Gomm and H. R. Hailles, *ibid.*, 1393 (1933).
- (3) W. E. Garner, "Chemistry of the Solid State," London 1955, Ch. 7 and 9.
- (4) W. E. Garner, *Proc. Roy. Soc. (London)*, **A246**, 203 (1958).
- (5) P. J. F. Griffiths and J. M. Groocock, *J. Chem. Soc.*, **672**, 3380 (1957).
- (6) G. Todd, *Chemistry and Industry*, 1005 (1958).
- (7) M. Stammler, J. E. Abel and J. V. R. Kaufman, *Nature*, **185**, 456 (1960).

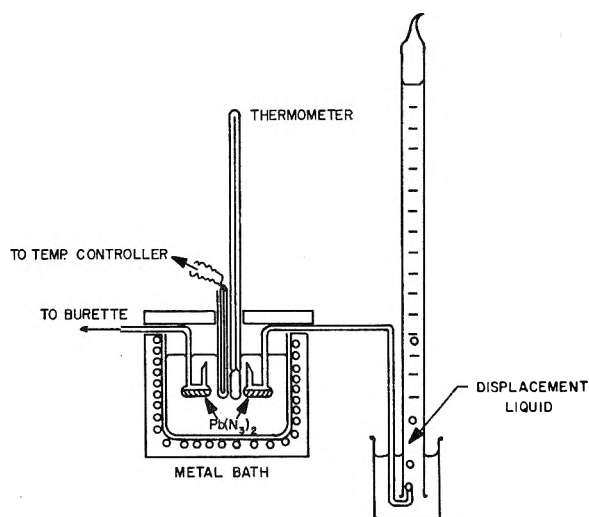


Fig. 1.—Slow decomposition apparatus.

over the displacement liquids, two mechanisms could be observed.

In the case of low water pressures, the decomposition curves (Fig. 2) are similar to those obtained under vacuum, except that the induction times are considerably increased with increasing water vapor pressures. At the beginning of the reaction a small amount of gas is evolved. The hygroscopic displacement liquids are then drawn back into the outlet tubes, and finally the acceleratory reaction starts. The maximum reaction rates  $(d\alpha/dt)_{max}$  in the straight portion of the curves, together with the aqueous tensions  $p_{H_2O}$  (25°), the densities of the displacement liquids and the induction times  $t_i$  (arbitrarily defined as the intersection of the time axis with the tangent to the steepest part of the curves) are shown in the legend of Fig. 2. Curve 6 was obtained using first a dilute phosphoric acid as the displacement liquid and then replacing it after 360 hours by concentrated

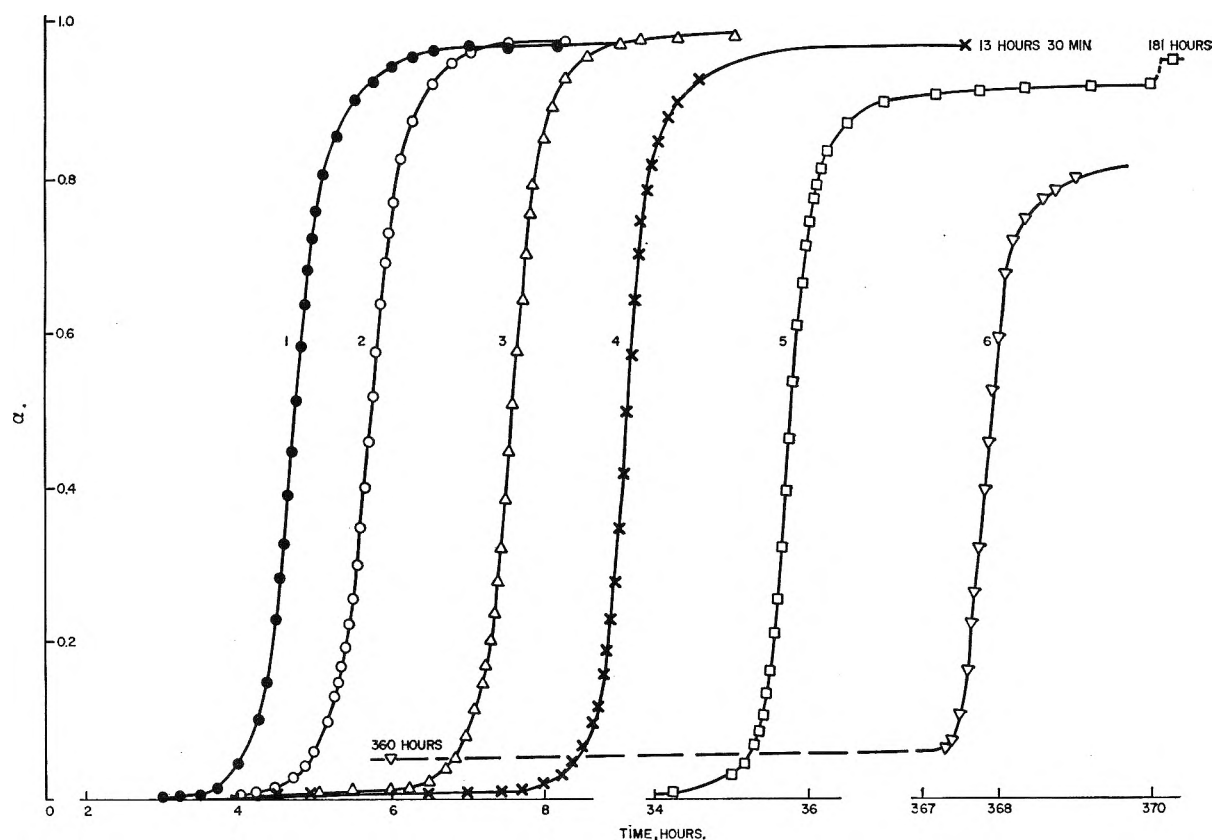


Fig. 2.—Slow decomposition of  $\alpha$ -Pb(N<sub>3</sub>)<sub>2</sub> under relatively low water vapor pressures ( $t = 240^\circ$ ).

Curve N <sub>r</sub>	Displacement liquid	$\rho$ (25°) (g./cm. <sup>3</sup> )	$p_{H_2O}$ (25°) (mm.)	$(d\alpha/dt)_{max} \times 10^2$ (min. <sup>-1</sup> )	$t_i$
1	H <sub>2</sub> SO <sub>4</sub>	1.831	<0.1	2.1 <sub>5</sub>	4 hr. 20 min.
2	H <sub>3</sub> PO <sub>4</sub>	1.695	2.0	2.0	5 hr. 20 min.
3	H <sub>3</sub> PO <sub>4</sub>	1.580	6.0	2.2 <sub>3</sub>	7 hr. 13 min.
4	H <sub>2</sub> SO <sub>4</sub>	1.513	3.7	2.5 <sub>5</sub>	8 hr. 45 min.
5	Diocetyl phthalate	...	...	2.3 <sub>5</sub>	35 hr. 25 min.
6	{ H <sub>3</sub> PO <sub>4</sub> and H <sub>2</sub> SO <sub>4</sub> (after 360 hr.)	1.511 1.831	8.9 <0.1	2.2	367 hr. 30 min.

of 0.34. The reaction rate  $d\alpha/dt$  in the final stage preceding explosion was  $5.6 \times 10^{-2} \text{ min.}^{-1}$ .

All subsequent experiments were carried out at 240°. Depending upon the water vapor pressure

sulfuric acid. For curves 1-4, decomposition to metallic lead is nearly quantitative ( $\alpha = 0.95$ ), within a few hours after the maximum rate has been reached. With curve 5, 145 hours are required to

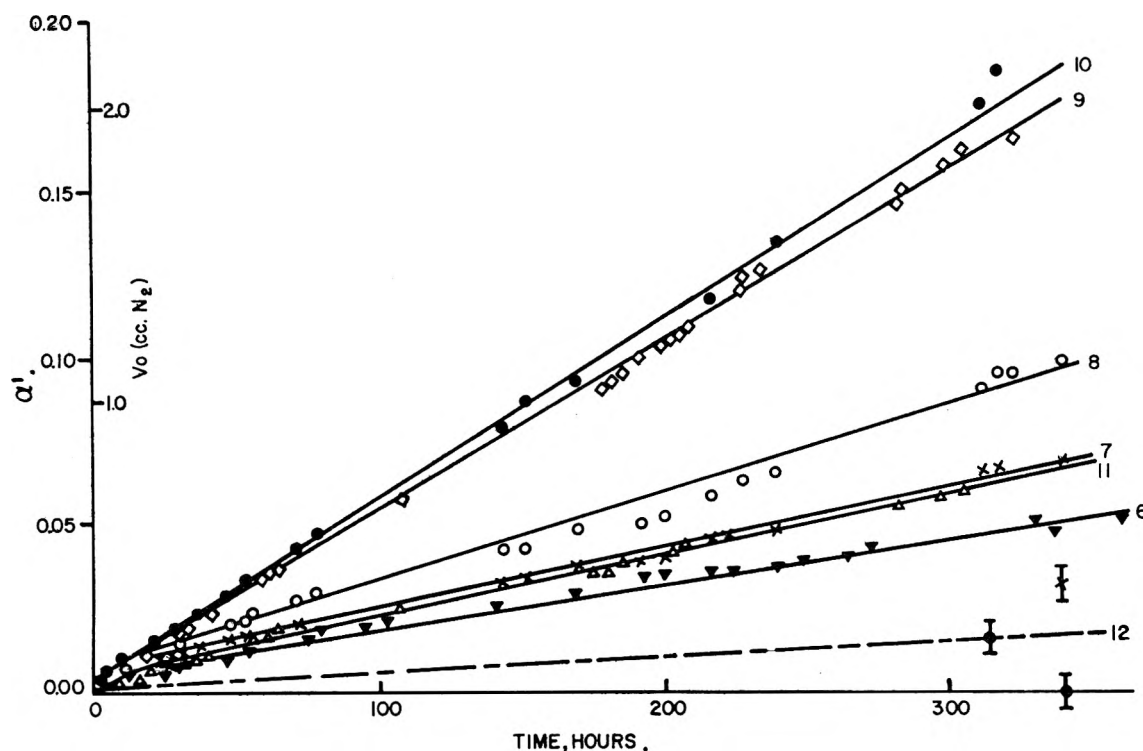


Fig. 3.—Slow decomposition of  $\alpha$ - $\text{Pb}(\text{N}_3)_2$  under relatively high water vapor pressures ( $t = 240^\circ$ )

Curve $N_r$	Displacement liquid	$\rho$ (25°) (g/cm. <sup>3</sup> )	$p_{\text{H}_2\text{O}}$ (25°) (mm.)	$d\alpha'/dt \times 10^6$ (min. <sup>-1</sup> )	$(d\alpha'/dt)_H \times 10^5$ (min. <sup>-1</sup> )	$\text{NH}_4\text{N}_3$ (mg.)
6	$\text{H}_3\text{PO}_4$	1.511	8.9	0.22	0.21	..
7	$\text{H}_3\text{PO}_4$	1.434	12.1	.31	0.34	0.28
8	$\text{H}_3\text{PO}_4$	1.301	18.0	.43	0.52	0.79
9	$\text{H}_2\text{SO}_4$	1.150	19.0	.83	1.12	..
10	$\text{H}_3\text{PO}_4$	1.153	21.7	.89	1.20	1.21
11	$\text{NaOH}$	1.001	23.0	(.31)	..	..

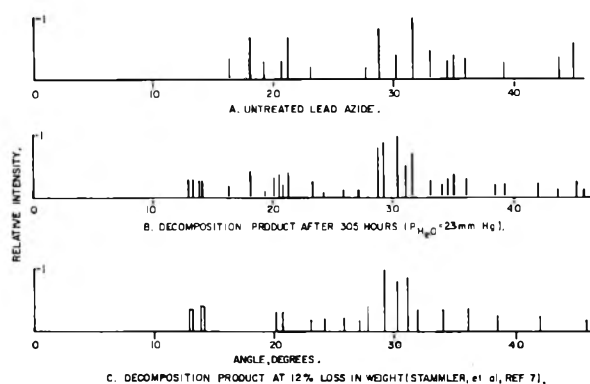


Fig. 4.—Comparison of X-ray diagrams ( $\text{CuK}\alpha$ ).

reach a value of 0.92 from the maximum. With curve 6 the end value is about 0.85. The reason for this is given later in the discussion.

When displacement liquids which have a relatively high water vapor pressure are used the results are different (Fig. 3). No acceleratory stage is observed and the slopes of the curves become fairly constant after about 10 hours, their magnitude depending on the water vapor pressure over the displacement liquids. The anomalous slope of curve 11 is explained in the discussion. In all of these reactions a white sublimate of ammonium azide could be observed in the colder portions of the outlet tubes. The amounts for curves 7, 8 and

10 are given in the legend of Fig. 3. Of all of the displacement liquids, only the  $\text{NaOH}$  solution showed a positive azide reaction.

X-Ray diagrams of the decomposition products (Fig. 4) indicate a mixture of undecomposed lead azide and a substance which has been identified by Stammer, *et al.*,<sup>7</sup> as the decomposition product associated with the first plateau (11.8–12.4% loss in weight). The intensity of the X-ray reflections ascribed to this substance is greatest with the sample decomposed over  $\text{NaOH}$ . Apparently it has the same X-ray structure as the first decomposition product obtained by Todd,<sup>6</sup> although the exact angles of his reflections cannot be reconstructed due to the reduced scale of the reproduction.

### Discussion

Since lead azide is prepared from aqueous solutions it presumably contains a small amount of water either adsorbed or enclosed in the crystals.<sup>8</sup> The desorption of water constitutes the first step in the heating process. Since the volume of the vessel is very small, the water vapor pressure is

(8) The approximate amount of water was determined by heating a sample of lead azide *in vacuo* at  $240^\circ$ . An increase of pressure corresponding to about 1% decomposition was observed during the first 5 minutes. The gas could be almost completely frozen out with liquid nitrogen. A mass spectrogram of the frozen gas showed a mixture of  $\text{H}_2\text{O}$  and  $\text{HN}_3$  the latter being a hydrolysis product formed according to eq. 1 from lead azide and the original  $\text{H}_2\text{O}$ .



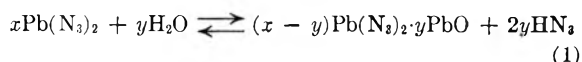
relatively high. The thermally created "germ nuclei" cannot develop into "growth nuclei" which would normally catalyze the decomposition since they react with water vapor. An autocatalytic reaction is possible only when the water vapor pressure is reduced to a small value (less than 8.9 mm. at 240°). This is effected by absorption of the water vapor in the hygroscopic displacement liquids and by a hydrolysis reaction with the lead azide. The fact that the hygroscopic displacement liquids are drawn back into the outlet tubes after the initial evolution of a small amount of gas indicates that the absorption of water vapor at this stage is faster than the evolution of nitrogen. Acids having a low water vapor pressure absorb water much faster than the more dilute acids; consequently shorter induction periods are observed. This observation is, however, not completely general since curve 4 does not lie between curves 2 and 3. Conceivably, other less controllable factors, like the volume of the vessels, the length and diameter of the outlet tubes, the contact area between the gas bubbles leaving the outlet tubes and the displacement liquids, and the viscosity of the displacement liquids influence the diffusion characteristics of the water vapor. The very long induction period observed for dioctyl phthalate (curve 5) can be easily explained by assuming that no water is absorbed; instead water reacts with the lead azide to form a basic lead azide which is apparently less decomposable. Consequently, the decomposition is not as complete as in the case of the curves obtained for hygroscopic liquids. The same is true for sample 6 which was first decomposed under a water vapor pressure of 8.9 mm. (Fig. 3). Only the undecomposed lead azide and not the basic lead azide is further decomposed after the displacement liquid has been replaced by concentrated sulfuric acid.

The reason why previous authors<sup>1-5</sup> found relatively short induction periods under vacuum may be explained as follows: Vacuum systems generally have a volume in the liter range, and water released upon heating would expand throughout the whole volume. The water vapor pressure would be only about 10<sup>-4</sup> times as large as in the present case where vessels of about 0.4 cc. have been used. This water vapor pressure is not sufficient to prevent the "germ nuclei" from growing. This concept of "catalyst poisoning" can also be applied to the slow decomposition of other substances.

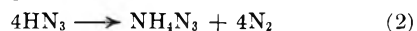
It is interesting to note that long induction periods occur with the azides of metals which are more electronegative than lead. Garner and Reeves<sup>9</sup> observed this phenomenon when decomposing alkaline earth azides under vacuum. The authors assumed that the initial growth of the small nuclei is a very slow process. They are, however, aware of the difficulties involved in their assumption for, as they stated, nucleation commences in the disturbed areas of the lattice where the rate of nuclear growth can be expected to be fast. The present concept of catalyst poisoning avoids this difficulty. Due to the high reactivity of the alka-

line earth metals, the very small aqueous tensions which can be expected in vacuum systems, along with traces of oxygen due to unavoidable leakage, will be sufficient to react with the "germ nuclei" before they can grow. The long induction periods for alkali azides,<sup>10</sup> and lithium aluminum hydride<sup>11</sup> and the absence of the induction period with silver azide<sup>12</sup> may also be used as an argument for the concept of catalyst poisoning.

By increasing the aqueous tensions over the displacement liquids (Fig. 3) the autocatalytic reaction is suppressed, and a hydrolysis reaction predominates, yielding HN<sub>3</sub> and a basic lead azide



Since this reaction is an equilibrium reaction its rate should become zero, if HN<sub>3</sub> is not removed from the equilibrium. The volume increase represented by curves 6-11 is mainly due to the thermal decomposition of hydrazoic acid formed, the products being nitrogen, which causes the increase in volume, and ammonia, which combined with excess hydrazoic acid to form solid ammonium azide. The equation is



This reaction has been studied by Meyer and Schumacher<sup>13</sup> who found that it is heterogeneous and of the first order. Consequently the rate of the reaction depends on the surface area of the vessel and of the solids contained in the vessel, and the concentration of the hydrazoic acid. The initial rapid evolution of nitrogen observed on heating of the PbN<sub>6</sub> crystals is attributed to a relatively high water vapor pressure produced by the desorption of water. When the water vapor pressure over the azide is the same as that over the displacement liquid, water for hydrolysis is supplied by the displacement liquid. The relatively low nitrogen evolution observed for curve 11 (dil. NaOH) which should have been above curve 10 is due to absorption of hydrazoic acid in the NaOH solution, whereon the concentration of the acid in the gas atmosphere is reduced.

Since the amount of ammonium azide is known, the volume of nitrogen produced by the decomposition of HN<sub>3</sub> can be determined. When this is subtracted from the nitrogen found for the over-all decomposition curves of Fig. 3 (slope  $d\alpha'/dt$ ) a small volume of gas remains. The presence of this residual volume may have two causes.

First, it is possible that hydrazoic acid is carried over into the buret with the nitrogen, and adds to its volume. The high vapor pressure of hydrazoic acid (509 mm. at 25°<sup>14</sup>) does not exclude this possibility. The actual pressure of HN<sub>3</sub> in the vessel which, according to eq. 1, is given by the water vapor pressure and the equilibrium constant

(10) W. E. Garner and D. J. B. Marke, *J. Chem. Soc.*, 657 (1956).

(11) W. E. Garner and E. W. Haycock, *Proc. Roy. Soc. (London)*, **A211**, 335 (1952).

(12) B. E. Bartlett, F. C. Tompkins and D. A. Young, *ibid.*, **A246**, 206 (1958).

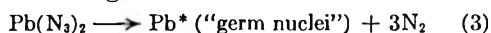
(13) R. Meyer and H. J. Schumacher, *Z. physik. Chem.*, **A170**, 33 (1934).

(14) P. Gunther, R. Meyer and F. Müller-Skjold, *ibid.*, **A175**, 164 (1935).

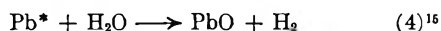
(9) W. E. Garner and L. E. Reeves, *Trans. Faraday Soc.*, **51**, 694 (1953).

is not known. It should, however, be lower than the water vapor pressure, since, due to the greater acidity of hydrazoic acid one should expect an equilibrium constant which is much less than unity. Unfortunately the ammonium azide obtained in the test with sodium hydroxide as the displacement liquid (curve 11) was used for sublimation tests and not weighed. If in this case no difference would have been observed between the amount of nitrogen due to the reaction of eq. 2 and the observed amount, then the residual volume found with the acid displacement liquids would be solely that of  $\text{HN}_3$ .

The second possibility for the presence of a residual gas volume may be seen in both the non-catalytic starting reaction



and the reaction between water and the "germ nuclei"



The combined rate of these reactions is  $0.85 \times 10^{-6} \text{ min.}^{-1}$  (curve 12) which is approximately 1/30,000 that of the maximum reaction rate observed for curves 1-6) (Fig. 2). Since the first possibility cannot be excluded, this value has to be considered as an upper limit. The reaction rates of the hydrolysis reaction can be obtained by subtracting the rate associated with curve 12, from the rates  $d\alpha'/dt$  taken from curves 6-10 (Fig. 3) and by multiplying the difference by a factor of 1.5, since part of the  $\text{HN}_3$ -nitrogen is bound in ammonium azide and does not show up volumetrically. This holds only for the acid displacement liquids in which no hydrazoic acid could be detected. The corresponding values  $(d\alpha/dt)_H$  are listed in the legend of Fig. 3. The values for curve 11 cannot be calculated since part of the  $\text{HN}_3$  was removed from the equilibrium by absorption in the  $\text{NaOH}$  solution.

The reaction rates found by Stammer, *et al.*, are much greater than those of the hydrolysis reaction under consideration. The first intermediate ( $\alpha = 0.5$ , if the structure proposed later is assumed) was reached after 6 hours at a temperature of only

(15) According to the phase rule, only two solid phases are permitted in the system described by the hydrolysis reaction in eq. 1. As long as  $\text{Pb}(\text{N}_3)_2$  is present,  $\text{PbO}$  will be converted into a basic lead azide (first intermediate).

200°. The reaction rate in the initial, practically linear portion of the curve was  $0.16 \times 10^{-2} \text{ min.}^{-1}$ . At 240° in air, Todd obtained the first decomposition step as early as 30 minutes; this corresponds to a reaction rate of  $1.7 \times 10^{-2} \text{ min.}^{-1}$  which comes close to our maximum reaction rate under dry nitrogen.

The question arises as to whether it is the oxygen or the humidity of the air that causes such high reaction rates. In work still in progress tests have been run under dry air and oxygen at 240° using the apparatus shown in Fig. 1 with concentrated sulfuric acid as displacement liquid. These tests yielded reaction rates which, for as long as 100 hours for air and 132 hours for oxygen, were in the very low range of  $10^{-5} \text{ min.}^{-1}$ . After this time the oxygen was consumed, and the reaction followed the pattern of curves 1-5, yielding lead as the final decomposition product. Obviously dry oxygen does not accelerate the reaction. The only way oxygen can react is with the lead nuclei and, since they are formed very slowly, the effect of oxygen is very small.

Thus the fundamental reaction occurring in the experiments of Todd<sup>6</sup> and Stammer, *et al.*,<sup>7</sup> can be considered as a hydrolysis reaction, since both worked in air at ambient humidity. Their humidity conditions correspond to the conditions of the present tests run under relatively high water vapor pressures (Fig. 3). Since, however, their decomposition experiments were carried out under conditions of dynamic air flow, the atmospheric concentration of hydrazoic acid must have been below that encountered under the static conditions of the present experiments. Accordingly, the equilibrium of the hydrolysis reaction was shifted towards basic lead azide which explains the high rate of reaction observed by them.

There is still some doubt as to the formula for the basic lead azide of the first intermediate step. The formula  $\text{Pb}(\text{N}_3)_2 \cdot \text{PbO}$  would correspond to a loss in weight of 11.7% in agreement with the values found by Stammer, *et al.* The analytical values of Todd likewise point towards this direction.

**Acknowledgment.**—The author is indebted to Drs. R. C. Ling, W. R. Hess and M. Stammer and Mr. J. Alster for many helpful discussions.

THE  $\gamma$ -RADIOLYSIS OF SOLUTIONS OF HYDROGEN CHLORIDE IN CYCLOHEXANE

By P. J. HORNER AND A. J. SWALLOW

T.I. Research Laboratories, Hinxton Hall, Cambridge, England

Nuclear Technology Laboratory, Department of Chemical Engineering and Chemical Technology, Imperial College, London S.W. 7, England

Received October 28, 1960

Solutions of hydrogen chloride in cyclohexane, when irradiated with  $\gamma$ -rays, give hydrogen with  $G = 6.05$  compared with  $G = 4.85$  from cyclohexane alone. When iodine is present ( $4 \times 10^{-4} M$ ) the yield for iodine removal is  $G = 7.0$  atoms removed per 100 e.v., compared with  $G = 4.8$  in the absence of hydrogen chloride. Solutions of hydrogen chloride also differ from pure cyclohexane in that they become yellow on irradiation, and give cyclohexyl chloride and a highly unsaturated material of high molecular weight. No cyclohexene is produced. Many of these results can also be obtained with ultraviolet light instead of  $\gamma$ -rays. The facts cannot be explained by any existing theory, and it is concluded that excited molecules must be responsible for the effects.

Very little is known about those stages which are intermediate between the passage of an ionizing particle through matter and the formation of free radicals and molecular products. An attempt to study these stages was made by Williams and Hamill<sup>1</sup> who irradiated solutions of various substances in hydrocarbons. Williams and Hamill found that the minor component, for example methyl iodide, became involved in reaction, and attributed this to the capture of electrons by the solute. However as Williams and Hamill pointed out, many of their results can also be explained in other ways, for example transfer of positive charge may explain some of the results, while transfer of excitation energy from solvent to solute, as in the photochemistry of similar systems,<sup>2</sup> may be occurring in other cases. A simple system of the type studied by Williams and Hamill has now been selected for further study. Cyclohexane was chosen as solvent because its radiation chemistry is relatively simple<sup>3</sup> and because its physical properties are well understood. Hydrogen chloride was chosen as solute because it played a special role in Williams and Hamill's experiments, and because its ionization potential and other properties are known, and stand in a favorable relationship to those of cyclohexane.

## Experimental Methods

The cyclohexane used for most of this work was a grade prepared specially pure for spectroscopy, obtained from British Drug Houses. The purity of this material was examined spectrophotometrically using 10 cm. cells. Benzene and possibly some aliphatic unsaturation were present, but the concentration of benzene was below  $5 \times 10^{-4} M$ . For some experiments (including all irradiations with ultraviolet light) the cyclohexane was purified further by fractional distillation followed by passage through a silica gel column. This procedure removed all but slight traces of impurity, the benzene concentration being reduced by a factor of ten at least. The two grades of cyclohexane were dried by distillation from  $P_2O_5$  *in situ*. They gave identical yields of hydrogen on  $\gamma$ -irradiation, and both gave the same results in the iodine removal experiments. Cyclohexene was the purest available grade, and was purified further by distillation before use. Other chemicals, including iodine, ammonium chloride and sulfuric acid, were of reagent quality. Hydrogen chloride was prepared *in vacuo* by tipping a weighed amount of ammonium chloride into concentrated sulfuric acid. The hydrogen chloride was then distilled into the vessel containing the cyclohexane. Trans-

fer into the vessel was quantitative as shown by titration. The concentration in the solution was estimated from the volumes of the cyclohexane and the vessel, using the solubility data of Wiegner.<sup>4</sup>

All solutions were thoroughly degassed to a pressure of about  $10^{-4}$  mm., and were sealed in all-glass vessels before irradiation. In the case of the solutions for ultraviolet irradiation, degassing was with an oil diffusion pump using silicone oil, to avoid the possible presence of traces of mercury vapor in the system. The vessels used for the  $\gamma$ -irradiations were of three types. The type used for determinations of gas production consisted of a glass tube 14–15 mm. in external diameter, fitted with a break seal at the lower end, and sealed off at the top. The total capacity was about 12.5–13 ml. These vessels were filled with 12 ml. of cyclohexane. A second type of vessel was used for experiments where relatively large amounts of product were needed, as in the determination of cyclohexyl chloride and involatile residues. These vessels were also used for cyclohexene determinations. The vessels consisted of a glass tube approximately 125 ml. in capacity, but without a break seal. One hundred-ml. quantities were irradiated in these vessels. The third type of vessel, used for iodine scavenging experiments, was U-shaped. One limb consisted of a spectrophotometer cuvette, the other of an irradiation tube. During  $\gamma$ -irradiation the cuvette was shielded with lead. The total capacity of the vessel was about 17 ml., the volume of cyclohexane used being 4 ml. Ultraviolet irradiation vessels consisted of a quartz cylinder 2.2 cm. external diameter and 2.2 cm. deep (light path 2.0 cm.), sealed on a tube (for filling) 15 mm. external diameter and 7.3 cm. long. A break seal was also included. Six-ml. quantities of cyclohexane were used in these vessels.

$\gamma$ -Irradiations were conducted with a 500 curie cobalt-60 irradiation unit constructed by Nuclear Engineering Ltd. The Fricke dosimeter (in 0.1 N  $H_2SO_4$ ) was used to measure the dose,  $G$  being taken as 15.5.<sup>5</sup> The dose in the system was obtained by multiplying the dose received in the Fricke dosimeter by the ratio of the electron densities of cyclohexane and water. Dose-rates were 400–4,000 rad. per minute. Ultraviolet irradiations were with a hydrogen discharge lamp made by Thermal Syndicate. The quartz irradiation cylinder was placed flat against the window of the lamp in such a way that the liquid was irradiated directly, without vapor or air between it and the lamp.

Radiolytic gas was measured volumetrically, special care being taken to remove all gas from solution. After measurement of total volume the gas was transferred to a rising temperature gas chromatographic apparatus containing an alumina column with hydrogen as carrier and a cathetometer for detection. Gases other than hydrogen were detectable in this way, the remainder of the radiolytic gas being taken to be hydrogen. Cyclohexyl chloride was identified by comparison with authentic samples using gas phase chromatography with *n*-octane as marker. It was estimated in the same way after a preliminary concentration by distillation of the irradiated solution. Some loss occurred at this stage and was allowed for in the final calculation. Io-

(1) R. R. Williams and W. H. Hamill, *Radiation Res.*, **1**, 158 (1954).  
(2) W. West, *Trans. Faraday Soc.*, **28**, 688 (1932); W. West and W. E. Miller, *J. Chem. Phys.*, **8**, 849 (1940).  
(3) H. A. Dewhurst, *J. Phys. Chem.*, **63**, 813 (1959).

(4) F. Wiegner, *Z. Elektrochem.*, **47**, 163 (1941).  
(5) J. L. Haybittle, R. D. Saunders and A. J. Swallow, *J. Chem. Phys.*, **25**, 1213 (1956).

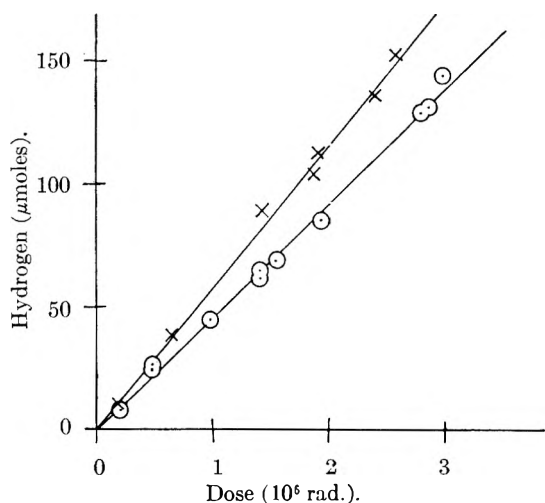


Fig. 1.—Production of hydrogen in  $\gamma$ -irradiated cyclohexane: X, with HCl; O, no HCl.

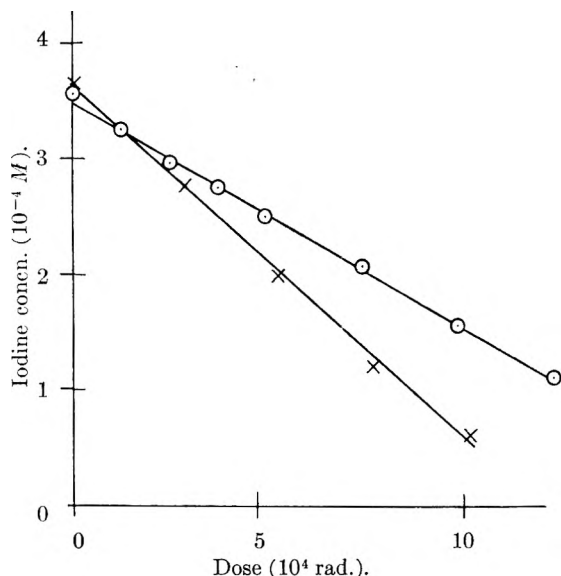


Fig. 2.—Rate of removal of iodine in  $\gamma$ -irradiated cyclohexane: X, with HCl; O, no HCl.

dine concentrations were measured spectrophotometrically using a Unicam SP600 spectrophotometer. The molar extinction coefficient of iodine in cyclohexane at  $520\text{ m}\mu$  was taken to be 940.<sup>8</sup> Ultraviolet absorption curves were measured with a Unicam SP500 spectrophotometer. Infrared measurements were done in the University Chemical Laboratory, Cambridge, by kind permission of Dr. N. Sheppard. Organic microanalyses were performed in the microanalytical laboratory of the Chemistry Department, Imperial College.

### Results

The production of hydrogen in  $\gamma$ -irradiated cyclohexane is shown in Fig. 1 as a function of dose. No gas other than hydrogen is produced, either in the absence or in the presence of hydrogen chloride. For pure cyclohexane the hydrogen yield calculated from Fig. 1 is  $G = 4.85$ . This is significantly lower than  $G = 5.85$  as found by Burton, Chang, Lipsky and Reddy,<sup>7</sup> but does not differ appreciably from  $G = 5.2$ – $5.4$  as found by most other workers.<sup>8</sup>

(6) E. N. Weber, P. F. Forsyth and R. H. Schuler, *Radiation Res.*, **3**, 68 (1955); we have confirmed this figure.

(7) M. Burton, J. Chang, S. Lipsky and M. P. Reddy, *ibid.*, **8**, 203 (1958).

The hydrogen yield for cyclohexane containing  $0.20\text{ M}$  hydrogen chloride is calculated from Fig. 1 to be  $G = 6.05$ .

Dissolved iodine ( $10^{-3}\text{ M}$ ) reduced the hydrogen yield from pure cyclohexane by 10–15% (dose  $\sim 2 \times 10^{19}$  e.v./g.) in agreement with results by other workers.<sup>7,9</sup> Iodine produced a similar decrease from cyclohexane containing  $0.20\text{ M}$  hydrogen chloride. Cyclohexane ( $3 \times 10^{-3}\text{ M}$ ) produced less than 5% change in hydrogen yield, either in the absence or in the presence of hydrogen chloride.

The loss of iodine from a  $4 \times 10^{-4}\text{ M}$  solution of iodine in cyclohexane is shown in Fig. 2 as a function of dose. For pure cyclohexane the yield calculated from the average of three such experiments is  $G = 4.8 \pm 0.5$  atoms removed per 100 e.v., compared with  $G = 5.6 \pm 0.3$  as found by Fessenden and Schuler.<sup>10</sup> These results are in fair agreement within the experimental error of the two determinations. Hydrogen chloride ( $0.016\text{ M}$ ) produces a marked increase in iodine consumption, the yield calculated from curves like those shown in Fig. 2 being  $G = 7.0$  atoms removed per 100 e.v.

It was noted that whereas pure cyclohexane solutions remained almost colorless on irradiation, solutions containing hydrogen chloride became yellow. A typical absorption curve of an irradiated solution of hydrogen chloride in cyclohexane ( $0.20\text{ M}$ ,  $\gamma$ -ray dose  $\sim 3 \times 10^{19}$  e.v./g.) is shown in Fig. 3 together with the curve for a similar solution which had been irradiated with ultraviolet light (30 hours) instead of  $\gamma$ -rays. Neither hydrogen chloride nor cyclohexyl chloride show any absorption in this region at the concentrations present, but it seems probable that the shape of both curves can be partly accounted for by the presence of dienes.

Examination of  $\gamma$ -irradiated solutions of hydrogen chloride in cyclohexane by gas phase chromatography showed cyclohexyl chloride to be the only irradiation product present with a boiling point less than about  $150^\circ$ . However, an unidentified high boiling material was also detected ("Polymer"). Attempts were made to measure cyclohexyl chloride formed at low dose levels by hydrolyzing the irradiated solution with alcoholic potassium hydroxide and precipitating chloride as silver chloride, but these were unsuccessful, and the yield was finally estimated by gas phase chromatography for solutions ( $0.12\text{ M HCl}$ ) given a  $\gamma$ -ray dose of  $\sim 2.5 \times 10^{21}$  e.v./g. The result was  $G$  (cyclohexyl chloride) =  $2.5 \pm 0.5$ . The "polymer" was estimated by evaporating the irradiated solution ( $\sim 2.5 \times 10^{21}$  e.v./g.) to constant weight in an oven at  $120^\circ$ . In the case of pure cyclohexane this technique gave a yield for cyclohexane converted to polymer of  $G = 4.2$  in excellent agreement with independent determinations of the same

(8) R. H. Schuler and A. O. Allen, *J. Am. Chem. Soc.*, **77**, 507 (1955); G. E. Adams, J. H. Baxendale and R. D. Sedgwick, *J. Phys. Chem.*, **63**, 854 (1959); W. S. Guentner, T. J. Hardwick and R. P. Nejak, *J. Chem. Phys.*, **30**, 601 (1959); E. S. Waight and P. Walker, *J. Chem. Soc.*, 2225 (1960); G. R. Freeman, *J. Chem. Phys.*, **33**, 71 (1960).

(9) R. H. Schuler, *J. Phys. Chem.*, **61**, 1472 (1957).

(10) R. W. Fessenden and R. H. Schuler, *J. Am. Chem. Soc.*, **79**, 273 (1957).

quantity,<sup>11</sup> and with  $G = 2.0$  for dicyclohexyl (i.e.,  $G = 4.0$  for cyclohexane converted) in the electron irradiation of cyclohexane.<sup>3,12</sup> In the case of irradiated cyclohexane-hydrogen chloride solutions (0.12  $M$ ) the measured yield for loss of cyclohexane to give polymer was  $G = 2.8$ , but the product (dark in color) was later found to absorb oxygen rapidly from the air, so that the true yield must be somewhat less than this. Elementary analysis of a sample of this polymer evaporated to dryness *in vacuo* showed its empirical formula to be  $C_6H_{7.6}Cl_{0.1}$ .

Irradiated solutions were examined by infrared spectroscopy for the presence of cyclohexene, which absorbs at  $13.95 \mu$ . Irradiated pure cyclohexane absorbed at  $13.95 \mu$  consistent with published results, but irradiated cyclohexane-HCl (0.12  $M$ ,  $\sim 2.5 \times 10^{21}$  e.v./g.) showed little or no absorption at this wave length. From these experiments it is concluded that the yield of cyclohexene in the cyclohexane-HCl system must be less than  $G = 0.4$ , and may be zero.

Measurements were made of the yield of hydrogen from cyclohexane irradiated with ultraviolet light. The results for pure cyclohexane were much less reproducible than for the  $\gamma$ -irradiations, possibly because small traces of impurities play an important part by absorbing light. It was found that the presence of hydrogen chloride (0.04  $M$ ) doubled the yield of hydrogen from cyclohexane. Complete spectroscopic data are available for hydrogen chloride,<sup>13</sup> but although it is known that cyclohexane absorbs little light above  $1700\text{--}1750 \text{ \AA}$ ,<sup>14</sup> the actual extinction coefficients in this region do not appear to be known. Hence it is impossible to be certain whether the increased hydrogen yield is caused by the direct absorption of light by hydrogen chloride, which then splits into atoms which give molecular hydrogen, or is caused by some other effect.

In other experiments with ultraviolet-irradiated solutions it was noted that the solutions containing hydrogen chloride became yellow (Fig. 3), whereas the pure cyclohexane remained almost colorless. Also cyclohexyl chloride was detected by gas phase chromatography in the irradiated solutions containing hydrogen chloride.

### Discussion

Williams and Hamill found that hydrogen chloride (0.23  $M$ ) inhibited the formation of methyl radicals from methyl iodide dissolved in cyclohexane. Our results confirm that hydrogen chloride can exert a powerful effect on a radiolytic reaction, and show that the yield and even the nature of the products from cyclohexane are quite different in the presence of HCl. The main products become cyclohexyl chloride ( $G = 2\text{--}3$ ), unsaturated "polymer" ( $G_{\text{cyclohexane}} = 2\text{--}3$ ), and

(11) J. Lamborn and A. J. Swallow, in preparation.

(12) With  $\gamma$ -rays at low dose rates, as in the present experiments, the polymer would not be pure dicyclohexyl (H. A. Dewhurst and R. H. Schuler, *J. Am. Chem. Soc.*, **81**, 3210 (1959) but the yield should still be close to  $G = 4$  as found here.

(13) J. Romand, *Ann. Phys.*, 12th series, **4**, 529 (1949).

(14) G. Scheibe and H. Grieneisen, *Z. physik. Chem.*, **26**, 52 (1934); L. W. Pickett, M. Muntz and E. M. McPherson, *J. Am. Chem. Soc.*, **73**, 4862 (1951).

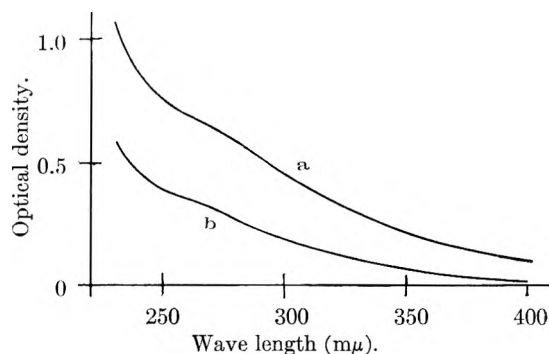
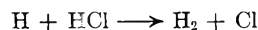


Fig. 3.—Absorption spectra of yellow colors produced by irradiation of cyclohexane-HCl: a, ultraviolet; b,  $\gamma$ -rays.

hydrogen ( $G = 6.05$ ). The rough material balance is reasonably good.

In seeking an explanation of our results it should be noted that several phenomena which are often invoked to explain results in radiation chemistry cannot be occurring in the present system. First direct action. If, in the absence of full information, we assume the importance of direct action to be proportional to the electron fraction of the solute, then in the most concentrated solutions studied here, direct action on hydrogen chloride, even if 100% efficient at causing homolytic fission, could only give products at the rate of 0.43 molecule per 100 e.v. absorbed in the whole system (assuming each atom produces one molecule of product). The actual amount of change due to direct action will be very much less than this. Secondly, the ionization potential of cyclohexane is 11.0 e.v. and of hydrogen chloride 12.8 e.v. so that transfer of positive charge cannot make a significant contribution. Thirdly it does not seem possible to explain the results on the assumption that hydrogen chloride does not affect the primary radiation act on cyclohexane, but does enter into subsequent free radical reactions. In particular, the activation energy for the reaction



is low enough for this reaction to be favored over the corresponding abstraction of hydrogen from cyclohexane, but the chlorine atom so produced would abstract hydrogen from cyclohexane rather than enter into other reactions such as addition to the double bond of cyclohexene or combination with a cyclohexyl radical. Hence the over-all reaction should be unaffected by hydrogen chloride. Fourthly the results of Leprince and Limido<sup>15</sup> show that hydrogen chloride does not react with cyclohexene in the absence of a catalyst such as stannic chloride, so that this reaction cannot be playing a part in the present system.

Magee and Burton have concluded,<sup>16</sup> and Williams and Hamill have implied,<sup>1</sup> that hydrogen chloride can capture electrons in irradiated systems presumably according to



From the hydrogen-chlorine bond strength and the electron affinity of the chlorine atom, this reaction

(15) P. Leprince and J. Limido, *Compt. rend.*, **244**, 2044 (1957).

(16) J. L. Magee and M. Burton, *J. Am. Chem. Soc.*, **73**, 523 (1951).

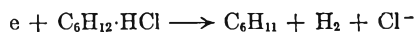
is endothermic to the extent of 0.6 e.v., and so could only occur before electrons have slowed down to thermal energies. From early experiments in the gas phase, the probability of electron capture in this reaction reaches a maximum at 0.5 e.v.<sup>17</sup> but more recent work indicates that the probability is at a maximum at a slightly higher value.<sup>18</sup> The recent data are more extensive, and in better agreement with the thermochemistry of the system. To calculate the yield for electron capture we may accept provisionally the figure of  $5 \times 10^{-4}$  for the maximum probability of capture at a collision.<sup>17</sup> For simplicity of calculation we can further assume that the capture probability is  $3 \times 10^{-4}$  in the range 1.5–0.5 e.v., and zero outside this range. Now if we assume with Magee<sup>19</sup> that an electron loses about 2% of its energy per collision (the exact value depends on the medium, but no value is available for cyclohexane), then the electron collides about fifty times in slowing down from 1.5 to 0.5 e.v. For the highest hydrogen chloride concentration employed in our experiments, about 1%, the number of collisions with HCl would be 0.5. Hence the probability of a given electron being captured by hydrogen chloride is at most  $1.5 \times 10^{-4}$ . Assuming a yield of  $G = 3$  for the production of electrons, the yield for electron capture by HCl is  $G < 4.5 \times 10^{-4}$ , which is negligible. The principal uncertainties in this calculation are the assumption of the values of  $3 \times 10^{-4}$  for the capture probability and of 2% for the percentage energy loss per collision, but these values between them would have to be low by at least a factor of  $10^{-3}$  to affect the argument, and this seems unlikely. The argument so far applies to the gas

(17) N. E. Bradbury, *J. Chem. Phys.*, **2**, 827 (1934); H. S. W. Massey, "Negative Ions," 2nd edition, Cambridge, 1950, p. 76.

(18) R. E. Fox, *J. Chem. Phys.*, **26**, 1281 (1957).

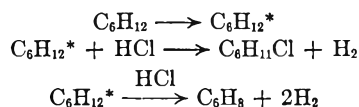
(19) J. L. Magee, *Ann. Rev. Nuclear Sci.*, **3**, 171 (1953).

phase. In the liquid phase it is possible that electron capture by "solvated" hydrogen chloride might be associated with the formation of molecular hydrogen in the reaction



but this reaction is endothermic to the extent of 0.1 e.v., and the above argument still applies. The conclusion that hydrogen chloride does not capture electrons in the present system is reinforced by our results with ultraviolet light of a wave length which could not produce ionization. The effects obtained are very similar to those with  $\gamma$ -rays, showing that the  $\gamma$ -ray result should be explicable without postulating electron capture.

In view of the above process of elimination we are inclined to conclude that the radiolysis products must arise in some way from the reactions of excited molecules. Unfortunately no reactions seem to have been reported in the literature which could provide a precedent for the present case. The simplest reaction scheme would be



but this is highly speculative and further work is required. It may well be that similar reactions of excited molecules are occurring in other systems, for example those studied by Williams and Hamill, but that knowledge of their existence has so far been obscured by other possibilities.

**Acknowledgments.**—The authors wish to thank Mr. W. H. T. Davison and Mr. D. G. Lloyd for their coöperation in this work, and many colleagues for helpful discussions of this puzzling system; also the Chairman of Tube Investments Ltd. for permission to publish this paper.

## THE MECHANISM OF OXIDATION BY HYDROGEN ATOMS IN AQUEOUS SOLUTION. I. MASS TRANSFER AND VELOCITY CONSTANTS

By GIDEON CZAPSKI, JOSHUA JORTNER AND GABRIEL STEIN

*Department of Physical Chemistry, Hebrew University, Jerusalem, Israel*

*Received October 31, 1960*

The conditions of the oxidation of various scavengers in aqueous solution by atomic hydrogen introduced from the gas phase were investigated experimentally and theoretically. Approximate equations are derived for the kinetics in the case of purely diffusion controlled mass transfer of H atoms and for the case of forced convection. First-order reaction with the scavenger in competition with second-order recombination, as well as consecutive scavenging mechanisms are considered. The results are compared with the treatment based on homogeneous kinetics.

In the investigation<sup>1</sup> of the reactions of H atoms with various scavengers atomic hydrogen was produced in the gas phase and introduced into the aqueous solution containing the scavenger. In this heterogeneous system we assumed, in view of the vigorous bubbling and stirring occurring under our experimental conditions, that homogeneous kinetics will provide a good approximation

(1) (a) G. Czapski and G. Stein, *Nature*, **182**, 598 (1958); (b) G. Czapski and G. Stein, *J. Phys. Chem.*, **63**, 850 (1959); (c) G. Czapski, J. Jortner and G. Stein, *ibid.*, **63**, 1769 (1959); (d) G. Czapski and G. Stein, *ibid.*, **64**, 219 (1960).

to the actual situation. In the present paper this assumption is examined and the conditions under which our work is carried out is investigated both experimentally and theoretically.

Mass transfer problems in heterogeneous systems are of great interest in several fields of chemical kinetics. They have been investigated<sup>2–5</sup> mainly

(2) L. L. Bircumshaw and A. C. Riddeford, *Quart. Rev.*, **6**, 157 (1952).

(3) T. K. Sherwood, "Mass Transfer between Phases," Pennsylvania State University, 1959.

(4) P. V. Danckwerts, *Trans. Faraday Soc.*, **46**, 300 (1950).

to establish the rate of transfer of the reacting species under the effect of chemical reaction. Under our experimental conditions there is vigorous bubbling and stirring by the  $H_2$  gas. We assume that under these conditions the actual rate of introduction of atomic H will be independent of changes in scavenger concentration. We also assume that scavenger concentration is constant and scavenger depletion does not occur during the reaction. Thus not the "film theory"<sup>5</sup> which predicts linear increase of the mass transfer coefficient with the scavenger concentration for pseudo first-order reactions, but an approach similar to that of the "penetration theory"<sup>3</sup> will be adopted.

In our case there is competition between the second-order recombination of H atoms and their first-order reaction with the dissolved scavenger. The application of non-homogeneous kinetics to this system will enable us to establish the reaction mechanisms and determine the rate constants in the extreme case of completely non-homogeneous conditions; compare these values with those obtained from treatment assuming homogeneous conditions and to estimate how far under our experimental conditions one or other of these extreme cases is approached.

### Experimental

Under our conditions atomic hydrogen is produced by a high frequency discharge in pure  $H_2$  gas at pressures of  $\sim 30$  mm. and it reaches the reaction vessel, being pumped through it at a velocity of the order of 150 liter  $min^{-1}$ . H atoms are by then present in high dilution in the  $H_2$  gas. The bubbling introduces H atoms by repeated brief exposures of the surface elements of the liquid phase. The exposure period is of the order of 0.1 sec. Vigorous stirring occurs and mass transfer is by diffusion and forced convection. We assume accordingly continuous renewal of the phase boundary.

**Efficiency of Forced Convection.**—To investigate the efficiency of stirring by bubbling stroboscopic photography was used under usual conditions of operation. Photographs were obtained using a Dumont Oscillograph Record Camera Type 321-A at film travel velocities of 3600 and 10800 inches per minute. The light source used was Strobolux Type 618-A, the trigger circuit was Strobotac Type 631-B58, both instruments manufactured by General Radio Co. Flash duration was  $5 \times 10^{-6}$  sec. The time intervals used were  $1/60$  and  $1/180$  sec. From consecutive photographs obtained at known time intervals and from the known dimensions of the reaction vessel we estimate that the velocity of the liquid under stirring is of the order of 100 cm.  $sec^{-1}$ .

**Effect of Changing Bubbler Size.**—The reduction of  $Ag^+$  ions by H atoms is independent of  $Ag^+$  concentration in the region above 0.05  $M$ .<sup>6</sup> In this concentration region it was found that changing the bubbler diameter from 1 to 6 mm. had no effect on the reduction yield. There was no change in the reduction yield when the solution volume was changed by a factor of three. These observations indicate that the dose of H atoms is constant.

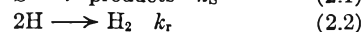
The effect of mass transport was investigated in the oxidation of  $10^{-2} M Fe^{2+}$  solutions in 0.8  $N H_2SO_4$  by H atoms. In this region the oxidation yield is dependent on  $Fe^{2+}$  ion concentration. The inlet tube was exchanged for one ending above the surface of the solution. When the gas was passed above the quiescent solution about 20% of the oxidation yield under bubbling conditions was obtained. Next, arrangements were made for stirring with a magnetic stirrer. When the solution was vigorously stirred and the gas passed above it the yield was about 50% of that obtained under bubbling conditions. These results show the importance of mass transfer processes in these systems.

However when the gas was bubbled through the solution, additional vigorous stirring with a magnetic stirrer had no effect on the yield. This indicates that the assumption of constant scavenger concentration is justified.

**The Steady-state Treatment.**—The mathematical treatment of the problem is based on the assumption that the concentration change at a certain point is due to transport processes and chemical reaction occurring simultaneously

$$\partial c/\partial t = (\partial c/\partial t)_{transport} + (\partial c/\partial t)_{reaction} \quad (1)$$

We consider now the kinetic scheme



where  $k_S$  denotes the velocity constant of the reaction of H atoms with the scavenger, S, and  $k_r$  that of the recombination reaction. Thus

$$-(\partial[H]/\partial t)_{reaction} = k_S[S][H] + k_r[H]^2 \quad (3)$$

the rate constants being in units of  $mole^{-1} cm.^3$ .

Throughout this treatment steady state is assumed. The justification of this assumption in some simple cases will be given. Setting

$$\partial[H]/\partial t = 0 \quad (4)$$

we get

$$(\partial[H]/\partial t)_{transport} = k_S[S][H] + k_r[H]^2 \quad (5)$$

The solution of equation 5 has to be subjected to the boundary conditions

$$X \longrightarrow \infty \quad [H] = 0 \quad \text{and} \quad d[H]/dX = 0 \quad (6)$$

where  $X$  represents the distance from the boundary, and subject to the law of mass conservation

$$\int (\partial[H]/\partial t)_{transport} dV = A \quad (7)$$

where  $V$  is the total volume of the system and  $A$  is the rate of introduction of atomic hydrogen expressed in moles  $sec^{-1}$ . A one-dimensional model for transport processes will be employed. Thus we set

$$dV = \varphi dX \quad (8)$$

where  $\varphi$  is the mean surface area for the mass transfer process.

**The Diffusion Model.**—First we shall assume that during the brief exposure of the surface mass transfer occurs by diffusion only

$$(\partial[H]/\partial t)_{transport} = D(\partial^2[H]/\partial X^2) \quad (9)$$

where  $D$  is the diffusion coefficient of H atoms, for which we assume a value of  $4 \times 10^{-6} cm.^2 sec^{-1}$ . Two simple cases will be considered. For a first-order reaction, as in 2.1, from equations 5 and 9.

$$\partial^2[H]/\partial X^2 = \beta[H] \quad (10)$$

where  $\beta = k_S[S]/D$ , leading to the solution

$$[H] = [H]_0 e^{-\beta^{1/2} X} \quad (11)$$

where  $[H]_0$  is the concentration of H atoms at the surface,  $X = 0$ , obtained by applying condition 7.

$$[H]_0 = A/\sqrt{k_S[S]D}\varphi \quad (12)$$

For a second-order reaction as in equation 2.2

$$\partial^2[H]/\partial X^2 = \alpha[H]^2 \quad (13)$$

where  $\alpha = k_r/D$ . The solution is

$$[H] = 1/[(1/[H]_0) + \sqrt{(\alpha/6) X}]^2 \quad (14)$$

where

(5) A. Wheeler, *Advances in Catalysis*, **3**, 249 (1951).

(6) G. Czapski and G. Stein, to be published.

$$[H]_0 = (1/\varphi^{2/3})(3A^2/2k_r D)^{1/3} \quad (15)$$

We attempt now to consider the general case where competition between second-order recombination and first-order scavenging reaction occurs. We obtain the equation

$$\partial^2[H]/\partial X^2 = \alpha[H]^2 + \beta[H] \quad (16)$$

the proper solution of which is

$$[H] = (6\beta/\alpha)\{(ae^{-\sqrt{\beta}X})/(1 - ae^{-\sqrt{\beta}X})\} \quad (17)$$

where

$$a = \left\{ \left( \frac{2}{3} \alpha[H]_0 + \beta \right)^{1/2} - \beta^{1/2} \right\} / \left\{ \left( \frac{2}{3} \alpha[H]_0 + \beta \right)^{1/2} + \beta^{1/2} \right\} \quad (18)$$

$[H]_0$  is again determined by applying equation 7 in the form

$$A = \int (k_r[H]^2 + k_s[S][H]) dV \quad (19)$$

Applying the expressions

$$\begin{aligned} \int [H] dX &= (6\beta^{1/2}/\alpha) \{a/(1-a)\} \\ \int [H]^2 dX &= (6\beta^{3/2}/\alpha^2)(3a^2 - a^3)/(1-a)^3 \end{aligned} \quad (20)$$

equation 19 is now obtained in the form

$$2\Delta^3 + 3\Delta^2 + \Delta = W \quad (21)$$

where

$$\Delta = a/(1-a) \quad (22)$$

$$W = (k_r A) / \{6(k_s[S])^{2/3} D^{1/2} \varphi\} \quad (23)$$

The yield,  $Y$ , of the scavenging reaction 2.1 will be given by

$$Y = k_s[S] \int [H] dV \quad (24)$$

Thus we obtain

$$Y = A\Delta/W \quad (25)$$

$Y$  is expressed in units of mole sec.<sup>-1</sup>.

In practice equation 21 was solved numerically for values of  $W$  from 100 to 0.001. The best value of  $k_s\varphi^{2/3}$  was obtained by trial and error. Using selected values of  $k_s\varphi^{2/3}$ ,  $W$  was calculated from eq. 23 and then  $\Delta$  was obtained. Hence  $Y$  was calculated from eq. 25. This procedure was repeated until best agreement with experiment was obtained.

It is of interest to test the limiting values of the solutions of eq. 21.

For high concentrations of  $S$ ,  $W \rightarrow 0$  and thus  $\Delta \rightarrow 0$ . Therefore  $\Delta \gg \Delta^2$ ,  $\Delta^3$  and thus  $\Delta = W$  and  $Y = A$ . For very low concentrations of  $S$ ,  $W \rightarrow \infty$  and thus  $\Delta = (1/2W)^{1/2}$ . We then obtain

$$Y_{([S] \rightarrow 0)} = k_s[S]\varphi^{2/3} (18DA/k_r^2)^{1/3} \quad (26)$$

This result can be readily obtained from equations 14 and 24.

**Time Dependent Solution.**—In order to test the adequacy of the steady-state treatment the time dependent solution was considered, for the first-order reaction. Equation 27

$$\partial[H]/\partial t = D\partial^2[H]/\partial X^2 - k_s[S][H] \quad (27)$$

can be solved using Danckwerts' treatment<sup>4</sup> or the Laplace transform method.<sup>7</sup> Equation 27 is solved under the initial conditions of  $[H] = 0$  for  $t = 0$ , and  $[H] = [H]_0$  for  $t > 0$  at  $X = 0$ . The solution is obtained in the form

(7) J. Crank, "The Mathematics of Diffusion," Oxford Univ. Press, 1956, p. 18ff.

$$[H] = ([H]_0/2) [\exp(-X\sqrt{k_s[S]/D}) \operatorname{erfc}\{(X/2\sqrt{Dt}) - (k_s[S]t)\} + \exp(X\sqrt{k_s[S]/D}) \operatorname{erfc}\{(X/2\sqrt{Dt}) + (k_s[S]t)\}] \quad (28)$$

The total amount of H atoms absorbed per unit time is given by

$$\int D \operatorname{grad} [H] d\varphi = ([H]_0/\sqrt{k_s[S]D}) \{(\operatorname{erf} \sqrt{k_s[S]t}) + \exp(-k_s[S]t)/\sqrt{\pi k_s[S]t}\} \quad (29)$$

For a sufficiently high value of  $t$ , when  $\operatorname{erf} \sqrt{k_s[S]t} \cong 1$ , expressions 28 and 29 reduce to equations 11 and 12 obtained under steady-state approximation. The required condition is that

$$t \sim (k_s[S])^{-1} \quad (30)$$

Under our experimental conditions  $k_s$  is of the order of  $10^5$  liter mole<sup>-1</sup> sec.<sup>-1</sup>,  $[S] \sim 10^{-3}$  to  $1 M$ , so that the steady-state approximation appears to be reasonable. It is interesting to point out that the condition of 30 is almost identical with the condition for the application of steady-state treatment in homogeneous kinetics, which we considered previously.<sup>10</sup> However this solution yields only the lower limit for the time required for the establishment of steady-state conditions.

**Forced Convection Model.**—In the preceding treatment we restricted the role of stirring to ensure quasi homogeneous scavenger concentration and assumed that scavenger depletion can be neglected. We shall now consider the effect of stirring on the mass transfer process. The quantitative treatment for forced convection will be based on the well known general equation

$$(\partial[H]/\partial t)_{\text{transfer}} = D \operatorname{div} \operatorname{grad} [H] - \mathcal{U} \operatorname{grad} [H] \quad (31)$$

where  $\mathcal{U}$  is the velocity vector of the liquid with component  $u$  parallel to the  $x$  axis. For the one-dimensional case under steady-state conditions  $D(\partial^2[H]/\partial X^2) - u(\partial[H]/\partial X) - k_s[S][H] - k_r[H]^2 = 0$  (32)

In the case when recombination may be neglected eq. 32 reduces to

$$\partial^2[H]/\partial X^2 - \gamma(\partial[H]/\partial X) - \beta[H] = 0 \quad (33)$$

where  $\gamma = u/D$ . The solution is

$$[H] = (A\eta/k_s[S]\varphi)e^{-\eta X} \quad (34)$$

where

$$\eta = -u/2D + \{(u^2/4D^2) + (k_s[S]/D)\}^{1/2} \quad (35)$$

It will be seen that transport by diffusion can be neglected compared with transport by convection, when

$$u^2/4D^2 \gg k_s[S]/D \quad (36)$$

or alternatively when

$$u \gg 2\sqrt{k_s[S]D} \quad (36)$$

Using the numerical values of  $k_s[S] = 10^4$  sec.<sup>-1</sup> and  $D = 4 \times 10^{-5}$  cm.<sup>2</sup> sec.<sup>-1</sup> it is found that when  $u \gg 1.2$  cm. sec.<sup>-1</sup> mass transport by convection only has to be considered. For these relatively high  $u$  values eq. 34 is reduced to the form

$$[H] = (A/u\varphi)e^{-k_s[S]X/u} \quad (34')$$

We shall now consider the general case when diffusion can be neglected in comparison by convection. Equation 32 will be given in the form

$$\partial[H]/\partial X + \omega[H] + \epsilon[H]^2 = 0 \quad (37)$$



where  $\omega = k_s[S]/u$  and  $\epsilon = k_r/u$ . The solution is

$$[H] = \omega b e^{-\omega X} / (1 - b \epsilon e^{-\omega X}) \quad (38)$$

where  $b = [H]_0 / (\omega + \epsilon[H]_0)$ . Application of condition 7 gives

$$b = Au / (k_s[S]\varphi u + k_r A) \quad (39)$$

and by using eq. 24 the yield is given by

$$Y = (k_s[S]\varphi u / k_r) \ln \{1 + (Ak_r / k_s[S]\varphi u)\} \quad (40)$$

Experimental results can be fitted to equation 40 by choosing the best value for the parameter  $(k_s\varphi u)$ .

**Comparison with Homogeneous Kinetics.**—The results of the present treatment based on heterogeneous kinetics will now be compared with the homogeneous kinetic treatment. The steady-state treatment of the competitive reactions of equations 2.1 and 2.2 based on homogeneous kinetics leads to

$$Y = \tau[S]^2 V \{ \sqrt{1 + (2A/\tau[S]^2 V)} - 1 \} \quad (41)$$

where  $t = k_s^2/2k_r$ . In the scavenger concentration region where  $[S]$  is sufficiently low and the steady state concentration of the H atoms is determined by the recombination reaction, the homogeneous kinetic treatment leads to the result

$$Y_{([S] \rightarrow 0)} = k_s[S](AV/k_r)^{1/2} \quad (42)$$

The most reliable values for the scavenging rate constant were obtained from experiments at low scavenger concentrations. We shall therefore compare the values of apparent rate constant obtained for the homogeneous treatment according to equation 42, with the value obtained in the case of purely diffusion controlled kinetics, for which at low scavenger concentrations equation 26 holds. We obtain for the ratio of the apparent rate constants obtained from homogeneous and diffusion controlled treatments

$$\frac{k_s^{\text{diff}}}{k_s^{\text{homo}}} = \frac{(k_r A)^{1/2} V^{1/2}}{18^{1/2} D^{1/2} \varphi^{3/2}} \cong \frac{500}{\varphi^{3/2}} \quad (43)$$

where the numerical value is obtained by setting  $A = 5 \times 10^{-8}$  mole sec.<sup>-1</sup> and  $V = 25$  cm.<sup>3</sup>. The effective area  $\varphi$  can only be approximately estimated under our conditions of bubbling; it is of the order of 10 cm.<sup>2</sup>. Thus we conclude that were the situation such, that forced convection is completely absent and mass transfer is by diffusion only, the rate constant evaluated from homogeneous kinetics would be an underestimate by some two orders of magnitude.

We shall now compare with this most extreme case our actual experimental conditions where forced convection occurs. It was shown that when the linear velocity of stirring,  $u$ , exceeds 1.2 cm. sec.<sup>-1</sup>, transport by convection outweighs transport by diffusion. Under these conditions at low scavenger concentrations we obtain for the yield

$$Y_{([S] \rightarrow 0)} = \frac{k_s^{\text{f.c.}}[S]\varphi u}{k_r} \ln \frac{Ak_r}{k_s^{\text{f.c.}}[S]\varphi u} \quad (44)$$

and for the ratio of the apparent rate constants obtained from homogeneous and forced convection treatments

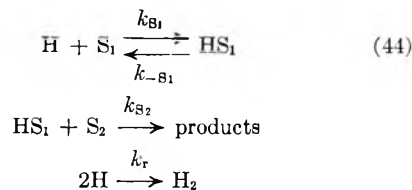
$$\frac{k_s^{\text{f.c.}}}{k_s^{\text{homo}}} = \frac{(AV/k_r)^{1/2}}{(\varphi u/k_r)(\ln Ak_r - \ln B)} \cong \frac{400}{\varphi u} \quad (45)$$

where  $B = k_s^{\text{f.c.}}[S]\varphi u$ . As  $[S] \rightarrow 0$ ,  $-\ln B$  may be neglected compared with  $\ln AK_r$  and introducing

then the numerical values the final result shown is obtained. We see that as expected the existence of forced convection expressed through the introduction of the stirring velocity, brings the constant obtained by the homogeneous treatment nearer to the true value. The treatment is necessarily very approximate, but it does show, that as the value of  $\varphi u \rightarrow 100$  cm.<sup>3</sup>sec.<sup>-1</sup>, the experimental constants obtained under our conditions of forced convection will approach within an order of magnitude those obtained assuming homogeneous kinetics.

**Consecutive Scavenging Mechanism.**—We shall now examine the question whether the assumption of homogeneous kinetics in a case where diffusion and/or forced convection occur may lead to the derivation of reaction mechanisms which correspond to the true state of affairs.

We shall consider that the reactions of H atoms with scavengers may proceed by a composite mechanism involving the formation of a reactive intermediate. The general kinetic scheme can be represented as



Considering mass transfer by diffusion only we obtain

$$\begin{aligned} D(\partial^2[H]/\partial X^2) &= k_{S_1}[S_1][H] + k_r[H]^2 - k_{-S_1}[HS_1] \\ D'(\partial^2[HS_1]/\partial X^2) &= -k_{S_1}[S_1][H] + k_{-S_1}[HS_1] + \\ &\quad k_{S_2}[S_2][HS_1] \end{aligned} \quad (45)$$

where  $D$  and  $D'$  are the diffusion coefficients of H atoms and of the  $HS_1$  intermediate complex. Assuming no depletion of the scavengers  $S_1$  and  $S_2$  the yield will be

$$Y = k_{S_2}[S_2] \int [HS_1] dV \quad (46)$$

The system of diffusion equations 45 was solved under the following simplifying assumptions: as  $D > D'$  and  $[H] > [HS_1]$ , the diffusion of the active intermediate  $HS_1$  was neglected and its concentration was expressed by ordinary steady-state expression. A similar approach was employed by Semenov<sup>8</sup> for some gas phase reactions. We obtain

$$[HS_1] = (k_{S_1}[S_1][H]) / (k_{-S_1} + k_{S_2}[S_2]) \quad (47)$$

The two diffusion equations are then replaced by the single one

$$\partial^2[H]/\partial X^2 = \alpha[H]^2 + \beta_1[H] \quad (48)$$

$$\beta_1 = k_{S_1}[S_1] / (D \{ (k_{-S_1}/k_{S_2}) + [S_2] \}) \quad (49)$$

The expression obtained is identical with eq. 16. Solving according to condition 24 leads to

$$Y = A \Delta_1 / W_1 \quad (50)$$

$$W_1 = k_r A / 6D^{1/2} k_{S_1}^{3/2} [S_1]^{3/2} e_{S_2}^{3/2} \quad (51)(a)$$

$$e_{S_2} = [S_2] / \{ (k_{-S_1}/k_{S_2}) + [S_2] \} \quad (b)$$

$\Delta_1$  is obtained from

$$2\Delta_1^3 + 3\Delta_1^2 + \Delta_1 = W_1 \quad (52)$$

Considering now the case of forced convection

(8) N. N. Semenov, "Some Problems in Chemical Kinetics and Reactivity," Princeton Univ. Press, 1959.

when diffusion can be neglected, the corresponding equations are

$$\begin{aligned} -\partial[\text{H}]/\partial X &= k_{S_1}[\text{S}_1][\text{H}] + k_r[\text{H}]^2 - k_{-S_1}[\text{HS}_1] \\ -\partial[\text{HS}_1]/\partial X &= -k_{S_1}[\text{H}][\text{S}_1] + \\ &\quad k_{-S_1}[\text{HS}_1] + k_{S_2}[\text{S}_2][\text{HS}_1] \end{aligned} \quad (53)$$

and by applying equation 47 the yield is

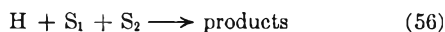
$$Y = \{(k_{S_1}\varphi[\text{S}_1]e_{S_2})/k_r\} \ln \{1 + (k_r A/k_{S_1}\varphi[\text{S}_1]e_{S_2})\} \quad (54)$$

In the case of homogeneous kinetics the reaction scheme of consecutive scavenging leads to the expression

$$Y = (\tau_1 e_{S_2}^2 [\text{S}_1]^2 / V) \{ (1 + (2AV/\tau_1 e_{S_2}^2 [\text{S}_1]^2))^{1/2} - 1 \} \quad (55)$$

where  $\tau_1 = k_{S_1}^2 / 2k_r$ .

Some general conclusions may now be derived regarding these results for homogeneous and heterogeneous kinetics. For high  $\text{S}_2$  concentrations  $e_{S_2} \rightarrow 1$  and the equations reduce to those obtained for the case of a single scavenger. Therefore the rate-determining step in this case involves the formation of the  $\text{HS}_1$  intermediate complex. At lower  $\text{S}_2$  concentrations  $e_{S_2}$  is less than unity and for  $\text{S}_2 \ll k_{-S_1}/k_{S_2}$  the kinetic equations become equivalent to those obtained for the triple collision mechanism



It is found then that in this approximation both heterogeneous and homogeneous treatments lead to the result that the yield is dependent on the concentration function  $e_{S_2}[\text{S}_1]$  alone, when the con-

secutive scavenging mechanism is the actually operating one.

### Conclusions

The impetus for the present investigation was given by one of the referees of the original draft of what forms now Part II of the present work. He requested detailed examination of those assumptions which were made in that and previous papers based on estimation of the experimental conditions, without a quantitative basis.

As the result of the present work we conclude regarding the absolute value of the rate constants, that under our conditions of vigorous stirring and bubbling the constants derived under the assumption of homogeneous kinetics are probably lower by not more than one order of magnitude than the true ones. As we cannot determine either  $u$  or  $\varphi$  accurately, no closer estimate is possible of the degree of agreement. However comparison of the values thus obtained by us with values derived from other experimental investigations support this conclusion. This point will be discussed in the following papers. Similarly, reaction mechanisms derived under these conditions under the assumption that homogeneous kinetics may be applied are the mechanisms arrived at also when heterogeneous kinetics are assumed.

In view of these conclusions homogeneous kinetics will be employed in some future papers, with due reference to the considerations now obtained.

## THE MECHANISM OF OXIDATION BY HYDROGEN ATOMS IN AQUEOUS SOLUTION. PART II. REACTION MECHANISMS WITH DIFFERENT SCAVENGERS

BY GIDEON CZAPSKI, JOSHUA JORTNER AND GABRIEL STEIN

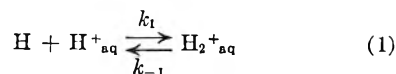
*Department of Physical Chemistry, Hebrew University, Jerusalem, Israel*

*Received October 31, 1960*

The mechanism of oxidation by hydrogen atoms of various acceptors is discussed. It is shown that two alternative pathways exist for the oxidation of ions dissolved in water. One involves the relatively slow reaction of H atoms with  $\text{H}^+_{\text{aq}}$  to form  $\text{H}_2^+_{\text{aq}}$ , which oxidizes acceptors, e.g.,  $\text{I}^-_{\text{aq}}$ . Alternatively other acceptors, e.g., metal cations may directly form intermediate complexes with H, with faster rate constants. The intermediate hydride complex may react with  $\text{H}^+_{\text{aq}}$ , yielding molecular hydrogen. When this faster, hydride complex, pathway is available, the slower  $\text{H}_2^+$  mechanism may not be of kinetic importance. The experimental results for the oxidation of  $\text{Fe}^{2+}$  ions by H atoms can be adequately explained by this mechanism. The results of radiation chemical and photochemical experiments are discussed.

Investigations of the radiation chemistry<sup>1,2</sup> of aqueous solutions of ferrous ions led to the assumption that H atoms may act as oxidizing agents in acid solutions. Evidence from the photochemistry of ferrous<sup>3,4</sup> and of iodide<sup>5,6</sup> ions was adduced to support this view. Recently using hydrogen atoms generated externally and introduced as such into the aqueous solutions it was shown that hydrogen

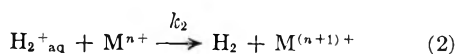
atoms are indeed capable of oxidizing ferrous to ferric ions<sup>7-9</sup> and iodide to iodine.<sup>10</sup> The reaction was shown to be pH dependent.<sup>9,10</sup> However the actual mechanism was not finally established. Namely it was proposed<sup>1,2</sup> that the oxidation involves the formation of  $\text{H}_2^+_{\text{aq}}$  ion according to



which acts as the actual oxidizing species

- (1) J. Weiss, *Nature*, **165**, 728 (1950).
- (2) T. Rigg, G. Stein and J. Weiss, *Proc. Roy. Soc.*, **211A**, 375 (1952).
- (3) T. Rigg and J. Weiss, *J. Chem. Phys.*, **20**, 1194 (1952).
- (4) J. Jortner and G. Stein, to be published.
- (5) T. Rigg and J. Weiss, *J. Chem. Soc.*, 4198 (1952).
- (6) J. Jortner, R. Levine, M. Ottolenghi and G. Stein, *J. Phys. Chem.*, in press.

- (7) G. Czapski and G. Stein, *Nature*, **182**, 598 (1958).
- (8) T. W. Davis, S. Gordon and E. J. Hart, *J. Am. Chem. Soc.*, **80**, 4487 (1958).
- (9) G. Czapski and G. Stein, *J. Phys. Chem.*, **63**, 850 (1959).
- (10) G. Czapski, J. Jortner and G. Stein, *ibid.*, **63**, 1769 (1959).



This mechanism was investigated in detail<sup>10</sup> and it was found that it was in agreement with the results obtained in the oxidation of iodide ions by atomic hydrogen. It was also compared with alternative mechanisms: the pH independent mechanism<sup>11</sup> of H abstraction from the hydration layer; the mechanism involving<sup>12,8</sup> triple collision between  $\text{H}, \text{H}^+_{\text{aq}}$  and the ion to be oxidized; and a mechanism in which  $\text{H}^+_{\text{aq}}$  was assumed to form a complex with the ion. None other than the mechanism involving  $\text{H}_2^+_{\text{aq}}$  agreed with the results. The value obtained for  $k_1$ , the velocity constant of the formation of  $\text{H}_2^+$  according to reaction 1 was found to be  $10^2$ – $10^3$  mole liter<sup>-1</sup> sec.<sup>-1</sup> by applying homogeneous kinetics. However the mechanism of the oxidation of the ferrous ion by H atoms could not be decided and consideration of the available evidence led to the conclusion<sup>13</sup> that in this case another mechanism may be operating. It was suggested<sup>13</sup> that in this alternative mechanism the hydride forming properties of the H atom may be of importance. The mechanism involving intermediate hydride complex formation was shown<sup>14</sup> to be consistent with the mechanism of homogeneous activation of  $\text{H}_2$  by solutions of metal ions and<sup>15</sup> with the results of radiation chemical experiments.<sup>16</sup> In the present paper our detailed results of the reinvestigation of the oxidation of ferrous ions by atomic hydrogen are reported and the mechanism operating discussed in detail.

### Experimental

**Procedure.**—The production of atomic hydrogen by electrodeless discharge at 30 Mc. was as described previously.<sup>9,10</sup> Atomic hydrogen was passed for 10 minutes through 25 ml. of the evacuated solution maintained at  $\sim 4^\circ$ . The pumping velocity in the present series of experiments was 150 liter min.<sup>-1</sup>. In order to improve reproducibility, no air was admitted after completing the run and full hydrogen atmosphere was maintained during the opening of the reaction vessel for analysis. With these precautions reproducibility was better than in our previously reported experiments. Each experiment was repeated at least three times and reproducibility was  $\pm 15\%$  or better.

**Determination of the dose of H atoms** was carried out using the reduction of  $10^{-3}$  M ferricyanide solutions.<sup>17</sup> During the runs the constancy of the dose was checked by the oxidation of 0.05 M  $\text{Fe}^{2+}$  solutions in 0.8 N  $\text{H}_2\text{SO}_4$ . The dose in the present series of experiments was  $1.2 \times 10^{-6}$  mole liter<sup>-1</sup> sec.<sup>-1</sup>.

**Analysis.**—The ferric ion concentration was determined by absorption measurements at 305 m $\mu$  in 1 cm. cells using a Beckman DU Spectrophotometer. The dependence of the molar absorption coefficient on the concentration of the sulfate ion and sulfuric acid concentration was determined in  $\text{H}_2\text{SO}_4$  solutions in the pH region 0.4–3.0, containing 0.01–0.2 M  $\text{Na}_2\text{SO}_4$ . Identical results were obtained by replacing  $\text{Na}_2\text{SO}_4$  by  $\text{FeSO}_4$ . The experimental results were duly corrected for the effect of sulfate ion concentration.

**Materials.**—A.R. ferrous ammonium sulfate and sulfuric acid were used. Solutions were prepared in triply distilled water. Matheson's electrolytic hydrogen was further purified by passing through palladized asbestos.

(11) N. Uri, *Chem. Revs.*, **50**, 376 (1952).

(12) J. P. Ethier and F. Haber, *Naturwiss.*, **18**, 266 (1930).

(13) G. Stein, *Disc. Faraday Soc.*, **29**, 235 (1960).

(14) J. Halpern, G. Czapski, J. Jortner and G. Stein, *Nature*, **186**, 629 (1960).

(15) G. Czapski and J. Jortner, *ibid.*, **188**, 50 (1960).

(16) F. S. Dainton and D. B. Peterson, *ibid.*, **186**, 878 (1960).

(17) G. Czapski and G. Stein, *J. Phys. Chem.*, **64**, 219 (1960).

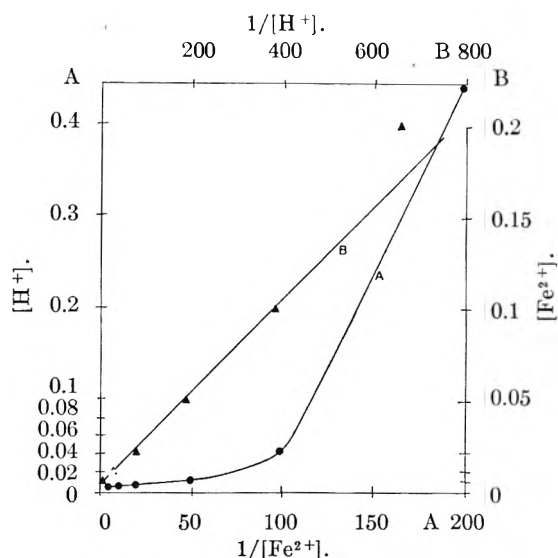


Fig. 1A.—Plot of the experimental results for the oxidation of  $\text{Fe}^{2+}$  according to the  $\text{H}_2^+$  mechanism.  $Y = 0.34A$ .  
B.—Plot of the experimental results for the oxidation of  $\text{Fe}^{2+}$  according to the hydride mechanism.

### Results

The oxidation of  $\text{Fe}^{2+}$  ions in acid solution by H atoms was investigated in the pH range of 0.4–3.0 and ferrous ion concentration of 0.001 to 0.2 M. The experimental results are presented in Table I. The reaction is found to be pH dependent in agreement with previous results.<sup>9</sup> The known ratio of the rate constants<sup>18,9</sup> of the reduction of  $\text{Fe}^{3+}$  and oxidation of  $\text{Fe}^{2+}$  by H atoms indicates that the decrease in the oxidation yield cannot be assigned to the back reaction between  $\text{Fe}^{3+}$  ions formed and H atoms. The dependence of the yield on  $\text{Fe}^{2+}$  concentration and the concentration of  $\text{H}^+$  ions is attributed to the competition with the recombination reaction



Our experimental results cannot be reconciled with the oxidation mechanism involving the hydrogen molecule ion as an intermediate. In the preceding paper the problem of analyzing the results obtained by the method of H atom production and introduction into aqueous solutions was discussed. It was shown that both the homogeneous and the heterogeneous kinetic approach to the treatment of the experimental results leads to the conclusion that for the consecutive scavenging reaction scheme the yield is a function of  $e_{s_2}[\text{S}_1]$ , where  $e_{s_2} = [\text{S}_2] / \{(k_{-s_1}/k_{s_2}) + [\text{S}_2]\}$ , as defined in the preceding paper.

By applying these conclusions to the oxidation mechanism involving  $\text{H}_2^+$  we see that the oxidation yield should be dependent on  $[\text{H}^+][\text{Fe}^{2+}] / \{(k_{-1}/k_2) + [\text{Fe}^{2+}]\}$ . When for different  $\text{Fe}^{2+}$  and  $\text{H}^+$  concentrations the same yield is obtained, this function should remain constant. In other words for different scavenger concentrations which give the same oxidation yield, the plot of  $[\text{H}^+]$  vs.  $1/[\text{Fe}^{2+}]$  should result in a straight line. Such results for  $Y = 0.34A$  are presented in Fig. 1A.

(18) W. G. Rothschild and A. O. Allen, *Rad. Res.*, **8**, 101 (1958).



the ferrous-hydride mechanism. The rate constant for reaction 3 can be estimated. The results of the homogeneous kinetics yield the value of  $k_3$   $10^4$  mole<sup>-1</sup> liter sec.<sup>-1</sup> which is a lower limit. Estimating the effective surface area as  $\varphi \sim 10$  cm.<sup>2</sup> the heterogeneous treatment leads to  $k_3 \sim 10^5$  mole<sup>-1</sup> liter sec.<sup>-1</sup>. Considering the value of the ratio  $k_{-3}/k_4$  obtained it should be pointed out that some dependence of this ratio on  $\text{Fe}^{2+}$  concentration was observed, the ratio decreasing with decreasing  $\text{Fe}^{2+}$ . Thus at 0.01 and 0.02 M  $\text{Fe}^{2+}$  the experimental results for the diffusion treatment were in better agreement with the value of  $k_{-3}/k_4 = 0.02$ . This may be due for example to the diffusion of intermediates which is neglected in our treatment. However our experimental results do not enable us to establish the value with greater accuracy.

### Discussion

The oxidation mechanism of the  $\text{Fe}^{2+}$  ion proceeds by hydride formation. However when we attempt to analyze the results previously obtained<sup>19</sup> for the oxidation of iodide ions by H atoms according to this mechanism a satisfactory agreement cannot be obtained. Figure 2 indicates that at a constant oxidation yield the function  $[\text{I}^-][\text{H}^+]/(\gamma + [\text{H}^+])$  is not constant while as it was previously demonstrated<sup>11</sup> the oxidation yield is a function of  $[\text{H}^+][\text{I}^-]/(0.1 + [\text{I}^-])$ . Thus it agrees with the oxidation mechanism involving  $\text{H}_2^+$  as an intermediate. The oxidation mechanism proposed for the ferrous ion is in agreement with the pH dependence of the yield in radiation chemical and photochemical experiments. The region in which pH dependence is observed due to competition with recombination, will depend on the rate of introduction of H atoms. A reinvestigation of the photochemical oxidation of ferrous ions in evacuated acid solution showed<sup>4</sup> that up to pH 2.4 the pH dependence of the initial quantum yield was due to the pH dependence of the primary photochemical H atom formation only, in 0.02 M  $\text{Fe}^{2+}$  and rate of formation of H atoms =  $3 \times 10^{-7}$  mole liter<sup>-1</sup> sec.<sup>-1</sup>. In radiation chemical experiments<sup>18,20</sup> at  $10^{-3}$  M  $\text{Fe}^{2+}$  and rate of formation of H atoms =  $3 \times 10^{-8}$  mole liter<sup>-1</sup> sec.<sup>-1</sup> no pH dependence was observed up to pH 2.1. Treating these systems according to the steady-state approach of eq. V, it appears that the condition for the independence of  $Y$  of pH and  $[\text{Fe}^{2+}]$  will prevail when

$$A/V \ll k_3^2 e_{\text{H}^+} [\text{Fe}^{2+}]^2 / 4k_r \quad (\text{VI})$$

Setting  $k_3 \cong 10^5$  mole<sup>-1</sup> liter sec.<sup>-1</sup> and  $k_{-3}/k_4 = 0.05$  the inequality VI is fulfilled both for the photochemical and radiation chemical experiments. This comparison is qualitative only, as it is not clear whether the assumption of initial homogeneous distribution of the radicals in radiation chemistry is adequate when competition between first- and second-order reactions occur.

In our treatment it was assumed that the recombination reaction  $r$  itself is pH independent. The possible reactions  $\text{FeH}^{2+} + \text{H}$  and  $\text{H}_2^+ + \text{H}$

(19) Correction of error. In ref. 10 the ordinate of Figs. 1, 2, 4, 5 and 6 has to be multiplied by a factor of 300.

(20) A. O. Allen and W. G. Rothschild, *Rad. Res.*, **7**, 591 (1957).

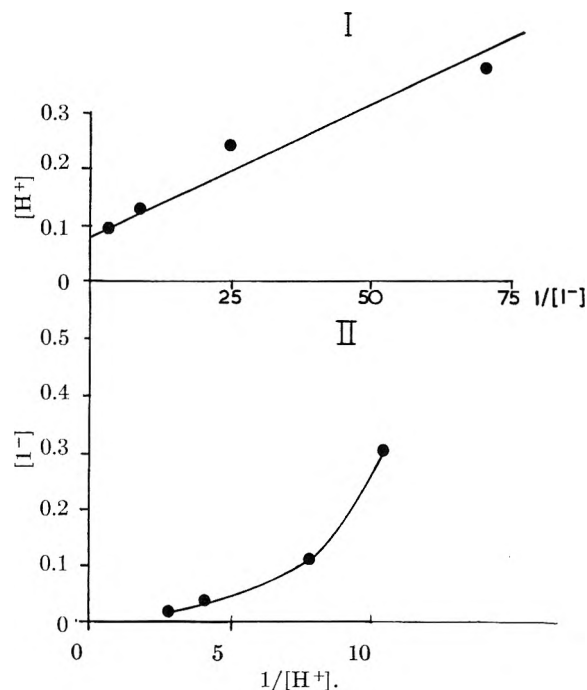


Fig. 2.—Plot of the experimental results of ref. 10 for the oxidation of  $\text{I}^-$  by H atoms: I,  $\text{H}_2^+$  mechanism; II, hydride mechanism.

are not included in the kinetic scheme. It is assumed<sup>9</sup> that since in these molecules the bond energies  $\text{Fe}^{2+}-\text{H}$  and  $\text{H}-\text{H}^+$  have to be considered, these reactions will be activation controlled, and will be slower than the diffusion controlled reaction  $r$ .

When the competitive reactions between  $\text{Fe}^{2+}$  ions on the one hand and other scavengers, e.g., molecular  $\text{O}_2$ <sup>18</sup> or methanol<sup>21</sup> were investigated it was found that the ratio of the rate constants was nearly independent of pH within a rather wide pH range. Radiation chemical experiments<sup>18</sup> showed that  $k_{\text{H}+\text{O}_2}/k_{\text{H}+\text{Fe}^{2+}}$  is 1200 at pH 0.35 and 1500 at pH 2.1. Photochemical experiments<sup>4</sup> gave for this ratio the value of  $900 \pm 300$  at pH 0.35 and  $1500 \pm 400$  at pH 2.4. According to the mechanism now proposed the competition is seen to be between the ferrous ion and the acceptor,  $\text{O}_2$  or methanol, for H atoms,  $\text{H}^+$  not being involved at this stage, since its reaction with H is slower. This will be the case as long as the dissociation reaction of the complex may be neglected in comparison with its reaction with  $\text{H}^+$ . The value of  $k_{-3}/k_4 = 0.05-0.02$  mole liter<sup>-1</sup> is consistent with the results of Baxendale and Hughes.<sup>21</sup> Similarly it can be shown<sup>15</sup> that the results of Dainton and Peterson<sup>16</sup> for the competition between  $\text{Fe}^{2+}$  and  $\text{N}_2\text{O}$  for H atoms leads to the value of  $k_{-3}/k_4 = 0.05$ , in excellent agreement with our experimental results. However in order to explain the results of Rothschild and Allen<sup>18</sup>  $k_{-3}/k_4$  should be of the order of 0.01. Our photochemical experiments indicate that at pH values higher than 2.1 deviations already occur from constancy of the ratio of rate constants. These discrepancies may be due to specific reactions of the  $\text{O}_2$  molecule with inter-

(21) J. H. Baxendale and G. Hughes, *Z. physik. Chem. N. F.*, **14**, 323 (1958).

mediates, and may be related to the nature of the H atom equivalent present in irradiated solutions. Thus the special case of O<sub>2</sub> remains to be fully explained and deserves more detailed investigation in the future.

The nature of the FeH<sup>2+</sup> complex should be briefly considered. This may in all probability be a *ferric hydride* possibly consisting of a Fe<sup>3+</sup>H<sup>-</sup> "charge transfer" complex in which a labile ion pair is formed. Similar intermediates were recently postulated in the homogeneous activation of H<sub>2</sub> in solution by some transition and post-transition cations.<sup>22</sup> For the negative iodide ion the formation of such an ion pair is unlikely.

The possibility of such hydride complex intermediates was also postulated by Krasna and Rittenberg<sup>23</sup> in the enzymatic activation of molecular hydrogen by the enzyme hydrogenase of *Proteus vulgaris*, and recently reinvestigated in the case of *Desulfovibrio*.<sup>24</sup> The enzyme is considered to contain iron.

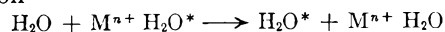
The rate of exchange of solvent molecules from the hydration layer of some transition cations with

(22) J. Halpern, *Quart. Rev.*, **10**, 463 (1956); *J. Phys. Chem.*, **63**, 398 (1959).

(23) A. I. Krasna and D. Rittenberg, *J. Am. Chem. Soc.*, **76**, 3015 (1954).

(24) A. I. Krasna, E. Riklis and D. Rittenberg, *J. Biol. Chem.*, **235**, 2717 (1960).

the medium was shown from n.m.r. measurements<sup>25</sup> to be of the order of 10<sup>6</sup> liter mole<sup>-1</sup> sec.<sup>-1</sup> for the reaction



which is of the same order of magnitude as the upper value for the rate of formation of the ferrous complex with H atoms derived in the present work.

According to the mechanism now proposed the oxidation of non-labile ferrous complexes, e.g., ferrocyanide, will not occur by the hydride mechanism, but by the H<sub>2</sub><sup>+</sup> mechanism, in agreement with our previous results.<sup>17</sup>

Combining the value now obtained of  $k_3 \sim 10^5$  liter mole<sup>-1</sup> sec.<sup>-1</sup> for the rate of reaction of Fe<sup>2+</sup> with H atoms, with the value of the ratio of the rate constants between H atoms and Fe<sup>2+</sup> or O<sub>2</sub>, respectively, gives an approximate value of  $k_{\text{H}+\text{O}_2} \cong 10^8 - 10^9$  liter mole<sup>-1</sup> sec.<sup>-1</sup>, in reasonable agreement with the results of Riesz and Hart.<sup>26</sup> However in this respect one has to bear in mind the reservations regarding the possible specific reactions of O<sub>2</sub> with intermediates in irradiated solutions.

We thank Prof. J. Halpern for valuable comments. This investigation was supported by the Israel Atomic Energy Commission.

(25) R. E. Connick and R. E. Poulson, *J. Chem. Phys.*, **30**, 759 (1959).

(26) P. Riesz and E. J. Hart, *J. Phys. Chem.*, **63**, 859 (1959).

## THE ROLE OF HYDROGEN ATOMS IN THE DECOMPOSITION OF HYDROGEN PEROXIDE AND IN THE RADIATION CHEMISTRY OF WATER

BY GIDEON CZAPSKI, JOSHUA JORTNER AND GABRIEL STEIN

*Department of Physical Chemistry, Hebrew University, Jerusalem, Israel*

*Received October 31, 1960*

Atomic hydrogen generated by an electrodeless high frequency discharge in H<sub>2</sub> gas and introduced into aqueous solutions reacts with 10<sup>-4</sup>-10<sup>-5</sup> M H<sub>2</sub>O<sub>2</sub> with a velocity constant of  $k \cong 10^5$  liter mole<sup>-1</sup> sec.<sup>-1</sup>, unaffected by changing the pH from 1 to 13. The reactions involved are discussed and compared with those postulated for the radiolysis of aqueous H<sub>2</sub>O<sub>2</sub> solutions.

In the radiolysis of dilute aqueous solutions electrons are one of the primary products. Electrons may react directly with suitable acceptors, or may form H atoms through reacting with water, with H<sub>aq</sub><sup>+</sup> or with H<sub>2</sub>O<sup>+</sup>. H atoms themselves may also result directly from, e.g., the dissociation of excited water molecules or by dissociative electron capture by H<sub>2</sub>O. The ratio  $e_{\text{aq}}/\text{H}$  may depend on the pH.

Once formed, H atoms may react with H<sub>aq</sub><sup>+</sup> to form H<sub>2aq</sub><sup>+</sup> ions. The ratio H/H<sub>2aq</sub><sup>+</sup> will depend on the pH.

In addition to these general considerations recently experimental evidence became available showing that two different forms of H atom equivalent are present in irradiated solutions, these two exhibiting widely different reactivity with specific acceptors. Thus Barr and Allen<sup>1</sup> have recently obtained evidence that the two forms show very

different velocity constants with H<sub>2</sub>O<sub>2</sub>. The possible pairs considered were e<sub>aq</sub> and H or alternatively H and H<sub>2</sub><sup>+</sup>. No decision was made between the two alternatives.

Allan and Scholes<sup>2</sup> investigating the reactions in irradiated aqueous solutions of some organic acceptors, came to similar conclusions, but identified the pair of reactants as the electron in water and H atoms. The considerations of Weiss<sup>3</sup> point in the same direction.

To differentiate between the two possibilities and provide evidence for the identification of the species involved in the radiolysis of water, we investigated the rate of reaction of atomic hydrogen with H<sub>2</sub>O<sub>2</sub> in dilute aqueous solution.

### Experimental

Atomic hydrogen was produced as described before,<sup>4</sup> by an electrodeless high frequency discharge at 30 Mc. in

(1) N. F. Barr and A. O. Allen, *J. Phys. Chem.*, **63**, 928 (1959).

See also A. O. Allen and H. A. Schwarz, *Proc. Int. Conf. Peaceful Uses of Atomic Energy*, **29**, 30 (1958).

(2) J. T. Allan and G. Scholes, *Nature*, **187**, 218 (1960).

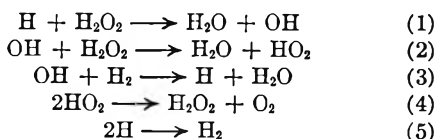
(3) E. Hayon and J. Weiss, *Proc. Int. Conf. Peaceful Uses of Atomic Energy*, **29**, 80 (1958); J. Weiss, *Nature*, **186**, 751 (1960).

(4) G. Czapski and G. Stein, *J. Phys. Chem.*, **63**, 850 (1959).

H<sub>2</sub> gas at 30 mm. pressure. The dose rate in the present series of experiments was  $A = 2 \times 10^{-7}$  mole liter<sup>-1</sup>sec.<sup>-1</sup> determined by the ferricyanide dosimeter.<sup>5</sup> The gas was pumped through the solution at a velocity of 150 liter min.<sup>-1</sup>, producing a very vigorous bubbling and stirring. Experiments were carried out at about 4°. Blank experiments were carried out by passing H<sub>2</sub> through the solution without discharge. In the absence of H atoms no decomposition was observed. Initial and final H<sub>2</sub>O<sub>2</sub> concentrations were determined iodometrically at the higher concentrations, and below [H<sub>2</sub>O<sub>2</sub>] = 10<sup>-5</sup> M by the oxidation of FeSO<sub>4</sub>. Water was triply distilled. H<sub>2</sub>O<sub>2</sub> was Hopkin and Williams' Analar.

### Results and Discussion

In neutral solutions, at pH~6, the decomposition was investigated at several concentrations of H<sub>2</sub>O<sub>2</sub>. The results are shown in Table I. We assume the mechanism



Our solutions were saturated with H<sub>2</sub> gas at 30 mm. pressure. Assuming that the solubility of H<sub>2</sub> is  $0.8 \times 10^{-3}$  M per atmosphere, the H<sub>2</sub> concentration in the solution is  $3 \times 10^{-5}$  M. The rate constants  $k_2$  and  $k_3$  are about equal.<sup>1</sup> We shall neglect reaction 2 compared with reaction 3 for H<sub>2</sub>O<sub>2</sub> concentrations of 10<sup>-5</sup> M or lower. We shall also disregard the radical recombinations H + OH and OH + OH. Under these simplifying conditions, assuming homogeneous kinetics (the justification for which was discussed separately<sup>6</sup> and is considered again in the Appendix) steady-state treatment gives

$$-d[\text{H}_2\text{O}_2]/dt = [\text{H}_2\text{O}_2]k_1A^{1/2}/k_6^{1/2} \quad (6)$$

Setting<sup>7</sup>  $k_6 = 10^{10}$  liter mole<sup>-1</sup>sec.<sup>-1</sup>, the values of  $k_1$  shown in Table I are obtained. Of the significance of these values it may be said that as the concentration of H<sub>2</sub>O<sub>2</sub> increases to 10<sup>-4</sup> M or higher, reaction 2 may no longer be neglected; as the concentration increases further, the chain decomposition of H<sub>2</sub>O<sub>2</sub>, negligible below  $5 \times 10^{-6}$  M becomes of increasing importance. On the other hand at concentrations of 10<sup>-5</sup> M and lower, the determination of H<sub>2</sub>O<sub>2</sub> becomes less accurate. We thus conclude that from these experiments  $k_1 = 1 \times 10^6$  liter mole<sup>-1</sup>sec.<sup>-1</sup>. This value should be compared with that of  $k_1$  in the gas phase, which is of the order of 10<sup>6</sup> liter mole<sup>-1</sup>sec.<sup>-1</sup>.<sup>8</sup>

To investigate the pH dependence of  $k_1$  the experiments shown in Table II were carried out in approximately 10<sup>-4</sup> M H<sub>2</sub>O<sub>2</sub>, where analytical accuracy is good. The results show that from pH~1 to ~13 the decomposition yield is approximately independent of pH. As to the absolute value of  $k_1$  these experiments at about 10<sup>-4</sup> M H<sub>2</sub>O<sub>2</sub> probably give a slightly too low value for the reasons discussed above.

The rate constant for the reaction of H atoms with O<sub>2</sub> was recently found<sup>9</sup> to be 10<sup>8</sup> to 10<sup>9</sup> liter

TABLE I  
DECOMPOSITION OF UNBUFFERED H<sub>2</sub>O<sub>2</sub> SOLUTIONS BY ATOMIC HYDROGEN AT 4°

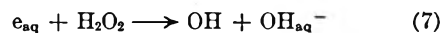
[H <sub>2</sub> O <sub>2</sub> ]initial, mole l. <sup>-1</sup>	[H <sub>2</sub> O <sub>2</sub> ]final, mole l. <sup>-1</sup>	ΔC, mole l. <sup>-1</sup>	ΔC/ [H <sub>2</sub> O <sub>2</sub> ] mean	k <sub>1</sub> , 10 <sup>4</sup> l. mole <sup>-1</sup> sec. <sup>-1</sup>
	6.15 × 10 <sup>-6</sup>			
7.02 × 10 <sup>-6</sup>	5.85 × 10 <sup>-6</sup>	1.02 × 10 <sup>-6</sup>	0.16	6.0
	0.78 × 10 <sup>-6</sup>			
1.01 × 10 <sup>-5</sup>	0.67 × 10 <sup>-5</sup>	0.26 × 10 <sup>-5</sup>	.29	10.5
	0.78 × 10 <sup>-5</sup>			
	3.30 × 10 <sup>-5</sup>			
4.04 × 10 <sup>-5</sup>	3.26 × 10 <sup>-5</sup>	0.81 × 10 <sup>-5</sup>	.23	8.4
	3.21 × 10 <sup>-5</sup>			
	0.815 × 10 <sup>-4</sup>			
1.00 × 10 <sup>-4</sup>	0.860 × 10 <sup>-4</sup>	0.15 × 10 <sup>-4</sup>	.16	6.0
	0.865 × 10 <sup>-4</sup>			

mole<sup>-1</sup> sec.<sup>-1</sup>. By an independent method we reached<sup>6</sup> a similar result. Barr and Allen<sup>1</sup> have shown that one of the species in which the hydrogen atom equivalent appears in irradiated solutions reacts with H<sub>2</sub>O<sub>2</sub> at a rate comparable to that with which it reacts with O<sub>2</sub>. The other form, obtainable also by the reaction of OH radicals with molecular H<sub>2</sub>, reacts with O<sub>2</sub> so much faster than with H<sub>2</sub>O<sub>2</sub>, that added H<sub>2</sub>O<sub>2</sub> is not an efficient scavenger for it in the presence of O<sub>2</sub>.

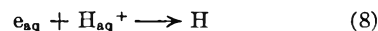
Our results are entirely consistent with the assumption that this species, reacting relatively slowly with H<sub>2</sub>O<sub>2</sub>, is the H atom, as  $k_1$  is found to be some 10<sup>3</sup> times lower than  $k_{\text{H} + \text{O}_2}$ .

This conclusion agrees also with the finding of Bunn, *et al.*,<sup>10</sup> that reaction 3 leads to the formation of atomic hydrogen and does not proceed by charge transfer.

We conclude therefore that the pair of reactive entities under the conditions of irradiation discussed by Barr and Allen<sup>1</sup> is e<sub>aq</sub> and atomic H. We thus agree with the conclusions of Allan and Scholes.<sup>2</sup> We consider that the fast radiation-induced decomposition process of H<sub>2</sub>O<sub>2</sub> in neutral solutions is



In acid solution the process



will proceed efficiently. On the other hand the formation of H<sub>2aq</sub><sup>+</sup> from H and H<sub>aq</sub><sup>+</sup> is a relatively slow process<sup>11</sup> with  $k_{\text{H} + \text{H}^+} \sim 10^3$  liter mole<sup>-1</sup>sec.<sup>-1</sup>. We thus conclude that the acid form of the primary radiation product, electron in water, is the H atom as such. These results are consistent with the sequence  $e_{\text{aq}} \xrightarrow{\text{H}^+} \text{H} \xrightarrow{\text{H}^+} \text{H}_{2\text{aq}}^+$ , as the pH decreases.

H<sub>2aq</sub><sup>+</sup> will become kinetically important at low pH values only in systems where no other acceptor can directly and rapidly react with e<sub>aq</sub> or H atoms by other pathways. Recently additional experimental evidence has been accumulating regarding specific reactions of electrons with suitable acceptors in the radiolysis of water.

(10) D. Bunn, F. S. Dainton, G. A. Salmon and T. J. Hardwick, *Trans. Faraday Soc.*, **55**, 1760 (1960).

(11) G. Czapski, J. Jortner and G. Stein, *J. Phys. Chem.*, **63**, 1769 (1959).

(5) G. Czapski and G. Stein, *J. Phys. Chem.*, **64**, 219 (1960).

(6) G. Czapski, J. Jortner and G. Stein, *ibid.*, **65**, 956, 960 (1961).

(7) H. L. Friedmann and A. H. Zeltman, *J. Chem. Phys.*, **28**, 878 (1959).

(8) K. H. Geib, *Z. physik. Chem.*, **A169**, 161 (1934).

(9) P. Riesz and E. J. Hart, *J. Phys. Chem.*, **63**, 859 (1959).

TABLE II  
THE pH DEPENDENCE OF THE DECOMPOSITION OF H<sub>2</sub>O<sub>2</sub> SOLUTIONS

Soln.	pH approx.	[H <sub>2</sub> O <sub>2</sub> ]initial, mole l. <sup>-1</sup>	[H <sub>2</sub> O <sub>2</sub> ]final, mole l. <sup>-1</sup>	ΔC, mole l. <sup>-1</sup>	ΔC/[H <sub>2</sub> O <sub>2</sub> ]mean
			0.950 × 10 <sup>-4</sup>		
H <sub>2</sub> SO <sub>4</sub> 0.16 N	1	1.12 × 10 <sup>-4</sup>	.934 × 10 <sup>-4</sup>	0.18 × 10 <sup>-4</sup>	0.18
No addition	6	1.00 × 10 <sup>-4</sup>	.85 × 10 <sup>-4</sup>	.15 × 10 <sup>-4</sup>	.16
NaOH 4 × 10 <sup>-4</sup> N	10	0.99 × 10 <sup>-4</sup>	.855 × 10 <sup>-4</sup>	.135 × 10 <sup>-4</sup>	.15
			.52 × 10 <sup>-4</sup>		
NaOH 0.1 N	13	0.63 × 10 <sup>-4</sup>	.57 × 10 <sup>-4</sup>	.85 × 10 <sup>-6</sup>	.14

These data include the increased hydrogen yields in aqueous monochloroacetic acid<sup>3</sup> and aqueous methanol<sup>12</sup> at low pH, the pH dependence of the ratio of the reduction of Cu<sup>2+</sup> and formic acid,<sup>12,13</sup> and the relative stability of H<sub>2</sub>O<sub>2</sub> in acid solution under irradiation.<sup>14</sup> Similar to the case of H<sub>2</sub>O<sub>2</sub> in acid solution is that of N<sub>2</sub>O<sup>15</sup> where Dainton and Peterson attributed the sharp drop in decomposition at lower pH values to the formation of the acid form of H atoms. The analysis of their results<sup>16</sup> shows that the reaction of H atoms as such with N<sub>2</sub>O is a relatively slow process, with a rate constant of the order of 10<sup>3</sup>–10<sup>4</sup> liter mole<sup>-1</sup> sec.<sup>-1</sup>. It may be concluded accordingly that the precursor of atomic hydrogen in irradiated neutral solutions is the electron in water, while the acid form is the H atom as such.

The present work provides also good support for the considerations<sup>6</sup> regarding the absolute value of the rate constants obtained by the present method. The value of  $k_1 = 10^6$  liter mole<sup>-1</sup> sec.<sup>-1</sup> was obtained by the application of homogeneous kinetics. It was shown<sup>6</sup> by comparison with heterogeneous kinetics that under our experimental conditions rate constants derived from homogeneous kinetics are lower by probably not more than one order of magnitude than the true one, and may possibly closely correspond to it. We see that in the present case not only does the value of  $k_1$  thus obtained agree well with the results of radiation chemistry, but is consistent with the value of  $k_1$  obtained from gas phase experiments.

### Appendix

In this paper homogeneous steady-state kinetics were applied. It is interesting to compare the results with those obtained by applying mass transport controlled kinetic processes. This problem was discussed in detail.<sup>6</sup> In the present case for

(12) J. H. Baxendale and G. Hughes, *Z. physik. Chem. N. F.*, **14**, 323 (1958).

(13) D. M. Donaldson and N. Miller, *Rad. Res.*, **9**, 487 (1958).

(14) T. J. Sworski, *J. Am. Chem. Soc.*, **76**, 4687 (1954).

(15) F. S. Dainton and D. B. Peterson, *Nature*, **186**, 878 (1960).

(16) G. Czapski and J. Jortner, *ibid.*, **188**, (1960).

purely diffusion controlled conditions the homogeneous steady-state equations should be replaced by

$$D_H \partial^2 [H] / \partial X^2 = k_1 [H] [H_2O_2] - k_2 [OH] [H_2] + k_3 [H]^2 \quad (1a)$$

$$D_{OH} \partial^2 [OH] / \partial X^2 = k_2 [OH] [H_2] - k_1 [H] [H_2O_2] \quad (2a)$$

where  $D_H$  and  $D_{OH}$  are the diffusion coefficients of H and of OH. As  $D_H > D_{OH}$  and  $[H] > [OH]$ , the diffusion of the OH radical is neglected and we set  $D_{OH} \partial^2 [OH] / \partial X^2 = 0$ . Hence we obtain

$$D_H \partial^2 [H] / \partial X^2 = k_3 [H]^2 \quad (3a)$$

The solution of this equation is subject to the boundary conditions  $[H] \rightarrow 0$  and  $\partial [H] / \partial X \rightarrow 0$  when  $X \rightarrow \infty$ , and to the relation

$$D_H \int \partial^2 [H] / \partial X^2 dV = A^* \quad (4a)$$

where  $V$  is the total volume of the system and  $A^*$  is the total dose rate in mole sec.<sup>-1</sup>. The decomposition yield of H<sub>2</sub>O<sub>2</sub> is obtained in the form

$$d[H_2O_2] / dt = k_1 [H_2O_2] / V \int [H] dV \quad (5a)$$

The solution of equation 3a is given by<sup>6</sup>

$$H = 1 / \{ \varphi^{2/3} (2k_1 D_H / 3A^*)^{1/3} + (k_1 / D_H)^{1/2} X \}^2 \quad (6a)$$

where  $\varphi$  is the effective mean surface for the diffusion process estimated<sup>6</sup> as of the order of 10 cm.<sup>2</sup>. The decomposition yield is

$$d[H_2O_2] / dt = (k_1 [H_2O_2] \varphi^{2/3} / V) (18 D_H A^* / k_1)^{1/3} \quad (7a)$$

Setting  $D_H = 4 \times 10^{-5}$  cm.<sup>2</sup> sec.<sup>-1</sup>,  $A^* = 5 \times 10^{-9}$  mole sec.<sup>-1</sup>,  $V = 25$  cm.<sup>3</sup>,  $k_1 = 10^{13}$  cm.<sup>3</sup> mole<sup>-1</sup> sec.<sup>-1</sup> and by using the data of Table I we get  $k_1 \varphi^{2/3} = 2 \times 10^7$  liter mole<sup>-1</sup> sec.<sup>-1</sup> cm.<sup>4/3</sup> and thus  $k_1$  is of the order of 10<sup>6</sup> liter mole<sup>-1</sup> sec.<sup>-1</sup>.

We thus see that the homogeneous kinetic treatment gave a lower limit of  $k_1$ , while as discussed previously, the purely diffusion controlled treatment leads to an upper value for  $k_1$ . In the actual forced convection situation of our experiments the employment of homogeneous kinetic will probably yield a value for the rate constant which is in agreement with the true value to better than one order of magnitude.



# DEGRADATION OF POLYMETHYL METHACRYLATE BY ULTRAVIOLET LIGHT

BY ALLAN R. SHULTZ

Contribution No. 191 from the Central Research Department, Minnesota Mining and Manufacturing Company, St. Paul 19, Minn.

Received November 7, 1960

Four polymethyl methacrylate films, having thickness 0.021, 0.107, 0.220 and 0.465 cm., were degraded by 2537 Å. wave length light. The irradiations were conducted in air at 26°. Polymer chain scissions produced by the absorbed photons were computed by application of theory to the benzene and 50:50 butanone:isopropyl alcohol solution viscosities of the original and irradiated films. The quantum yield for random chain scission under the above conditions is  $\varphi_d$  (2537 Å.) =  $2.3 \times 10^{-3}$  (scissions/absorbed photon). The extent of agreement with theory and the nature of deviations from theory of the experimental dose-effect relations observed are analyzed. A change of the light absorption coefficient with ultraviolet light exposure is a complicating factor.

## Introduction

Photolytic degradation of polymer films is of considerable practical interest. Published quantitative studies in this area, however, are not numerous. Quantum yield determinations have been made for ultraviolet light-induced changes in natural rubber,<sup>1</sup> cellulose,<sup>2-4</sup> cellulose acetate,<sup>5</sup> polyethylene,<sup>6</sup> polymethyl methacrylate,<sup>7-9</sup> polyethylene terephthalate,<sup>10</sup> polymethyl vinyl ketone<sup>11</sup> and polymethyl isopropenyl ketone.<sup>11</sup> The changes measured were gas evolution,<sup>1,3</sup> monomer production,<sup>7-9,11</sup> new functional group formation<sup>3,6</sup> and degree of polymerization decrease.<sup>2-5,7-11</sup> Sensitized crosslinking of polymer films by light,<sup>12-19</sup> using ketones and other photo-labile molecules as radical sources, is receiving increasing attention with some quantitative investigations evolving. This latter area involves radical attack by external agents rather than direct photolytic action by polymer unit-absorbed quanta.

The present investigation was undertaken to determine the quantum yield for random scission of pure polymethyl methacrylate by 2537 Å. light. The change in viscosity-average molecular weight as a function of film thickness is compared with theory.<sup>20</sup>

## Experimental

**Monomer Purification and Polymerization.**—Inhibited methyl methacrylate monomer (Monomer-Polymer Corp.) was washed successively with 5% NaNO<sub>2</sub>, 5% NaHSO<sub>3</sub>, 5% NaOH and water. After drying over MgSO<sub>4</sub>, 0.2% by weight of phenyl-β-naphthylamine was added and the monomer was distilled through a short glass helices-packed column at 100 mm. and 46° with nitrogen bleeding. The central cut, consisting approximately 80% of the initial monomer, was retained for polymerization.

Forty-five thousandths g. of lauroyl peroxide was added per 100 ml. of monomer and the solution was saturated with N<sub>2</sub> by sparging. Four pairs of glass plates (30 × 30 cm.) were spaced with stainless steel rod or shim separators, their edges were taped together with "Scotch" Brand Polyester Film Tape (#853) having solvent-resistant adhesive, and the separators were removed in the final stages of closure. The monomer-peroxide solution was syringed into these four spaced-plate pairs at room temperature, allowance in volume being made for complete fill of the enclosures at 40°. Polymerization was accomplished in 64 hours at 40.0 ± 0.02 in a water-bath, then 24 hours at 55° in an air oven followed by 18 hours at 100° in an air oven. The oven stages were employed to assure complete decomposition of the peroxide and essentially 100% conversion of monomer to polymer. The films were removed from the glass plates by cooling from 100° under a water tap and stripping the tape edgings. Despite reasonable flexibility of the tape binding, lack of any release agent and the normal 20-21% contraction during polymerization caused some irregular surface patterning in the four polymethyl methacrylate films. Large areas of apparently smooth, parallel-surfaced films were selected for the irradiation studies. Micrometer measurements on ten samples of each of the four films gave: film A, 0.0207 ± 0.0018 cm.; film B, 0.1070 ± 0.0023 cm.; film C, 0.2200 ± 0.0013 cm.; film D, 0.4650 ± 0.0007 cm. The similar absolute thickness variations in the first three films suggest that deviations of the glass plate surfaces from planarity may have been the controlling factor. Film D exhibits a surprisingly small thickness variation.

**Light Absorption Measurements.**—One 2.5 × 2.5 cm. sample of each film A, B and C was measured against air for apparent optical density, (O.D.)<sub>app.</sub>, in a Cary Model 11 Spectrophotometer. The wave length region covered was 2400 to 4000 Å. Correction for a single reflection at both the incident and excident film-air interfaces was calculated from (O.D.)<sub>app.</sub> for films A and C using the relation O.D. = (O.D.)<sub>app.</sub> + 2 log (1 - r). r is the fraction of light lost to specular reflection at an interface. Assuming the absorption to obey Lambert's law,  $I = I_0 e^{-kL}$ , the absorption coefficient, k, may be calculated as  $k = 2.303 [(O.D.)_{app.} + 2 \log (1 - r)] L^{-1}$ . At 2537 Å. we obtained  $k = 18.4 \text{ cm.}^{-1}$  and  $(1 - r) = 0.944$ . This k agrees fairly well with  $k = 19.6 \text{ cm.}^{-1}$  determined in chloroform solutions for a thermally-initiated polymethyl methacrylate which had been carefully precipitated, washed and vacuum dried to remove monomer.<sup>21</sup> A benzoyl peroxide-initiated polymethyl methacrylate ( $\bar{M}_n = 125,000$ ) was reported<sup>7</sup> to have a  $k = 2.303 \epsilon C = 2.303 \times 1.32 \times 12.1 = 36.8 \text{ cm.}^{-1}$ .

- (1) L. Bateman, *J. Polymer Sci.*, **2**, 1 (1947).
- (2) H. F. Sauer and W. K. Wilson, *J. Am. Chem. Soc.*, **71**, 958 (1949).
- (3) J. H. Flynn, W. K. Wilson and W. L. Morrow, *J. Research Natl. Bur. Standards (U. S.)*, **60**, 229 (1958).
- (4) J. H. Flynn, *J. Polymer Sci.*, **27**, 83 (1958).
- (5) A. Sippel, *Z. Elektrochem.*, **56**, 775 (1952).
- (6) A. R. Burgess, *Chemistry and Industry*, **78** (1952); N.B.S. Circ. **525**, 149 (1953).
- (7) P. R. E. J. Cowley and H. W. Melville, *Proc. Roy. Soc. (London)*, **210A**, 461 (1952).
- (8) P. R. E. J. Cowley and H. W. Melville, *ibid.*, **211A**, 320 (1952).
- (9) P. R. E. J. Cowley and H. W. Melville, N.B.S. Circ. **525**, 59 (1953).
- (10) K. R. Osborn, *J. Polymer Sci.*, **38**, 357 (1959).
- (11) K. F. Wissbrun, *J. Am. Chem. Soc.*, **81**, 58 (1959).
- (12) M. J. Roedel, U. S. Patent 2,484,529, October, 1949.
- (13) G. Oster, Belgian Patent 553,515, January, 1957.
- (14) G. Oster, G. K. Oster and H. Moroson, *J. Polymer Sci.*, **34**, 671 (1959).
- (15) H. Moroson, Ph.D. Thesis, Polytechnic Institute of Brooklyn, 1959. L.C. Card No. Mic 59-1775.
- (16) A. Charlesby, C. S. Grace and L. G. Penhale, *J. Polymer Sci.*, **34**, 681 (1959).
- (17) C. S. Grace and A. Charlesby, Paper No. IC7, IUPAC Polymer Symposium, Wiesbaden, October, 1959.
- (18) E. B. Atkinson, A. E. Hoisfield and M. R. Pettit, Paper No. IV C9, IUPAC Polymer Symposium, Wiesbaden, October, 1959.
- (19) H. Wilski, *Angew. Chem.*, **71**, 612 (1959).
- (20) A. R. Shultz, *J. Chem. Phys.*, **29**, 200 (1958).

(21) Unpublished data, this Laboratory.

This high value might be nearly accounted for by the contribution of 1/1250 mole fraction concentration of benzoate end-groups, but not quite on the basis of the same mole fraction of phenyl groups. In the present study lauroyl peroxide was purposely chosen to avoid the complicating effects of excessive initiator fragment light absorption. Further sources for reference on the ultraviolet light absorption of polymethyl methacrylate are available.<sup>22,23</sup>

Changes in ultraviolet absorption of films A and B were followed as a function of 2537 Å. irradiation exposure by comparison with initially O.D.-matched non-irradiated films in the Cary spectrophotometer split beam.

**Irradiation Apparatus and Procedure.**—The ultraviolet light irradiation facility consists of seven 30-watt General Electric low-pressure mercury vapor lamps (germicidal) mounted in an aluminum reflector with parabolic cross-section. Positioned in the center of this horizontal lamp bank is a vertical 16 × 16 × 26 cm. cardboard box with non-gloss black interior. A 16 × 16 × 3 mm. Corning #9863 glass filter is interposed between the lamps and the sample platform. The average lamp-to-sample platform distance is about 22 cm. No collimation of the incident light other than that imposed by the apparatus geometry was attempted. Maximum possible angle of incidence of light to the film surface is 32°. The corresponding angle of refraction in the film is about 21°. Assuming an optically smooth incident surface, the maximum ratio of light path travelled in the film to the normal path is 1.07.

The lamp and filter combination chosen assures that approximately 100% of the light energy striking the films is of 2537 Å. wave length. Radiation flux was determined with an Eppley thermopile at sample position using a Leeds and Northrup portable potentiometer as the voltage sensing instrument. The thermopile had been previously calibrated<sup>24</sup> against a N.B.S. standard light source (C-744) which gave a radiant energy flux of 45 μ watts/cm.<sup>2</sup> at 2 meters when operating at 0.3 amp. The incident flux at sample position in the irradiation facility was found to be 580 μ watts/cm.<sup>2</sup>. The entering intensity in the PMMA film is therefore  $I_0 = 0.944 \times 580 = 550 \mu \text{ watts/cm.}^2 = 7.0 \times 10^{14}$  (2537 Å. photons) cm.<sup>-2</sup> sec.<sup>-1</sup>. Insertion of the thermopile into the sample position at irregular intervals revealed less than ±10% variation in the incident light intensity during the irradiation period.

The PMMA films were cut into rectangular strips of approximately 0.2 g. weight (less for the thinnest films) and were irradiated in air (R.H. ~25%, temp. ~26°) for times equally spaced logarithmically, up to 192 hours.

**Solution Viscosity Measurements.**—Solution viscosities on the original and irradiated PMMA were measured in a Cannon-Fenske capillary viscosimeter at 25.0 ± 0.02°. Reagent grade benzene (flow time 79.0 sec.) and a 50:50 by volume mixture of reagent grade methyl ethyl ketone: isopropyl alcohol (flow time 86.4 sec.) were the solvent systems. No kinetic energy or shear corrections were made. Intrinsic viscosities,  $[\eta]$ , of the original PMMA films were obtained by extrapolating  $(\eta) = (\ln \eta_{rel})/c$  and  $\eta_{sp}/c$  against  $c$  plots of at least four concentrations to  $c = 0$ . Single concentration determinations on irradiated film solutions were made (relative viscosity range 1.1 to 1.4) using the relations

$$\text{benzene: } [\eta] = \langle \eta \rangle + 0.13 \langle \eta \rangle^2 c$$

$$\text{MEK-isopropyl alc.: } [\eta] = \langle \eta \rangle - 0.40 \langle \eta \rangle^2 c$$

### Results and Discussion

Table I lists the intrinsic viscosity of the non-irradiated PMMA films in benzene and in the MEK-isopropyl alcohol mixture (hereafter called the critical consolute mixture, CCM). Weight-average molecular weights (g./mole),  $\bar{M}_w$ , were calculated by the relations

$$\text{benzene}^{25}: \log \bar{M}_w = (4.102 + \log [\eta])/0.73 \quad (1)$$

$$\text{CCM}^{26}: \log \bar{M}_w = 2(3.228 + \log [\eta]) + 0.053 \quad (2)$$

TABLE I

INTRINSIC VISCOSITIES AND CALCULATED WEIGHT-AVERAGE MOLECULAR WEIGHTS OF ORIGINAL POLYMETHYL METHACRYLATE FILMS

Film	$[\eta]$ (dl. g. <sup>-1</sup> )		$\bar{M}_w \times 10^{-6}$	
	Benzene	CCM	Benzene	CCM
A	8.7	1.60	8.1	8.3
B	6.5	1.35	5.4	5.9
C	8.8	1.70	8.2	9.3
D	8.2	1.55	7.4	7.7

Equation 1 was derived from a light-scattering and viscosity study of nonfractionated PMMA. Equation 2 is the relation determined in ref. 26 modified by the logarithm of  $\bar{M}_w/\bar{M}_v$  assuming the fractions studied in ref. 26 to be "monodisperse" in mol. wt. and assuming the present samples to possess a most probable distribution of molecular weights. The general agreement in molecular weights calculated from the data in these two systems is good. If an allowance had been made for appreciable residual heterogeneity in the ref. 26 fractions the agreement would be even better. The 12% difference in  $\bar{M}_w$ (calcd.) values for film C may reside in filtering difficulty in the CCM solution, allowing evaporation losses prior to viscosity measurement. A calculated value of  $[\eta]$  (CCM) = 1.62 would place film C in better relation to the other films. Higher concentrations of PMMA in the CCM exhibited peculiar flow memory in the capillary viscosimeter, suggesting, possibly, phase separation incidence.

Exposure times and intrinsic viscosities of the irradiated films are given in Table II. Radiation absorption in the upper surface of the films, based upon the original absorption coefficient, is  $R_0 = k\bar{t}I_0$ .  $k = 18.4 \text{ cm.}^{-1}$ ,  $\bar{v} = 0.844 \text{ cm.}^3 \text{ g.}^{-1}$ ,  $I_0 = 2.52 \times 10^{18} \text{ photons cm.}^{-2} \text{ hr.}^{-1}$ , and  $t =$  irradiation time in hours. Of somewhat more intrinsic theoretical interest is the quantity  $0.5\bar{M}_{w0}R_0\bar{N}^{-1}$ , where  $\bar{M}_{w0}$  is the weight-average molecular weight (g./mole) of the non-irradiated polymer and  $\bar{N}$  is Avogadro's number.  $0.5\bar{M}_{w0}R_0\bar{N}^{-1}$  is the number of photons absorbed at the upper film surface per original number-average molecule assuming an initial most probable distribution of molecular weights. Introducing the quantum yield for chain scission,  $\varphi_d$ , we arrive at the quantity  $0.5\varphi_d\bar{M}_{w0}R_0\bar{N}^{-1} \equiv -R_0/R^*$ , the number of scissions per original number-average molecule at the upper surface.

Theory<sup>20</sup> predicts that the number of new viscosity-average molecules produced per original viscosity-average molecule,  $([\eta]_0/[\eta])^{1/a} - 1$ , (where  $a$  is the viscosity-molecular weight exponent in  $[\eta] = KM^a$ ) is related to  $-R_0/R^*$  by<sup>27</sup>

$$([\eta]_0/[\eta])^a - 1 = (kL)^{1/a} \left\{ \left[ \sum_{n=0,1,2,\dots} (a+n)^{-1} \left( -\frac{R_0}{R^*} y + 1 \right)^{-(a+n)} \right] y = e^{-kL} \right\}^{-1/a} - 1 \quad (3)$$

Experimental plots of  $([\eta]_0/[\eta])^{1/a} - 1$  vs.  $0.5\bar{M}_{w0}$

(25) E. F. Casassa, C. E. Hecht and R. L. Cleland, unpublished data, Massachusetts Institute of Technology, ca. 1951.

(26) S. N. Chinai and C. W. Bondurant, Jr., *J. Polymer Sci.*, **22**, 555 (1956).

(27) Note:  $+(R_0/R^*)y$  inadvertently appeared in eq. 12 of ref. 20 in place of the correct quantity  $-(R_0/R^*)y$ .

(22) J. W. Goodeve, *Trans. Faraday Soc.*, **34**, 1239 (1938).

(23) Per Olof Kinell, "Spectrophotometric Study of Polymethyl Methacrylate," Almqvist and Wiksells Boktryckeri AB, Uppsala, 1953.

(24) Richard L. Weiher, this Laboratory.

TABLE II

INTRINSIC VISCOSITY DATA FOR 2537 Å. LIGHT-IRRADIATED POLYMETHYL METHACRYLATE FILMS

Irrad. time, hr.	[ $\eta$ ] (Benzene)				[ $\eta$ ] CCM			
	A	B	C	D	A	B	C	D
0	8.7	6.5	8.8	8.2	1.60	1.35	1.70	1.55
0.375	6.3	..	..	..	1.58	..	..	..
.75	6.9	5.9	..	..	1.46	1.32	..	..
1.5	5.9	5.8	7.5	..	1.28	1.25	1.62	..
3	4.73	4.80	7.2	..	1.06	1.11	..	..
6	3.04	4.08	6.2	7.2	0.69	1.00	1.19	1.44
12	1.67	2.92	4.84	6.9	.481	0.68	1.02	1.39
24	1.06	2.25	..	6.7	.330	.66	0.88	1.35
48	0.62	1.99	3.44	6.9	.257	.50	.74	1.32
96	0.493	1.73	2.70	6.1	.220	.360	.65	1.17
192	..	1.03	2.08	6.1	.132	.346	.57	1.11

$R_0\bar{N}^{-1}$  on a log-log scale should therefore superpose upon corresponding theoretical log-log plots of  $([\eta]_0/[\eta])^{1/a} - 1$  vs.  $-R_0/R^*$  by a simple translation along the  $-R_0/R^*$  axis. The series in eq. 3 converges very slowly. Alternative forms,<sup>20</sup> applicable for  $a = 0.50$  and  $a = 1.00$ , are more convenient for numerical evaluation.

Figure 1 shows the benzene solution viscosity data for the light-irradiated films A, B, C and D superposed upon the theoretical curves for  $kL = 0.38, 1.97, 4.05$  and  $8.56$ , respectively. The limiting curves for  $a = 0.50$  and  $a = 1.00$  are drawn for each film. A good fit of the data to theory is found for films A, B and C over a large exposure range. The abscissa translation giving the correspondence is revealed by the vertical arrow which indicates the exposure at which  $0.5 \varphi_d \bar{M}_{w0} R_0 \bar{N}^{-1} = 1$ . It should be remarked that the same translation was made for all four films. From the exposure indicated by the arrow we calculated  $\varphi_d = 2.3 \times 10^{-3}$  scissions/photon as the quantum yield for random fracture of the polymer chains by the absorbed 2537 Å. light. It is difficult to assess the uncertainty in this quantum yield arising from the several uncertainties in the measurements involved. An estimate of  $\pm 25\%$  uncertainty in  $\varphi_d$  is not unreasonable.

Figure 2 is a plot of the CCM solution viscosity data superposed on the corresponding  $a = 0.50$  theoretical curves. The fit is much poorer than for the benzene solution data. The axis translation chosen fits the film A data (upper curve) to theory at  $([\eta]_0/[\eta])^2 - 1 = 1$  and gives a good fit of the film B data. The calculated quantum yield from the plot is  $\varphi_d = 2.0 \times 10^{-3}$  scissions/photon, but its reliability is not equal to that of the benzene solution data result. The film C data (second from bottom in Fig. 2) do not match theory even though an adjusted  $[\eta]_0 = 1.62$  was used in the construction. A viscosity-molecular weight exponent of  $a = 0.60$  would give a fairly good fit of the film A and B data to theory, but there is no justification for belief in such a high exponent.<sup>26</sup> At present we must assume that experimental difficulties, especially in the viscosity measurements, are the principal sources of the greater CCM-data divergencies from theory.

Figure 3 compares the film A and D solution viscosity data for both the benzene and CCM systems with the corresponding theoretical curves. Although in the above paragraph we emphasized the lack of fit of the CCM data with theory, it

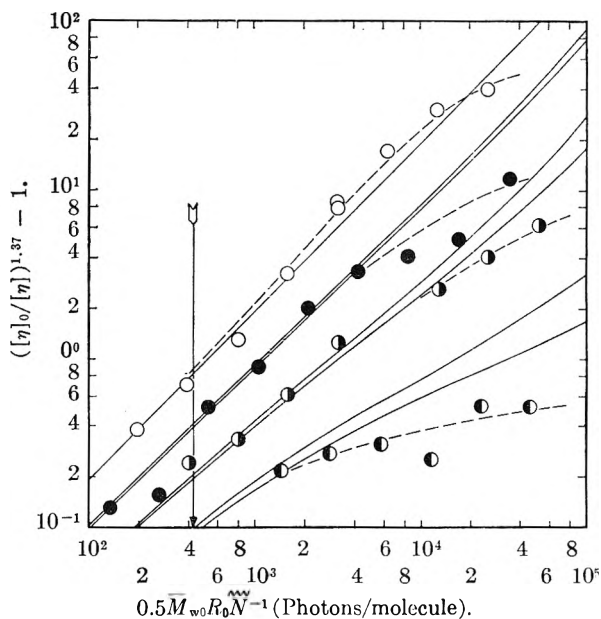


Fig. 1.—The number of new viscosity-average molecules per original viscosity average molecule,  $([\eta]_0/[\eta])^{1.37} - 1$ , plotted against the number of photons absorbed per original number-average molecule in the incident surface,  $0.5 \bar{M}_{w0} R_0 \bar{N}^{-1}$ . The solid lines are theoretical curves. Benzene solution-viscosity data for films A( $\circ$ ), B( $\bullet$ ), C( $\bullet$ ) and D( $\bullet$ ) are superposed.

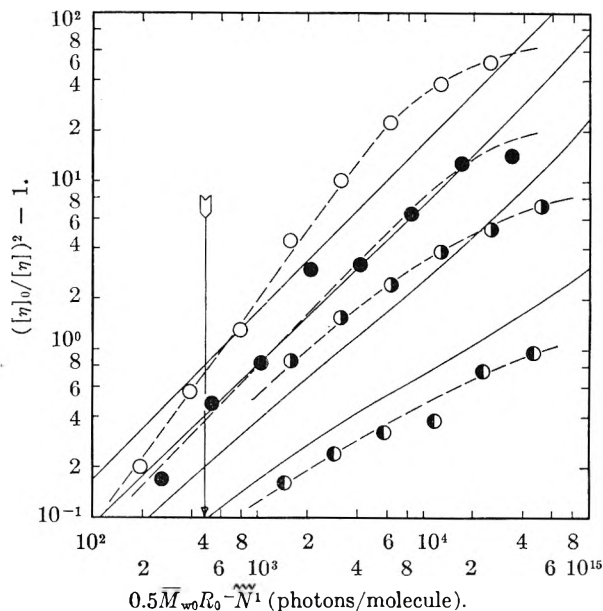


Fig. 2.—Same plot as Fig. 1 but for the butanone:isopropyl alcohol solution viscosity data. The viscosity-molecular weight exponent is  $a = 0.50$ . As in Fig. 1 the theoretical curves were calculated, top-to-bottom, for  $kL = 0.38, 1.97, 4.05$  and  $8.56$ , respectively.

should be noted that considerable correspondence does exist.

Real and understandable systematic deviations of experimental data from simple theory are apparent in Figs. 1, 2 and 3. Focussing attention upon Fig. 1 we note that the experimental curve for film A develops a gradual "positive" deviation from theory as exposure progresses, but finally exhibits "negative" deviation at the highest exposure. The film B and C data do not show deviations from

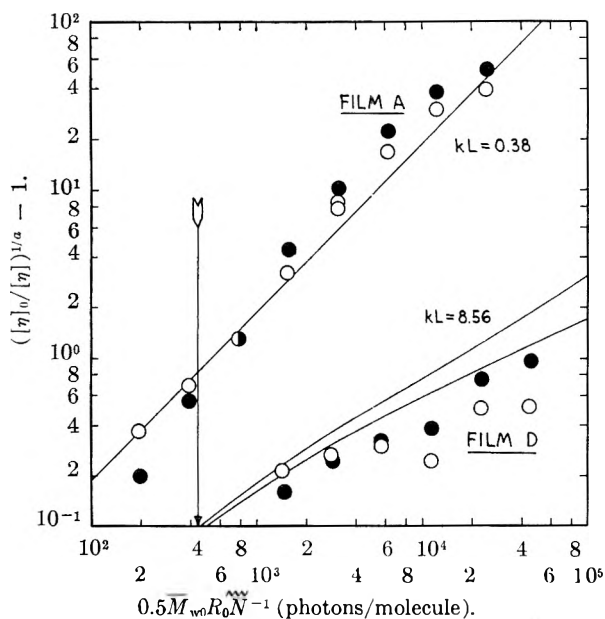


Fig. 3.—A combined plot of  $([\eta]_0/[\eta])^{1/a} - 1$  vs.  $0.5\varphi_d M_w R_0 \bar{N}^{-1}$  (theoretical) and vs.  $0.5M_w R_0 \bar{N}^{-1}$  (experimental) for films A and D benzene viscosity data (open circles) and butanone:isopropyl alcohol viscosity data (solid circles). The same horizontal translation of axes was made for all the data. The arrow indicates  $\varphi_d = 2.3 \times 10^{-3}$  scissions/absorbed photon.

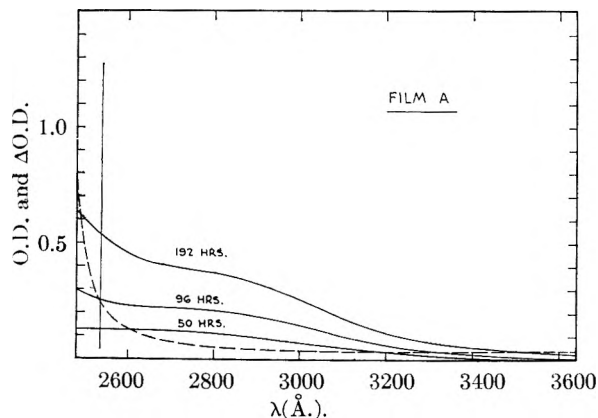


Fig. 4.—Original apparent optical density (broken line) and increases in optical density (solid lines) for a film A sample as functions of wave length and total 2537 Å. wave length light exposure times.

theory until high exposures are reached; they then deviate in a "negative" sense. Film D data exhibit "negative" deviations from theory at nearly all exposures studied. The cause of these systematic deviations is discovered by studying the changes in optical density occurring during the irradiation. Figure 4 shows the original apparent optical density curve (broken line) for a film A sample and the increases in optical density (solid lines) observed after chosen total irradiation times. Figure 5 is a similar plot for a thick film B sample over the same wave length region (2480–3640 Å.). A broad absorption peak centered at  $\sim 2850$  Å. and having an approximate width at half height of 900 Å. is produced by the 2537 Å. light irradiation (cf. Fig. 5). Exact peak location is prevented by the tail of the strong shorter wave length absorption. At 2537 Å. the apparent optical density

of the film B sample has the values 1.00, 1.28, 1.65 and 2.03 at 0, 50, 96 and 192 hours exposure, respectively. Apparent O.D. values at 2537 Å. of the film A sample are 0.22, 0.35, 0.48 and 0.76, at 0, 50, 96 and 192 hours exposure, respectively. An average film A sample therefore progressed from 32% absorption of the entering 2537 Å. light in the initial stages of irradiation to 80% adsorption of this light after 192 hours exposure. The near coincidence of the data at higher exposures with the theoretical curves (Fig. 1) is thus somewhat of an artifact. The light absorbed by the new chromophores is effective in polymer chain scission, thus producing an *apparent increase* in the degradation effectiveness with increasing exposure of the thin film A. The scission yield of this new absorption relative to the original absorbing structure is not, under present mathematical construction, calculable. It appears to be roughly comparable. Film D, which initially absorbed nearly 100% of the entering 2537 Å. light exhibits an *apparent decrease* in scission efficiency with increasing exposure. No sensible increase in total absorbed quanta could be caused by the new absorption. The more precipitous attenuation produced further skews the scission distribution in depth and decreases the number of scissions per viscosity-average molecule in the total polymer film. This effect, which is most readily discernible in the film D sample, becomes evident in all the films studied at high exposure.

The curve fitting method employed in Fig. 1 constitutes, in essence, a double extrapolation of the experimental results to the limit of zero film thickness and zero exposure. This minimizes the error introduced by the new absorbing groups into the calculated scission efficiency. Especially when the film thickness range and new absorber scission efficiency embrace the positive-to-negative apparent efficiency contribution is the introduced uncertainty minimized.

Inspection of the form of the new ultraviolet absorptions produced in films A and B reveals some interesting, although not definitive, characteristics. Film A does not show the formation of the well defined absorption peak near 2850 Å. which is noted in film B. The rise in absorption below 2700 Å. which is common to both films is more pronounced, relatively, in the thinner film and masks the 2850 Å. peak. The 2850 Å. peak may be associated with a ketonic or aldehydic carbonyl grouping in a volatile product. The broken dot-dash curve in Fig. 5 represents the 192 hr.-exposure film B sample after subsequent 70° heating for 13 hours under vacuum. The form of the resultant absorption curve approaches that of the thinner film.

The nature and origin of the new chromophores is open to speculation. If they are photooxidation products of the polymer structural units (this is possible since the film irradiations were conducted in air) they might or might not be necessary precursors to chain scission. The latter is believed true since no definite induction period is observed in the degradation. Oxygen might enter into the photochemical reaction which produces stabilized chain

ruptures from initial light-absorption activated chain units. This is neither proven nor disproven by the limited chemical evidence at hand. The possibility that the new absorptions might be due to methyl pyruvate produced by photooxidation of residual monomer in the polymer films was explored.<sup>28</sup> Although this source of the chromophore seemed logical, subsequent experiments proved that neither the magnitude nor the position of the new absorption could be explained on this basis.

The increased absorption by ultraviolet-irradiated PMMA in the near ultraviolet and blue region of the spectrum and the effect of certain additives upon it has been the subject of an optical and chemical analytical study.<sup>29</sup> This visible "yellowing" may be similar in chemical origin to that caused by high-energy electron irradiation.<sup>30</sup>

The quantum yield for random scission,  $\varphi_d = 2.3 \times 10^{-3}$ , found in the present study is comparable to quantum yields determined for ultraviolet-degradation of other solid polymers at or near room temperature.<sup>10</sup> It is in no manner comparable to the quantum yield, 0.1–0.2, reported for photo-initiation of PMMA depolymerization by 2537 Å. light in the 150–195° temperature range.<sup>7–9</sup> If these two processes originate in the same photochemical act, the greater mobility of the polymeric and low molecular weight-scission fragments at the elevated temperatures must be credited with cage-recombination prevention. There is reason<sup>8,31</sup> for belief that the photo-initiation of depolymerization occurred principally at some terminal end-groups of the PMMA chains. This belief is questionable when scrutinized in the light of the reported  $10^{-1}$  quantum yield. These investigators suggested reasonable end groups formed by disproportionation between two polymer radicals. One of the two terminal end groups (the saturated, hydrogen-atom acceptor) thus formed would have an ultraviolet-absorption coefficient indistinguishable from the repeating units in the chains. The other terminal end group (unsaturated, hydrogen-atom donor) should have an absorption coefficient at 2537 Å. essentially equal to monomeric methyl methacrylate which we measured for our monomer at 23° in chloroform to be  $k_{\text{MMA}}(2537 \text{ Å.}) = 1.71 \times 10^3 \text{ cm.}^{-1}$ . Considering, *e.g.*, a PMMA having a number-average degree of polymerization  $\overline{DP}_n = 1250$  only 1/2500 of the polymer units would be of this conjugated unsaturated ester structure. Since the  $k$  contributions of units in a mixture may be satisfactorily summed on a volume-fraction basis, the contribution of this terminal unit would be  $(1/2500) \times 1.71 \times 10^3 = 0.68$ . This is only 0.0185 of the over-all PMMA  $k(2537 \text{ Å.}) = 36.8$  value reported.<sup>8</sup> Even if the quantum yield for depolymerization initiation were unity for photons absorbed by such sites the observed quantum yield would be  $< 0.02$ . Extensive energy transfer from

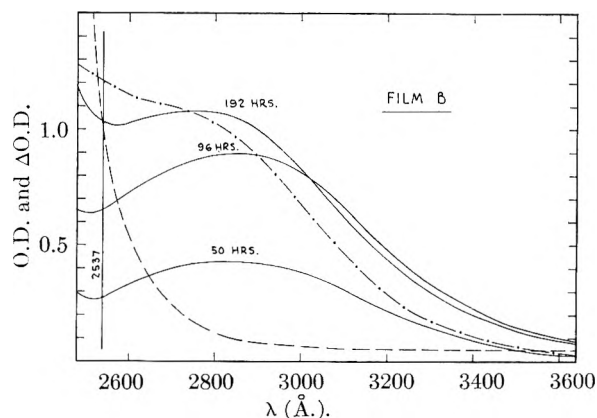


Fig. 5.—Original apparent optical density (lower broken line) and increases in optical density (solid lines) for a film B sample as functions of wave length and total 2537 Å. wave length light exposure times. The upper broken line is the residual optical density increase in the 192 hour sample after subsequent 70° heating for 13 hours under vacuum.

random absorption sites to the chain ends is not reasonable.

As mentioned previously (Experimental: Light Absorption Measurements) approximately one-half of the  $k(2537 \text{ Å.}) = 36.8 \text{ cm.}^{-1}$  value reported by Cowley and Melville<sup>7</sup> could be accounted for by aromatic initiator fragments on the *starting ends* of the PMMA chains. The quantum yield of  $10^{-1}$  for depolymerization initiation might then be explained by a depolymerization initiation efficiency of 0.2 for photons absorbed by these initiator fragments. This would require, however, that the polymer chain unzipping progress in the *same* chain direction as polymerization had occurred. Molecular reversibility of the two processes (polymerization and depolymerization) would thus not be represented. It would be very interesting to learn whether chain depropagation can be initiated and sustained in this directional sense. There is obviously another alternative explanation of end-initiated depropagation. Radicals produced from photolysis of the initiator fragment ends, or of other groups, may add into the disproportionation-produced terminal double bonds of the PMMA and initiate depropagation in the more conventionally expected manner.

It is of some interest to compare the total energy absorptions per chain scission,  $E_d$ , in PMMA undergoing sub-ionizing ultraviolet light irradiation and undergoing ionizing irradiation. High-energy and  $\gamma$ -rays produce scissions in PMMA at room temperature with  $E_d = 60$  electron volts.<sup>32–35</sup> A photon of 2537 Å. light has an energy of 4.88 e.v. A quantum yield of  $2.3 \times 10^{-3}$  therefore leads to  $E_d(2537 \text{ Å.}) = 2100$  e.v. On an energy absorbed basis ultraviolet light is much less efficient in this degradation process at room temperature than are ionizing radiations. In our present treatment of PMMA degradation by light we have assumed

(32) P. Alexander, A. Charlesby and M. Ross, *Proc. Roy. Soc. (London)*, **A223**, 392 (1954).

(33) A. R. Shultz, P. I. Roth and G. B. Rathmann, *J. Polymer Sci.*, **22**, 495 (1956).

(34) L. A. Wall and D. W. Brown, *J. Research Natl. Bur. Standards*, **57**, 131 (1956).

(35) A. R. Shultz, *J. Polymer Sci.*, **35**, 369 (1959).

(28) The author is indebted to Dr. C. E. Barnes for this suggestion.

(29) J. Haslam, S. Grossman, D. C. M. Squirrel and S. F. Loveday, *The Analyst*, **78**, 92 (1953).

(30) S. H. Pinner and A. J. Swallow, *Plastics (London)*, **22**, 194 (1957).

(31) R. Simha, *J. Polymer Sci.*, **9**, 465 (1952).

negligible chain-to-chain crosslinking during exposure. This is known to be true during PMMA degradation by ionizing radiations.<sup>33</sup> Moderate extents of concurrent crosslinking would not sensibly affect the viscosity-molecular weight observations.<sup>36,37</sup> A certain parallelism between effects of ionizing radiations and ultraviolet light on poly-alkyl-methacrylates might be remarked in passing. Increasing length of alkyl side chains in the homogeneous poly-*n*-alkyl-methacrylates favors increasing chain-to-chain crosslinking relative to backbone scission under ionizing radiation.<sup>35,38,39</sup> Beyond poly-*n*-hexyl methacrylate

(36) B. H. Zimm and R. W. Kilb, *J. Polymer Sci.*, **37**, 19 (1959).

(37) R. W. Kilb, *ibid.*, **38**, 403 (1959).

(38) R. K. Graham, *ibid.*, **38**, 209 (1959).

(39) A. R. Shultz, P. I. Roth and J. M. Berge, Paper presented at the 135th National American Chemical Society Meeting, Boston, Mass., April, 1959.

crosslinking predominates over scission and infinite networks are formed. A similar progression occurs in poly-alkyl-methacrylate films undergoing ultraviolet light irradiation in air; infinite network formation occurs at shorter side-chain lengths than under ionizing radiation conditions.<sup>40</sup> Quantitative investigations of polymer reactions under light and ionizing radiations should permit comparison beneficial to basic interpretations in both areas.

**Acknowledgments.**—The assistance of Mr. James B. Watrud in executing a large portion of the experimental work is gratefully acknowledged. The aid of Mr. Floyd C. Vincent in performing the ultraviolet spectrophotometric measurements is also appreciated.

(40) R. L. Feller, Mellon Institute of Industrial Research, private communication, May, 1957.

## KINETIC SALT EFFECTS BY THE TETRAALKYLAMMONIUM IONS

BY ANTONIO INDELLI

*Chemistry Department of the University of Ferrara, Ferrara, Italy*

*Received November 6, 1960*

The salt effects produced by tetraalkylammonium salts have been measured in five reactions involving anions. For the bromate-iodide and the iodate-iodide reactions the effects are in agreement with the Brønsted-Debye theory. For the ethyl oxalate-hydroxide reaction the effects are lower than normal. For the ferricyanide-iodide reaction the effects are opposite to those predicted by the Brønsted-Debye theory. The activated complexes have charges 0, -1, -2 and -5, respectively. These results are interpreted in terms of short range interactions, which are more important when the negative charge of the activated complex is high and when non-electrostatic factors are involved. The results for the bromoacetate-thiosulfate reaction are closer to the predictions of the Brønsted-Debye theory than those for the ethyl oxalate-hydroxide reaction. This fact is discussed on the basis of the absence of non-electrostatic factors, and of the organic character of the tetraalkylammonium salts.

Differences between the salt effects of the tetraalkylammonium and the alkali-metal salts have been reported in several occasions. In some cases these differences have been attributed to the failure of the tetraalkylammonium ions to form ion pairs with the reacting anions.<sup>1,2</sup> Association phenomena have been considered by Kurz and Gutsche too.<sup>3</sup> In some other instances the micelle formation by these large organic ions seems to be relevant.<sup>4</sup> Previous work on kinetic salt effects in reactions between anions seems to indicate that the higher the negative charge of the activated complex, the more anomalous the effects of the tetraalkylammonium salts. In the reaction of potassium ethylmalonate with sodium hydroxide tetraethylammonium nitrate has a smaller effect than sodium or potassium nitrate.<sup>5</sup> In the reaction of persulfate with iodide tetramethylammonium bromide has a much smaller accelerating effect than sodium or potassium chloride, and tetraethylammonium bromide has a still smaller effect, and has a retarding effect in a certain range of concentrations.<sup>6</sup> In the reaction of trimetaphosphate

with sodium hydroxide tetramethylammonium chloride has a retarding effect, in qualitative disagreement with the Brønsted-Debye theory on the salt effects.<sup>7</sup> Therefore we thought it interesting to study the salt effects of some tetraalkylammonium salts on a series of reactions of different charge type. In all cases solutions as dilute as possible were used, to minimize the differences in the activity coefficients arising from the different ionic radii.

### Experimental

**Materials.**—Most of the chemicals were Erba RP products and were recrystallized from conductivity water. Tetramethylammonium nitrate was prepared and purified as described in a previous paper.<sup>8</sup> Tetraethylammonium perchlorate was an Erba RS product, specially purified for polarographic use; it was found to be ash-free, neutral and with no buffer action. Tetra-*n*-butylammonium perchlorate was prepared from tetra-*n*-butylammonium bromide in aqueous solution, by precipitating with perchloric acid, and was recrystallized three times from conductivity water. Potassium ethyloxalate was prepared from the diethyl ester by the Nielsen's method,<sup>9</sup> and was recrystallized from absolute ethanol. Sodium bromoacetate was prepared by neutralizing an aqueous solution of monobromoacetic acid Erba RP, which had been standardized with sodium hydroxide; it was kept in a refrigerator and diluted just before use. It contained only a barely detect-

(1) R. M. Healy and M. L. Kilpatrick, *J. Am. Chem. Soc.*, **77**, 5258 (1955).

(2) J. R. VanWazer, E. J. Griffith and J. F. McCullough, *ibid.*, **77**, 287 (1955).

(3) J. L. Kurz and C. D. Gutsche, *ibid.*, **82**, 2175 (1960).

(4) E. F. J. Duynstee and E. Grunwald, *ibid.*, **81**, 4540, 4542 (1959).

(5) A. Indelli, G. Nolan, Jr., and E. S. Anis, *ibid.*, **82**, 3237 (1960).

(6) A. Indelli and J. E. Prue, *J. Chem. Soc.*, 107 (1959).

(7) A. Indelli, *Ann. Chim. (Rome)*, **48**, 332 (1958).

(8) A. Indelli, *ibid.*, **48**, 345 (1958).

(9) R. F. Nielsen, *J. Am. Chem. Soc.*, **58**, 206 (1936).

able trace of bromide ions. All the water used for the solutions and the runs was prepared as described in previous papers.<sup>6</sup>

**Procedures.**—The experiments on the reactions between bromate and iodide and between iodate and iodide were performed as described in previous papers.<sup>10,11</sup> The reaction between ferricyanide and iodide was followed by adding some starch to the reaction mixture and by titrating the iodine with a  $\text{Na}_2\text{S}_2\text{O}_3$  solution delivered from an "Aglar" microsyringe. Very small and almost constant amounts of titrating solution were added and the end-point was taken when the last amount failed to give any discoloration. The sharpness of the end-point was satisfactory and ten of such titrations were performed during each run, the total amount of added  $\text{Na}_2\text{S}_2\text{O}_3$  corresponding to about 0.4% of the ferricyanide. Preliminary experiments showed that no appreciable reaction of the ferricyanide with the thiosulfate or the tetrathionate did occur.

The reaction between potassium ethyloxalate and sodium hydroxide was followed with a method similar to that used for the reaction of potassium ethylmalonate with sodium hydroxide,<sup>6</sup> only minor modifications being introduced. The samples and the quenching solution of potassium hydrogen phthalate were measured by volume, whereas the titrations were performed with a weight buret. The color of the indicator during the titrations was compared with that of a buffer solution, freshly prepared, having exactly the same volume and the same indicator concentration. In this way more accurate end-points were obtained.

The reaction of sodium bromoacetate with sodium thiosulfate was also followed with a sampling technique. At suitable intervals 100-ml. samples of the reacting mixture were withdrawn from a polyethylene reaction bottle and were titrated with a 0.00032 *M* solution of iodine, the polarized platinum electrode being used as an indicator. The reaction was followed for eight to eleven days, which corresponded to about 30 to 40% reaction.

The temperature was kept to 25.0° with a water thermostat in all cases, but for the reaction bromoacetate-thiosulfate where an air thermostat was used. The accuracy was about 2 to 4% for the reactions iodate-iodide and bromate-iodide, 5 to 8% for the reaction ferricyanide-iodide, 2 to 3% for the reaction ethyloxalate-hydroxide and 1 to 2% for the reaction bromoacetate-thiosulfate.

## Results

Table I reports the rate constants for the five reactions in the presence of tetraalkylammonium salts, and for comparison the reaction rate constants obtained in the presence of potassium nitrate. The latter data are taken from previous papers.<sup>10-13</sup> The correlation with the charge of the activated complex is satisfactory, except in the case of the thiosulfate-bromoacetate reaction, and in fact the difference between potassium nitrate and the tetraalkylammonium salts increases when the charge of the activated complex increases. For the ferricyanide-iodide reaction, where the charge of the activated complex is  $-5$ ,<sup>12</sup> the salt effect is reversed. The results obtained by Kurz and Gutsche<sup>3</sup> and by Duynstee and Grunwald<sup>4</sup> are also in agreement with this general trend. The charge of the activated complex, however, is not the only influential factor. Actually the effects of the tetraalkylammonium salts on the bromoacetate-thiosulfate reaction are more normal than the corresponding ones in the persulfate-iodide reaction,<sup>6</sup> where the activated complex has the same charge of  $-3$ , and then those on the ethyloxalate-hydroxide reaction where the activated complex has charge  $-2$ . The effects on this last reaction are also less normal than those on the very similar reaction be-

tween ethylmalonate and hydroxyl ions.<sup>5</sup> It seems therefore that another important factor in determining these salt effects must be non-electrostatic in nature, and in fact activation energy measurements show that prominent non-electrostatic effects are present in the persulfate-reaction and absent in the bromoacetate-thiosulfate reaction.<sup>14-17</sup> On the other hand the presence of non-electrostatic effects in the ethyloxalate-hydroxide reaction is also suggested by the abnormal salt effects by multivalent cations,<sup>18</sup> and by the geometry of the activated complex.<sup>14</sup> The same considerations suggest that the non-electrostatic effects should be more important in this reaction than in the ethylmalonate-hydroxide.

The tetramethylammonium nitrate has a remarkable accelerating action on the bromoacetate-thiosulfate reaction. This could be correlated with the organic nature of the cation, as it is known that this reaction is accelerated by organic substances,<sup>19</sup> and shows also abnormal salt effects in the presence of large organic anions.<sup>20</sup> On the other hand tetraalkylammonium and other large organic ions have abnormal salt effects on some first-order reactions.<sup>21,22</sup>

## Discussion

The simplest interpretation of the above results is that the greater the negative charge of the activated complex, the greater is the importance of the short range actions on the part of the cations. The presence of non-electrostatic effects should enhance the importance of the short range actions because the decrease in the repulsion between the reactants, or the increase of probability of formation of the activated complex, is accompanied by a decrease of the intrinsic energy barrier which must be overcome to form the products.<sup>14</sup> A polarization of the reactants or of the activated complex seems to be a reasonable explanation for these non-electrostatic effects. A similar phenomenon has been postulated to account for some salt effects in the aromatic nucleophilic substitution reactions.<sup>23</sup> The tetraalkylammonium ions, because of their large size, cannot have a great short range action, and therefore cannot have an accelerating action comparable to that of the smaller sodium or potassium ions. Moreover, due to their polarizability, they can cluster around a highly charged activated complex and prevent the smaller ions to get near enough the activated complex to exert any appreciable short range action. A rather similar mechanism has been postulated by Davies and Dwyer to explain the retarding action that large anions and

(13) A. Indelli, *ibid.*, 1, 143 (1960).

(14) A. Indelli and E. S. Amis, *J. Am. Chem. Soc.*, 82, 332 (1960).

(15) H. G. Davis and V. K. LaMer, *J. Chem. Phys.*, 10, 585 (1942).

(16) P. A. H. Wyatt and C. W. Davies, *Trans. Faraday Soc.*, 45, 774 (1949).

(17) C. W. Davies and I. W. Williams, *ibid.*, 54, 1547 (1958).

(18) J. I. Hoppé and J. E. Prue, *J. Chem. Soc.*, 1775 (1957).

(19) V. K. LaMer and M. E. Kammer, *J. Am. Chem. Soc.*, 57, 2669 (1935).

(20) J. A. Erikson and E. C. Lingafelter, *J. Colloid Sci.*, 4, 591 (1949); 10, 71 (1955).

(21) J. P. Hunt and R. A. Plane, *J. Am. Chem. Soc.*, 76, 5960 (1954).

(22) A. Jensen, F. Basolo and H. M. Neumann, *ibid.*, 80, 2354 (1958).

(23) J. D. Reinheimer, W. F. Kieffer, S. W. Frey, J. C. Cochran and E. W. Barr, *J. Am. Chem. Soc.*, 80, 164 (1958).

(10) A. Indelli, G. Nolan, Jr., and E. S. Amis, *J. Am. Chem. Soc.*, 3233 (1960).

(11) A. Indelli, *J. Phys. Chem.*, 65, 240 (1961).

(12) A. Indelli, *Ann. univ. Ferrara Nuova Serie*, 1, 129 (1960).

TABLE I  
 REACTION RATE CONSTANTS IN THE PRESENCE OF TETRAALKYLAMMONIUM SALTS

Reactants concn. <sup>a</sup> and units of $k'$	Added salt concn. <sup>a</sup>	$k'$ in presence of			
		KNO <sub>3</sub>	Me <sub>4</sub> NNO <sub>3</sub>	Et <sub>4</sub> NClO <sub>4</sub>	Bu <sub>4</sub> NClO <sub>4</sub>
KBrO <sub>3</sub> = 8.3; KI = 25; HNO <sub>3</sub> = 25; $k' = 10^{-2} k$ (1.3 equiv. <sup>-3</sup> sec. <sup>-1</sup> ); $k'_0 = 7.24^b$	100	6.1		6.14	
	200	5.6		5.45	
KIO <sub>3</sub> = 0.83; KI = 3.75; HNO <sub>3</sub> = 5.0; $k' = 10^{-9} k$ (1.4 equiv. <sup>-4</sup> sec. <sup>-1</sup> ); $k'_0 = 6.4^b$	20	5.8	5.8	5.7	
	40	5.4	5.3	5.4	
	100	4.81	4.72	4.77	
	200	4.17	4.14	4.14	
	200	2.69	2.40	2.45	
K <sub>3</sub> Fe(CN) <sub>6</sub> = 100; KI = 400; $k' = 10^4 k$ (1.2 equiv. <sup>-2</sup> sec. <sup>-1</sup> ); $k'_0 = 2.45^b$	400	3.31	2.44	1.92	
	800	3.97	2.06	1.43	
	1600	5.3	1.99	0.56	
	16	5.62	5.94	5.81	5.84
Na <sub>2</sub> S <sub>2</sub> O <sub>3</sub> = 1.5; BrCH <sub>2</sub> COONa = 1.5; $k' = 10^3 k$ (1. equiv. <sup>-1</sup> sec. <sup>-1</sup> ); $k'_0 = 5.21^b$	40	6.28	6.43	6.25	6.17
	80	6.86	7.21	6.83	
	160	7.92	8.06	7.49	
	53	5.61	5.63	5.60	5.46
EtC <sub>2</sub> O <sub>4</sub> K = 8.3; NaOH = 8.3; $k' = 10 k$ (1. equiv. <sup>-1</sup> sec. <sup>-1</sup> ); $k'_0 = 5.21^b$	107	5.97	5.79	5.72	
	213	6.52	5.91	5.86	
	427	7.02	6.36	6.16	

<sup>a</sup> Concentration units = 10<sup>-4</sup> mole l.<sup>-1</sup>. <sup>b</sup>  $k'_0 = k'$  in the absence of added salt.

cations have on the racemization of tris-dipyridyl-nickel.<sup>24</sup>

The short range actions can, to a certain extent be considered as due to ionic association,<sup>6,7,25,26</sup> and if this model is assumed the action of the tetraalkylammonium salts can be considered as a "secondary salt effect." In fact one can say that the "dissociation constant" of the "ion pairs" has been increased by the presence of the tetraalkylammonium ions. However, the consistent difference between the action of the tetraethyl- and the tetramethylammonium salts is conflicting with this interpretation. It might be interesting to observe that tetraalkylammonium and perchlorate ions are often used in kinetic work to avoid the formation of ion pairs with reacting anions and cations, respectively: both of these kind of salts have often a "salting in" effect on non-electrolyte solutions.<sup>27</sup>

(24) N. R. Davies and F. P. Dwyer, *Trans. Faraday Soc.*, **50**, 24 (1954).

(25) E. A. Guggenheim, *Disc. Faraday Soc.*, **24**, 53 (1957).

(26) G. Scatchard, *Natl. Bur. Standards (U. S.), Circ. No.*, **534**, 185 (1953).

These results do not seem to support the Olson and Simonson claim that either the Brønsted original equation or the Debye-Hückel theory is unsound.<sup>28</sup> They show once more, however, that the combination of the two leads to a rather poor approximation, which in many cases, and particularly for reactions between ions of the same sign, cannot be useful. The treatment of Scatchard can probably account for part of the unusual salt effects exhibited by the tetraalkylammonium ions, because of the great importance that the ionic radii have in this calculation,<sup>26</sup> but a consideration of the non-electrostatic effects seems also necessary. Therefore the salt effects can depend both upon the structure and the charge of the activated complex, so that they can probably give useful indications on the mechanism of many ionic reactions.

**Acknowledgments.**—Thanks are due to Ambrogio Giacomelli for valuable assistance with the experiments.

(27) F. A. Long and W. F. McDevit, *Chem. Revs.*, **51**, 119 (1952).

(28) A. R. Olson and T. R. Simonson, *J. Chem. Phys.*, **17**, 1167 (1949).



# INTERACTIONS OF DIPOLAR IONS WITH IONIZED POLYMERS. ELECTROSTATIC AND SPECIFIC EFFECTS

BY JEHUDA FEITELSON

*Department of Physical Chemistry, The Hebrew University, Jerusalem, Israel*

*Received November 19, 1960*

The purely electrostatic interactions between a highly swollen cation-exchange resin and large dipolar molecules (amino acids) were calculated and compared with the values derived from chromatographic data. As this resin approximates the model of a fairly dilute polyelectrolyte solution studied by Fuoss, Katchalsky and Lifson, their theory was used to estimate the electrostatic field in the resin gel. Glycine,  $\beta$ -alanine,  $\gamma$ -aminobutyric acid, diglycine and leucine were only slightly attracted by the polyelectrolyte chains in agreement with the calculated interactions. Phenylalanine, however, was strongly attracted by the polymer chains a specific effect which may be due to short range forces between the benzene rings of the resin and that of phenylalanine.

## Introduction

The electrochemical properties of high polymers influence both their thermodynamic properties<sup>1</sup> and their reactivity, especially with ionized reactants.<sup>2</sup> The electrostatic interactions involved, which are particularly interesting to biochemists and investigators of synthetic polymers, are not restricted to ions; polar molecules also should be affected by the powerful electrostatic fields. In that event, the behavior and, therefore, the reactivity of many uncharged molecules should be influenced by the presence of ionized polymers.

We have investigated the purely electrostatic polyion-dipole interactions in an ion-exchange resin of very low crosslinkage. Such resins are highly swollen in very dilute salt solutions because of osmotic forces, and their polyelectrolyte chains between crosslinkages approximate stretched polymer chains. The electrostatic field of such molecules has been evaluated,<sup>3,4</sup> and this model was used in our study. We choose amino acids at their isoelectric point as the dipole species because of their large dipole moments and because of the possible importance of such interactions in biological systems; following the advances in protein biosynthesis, for instance, the interactions of DNA and RNA with amino acids have recently been studied.<sup>5,6</sup>

The concentration of dipolar molecules as a function of their distance from the polyion in the resin has been estimated, and the average concentration in the gel compared to that in the ambient solution.

The interactions between small molecules and polymers are often investigated by equilibrium dialysis<sup>5,6</sup> and characterized by interaction constants. Only very strong interactions can be observed by this method since it depends on the change of concentration in an appreciable volume caused by the presence of polymer in a dilute solution.

On the other hand, in multi-plate chromato-

graphic columns the effect is very much enhanced during successive equilibria along the column. The ionized resin is the stationary phase, and even weak interactions exert an observable effect on the rate of advancement of the solute band. This method has been employed here.

## SYMBOLS

$a$	radius of polyelectrolyte rod
$h$	length of polyelectrolyte rod
$r$	distance from rod center to center of dipolar molecule
$R$	half the distance between the centers of two rods; $\pi R^2 h =$ volume per rod in soln.
$\varphi$	angle between field and direction of dipole
$\psi$	electrostatic potential
$C_0$	concn. of dipoles at $d\psi/dr = 0$
$C_r$	actual dipole concn. at distance $r$ from rod
$f$	activity coefficient of dipolar ion
$e$	the elementary charge
$l$	charge separation
$\mu$	dipole moment = $e \times l$
$h$	length of polyion rod

The subscripts "i" and "o" denote the inner-resin and outer-solution phases, respectively.

## Theoretical

The following model was adopted: The polyelectrolyte chains are pictured as parallel cylindrical rods carrying the uniformly distributed charge of the actual polymer of equal length. The counterions assume a Boltzmann distribution in the liquid surrounding the charged rod, thus preserving electroneutrality. The potential field of such a system in the absence of added salt has been evaluated by Fuoss, Lifson and Katchalsky<sup>3</sup> and independently by Alfrey, Berg and Morawetz<sup>4</sup>; The expression for the electrostatic potential is given by<sup>3</sup>

$$\psi(r) = \frac{kT}{e} \ln \left\{ \frac{2\lambda}{|\beta|^2} \frac{r^2}{R^2 - a^2} \sin^2(|\beta| \ln Ar) \right\} \quad (1)$$

where  $\lambda$  is a parameter dependent on the charge density, and  $\beta$  and  $A$  are integration constants.

It is assumed that the addition of a small amount of dipolar molecules of a concentration much lower than that of the gegenions does not influence the electrical potential appreciably. The dielectric constant throughout the solution is assumed to be uniform and to equal that of the solvent.

The electrostatic energy of a dipole of charge separation  $l$  in the polyelectrolyte field at a point  $r$  is

$$W_r = e\psi_{r-l \cos \varphi/2} - e\psi_{r+l \cos \varphi/2} = e(d\psi/dr)_r l \cos \varphi = (d\psi/dr)_r \mu \cos \varphi \quad (2)$$

which is valid as a first approximation for small

(1) Summarized by R. A. Marcus, *J. Chem. Phys.*, **23**, 1056 (1955).

(2) H. E. Deuel, "Kolloidische Untersuchungen an Pektinstoffen," ETH Zurich, 1943; A. Katchalsky and J. Feitelson, *J. Polymer Sci.*, **13**, 385 (1954); H. Landenheim, B. M. Loebel and H. Morawetz, *J. Am. Chem. Soc.*, **81**, 20 (1959).

(3) R. M. Fuoss, A. Katchalsky and S. Lifson, *Proc. Natl. Acad. Sci. U. S.*, **37**, 579 (1951).

(4) T. Alfrey, P. W. Berg and H. Morawetz, *J. Polymer Sci.*, **7**, 543 (1951).

(5) G. Zubay and P. Doty, *Bioch. Biophys. Acta*, **29**, 47 (1958).

(6) Ch. D. Jardetzky, *J. Am. Chem. Soc.*, **80**, 1125 (1958).

charge separations. The value of  $(d\psi/dr)_r$  can be found by differentiating eq. 1

$$(d\psi/dr)_r = (2kT/\epsilon r)(1 + |\beta \cot \beta| \ln Ar) \quad (3)$$

If a Boltzmann distribution in the polyelectrolyte field is assumed, the concentration of dipoles, with their axes at an angle  $\varphi$  to the field, at a distance  $r$  from the rod is

$$C_r = C_0 \exp\left(-\frac{d\psi}{dr} \frac{\mu \cos \varphi}{kT}\right)$$

Taking all possible dipole orientations into account, we find the concentration of dipoles at  $r$  by integrating over the angle  $\varphi$

$$C_r = C_0/2 \int_0^\pi \exp\left(-\frac{d\psi}{dr} \frac{\mu \cos \varphi}{kT}\right) \sin \varphi d\varphi = \\ C_0/2 \int_{-1}^1 \exp\left(-\frac{d\psi}{dr} \frac{\mu \cos \varphi}{kT}\right) d \cos \varphi$$

This assumes that the energy of each dipole is independent of whether its inclination towards the field is in the plane of the cylinder axis or in any other plane; therefore the effect of the curvature of the polymer rod is neglected. It has been found,<sup>7</sup> however, that this factor has only a small effect on our calculations.

In this case integration over  $\cos \varphi$  yields

$$C_r = C_0 \sinh\left(\frac{d\psi}{dr} \frac{\mu}{kT}\right) / \frac{d\psi}{dr} \frac{\mu}{kT} \quad (4)$$

The amount of dipoles in the polyelectrolyte gel  $N$  is given by integrating over the volume of the gel penetrable by dipoles

$$N = \int_a^R C_r 2\pi r h dr = \\ C_0 2\pi h \int_a^R \left[ \sinh\left(\frac{d\psi}{dr} \frac{\mu}{kT}\right) / \frac{d\psi}{dr} \frac{\mu}{kT} \right] r dr \quad (5)$$

The amount of dipoles in a similar volume of solution at  $d\psi/dr = 0$  is therefore

$$N_0 = \int_a^R C_0 2\pi r h dr = C_0 \pi h (R^2 - a^2)$$

The average concentration in the ion-exchange gel can be defined as

$$C_i = \int_a^R C_r 2\pi r h dr / \int_a^R 2\pi r h dr \quad (6)$$

while the concentration in the ambient solution is  $C_0$ . The distribution coefficient between resin and solution is

$$K_o^i = C_i/C_0 = 2\pi h \int_a^R C_r r dr / 2\pi h C_0 \int_a^R r dr = \\ \frac{\int_a^R \left[ \sinh\left(\frac{d\psi}{dr} \frac{\mu}{kT}\right) / \frac{d\psi}{dr} \frac{\mu}{kT} \right] r dr}{1/2(R^2 - a^2)} \quad (7)$$

The integral has been evaluated numerically for different values of  $l$ .

The boundaries of integration must be further specified. The volume per rod available to dipolar ions is  $(R^2 - a^2)/\pi h$ . Here  $R$ , the average mid-distance between two rod centers, is defined by Lifson and Katchalsky<sup>8</sup> by

$$C_m = 1000/\pi b R^2 N \quad (8)$$

where  $C_m$  is the monomolar polymer concentration and  $b$  the length of the monomer unit. Instead of

(7) J. Feitelson, unpublished results.

(8) S. Lifson and A. Katchalsky, *J. Polymer Sci.*, **13**, 43 (1954).

summing over all the polyelectrolyte molecules in the gel, we have integrated over the volume of the gel shaped as one long cylinder of potential distribution similar to that in the gel. The dipolar molecules are free to achieve any orientation in the range  $r = a + l/2$  to  $r = R$ , but between  $r = a$  and  $r = a + l/2$  the rotation is restricted so that  $\cos \varphi$  can have values only between  $+2(r - a)/l$  and  $-2(r - a)/l$ . For the latter range,  $(d\psi/dr) \cdot (\mu/kT)$  in eq. 5 becomes

$$\frac{d\psi}{dr} \frac{\mu}{kT} \frac{2(r - a)}{l} = 2 \frac{d\psi}{dr} \frac{\epsilon(r - a)}{kT}$$

The integration of eq. 5 and 7 should therefore be carried out in two parts, from  $a$  to  $a + l/2$  and from  $a + l/2$  to  $R$ .

Since the dipolar molecules have no net charge, their activities in the resin and in solution are equal at equilibrium

$$C_i f_i = C_o f_o$$

and

$$K_o^i = C_i/C_o = f_o/f_i$$

yields the activity coefficient ratio. If the experimental value of this ratio agrees with the calculated one and the differences for different dipolar ions depend on the respective dipole moments only, it can be assumed that the activity coefficients in the resin are determined mainly by electrostatic forces. Specific group interactions should change the ratio appreciably.

It has been shown previously that the distribution of a substance between an ion-exchange resin and solution can be determined by chromatography.<sup>9</sup> The distribution coefficient is given by

$$K_o^i = (\Delta V/\Delta X - \delta)/(1 - \delta)$$

where  $\Delta V$  is the eluant volume needed for the elution of the maximum of the band,  $\Delta X$  is the volume of the column and  $\delta$  the void volume fraction of the column.

If a part of the resin volume is inaccessible to solute molecules, as is the volume occupied by the polyelectrolyte rods in our model, the expression becomes

$$K_o^i = (\Delta V/\Delta X - \delta)/(1 - \delta - \delta') \quad (9)$$

where  $\delta'$  denotes the volume occupied by the polymer rods in 1 ml. of column.

The value of  $K_o^i$  for dipolar ions can therefore be calculated by eq. 7 and also determined chromatographically, *i.e.*, from the distribution of dipoles between the polymer phase and the ambient solution.

**Methods and Materials.**—The ion-exchange resin employed was a Zeokarb-225 preparation, nominally containing 1% divinylbenzene, supplied by the Permutit Co. Ltd. of London. The average diameter of the beads was 70  $\mu$ . Its exchange capacity, determined by displacing the  $H^+$  ions from a known amount of resin in a column and titrating the acid with sodium hydroxide was 0.53 meq. per ml. of swollen polymer. The water content, which was measured by drying a sample of fully swollen resin *in vacuo* at 110° to constant weight, was 92% by weight.

To measure the void volume fraction  $\delta$ , the water held between the resin particles was separated by centrifugation.<sup>9</sup> The value obtained,  $\delta = 0.34-0.36$ , was checked by measuring the elution volume of cysteic acid at pH 6.5, which is a negatively charged molecule at this pH. Thus, it does

(9) J. Feitelson, *Arch. Biochem. and Biophys.*, **79**, 177 (1959).

not enter the negative resin at very low salt concentration and appears in the eluate after  $\Delta X \times \delta$  ml.

**Chromatography.**—Since the adsorption of dipolar ions is weak, the elution volumes  $\Delta V$  of our substances differed very little from the column volume  $\Delta X$ . It was therefore important to measure the elution volumes precisely. A resin slurry in equilibrium with buffer was allowed to settle to a height of about 105 cm. in columns of 1 cm. diameter with sintered glass at the bottom. After additional buffer had flowed through the column, the height of resin was marked and the column loaded with about 0.2 ml. of 0.05–0.08% solution of the dipolar ion. Elution with buffer was started, and the effluent obtained from the time of introduction of the solute to the appearance of the dipolar ion was collected in a weighed measuring cylinder; then successive 1-ml. fractions were collected and analyzed by the ninhydrin method according to Moore and Stein.<sup>10</sup> The volume of all fractions was determined gravimetrically; blanks were run to determine the loss by evaporation. The flow rate was about 2.5 ml. per hour, *i.e.*, 3.2 ml./hour/cm.<sup>2</sup> of column cross-section and the temperature was  $25 \pm 2^\circ$ .

$\Delta X$  was found by calibration of the empty columns with water to the previously mentioned mark (resin height).

The buffer solution, prepared from Analar-grade sodium phosphate and triply distilled water, was 0.02 *N* in  $\text{Na}^+$  ions. The amino acids and peptide were obtained from the Nutritional Biochemicals Co.

### Results and Discussion

By using the theory of Fuoss, Katchalsky and Lifson,<sup>3</sup> we can plot the electrostatic potential near the ion-exchange polyelectrolyte chains. In our experiments the polyelectrolyte concentration in the gel was 0.53 meq./ml. and  $R$  as given by eq. 8 is 19.6 Å. A diameter of 6 Å. for the rods seems to be a reasonable value and the relevant parameter  $\gamma$  was therefore 1.888. With  $\lambda = 2.830$ ,  $\beta$  and  $A$  in eq. 1 can be found from the theory;  $d\psi/dr$  was estimated by eq. 3. Approximate values for the dipole moments, calculated from dielectric increment data,<sup>11</sup> are given along with the charge separations in the dipolar ions in Table I.

TABLE I

DIPOLE MOMENTS  $\mu$  AND CHARGE SEPARATIONS  $l$  OF DIPOLAR IONS

	$\mu$ (Debye)	$l$ , Å.
Glycine	15.2	3.1
Leucine	15.8	3.2
$\beta$ -Alanine	18.7	3.9
$\gamma$ -Aminobutyric acid	22.6	4.7
Diglycine	26.5	5.5

TABLE II

DISTRIBUTION COEFFICIENTS AND INTERACTION ENERGIES OF DIPOLAR IONS IN AN ION-EXCHANGE RESIN

	$K_o^i$ calcd. for (a) = 0.1 Å.	$RT \ln f_i/f_o$ cal./mole	$K_o^i$ calcd. for (a) = 1.0 Å.	$RT \ln f_i/f_o$ cal./mole	$K_o^i$ obsd.	$RT \ln f_i/f_o$ cal./mole obsd.	$K_o^i$ obsd. $K_o^i$ calcd.
Glycine	1.09	51	1.05	29	1.08	47	1.02
Leucine	1.10	56	1.05	29	1.10	56	1.04
$\beta$ -Alanine	1.17	94	1.08	47	1.10	56	1.02
$\gamma$ -Aminobutyric acid	1.31	161	1.11	62	1.12	69	1.01
Diglycine	1.34	180	1.15	83	1.19	105	1.03
Phenylalanine			$\leq 1.10$		1.55	260	1.45

<sup>a</sup>  $r_{\min}$  is the shortest distance between the center of the dipole or charged group and the center of the polyelectrolyte rod.

The dipolar molecules discussed here have a certain volume. The charges are embedded in the bulk near the ends. Therefore, the distance of closest approach of the center of the molecule or a charged group to the polyelectrolyte rod was assumed to be 1 Å.;  $r_{\min} = a + 1$  Å. For comparison values are also given for an approach of 0.1 Å. Inspection of the potential curve shows that

even for molecules with large dipole moments, the linear approximation expressed in eq. 1 holds well except for an approach nearer than 1 Å.; therefore eq. 1 was used throughout. Using Simpson's rule, we estimated the integral in eq. 7 from  $a + 1$  to  $a + l/2$ , and separately from  $a + l/2$  to  $R$ ; dividing by  $1/2[R^2 - (a + 1)^2]$  gave the distribution coefficients. The interaction energies were expressed as  $RT \ln f_i/f_o$ . The experimental values of  $K_o^i$  were estimated from the measured elution volumes by eq. 9.  $\delta$  was taken to be  $\pi a^2 h / \pi R^2 h = 0.025$ . The experimental error in  $K_o^i$  is not more than  $\pm 0.02$ .

A polyelectrolyte chain is of course not a cylindrical rod and the model adopted is, therefore, only a crude approximation for an ion-exchange resin in a dilute buffer solution. The latter is essential in our experiments to maintain the system at a constant *pH*. Because of the Donnan equilibrium set up between resin and solution it can, however, be assumed that the free salt concentration in the resin will not exceed a few thousandths normal when in contact with 0.02 *N*  $\text{Na}^+$  ions. This low free salt concentration in the resin should not alter the potential appreciably.

Dipolar ions can undergo both acidic and basic dissociation. Since the cationic form is strongly adsorbed and the anionic form repelled by our resin, the presence of either would greatly influence the chromatography. At the isoelectric point both influences cancel to some extent and if the basic and acidic *pK*'s are far enough apart, the absolute amounts of the ionic forms will be negligible. To make sure that we were not measuring ionic effects, experiments were carried out at different *pH*'s in the vicinity of the isoelectric point in the resin.<sup>12</sup> If a change of 1 *pH* unit gives rise to no change in absorption, it can safely be assumed that practically no ionic interactions are involved; change of 1 *pH* unit alters the concentration of the ionic form and thereby the contribution of its distribution coefficients by a factor of 10.

The results in Table II show that the dipolar molecules are only slightly attracted by the resin;

both the calculated and observed values of  $K_o$

(10) S. Moore and W. H. Stein, *J. Biol. Chem.*, **176**, 367 (1948).

(11) E. J. Cohn and J. T. Edsall, "Proteins Amino Acids and Peptides," Reinhold Publ. Corp., New York, N. Y., 1943, pp. 147, 152, 296.

(12) The *pH* in the cationic resin is lower than that in the ambient solution, the difference being governed chiefly by the predominant  $\text{Na}^+$  ion distribution between the two phases. Since, however, only concentrations can easily be measured but activities are involved in the Donnan equation, the real *pH* difference is not known.

are close to unity. There is some tendency for  $K_o^i$  to increase with the dipole moment. Since many assumptions are involved, too much significance should not be attached to the absolute values of  $K_o^i$  and the interaction energies. The agreement with the calculated values under these conditions is very good. It indicates that in these cases purely electrostatic forces prevail and that a distance of a closest approach to the rod of 1 Å. is a good assumption. The data also show that the isopropyl side chain of leucine does not appreciably influence its absorption. On the other hand, the comparatively high distribution coefficient observed for phenylalanine, which has a dipole moment similar to that of glycine, shows clearly that here specific forces play an important part. These forces are probably of the nature of interactions between benzene rings.

In a comparison of our results with the sequence of elution peaks in a Moore and Stein amino acid separation,<sup>13</sup> some points must be borne in mind. One of the factors governing the separation of

(13) S. Moore and W. H. Stein, *J. Biol. Chem.*, **211**, 893 (1954); *Anal. Chem.*, **30**, 1185 (1958).

amino acids is the difference in their dissociation constants. This has no influence on our experiments since they were conducted at the respective isoelectric points of the dipolar ions. The so-called sieve effects, caused by the limited pore sizes of crosslinked resins can be assumed to be absent in our highly swollen resin. The relatively slow elution of phenylalanine which we observed is less prominent in the Moore and Stein separations<sup>11</sup>; in the latter this effect may be overshadowed by other factors. Also at the lower temperatures of our experiments, benzene ring interactions may be more pronounced.

The data also show that from interactions like the ones described here, between a highly charged polymer and large dipolar molecules, no great changes of concentration are to be expected. No strong dipole binding is observed unless specific forces are involved. However, interactions of this kind may play a part in polymer reactivity since the concentration of dipolar ions near the polyelectrolyte chain is appreciably increased;  $(d\psi/dr)(\mu/kT) = 2.1$  means a twofold increase in concentration (see eq. 4). This should be taken into account in any consideration of reaction rates.

## KINETICS OF THE CATALYTIC ISOMERIZATION-DEHYDROISOMERIZATION OF METHYLCYCLOPENTANE

By J. H. SINFELT AND J. C. ROHRER

*Esso Research and Engineering Company, Linden, New Jersey*

*Received November 23, 1960*

The kinetics of isomerization-dehydroisomerization of methylcyclopentane to form cyclohexane and benzene over a platinum-on-alumina catalyst were investigated at 427 and 471°, at hydrogen pressures ranging from 0 to 20 atm. and methylcyclopentane pressures ranging from 0.1 to 10 atm. The reaction rate was found to pass through a maximum with increasing hydrogen pressure. In the absence of hydrogen no isomerization-dehydroisomerization to cyclohexane and benzene could be detected. It is suggested that at low hydrogen pressures the reaction rate is limited by the dehydrogenation activity of the catalyst, with the primary function of the hydrogen being to keep the platinum free of surface residues. At sufficiently high hydrogen pressures, however, it is suggested that the acid activity of the catalyst is controlling. The rate then decreases with increasing hydrogen pressure because of the inverse effect of hydrogen on the equilibrium concentration of methylcyclopentene intermediates.

### Introduction

The isomerization of saturated hydrocarbons in the presence of hydrogen over metal-acidic oxide catalysts is a well-known reaction.<sup>1-3</sup> The metal-acidic oxide catalysts have been termed dual-function catalysts. The metal, usually platinum or nickel, is a source of hydrogenation-dehydrogenation activity, while the support, for example, alumina or silica alumina, imparts acidic properties to the catalyst. Considerable experimental evidence has been accumulated which indicates that isomerization of saturated hydrocarbons over these catalysts proceeds *via* olefin intermediates.<sup>4-7</sup>

According to this mechanism, olefins are generated on metal dehydrogenation sites, from which they migrate to acidic sites to isomerize. Either the dehydrogenation or the acidic function of the catalyst may be limiting, depending on the catalyst and reaction conditions.

The role of hydrogen in isomerization appears somewhat complex. On the one hand, increasing hydrogen pressure was found to decrease the rate of isomerization of *n*-pentane over a Pt-Al<sub>2</sub>O<sub>3</sub> catalyst at 372°. On the other hand, Ciapetta and Hunter<sup>1</sup> found that, in the complete absence of hydrogen, nickel-silica-alumina catalysts show no activity for isomerization. Thus, two opposite effects of hydrogen have been observed.

In the present paper, kinetic data are presented for the isomerization - dehydroisomerization of methylcyclopentane to form cyclohexane and benzene over a Pt-Al<sub>2</sub>O<sub>3</sub> catalyst. In view of the complicated nature of the role of hydrogen suggested in previous studies on paraffin isomerization, the kinetics were investigated over a wide range

(1) F. G. Ciapetta and J. B. Hunter, *Ind. Eng. Chem.*, **45**, 147 (1953).

(2) F. G. Ciapetta, *ibid.*, **45**, 159 (1953).

(3) H. Heinemann, G. A. Mills, J. B. Hattman and F. W. Kirsch, *ibid.*, **45**, 130 (1953).

(4) F. G. Ciapetta, *ibid.*, **45**, 162 (1953).

(5) G. A. Mills, H. Heinemann, T. H. Milliken and A. G. Oblad, *ibid.*, **45**, 134 (1953).

(6) P. B. Weisz and E. W. Swegler, *Science*, **126**, 31 (1957).

(7) J. H. Sinfelt, H. Hurwitz and J. C. Rohrer, *J. Phys. Chem.*, **64**, 892 (1960).

of hydrogen pressures. This has resulted in a clearer picture of the role of hydrogen.

### Experimental

**Procedure.**—The reaction rate measurements were made in a flow system. Methylcyclopentane was passed over the catalyst in the presence of hydrogen, and the reaction products were analyzed by a combination of three chromatographic columns coupled directly to the reactor outlet. The reactor was a 1/2 inch i.d. stainless steel tube with a total volume of about 20 cc., and was surrounded by an electrically heated aluminum block to maintain isothermal operation. The catalyst charge varied from 5 to 15 g. depending on the temperature of the run. The catalyst was diluted with inert ceramic beads to fill the reactor volume.

The catalyst was pretreated with flowing hydrogen for three hours at 527° prior to introducing the methylcyclopentane. In making the rate measurements, the methylcyclopentane was passed over the catalyst for 30 minute reaction periods at each set of conditions. Between reaction periods hydrogen was passed over the catalyst for 90 minutes at the pressure to be used in the following reaction period. The reaction products were sampled near the end of each of the reaction periods to ensure that steady state conditions had been attained.

The three chromatographic columns contained polyethylene glycol, hexamethylphosphoramide and squalane, all impregnated on firebrick. The polyethylene glycol column was used for the determination of benzene, the hexamethylphosphoramide for C<sub>5</sub> and lighter paraffins, and the squalane for methylcyclopentane and the hexanes. The polyethylene glycol and squalane columns were 1/4 inch i.d., 4 meters in length, and were operated at 95°. The hexamethylphosphoramide column was 16 meters long and was operated at 40°. The columns gave excellent resolution of the reaction products.

**Materials.**—Phillips pure grade methylcyclopentane (> 99 mole % purity) was used in all the runs. The methylcyclopentane was dried with Drierite (CaSO<sub>4</sub>) to less than 5 p.p.m. water before using. The hydrogen was passed through a Deoxo unit containing palladium catalyst to convert trace amounts of oxygen to water, and then dried over Linde 5A molecular sieves. The platinum on alumina catalyst used in the present study contained 0.3% platinum, and was prepared by impregnation of alumina with aqueous chloroplatinic acid. The surface area of the alumina was approximately 145 m<sup>2</sup>/g.

### Results

The major reactions of methylcyclopentane in the presence of hydrogen over Pt-Al<sub>2</sub>O<sub>3</sub> catalyst can be conveniently classified into two types: (a) conversion to six-membered ring hydrocarbons, cyclohexane and benzene, termed isomerization-dehydroisomerization, and (b) hydrocracking reactions leading to destruction of the ring. Some dehydrogenation to methylcyclopentenes is also observed. The present paper is primarily concerned with the isomerization-dehydroisomerization of methylcyclopentane. At the conditions of this study, the major product of isomerization-dehydroisomerization is benzene. At lower temperatures and higher hydrogen pressures, the major product would be cyclohexane. At the low conversion levels investigated in this work, the products of the hydrocracking reactions were almost exclusively hexanes, there being little secondary cracking to C<sub>1</sub>-C<sub>5</sub> hydrocarbons. Typical distributions of products from methylcyclopentane (MCP) at 471° are shown in Table I.

Rates were measured at low methylcyclopentane conversions (0.5-15%). The partial pressures of methylcyclopentane and hydrogen then do not vary greatly through the reactor. The rate  $r$ , given by

TABLE I

DISTRIBUTION OF PRODUCTS FROM METHYLCYCLOPENTANE

Temp., °C.	471	471	471
Space velocity, $F/W$	0.30	0.30	0.30
Pressure, atm.			
MCP	1.0	1.0	1.0
H <sub>2</sub>	0.0 <sup>a</sup>	6.0	20.0
Composition, mole %			
C <sub>1</sub> -C <sub>5</sub> <sup>b</sup>		0.3	
2-Methylpentane		1.3	2.4
3-Methylpentane		1.0	1.4
<i>n</i> -Hexane	0.3	2.4	3.2
MCP	99.5	85.6	88.1
Cyclohexane		0.4	0.3
Benzene		5.9	3.4
Methylcyclopentenes <sup>c</sup>	0.2	2.9	1.0

<sup>a</sup> N<sub>2</sub> at 6.0 atm. substituted for H<sub>2</sub>. <sup>b</sup> Mole % MCP converted to C<sub>1</sub>-C<sub>5</sub>. <sup>c</sup> Contain small amounts of hexenes.

$$r = F\Delta x/W \quad (1)$$

where  $F$  is the feed rate in moles of methylcyclopentane per hour,  $W$  is the weight of catalyst in grams, and  $\Delta x$  is the fraction of methylcyclopentane converted in a particular reaction, then corresponds closely to the conditions at the reactor inlet. The approach in studying the kinetics is to measure  $r$  as a function of the partial pressures of methylcyclopentane and hydrogen at the reactor inlet. In determining the rate  $r_I$  of the isomerization-dehydroisomerization reaction,  $\Delta x$  is taken as the conversion to cyclohexane plus benzene, while for determining the rate  $r_{HC}$  of hydrocracking,  $\Delta x$  is taken as the conversion to C<sub>3</sub> and lower molecular weight paraffins. Reaction rates, expressed as g. moles of methylcyclopentane converted per hour per g. of catalyst to cyclohexane and benzene ( $r_I$ ) or hydrocracked ( $r_{HC}$ ) are shown in Table II as a function of hydrogen and methylcyclopentane pressures ( $p_H$  and  $p_M$ , respectively, expressed in atm.) at 427 and 471°.

The presence of hydrogen was found to be necessary for isomerization-dehydroisomerization, since no cyclohexane or benzene could be detected when nitrogen was substituted for hydrogen. Furthermore, the rate was found to pass through a maximum with increasing hydrogen pressure, so that at sufficiently high hydrogen pressures the rate decreased with increasing hydrogen pressure.

The rate of hydrocracking of the methylcyclopentane ring was for the most part found to increase with increasing hydrogen pressure, with a possible maximum occurring at 427°. In the complete absence of hydrogen the rate of cracking of the ring was not zero, but was quite low compared to the rates at higher hydrogen pressures.

The effect of methylcyclopentane pressure on both the rates of isomerization-dehydroisomerization and hydrocracking at 471° was found to depend on hydrogen pressure. At 20 atm. hydrogen pressure the rates were found to increase with increasing methylcyclopentane pressure. At 2 atm. hydrogen pressure, however, the rates were actually found to decrease with increasing methylcyclopentane pressure over the range studied, indicating that the rates pass through a maximum at a lower methylcyclopentane pressure. This

also appears to be the case at 427°, although the effect is not so pronounced.

TABLE II

SUMMARY OF RATE DATA ON METHYLCYCLOPENTANE

Temp., °C.	$p_M$	$p_H$	$F/W$	$\tau_I$	$\tau_{HC}$
427	1.0	0 <sup>a</sup>	0.067	0	0.0002
427	0.1	2.0	.074	0.0066	.0023
427	0.33	2.0	.067	.0051	.0024
427	1.0	2.0	.067	.0048	.0020
427	1.0	6.0	.065	.0051	.0064
427	1.0	20.0	.032	.0022	.0051
471	1.0	0 <sup>a</sup>	0.30	0	0.0009
471	0.1	2.0	.31	0.0077	.0048
471	0.33	2.0	.30	.0061	.0045
471	1.0	2.0	.31	.0028	.0026
471	1.0	6.0	.30	.019	.014
471	1.0	20.0	.30	.011	.021
471	10.0	20.0	.52	.036	.036

<sup>a</sup> N<sub>2</sub> substituted for H<sub>2</sub>.

### Discussion

It is generally accepted that isomerization or dehydroisomerization of saturated hydrocarbons over dual function catalysts involves olefin intermediates. According to this mechanism methylcyclopentane would first dehydrogenate on Pt sites to methylcyclopentenes which migrate to acidic sites to isomerize to cyclohexene. The cyclohexene then returns to Pt sites where it is either hydrogenated to cyclohexane or dehydrogenated to benzene, the relative amounts of these products depending on reaction conditions. If the isomerization step is rate limiting, the concentration of each of the methylcyclopentene intermediates formed in the initial dehydrogenation step will approach an equilibrium value, which is inversely proportional to hydrogen pressure. The over-all rate will then decrease with increasing hydrogen pressure, in agreement with the present data on methylcyclopentane for hydrogen pressures ranging from 6 to 20 atmospheres, and with previously reported data on *n*-pentane isomerization at 372°. However, it does not account for the effect of hydrogen at lower pressures, where the rate actually increases with hydrogen pressure. Thus, the role of hydrogen appears to be more than one of limiting the concentration of intermediate methylcyclopentenes attainable at equilibrium.

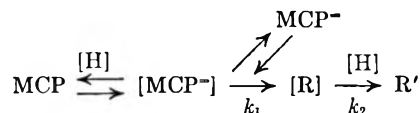
In the absence of hydrogen the dehydrogenation activity of the catalyst appears to be quite small. For example, the conversion of methylcyclohexane to toluene at 471°, 1.0 atm. methylcyclohexane pressure, and  $F/W = 1.0$  is about two hundred-fold lower in the absence of hydrogen. Since only

$p_H$ , atm.	% Conversion
0	0.3
10	64

Pt sites are required for dehydrogenation,<sup>5</sup> the effect of hydrogen appears to be associated with the Pt. It is suggested that in the absence of hydrogen the platinum is almost completely covered with hydrogen deficient hydrocarbon residues, formed by side reactions involving extensive dehydrogenation and polymerization. The primary

role of hydrogen is then to keep the surface clean. Studies on the dissociative adsorption of hydrocarbons, such as cyclohexane and cyclopentane, over a variety of metals have given direct evidence for the formation of such residues, and for their removal by reaction with hydrogen.<sup>8</sup> Studies on adsorption of benzene over platinum catalysts<sup>9</sup> furnish additional evidence for the ability of hydrogen to clean up platinum surfaces.

For isomerization-dehydroisomerization of methylcyclopentane at low hydrogen pressures, it is then suggested that the rate-limiting step is the formation of the intermediate methylcyclopentenes *via* the reaction scheme



in which the brackets refer to species on the surface, MCP refers to methylcyclopentane, MCP<sup>-</sup> to methylcyclopentenes, and [R] represents the surface residue. According to this picture MCP dehydrogenates on the surface to [MCP<sup>-</sup>], which can then either desorb or undergo further dehydrogenation and polymerization reactions to form the residue [R]. The surface residue is also being continuously removed to the gas phase as hydrocarbons R' by a hydrogen clean-up reaction involving adsorbed hydrogen [H]. If we make the simplifying assumption that a steady state concentration of surface residue is approached, we can write

$$\frac{d\theta_R}{dt} = k_1\theta_{M'} - k_2\theta_R\theta_H = 0 \quad (2)$$

where  $\theta_{M'}$ ,  $\theta_R$  and  $\theta_H$  represent coverage of the platinum sites by methylcyclopentenes, residue and hydrogen, respectively. The first term  $k_1\theta_{M'}$  is the rate of formation of residue from adsorbed methylcyclopentenes, while the second term  $k_2\theta_R\theta_H$  is the rate of removal by reaction with adsorbed hydrogen. Here the rate of removal has been assumed to be proportional to the first power of  $\theta_H$ , although it might well depend on a higher power of  $\theta_H$ , depending on the detailed nature of the removal reaction. At sufficiently low hydrogen pressures  $\theta_H$  becomes very small so that the surface is almost completely covered with residue, *i.e.*,  $\theta_R$  approaches unity. At such conditions  $\theta_{M'}$  can be approximated by

$$\theta_{M'} = (k_2/k_1)\theta_H \quad (3)$$

The over-all rate of isomerization-dehydroisomerization is in turn determined by the rate of formation of the intermediate methylcyclopentenes in the gas phase, as given by

$$r = k'\theta_{M'} \quad (4)$$

where  $k'$  is a rate constant for desorption. Since  $\theta_{M'}$  increases with increasing hydrogen pressure,  $\theta_H$  will also increase, thus accounting for the promotional effect of hydrogen pressure on the rate. Furthermore, since methylcyclopentane and

(8) A. K. Galwey and C. Kemball, *Trans. Faraday Soc.*, **55**, 1959 (1959).

(9) R. C. Pitkethly and A. G. Goble, Paper No. 91, Section II, Proceedings of the Second International Congress on Catalysis, Paris, France, 1960.

hydrogen may compete for active sites, increasing methylcyclopentane pressure at constant hydrogen pressure would decrease  $\theta_H$ . According to equation 3,  $\theta_M'$  would then actually decrease, and this in turn would result in a decrease in the rate. This is consistent with the data at 2 atm. hydrogen pressure showing a decrease in rate with increasing methylcyclopentane pressure.

The temperature coefficient of the reaction rate depends markedly on hydrogen pressure. At very low hydrogen pressures the temperature coefficient is quite small and can even be negative, indicating that  $k_1$  increases faster than  $k_2$  with temperature or that  $\theta_H$  decreases with temperature.

At very high hydrogen pressures coverage of Pt by residues ceases to be a limiting factor and equation 3 no longer holds. The acidic function of the catalyst, rather than the platinum, then becomes limiting, and the temperature coefficient is much higher.

The conclusions on methylcyclopentane isomerization-dehydroisomerization reached in the present study would be expected to apply equally well in the isomerization of *n*-paraffins, since the reaction mechanisms are in all probability the same. The complex role of hydrogen would appear to be characteristic of reactions which depend on both the dehydrogenation and acidic functions of the catalyst.

## THE OSMOTIC AND ACTIVITY COEFFICIENTS OF SOME BOLAFORM SULFONATES<sup>1</sup>

BY O. D. BONNER AND O. C. ROGERS

*Department of Chemistry, University of South Carolina, Columbia, South Carolina*

*Received November 23, 1960*

Osmotic and activity coefficients have been determined for some disulfonic acids and their salts. These data were determined for the more concentrated solutions by isopiestic comparison of solutions of the sulfonates with solution of sodium chloride or lithium chloride. A specially constructed vapor pressure comparison apparatus was used for comparisons of the dilute solutions. The sulfonate groups appear to act osmotically independent of one another at high concentrations where  $1/K$  is small relative to the distance of separation. In dilute solutions the separation of the anionic groups results in osmotic coefficients larger than for normal 2,1 electrolytes. There appears to be micelle formation in disulfonates where the groups are separated by several methylene linkages.

### Introduction

Considerable interest has been shown in recent years in the osmotic properties of various aromatic sulfonic acids and their salts as related to the interpretation of ion-exchange equilibrium studies on sulfonated polystyrene-divinylbenzene copolymers. The osmotic and activity coefficients of several monosulfonic acids and salts have been determined and the degree of dissociation correlated with the molar volume of the parent hydrocarbon.<sup>2</sup>

An attempt is being made in this work to investigate qualitatively two effects which must be considered in order to make valid a comparison of data for a cross-linked polymer with similar data for a soluble electrolyte having a structure similar to the monomer units present in the polymer. It is necessary, first, to note the interaction between two similar ionic groups in a polymer as a function of the distance of separation between these groups. Of importance also is the determination of the effect of polymerization on the osmotic properties of electrolytes. The magnitude of both of these effects can be evaluated from measurements of certain disulfonic acids and by comparison of these data with those for similar monosulfonic acids. These disulfonic acids are a peculiar type of 2,1 electrolyte and are referred to as "bolaform" electrolytes, a term first used by Fuoss and co-workers to describe electrolytes that have two identical ionic

groups which are separated by relatively great distances.<sup>3</sup>

The osmotic properties of two such disulfonic acids, *m*-benzenedisulfonic acid and 4,4'-bibenzyl-disulfonic acid, have already been reported.<sup>4</sup> However, due to the difficulty in making precise measurements in dilute solutions by the isopiestic method, considerable uncertainty exists in the activity coefficients of these 2,1 electrolytes caused by the extrapolation of osmotic data to infinite dilution. Since the osmotic coefficients are obtained directly from the isopiestic data without extrapolation, these data, except for the most dilute solutions, are probably correct. In this work *m*-benzenedisulfonic acid and 4,4'-bibenzyl-disulfonic acid were reinvestigated along with two new disulfonic acids and the sodium lithium salts of these acids.

A sensitive vapor pressure comparison apparatus was constructed for this purpose in order to supplement the isopiestic data in dilute solutions. The apparatus is essentially a wet bulb thermometer of high sensitivity. Osmotic data can be obtained between 0.01 and 0.15 molal with an accuracy of better than one per cent.

### Experimental

**Vapor Tension Apparatus.**—This apparatus is similar to that described by Brady, *et al.*,<sup>5</sup> except that a d.c. rather than an a.c. source is used. The constant humidity cham-

(1) This work was supported by the Atomic Energy Commission under Contract No. AT-(40-1)-1437.

(2) O. D. Bonner and O. C. Rogers, *J. Phys. Chem.*, **64**, 1499 (1960).

(3) R. M. Fuoss and D. Edelson, *J. Am. Chem. Soc.*, **73**, 269 (1951)

(4) O. D. Bonner, V. F. Holland and L. L. Smith, *J. Phys. Chem.* **60**, 1102 (1956).

(5) A. P. Brady, H. Huff and J. W. McBain, *ibid.*, **55**, 304 (1951).

ber is an unsilvered Dewar flask which is inside a heavy walled resin reaction flask. Both flasks are completely immersed in a constant temperature bath maintained at  $25 \pm 0.01^\circ$ . Temperature fluctuations in the bath are effectively damped before reacting the humidity chamber. Details of the apparatus are as follows.

In the pipet system the outer glass tube is fixed firmly in the rubber stopper in the resin reaction flask and above the water level of the constant temperature bath. A second glass tube fits snugly inside the larger tube and serves as a guide for the flexible tip pipet. The guide tube has a  $90^\circ$  bend about  $1/2$  inch from the end so that by turning the guide, the pipet tip can be rotated from one thermistor to the other. The tip of the pipet is made of 0.05 inch i.d. Teflon tubing, sealed to the glass pipet with sealing wax. A small rubber washer, approximately  $1/16$  inch in diameter, is placed around the thermistor just above the oxide lead to ensure that the drops all have the same thermal contact with that portion of the thermistor that is thermally sensitive.

The resistance changes of the thermistors are measured by incorporating them as two arms of a Wheatstone bridge. Each thermistor has a resistance of about 100,000 ohms at  $25^\circ$  with a sensitivity of about 5,000 ohms/ $^\circ\text{C}$ . at this temperature. A 100,000 and a 90,000 ohm carbon resistor along with a 10,000 ohm variable resistance form the other two arms of the bridge. Both fixed resistors are placed in a small Dewar flask to damp out the effect of temperature fluctuations on the resistance. The source of potential is a 1.5 volt dry-cell in series with a 150,000 ohm resistor. The detector is a Hewlett Packard Model 425A microvolt-ammeter with a detection limit of 0.1 microvolt. The sensitivity of the detector is such that a change of one ohm at the balance point gives a deflection of 1 microvolt or about one centimeter on the scale of the instrument, thus the bridge is easily balanced to  $\pm 0.5$  ohm.

All leads to the thermistors and resistors in the bridge are shielded monoconductor cable, with all shields and the chassis of the instrument connected to a common ground. The thermistors were aged in an oven at  $120^\circ$  with a 1.5 volt battery connected directly across the leads for about two weeks. This aging process seems to reduce spasmodic changes in the absolute resistance of the thermistors.

In an actual experimental determination, the pipets are filled with the two solutions to be compared, the reference solution and the unknown solution, and inserted into the pipet guides. About 30 minutes are needed for the pipets and solutions to adjust to the temperature of the humidity cell. The solutions are placed on the thermistors by bringing the tip of the pipet against the thermistor probe, opening the stopcock and allowing several drops to run down the thermistor, washing away previous solution. The stopcock is closed before the last drop is large enough to fall off, but not before it is of sufficient size to completely cover the sensitive tip of the thermistor. After the reference solution has been placed on one thermistor and the unknown solution placed on the other thermistor, the variable resistor is adjusted until the detector indicates the null point has been reached. About 6 to 8 minutes are needed for the system to come to thermal equilibrium and give a constant resistance reading. After recording the resistance, the pipets are rotated and the drops placed in the opposite order on the thermistors and the resistance reading again observed. This cycle is repeated several times and the data averaged to minimize errors.

**Preparation and Purification of Compounds.**—In this work four disulfonic acids and certain salts of these acids were prepared. The purity of the disulfonates was determined in the following manner. About 5 meq. of the recrystallized dried sodium or potassium salt of the sulfonate was accurately weighed and dissolved in distilled water. This solution was passed through a column containing Dowex 50-X8 cation-exchange resin in the hydrogen form and the number of milliequivalents of sulfonate determined by titrating the hydrogen ions in the effluent solution with standard base. The experimental and calculated equivalent weights checked within 0.1% in all instances.

***m*-Benzenedisulfonic Acid.**—*m*-Benzenedisulfonic acid is available, commercially, in the technical grade. The acid was recrystallized from ether and dried in a vacuum oven. The salts were prepared by neutralization with the appropriate standardized base.

**4,4'-Bibenzylidenedisulfonic Acid.**—Bibenzyl was obtained commercially and sulfonated by heating a mixture of 50 g.

of bibenzyl with 100 g. of concentrated sulfuric acid to about  $60^\circ$  for two hours. The reaction mixture was neutralized with barium hydroxide and the hot solution filtered to remove the barium sulfate. On cooling and adding methanol, the barium sulfonate precipitated and was further purified by additional recrystallizations of the barium salt from methanol-water solvent. The pure acid was prepared by passing an aqueous solution of the barium sulfonate through an ion-exchange column in the hydrogen form. The salts were prepared by neutralization of the acid with the appropriate base.

**1,8-Diphenyloctanedisulfonic Acid.**—1,8-Diphenyloctanedisulfonic acid was prepared by hydrogenation followed by sulfonation of 1,8-diphenyloctatetraene. 1,8-Diphenyloctatetraene was prepared by the condensation of succinic acid and cinnamaldehyde in the presence of lead oxide and acetic anhydride according to the method of Kuhn.<sup>6</sup>

The catalytic hydrogenation of the olefin was carried out in acetic acid media. A suspension of 8 g. of 1,8-diphenyloctatetraene and 1 g. of 5% palladium-on-charcoal in 150 ml. of acetic acid was agitated under a hydrogen pressure of 30 p.s.i. at a temperature of  $70^\circ$  until all the yellow color disappeared. The palladium-on-charcoal was removed by filtration and the acetic acid removed by distillation. The remaining hydrocarbon was distilled under reduced pressure (b.p.  $146^\circ$  at 1 mm.).

The hydrocarbon was sulfonated in the following manner: 10 g. of 1,8-diphenyloctane and 10 g. of concentrated sulfuric acid were stirred rapidly on a water-bath at about  $60^\circ$ . Fuming sulfuric acid (20%) was added dropwise until a total of 5 ml. had been added. The mixture formed a brown paste which was stirred for 1 hour at  $60^\circ$ . The paste was poured into 100 ml. of concentrated hydrochloric acid and cooled to  $0^\circ$ . The disulfonic acid formed a gelatinous precipitate which was separated by means of a centrifuge.

The precipitate was washed twice with cold hydrochloric acid and the excess hydrochloric acid removed with a water aspirator pump. The disulfonic acid was carefully neutralized with concentrated sodium hydroxide and the sodium disulfonate recrystallized twice from methanol-water solvent. The pure acid was prepared by ion exchange and the salts prepared by neutralization with base. The experimentally determined equivalent weight and that calculated for the disodium sulfonate agree within 0.1%.

The positions of the sulfonate groups on the rings can only be assumed to be 4,4' because of the analogy with the bibenzyl system.

**1,14-Diphenyltetradecanedisulfonic Acid.**—The disulfonic acid was prepared by sulfonating the parent hydrocarbon 1,14-diphenyltetradecane, which was prepared by the reduction of 1,14-diphenyl-3,12-tetradecadiene. The diketone was prepared by reacting di- $\beta$ -phenylethylcadmium with sebacyl chloride according to the method of Soffer and co-workers.<sup>7</sup>

The diketone was reduced by the Wolff-Kishner reduction as described by Soffer and co-workers<sup>8</sup> in an earlier paper.

About 20 g. of the hydrocarbon and 5 ml. of concentrated sulfuric acid were stirred on a water-bath at  $60^\circ$  while 10 ml. of 20% fuming sulfuric acid was added slowly. The mixture was heated and stirred for two hours and the dark brown slurry cooled to  $0^\circ$  and neutralized with 10% sodium hydroxide. The sodium salt was only slightly soluble and was removed by filtration. For additional purification the salt was recrystallized three times from water.

The pure acid was prepared by ion exchange as in the previous systems. The sodium, lithium and potassium salts were all too insoluble to be used in this work. The experimentally determined equivalent weight and that calculated for the disodium sulfonate agree within 0.1%.

## Results and Discussion

The calculation of the osmotic coefficients from the vapor tension data was accomplished by the use of the interpolation equation

$$vm\phi = v_2m_2\phi_2 - \frac{\Delta R_{12}}{\Delta R_1 + \Delta R_2} (v_2m_2\phi_2 - v_1m_1\phi_1)$$

(6) R. Kuhn, *Helv. Chim. Acta*, **11**, 93, 138 (1928).

(7) M. D. Soffer, N. S. Strauss, M. D. Trail and K. W. Sherk, *J. Am. Chem. Soc.*, **69**, 1864 (1947).

(8) M. D. Soffer, M. B. Soffer and K. W. Sherk, *ibid.*, **67**, 1435 (1945).



TABLE I  
 TABLE OF OSMOTIC COEFFICIENTS AT 25°C<sup>a</sup>

Molality	$\sqrt{m}$	1	2	3	4	5	6	7	8	9
0.01	0.100	0.923	0.921	0.922	0.847	0.898	0.888	0.923	0.923	0.302
.02	.141	.900	.896	.897	.824	.859	.858	.850	.868	.236
.03	.173	.885	.881	.882	.813	.849	.847	.732	.804	.228
.04	.200	.877	.875	.875	.807	.843	.841	.658	.732	.225
.05	.224	.876	.873	.870	.802	.838	.836	.607	.662	.223
.06	.245	.878	.873	.867	.799	.834	.830	.566	.614	.222
.07	.265	.879	.874	.865	.795	.829	.826	.530	.576	.222
.08	.283	.880	.876	.864	.791	.827	.822	.502	.550	.222
.09	.300	.882	.878	.863	.789	.824	.818	.479	.527	.222
.10	.316	.884	.880	.862	.787	.822	.815	.462	.508	.222
.15	.387				.777	.812	.797			
.20	.447	.908	.902	.864	.769	.805	.781	.380	.412	.232
.30	.548	.937	.931	.872	.758	.796	.751	.372	.407	.238
.40		.969	.957	.880	.750	.788	.719	.379	.418	.244
.50		.998	.983	.889	.748	.787		.391	.430	.250
.60		1.028	1.010	.899	.751	.789		.411	.445	.257
.70		1.058	1.038	.910	.760	.797		.434	.463	.266
.80		1.088	1.065	.921	.770	.811		.455	.485	.274
.90		1.119	1.092	.932	.783	.828		.476	.506	.284
1.00		1.151	1.121	.944	.798	.844		.498	.529	.297
1.20		1.223	1.179	.967	.836	.877		.543	.575	.326
1.40		1.292	1.238	.992	.877			.585		.365
1.60		1.362	1.292	1.016	.921			.633		.411
1.80			1.342	1.040	.969			.684		.462
2.00			1.394	1.063	1.021			.735		.517
2.50			1.510	1.117	1.162					
3.00				1.164	1.307					
3.50					1.449					
4.00					1.590					
4.50					1.742					
5.00					1.894					

<sup>a</sup>1, *m*-benzenedisulfonic acid; 2, lithium *m*-benzenedisulfonate; 3, sodium *m*-benzenedisulfonate; 4, 4,4'-bibenzyliddisulfonic acid; 5, lithium 4,4'-bibenzyliddisulfonate; 6, sodium 4,4'-bibenzyliddisulfonate; 7, 1,8-diphenyloctanedisulfonic acid; 8, lithium 1,8-diphenyloctanedisulfonate; 9, 1,14-diphenyltetradecanedisulfonic acid.

where  $\nu m\phi$  is the osmotic concentration of the unknown solution,  $\nu_1 m_1 \phi_1$  and  $\nu_2 m_2 \phi_2$  are the osmotic concentrations of the two reference solutions. Reference solution number 1 has a slightly lower osmotic concentration than the unknown solution and reference solution number 2 has an osmotic concentration slightly greater than that of the unknown solution.  $\Delta R_1$  is the observed resistance difference when the unknown solution is compared to reference solution number 1 and  $\Delta R_2$  is the corresponding resistance difference when the unknown solution and reference solution number 2 are compared. After obtaining a value for the osmotic concentration,  $\nu m\phi$ , the osmotic coefficient is obtained by dividing the osmotic concentration by  $\nu m$ ,  $\nu$  being the number of ions formed on complete dissociation ( $\nu = 3$  for these bolaform electrolytes), and  $m$  is the molality.

The isopiestic technique and apparatus was similar to that described in a publication by Robinson and Sinclair.<sup>9</sup> The osmotic coefficients are obtained from the isopiestic data from the relation that at equilibrium

$$\nu m\phi = \nu_r m_r \phi_r$$

where the subscript *r* refers to the reference solution. Solving for the osmotic coefficient of the unknown one obtains

(9) R. A. Robinson and D. A. Sinclair, *J. Am. Chem. Soc.*, **56**, 1830 (1934).

$$\phi = \frac{\nu_r m_r}{\nu m} \phi_r = R \phi_r$$

where  $R$  is defined as the isopiestic ratio and  $\phi_r$  is the osmotic coefficient of the reference solution at molality  $m_r$ .

In order to calculate the activity coefficients from the osmotic data, a plot was made of the osmotic coefficients against concentration, using the osmotic coefficients from both the vapor tension and the isopiestic measurements. Coefficients calculated from both types of measurements fitted nicely on a single smooth curve and values for the isopiestic ratio  $R$  were calculated for the entire concentration range. Robinson and Sinclair<sup>9</sup> developed the following relationship for the calculation of activity coefficients

$$\ln \gamma_{\pm} = \ln \gamma_r + \ln R + 2 \int_{\sqrt{m_r \gamma_r} = 0}^{\sqrt{m_r \gamma_r}} \frac{R - 1}{\sqrt{m_r \gamma_r}} d\sqrt{m_r \gamma_r}$$

where  $\gamma^+$  and  $\gamma_r$  are the activity coefficients of the unknown solution and the reference solution, respectively,  $R$  is the isopiestic ratio and  $m_r$  is the molality of the reference solution isopiestic with the unknown solution. This method involves the graphical integration of a plot of  $R - 1/\sqrt{m_r \gamma_r}$  vs.  $\sqrt{m_r \gamma_r}$  between the limits of  $\sqrt{m_r \gamma_r} = 0$  and the value of  $\sqrt{m_r \gamma_r}$  at the desired concentration.

A theoretical interpretation of the osmotic data

TABLE II  
TABLE OF ACTIVITY COEFFICIENTS AT 25<sup>o</sup>a

Molality	$\sqrt{m}$	1	2	3	4	5	6	7	8	9
0.01	0.100	0.781	0.766	0.766	0.565	0.727	0.695	0.797	0.811	0.1400
.02	.141	.718	.703	.705	.494	.644	.598	.691	.717	.0788
.03	.173	.677	.662	.663	.454	.602	.570	.564	.629	.0572
.04	.200	.648	.635	.636	.427	.572	.541	.480	.548	.0456
.05	.224	.630	.616	.615	.407	.558	.519	.420	.477	.0383
.06	.245	.618	.602	.599	.391	.530	.501	.373	.426	.0332
.07	.265	.607	.592	.586	.378	.515	.487	.336	.385	.0294
.08	.283	.599	.583	.575	.366	.502	.473	.306	.354	.0266
.09	.300	.591	.575	.566	.356	.490	.462	.282	.327	.0243
.10	.316	.585	.569	.557	.347	.480	.451	.262	.306	.0223
.15	.387	.565	.548	.525	.315	.441	.410	.198	.233	.0163
.20	.447	.557	.538	.507	.292	.415	.379	.161	.191	.0133
.30		.555	.535	.484	.261	.379	.335	.124	.141	.0097
.40		.565	.541	.469	.242	.354	.300	.105	.127	.0078
.50		.579	.550	.462	.228	.337		.092	.113	.0067
.60		.598	.564	.458	.219	.324		.084	.104	.0058
.70		.620	.582	.456	.212	.317		.079	.097	.0053
.80		.646	.604	.455	.208	.313		.075	.092	.0048
.90		.674	.625	.457	.205	.312		.072	.089	.0045
1.00		.706	.650	.460	.204	.312		.069	.086	.0042
1.20		.785	.710	.466	.205	.314		.067	.083	.0038
1.40		.874	.775	.476	.208			.065		.0036
1.60		.981	.849	.489	.215			.065		.0035
1.80			.927	.502	.224			.065		.0034
2.00			1.009	.516	.235			.067		.0034
2.50			1.257	.555						
3.00				.598						
3.50										
4.00										
4.50										

<sup>a</sup> See footnote a of Table I.

for bolaform electrolytes is somewhat more complicated than when only simple inorganic electrolytes are involved because of two major factors. First, the anion has a large mass of low dielectric organic material closely associated with the negatively charged sites, and second, the two negative charges of the divalent ion are separated by a flexible chain, which in the case of 1,14-diphenyltetradecanedisulfonic acid, can possibly be extended to 35 Å.

The first factor, that of the low dielectric organic material in close contact with the sulfonate group, has been investigated previously<sup>3</sup> by determining the osmotic properties of a series of monosulfonated aromatic compounds, starting with benzenesulfonic acid and observing the variation of the osmotic properties with the number of methyl groups added to the aromatic ring. The conclusion drawn from this work was that the added methyl groups cause a decrease in the osmotic and activity coefficients of the electrolytes. There was also observed a change in the order of increasing activity for the acids and salts of the acids. In the lowest molecular weight compound, benzenesulfonic acid, the order at any concentration for the osmotic coefficients was shown to be Li > H > Na. For the highest molecular weight compound, mesitylenesulfonic acid, the order was Li > Na > H. This shift in the position of the acid with respect to the lithium and sodium salts indicates a

decrease in the dissociation constant of the acid with increasing number of methyl groups.

In this work, the order for the osmotic coefficients of *m*-benzenedisulfonic acid and its salts is H > Li > Na over the entire concentration range. This is the only sulfonic acid investigated so far that has the osmotic coefficient of the acid greater than the salts over the entire concentration range. It is believed that the low ratio of organic matter to the number of sulfonate groups is responsible for the high activity.

The remaining disulfonic acids that were investigated in this work have a higher ratio of organic material to the number of sulfonate groups, and in each case the curve for the osmotic coefficient *vs.* concentration for the acid is below the curve for the corresponding lithium salt indicating that the acid strengths of the bolaform sulfonates are similar in magnitude to those of monosulfonic acids of similar equivalent weights.

The very rapid decrease of the osmotic and activity coefficients with increasing concentration for 1,8-diphenyloctanedisulfonic acid and the lithium salt of the acid and the even more rapid decrease for 1,14-diphenyltetradecanedisulfonic acid suggest micelle formation. Although the formation of micelles is usually attributed only to those compounds having an ionic or water-soluble group on one end and a long hydrophobic chain extending from the water-soluble group, the bolaform ions

appear to exist in some sort of entanglement that effectively reduced the number of particles present.

Additional evidence for the proposal of micelle formation is seen in the values of the osmotic coefficients of 1,14-diphenyltetradecanedisulfonic acid in the concentration range between 0.02 and 0.5 *m*. In this range, the osmotic coefficients are below 0.25. If the molecule were completely associated, the lower limit of the osmotic coefficient would ideally be 0.33, since the calculations are performed assuming the formation of three particles at infinite dilution.

The electrostatic effect of the two sulfonate groups being separated by a large distance on the osmotic properties of the electrolyte solutions is a somewhat more complicated problem. Very little theoretical work has been done in the field of bolaform electrolytes although Kirkwood<sup>10</sup> has proposed an equation for the calculation of the activity coefficients of zwitterions.

The osmotic and activity coefficients *vs.* concentration curves for the bolaform electrolytes differ somewhat from the curves obtained from normal uni-divalent electrolytes such as Na<sub>2</sub>SO<sub>4</sub> or CaCl<sub>2</sub>. For a normal divalent ion such as the calcium ion, the two unit charges can be thought of as being distributed in a centrosymmetrical manner about the surface of a small sphere, whereas in the case of the bolaform ion, the two charges are separated by a distance which is large when compared to the diameter of a calcium ion. It is then conceivable that in certain conditions of concentration and chain configuration the two sulfonate groups may have independent ion atmospheres and behave electrostatically as two separate monovalent ions.

Although Rice is primarily interested in ion pair formation and diffusion properties, it is believed that some of the general statements that are made in his papers are applicable to the interpretation of osmotic coefficients in dilute solutions. He has calculated the mean end to end distance of some bolaform electrolytes<sup>11,12</sup> consisting of two quaternary ammonium groups separated by various numbers of methylene groups and postulates that whereas the limiting behavior at infinite dilution is the same for bolaform ions and ordinary divalent ions, this similarity will not persist at higher concentrations. Specifically, Rice states that when  $1/K$  is less than  $R/2$ , the ion atmospheres may be thought of as independent,  $K$  being the reciprocal of the average radius of the ionic atmosphere, and  $R$  the distance of separation of the two charged groups. However, when  $1/K$  becomes approximately equal to  $R$ , the ion atmospheres overlap and form an oblong casing around the bolaform ion. According to these statements of Rice, we may calculate that for a bolaform electrolyte with  $R = 35 \text{ \AA.}$ , the ionic atmospheres will be independent at concentrations greater than 0.02 molal (where  $1/K = R/2$ ). For smaller bolaform electrolytes, the sulfonate groups become independent at higher concentrations.

Although the foregoing discussion predicts deviations from normal 2-1 electrolyte behavior for bola-

form electrolytes, no statement is made as to the direction of the deviation. We may write the limiting law type equation for the slope of the osmotic coefficient *vs.* the square root of molality curve as

$$d\phi/d\sqrt{m} = -\frac{2.303}{3} A z_+ z_- K$$

where  $K = (\mu/m)^{1/2}$ ,  $\mu$  is the ionic strength, and  $A$  is 0.509 for water at 25°. We may then proceed to evaluate  $K$  for various types of electrolytes

- (A) Normal 1-1 electrolyte  $K = 1$   
 $d\phi/d\sqrt{m} = -0.39$   
 (B) Normal 2-1 electrolyte  $K = \sqrt{3}$   
 $d\phi/d\sqrt{m} = -1.35$   
 (C) For the special case of a bolaform electrolyte treated as two 1-1 electrolytes  $K = \sqrt{2}$   
 $d\phi/d\sqrt{m} = -0.55$

Although it is realized that the limiting law does not hold accurately in solutions above 10<sup>-3</sup> molal, these calculations suggest that the independent nature of the charged groups in the bolaform ion will cause deviations that will give osmotic coefficients slightly larger than those of normal divalent ions.

The experimental data for 1,8-diphenyloctanedisulfonic acid and lithium salt tend to support this idea. In dilute solutions the osmotic coefficients are larger than those calculated using the theoretical 2-1 limiting slope and also larger than the values for solutions of CaCl<sub>2</sub>, the osmotic coefficients of CaCl<sub>2</sub> being among the highest of the normal 2-1 electrolytes.

Perhaps the best correlation between the monosulfonate and disulfonate osmotic data is shown in the investigations of the *p*-toluenesulfonates and the 4,4'-bibenzylidisulfonates. The cross-over of the osmotic coefficient *vs.* concentration curves for *p*-toluenesulfonate<sup>13</sup> is matched by a similar cross-over which occurs with 4,4'-bibenzylidisulfonic acid and sodium 4,4'-bibenzylidisulfonate. The similarity of the bibenzyl sulfonates to two molecules of the toluene sulfonates is of course apparent. In concentrated solutions where  $1/K$  becomes very small it would be expected that solutions of these two sulfonates would behave nearly identically. Osmotic coefficients of *p*-toluenesulfonic acid in concentrated solutions have been determined from isopiestic comparison with solutions of lithium chloride and these data are given in Table III. A comparison of *p*-toluenesulfonic acid data with bibenzylidisulfonic acid data is possible if the disulfonate is considered to be equivalent to two 1-1 electrolytes. For this purpose weight normality,  $N$ , rather than molality may be used to express concentrations and the number of ions per unit,  $\nu'$ , is taken to be 2. An apparent osmotic coefficient,  $\phi'$ , may then be calculated from isopiestic comparison with a reference solution when the relationship

$$\nu_r m_r \phi_r = \nu' N \phi' = (2)(2m)\phi'$$

is utilized. The true coefficient  $\phi$  is thus related to  $\phi'$  as

(13) O. D. Bonner, G. D. Easterling, D. L. West and V. F. Holland, *ibid.*, **77**, 242 (1955).

(10) J. G. Kirkwood, *J. Chem. Phys.*, **2**, 351 (1934).

(11) S. A. Rice, *J. Am. Chem. Soc.*, **78**, 5247 (1956).

(12) S. A. Rice, *ibid.*, **80**, 3207 (1958).

$$3m\phi = 4m\phi' \text{ or } \phi' = 3/4\phi$$

This treatment of disulfonates is formally equivalent to that of previous investigators<sup>14-17</sup> in the field of polyelectrolytes. Identical results are obtained if one considers the solvent activity of solutions of the two electrolytes as a function of the concentration as obtained from  $\nu m\phi$  vs. concentration plots.

TABLE III

OSMOTIC COEFFICIENTS OF *p*-TOLUENESULFONIC ACID AT 25°  
IN CONCENTRATED SOLUTIONS

<i>m</i>	$\phi$	<i>m</i>	$\phi$	<i>m</i>	$\phi$
5.0	0.942	7.0	1.113	9.0	1.284
5.5	.984	7.5	1.160	9.5	1.324
6.0	1.028	8.0	1.204	10.0	1.361
6.5	1.072	8.5	1.245		

The electrolytes behave in the expected manner at low concentrations with the osmotic coefficients for *p*-toluenesulfonic acid being greater than the

(14) E. Glueckauf, *Proc. Roy. Soc. (London)*, **214**, 207 (1952).

(15) J. Duncan, *ibid.*, **214**, 344 (1952).

(16) D. Reichenberg, *Research*, **6**, 98 (1953).

(17) G. E. Boyd and B. A. Soldano, *Z. Elektrochem.*, **57**, 162 (1953).

apparent osmotic coefficients for bibenzylsulfonic acid. The osmotic coefficient vs. concentration (or  $\nu m\phi$  vs. concentration) curves approach one another as the concentration is increased and actually cross at about 8.5 weight normal, at which point  $1/K$  is approximately 1.1 Å. The osmotic behavior of the two electrolytes becomes identical then with a separation of the ionic groups greater than about 2.2 Å. This may be compared with a distance of about 15 Å. between the bibenzyl sulfonate groups when the molecule is fully extended. The actual cross of the curves is unexpected but may be explained in terms of hydrogen bonding. At these concentrations the sulfonic acids are roughly 50% dissociated. The undissociated sulfonic acid molecules would be expected to form hydrogen bonds, thus decreasing the hydration<sup>18</sup> of the sulfonate group and decreasing at the same time the osmotic coefficient. The ability of the bibenzyl sulfonates to form hydrogen bonds should be less than that of *p*-toluenesulfonic acid since these bonds are structurally not possible between sulfonate groups of the same molecule.

(18) R. H. Stokes and R. A. Robinson, *J. Am. Chem. Soc.*, **70**, 1870 (1948).

## SOLVENTS HAVING HIGH DIELECTRIC CONSTANTS. XII. REACTION OF SODIUM PHENOXIDE WITH ALKYL IODIDES IN THESE MEDIA<sup>1,2</sup>

BY LYLE R. DAWSON, JERRY E. BERGER AND HARTLEY C. ECKSTROM

*Department of Chemistry, University of Kentucky, Lexington, Ky.*

*Received November 30, 1960*

Second-order reaction rate constants have been obtained for the reaction between sodium phenoxide and alkyl iodides in *N*-methylacetamide and in mixtures of *N*-methylacetamide with *N,N*-dimethylacetamide as solvents. The Arrhenius activation energy for the reaction *n*-propyl iodide with sodium phenoxide in *N*-methylacetamide (dielectric constant = 165.3) is 19.39 kcal./mole, and in a mixture with a dielectric constant equal to 120.0 it was 18.38 kcal./mole. Reaction rate data obtained as a function of dielectric constant using solvent mixtures rich in *N*-methylacetamide revealed that the reaction is slower than predicted in these solvents. The observed deviations may be attributed to preferential solvation resulting in a localized higher dielectric constant in the vicinity of the solute particles and to viscosity effects. Second-order rate constants were observed to decrease as the initial concentration of sodium phenoxide was increased with that of the alkyl iodide held invariant.

Electrolyte solutions using solvents with high dielectric constants have been investigated extensively by this Laboratory.<sup>3</sup> These studies have included the determination of conductances, dielectric constants, viscosities, diffusion characteristics, transference numbers and solubilities in *N*-methylacetamide and related solvents and in their mixtures. However, very few homogeneous reaction kinetics investigations have been made in these solvent systems of high dielectric constant.

It was the purpose of the present research to study a reaction between neutral molecules and ions in *N*-methylacetamide as a solvent and in solvent mixtures of *N*-methylacetamide and *N,N*-dimethylacetamide with the objective of learning

the effects of the structure of the reacting neutral molecule, temperature, dielectric constant and concentration upon the kinetics of the reaction, as well as the effect, if any, of preferential solvation.

The reaction chosen was the ether synthesis employing sodium phenoxide and alkyl iodides. Its choice is an obvious one because of the ease in modifying the structures of both the ion and the neutral molecule. Also, the reaction between sodium phenoxide and alkyl iodides has the advantages that it may be followed quantitatively; it is free from complicating competing reactions and it is free from reverse changes. Furthermore, ether syntheses employing similar reactants have been studied by Segaller<sup>4</sup> in alcoholic solutions, by Mitchell<sup>5</sup> and by Woolf<sup>6</sup> in ethanol—also by Quayle and Royals,<sup>7</sup> and by Dostrovsky and Hughes.<sup>8</sup>

(1) Taken from a Ph.D. dissertation submitted by J. E. Berger.

(2) This work was supported in part by a research grant from the U. S. Atomic Energy Commission.

(3) L. R. Dawson, E. D. Wilhoit, R. R. Holmes and P. G. Sears, *J. Am. Chem. Soc.*, **79**, 3004 (1957); L. R. Dawson and C. Berger, *ibid.*, **79**, 4269 (1957); W. D. Williams, J. A. Ellard and L. R. Dawson, *ibid.*, **79**, 4652 (1957).

(4) D. Segaller, *J. Chem. Soc.*, **103**, 1154, 1421 (1913); **105**, 112 (1914); **106**, 105 (1914).

(5) J. A. Mitchell, *ibid.*, **1792** (1937).

(6) S. Woolf, *ibid.*, **1172** (1938).

### Experimental

**Materials.**—N-Methylacetamide was prepared and purified by previously described methods which have been developed in this Laboratory.<sup>9</sup>

N,N-Dimethylacetamide was treated with solid KOH at 0° for 36 hours to remove water and acidic contaminants. The organic phase was refluxed at reduced pressure in the presence of freshly ignited CaO for 8 hours. Final distillation of this solvent was carried out at reduced pressure using a 120 cm. column packed with glass helices.

Sodium phenoxide was prepared as follows: Metallic sodium weighing several grams was converted to sodium shot<sup>10</sup> in anhydrous sulfur-free toluene. A known quantity of this sodium shot (approx. 5 g.) was placed in a one-liter flask containing 425 ml. of anhydrous sulfur-free toluene. The flask was equipped with a mechanical stirrer, an addition funnel and a reflux condenser to which a magnesium perchlorate-Ascarite drying tube was attached. Reagent grade phenol representing 5% excess over the stoichiometric quantity was dissolved in 225 ml. of toluene and added dropwise over an interval of two hours. During the addition step, the reaction mixture was stirred vigorously and maintained at temperatures between the ambient room temperature and the boiling point of the solvent. Following the addition step, heating was increased gradually until a state of gentle reflux was attained. Heating and stirring were continued for approximately 24 hours.

After the reaction mixture had cooled, the product was filtered *in situ* by inserting a porous glass tube connected to vacuum. The sodium phenoxide was washed repeatedly with toluene; in each case the toluene was removed by the "inverse filtering" technique. The white product was stored as a slurry in Skelly A solvent. To use, small portions of the slurry were withdrawn, filtered and dried in the absence of water vapor, carbon dioxide and oxygen.

To determine equivalent weights, samples of the salt were dissolved in water and titrated with dilute aqueous HCl. Repetitive determinations on samples from different preparations yielded an average value of 117.2 (calculated value for C<sub>6</sub>H<sub>5</sub>ONa is 116.1). The experimental equivalent weight value was unaltered by additional washings with inert solvents. This discrepancy, which is less than 1%, may be due to the effect of phenol (liberated during hydrolysis) on the end-point.

The solid sodium phenoxide was stored before use in a vacuum desiccator over magnesium perchlorate at pressures not exceeding 1 mm. (abs.). The salt can be stored for long periods of time as a slurry in an inert solvent.

The alkyl iodides were washed free of color using dilute aqueous NaOH. Successive extractions were made with distilled water until the aqueous phase was neutral. The alkyl iodides were dried over CaCl<sub>2</sub> for several hours and distilled through a 20 cm. column packed with glass helices. The colorless middle fractions were stored at 0° in the presence of freshly etched silver foil. This technique permitted these photosensitive compounds to be stored for relatively long periods of time without the appearance of colored impurities.

**Apparatus and Procedure.**—The reaction vessel was a water jacketed 50-ml. buret. Thermostatically controlled water was pumped through the water jacket to maintain the temperature of the buret within ±0.05° of the desired value. The temperature at a particular setting was determined by a calibrated thermometer.

Time intervals were measured to within 0.1 second by means of two stop watches so mounted that one watch could be stopped and the other started simultaneously.

Alkyl iodide solutions were prepared volumetrically at the temperature of the experiment. The necessary quantity of alkyl iodide was placed in a tightly stoppered volumetric flask and weighed. Buoyancy corrections were made in all cases. The flasks then were chilled in Dry Ice-acetone to prevent volatility losses of the alkyl iodides during the addition of N-methylacetamide. The solution was placed in a water thermostat at the temperature of the experiment and

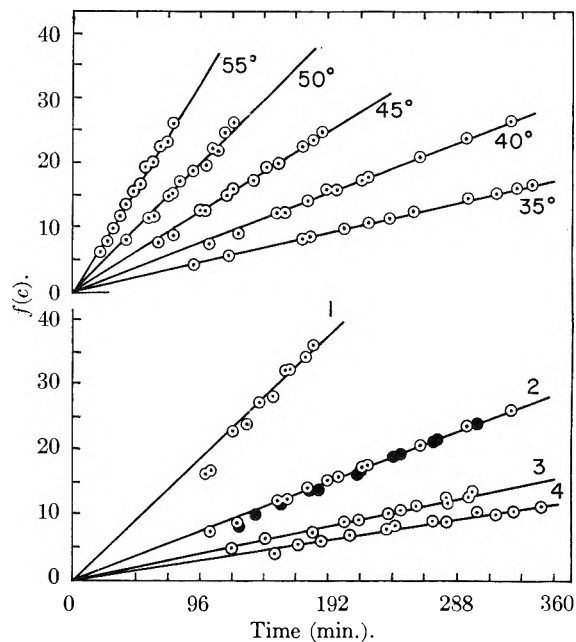


Fig. 1.—Lower ordinate: second-order type plots for the reaction of sodium phenoxide with alkyl iodides in N-methylacetamide at 40°. Curve 1, ethyl iodide; curve 2 -O- n-propyl iodide, -●- n-butyl iodide; curve 3, *i*-propyl iodide; curve 4, *i*-butyl iodide. Upper ordinate: second-order type plots for the reaction of sodium phenoxide with *n*-propyl iodide in N-methylacetamide. Reaction rate constant at 35° is 0.048 (moles/l.)<sup>-1</sup> min.<sup>-1</sup>; at 40°, 0.080; at 45°, 0.129; at 50°, 0.206; at 55°, 0.336.

the final volume adjustment was made by the addition of N-methylacetamide.

Sodium phenoxide solutions were prepared volumetrically at the temperature of the experiment and then analyzed for phenoxide content. Aliquots of the sodium phenoxide solution were placed in a known (excess) quantity of dilute aqueous HCl. Dilute aqueous NaOH was used to back titrate the sample to the brom thymol blue equivalence point.

To obtain reaction rate data, volumetric pipet (maintained at the temperature of the experiment) was used to transfer 25 ml. of the alkyl iodide solution to a 100-ml. flask equipped with a ground glass stopper. This mixing flask was maintained at the temperature of the experiment. From a second volumetric pipet (maintained at this same temperature) 25 ml. of sodium phenoxide solution was added to the flask. The start of flow from this second pipet into the flask was taken as zero time. The mixing flask was stoppered and shaken violently for approximately 30 seconds. The content of the flask was poured rapidly into the reaction buret. The top of the buret was kept stoppered to avoid vapor losses.

Quenching solutions consisted of 25 ml. of distilled H<sub>2</sub>O, 10 ml. 0.05059 *N* aqueous HCl and several drops of brom thymol blue. At different time intervals, 5-ml. samples of the reaction mixture were drained into the quenching solutions. The stop watches were stopped and started simultaneously when the sample began to drain from the buret tip. Immediately prior to each sample withdrawal, the small volume of the reaction mixture in the stopcock bore and buret tip was discarded. This procedure eliminated errors caused by the reaction taking place in the exposed buret tip. Sample sizes were chosen such that the quenching acid was present in excess. Back titration was done with 0.03056 *N* aqueous NaOH.

Rate constants were obtained for each point from the second-order reaction equation

$$\frac{1}{B_0 - A_0} \ln \frac{A_0 B}{B_0 A} = f(c) = kt \quad (1)$$

where  $A_0$  and  $B_0$  are the initial concentrations of the reactants at the time zero,  $A$  and  $B$  the concentrations at time  $t$ , and  $k$  is the rate constant. The average rate constants

(7) O. Quayle and E. E. Royals, *J. Am. Chem. Soc.*, **64**, 226 (1942).

(8) I. Dostrovsky and E. D. Hughes, *J. Chem. Soc.*, 157 (1946).

(9) L. R. Dawson, P. G. Sears and R. H. Graves, *J. Am. Chem. Soc.*, **77**, 1986 (1955).

(10) Louis F. Fieser, "Experiments in Organic Chemistry," D. C. Heath and Co., New York, N. Y., 1941, p. 385.

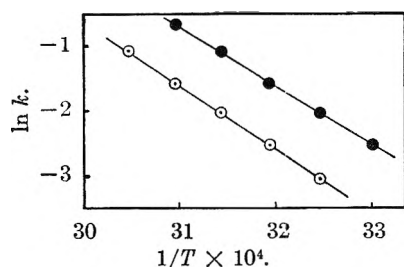


Fig. 2.—O—O—O, the logarithm of reaction rate constant *vs.* reciprocal of absolute temperature for the *n*-propyl iodide-sodium phenoxide reaction in N-methylacetamide. ●—●—●, the logarithm of reaction rate constant *vs.* reciprocal of absolute temperature for the *n*-propyl iodide-sodium phenoxide reaction in a mixed solvent composed of 79.97 wt. % N-methylacetamide and 20.03 wt. % N,N-dimethylacetamide (dielectric constant = 119.9).

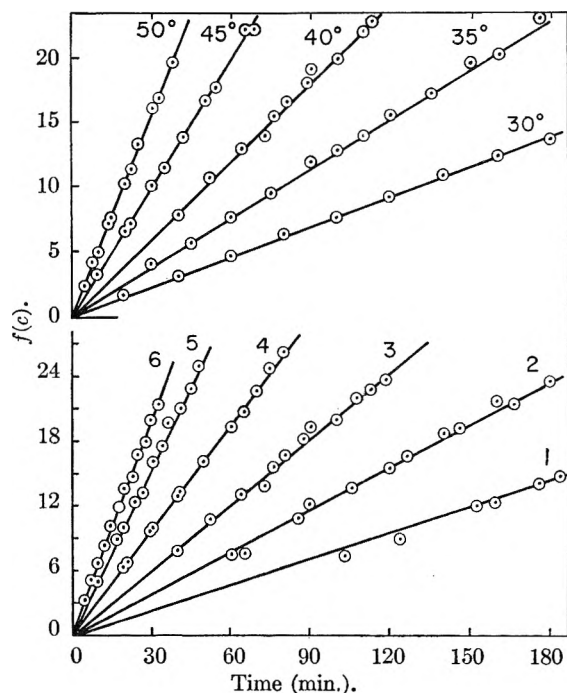


Fig. 3.—Lower ordinate: second-order type plots for the reaction of sodium phenoxide with *n*-propyl iodide in mixtures of N-methylacetamide and N,N-dimethylacetamide at 40°. Curve 1, 100 wt. % N-methylacetamide, reaction rate constant  $k = 0.0801$  (moles/l.)<sup>-1</sup> min.<sup>-1</sup>, dielectric constant  $D = 165.3$ ; curve 2, 90.01 wt. % NMA,  $k = 0.1308$ ,  $D = 140.8$ ; curve 3, 79.97 wt. % NMA,  $k = 0.2022$ ,  $D = 119.9$ ; curve 4, 70.07 wt. % NMA,  $k = 0.3245$ ,  $D = 102.5$ ; curve 5, 60.08 wt. % NMA,  $k = 0.5150$ ,  $D = 88.2$ ; curve 6, 55.13 wt. % NMA,  $k = 0.6564$ ,  $D = 81.3$ . Upper ordinate: second-order type plots for the reaction of sodium phenoxide with *n*-propyl iodide in a mixed solvent composed of 79.97 wt. % N-methylacetamide and 20.03 wt. % N,N-dimethylacetamide (dielectric constant = 119.9). Reaction rate constant at 30° is 0.0787 (moles/l.)<sup>-1</sup> min.<sup>-1</sup>; at 35°, 0.1283; at 40°, 0.2022; at 45°, 0.3343; at 50°, 0.5180.

were obtained by the least squares treatment of the  $f(c)$  *vs.*  $t$  data.<sup>11</sup> Activation energies were obtained in the customary way from Arrhenius plots.

**Conductance and Dielectric Constant Measurements.**—The conductance of sodium phenoxide in N-methylacetamide at 40° was determined by methods which have been reported previously by this Laboratory.<sup>12</sup> The dielectric

constants of mixtures of N-methyl- and N,N-dimethylacetamide at 40° were determined in a manner similar to that reported by Eckstrom, Berger and Dawson.<sup>13</sup>

### Results and Discussion

Second order plots of  $f(c)$  from eq. 1 *vs.* time for the reaction of sodium phenoxide with the five alkyl iodides in pure N-methylacetamide at 40° are shown in Fig. 1. Comparison of the reactivities is given in Table I.

TABLE I

COMPARISON OF THE REACTIVITIES OF SEVERAL ALKYL IODIDES WITH SODIUM PHENOXIDE IN N-METHYLACETAMIDE AT 40°

Alkyl iodide	$k$ (moles/l.) <sup>-1</sup> min. <sup>-1</sup>	Relative reactivity	Relative reactivity <sup>b</sup>
Ethyl	0.196	5.94 <sup>a</sup>	2.48 <sup>b</sup>
<i>n</i> -Propyl	.080	2.42	1.01
<i>n</i> -Butyl	.079	2.39	1.00
<i>i</i> -Propyl	.044	1.33	..
<i>i</i> -Butyl	.033	1.00	..

<sup>a</sup> Reactivity of *i*-butyl iodide taken as unity. <sup>b</sup> Reactivity of *n*-butyl iodide taken as unity.

Apparently the attack of a phenoxide ion on the alkyl iodide is made with approximately equal efficiency for straight-chain halides possessing three or more carbon atoms. Since the branched chain aliphatic halides are less reactive than the analogous normal aliphatic halides, the number of effective collisions must have decreased as steric effects become operative. Unfortunately, tertiary aliphatic iodides could not be studied because of solvolysis and side reactions.

When only the normal aliphatic iodides are considered, the relative reactivities are given in the last column of Table I. This order is to be expected and has been observed by other investigators using different solvents and different salts.<sup>14,15</sup> In ethanol solutions, Segaller<sup>4</sup> obtained values of 1.00, 1.05 and 2.63 for the same reacting species. The observations of several other authors<sup>16</sup> confirm the fact that little change in reaction rate is observed for SN<sub>2</sub> reactions of primary aliphatic halides as the carbon chain is lengthened past *n*-propyl.

Rate data for the reaction of *n*-propyl iodide with sodium phenoxide at five temperatures are given in Fig. 1. The rate constant increases by a factor of approximately 2.6 for each ten degree rise in temperature. Segaller<sup>17</sup> obtained higher temperature coefficients for comparable reactions in ethanolic solutions. In studying various alkyl iodide-sodium eugenoxide reactions, Woolf<sup>18</sup> reported temperature coefficients of 2.5 compared to a value of 3.0 reported by Segaller.

The Arrhenius activation energy plot is given in Fig. 2 from which an activation energy of 19.39 kcal./mole is obtained. For this same reaction in ethanolic solution, Segaller<sup>17</sup> obtained a value of 21.8 kcal./mole. For the reaction of *n*-butyl iodide with sodium phenoxide in ethanolic solution,

(13) H. C. Eckstrom, J. E. Berger and L. R. Dawson, *J. Phys. Chem.*, **64**, 1458 (1960).

(14) A. Menshutkin, *Z. physik. Chem.*, **4**, 273 (1899).

(15) Burke and Donnay, *J. Chem. Soc.*, **85**, 555 (1904).

(16) T. I. Crowell, *J. Am. Chem. Soc.*, **75**, 6046 (1953).

(17) D. Segaller, *J. Chem. Soc.*, **105**, 106 (1914).

(18) S. Woolf, *ibid.*, 1172 (1937).

(11) The calculations were performed on an IBM 650 by Dr. J. W. Hamblen of the University of Kentucky computing Center.

(12) L. R. Dawson, P. G. Sears and R. H. Graves, *J. Am. Chem. Soc.*, **77**, 1986 (1955); L. R. Dawson, E. D. Wilhoit and P. G. Sears, *ibid.*, **78**, 1569 (1956).

Quayle and Royals<sup>7</sup> obtained an activation energy of 19.53 kcal./mole. Using the activation energy 19.39 kcal./mole at 313°K., the fraction of effective collisions was found to be  $2.93 \times 10^{-14}$  and a frequency factor of  $0.455 \times 10^{11}$  l./mole-sec. By interpolating Segaller's data to obtain a rate constant at 313°K., a frequency factor of  $1.04 \times 10^{11}$  l./mole-sec. is obtained. These values agree well with the collision theory value of about  $10^{11}$  for most examples.

To determine the effects of dielectric constant on the reaction of *n*-propyl iodide with sodium phenoxide, mixed solvents of *N*-methylacetamide and *N,N*-dimethylacetamide were used to vary the dielectric constant from approximately 165.3 to 81.3. In Fig. 3 the second-order function  $f(c)$  is plotted against time for pure *N*-methylacetamide and for five mixtures. One should expect the logarithm of the reaction rate constant for ion-neutral molecule reaction to be a linear function of the reciprocal of the dielectric constant. A small but definite deviation from linearity is discernable in Fig. 4. It can be argued that this deviation is the result of (1) the localized higher dielectric constant in the vicinity of solute particles and (2) the viscosity effect which would retard the reaction in mixtures rich in *N*-methylacetamide.

The localized higher dielectric constant in the vicinity of solute particles could be the result of preferential absorption of the more polar constituent, *N*-methylacetamide, by phenoxide ions and the polar iodide molecules. Hence, in the vicinity of these solute entities there could be a higher dielectric constant than in the bulk solvent phase. If this were the case, the observed rate constants could actually correspond to those characteristic of media of higher dielectric constant. This would tend to move upward these points lying near the top of Fig. 4 and tend to make the results linear. The concept of preferential solvation is not a new idea, but is one that has been used to explain other physical phenomenon of solutions.<sup>19,20</sup>

Viscosity effects could contribute to the acceleration of the reaction in the mixed solvent systems since *N*-methylacetamide is approximately 4 times more viscous than the corresponding dimethyl compound. As in the case of dielectric constants, the addition of small quantities of *N,N*-dimethylacetamide to *N*-methylacetamide may greatly decrease the viscosity of the resulting mixture. The depolymerization of *N*-methylacetamide aggregates has been observed by viscosity studies of dimethylformamide-*N*-methylacetamide mixtures.<sup>19</sup> If the reaction rate is governed by the ability of the phenoxide ions and the *n*-propyl iodide molecules to move through the medium, then it seems reasonable to expect increases in the rate constant with decreases in viscosity.<sup>21</sup>

An approximately 80 weight % *N*-methylacetamide—20 weight % *N,N*-dimethylacetamide

(19) L. R. Dawson and W. W. Wharton, *J. Electrochem. Soc.*, (in press).

(20) H. Sadek and R. M. Fuoss, *J. Am. Chem. Soc.*, **72**, 301 (1950), corrections *ibid.*, **72**, 5803 (1950); R. C. Miller and R. M. Fuoss, *ibid.*, **75**, 3076 (1953); F. M. Sacks and R. M. Fuoss, *ibid.*, **75**, 5172 (1953).

(21) E. A. Moelwyn-Hughes, "The Kinetics of Reactions in Solution," Clarendon Press, Oxford, 1947, p. 218.

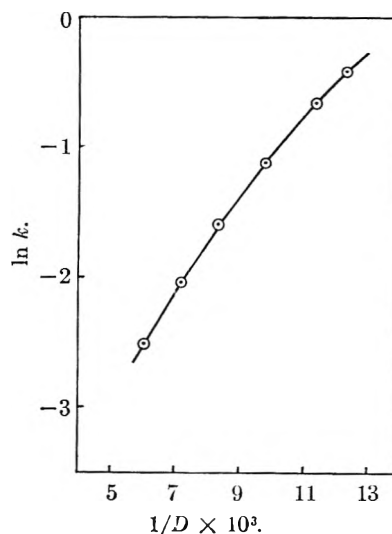


Fig. 4.—The logarithm of reaction rate constant vs. reciprocal of dielectric constant for the reaction of sodium phenoxide with *n*-propyl iodide at 40°.

solvent mixture with the *n*-propyl iodide—sodium phenoxide reaction system was studied as a function of temperature. Data, in the form of second-order plots, are presented in Fig. 3. The activation energy of 18.38 kcal./mole was obtained from Fig. 2 with values of  $1.48 \times 10^{-13}$  for the fraction of effective collisions and of  $0.228 \times 10^{11}$  l./mole-sec. for the frequency factor. These results imply that there are more effective collisions in the mixed solvents and that the reaction rate is less dependent upon temperature changes. These data lend evidence of depolymerization and selective solvation of *N*-methylacetamide when *N,N*-dimethylacetamide is added to the system. In pure *N*-methylacetamide temperature increases undoubtedly cause degradation of polymer chains, thus increasing reaction rate, but in the mixed solvent extensive degradation has been accomplished already by the introduction of the second component. This argument is supported by the fact that the rate constants for this selected reaction at a given temperature are higher in the mixed solvent than in pure *N*-methylacetamide; this is apparent from Fig. 3. It also seems plausible that the ultimate structure of the mixed solvent would be less responsive to temperature changes than that of *N*-methylacetamide, thus resulting in a lower activation energy.

When the concentration of the *n*-propyl iodide was held invariant and the initial concentration of sodium phenoxide was varied, the reaction rate constant was observed to decrease by about 6% as the initial phenoxide concentration was increased from 0.03 to 0.07 M. Segaller<sup>4</sup> was the first to observe this phenomenon in the alkyl iodide—sodium phenoxide reaction in ethanol. Quayle and Royals<sup>7</sup> also noticed this behavior in the reaction of *n*-butyl bromide with the sodium salts of phenol, thiophenol and *n*-butyl mercaptan. Woolf<sup>18</sup> and Mitchell<sup>5</sup> also obtained similar results in their studies of the reactions of alkyl iodides with sodium eugenoxide and sodium guaiacoxide, respectively. In each of these literature reports,

and in the present investigation, the second-order rate constant decreased as the concentration of the sodium salt was increased.

A concentration effect of this nature is taken customarily as evidence that the reaction under consideration is ionic in nature and that the rate constant is dependent on the degree of ionization. To interpret this effect Acree<sup>22</sup> and his collaborators postulated a "dual hypothesis" which assumed that both ions and neutral molecules of the salt are capable of reacting, thus the observed rate constant is a combination of an ionic rate constant and a molecular rate constant with the degree of dissociation as the variable parameter. Conductance

(22) H. C. Robertson and S. F. Acree, *J. Am. Chem. Soc.*, **37**, 1902 (1915).

data for sodium phenoxide in N-methylacetamide showed a linear Kohlrausch plot to concentrations approaching 0.1 mole/l. The slope of the conductance curve was  $-18.23$ ; the theoretical slope is  $-13.21$ . Using the well known Shedlovsky modification of the Onsager equation the limiting equivalent conductance was found to be  $17.50 \text{ ohms}^{-1}$  with a dissociation constant of 0.33. In the case of the dilute solutions used in this work where the dielectric constant ranged from 81.3 to 165.3, the sodium phenoxide may be considered essentially completely dissociated. It seems probable that an invariant value of the rate constants might be obtained by incorporating activity coefficients, but these studies were outside the scope of the present work.

## THE CONDUCTANCES OF A NUMBER OF ACIDS AND DIVALENT METAL SALTS IN ANHYDROUS ETHANOLAMINE

BY PHILIP W. BREWSTER, FREDERIC C. SCHMIDT<sup>1</sup> AND WARD B. SCHAAP

Contribution No. 987 from the Department of Chemistry, Indiana University, Bloomington, Ind.

Received December 14, 1960

The conductances of solutions of three halogen acids and benzoic acid, some simple salts of strontium and barium, and salts of lead have been studied in anhydrous ethanolamine. The phoreograms in the dilute regions are normal in the case of the alkaline earth metal salts, but have positive slopes in the case of the acids and the lead salts. An explanation for these cases is suggested in terms of suppression of solvent ionization and complex ion formation.

### Introduction

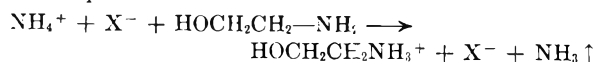
In a previous paper<sup>2</sup> it was shown that anhydrous ethanolamine has an extremely high solvent conductance, no doubt due to the high auto-ionization of the solvent. It was further shown that salts of the alkali metals have high ion-pair dissociation constants, and it was therefore of interest to examine the conductance of the halogen acids in this medium. Salts of lead were investigated to study the effects of stable complex formation involving the amine solvent.

### Experimental

The bridge and accessories have been previously described.<sup>3</sup>

The salts of lead and the alkaline earth salts were weighed in small tared cups and added to the cell in the normal way. The conductance curves of the acids, however, were obtained by adding concentrated solutions of the acids (hydrohalides of ethanolamine) in ethanolamine from a calibrated 10-ml. micropipet-buret (Emil Greiner Corp.). Results for KI with this method were in excellent agreement with those obtained by adding the concentrated solution by means of a tared syringe into a cell sealed by a serum cap.

The solutions of halogen acids were prepared by adding reagent grade ammonium halides to pure anhydrous ethanolamine and pumping off the liberated ammonia, according to the equation



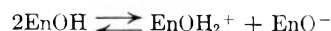
The reaction is completely stoichiometric. The mono and dihydro halide can be made at will. All other metal salts used were also reagent grade or Johnson-Matthey "Specpure" grade.

**Acids in Ethanolamine.**—The experimental conductance values are given in Table I. It will be seen that these are anabatic in the case of the acids to the extent of having positive slopes, the slope decreasing with increasing concentration. It appears that the high auto-ionization of the solvent is being suppressed to some extent by the presence of the acidic solute. Thus, subtraction of the total solvent correction from the conductance of the solutions leads to a *large over-correction* in the most dilute regions. Since the solvent correction becomes relatively less important as concentration of solute increases, the curves finally attain the normal negative slopes at concentrations greater than about 0.3 molar. In order to obtain some idea of the true nature of the acid curves it was decided to allow for the suppression of solvent ionization. The calculations are based on the following data and assumptions.

The specific conductance of the pure solvent =  $11.0 \times 10^{-6}$ . Making reasonable assumptions regarding the mobilities of the solvo-cations and solvo-anions, we estimate  $\Lambda_0$  (solvent) = 7.5.

Then, from the specific conductance of the solvent the concentration of solvoions is estimated by  $\lambda = 1000L/C$ , thus  $C = 1.4 \times 10^{-3}$  moles/l.

Now  $C = [\text{EnOH}_2^+] = [\text{EnO}^-]$  in pure ethanolamine, since the solvent ionizes according to the equation



(The above notation is for convenience and is not to be implied that the hydroxyl group is responsible for the ionization.) (The proton is presumably located on the amino end of the chain.) The ion

(1) Address all correspondence to F. C. Schmidt. This investigation was carried out under A. E. C. contract No. AT(11-1)256.

(2) P. W. Brewster, F. C. Schmidt and W. B. Schaap, *J. Am. Chem. Soc.*, **81**, 5532 (1959).

(3) B. B. Hibbard and F. C. Schmidt, *ibid.*, **77**, 225 (1955).



TABLE I  
DATA FOR CONDUCTANCES OF VARIOUS SALTS IN ANHYDROUS

ETHANOLAMINE ( $T = 25.0^\circ$ )			
$c \times 10^4$	$\Lambda$	$c \times 10^4$	$\Lambda$
Hydrochloric acid		Hydriodic acid	
0.82501	4.610	2.0113	4.822
3.2962	4.763	1.9844	5.101
4.4102	4.802	4.3876	5.219
6.2771	4.865	5.2678	5.260
8.5349	4.922	6.6003	5.309
11.138	4.987	10.340	5.441
16.013	5.116	12.159	5.521
23.274	5.276	15.606	5.650
31.203	5.412	23.569	5.882
43.736	5.582	29.705	6.071
49.879	5.640	42.350	6.235
62.197	5.689	53.795	6.355
71.571	5.730	59.933	6.402
88.131	5.699		
Solvent conductance: $11.056 \times 10^{-6}$		Solvent conductance: $11.593 \times 10^{-6}$	
Hydrobromic acid		Benzoic acid	
0.31042	5.154	3.5816	3.512
0.82253	5.228	7.8686	3.657
3.7301	5.356	11.561	3.775
4.8146	5.411	15.255	3.881
7.5625	5.529	19.103	3.981
13.581	5.752	26.175	4.126
18.767	5.900	33.955	4.237
28.179	6.122	40.941	4.309
42.518	6.342	51.543	4.386
52.872	6.436		
66.069	6.527		
Solvent conductances: $11.315 \times 10^{-6}$		Solvent conductances: $11.144 \times 10^{-6}$	
Lead iodide		Lead nitrate	
1.9162	5.140	9.1936	5.869
3.1286	5.082	1.9387	5.534
4.6365	5.221	5.2110	5.668
5.1193	5.187	7.2896	5.789
7.0953	5.282	13.869	5.980
12.632	5.428	19.433	6.095
17.395	5.546	24.802	6.218
25.176	5.751	30.268	6.320
		35.988	6.401
		41.852	6.451
		53.352	6.523
		63.160	6.566
		76.194	6.568
		94.355	6.566
		120.57	6.542
Solvent conductance: $11.316 \times 10^{-6}$		Solvent conductance: $11.140 \times 10^{-6}$	
Barium nitrate		Barium chloride	
5.5254	4.931	6.5921	4.429
9.9773	4.743	10.796	4.375
13.311	4.618	16.180	4.338
16.915	4.469	21.445	4.322
20.683	4.328	27.494	4.312
26.409	4.154	34.555	4.278
31.014	4.037	42.568	4.225
37.713	3.885	50.922	4.186
46.290	3.731	62.905	4.124
57.548	3.564		
70.479	3.442		

Solvent conductance: $11.214 \times 10^{-6}$		Solvent conductance: $11.163 \times 10^{-6}$	
Strontium nitrate		Lead bromide	
4.4686	5.489	1.9973	5.332
7.1506	5.265	3.9641	5.414
10.868	5.042	5.7773	5.517
15.664	4.853	8.2977	5.609
21.002	4.670	11.994	5.702
26.233	4.490	15.474	5.806
32.489	4.355	18.572	5.894
39.653	4.216	22.186	5.970
49.110	4.093	25.928	6.089
60.468	3.941	32.257	6.104
Solvent conductance: $11.559 \times 10^{-6}$		Solvent conductance: $11.323 \times 10^{-6}$	

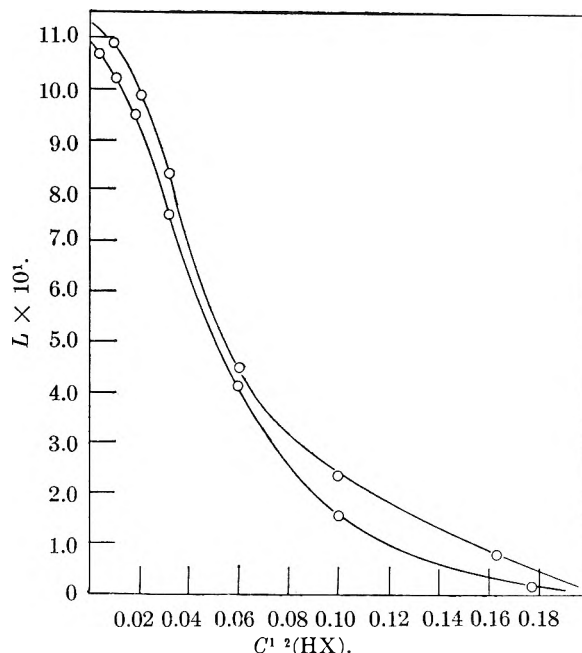
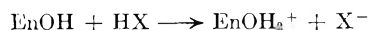


Fig. 1.—Solvent correction curve for acids in ethanolamine.

product constant of the pure solvent is then given by the expression

$$K_s = [\text{EnO}^-][\text{EnOH}_2^+] = (1.4 \times 10^{-3})^2 = 2 \times 10^{-6}$$

Addition of low concentrations of a strong acid (HX) to the solvent will result in solvation of the acid



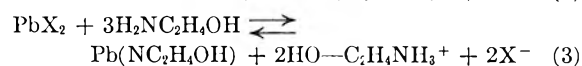
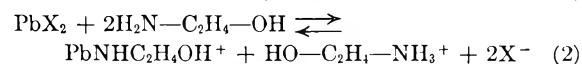
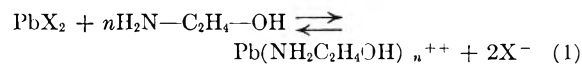
Thus the true total  $[\text{EnOH}_2^+] = C_{\text{HX}} + x$ , where  $C_{\text{HX}}$  is the concentration of acid added and  $x$  represents the  $[\text{EnOH}_2^+]$  arising from the solvent ionization. However,  $x$  is also equal to  $[\text{EnO}^-]$ . Thus,  $(C_{\text{HX}} + x)[\text{EnO}^-] = (C_{\text{HX}} + x)x = 2 \times 10^{-6}$  and  $x = -C_{\text{HX}} \pm \sqrt{C_{\text{HX}}^2 + 8 \times 10^{-6}/2}$ . A series of values of  $x$  for different values of  $C_{\text{HX}}$  can be calculated, and a new solvent correction curve can be drawn for each  $\Lambda_0$  value assumed for the solvoions. Two of these curves are shown in Fig. 1, the lower one is based on the assumption that  $\Lambda_0 = 7.5$  and the upper one assumes  $\Lambda_0 = 6.5$ . It will be seen from these curves that solvent ionization is essentially completely suppressed by the dissolved solute above  $C^{1/2} = 0.1$ . The results of applying the corrections to the conductance of

the four acids can be seen in the table. The phoreograms when plotted now show the expected negative slope in the more concentrated regions. The correction is obviously of the right order, but too much should not be expected, since it is assumed that all acids are completely dissociated, a fact unlikely to be true at higher concentration, and because of the uncertainty in the value of  $\Lambda_0$  of the solvent. The corrected values shown are based on a calculation assuming  $\Lambda_0$  (solvent) = 7.0. The phoreograms for HCl and HBr extrapolated to approximately the same value, but HI extrapolates somewhat lower. Data from the alkali salts presented in the previous paper would require that the halogen acids extrapolate roughly to the same limiting conductance.

The corrected curve for benzoic acid is typical of a weaker electrolyte. At present it appears that the simple, calculated solvent correction outlined above is approximately correct, but is certainly not exact in this simple form.

**Lead Salts.**—The phoreograms of these salts resemble those of the acids, being anabatic in the most dilute regions, then leveling out and becoming almost parallel with the concentration axis. The explanation of this must again involve a suppression of the solvent conduction, but in the cases of these cations, the protons arise from the solvolysis of the cations. It is entirely possible that the lead ion, like ions of silver and mercury, is able to undergo solvolytic reactions in anhydrous ethanolamine. Such reactions are known to take place with these ions in liquid ammonia, a much less ionized solvent than the amine in question.

The following equilibria are postulated to exist when a lead salt dissolves in ethanolamine



Reactions 2 and 3, *i.e.*, the formation of the amide and the imide, involve the formation of varying

amounts of free halogen acid, and therefore a comparison of the conductance of the lead salt with that of the corresponding halogen acid should indicate which of the above reactions is predominant.

Reaction 1 can be quickly discounted, since this is simple solvation and should lead to a conductance curve with a normal negative slope. Reaction 3 gives rise to an equivalent quantity of free halogen acid and therefore should, because of the un-ionized nature of the lead imide produced, give a phoreogram superimposable upon that of the corresponding halogen acid. Reaction 2 would by similar reasoning be expected to give a conductance curve with slope intermediate between these two extremes, since only one-half equivalent of free halogen acid is produced in the reaction and the suppression of the solvent conductance is correspondingly less.

Comparison of the conductance curves of HBr and  $\text{PbBr}_2$  shows these to have very similar slopes and to be nearly superimposable. Thus it would seem that reaction 3 is essentially the *only* reaction occurring in the case of  $\text{PbBr}_2$ . The phoreogram for  $\text{PbI}_2$  has a smaller slope than that of HI and  $\text{PbI}_2$  shows less conductance than HI at a given concentration. This behavior would be expected, if in this case reaction 2 played a part, or if the iodide ion partially complexed the lead to form a complex such as  $\text{PbI}_4^{2-}$ , which is known to be very stable in aqueous solutions. Cadmium halides complex readily with halide ions to give a stable  $\text{CdX}_4^{2-}$  ion.

**Alkaline Earth Salts.**—The conductance values for three alkaline earth salts are given also in Table I. No Fuoss-Kraus extrapolation for these salts was attempted since the ion-pair dissociation constant so obtained would be complicated by the possibility of the existence of two ion-pair equilibria. As with the alkali metal salts, the experimental Onsager slopes are greater than the calculated values. The Kohlrausch difference for  $1/2$ - $(\text{Ba}(\text{NO}_3)_2-\text{BaCl}_2)$  is 0.45 unit and is in excellent agreement with 0.42 obtained from the means of the differences for sodium and potassium salts, *i.e.*,  $(\text{NaNO}_3-\text{NaCl})$  and  $(\text{KNO}_3-\text{KCl})$ .

RATE OF REACTION,  $O + H_2 \rightarrow OH + H$ , IN FLAMES

BY C. P. FENIMORE AND G. W. JONES

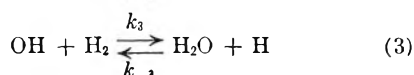
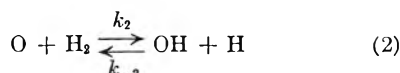
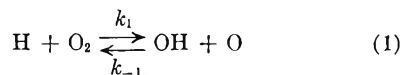
General Electric Research Laboratory, Schenectady, N. Y.

Received December 16, 1960

By probing low pressure flames of  $H_2-O_2-N_2-N_2O$ , and using the ratios of rate constants previously determined in flames, we find that the rate constant for the reaction of oxygen atoms with hydrogen molecules is  $2.5 \pm 0.4 \times 10^8$  l. mole<sup>-1</sup> sec.<sup>-1</sup> at 1660°K. and  $3.0 \pm 0.3 \times 10^8$  at 1815°. These values agree with a long extrapolation of Baldwin's results at about 800°K., and combine with them to give  $k = 2.5 \times 10^8 e^{-7.7 \text{ kcal./RT}}$  l. mole<sup>-1</sup> sec.<sup>-1</sup>.

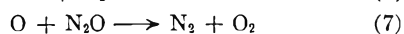
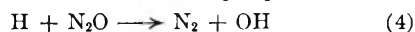
## Introduction

Of the three important bimolecular reactions in  $H_2-O_2$  mixtures



$k_1^{1-4}$  and  $k_3^{5,6}$  are moderately well known over a considerable range of temperature, but  $k_2^2$  has not been measured above 820°K. and estimates of its value at high temperatures would be worthwhile. Measurement of  $k_2$  in some  $H_2-O_2-N_2-N_2O$  flames are reported in this paper.

Nitrous oxide is included in the reactants because its irreversible decomposition in low pressure  $H_2-O_2$  flames allows the measurement of radical concentrations. It reacts chiefly by



of which (4) is the fastest by far.

It is assumed that no important reaction of oxygen atoms has been omitted, so that we can write out the expression for  $d[O]/dt$  due to the chemical reactions above and solve the resulting expression for  $k_2$ . Any consumption of oxygen atoms in the recombinations  $2O + M \rightarrow O_2 + M$  or  $O + H + M \rightarrow OH + M$  has been ignored, but these termolecular recombinations must be small compared to the reverse of reaction 1 which is included. Another simplification may as well be made from the start; it will always be possible to neglect the reverse of reaction 2 in the region where  $k_2$  is evaluated, as will be shown, and to choose this region so that  $d[O]/dt$  is approximately zero. Then

$$k_2 = \frac{-d[O]_2/dt + k_5[N_2O][M] - d[NO]/2dt}{[H_2][O]}$$

and everything on the right side of this expression can be measured.

The rates of change of  $[O_2]$  and  $[NO]$  can be obtained by probing flat, one dimensional flames and

correcting the traverses for diffusion. The composition traverses also allow estimates of  $k_5[N_2O][M]$  and  $[H_2]$  at any point.

$[O]$  can be estimated in two independent ways. First, since the nitric oxide formed in reaction 6 does not undergo appreciable decomposition,  $[O]$  can be obtained from

$$d[NO]/dt = 2k_6[O][N_2]$$

Second, it can also be estimated from the three reactions 4, 3 and 1 because

$$-d[N_2O]/dt = k_4[H][N_2O]$$

accounts for most of the decomposition of nitrous oxide and gives an estimate of  $[H]$  which can be substituted into

$$d[H_2O]/dt = k_3[OH][H_2] - k_{-3}[H_2O][H]$$

to get  $[OH]$ . Both  $[H]$  and  $[OH]$  can then be substituted in

$$-d[O_2]/dt + k_7[O][N_2O] = k_1[H][O_2] - k_{-1}[OH][O]$$

to get  $[O]$ . In the last expression, the term in  $k_7$  can be omitted whenever  $d[NO]/dt$  is small compared to  $-d[O_2]/dt$  because  $k_7 < k_6/2$ .

Although the determination of  $[O]$  from reactions 4, 3 and 1 may seem involved, this method has two advantages over the simpler determination by reaction 6. It does not really depend on the separate values of  $k_4$ ,  $k_3$ ,  $k_1$  but only on their ratios; and since these constants were measured relative to one another in the temperature range in which we use them, the ratios are probably more accurate than the separate values.  $[O]$  from reaction 6 does of course depend on the separate value of  $k_6$ .

Also the reaction rates one uses in (4), (3) and (1) are fairly large and can be tested for internal consistency. In a region where  $d[O]/dt$  and  $d[OH]/dt$  are small, one should have  $-d[N_2O]/dt - 2d[O_2]/dt = d[H_2O]/dt + d[NO]/dt$  since oxygen must be conserved. This relation holds experimentally within 10%, and  $d[NO]/dt$  is always small compared to the three other terms in the equality. Therefore the three larger terms are at least consistent among themselves. The small  $d[NO]/dt$  used in the determination of  $[O]$  via reaction 6 cannot be tested in the same way because it does not make a very significant contribution to the conservation of oxygen or nitrogen.

The values adopted for the rate constants are quoted in Table I.  $k_1$ ,  $k_3$ ,  $k_4$  and  $k_5$  are correct relative to one another to perhaps 30%, and  $k_1$  and  $k_3$  also agree within a factor of two with independent estimates in the literature.  $k_5$  is obtained from a correlation of much of the data on the pseudo-unimolecular, thermal decomposition of nitrous oxide.<sup>7</sup> The limiting low pressure con-

- (1) N. N. Semenov, *Acta Physicochim.*, **20**, 290 (1945).
- (2) R. R. Baldwin, *Trans. Faraday Soc.*, **52**, 1344 (1956).
- (3) G. L. Schott and J. L. Kinsey, *J. Chem. Phys.*, **29**, 1177 (1958).
- (4) C. P. Fenimore and G. W. Jones, *J. Phys. Chem.*, **63**, 1154 (1959).
- (5) L. Avramanko and R. Lorentso, *Zhur. Fiz. Khim.*, **24**, 207 (1950).
- (6) C. P. Fenimore and G. W. Jones, *J. Phys. Chem.*, **62**, 693 (1958).

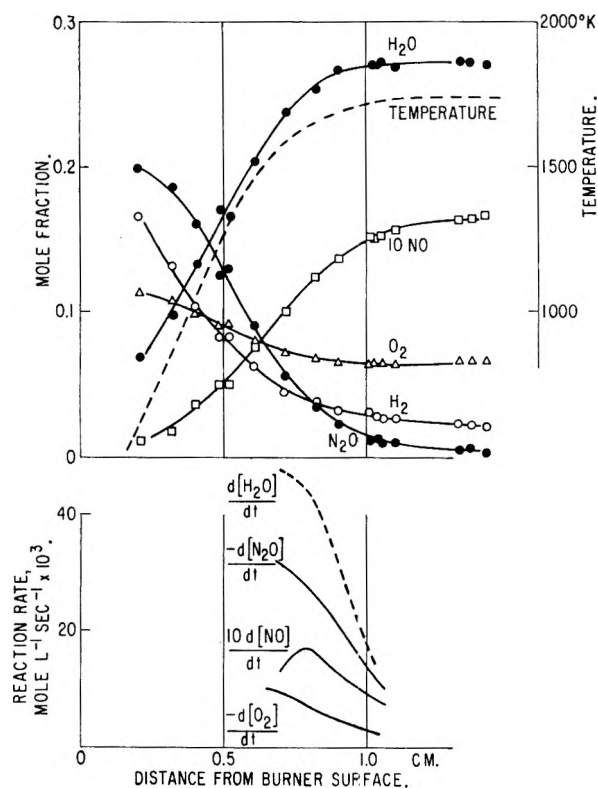


Fig. 1.—Traverses through a flame of reactant composition  $H_2 + 0.66N_2O + 1.81$  air burnt at 2 cm. pressure of mercury with a mass flow of  $2.32 \times 10^{-3}$  g. cm. $^{-2}$  sec. $^{-1}$ . Calculated reaction rates are plotted in the lower part of the graph.

stant listed is appropriate to initially pure nitrous oxide where  $[M]$  represents initial  $[N_2O]$ . If  $[M]$  represents the total concentration of a mixture of other gases, as it does in our flames, the

TABLE I  
BIMOLECULAR RATE CONSTANTS<sup>a</sup>

Reaction	Rate constant, mole l. $^{-1}$ sec. $^{-1}$	Ref.
1	$6 \times 10^{11} e^{-18/P.T}$	4
3	$2.5 \times 10^{11} e^{-10/R.T}$	6
4	$4 \times 10^{11} e^{-16.3/R.T}$	4
5	$4 \times 10^{12} e^{-59/K.T}$	7
6	$1 \times 10^{11} e^{-28/R.T}$	8
7	$k_7 < k_6/2$	9

<sup>a</sup> For reactions 1, 2 and 3, the rate constants for the reverse reactions can be obtained from the constants for the forward reactions and the equilibrium constants;  $k_1/k_{-1} = 35e^{-16.6/R.T}$ ,  $k_2/k_{-2} = 2e^{-8.0/R.T}$ ,  $k_3/k_{-3} = 0.25e^{15.5/R.T}$ .

pre-exponential factor of  $k_5$  could be wrong by a factor of about two, and we will discuss this possibility later. For any use we make of  $k_7$ , it will be enough to know that at the temperatures of interest  $k_7$  is smaller than  $k_6$ .

The diffusion corrections to get  $d[NO]/dt$ ,  $-d[O_2]/dt$ ,  $-d[N_2O]/dt$ ,  $d[H_2O]/dt$  from experimental composition traverses caused us some trouble. With the diffusion coefficients  $D_{NO}$ ,  $D_{O_2}$ , etc., assumed the chemical reaction rates were

(7) H. S. Johnston, *J. Chem. Phys.*, **19**, 663 (1951).

(8) C. P. Fenimore and G. W. Jones, 8th Combustion Symposium at Pasadena, Calif., Sept. 1960.

(9) F. Kaufman, N. J. Gerri and R. E. Bowman, *J. Chem. Phys.*, **25**, 106 (1956).

calculated just as before.<sup>4</sup> The flames were 60 to 70% nitrogen, and we first tried approximate  $D_{NO}$  values appropriate to binary NO- $N_2$  mixtures.<sup>10</sup> These gave too great a correction however, and resulted in negative calculated values of  $d[NO]/dt$  in the early parts of some flames. After several trials in different runs, we eventually used

$$D_{NO} = 2.3 \times 10^{-4} T^{1.67} \text{ cm.}^2 \text{ sec.}^{-1}$$

in all flames at 4 cm. pressure of mercury. For other species, the diffusion coefficient was taken from  $D_{NO}$  under the assumption that  $D$  was inversely proportional to the square root of the molecular weight. For other pressures, it was assumed that  $D$  varied inversely with pressure. The value chosen for  $D_{NO}$  is near the greatest value which did not overcorrect the nitric oxide traverse.

The calculation of  $[O]$  by means of reaction 6 is considerably more sensitive to changes in the diffusion coefficient than is the calculation *via* (4), (3) and (1). A smaller  $D_{NO}$  decreases the maximum  $[O]$  as calculated from (6).

### Experimental

The arrangement was the same as used before. It included a water-cooled, porous, flat flame burner<sup>11</sup> of 31.1 cm. $^2$  surface area mounted in a bell jar which was also equipped with a movable quartz probe ( $\sim 0.1$  mm. diam.), movable quartz coated thermocouple (made of butt-welded Pt-Pt, Rh wires 0.012 mm. diam.), pumps, and externally mounted cathetometer. The reactants were metered through critical flow orifices. Thermocouple readings were corrected for radiation<sup>11</sup> to get temperature traverses. Composition traverses of the stable components were obtained from mass spectrometric analyses of samples drawn through the quartz probe at critical flow rates.

**Determination of  $k_2$ .**—The upper half of Fig. 1 presents typical traverses through a flame burnt at 2 cm. pressure. The lower part of the figure shows reaction rates calculated from the traverses.  $[O]$  as calculated from

$$[O] = d[NO]/2k_6[N_2O]dt$$

attains a maximum value of  $6.0 \times 10^{-6}$  mole l. $^{-1}$  at 0.8 to 0.95 cm. from the burner surface.

Calculating  $[O]$  in the alternate way described above, we find that

$$[H] = -d[N_2O]/k_4[N_2O]dt$$

is relatively constant through most of the flame. At a position 0.8 to 0.95 cm. from the burner surface,  $[H] = 1.4 \times 10^{-6}$  mole l. $^{-1}$ ; and then in turn,  $[OH] = 0.83 \times 10^{-6}$  from reaction 3 and  $[O] = 3.7 \times 10^{-6}$  from reaction 1.

The  $[O]$  obtained from reactions 4, 3 and 1 is smaller by a factor of 1.6 than  $[O]$  calculated from reaction 6. A similar discrepancy occurs in all the flames, by a factor of 3.6 in the worst case and 1.6 in the best, and always in the sense that  $[O]$  from reaction 6 is the larger.

Since  $[O]$  from reaction 6 is more sensitive to a change in the diffusion coefficient, we trust it less. Other reasons for preferring the smaller  $[O]$  from reactions 4, 3 and 1 have been given in the introduction; and we use the smaller  $[O]$  for estimating  $k_2$ .

For the flame described in Fig. 1, at 0.8 to 0.95

(10) A. A. Westenberg, *Combustion and Flame*, **1**, 346 (1957).

(11) W. E. Kaskan, "6th Symposium on Combustion," Reinhold Publ. Corp., New York, N. Y., 1957, p. 134.

cm. from the burner surface, the reverse of (2) is small compared to the forward reaction. This is apparent because the product of reaction partners for the forward process,  $[O][H_2]$ , is twenty times the product for the reverse,  $[OH][H]$ ; but the equilibrium constant,  $k_2/k_{-2}$ , is of order unity.

$d[O]/dt$  is very small in the region 0.8 to 0.95 cm. from the burner surface, so we substitute into

$$k_2 = \frac{-d[O]_2/dt + k_5[N_2O][M] - d[NO]/2dt}{[O][H_2]}$$

to get  $k_2 = 2.8 \times 10^8$  l. mole<sup>-1</sup> sec.<sup>-1</sup> at 1675°K. The term,  $k_5[N_2O][M]$ , is small compared to  $-d[O_2]/dt$  and could have been omitted in this example.

Estimates of  $k_2$ , obtained in a similar way in each flame, are listed in Table II. The first four runs are fuel rich flames, the last two are fuel lean. The last column of Table II gives the percentage contribution of the term  $k_5[N_2O][M]$  to the value of  $k_2$ . If  $k_5$  were wrong, only runs no. 2 and 3 would be affected.

TABLE II  
ESTIMATES OF  $k_2^{-1}$

Run	P, cm.	T, °K.	$[O] \times 10^6$ , mole l. <sup>-1</sup>	$k_2 \times 10^{-8}$ , l. mole <sup>-1</sup> sec. <sup>-1</sup>	$k_5$ term, <sup>a</sup> %
1	4	1825	1.2	3.0	~0
2	6	1830	0.4	1.7	75
3	4	1790	8	1.8	33
4	4	1640	8	2.0	~0
5	2	1675	3.7	2.8	~0
6	4	1670	3.0	2.8	~0

<sup>a</sup> Contribution of the term,  $k_5[N_2O][M]$ , to the value deduced for  $k_2$  if  $k_5$  is assumed to have the value in Table I. Actually  $k_5$  is eventually assumed to be 2.25 times larger than this value, see text, and the eventual values of  $k_2$  in runs 2 and 3 are  $3.3$  and  $2.6 \times 10^8$ , respectively.

As they stand, the first three runs in Table II average to  $k_2 = 2.2 \times 10^8$  at about 1815°K. with a mean deviation of 26%. But  $k_5$  is not known better than to a factor of about two, as was explained in the Introduction, and it is legitimate to vary the pre-exponential factor of  $k_5$  in order to get the best agreement in  $k_2$ . If  $k_5$  is multiplied by 2.25, the average deviation in  $k_2$  decreases to only 8% and the average becomes identical with the only value of  $k_2$  which is independent of  $k_5$ . Therefore we increase the  $k_5$  given in Table I and accept  $k_2 = 3.0 \pm 0.3 \times 10^8$  at 1815°.

The last three runs give an average at 1660°K. of  $k_2 = 2.5 \pm 0.4 \times 10^8$ , independent of  $k_5$ .

**Comparison with Other Work.**—Baldwin<sup>2</sup> deduced from the low pressure limit of explosions in  $H_2-O_2-N_2$  mixtures that  $k_2$  (or  $k_3$ ) =  $2.0 \times 10^7$  l. mole<sup>-1</sup> sec.<sup>-1</sup> at 793°K. The ambiguity arose because reactions 2 and 3 have an identical dependence on  $[H_2]$ ; but since  $2 \times 10^7$  is only  $1/10^5$  or  $1/20^6$  of the value expected for  $k_3$  from other work, it is probably  $k_2$ . He also reported an activation energy of 9.2 kcal., but disclaimed much accuracy; for  $k_2$  was reproducible only within  $\pm 12\%$  at constant temperature, and the variation over the whole temperature range was 44%. Perhaps it is not unfair to suggest that his error might have been  $\pm 3$  kcal.

If his estimate at 793° is extrapolated to 1815°, using 9.2 kcal. activation energy, it gives  $k_2 = 5.4 \times 10^8$  as compared to our observed  $3 \times 10^8$ . This is good agreement. His and our estimates combine to

$$k_2 = 2.5 \times 10^8 e^{-7.7/RT} \text{ l. mole}^{-1} \text{ sec.}^{-1}$$

and 7.7 is the same as 9.2 kcal. within the probable error of the latter. If the pre-exponential factor is taken proportional to  $T^{n/2}$ , part of the temperature dependence is absorbed by this factor, and  $E_2$  becomes 6.4 rather than 7.7 kcal.

In much the same way as Baldwin, but with less complete data and interpretations, Azatian and co-workers<sup>12</sup> found  $k_2 = 9 \times 10^{10} e^{-12.1/RT}$  at 840 to 930°K. from the lower explosion limits of  $CO-O_2$  mixtures containing 0.76 to 8.0% added hydrogen. Their result extrapolates to twice Baldwin's estimate at 793° and to ten times our estimate at 1815°. It is not possible to reconcile our measurements with those of Azatian, *et al.*, and still maintain an activation energy of  $9 \pm 3$  kcal.

**NOTE ADDED IN PROOF.**—Clyne and Thrush<sup>13</sup> reported just recently an estimate of  $k_2 = 1.2 \times 10^{10} e^{-9.2/RT}$  l. mole<sup>-1</sup> sec.<sup>-1</sup> at 409 to 733°K. by a very different method; O atoms were generated in known concentration by titrating N atoms with nitric oxide, and the decay of the O atoms when mixed with hydrogen was followed by the radiation from the O + NO emission. Their estimate of  $k_2$  is systematically larger than the expression deduced in this paper by a factor of 2 to 3; but a disagreement of this order is perhaps within the error of any of the data.

(12) V. V. Azatian, V. V. Voevodskii and A. B. Nalbandian, *Dokl. Akad. Nauk. SSSR*, **132**, 864 (1960).

(13) M. A. A. Clyne and B. A. Thrush, *Nature*, **189**, 135 (1961).

# COMPOUND REPETITION IN OXIDE-OXIDE INTERACTIONS. THE SYSTEM $\text{Cs}_2\text{O}-\text{Nb}_2\text{O}_5$

BY ARNOLD REISMAN AND JOAN MINEO

*Watson Laboratory of International Business Machines, Yorktown Heights, N. Y.*

*Received December 16, 1960*

In order to test the predictions made in a previous paper,<sup>1</sup> the mixed oxide system  $\text{Cs}_2\text{O}-\text{Nb}_2\text{O}_5$  was investigated using differential thermal, X-ray and density analyses. Five compounds were identified in the region 0–66 mole %  $\text{Cs}_2\text{O}$ . Except for a compound melting congruently at approximately 27.7 mole %  $\text{Cs}_2\text{O}$  ( $5\text{Cs}_2\text{O}\cdot 13\text{Nb}_2\text{O}_5$ ) and 1415°, the remaining compounds,  $2\text{Cs}_2\text{O}\cdot 15\text{Nb}_2\text{O}_5$ ,  $\text{Cs}_2\text{O}\cdot 2\text{Nb}_2\text{O}_5$ ,  $2\text{Cs}_2\text{O}\cdot 3\text{Nb}_2\text{O}_5$  and  $\text{Cs}_2\text{O}\cdot \text{Nb}_2\text{O}_5$  melt incongruently at 1403, 1153, and 972 and 857°, respectively. The 2:15 and 5:13 compounds are isomorphous with the analogous rubidium compounds and the remainder are not. The trends observed in the lower weight members of the series have been found to continue. Thus, the barely emerged compound  $\text{Rb}_2\text{O}\cdot 4\text{Nb}_2\text{O}_5$  has no cesium analog, and the greatly submerged  $4\text{Rb}_2\text{O}\cdot 3\text{Nb}_2\text{O}_5$  composition also fails to repeat.

## Introduction

In previous articles,<sup>1–4</sup> an attempt has been made to test the validity of the Goldschmidt hypothesis<sup>5</sup> concerning model behavior, and to gather information concerning compound repetition in a series of congener interactions. Since the latter objective has been approached primarily *via* a study of the series alkali oxide– $\text{Nb}_2\text{O}_5$ , it is evident that generalizations based on these systems require independent verification obtainable by investigations of similar series of interactions. Such studies involving, for example, the alkali oxides and the compound  $\text{V}_2\text{O}_5$ , whose structural and chemical attributes differ appreciably from those of  $\text{Nb}_2\text{O}_5$ , have been initiated and will be reported upon at a later date. As a first stage, however, partial verification of the ideas previously expressed depends on success at predicting the diagram of state for an unknown system in the series now under investigation.

Based on observations of progressive submergence of repeated compound fields with increasing ionicity of the alkali metal in the sequence lithium through rubidium, speculations were entertained concerning the composition of compounds to be expected in the system  $\text{Cs}_2\text{O}-\text{Nb}_2\text{O}_5$ .<sup>1</sup> These speculations led to predictions that two compound ratios present in the rubidium interaction would not repeat in the cesium system and that a third ratio might or might not recur. Related to the question of compound repetition is the question of whether compound ratios, not detected in the lower weight interactions, would appear. This phenomenon appears to depend on marked changes in interoctahedral coordination which appear to be coincident with the introduction of the potassium ion into the lattice. Consequently, new ratios were not expected in the cesium system.

## Experimental Procedure

**Reagents.**—Trona  $\text{Cs}_2\text{CO}_3$  and Fansteel "High Purity"  $\text{Nb}_2\text{O}_5$  served as the starting materials for all reactions. Pretreatment of the pentoxide has been described previously.<sup>1</sup> The carbonate was found to contain small quantities of iron, 0.5–1.0% by weight, but was essentially free of other impurities. The iron was removed by several iso-

thermal recrystallizations from water, and the final product was of the order 99.8%  $\text{Cs}_2\text{CO}_3$ .

**Sample Preparations.**—Samples for cooling, heating, density and X-ray analyses were prepared in the same manner as before,<sup>1–4</sup> except for reaction temperatures. These were as usual some 20° below solidus or incongruent transformation temperatures determined by preliminary cooling analysis from the melt.

**Differential Thermal, Density and X-Ray Analysis.**—The methods previously employed<sup>1–4</sup> were utilized without modification. For obvious reasons, liquidus data were acquired from cooling curve analyses. Data for four phase equilibria were gathered from both heating and cooling studies. Since most of the compositions were marked y moisture sensitive, tending to hydrolyze, solid state reacted samples were protected from moisture, and density studies were conducted in trichloroethylene.

## Discussion of Experimental Results

Tables I and II list the composite results of thermal, density and X-Ray studies. Figures 1 and 2 show the proposed construction of the thermal and density diagrams. Meaningful liquidus data could not be collected for alkali oxide compositions greater than 66 mole % for several possibly related reasons. In melts containing greater quantities of the alkali component, both platinum and gold–20% palladium crucibles were severely attacked in the time interval necessary to melt the samples and take them through their liquidus crystallizations. Appreciable volatilization of the alkali component also was observed in this region and the data were found to scatter much more than normally. In addition to the above, the latent heats associated with primary crystallizations diminished rapidly, even at differential sensitivities of 5  $\mu\text{v./inch}$ , although one would expect an increase in such anomalies as a compound peak is approached.

Attempts at resolving the diagram in this region using X-Ray techniques were not definitive. The problem of contamination by the container materials plus difficulties encountered in carrying reactions to completion in the solid state, and even slightly above the eutectic temperature, coupled with rather diffuse and inconsistent X-Ray patterns made interpretation difficult. Thermal and X-Ray data do, however, indicate the existence of one other compound to the right of 66 mole %  $\text{Cs}_2\text{O}$ . Since the present system shows a continuation of the behavior observed in the rubidium system in all other regions, it is assumed that the unresolved region includes a  $4\text{Cs}_2\text{O}\cdot \text{Nb}_2\text{O}_5$  compound.

In the pentoxide rich portions of the diagram,

(1) A. Reisman and F. Holtzberg, *J. Phys. Chem.*, **64**, 748 (1960).

(2) A. Reisman and F. Holtzberg, *J. Am. Chem. Soc.*, **80**, 6503 (1958).

(3) A. Reisman, F. Holtzberg and E. Banks, *ibid.*, **80**, 37 (1958).

(4) A. Reisman and F. Holtzberg, *ibid.*, **77**, 2115 (1955).

(5) V. M. Goldschmidt, *Skrift Norsk Vid. Oslo. Mat. Nat. Kl.*, **8**, 7 (1926).

TABLE I

THERMAL DATA FOR THE SYSTEM  $Cs_2O-Nb_2O_5$ 

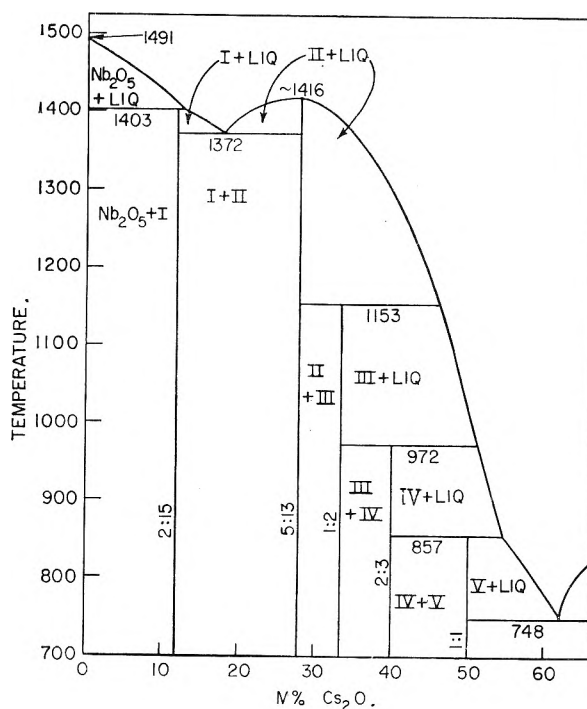
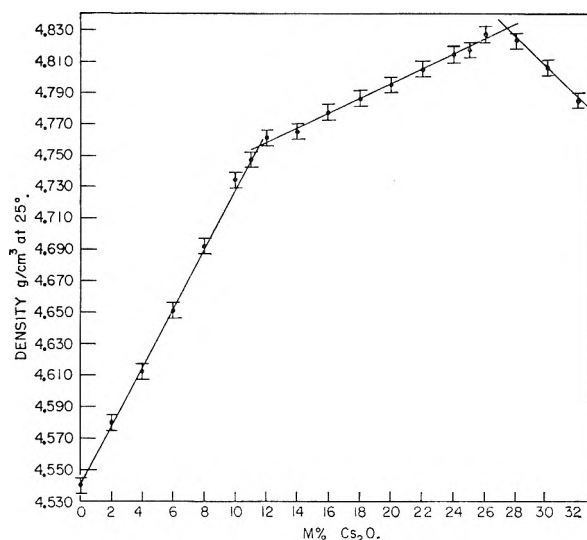
$Cs_2O$ , mole %	$Nb_2O_5$ , mole %	Liquidus	Solidus	Transitions	Primary phase
0	100	0	1491	1491	$Nb_2O_5$
2.5	97.5	1476	1399		$Nb_2O_5$
4.0	96.0	1469	1402		$Nb_2O_5$
6.0	94.0	1441	1399		$Nb_2O_5$
8.0	92.0	1437	1404		$Nb_2O_5$
10.0	90.0	1413	1406		$Nb_2O_5$
12.0	88.0	1409	1372		I
14.0	86.0	1392			I
16.0	84.0	1386	1377		I + II
18.0	82.0	1377	1371		I + II
20.0	80.0	1395	1367		II
22.0	78.0	1403	1363		II
24.0	76.0	1412	1357		II
26.0	74.0	1414			II
28.0	72.0	1411	1131		II
30.0	70.0	1410	1154		II
32.0	68.0	1403	1146		II
34.0	66.0	1381	965 <sup>a</sup>	1155	II
38.0	62.0	1331	971 <sup>a</sup>	1154	II
40.0	60.0	1294	968 <sup>a</sup>	1158	III
41.0	59.0		849 <sup>a</sup>	973 <sup>a</sup>	III
42.0	58.0	1245	859 <sup>a</sup>	1151 873 <sup>a</sup>	III
44.0	56.0	1197	857 <sup>a</sup>		III
46.0	54.0	1154	854 <sup>a</sup>		III
48.0	52.0	1097	854 <sup>a</sup>		III
50.0	50.0	1010	859 <sup>a</sup>		III
51.0	49.0		740 <sup>a</sup>		III
52.0	48.0	950	752 <sup>a</sup>	857 <sup>a</sup>	IV
54.0	46.0	870	747 <sup>a</sup>	856 <sup>a</sup>	IV
56.0	44.0	848	752 <sup>a</sup>		V
58.0	42.0	813	748 <sup>a</sup>		V
60.0	40.0	767	748 <sup>a</sup>		V
62.0	38.0	748	748		V + ? eutectic lies here
64.0	36.0	801	746		?
66.0	34.0	826	738		?

<sup>a</sup> Heating curve data only.

TABLE II

DENSITY DATA FOR THE SYSTEM  $Cs_2O-Nb_2O_5$  AT 25°

Mole % $Cs_2O$	Mole % $Nb_2O_5$	Density, g./cc. at 25°	Av.
0	100	4.540	4.540
2	98	4.580	4.580
4	96	4.612	4.612
6	94	4.651	4.651
8	92	4.692	4.692
10	90	4.734	4.734
11	89	4.747	4.747
12	88	4.763 4.758	4.761
14	86	4.766 4.763	4.765
16	84	4.779 4.774	4.777
18	82	4.786	4.786
20	80	4.795	4.795
22	78	4.805	4.805
24	76	4.813 4.815	4.814
25	75	4.815 4.819 4.817	4.817
26	74	4.828 4.825	4.827
28	72	4.824 4.824 4.822	4.823
30	70	4.805 4.806	4.806
32	68	4.787 4.783	4.785

Fig. 1.—Thermal diagram of the system  $Cs_2O-Nb_2O_5$ .Fig. 2.—Partial density diagram of the system  $Cs_2O-Nb_2O_5$ .

density measurements were employed to fix the composition of the niobium richest compound. Within the limits of experimental error, the intersection of density arms occurs at 11.6 mole %  $Cs_2O$  and 4.755 g./cm.<sup>3</sup> at 25°. As in the rubidium system, the smallest whole number ratio corresponding to this value is 2:15 (11.76 mole %). X-Ray examination of this compound which melts incongruently at 1402° showed it to be isomorphous with its rubidium analog.

As expected, the 1:4 compound, seen in the rubidium system, as a congruently melting compound just intersecting the liquidus arms on either side, does not occur heterogeneously. The liquidus field for the 2:15 compound terminates in a eutectic at 17.5 mole %  $Cs_2O$  and 1372°.

In the rubidium interaction, it was pointed out that the location of the 4:11 compound was effected *via* heating curve analyses, and was assigned a composition of 26.67 mole %  $\text{Rb}_2\text{O}$  based on these data. The concern at that time was whether this seemingly odd ratio was reasonable. Since the only volatile component is the alkali oxide, loss of this material would result in a displacement of the compound's apparent composition to higher pentoxide values rather than to the observed lower one. In the present study, the combining ratio for this compound was established using the density technique. Within the limits of error, the intersection of the arms is at 27.4 mole % and 4.831 g./cm.<sup>3</sup> at 25°, as compared to the more approximate value of 27 mole % given in the rubidium paper. Assuming that if anything, the mole fraction indicated by the density data lies to the left of the true point, a small number value of 5:13 was assigned to this compound. This ratio corresponds to 27.7 mole %  $\text{Cs}_2\text{O}$ , and is assumed to be more representative than the 4:11 value previously assigned. The 5:13 compound melts at 1415° and is isomorphic with its rubidium analog.

The 1:2 compound melting at 1155° and 46 mole %  $\text{Cs}_2\text{O}$  was readily located with X-ray and heating curve analyses. X-Ray analysis indicated that this compound is not isomorphic with its rubidium analog.

As expected, a compound having a base to acid ratio of 2:3 was resolved using X-ray and thermal techniques. This material melts incongruently at 975° and 51 mole %, and its liquidus field is appreciably submerged. It is not improbable that a similar ratio would fail to reappear in the next higher interaction. The 2:3 analogs are not isomorphic with one another. The meta compound which is slightly submerged in the rubidium interaction is now almost completely submerged. It melts incongruently at 850° and 56 mole % and its field of primary crystallization terminates in a eutectic at 748° and 62 mole %. This compound is not isomorphic with its rubidium counterpart.

As expected, the highly submerged 4:3 rubidium compound fails to have a stable analog in the cesium system lending some further support to the ideas previously expressed.

While in general the present system shows a continuation of compound submergences with increasing atomic weight in a given congener series, there are two apparent inconsistencies for which no explanation suffices.—These involve the 2:15 and 1:2 compounds both of whose liquidus curves do not appear indicative of greater dissociation. While one cannot derive absolute data on the heat of fusion of a compound solely from solubility data, one can in certain cases make approximations which are indicative of the level of dissociation in the liquid phases. If the state of unit activity for a liquid compound is taken as that of the pure undissociated liquid, one can derive a freezing point equation where the activity term represents that of an ideal solution whose apparent activity and mole fraction difference is due to a dissociation process. Without going into the details of such a treatment, one can demonstrate that the effect of dissociation is to decrease the solubility of the material in question. This approach can be employed qualitatively in comparing the rubidium and cesium systems for the case of  $\text{Nb}_2\text{O}_5$  and consequently for the 2:15 analogs. If we assume that differences between the solubility curves of the  $\text{Nb}_2\text{O}_5$  in the two interactions are due to the differences in its idealized activity caused by different degrees of dissociation of the next adjacent compound, one would expect the  $\text{Nb}_2\text{O}_5$  solubility to decrease in the cesium system. In other words, the  $\text{Nb}_2\text{O}_5$  liquidus curve should be displaced to the right. A comparison of the curves, however, shows an apparent increase in solubility, indicating that the 2:15 cesium compound is less dissociated. In the case of the 1:2 compound whose disposition was unclear, two effects are observed. The temperature interval for its liquidus field is two to three times that in the rubidium system while its liquidus slope is almost coincident with that of the 5:13 compound. It is expected that plausible explanations for these possible inconsistencies will become evident from a study of the vanadium series where the pentoxide portion of the diagram is expected to exhibit less compound formation.

**Acknowledgment.**—The authors wish to express thanks to B. Agule for performing the density analyses.



# CONDUCTANCE OF THE ALKALI HALIDES. I. POTASSIUM CHLORIDE IN DIOXANE-WATER MIXTURES<sup>1,2</sup>

BY JOHN E. LIND, JR.,<sup>3</sup> AND RAYMOND M. FUOSS

Contribution No. 1648 from the Sterling Chemistry Laboratory of Yale University, New Haven, Conn.

Received December 16, 1960

The conductance of potassium chloride was measured at 25° in dioxane-water mixtures which cover the range 78.54–12.74 in dielectric constant. The data conform to the equation  $\Lambda = \Lambda_0 - S(c\gamma)^{1/2} + Ec\gamma \log c\gamma + Jc\gamma + J_2(c\gamma)^{3/2} - K_A c\gamma^2 \Lambda$  within a precision of 0.01–0.05%, thus establishing the validity of this functional form of the conductance equation for a typical inorganic salt. Association to ion pairs begins to be increasingly visible below  $D \approx 40$ ; at  $D = 12.74$ , the association constant is 1700. The contact distance  $a$  was found to vary from 2.5 to 6.4, depending on the method used to compute it; this variation suggests that the model and the theory need further refinements for the case of small ions in hydrogen bonding solvents.

The electrostatic theory of conductance<sup>4</sup> ascribes the decrease of equivalent conductance with increasing concentration to the effects of the ionic charges on mobility and on relative concentration of free ions, using as a model charged spheres to represent the ions and a structureless continuum to represent the solvent. This model and the theory based on it has been quite successful in accounting for the observed behavior of quaternary ammonium salts in a variety of solvents<sup>5</sup>; in these cases, the ions are large compared to the solvent molecules. In particular, the contact distance  $a_K$  between ion pairs obtained from the dependence of the association constant on dielectric constant agrees closely with the sum  $a_A$  of the radii obtained from the limiting conductances by applying an electrostatic correction to Stokes law. Also, the value of this parameter  $a_J$  obtained from the curvature of the phoreogram is in fair agreement with the other two values.

In order to test the theory and model further, we have started a systematic study of the alkali halides. These salts have small ions; since association depends on the Bjerrum parameter<sup>6</sup>  $b = e^2/aDkT$ , we would expect association to become significant at higher dielectric constants than for the quaternary salts. Also, deficiencies in the present theory might be expected to be magnified for the case of small ions. Water-dioxane was chosen as the first solvent system for investigation, due to the wide range of dielectric constant which can be covered. Since water is a hydrogen bonding solvent, and since the water molecule has a fairly large dipole moment in a small volume, ion-solvent interactions should be readily observable.

In this paper, we present a discussion of the conductance of potassium chloride in dioxane-water mixtures which cover the range  $12.74 \leq D \leq 78.54$ . The system conforms to the general theory, with some marked deviations in details:

(1), the ion size  $a_J$  depends on solvent composition; (2), the  $\log K_A - D^{-1}$  plot shows a slight curvature; and (3), the hydrodynamic distance  $a_A$  is unrealistically small. These discrepancies call for a more detailed theory, based on a model which takes into account the discrete structure of the solvent when ion and solvent molecule become comparable in size.

## Experimental

**Materials.**—Potassium chloride<sup>7</sup> was twice precipitated from concentrated aqueous solution by hydrogen chloride, washed with ice-water, dried and then fused in air at 800°. The spectrum showed no sodium lines, and a test with barium chloride showed that no sulfate had been picked up during the precipitation. The conductance of the twice recrystallized sample agreed within 0.03% of that of the once precipitated material; the slope of the  $\Lambda' - c$  curve<sup>8</sup> was 200.7 as compared with the weighted average 198.4 over the best available data on this salt. (Our maximum concentration was about 0.01 *N*; the above difference  $\Delta J = 2.3$  thus corresponds to 0.023  $\Lambda$ -units or 0.015% of the conductance.)

Dioxane was refluxed over potassium hydroxide for a day and next dried over barium oxide for a day. It was then stored over 10% sodium-lead alloy in a still-pot; after refluxing for a least two days, it was distilled through a 50 cm. column packed with glass beads into appropriate receivers; b.p. 101.3°. Distillation and storage of the dioxane was under nitrogen. Densities<sup>9</sup> ranged from 1.02716 to 1.02794 at 25°; the highest density was obtained after refluxing over the alloy for a week.

Nitrobenzene ( $D = 34.82$ ) and ethylene dichloride ( $D = 10.36$ ) were used as standards<sup>10</sup> to calibrate the cells used in determining the dielectric constants of the mixtures of dioxane and water. Nitrobenzene<sup>11</sup> was washed with equal volumes of 1 *N* sulfuric acid, saturated sodium carbonate solution and water. It was then dried successively over calcium chloride and barium oxide; after standing several days over activated alumina, it was distilled at 1 mm. through a Todd still at 50:1 reflux ratio; specific conductance,  $\kappa_0 = 4-14 \times 10^{-9}$  mho. Ethylene dichloride was washed with saturated sodium carbonate solution, dried with calcium chloride (saturated solution) followed by

(7) T. Shedlovsky, *J. Am. Chem. Soc.*, **54**, 1411 (1932).

(8) J. E. Lind, Jr., J. J. Zwolenik and R. M. Fuoss, *ibid.*, **81**, 1557 (1959).

(9) Density of dioxane: (a) 1.0311, C. P. Smyth and W. S. Walls, *J. Am. Chem. Soc.*, **53**, 2116 (1931); (b) 1.0286, J. A. Geddes, *ibid.*, **55**, 4832 (1933); (c) 1.02766, F. Hovorka, R. A. Schaefer and D. Dreisbach, *ibid.*, **58**, 2264 (1936); (d) 1.02687, P. R. Frey and E. C. Gilbert, *ibid.*, **59**, 1344 (1937); (e) 1.0276, C. H. Schneider and C. C. Lynch, *ibid.*, **65**, 1063 (1943); (f) 1.0280, P. C. Teague and W. A. Felsing, *ibid.*, **65**, 485 (1943); (g) 1.02802, B. Pesce and M. V. Lage, *Gazz. chim. ital.*, **74**, 131 (1944); (h) 1.02806, M. L. McGlashan and R. P. Rastogi, *Trans. Faraday Soc.*, **54**, 496 (1958).

(10) A. A. Maryott and E. R. Smith, "Tables of Dielectric Constants of Pure Liquids," NBS Circular 514, 1951.

(11) E. G. Taylor and C. A. Kraus, *J. Am. Chem. Soc.*, **69**, 1731 (1947).

(1) Presented at the Spring 1960 meeting of the American Chemical Society at Cleveland.

(2) This paper is based on part of a thesis presented by John E. Lind, Jr. to the Graduate School of Yale University in partial fulfillment of the requirements for the Degree of Doctor of Philosophy, June, 1960.

(3) National Science Foundation Fellow, 1957–1960.

(4) R. M. Fuoss and F. Accascina, "Electrolytic Conductance," Interscience Publishers, Inc., New York, N. Y., 1959.

(5) H. Sadek and R. M. Fuoss, *J. Am. Chem. Soc.*, **81**, 4507 (1959); E. Hirsch, *ibid.*, **82**, 1018 (1960); D. S. Berns and R. M. Fuoss, *ibid.*, **82**, 5585 (1960); J. E. Lind, Jr., and R. M. Fuoss, *ibid.*, **83**, 1828 (1961).

(6) See ref. 4 for definition of symbols used in this paper.

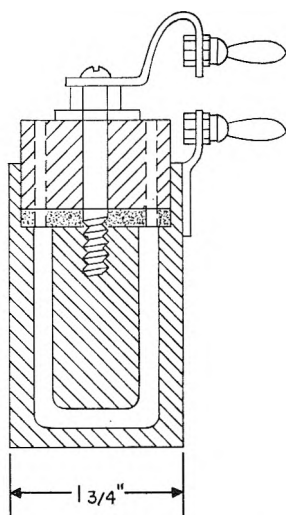


Fig. 1.—Cell for the megacycle bridge.

barium oxide and was distilled through the Todd still at 5:1 final reflux ratio; b.p., 83.3°.

**Apparatus.**—For measuring dielectric constants of the dioxane-rich mixtures, Sadek-Fuoss 3-terminal cells<sup>12</sup> and a General Radio 716C Schering Bridge with the 716-P4 guard circuit were used at 200 and 300 kc. In these measurements, the external electrode of the cell was grounded and the internal electrode was at high potential; the guard electrode was balanced to ground potential. Results with this simple circuit agreed within 0.1–0.2% with those obtained by using the less convenient circuit in which the cell is placed inside (but insulated from) a grounded container, with the outer electrode at high potential and the inner and guard electrodes balanced at ground potential. For the water-rich mixtures, the loss tangent was so high that the above bridge could not be balanced; hence for these, a General Radio 716-CSI bridge and a 2-terminal stainless steel cell were used at 1 megacycle. The cell is shown in Fig. 1; in order to minimize lead corrections, it plugs directly into the bridge panel. It is kept at 25° by a closely fitting grounded copper jacket through which thermostated oil is pumped. The electrodes are stainless steel; the supporting insulator is Teflon. The glass plate at the top of the cell avoids bubbles which would be trapped at a liquid-Teflon interface. The holes through the cover are closed with tapered Teflon pins after the inner electrode is seated. The cell constants were as follows: 3-terminal cells,  $C_v = 16.03$  pf. and 6.94, pf.; 2-terminal cell,  $C_v = 7.90$  pf. with 4.4 pf. lead capacity.

Densities were measured in a Sprengel pycnometer,  $V_0 = 19.3785$  ml. by calibration with water at 25°. Solution densities were measured at concentrations 2 to 4 times higher than those used in the conductance work; concentration  $c$  in equivalents per liter were calculated from the experimental weight concentration  $m$  moles per kg. solvent by the relation  $c/m = \rho_0 - \beta m$ , where  $\rho_0$  is the density of the mixed solvent and  $\beta$  is the experimentally determined coefficient. Its average value for  $KCl-C_4H_8O_2-H_2O$  is  $\beta = -0.027$ .

Viscosities were measured with an Ubbelohde viscometer which had a flow time of 471.3 sec. with water at 25°. Geddes<sup>9b</sup> data for dioxane-water mixtures between 40 and 80% dioxane were used for calibration. The kinetic energy correction was negligible. In filling this (and other containers), precautions were taken to avoid changes in composition of the mixtures due to evaporation of the relatively more volatile dioxane. In general, solutions were transferred from one container to another by nitrogen pressure, the nitrogen first passing through a saturator containing dioxane-water in the appropriate ratio; the container into which a mixture was transferred was previously swept out with nitrogen saturated with mixed vapor.

Conductances were usually measured at 1, 2.5 and 10 kc. and extrapolated to infinite frequency ( $R$  vs.  $f^{-1}$ ) in order to eliminate polarization errors; the correction did not

exceed 0.05%. For cell resistances greater than about 5000 ohms, the  $Rf^{-1}$  curves became concave-up at the high frequency end indicating a slight Parker effect. In these cases, measurements for extrapolation were made at 0.32, 0.64, 1.0 and 2.0 kc. Solvent conductances were measured at 2 kc. with the cell parallel to a calibrated  $10^6$  ohm resistor (General Radio Type 510). The maximum solvent correction was 0.7% and usually was much smaller. The bridge was built around a Leeds and Northrup Campbell-Shackleton Ratio Box, according to Shedlovsky's design.<sup>13</sup> Cell resistances were balanced against a Leeds and Northrup 4755 Decade Box, (supplemented by a General Radio 510F  $10^4$ – $10^6$  ohm decade resistor) which was calibrated to a precision of better than 0.003%. Lead resistances from bridge to cell and resistances of the leads built into the cells were measured to  $\pm 0.01$  ohm. Cell solutions were thermostated<sup>14</sup> to  $25 \pm 0.002^\circ$  in an oil-bath. Temperatures were measured using a platinum resistance thermometer and a Mueller bridge. Exploration showed that the stirring in the thermostat was adequate to ensure temperatures uniform to  $0.01^\circ$  in any given location; for a given run, the cell was always placed in the same spot in the bath for each point.

The conductance cells were constructed by sealing appropriate electrode capsules to 1-l. erlenmeyer flasks, equipped with ground glass caps. The electrodes were bright platinum; they were held rigidly with respect to each other by glass spacers fused over 10 mil. platinum wires welded to the corners of the electrodes, and with respect to the cell capsule by fusing a bracing glass rod to the bottom spacers of the electrodes. Metal-to-glass seals for the leads from the electrodes were made as recommended by Hnizda and Kraus,<sup>15</sup> using 15 mm. lengths of platinum tubing (1.5 mm. i.d., 0.05 mm. wall) and Corning 707 glass. In the final design, 1 mm. lead wires of silver were fused to platinum beads at the external ends of the platinum tubes, and were carried inside 6 mm. Pyrex tubes to the top of the cell, where the bridge leads could be attached by means of platinum-faced clips. For this design, the correction for cell leads was negligible.

The cells were calibrated with potassium chloride solutions by the LZP method<sup>8</sup> for constants 1.0 and greater; for smaller constants, calibration was by comparison with a directly calibrated cell. For comparison work, dilute aqueous sodium bicarbonate solution is the most convenient electrolyte we have yet encountered; the solutions can be poured back and forth repeatedly without change. Numerous cross-comparisons were made among all our cells; careful statistical analysis of the many data give the following self-consistent set of values for the cell constants: 10.8290  $\pm$  0.0016, 2.44376  $\pm$  0.00009, 1.06710  $\pm$  0.00019, 0.94272  $\pm$  0.00005, 0.39099  $\pm$  0.00004, 0.125052  $\pm$  0.00008 and 0.073993  $\pm$  0.000006.

**Technique.**—Salt samples (at least 20 mg.) were weighed in platinum boats on the microbalance to  $\pm 3 \gamma$ . Solutions were always made up by weight (corrected to vacuum); the calibration of the weights on the "kilo"-balance was made consistent with that of the weights for the microbalance by building up the calibration from the latter to the former, with an analytical balance as intermediate, using the Richards method.<sup>16</sup>

Conductance runs were made by the dilution method, starting with about one fifth<sup>17</sup> the final amount of solvent in the cell. After measuring the solvent conductance, the salt was added and the cell placed in the bath for equilibration. Since rate of solution was slow in the dioxane-rich mixtures, several of the low constant cells had a stirrer well in the bottom of the main chamber; this was connected to the bottom of the electrode capsule by an 8 mm. tube. A magnetic stirrer in the well then circulated liquid through the capsule into the cell and back. After temperature equilibrium, final resistance was measured. Then the cell was wiped free of thermostat oil after draining, washed with ethanol, wiped with a damp cloth, and weighed. Next,

(13) T. Shedlovsky, *ibid.*, **52**, 1793 (1930); H. Eisenberg and R. M. Fuoss, *ibid.*, **75**, 2914 (1953).

(14) J. J. Zwolenik, J. E. Lind, Jr., and R. M. Fuoss, *Rev. Sci. Instr.*, **30**, 575 (1959).

(15) V. F. Hnizda and C. A. Kraus, *J. Am. Chem. Soc.*, **71**, 1565 (1949).

(16) T. W. Richards, *ibid.*, **22**, 144 (1900); F. C. Eaton, *The Chemist Analyst*, **38**, 28 (1949).

(17) Ref. 4, pp. 245–6.

(12) H. Sadek and R. M. Fuoss, *J. Am. Chem. Soc.*, **76**, 5897 (1954).

it was uncapped in a "dry box" and the second portion of solvent was pumped in. After weighing, the cell was replaced in the thermostat. The "dry box" was a closed box, filled with nitrogen under slight pressure, in which all solution manipulations were carried out; open beakers of sodium hydroxide and alkaline pyrogallol were kept in the box to absorb carbon dioxide and oxygen.

The water used for preparing the mixtures was ordinary distilled water ( $\kappa_0 = 1.2 \times 10^{-6}$ ) from the laboratory still. It was first boiled for 0.5 hr. while nitrogen was bubbled through it to displace oxygen. Then it was allowed to cool in the nitrogen box and mixtures of water and dioxane were made in the box, the capped container being removed for weighing at appropriate times, of course. This container was a 2-l. flask with a graduated 180 ml. side chamber in which portions of solvent for addition to the conductance cells could be pregauged before being pumped into the cell. It was found that the solvent conductance remained stable for hours if the mixed solvent were sparged for 0.5 hr. before use with nitrogen through a glass frit; the nitrogen was first passed through a saturator filled with the same solvent mixture. In order to avoid errors due to possible changes of solvent composition, density, viscosity and dielectric constant were determined for each mixed solvent that was used for conductance work, rather than interpolating these quantities from plots of  $\rho$ ,  $\eta$  or  $D$  against composition. In other words, the solvents are identified primarily by the value of  $D$  rather than by composition.

An unexpected effect was observed during the conductance measurements: in those cells which had the small pumping well between the main chamber and the electrode capsule, the final resistance was found to be about 0.10% lower in the stirred solution than in an undisturbed solution. The systems required 30-40 min. to reach a steady state-resistance after switching the stirrer from off to on or *vice versa*. Both values were steady to 0.01% and the cycle high-low could be repeated at will, without hysteresis. We find that other workers have noticed similar effects.<sup>18-22</sup> Experiments ruled out adsorption or temperature gradients as the cause of the change. Since the values without agitation were slightly more reproducible, we report as final values of conductance those based on resistance measurements made on solutions at rest for at least 30 min. after stopping the stirrer.

### Results

The properties at 25° of the solvents used in the conductance work are summarized in Table I where  $w$  = weight % dioxane in the mixture,

TABLE I

PROPERTIES OF DIOXANE-WATER MIXTURES

No.	$w$	$\rho$	$D$	100 $\eta$	10 <sup>4</sup> $\kappa_0$
1	0.0	0.99707	78.54 <sup>a</sup>	0.8903	1.63
2	22.2	1.01585	60.16	1.330	0.58
3	43.65	1.03037	41.46	1.803	.45
4	56.7	1.03544	30.26	1.977	.24
5	61.7	1.03634	25.84	1.991	.16
6	69.9	1.03690	19.32	1.928	.094
7	75.0	1.03630	15.37	1.844	.040
8	78.8	1.03565	12.74	1.755	.028

<sup>a</sup> J. Wyman, Jr., *Phys. Rev.*, **35**, 613 (1930).

$\rho$  = density,  $D$  = dielectric constant,  $\eta$  = viscosity and  $\kappa_0$  = solvent conductance. The solvent conductances decrease systematically<sup>23</sup> as the dioxane content increases. Our densities run about 0.01% higher than those observed by Geddes<sup>9b</sup>; the scatter of the points on a  $\rho$ - $w$  curve runs ex-

actly parallel to the density of the dioxane used in preparing the mixtures. This observation suggests that dioxane holds the last traces of water with extreme tenacity; it will be recalled that it required a week's refluxing over Na-Pb alloy to get the density up from 1.027 to 1.028. Our dielectric constants run parallel to the most recent literature values<sup>24</sup> in absolute value; agreement is within 0.2% at the water-rich end and 0.8% at the dioxane-rich end of the  $D$ - $w$  curve. Our viscosities agree within 0.05% with the values reported by Geddes,<sup>9b</sup> after correction of these data to the present water standard.<sup>25</sup>

The conductance data ( $c$  = equivalent per liter,  $\Lambda$  = equivalent conductance) are summarized in Table II; the different systems are identified

TABLE II

CONDUCTANCE OF POTASSIUM CHLORIDE IN DIOXANE-WATER MIXTURES AT 25°

10 <sup>4</sup> $c$	$\Lambda$	$\Delta\Lambda$	10 <sup>4</sup> $c$	$\Lambda$	$\Delta\Lambda$
$D = 78.54$			$D = 25.84$		
99.697	141.275	-0.002	32.813	43.157	-0.007
78.577	142.117	+ .000	25.964	44.086	- .002
58.689	143.060	+ .000	19.479	45.154	+ .001
40.166	144.141	- .002	13.239	46.430	- .007
19.368	145.813	+ .001	6.756	48.237	+ .003
$D = 60.16$			$D = 19.32$		
71.619	94.237	+ .005	23.476	33.770	- .004
56.758	94.852	- .014	18.875	34.838	+ .004
43.004	95.566	+ .009	14.217	36.186	+ .007
14.966	97.589	- .001	9.455	37.981	- .010
			4.830	40.501	+ .004
$D = 41.46$			$D = 15.37$		
55.446	62.524	- .007	18.473	26.420	+ .000
45.892	63.079	+ .007	14.005	27.902	+ .010
33.716	63.890	+ .004	10.092	29.645	- .004
22.430	64.815	- .012	5.183	33.005	+ .002
11.671	66.031	+ .005			
$D = 30.26$			$D = 12.74$		
36.749	48.573	- .005	14.535	19.763	- .012
29.624	49.333	+ .006	11.549	20.944	+ .014
22.559	50.207	- .005	8.671	22.466	+ .010
15.362	51.319	- .002	5.912	24.549	- .016
8.514	52.706	+ .001	2.971	28.276	+ .007

by their dielectric constants. The quantity  $\Delta\Lambda$  is the difference between the observed conductance and the value calculated as described in the next section. The precision of the dilution method was tested by adding another portion of salt after the last dilution; for example, at  $D = 25.84$ , after the fifth point, enough salt was added to bring the concentration back to  $27.484 \times 10^{-4}$ . The conductance  $\Lambda = 43.876$  with  $\Delta\Lambda = 0.011$  fits the curve through the first five points within 0.03%. All of the resistances were quite stable; the most dilute solutions showed a drift of about 0.02% in half a day. Ordinarily, a run was completed in 5-6 hr.

(24) F. E. Critchfield, J. A. Gibson, Jr., and J. L. Hall, *ibid.*, **75**, 1991 (1953).

(25)  $\eta(\text{H}_2\text{O}, 25^\circ) = 0.008903$ ; J. F. Swindells, C. F. Snyder, R. C. Hardy and P. E. Golden, *Nat. Bur. Stand. Circ. Supp.* **440**, 700 (1958).

(18) G. S. Hartley and G. W. Donaldson, *Trans. Faraday Soc.*, **33**, 457 (1937).

(19) E. Swift, Jr., *J. Am. Chem. Soc.*, **60**, 728 (1938).

(20) A. B. Scott and H. V. Tartar, *ibid.*, **65**, 692 (1943).

(21) C. B. Monk, *ibid.*, **70**, 3281 (1948).

(22) H. M. Daggett, Jr., E. J. Bair and C. A. Kraus, *ibid.*, **73**, 799 (1951).

(23) The product of  $\kappa_0$  and solvent viscosity is proportional to the weight per cent. of water in the mixture.

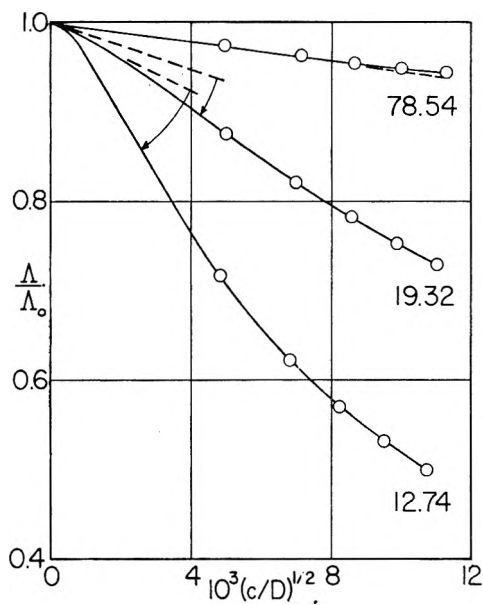


Fig. 2.—Plots of reduced conductance as a function of ionic charge density.

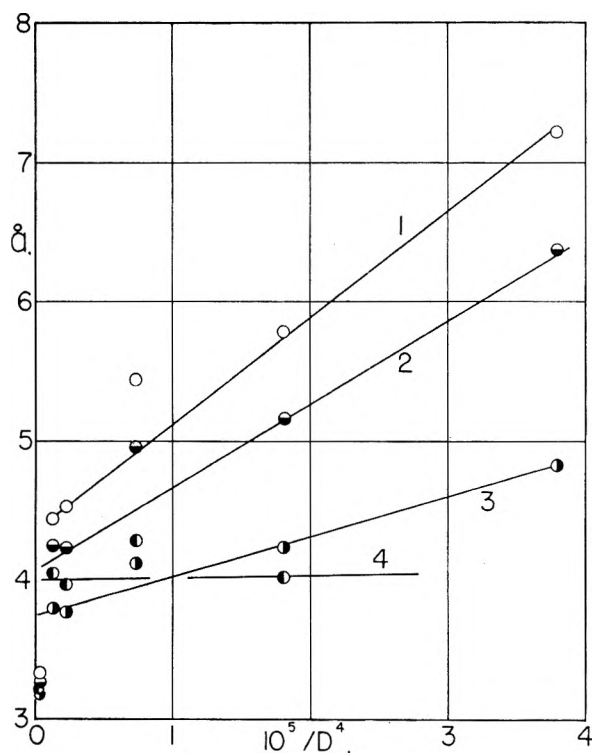


Fig. 3.—Systematic variation of computed contact distance with dielectric constant.

The standard deviation in  $[\Lambda(\text{obsd.}) - \Lambda(\text{calcd.})]$  increases from about 0.005 to 0.05% as  $D$  decreases from 78.54 to 12.74; this trend may be due to differential evaporation, despite our precautions (the conductance is much more sensitive to composition in the lower range of dielectric constants) or perhaps the functional form of the theoretical equation is not yet quite correct (in this case, the activity coefficient or still neglected  $c^{3/2}$  terms are suspects). The general pattern of  $\Delta\Lambda$  is systematic ( $- + + - +$ ) for nearly all

the runs, which suggests imperfect adequacy of the equation; the amplitude of the variation is, however, only 0.02  $\Lambda$ -units (independent of  $D$ ).

### Discussion

Inspection of the data of Table II shows that association of the ions of potassium chloride to pairs increases rapidly once the dielectric constant of the solvent drops below about 40, because the equivalent conductance decreases steadily more rapidly with increasing concentration as  $D$  decreases. This change is shown graphically in Fig. 2 where the reduced conductance  $\Lambda/\Lambda_0$  is plotted against  $(c/D)^{1/2}$ . (This choice of coordinates is convenient for comparing different systems;  $\Lambda/\Lambda_0$  eliminates the main effect of viscosity in the ordinate and  $(c/D)^{1/2}$  is proportional to  $\kappa a$  which is the theoretically significant independent variable in considering electrolytic systems.) In water, the curve lies above the limiting tangent, indicating at most only slight association, but at  $D = 19.32$ , the curve has become concave-up over the working range of concentration and at  $D = 12.74$ , the initial point is only about one-half the limiting value. This trend clearly shows the controlling role assumed by the (negative) association term in the conductance equation when ion pair formation is favored by low dielectric constant.

The data were analyzed by the IBM 650 Computer, using several modifications of Kay's program,<sup>26</sup> in order to obtain the parameters  $\Lambda_0$ ,  $a$  and  $K_A$  of the conductance equation

$$\Lambda = \Lambda_0 - S(c\gamma)^{1/2} + E c \gamma \log c \gamma + J(a)c\gamma + J_2(a)(c\gamma)^{3/2} - \frac{K_A c \gamma^2 \Lambda}{K_A c \gamma^2 \Lambda} \quad (1)$$

(Since the ions are small, the Einstein term  $F\Lambda c$  is set equal to zero.) The final values of the constants are summarized in Table III. Using these values, conductances at each experimental point were then computed by means of (1) in order to obtain the  $\Delta\Lambda$  values of Table II.

TABLE III  
CONSTANTS FOR POTASSIUM CHLORIDE IN DIOXANE-WATER MIXTURES AT 25°

$D$	$\Lambda_0$	$a$	$K_A$
12.74	39.45 ± 0.13	6.37 ± 0.20	1700 ± 40
15.37	42.34 ± .09	5.16 ± .15	498 ± 14
19.32	46.26 ± .04	4.96 ± .14	162 ± 5
25.84	52.32 ± .03	4.24 ± .18	34 ± 2
30.26	56.45 ± .03	4.25 ± .24	18 ± 2
41.46	69.13 ± .04	3.26 ± .49	1.2 ± 1.5
60.16	100.74 ± .01	3.31 ± .04	.....
78.54	149.893 ± .002	3.333 ± .003	.....

The first analysis was made neglecting the  $J_2$  term.<sup>27</sup> The latter includes arithmetical approximations from the third term in the series expansion of  $(1 + \kappa a)^{-1}$  in the electrophoresis term and the third term in the expansion of exponential integrals ( $E_i x \approx -0.5772 - \ln x + x$ ) in the relaxation term; in other words, it is a numerical correction to the  $c$  and  $c \log c$  terms of the general conductance

(26) R. L. Kay, *J. Am. Chem. Soc.*, **82**, 2099 (1960).

(27) Ref. 4, equations 14.102 and 14.103 contain misprints. The  $\theta_i$  in 102 should be preceded by a minus sign and the exponent of  $b$  in 103 is 2. The correct form of  $J_2$  is given as equation 3 by D. S. Berns and R. M. Fuoss, *J. Am. Chem. Soc.*, **82**, 5585 (1960).

equation rather than a  $c^{1/2}$  term of the latter arising from interionic forces.<sup>28</sup> A systematic variation (curve 1, Fig. 3) of the contact distance  $\bar{a}$  resulted; at  $D = 12.74$ ,  $\bar{a} = 7.21$  and at  $D = 41.46$ ,  $\bar{a} = 3.33$ . Recalculation retaining the  $J_2$  term reduced the variation, giving 6.37 and 3.26 (curve 2, Fig. 3).

This result suggested that the variation in  $a$  might be due to neglected higher terms in the theoretical equation rather than to inadequacy of the model (invariant spheres in a continuum) used in the theory. We therefore tried the inclusion of the next term in the activity coefficient, which was calculated by Gronwall, LaMer and Sandved.<sup>29</sup> In order to include the term in the computer program, an empirical interpolation formula was used which reproduces the tabulated values satisfactorily over the range  $0.02 \leq \kappa a \leq 0.18$ . The equation used for the activity coefficient was

$$-\ln f^2 = 2\beta'(c\gamma)^{1/2}/(1 + \kappa a) + (1.6368 \times 10^{-11}/a^3 D^3 T^3)(\kappa a - 0.01526) \quad (2)$$

Inclusion of this term decreases  $f^2$  and hence the association term in the conductance equation; since the latter has the opposite sign to the  $J$  term, a smaller  $J$  will result from a given set of data when (2) is used instead of the Debye-Hückel equation. Also, the effect will be greater the lower the dielectric constant, because the coefficient  $K_A$  is then increasing rapidly. A value of  $\bar{a}$  practically constant at 4.0 resulted (curve 4, Fig. 3). Numerically, nearly the same result can be achieved by going the other way in the approximation, *i.e.*, by using the point charge approximation

$$-\ln f^2 = 2\beta'(c\gamma)^{1/2} \quad (3)$$

which gives 4.84 and 3.18 (curve 3, Fig. 3), as compared to 6.37 and 3.26. Our conclusions therefore are that little weight should be given to the value of  $a$  from  $J$  when association is marked, and that salvation of the situation by invoking solvation is emphatically not warranted. The results of these calculations are summarized in Fig. 3 where the  $a$ -values are plotted against  $D^{-4}$ . The conclusion appears inevitable that some higher terms are missing in (1); some are certainly in the activity coefficient, and some arise from the  $c^{1/2}$  terms which were neglected in the present approximate solution of the fundamental equation of continuity. These missing terms will involve higher powers of  $b = e^2/aDkT$  than those at present included; since the leading term of  $J$  varies as  $D^{-3}$ , we chose  $D^{-4}$  as the abscissa scale in Fig. 3. The results suggest that  $\bar{a}$  for potassium chloride in dioxane-water mixtures is about 4.0; this is, however, larger than the value 3.3 found in water. On the other hand, it agrees well with the value  $3.8 \pm 0.4$  found in glycerol-water mixtures.<sup>30</sup>

At  $D = 12.74$ , potassium chloride is quite highly associated, with  $K_A = 1700$ . As the dielectric constant increases,  $K_A$  decreases, as shown in Table III. At  $D = 41.46$ , the computer derives from

(28) Ref. 4, pp. 185-187.

(29) T. H. Gronwall, L. V. LaMer and K. Sandved, *Physik. Z.*, **29**, 358 (1928).

(30) F. Accascina, *J. Am. Chem. Soc.*, **81**, 4995 (1959); F. Accascina and S. Petrucci, *Ric. Sci.*, **30**, 808 (1960).

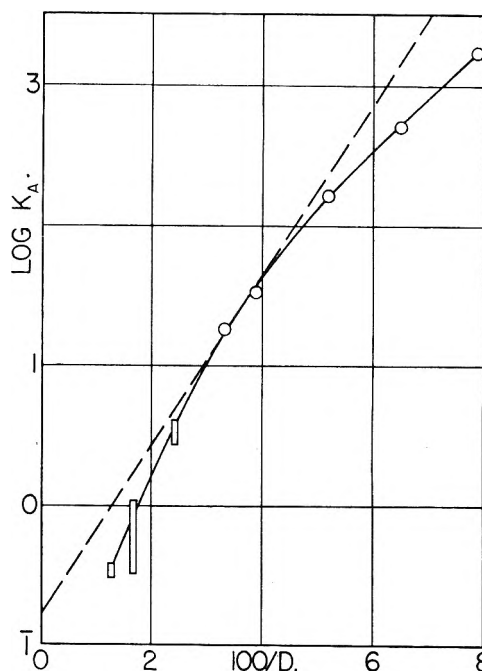


Fig. 4.—Dependence of association constant on dielectric constant. Dashed line—theoretical dependence for  $\bar{a} = 4.0$ .

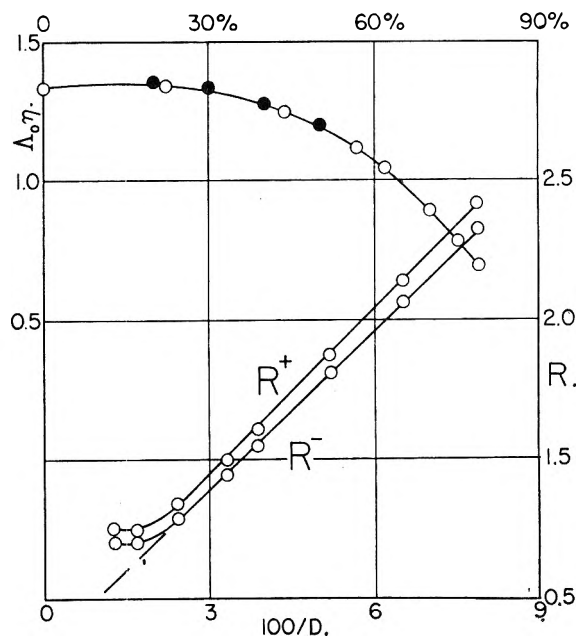


Fig. 5.—Walden products (scales left and top) and Stokes radii (scales right and bottom) for potassium chloride in dioxane-water mixtures.

the data  $K_A = 1.2 \pm 1.5$ , *i.e.*, within the precision of the measurement (0.01% for this run), the effects of association are barely detectable and at higher values of  $D$ , they become invisible to the computer. It would be incorrect, however, to conclude that association terminates abruptly near  $D \approx 40$ , as is shown by the results of calculation of  $a$  with  $K_A$  set equal to zero for higher dielectric constants. In (1), the  $J$  and  $K_A$  terms appear with opposite signs, and when  $D$  is large, both become essentially linear in concentration

( $\gamma \approx 1$ ,  $f \approx 1$ ,  $\Lambda \approx \Lambda_0$ ) and the computer program cannot separate the two terms, which effectively coalesce to become  $(J - K_A \Lambda_0)c$ . If  $K_A$  is set equal to zero in the program, the data then yield a numerical coefficient for the linear term, and clearly the value of  $a$  computed from it will be too small. For water, for example, the program for unassociated electrolytes (eq. 1 with  $\gamma = 1$ ,  $K_A = 0$ ) gives  $\hat{a} = 3.19$ , while the program for the unabbreviated equation gives  $d = 3.53$  with  $K_A = 0.10 \pm 0.10$ . The latter value agrees better with the extrapolation (Fig. 3) from the data at lower dielectric constant.

Association of potassium chloride even at high dielectric constant can be demonstrated in another way. By assuming a value for  $a$ , the conductance equation can be rearranged to a two parameter equation ( $\Lambda_0$  and  $K_A$ )

$$\Lambda_K \equiv \Lambda + S(c\gamma)^{1/2} - Ec\gamma \log c\gamma - Jc\gamma - J_2(c\gamma)^{3/2} = \Lambda_0 - K_A c\gamma^2 \Lambda \quad (4)$$

The corresponding  $\Lambda_K$  program, when applied to the data for the three systems of highest dielectric constant, using  $\hat{a} = 4.0$ , gave the values shown as open rectangles in Fig. 4, where  $\log K_A$  is plotted against  $1/D$ . These points from (4) lie on an extension of the curve through the points at lower  $D$ , where association is unambiguous. The value calculated for water agrees with the value  $K_A = 0.4$  estimated from the results obtained by Eigen and Wicke.<sup>31</sup> Theoretically the curve in Fig. 4 should be a straight line<sup>32</sup> corresponding to the equation

$$K_A = (4\pi Na^3/3000) \exp(e^2/aDkT) \quad (5)$$

This straight line, with  $\hat{a} = 4.0$ , is shown as the dashed line in Fig. 4. A vertical displacement by an amount corresponding to  $E_s \approx -kT$ , where  $E_s$  is the ion-solvent interaction energy introduced by Gilkerson,<sup>33</sup> would give fair numerical agreement between (5) and all the observed values with some systematic deviation. The present theory is, however, unable to account for the qualitative difference manifested by the curvature of the observed function. The slope of the curve through the data at low dielectric constants gives  $a_K = 6.7$ , which obviously is too large. Furthermore, an attempt to remove the curvature by assuming a larger linear term fails on two counts: it leads to even larger  $a_i$  values from the larger  $J(a)$  required and more significantly, substantially increases the deviation between calculated and observed values of the conductance. Smaller activity coefficients than those computed by the Debye-Hückel equation and/or a different theoretical interpretation of the linear coefficient for large values of  $b$  (small  $a$  or  $D$ ) would resolve the dilemma. Further theoretical work on these questions is in progress.

(31) M. Eigen and E. Wicke, *J. Phys. Chem.*, **58**, 702 (1954); Fig. 10 and Table I.

(32) R. M. Fuoss, *J. Am. Chem. Soc.*, **80**, 5059 (1958).

(33) W. R. Gilkerson, *J. Chem. Phys.*, **25**, 1199 (1956).

Finally, we consider the limiting conductances which are summarized in Table III. The Walden product for potassium chloride in dioxane-water mixtures goes through a slight maximum at about 15% dioxane, as shown in the curve of Fig. 5. The data (solid circles) of Dunsmore and Speakman<sup>34</sup> (0-50% dioxane) agree very well with our results. Using the equation<sup>35</sup>

$$R = 0.8194 \times 10^{-8}/\lambda_{0\eta} \quad (6)$$

where  $R$  is the Stokes radius,  $\lambda_0$  is the single ion limiting conductance and  $\eta$  is solvent viscosity, we find a systematic dependence of  $R$  on dielectric constant as has been observed for a number of other systems.<sup>35</sup> (The calculation is based on the value<sup>36</sup> of  $n^+ = 0.4905$  for the potassium ion of potassium chloride in water; it is assumed that  $n^+$  is independent of solvent composition to first approximation.) A plot of  $R$  against  $1/D$ , as shown in Fig. 5, has a hook upwards at high dielectric constant, corresponding to the maximum in the Walden product; evidently the hydrodynamic situation is quite complicated in the water-rich mixtures. But for solvents with more than about 40% dioxane, the curves become nearly linear; the equations

$$10^8 R(K^+) = 0.8603 + 19.56/D \quad (7)$$

and

$$10^8 R(Cl^-) = 0.8277 + 18.84/D \quad (8)$$

reproduce the data for  $D < 40$  within 0.2-1.0%. (The deviation is systematic and reflects the slight curvature of the line rather than scatter of the data from a smooth curve.) The sum of the values ( $a_A = 1.688$ ) of  $R_\infty$  for the two ions in a hypothetical solvent of infinite dielectric constant is considerably smaller than the sum of the crystallographic radii (3.14 Å). For large ions in organic solvents, we have found excellent agreement<sup>37</sup> between  $a_A$ ,  $a_K$  and contact distances obtained from molecular models; clearly, the ions of KCl are behaving differently. These ions are about the same size as water molecules, and as Sutherland<sup>38</sup> pointed out long ago, the model used by Stokes is not realistic for this case. To allow for the possibility of motion essentially without friction, due to the slipping of ions through holes in the liquid, he showed that the Stokes coefficient of  $6\pi\eta R$  becomes  $4\pi\eta R$ . Using this factor in (6), we find  $a_A(\text{corr.}) = 2.53$  which is considerably nearer the value obtained from the other sources considered in this discussion. The agreement, however, is far from perfect, and shows that more theoretical work is needed on the problem of the hydrodynamics of small ions, especially in hydrogen-bonding solvents.

(34) H. S. Dunsmore and J. C. Speakman, *Trans. Faraday Soc.*, **50**, 236 (1954).

(35) R. M. Fuoss, *Proc. Natl. Acad. Sci. U.S.A.*, **45**, 807 (1959).

(36) R. A. Robinson and R. H. Stokes, "Electrolytic Solutions," 2nd edition, Academic Press, Inc., New York, N. Y., 1959, p. 463.

(37) E. Hirsch and R. M. Fuoss, *J. Am. Chem. Soc.*, **82**, 1018 (1960).

(38) W. Sutherland, *Phil. Mag.*, **9**, 781 (1905).

# INTERPRETATION OF THE ELECTRIC MOMENTS OF POLYMETHYLENE DIHALIDES AND DICYANIDES

BY H. BRADFORD THOMPSON AND STEPHEN L. HANSON

*Department of Chemistry, Gustavus Adolphus College, St. Peter, Minnesota*

*Received December 22, 1960*

Electric moments for the series  $\text{Cl}(\text{CH}_2)_n\text{Cl}$  were determined in benzene solution at  $25^\circ$ : for  $n = 3$ , 2.10 Debye;  $n = 4$ , 2.10;  $n = 5$ , 2.36;  $n = 6$ , 2.26;  $n = 10$ , 2.60. These and published data on corresponding bromides and nitriles may be explained using a diamond lattice model including steric exclusion. The low moment for  $n = 4$  in each series is a natural consequence of this model. For best fit of data to theory, the *trans*  $\rightarrow$  *gauche* energy for rotation of a  $-\text{CH}_2\text{X}$  group relative to the adjoining chain is  $905 \pm 55$  cal. for chlorides,  $780 \pm 100$  cal. for bromides and  $930 \pm 100$  cal. for nitriles.

In at least four homologous series of molecules with polar groups at both ends of aliphatic carbon chains, the four-carbon member has been reported to have an abnormally low electric moment (Fig. 1). On this basis cyclic structures have been proposed by Rogers<sup>1</sup> in the case of the dibasic acids and by Smyth and Walls<sup>2,3</sup> for the corresponding ethyl esters. We wish here to report a similar anomaly in the polymethylene chlorides, and to treat these series in the light of present knowledge of rotational barriers, using an approach previously applied with success to halogen substituted propanes and neopentanes.<sup>4-6</sup> In this paper, the case of the chlorides, bromides and nitriles will be considered, and it will be shown that the assumption of an important cyclic rotational structure is in these series unnecessary, that the electric moments of the substituted butanes might be expected to be low in any event.

## Theoretical

The basic assumptions of the model employed here are given below in italics. Each assumption (or at least something very similar) has been described before. The entire set has, however, properties that deserve attention.

**The Diamond-lattice Model.**—A set of common assumptions used to approximate the geometry of hydrocarbons is<sup>5,7,8</sup>

*I. Each substance consists of an equilibrium mixture of rotational isomers (rotomers). In saturated non-cyclic hydrocarbons each rotomer is in the staggered position with respect to each internal rotation.*

*II. Bond angles at each carbon atom are assumed tetrahedral.*

*III. A set of bond lengths is assumed. Accordingly, all C-C bonds are assumed to be of equal length.*

These three requirements restrict the carbon skeleton to conformations like those of a series of atoms within a diamond crystal. This accordingly is called

the *diamond-lattice model*. Bond lengths selected for this paper are:<sup>9</sup> C-C, 1.54 Å.; C-H, 1.10 Å.; C-Cl, 1.77 Å.; C-Br, 1.94 Å.; C-CN, 1.46 Å.; C $\equiv$ N, 1.16 Å.

Next, some consideration must be given steric interactions between parts of the chain. The distances between atoms separated by one or two bonds are fully determined by the model. Interactions between atoms separated by three bonds will appear as part of the assumed barrier to rotation about the central bond. Thus the first case requiring special consideration is the five-carbon chain. There turn out to be four end-to-end distances, 2.51, 3.56, 4.36 and 5.03 Å. Of these, only 2.51 Å. represents any considerable squeeze for methyl or methylene groups. The conformation shown in Fig. 2, with the two end bonds lying parallel, is the only arrangement leading to this short end-to-end distance. Thus

*IV. A rotomer containing a five-atom segment arranged as in Fig. 2 is assumed to make no contribution to the observed properties of the substance, provided any alternative rotomer not containing this arrangement exists. Such a rotomer shall be said to be "excluded."*

Careful examination of the diamond lattice reveals an important consequence of this exclusion. The shortest closed path not containing an excluded chain segment is 14 atoms in length! An 11-atom chain can be found with its ends 2.51 Å. apart, but no shorter chain (of more than five atoms) has ends separated by less than 3.56 Å. Thus assumption IV may cover the only important steric interaction in medium-length chains.<sup>10</sup>

**Validity of the Exclusion.**—Structures like Fig. 2, where the X groups are methyls, have been shown to be excluded in *cis*-1,3-dimethylcyclohexane, where Pitzer<sup>11</sup> has estimated a destabilizing energy of at least 5.4 kcal. For halogens at X, Mizushima has pointed out that in the hexachlorocyclohexanes the arrangement in Fig. 2 occurs only when there is no alternative.<sup>7b</sup> The same appears to apply in a variety of substituted propanes and neopentanes.<sup>5,6</sup> However, since the present interpretation rests quite strongly on this exclusion, some further discussion seems appropriate.

Two chlorines terminating the chain in Fig. 3 are within 2.52 Å. of one another, while the sum of their van der Waals radii is 3.6 Å. By far the easiest way in which this crowding can be accom-

- (1) M. T. Rogers, *J. Phys. Chem.*, **61**, 1442 (1957).
- (2) C. P. Smyth and W. S. Walls, *J. Am. Chem. Soc.*, **53**, 527 (1931).
- (3) C. P. Smyth and W. S. Walls, *J. Chem. Phys.*, **1**, 200 (1933).
- (4) P. Trunel, *Ann chim.*, (11) **12**, 93 (1933).
- (5) H. B. Thompson and C. C. Sweeney, *J. Phys. Chem.*, **64**, 221 (1960).
- (6) H. B. Thompson and C. W. Lawson, *ibid.*, **64**, 1788 (1960).
- (7) S. I. Mizushima, "Structure of Molecules and Internal Rotation," Academic Press, Inc., New York, N. Y., 1954; a, p. 99; b, p. 81; c, p. 34.
- (8) A. Tobolsky, R. E. Powell and H. Eyring, in "The Chemistry of Large Molecules," R. E. Burk and O. Grummitt, Editors, Interscience Publishers, Inc., New York, N. Y., 1943, Ch. 5.
- (9) From the Table of Selected Bond Lengths in "Tables of Interatomic Distances," L. E. Sutton, Editor, The Chemical Society, London, 1958. Values have been rounded to the nearest 0.01 Å.

- (10) That smaller rings (except cyclohexane) are strained is well known. See for example N. L. Allinger, *J. Am. Chem. Soc.*, **81**, 5727 (1959). The diamond-lattice model can, of course, be applied to cyclohexane and related compounds.

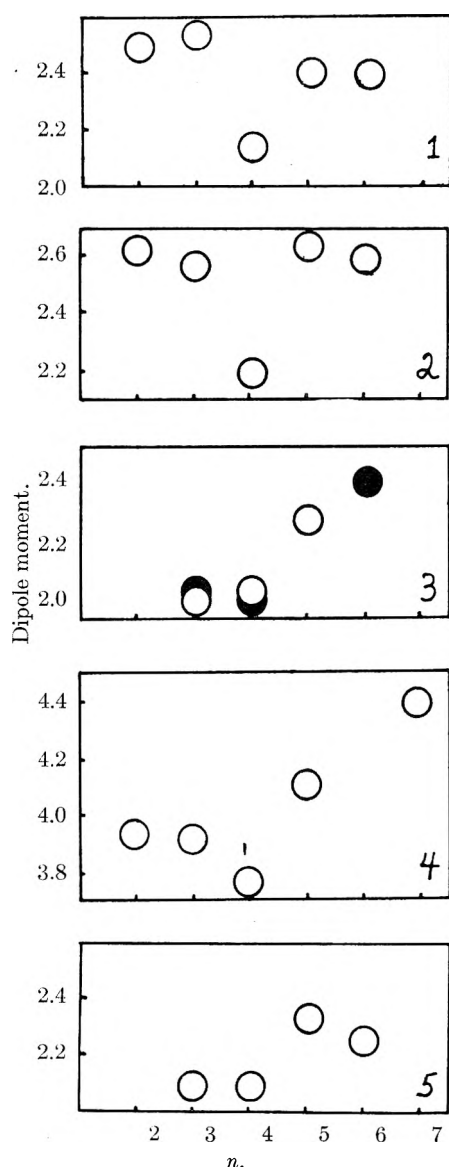


Fig. 1.—Electric dipole moment as a function of chain length in several homologous series. Dark circles for dibromides are in heptane, open circles in benzene at 25°. The acids are in dioxane solution, other moments in benzene: 1,  $\text{EtOOC}-(\text{CH}_2)_n-\text{COOEt}$  (ref. 2); 2,  $\text{HOOC}-(\text{CH}_2)_n-\text{COOH}$  (ref. 1); 3,  $\text{Br}-(\text{CH}_2)_n-\text{Br}$  (ref. 3); 4,  $\text{NC}-(\text{CH}_2)_n-\text{CN}$  (ref. 4); 5,  $\text{Cl}-(\text{CH}_2)_n-\text{Cl}$  (this paper).

modated is internal rotation. A rotation of each  $-\text{CH}_2\text{Cl}$  through 25° would increase the Cl-Cl distance to 3.3 Å., still a considerable squeeze. If the threefold barrier to rotation were in each case 2400 cal. high, this would require 1700 cal. Mutual repulsion of the two bond moments must add several hundred calories at this distance, and the resultant potential well must be quite narrow and steep, so it is not surprising that such rotomers make little contribution to over-all properties. The same argument will apply to bromide or cyanide groups. For bromides, the longer C-Br bond taken with the larger van der Waals radius<sup>12</sup> gives almost

(11) As quoted by W. G. Dauben and K. S. Pitzer in "Steric Effects in Organic Chemistry," M. S. Newman, Editor, John Wiley and Sons, Inc., New York, N. Y., 1956, p. 19.

(12) L. Pauling, "The Nature of the Chemical Bond," 2d Ed., The Cornell University Press, Ithaca, N. Y., 1940, p. 189.

exactly the same situation as for chlorides. While no accurate non-bonded distance for  $-\text{CN}$  groups side-by-side seems to be available, the C-N distance in adjacent molecules in crystalline HCN,<sup>13</sup> 3.35 Å., probably approximates the C-C approach. As the C-CN bond is shorter than the C-Cl bond, an even greater rotation will be necessary to accommodate nitrile groups. In addition, the group moment is almost twice that for C-Cl.

The case of methyl or methylene groups involves an even larger group (radius about 2 Å.<sup>12, 14, 15</sup>), again at a short C-C distance; again the exclusion assumption seems safe. Methylene-to-polar-group approach is somewhat trickier. Several cases have been cited in which, at greater distances, an attraction appears to exist.<sup>16</sup> This has been attributed to a weak hydrogen bond. In the present case, however, the C-Cl distance is 2.5 Å., very short even for a very strong hydrogen bond. In addition, the C-H-Cl system is far from linear, and the hydrogen approaches the chlorine from the rear. Finally, in chloropropane, where the chlorine and the methyl carbon nuclei are over 3 Å. apart, the attraction is apparently barely sufficient to overcome the usual repulsive interaction.<sup>17, 18</sup> Since the latter increases rapidly as the groups approach, exclusion seems a safe assumption here also.

**Calculation of Electric Moments.**—In a mixture of molecular species in the vapor or in dilute solution, the observed molar polarization will be an average properly weighted according to the mole fractions of the various species. The electronic and atomic polarizations of rotomers of the same compounds may with little error be expected to be equal. Accordingly the orientation polarization will be the appropriate weighted average, as will the square of the observed electric moment  $\mu$  at any temperature. Thus

$$\mu^2 = \frac{\sum_i \mu_i^2 N_i}{\sum_i N_i} \quad (1)$$

where  $\mu_i$  is the electric moment of the  $i$ th non-excluded rotomer and  $N_i$  is the relative number of molecules of this rotomer at equilibrium. Relative values of  $N_i$  for two different non-excluded rotomers in equilibrium should be given by

$$\frac{N_2}{N_1} = \frac{f_2}{f_1} e^{-(E_2 - E_1)/RT} \quad (2)$$

where  $f_1$  and  $f_2$  are partition functions for the two rotomers, and  $E_2$  and  $E_1$  are the energies of the rotational minima.<sup>7c</sup> Pitzer has shown<sup>19</sup> that the rotational-vibrational part of the ratio  $f_2/f_1$  is approximately unity. This approximation improves as classical behavior is approached. We will assume, then, that  $f_1$  and  $f_2$  need represent only factors  $g_1$  and  $g_2$  for the symmetry characteristics of the rotomers.

To the extent that the internal rotations are

(13) W. J. Dulmage and W. N. Lipscomb, *Acta Cryst.*, **4**, 330 (1951).

(14) A. E. Smith, *Acta Cryst.*, **6**, 224 (1952).

(15) H. M. M. Shearer and V. Vand, *ibid.*, **9**, 379 (1956).

(16) G. J. Szasz, *J. Chem. Phys.*, **23**, 2449 (1955).

(17) Y. Morino and K. Kuchitsu, *ibid.*, **28**, 175 (1958).

(18) C. Komaki, *et al.*, *Bull. Chem. Soc. Japan*, **28**, 330 (1955).

(19) K. S. Pitzer, *J. Chem. Phys.*, **14**, 239 (1946).



mutually independent, the exponential term may be expressed in terms of a product of factors for these individual rotations. Thus

$$\frac{N_2}{N_1} = \frac{g_2}{g_1} \prod_r e^{-\Delta E_r/RT} \quad (3)$$

where  $\Delta E_r$  is the energy difference associated with the  $r$ th internal rotation. At a given temperature each exponential term may be represented by a single factor  $x_r$ . Then

$$N_2/N_1 = g_2/g_1 \prod_r x_r \quad (4)$$

which will lead to the fifth assumption in our model.

V. For each bond about which rotation can occur, there is a factor defining the relative probabilities for each *gauche* conformation relative to the *trans* conformation. This factor depends only upon the temperature and the nature of the atoms attached directly to the atoms terminating the bonds in question.

The second statement in V is open to some question, though this approach has had considerable success in the statistical treatment of hydrocarbons.<sup>20,21</sup> In butane, pentane and hexane, for instance,  $\Delta E$  for the *gauche-trans* transition is, respectively, 770, 450 and 500 cal./mole.<sup>11</sup> This represents a range of values for  $x_r$  from 0.27 to 0.43. The wide variation here is due largely to the value for butane; 500 cal./mole seems to be generally satisfactory as an estimate in longer chains. Since we will deal here with heavy-atom skeletons at least five atoms long, a value of 0.40 for  $x$  might reasonably be expected to be in error by 10% or less. Furthermore, the electric moments predicted using this model turn out to be quite insensitive to the value of  $x_r$  associated with rotations along the carbon chain, as will be shown below. End group rotation might be a different matter. In this case, however, one always will have, in the present study, a  $\text{CH}_2\text{X}$  group at one end of the bond and a chain of at least three methylene groups on the other, so that constancy for  $x_r$  for a given homologous series may confidently be expected.

We will define the factors  $x_r$  and  $g_i$  relative to the completely extended hydrocarbon chain, with all rotations *trans*. On this basis, combining equations 1 and 4

$$\mu^2 = \frac{\sum_i (\mu_i^2 g_i \prod_r x_{r_i})}{\sum_i (g_i \prod_r x_{r_i})} \quad (5)$$

It remains now only to estimate  $\mu_i^2$  and the  $x_{r_i}$ 's for each rotomer.

In  $\text{X}-(\text{CH}_2)_n-\text{X}$ , where  $n$  is even, the two C-X bond moments are either opposed or fixed at an angle of  $70^\circ 32'$ , following the diamond-lattice model. If the C-X moment is  $m$ , the squares of the rotomer moments for these two orientations are, respectively, zero and  $8/3 m^2$ . Similarly, if  $n$  is odd, the C-X bonds lie either parallel or at the tetrahedral angle, and the square of the rotomer moment is either  $4m^2$  or  $4/3 m^2$ .

For  $\text{X}-(\text{CH}_2)_n-\text{X}$  the coefficients  $x_{r_i}$  take only three values under rule V: unity,  $x$ , the relative *gauche* population for  $-\text{CH}_2\text{X}$  rotation, and  $y$ ,

(20) K. S. Pitzer, *J. Chem. Phys.*, **8**, 711 (1940).

(21) N. Sheppard and G. J. Szasz, *ibid.*, **17**, 86 (1949).

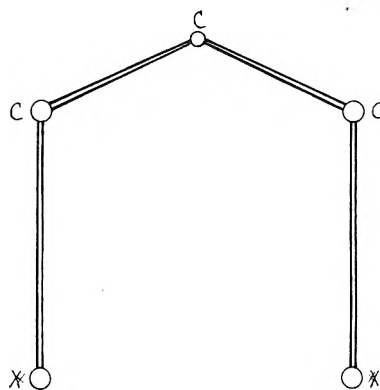


Fig. 2.—Sterically excluded chain segment conformation. This arrangement is excluded if  $\text{X} = \text{CN}, \text{Cl}, \text{Br}$  and/or  $\text{CH}_2$ .

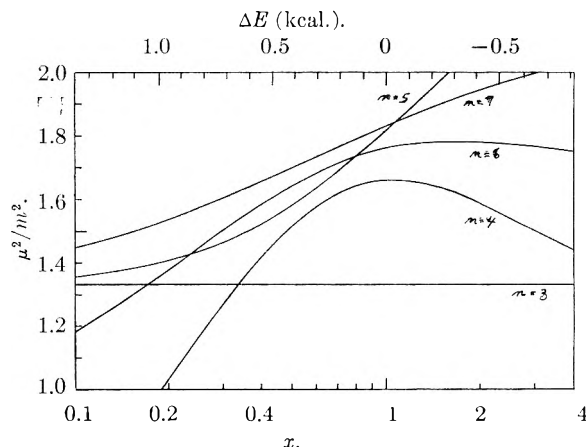


Fig. 3.—Electric moment as a function of end-positions parameter.  $\Delta E$  is the energy by which one *gauche* position is less stable than the *trans*.

the corresponding factor for rotation along the carbon chain. As we have seen, the value of  $y$  is fairly well established. The products in equation 5 will then take the form  $x^a y^b$  where  $a$  may take the values 0, 1 and 2 while  $b$  may take any integral value from 0 to  $n-3$ . Collecting terms in each combination of  $a$  and  $b$ , and for each value of the rotomer moment

$$\mu^2 = \frac{\sum_{a,b} x^a y^b (g_{ab1} \mu_1^2 + g_{ab2} \mu_2^2)}{\sum_{a,b} x^a y^b (g_{ab1} + g_{ab2})} \quad (6)$$

where the  $g$ 's are the numbers of non-excluded rotomers of each moment for each combination of  $a$  and  $b$ , and include the values  $g_i$  of equation 5.

It remains only to determine the form of equation 6 for each value of  $n$ . This is a trivial exercise for  $n=3$ , since all non-excluded rotomers have a squared moment of  $4/3 m^2$ .<sup>6</sup> For  $n=4$  a more complex situation results, in which ten rotomers, properly weighted for symmetry, must be considered. These are described in Table I. The resultant equation is

$$\frac{\mu^2}{m^2} = \frac{8}{3} \frac{4x + 2x^2 + 4xy}{1 + 4x + 4x^2 + 2y + 4xy + 2x^2y} \quad (7)$$

From the table one can see a possible reason for the low electric moments for  $n=4$ : all the excluded rotomers are of high moment.

Similar treatments for  $n = 5, 6$  and  $7$  produce equations 8-10 below. In each case the excluded rotomers include ones of both high and low moment.

$$\frac{\mu^2}{m^2} = \frac{4}{3} \frac{1 + 4x + 8x^2 + 4y + 12xy + 16x^2y + 2y^2 + 4xy^2 + 2x^2y^2}{1 + 4x + 4x^2 + 4y + 12xy + 8x^2y + 2y^2 + 4xy^2 + 2x^2y^2} \quad (n = 5) \quad (8)$$

$$\frac{\mu^2}{m^2} = \frac{8}{3} \frac{4x + 2x^2 + 2y + 16xy + 10x^2y + 4y^2 + 12xy^2 + 10x^2y^2 + 2y^3 + 2x^2y^3}{1 + 4x + 4x^2 + 6y + 20xy + 16x^2y + 8y^2 + 20xy^2 + 12x^2y^2 + 2y^3 + 4xy^3 + 2x^2y^3} \quad (n = 6) \quad (9)$$

$$\frac{\mu^2}{m^2} = \frac{4}{3} \frac{1 + 4x + 8x^2 + 8y + 36xy + 40x^2y + 18y^2 + 76xy^2 + 50x^2y^2 + 12y^3 + 44xy^3 + 16x^2y^3 + 2y^4 + 4xy^4 + 2x^2y^4}{1 + 4x + 4x^2 + 8y + 28xy + 24x^2y + 18y^2 + 52xy^2 + 38x^2y^2 + 12y^3 + 28xy^3 + 16x^2y^3 + 2y^4 + 4xy^4 + 2x^2y^4} \quad (n = 7) \quad (10)$$

The  $n = 7$  case involves over 200 different rotomers plus optical antipodes. The labor involved in attempting  $n = 8$  seemed excessive.

TABLE I  
ROTOMERS FOR X-(CH<sub>2</sub>)<sub>n</sub>-X

Con-formation <sup>a</sup>	$\mu^2/m^2$	Weight <sup>b</sup>	Gauche rotations	
			a	b
T T T	0	1	0	0
T T G	8/3	4*	1	0
G T G	8/3	2*	2	0
G T G'	0	2	2	0
T G T	0	2*	0	1
T G G	8/3	4*	1	1
T G G'	8/3	4*	Excluded	
G G G	0	2*	2	1
G G' G'	8/3	4*	Excluded	
G G' G	8/3	2*	Excluded	

<sup>a</sup> Notation of Shimanouchi and Mizushima. Compare Table 4.2 ref. 7a. <sup>b</sup> Weights relative to the TTT rotomer, with a factor of 2 included where an optical isomer (\*) also exists.

Figure 3 shows these curves for  $y = 0.4$  in the range  $x = 0.1$  to  $4$ . Values for  $y = 0.5$  differed from these by 0.03 or less, an encouraging result in light of the discussion in a previous section. In the range of interest in this study, predicted moment is two or three times as sensitive to changes in  $x$  as to changes in  $y$ . In addition,  $y$  is fairly precisely known—it seems unlikely that one would normally choose a value far from 0.4. Thus it seems appropriate to adopt this value for  $y$  and seek a best fit by varying  $x$ .

### Results and Discussion

**Electric Moments of the Dichlorides.**—Experimental moments in benzene at 25° determined in this Laboratory for the series Cl-(CH<sub>2</sub>)<sub>n</sub>-Cl are compared with values from the above treatment in Table II. The C-Cl bond moment used in calculating  $\mu^2/m^2$ , 1.97 D., is that for 1-chloropropane. This value is employed directly for all except 1,3-dichloropropane, where inductive effects have been estimated at 0.20 D. lowering of  $m$  in the corresponding bromide.<sup>22</sup> Two-thirds this lowering is assumed appropriate for the C-Cl moment, since the polarizability is in this case somewhat lower. This leads to 1.84 D. for  $m$ .

The best fit to our model is obtained for  $x = 0.22$ , corresponding to about 905 cal./mole favoring the *trans* position for each chain end. A lower limit for  $x$  can be set by assuming  $\mu$  to be 0.1 D. below the experimental value for the case  $n = 4$ . This leads to  $\mu^2/m^2 = 1.03$ ,  $x = 0.20$ , and  $\Delta E = 960$  cal. A similar estimate of the upper limit, using

TABLE II

ELECTRIC MOMENTS FOR Cl-(CH<sub>2</sub>)<sub>n</sub>-Cl

n	$\mu$	$\mu^2/m^2$	
		Obsd. <sup>a</sup>	Predicted <sup>b</sup>
n = 3	2.10 <sup>d</sup>	1.30	1.33
n = 4	2.10	1.14	1.09
n = 5	2.36	1.44	1.42
n = 6	2.27	1.33	1.41
n = 10	2.60	1.74	(2.00) <sup>c</sup>

<sup>a</sup> Assuming  $m = 1.97$  for  $n > 3$ ,  $m = 1.84$  for  $n = 3$ . <sup>b</sup> Assuming  $x = 0.22$ ,  $y = 0.40$ . <sup>c</sup> For complete relative freedom of the polar groups.

$n = 6$ , gives  $x = 0.24$  and  $\Delta E = 850$  cal. Thus a range  $\Delta E = 905 \pm 55$  cal. seems reasonable.

**Dibromides and Dinitriles.**—The data of Smyth and Walls (Fig. 1c) are treated in Table III. Values of  $m$  are those used by Smyth.<sup>22b</sup> The inductive lowering may be overestimated for  $n = 3$ .<sup>23</sup> Where values at 25° in both benzene and heptane were available the mean was used. In every case the range was 0.06 D. or less.

TABLE III

ELECTRIC MOMENTS FOR Br-(CH<sub>2</sub>)<sub>n</sub>-Br

n	$\mu$	$\mu^2/m^2$	
		Obsd. <sup>a</sup>	Predicted <sup>b</sup>
n = 3	2.00	1.38	1.33
n = 4	1.99	1.10	1.21
n = 5	2.27	1.43	1.45
n = 6	2.40	1.60	1.47
n = 9	2.57	1.83	
n = 10	2.55	1.80	(2.00) <sup>c</sup>

<sup>a</sup> Assuming  $m = 1.90$  for  $n > 3$ ,  $m = 1.70$  for  $n = 3$ . <sup>b</sup> Assuming  $x = 0.27$ ,  $y = 0.40$ . <sup>c</sup> See note c, Table II.

This time the best fit gives  $x = 0.27$  and  $\Delta E = 780$  cal. The assumption of 0.1 D. errors as used for the chlorides would barely bring the data in line with this fit, and would lead to an absurdly low estimated error. From inspection of Fig. 3, 0.23 and 0.32 seem reasonable extremes for  $x$ . The range thus obtained corresponds to  $\Delta E = 780 \pm 100$  cal.

Trunel's data (Fig. 1d) for the nitriles in benzene at 25° is treated in Table IV. The group moment is Trunel's value for C<sub>2</sub>H<sub>5</sub>CN. For  $n = 3$  a rough estimate of  $m$  has been made by applying the same percentage lowering as in the dichlorides. Whether such a crude estimate has anything but success to recommend it is debatable. The best fit,

(23) R. P. Smith and J. Rasmussen have reported more elaborate estimations of the individual rotomer moments for these series in a paper presented before the Division of Physical Chemistry at the 138th Meeting of the American Chemical Society, September, 1960, at New York, N. Y.

$x = 0.21$ , corresponds to  $\Delta E = 930$  cal. Reasonable limits would appear to be  $\pm 100$  cal.

TABLE IV  
ELECTRIC MOMENTS FOR  $\text{NC}-(\text{CH}_2)_n-\text{CN}$

$n$	$\mu$	$\mu^2/m^2$	
		Obsd. <sup>a</sup>	Predicted <sup>b</sup>
$n = 3$	3.91	1.39	1.33
$n = 4$	3.76	1.12	1.06
$n = 5$	4.10	1.33	1.41
$n = 7$	4.39	1.52	1.54
$n = 8$	4.50	1.60	
$n = 10$	4.95	1.93	(2.00) <sup>c</sup>

<sup>a</sup> Assuming  $m = 3.56$  for  $n > 3$ ,  $m = 3.32$  for  $n = 3$ . Assuming  $x = 0.21$ ,  $y = 0.40$ . <sup>c</sup> See note c, Table II.

### Experimental

Electric moments were calculated by the procedure of Halverstadt and Kumler.<sup>24</sup> Apparatus and method have been described previously.<sup>5</sup> Results are reported in Table V.

1,4-Dichlorobutane was twice fractionally distilled: b.p. 152.0–152.2° (730 mm.),  $d_4^{26}$  1.1348,  $n_D^{26}$  1.4531. 1,5-Dichloropentane was likewise twice fractionated: b.p. 180–180.4° (735 mm.),  $d_4^{25}$  1.0947,  $n_D^{25}$  1.4538.

1,6-Dichlorohexane was prepared by adding  $\text{SOCl}_2$  to 1,6-hexanediol at room temperature, then heating under reduced pressure to remove excess  $\text{SOCl}_2$  and by-products. The product was then fractionated under reduced pressure: b.p. 74.0–74.5° (6.5 mm.),  $d_4^{25}$  1.0720,  $n_D^{25}$  1.4544.

1,10-Dichlorodecane was similarly prepared from 1,10-decanediol: b.p. 135° (5 mm.),  $d_4^{25}$  0.9925,  $n_D^{25}$  1.4579.

A small sample of each product was dried overnight over  $\text{CaCl}_2$  before determining the electric moment.

### Conclusion

In the three homologous series considered here, the low electric moments of the substituted butanes are the natural consequence of steric factors, according to a model based on reasonable assumptions

(24) I. F. Halverstadt and W. D. Kumler, *J. Am. Chem. Soc.*, **64**, 2988 (1942).

TABLE V  
CALCULATION OF ELECTRIC MOMENTS FOR  $\text{Cl}-(\text{CH}_2)_n-\text{Cl}$

$n$	Empirical constants				$M_{RD}$	$\mu$
	$\epsilon_1$	$\alpha$	$v_1$	$\beta$		
4	2.2755	3.70	1.1446	-0.300	30.26	2.10
5	2.2752	4.30	1.1428	-0.305	34.88	2.36
6	2.2766	3.61	1.1446	-0.299	39.20	2.27
10	2.2732	3.61	1.1444	-0.308	58.04	2.60

within the framework of modern conformational analysis. It is possible from the observed moments in each series to estimate the relative energies of *gauche* and *trans* end-group positions.

The moments in the dibasic acids and esters will require further study. It seems likely, however, that no assumption of cyclic structure will be required here either. Recent studies in this Laboratory on substituted succinic acids appear to indicate that a low moment occurs in precisely those cases in which a cyclic structure is least probable.<sup>25</sup>

It is tempting to claim that the success of this model is strong evidence for the validity of the entire set of assumptions used. However, Smith and Rasmussen,<sup>26</sup> using quite a different exclusion assumption in place of IV above, also predict a low moment for  $n = 4$  for some values of  $x$ . This, of course, only strengthens the argument against assumption of cyclic or other special rotomer structures.

**Acknowledgment.**—This series of studies was initiated under a grant from Research Corporation. We are grateful also to Dr. Max T. Rogers for discussions which stimulated and assisted this work. Miss Marjorie Rawhouser checked and refined a number of the calculations.

(25) H. B. Thompson, L. Ebersson and J. V. Dahlen, to be published.  
(26) R. P. Smith, personal communication. See also ref. 23.

## THE COMPARATIVE ROLES OF OXYGEN AND INHIBITORS IN THE PASSIVATION OF IRON. III. THE CHROMATE ION

BY G. H. CARTLEDGE

Chemistry Division, Oak Ridge National Laboratory, Operated by Union Carbide Corporation for the U. S. Atomic Energy Commission, Oak Ridge, Tennessee

Received December 22, 1960

Polarization studies similar to those with the pertechnetate ion have been extended to the chromate ion in oxygen or helium, for the purpose of determining the relative contributions of the two oxidants to the total cathodic current on passive iron. It was found that the cathodic reduction of chromate ion on passive iron is similar to that of the pertechnetate ion in being slow, relative to the reduction of oxygen. Whereas the reduction product from the pertechnetate ion accelerates reduction processes on the electrode, this effect was not found with the chromate ion. It was found also that the fully passivated surface apparently contains a reducible component other than the passivating film itself. It is not easily destroyed by substitution of helium or carbon monoxide for oxygen, though a limited amount of electrochemical reduction suffices for its elimination without activation of the electrode.

The action of chromates as inhibitors for the corrosion of iron and steel is of particular interest because of their widespread use both for practical purposes and in studies of passive films. The preceding papers in this series<sup>1,2</sup> included reference to the principal recent studies bearing on the mechanism of this action. In view of the ability of the

chromate ion to form a film of mixed oxides by reaction with an active iron surface, it is of special importance to determine explicitly whether either the production of such film or the oxidation potential involved in its formation is the sole factor in the action of the inhibiting ion.

In certain experiments with  $\text{Cr}^{51}\text{O}_4^-$ , to be discussed at a later point, the results were interpreted on the assumption that the  $\text{Cr}_2^{51}\text{O}_3$  deposited on the

(1) G. H. Cartledge, *J. Phys. Chem.*, **64**, 1877 (1960).

(2) G. H. Cartledge, *ibid.*, **64**, 1882 (1960).

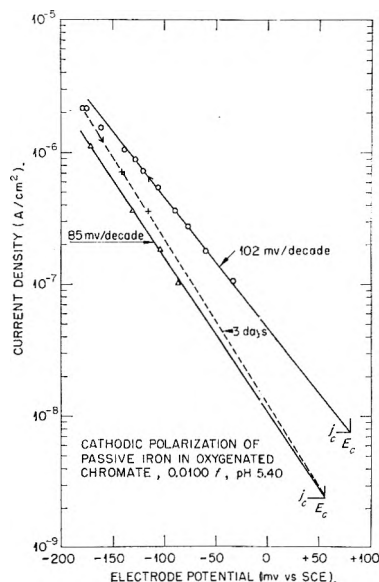


Fig. 1.—Cathodic polarization of an iron electrode passivated in an oxygenated chromate solution. Current densities are in amperes per  $\text{cm}^2$  of apparent surface. The extension of the dashed curve below the points marked x denotes an interval of 3 days before the second polarization indicated by the lower solid curve.

specimen measured the total corrosion, whether oxygen was present or not. Reduction of chromates at low acidities is notoriously slow, however. This was demonstrated for passivation of iron in previous experiments,<sup>3</sup> which showed that a deaerated  $10^{-3}$  *f* chromate solution at *pH* 6.5 and at  $57^\circ$  gave potentials on an iron electrode that were very unreproducible and considerably less noble than that observed in a deaerated pertechnetate solution or in an oxygenated chromate solution under the same conditions of acidity and temperature. Previous work<sup>2</sup> also demonstrated that the reduction of pertechnetate ions under inhibiting conditions is considerably slower than reduction of oxygen on the passive iron electrode. There is no known record of a direct comparison of the reduction rates on passive iron of oxygen and the various reducible ions used as inhibitors. The present work is intended to supply this information with respect to the chromate ion, as part of the basis for a consideration of the role of inhibitors in the passivation process.

### Experimental

The procedures and electrolytic iron used were the same as those of the preceding work,<sup>2</sup> except that no phthalate ion was used with the oxidizing inhibitor, since the chromate solutions possessed sufficient buffering capacity. It was found that the reduction of chromate ions is so slow that it is possible to subject a 0.0500 *f* solution of  $\text{K}_2\text{Cr}_2\text{O}_7$  to cathodic pre-electrolysis at a quite low potential. A divided cell was used and helium, purified by passage over copper turnings at  $425^\circ$ , was passed through the solution during electrolysis. A cylindrical platinum-gauze electrode 2.5 cm. in diameter and 5 cm. long served as cathode. Electrolysis at 1 ma. was conducted for 6 hr., the cathode potential being  $-675$  to  $-735$  mv. vs. S.C.E. At the conclusion of the electrolysis *pH* had risen to 5.98. A portion of the catholyte gave no precipitate when treated with ammonia and a hydrochloric acid extract of the cathode gave only the faintest turbidity when it was made weakly

ammoniacal, although the total charge passed could have reduced 4 mg. of Cr(VI) to Cr(III).

Both galvanostatic and potentiostatic measurements were made, as required, and the solution was vigorously stirred by a stream of either oxygen or oxygen-free helium. It was demonstrated that measurements in pre-electrolyzed solutions did not give significantly different results from those made in solutions of analytical-grade chromates recrystallized once from triply distilled water and dissolved in triply distilled water.

### Results

**Effects of Reduction Products.**—Figure 1 shows the results of cathodic polarization of a passivated iron electrode in oxygenated  $1.00 \times 10^{-2}$  *f* chromate at *pH* 5.40 (mixture of  $\text{CrO}_4^{2-}$  and  $\text{Cr}_2\text{O}_7^{2-}$ ). The curve is typical of a number of polarizations under the same conditions. It was observed that use of current densities above  $10^{-6}$  amp./ $\text{cm}^2$  for more than a few minutes with a freshly passivated electrode led to an increase in the overvoltage for a given current density. This effect is shown in Fig. 1 by the two points (x) on the dashed curve, which were taken with diminishing current density, and by the lower solid curve, which was taken three days later. The electrode was on open circuit during this interval. The increase of overvoltage here observed is just the reverse of the behavior found with the pertechnetate ion.<sup>2</sup> The shift was not observed on electrodes which had been passivated for longer times and polarized only at current densities less than a few  $\mu\text{a.}/\text{cm}^2$ .

An experiment was made to determine whether the cathodic processes are accelerated by deposition of  $\text{Tc}(\text{OH})_4$  on an electrode after passivation in chromate, as was observed in the polarizations presented in the previous paper.<sup>2</sup> Clearly, from thermodynamic considerations, chromate should oxidize  $\text{Tc}(\text{OH})_4$  back to  $\text{TcO}_4^-$ , so it was problematical how long such a deposit might be maintained. A heavy deposit was formed by passing a cathodic current of 10 ma. for 3 min. through the passivated iron electrode in an acidic sulfate solution containing  $\text{TcO}_4^-$ . The dull, dark gray color persisted when the electrode was returned to the chromate solution ( $1.00 \times 10^{-2}$  *f*, *pH* 5.50). The electrode was polarized potentiostatically at  $-75$  mv. in the oxygenated chromate solution both before depositing  $\text{Tc}(\text{OH})_4$  and again after the electrode containing  $\text{Tc}(\text{OH})_4$  had been oxygenated for 18.2 hr. The current density increased 1.9-fold after deposition of  $\text{Tc}(\text{OH})_4$ . The amount of technetium on the electrode was shown by  $\beta$ -counting to be approximately 21  $\mu\text{g}$ . The deposit was found to be covered over with  $\text{Cr}(\text{OH})_3$  formed by reaction with the chromate ions, however, since the usually effective anodic decontamination in acidic solution removed only a negligible amount of beta activity. A second anodic polarization in an alkaline medium removed both the precipitated chromium and technetium hydroxides, since the  $\beta$ -activity was diminished by 99.8%. An accelerating effect of precipitated  $\text{Tc}(\text{OH})_4$  on the cathodic processes was therefore observed, but doubtless in somewhat lower degree than would have characterized a completely superficial film.

**Sensitivity to Sulfate Ions.**—It was found previously that addition of sulfate ions disturbs the

(3) R. F. Sympton and G. H. Cartledge, *J. Phys. Chem.*, **60**, 1037 (1956).

inhibitory action of chromates, under marginal conditions, just as it affects the other inhibitors studied.<sup>1,3</sup> This effect was confirmed in the present experiments. After an electrode had been passivated in oxygenated  $1.00 \times 10^{-2} f$  chromate at pH 6.00 and subjected to cathodic polarization in oxygen, enough potassium sulfate was added to make the solution  $1.00 \times 10^{-2} f$  in sulfate without change of pH. The sulfate was added while the electrode was at  $-147$  mv. S.C.E. under a current density of  $1.32 \times 10^{-6}$  amp./cm.<sup>2</sup>. This potential remained essentially constant during 24 min., but severe pitting corrosion developed when the cell was left on open circuit over a weekend, the potential having fallen to  $-462$  mv.

**Effects of Deoxygenation.**—The effect of oxygen in the chromate system was investigated by polarization measurements over the range of acidities from pH 3.57 to 6.00. The lower pH values were chosen in order to include the acidity used in some of the work of Brasher and Kingsbury.<sup>4</sup> In Series I and II iron electrodes were passivated in oxygenated chromate solutions at pH values of 3.57 and 5.50, respectively. The effect of changing the gas stream from oxygen to helium or the reverse was determined both on open circuit and with a cathodic polarizing current. For Series I, the electrode was first held at  $-75$  mv. (S.C.E.) potentiostatically after 18.2 hr. in oxygenated chromate; the current density became stable at  $4.39 \times 10^{-6}$  amp./cm.<sup>2</sup>. Replacement of oxygen by helium with the same current passing caused the potential to fall rapidly past  $-200$  mv. To avoid activation of the electrode, the current was discontinued. The subsequent behavior of the system is given in Fig. 2, which shows the extreme rapidity and extent of the shift in potential caused by changing the atmosphere. After the solution had time to become saturated with oxygen the electrode was again held at  $-75$  mv., the required current density becoming stable at  $4.95 \times 10^{-6}$  amp./cm.<sup>2</sup>, in reasonable agreement with the value observed before the measurements in helium. The results of the experiment were further confirmed by potentiostatic polarizations of the same system at  $-150$  mv. S.C.E. in helium and then in oxygen. The current density attained at the constant potential was  $5.65 \times 10^{-8}$  amp./cm.<sup>2</sup> in helium, and this changed to  $1.03 \times 10^{-5}$  amp./cm.<sup>2</sup> after admission of oxygen. At the conclusion of the experiment, the iron was bright and free of visible film.

In Series II, at pH 5.50, passage of helium for 40 hr. led to a stable open-circuit potential of  $-185$  mv. The electrode was then anodically polarized at  $-75$  to  $-55$  mv. during 65 min. When the current was shut off, the potential shifted as shown in Fig. 3. Following these observations, the same electrode was again polarized galvanostatically in fresh oxygenated electrolyte three days later. It gave a good Tafel of slope 107 mv./decade, displaced 12 mv. positive to the one established by the three points potentiostatically determined before the long exposure to helium. The debasing which

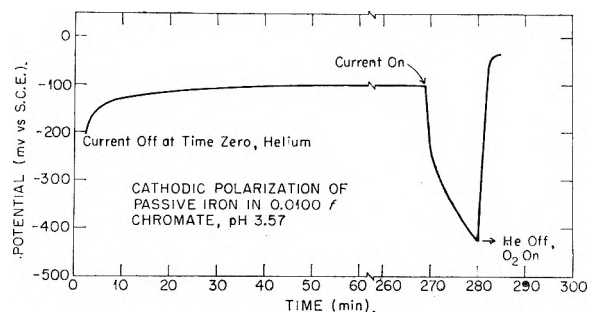


Fig. 2.—The effect of atmosphere on the cathodic polarization of passive iron in  $1.00 \times 10^{-2} f$  chromate at pH 3.57. Polarizing current density was  $4.39 \times 10^{-6}$  amp./cm.<sup>2</sup>. The curve is plotted from a continuous recording of the potential.

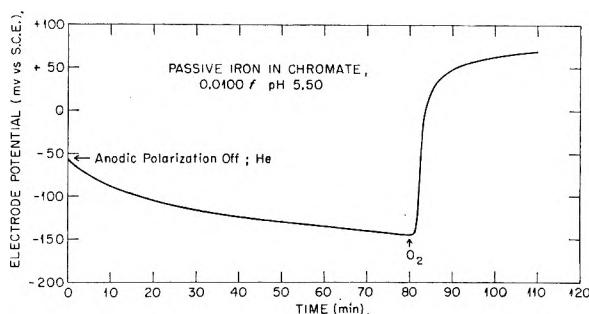


Fig. 3.—Passive iron in  $1.00 \times 10^{-2} f$  chromate at pH 5.50. After 40 hr. in helium, the electrode was anodically polarized in helium until time zero. Oxygen replaced helium after 80 min. Plotted from a continuous recording of the potential.

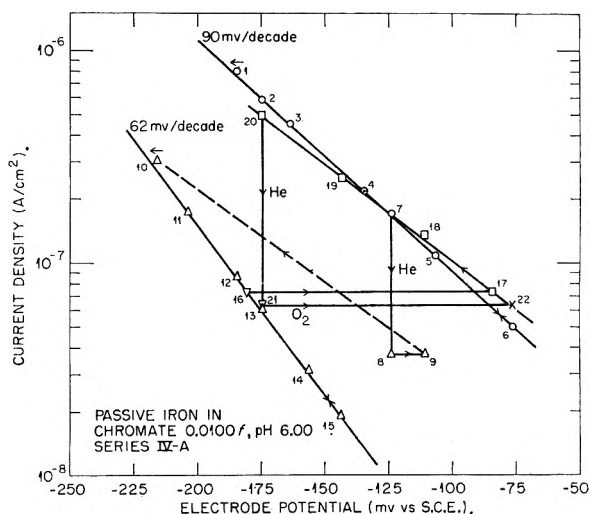


Fig. 4.—Cathodic polarization alternately in oxygen and in helium, starting at the point numbered 1.

occurs in an atmosphere of helium and the extremely fast ennobling when oxygen is admitted clearly demonstrate qualitatively the comparative reduction rates of the two oxidizing agents.

In several succeeding series of experiments, passivated electrodes were polarized in oxygenated chromate solutions and then the oxygen was displaced by bubbling either helium or carbon monoxide through the solution in order to obtain polarization curves for reduction of chromate alone. The conditions for Series III–VI were as follows:

(4) D. M. Brasher and A. H. Kingsbury, *Trans. Faraday Soc.*, **54**, 1214 (1958).

III. A preliminary potentiostatic measurement in oxygen, then in helium. A surface oxidant not removed by helium was apparently indicated. Data not given in detail.

IV. At  $pH$  6.00, alternately in oxygen and in helium, in two cycles. Series IV-A is Fig. 4; IV-B gave similar results; data not shown.

V. Phthalate at  $pH$  6.07–6.03 to determine whether the "excess nobility" observed under helium in Series III and IV depended upon the presence of chromate ions in solution.

VI. Chromate at  $pH$  values of 4.25 and 6.00, oxygen being displaced by either helium or carbon monoxide to determine if the latter exerted any specific effects in comparison with the inert gas, and whether the change of  $pH$  affected the results significantly with either gas.

In the preliminary potentiostatic experiment (Series III) it was found that passage of helium for 20 hr. did not lower the current density to a point on the Tafel line subsequently established in helium after the electrode had been subjected to some additional cathodic polarization. The observations suggested the possibility that the fully oxygenated surface contains a reducible component (besides the passivating film itself) that is not eliminated merely by passage of helium, even after 20 hr., but requires a certain minimum amount of cathodic polarization for its reduction.

**Series IV.**—Figure 4 (Series IV-A) is typical of several experiments of this type. An electrode was passivated for 69 hr. in oxygenated and pre-electrolyzed chromate,  $1.00 \times 10^{-2} f$  at  $pH$  6.00. The electrolyte was renewed and the polarization proceeded in the sequence indicated by the numerals attached to the points in Fig. 4. Points 1–6 and back to 7 correspond to a normal Tafel line for the oxygenated system. Substitution of helium caused a rapid fall in current density at a fixed potential of  $-124$  mv. Point 9 is a check on point 8 after the system had been on open circuit under helium overnight. A charge of  $0.5$  mc./cm.<sup>2</sup> was passed at point 10 without waiting for a steady-state potential, after which stable potentials were attained for points 11–16. In recording points 11–16 the elapsed time was 170 min.; potentials were generally considered sufficiently stable for the intended purpose if the value did not shift more than 1 mv. in about 15 min. Again it is seen that points 8–9 indicate considerably higher current densities than would correspond to the same potential on the Tafel given by points 11–16, in confirmation of the results of the preliminary experiments.

From point 16, admission of oxygen raised the potential at constant current density by almost 100 mv. in 15 min., following which points 17–20 were obtained. Except for the slightly higher (and more usual) polarizability, the curve fell very near the original curve taken in oxygen. During the measurements from points 16 to 20, oxygen passed for only 97 min. and current was on for the entire time. Introduction of helium at point 20 caused the current density at constant potential to fall to the curve previously established in helium, rather than to some higher value. From point 21, passage

of oxygen again caused the potential to become steady in 16 min. at point 22, which is seen to be accurately on the Tafel line observed in oxygen at the beginning of the second cycle of measurements. Exactly similar results were obtained in Series IV-B. It is seen from Fig. 4 that the "excess nobility" was clearly indicated in the first cycle by points 8, 9, but not in the second cycle, point 21.

**Series V-A.**—In this series, polarizations were made in a solution containing only a phthalate at  $1.00 \times 10^{-2} f$  and  $pH$  6.07–6.03, in order to determine whether the chromate ions were responsible for the effects observed under helium in Series III and IV. After sufficient potentiostatic data were obtained in oxygen to show that the electrode was normal,<sup>1</sup> the potential was held at  $-75$  mv. S.C.E. while passing helium. This potential is 56 mv. negative to the calculated Flade potential. In 3.3 hr. the current density fell only to 37% of its value in oxygen; the electrode was not activated. Furthermore, the potential ennobled rapidly when the current was cut off and came to  $+26$  mv. overnight, with helium still passing. Renewed polarization to  $-75$  mv. then required 25% of the original current density in oxygen. The current density was increased from  $4.80 \times 10^{-8}$  to  $4.75 \times 10^{-7}$  amp./cm.<sup>2</sup> until  $0.46$  mc./cm.<sup>2</sup> had been passed. The potential debased steadily and failed to enoble when the current density was reduced. Activation to  $-730$  mv. ensued on open circuit. The total charge passed during the polarization to potentials below  $-75$  mv. was  $0.55$  mc./cm.<sup>2</sup>.

In a similar experiment (V-B), the electrode was again passivated in oxygenated  $1.00 \times 10^{-2} f$  phthalate at  $pH$  6.03. When helium was passed for only 25 min. the current density fell to 40% of its former value, and was essentially stable at this point. The current density was then doubled in order to determine whether activation would result at this stage from passage of the amount of charge that produced activation in the preceding experiment after longer exposure to the helium atmosphere. At  $0.36$  mc./cm.<sup>2</sup>, rapid ennobling occurred on opening the circuit. The same result was obtained after passage of  $0.54$  and  $0.85$  mc./cm.<sup>2</sup>; although the potential had fallen finally to  $-150$  mv. S.C.E. and was still falling, the electrode was still not activated. The electrode was left on open circuit under helium, and 40 hr. later was found to be corroding at  $-760$  mv. S.C.E. The solution was colorless and free of turbidity, but gave a strong test for iron ions and turned brown on exposure to air. The experiment makes it clear that the persistence of a reducible component after exposure to helium does not arise from any chromium species on the electrode.

**Series VI.**—The measurements of this series were made in chromate solutions to determine (1) whether similar results would be obtained at a lower  $pH$  value and (2) whether any difference would arise from use of carbon monoxide, instead of helium, to displace oxygen. Helium was used in Series VI-A with  $1.00 \times 10^{-2} f$   $Cr_2O_7^{2-}$  at  $pH$  4.25. The results gave curves almost identical with those of the first cycle shown in Fig. 4, except for a

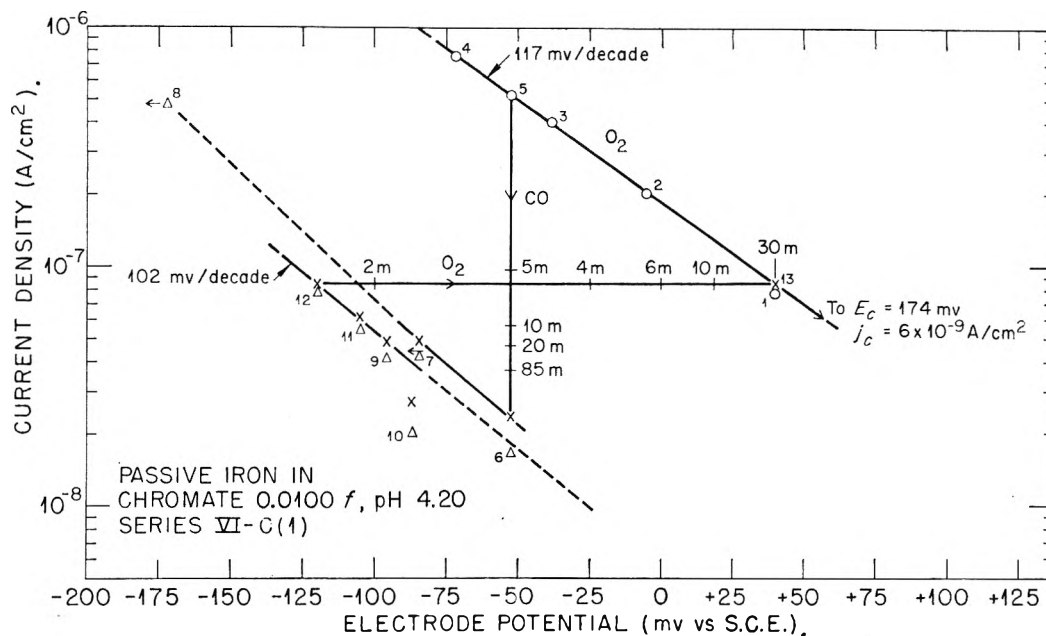


Fig. 5.—Cathodic polarization in oxygen or carbon monoxide. The numerals followed by "m" give the time in min. at which the current density or potential reached the indicated value after the atmosphere was changed. For the polarization in helium, data points are denoted by  $\Delta$ ; the x's represent current densities corrected by a constant corrosion current density of  $6 \times 10^{-9}$  amp./cm.<sup>2</sup>.

displacement of 130 mv. in the noble direction due to the reduction of the pH value. For the experiments in which oxygen was displaced by carbon monoxide, C.P. cylinder gas was passed through a trap at Dry Ice temperature to remove traces of carbonyls, then over copper turnings at 365°, Ascarite, fiber-glass and a water saturator. The electrolyte was again  $1.00 \times 10^{-2} f \text{Cr}_2\text{O}_7^{2-}$  at pH 4.25 or  $1.00 \times 10^{-2} f \text{CrO}_4^{2-}$  at pH 6.00. In Series VI-B the polarization was carried through two cycles under CO, exactly as was shown for helium in Fig. 4. Again, the minimum current density was not reached on passing CO in the first cycle, but the corresponding point fell nicely on the Tafel in the second cycle. Figure 5 (Series VI-C(1)) is representative of several experiments done at the lower pH. Except that the Tafel slopes tended to indicate a somewhat higher polarizability, the results do not appear to be significantly different from those obtained with helium at either pH value. With both gases and at both pH values exposures of 5–8 hr. reduced the cathodic current density for the fixed potential to 6–8% of its value in oxygen, the final current density being so near the passive corrosion current density as to be difficultly measurable.

### Discussion

**Relative Reduction Rates.**—The results make it evident that reduction of chromate ions furnishes only a small fraction of the total cathodic current when oxygen is present under the conditions of these experiments, the difference being about two orders of magnitude. This is in agreement with numerous analyses of stripped films reported in the literature, which uniformly show an excess of iron oxide over the stoichiometrically equivalent amount of chromium(III) oxide, when passivation is effected in the presence of an ample supply of oxygen.

At first sight this conclusion seems to be out of harmony with results obtained by Cohen and Beck<sup>5</sup> and by Brasher and co-workers.<sup>4,6,7</sup> According to Cohen and Beck, from 1–3  $\mu\text{g.}$  of Cr/cm.<sup>2</sup> goes into the film in a very few minutes when a solution containing 50 p.p.m. of  $\text{Na}_2\text{CrO}_4$  is admitted to a specimen of iron that has been freshly reduced in hydrogen. It was reported that the same amount is taken up when air is present. In these experiments the air-formed film was reduced and oxygen evidently was rather well eliminated. The  $\text{Cr}^{51}$  counted therefore corresponded to the product from the initially fast reaction of  $\text{Cr}^{61}\text{O}_4^{2-}$  and active iron, together with any chromate ions adsorbed from solution. Their data show about 2  $\mu\text{g.}$  of Cr/cm.<sup>2</sup> after an exposure of 3 min. In electrical terms, this quantity represents an average current density of  $7 \times 10^{-5}$  amp./cm.<sup>2</sup> over the 3 min. Even this average value is a rather large current density on film-covered iron, according to the present measurements, and suggests that, when Cohen and Beck's solution was not deaerated, diffusion control limited the participation of oxygen in the cathodic process, especially in the fast, early stages of reaction. The contradiction is therefore probably only apparent.

Brasher, *et al.*, as well as Powers and Hackerman<sup>8</sup> found that no  $\text{Cr}^{51}$  went into the film in neutral or alkaline solution when air was present, although Brasher, *et al.*, reported that, at pH 4.2, removal of oxygen made no difference in the uptake of  $\text{Cr}^{51}$  by specimens already having had some exposure to air. The method of excluding oxygen

(5) M. Cohen and A. F. Beck, *Z. Elektrochem.*, **62**, 696 (1958).

(6) D. M. Brasher, A. H. Kingsbury and A. D. Mercer, *Nature*, **180**, 27 (1957).

(7) D. M. Brasher and C. P. De, *ibid.*, **180**, 28 (1957).

(8) R. A. Powers and N. Hackerman, *J. Electrochem. Soc.*, **100**, 314 (1953).

during the subsequent counting experiments was not stated. It was to match the pH (4.2) used in one of the experiments by Brasher, *et al.*, that certain of the present measurements were conducted. The data showed unequivocally the same excess reduction of oxygen as was observed at pH values of 5.5 and 6.0. Further, the uptake of chromium in 28 days at pH 4.2 was found by Brasher, *et al.*, to be  $0.6 \mu\text{g./cm.}^2$ , the solution being exposed to air. (The fast gain of  $0.1 \mu\text{g.}$  attributed to adsorption is subtracted.) If this quantity is converted to electrical terms it represents an average corrosion rate of  $1.45 \times 10^{-9}$  amp./cm.<sup>2</sup> Since the Cr<sup>51</sup> counted includes that deposited during the early stages of the experiment when reaction was most rapid, this calculated average corrosion rate must be considerably higher than the steady-state corrosion rate reached after full passivation. Yet the steady-state corrosion rate at pH 4.2 is of the order of  $1.1 \times 10^{-8}$  amp./cm.<sup>2</sup> in a sulfate solution, according to Vetter,<sup>9</sup> and rates averaging only slightly less than this were indicated in the present measurements in the chromate solution. It is probable, therefore, that the total corrosion rate was not measured by the Cr<sup>51</sup> counts in the experiments of Brasher, *et al.* Considering the small currents involved, it is easy to appreciate the extreme precautions required in the exclusion of oxygen, if reliable corrosion rates are to be measured by counting the Cr<sup>51</sup> deposited by reduction. As shown in a previous paper,<sup>2</sup> corresponding experiments started with the pertechnetate ion in 1953 have given no increase in  $\beta$ -activity since stabilization of the count arising from the initial reactions.<sup>10</sup>

**Reducible Species on the Electrode.**—The measurements represented by Figs. 4 and 5 raise a question regarding the number and identity of reducible species at the passivated interface. As indicated previously, the experiments of Series III made it appear that the removal of oxygen by a stream of helium did not produce the maximum diminution of the current density for a fixed potential, even when the gas was passed for many hours. It seemed as though a certain small amount of cathodic polarization was necessary for this to occur, although subsequent admission of oxygen rapidly restored the electrode to the state it had before passage of helium. The possible cathodic processes are reduction of: (1) O<sub>2</sub> from the solution, (2) some chromate species from solution, (3) constituents of the passive film itself which is variously regarded as consisting of chemisorbed oxygen or an iron(III) oxygen compound, or, conceivably, (4) some other reducible species in the film or the solution phase not included in the previous categories and not removable except by electrochemical reduction.

(9) K. J. Vetter, *Z. Elektrochem.*, **59**, 67 (1955).

(10) The large difference between the rates of reduction of oxygen and chromate ions observed in the present experiments makes it impossible to assume that mere transport of electrons through the passive film itself is rate determining, as was done by O. Kubaschewski and D. M. Brasher, *Trans. Faraday Soc.*, **55**, 1200 (1957). The rate-determining process clearly depends upon the identity of the reducible species at the surface, since the same underlying film is involved in both cases, and the field at the interface and through the film derives from a complex of interactions at the surface.

Experiments such as that illustrated in Fig. 5 show that reduction of the current density due to displacement of oxygen by an indifferent gas proceeds very rapidly. In Fig. 5, the times given were counted from the moment of changing the gas at the entrance to the purification train, which included a water saturator, as well as perhaps 200 ml. of gas volume. Nevertheless, 80–90% of the decrease in current density regularly occurred within 10 min. No difference between helium and carbon monoxide was observed in this respect, which suggests that only a diminution of the concentration of oxygen by physical means is involved. If the persisting cathodic process arose from traces of oxygen remaining in the helium, one would not expect the spontaneous activation under helium observed in Series V-A and B.

It is believed that reduction of chromate is approximately responsible for the results corresponding to the Tafel curves at the highest overvoltages after some polarization in helium ( $0.5$ – $1$  mc./cm.<sup>2</sup>). The facts that the potentials in helium never fell into the active region and that oxygen so quickly restored the noble potential after polarization in helium in both phthalate and chromate systems seem to demonstrate that the passive film itself was never destroyed: that is, its rate of reduction was very slow in comparison with that of other cathodic processes. As noted in Series V, use of streaming helium in the phthalate system led to a decrease of the current density for a constant potential to only 25–40% of its value in oxygen. Furthermore, the potential re-nobled upon opening the circuit after helium had passed for only an hour and a total of  $0.85$  mc./cm.<sup>2</sup> had been passed through the electrode (Series V-B), although in V-A such re-nobling did not occur when the system was polarized by only  $0.46$  mc./cm.<sup>2</sup> after 22 hr. under helium. In other words, the corrosion current which continues on open circuit under helium apparently can substitute for applied cathodic current if the system remains on open circuit under helium for a sufficient time.

Reducible iron species in solution would, of course, give the persistent effect if present in sufficient concentration. In other experiments<sup>11</sup> it was found that some iron species from the solution phase went into the film during passivation of stainless steel in sulfuric acid to which Fe<sup>65,69</sup> was added. It was observed also<sup>1</sup> that brown complexes of iron(III) formed in phthalate solutions when conditions were such that passivation was not quite attained, and, at the same time, a visible film formed on the electrode. It is therefore evident that there are interactions between soluble iron ions and the film during passivation. Since the solutions were always renewed in the present experiments before polarization measurements were started, it is most likely that the cathodic polarization was required to reduce some component on the electrode, rather than one in the solution. If a component of the film was actually removed, however, the film structure responsible for passivity was apparently not thereby destroyed when chromate was present. The evidence for some additional reducible com-

(11) G. H. Cartledge, *J. Electrochem. Soc.*, **104**, 420 (1957).



ponent on the electrode is suggestive, though by no means conclusive.

**Steady State Potentials.**—Both the present measurements and those previously obtained at 57°<sup>3</sup> indicate that the chromate ion in the pH range of 3.57–6.0 and in the absence of oxygen causes the potential slowly to approach a value which appears to be a reasonably steady mixed potential corresponding to a considerably reduced corrosion current density (Figs. 2 and 3). The potentials are distinctly less noble than the calculated Flade potential, however, and something like 200 mv. less noble than that given by the pertechnetate ion in spite of its lower oxidation–reduction potential. When oxygen is present, freshly passivated electrodes show cathodic polarization curves in pertechnetate and chromate solutions at pH 5–6 which are within 25–50 mv. of each other, the overvoltage being higher in the chromate solution. The chromate system differs from the pertechnetate system in that the reduction product of the chromate ion increases the cathodic overvoltage somewhat, whereas  $Tc(OH)_4$  definitely decreases it.

The polarizations in helium required considerable time to reach essentially stable states, but gave an approximation to Tafel lines covering current densities in the neighborhood of  $10^{-7}$  amp./cm.<sup>2</sup>. If it may be assumed that the cathodic reaction under these conditions consists in reduction of  $CrO_4^{2-}$  to  $Cr(OH)_3$ , a theoretical reversible potential may be calculated for this couple. A long extrapolation of the Tafel line to this potential suffices to give a crude value of the exchange current for the reaction on the passive electrode, for comparison with similar extrapolations in the reduction, respectively, of oxygen and pertechnetate ions.<sup>1,2</sup> For the six polarizations in the chromate system in helium or carbon monoxide at pH values of 4.2 and 6.0, four agree closely in extrapolating to log  $j_0$  values

between –15 and –16, the other two being –14 and –17, respectively. Corresponding values for reduction of the pertechnetate ion are ca. –8, whereas for oxygen in the phthalate system the value averages –17. Apparently it is somewhat higher for oxygen in the chromate system.

**Summary.**—The experiments lead to the conclusions: (1) that reduction of oxygen on the passive surface is about two orders of magnitude faster than that of chromate at potentials near the Flade potential; (2) that the chromate reduction product does not accelerate the reduction processes, as  $Tc(OH)_4$  does; (3) that reduction of chromate ions and of oxygen have comparable exchange current densities under the conditions of these experiments, so that the greater contribution of oxygen to the total cathodic process derives chiefly from its more noble reversible potential under the conditions assumed; (4) that there is some evidence that the fully passivated surface contains a persistently held reducible constituent other than the passive film itself and not dependent upon the presence of chromate ions for its formation. The bearing of the results upon the mechanism of passivation will be considered more fully after presentation of the results of a similar study of osmium (VIII) oxide in a forthcoming paper.

**Acknowledgment.**—The author is indebted to Dr. Dieter Spahrbiel for conducting a few additional experiments like that shown in Fig. 4. A low-carbon steel was used and the results were similar in general. The current density at a fixed potential in helium was about two orders of magnitude below that in oxygen, however, and so near the corrosion current density that the existence of the “singular point” could not be established reliably. It is also a pleasure to acknowledge helpful discussions with Dr. E. J. Kelly.

## LATERAL INTERACTION ON A SMOOTH SURFACE

By J. G. ASTON AND H. CHON

No. 115 from the Cryogenic Laboratory of the College of Chemistry and Physics, The Pennsylvania State University, University Park, Penna.

Received December 23, 1960

A simple expression for the lateral interaction energy of the mobile layer on a uniform surface is obtained using a two-dimensional van der Waals equation of state. When van der Waals constants derived from the usual three dimensional ones are used, this expression is in agreement with the experimental results for the rare gases on graphitized carbon black. The differential heats of adsorption after subtracting the lateral interaction energy indicate little heterogeneity.

### Introduction

The lateral interaction energy of the adsorbed gases on a uniform surface was expressed in a simple way by Aston and Greyson<sup>1</sup> in terms of the three-dimensional van der Waals constants. They compared the expression for the lateral interaction in a mobile layer with the experimental results of the rare gases on graphitized carbon black<sup>2</sup> and

found the experimental values near the monolayer were considerably lower than the calculated values. This was attributed to reduction of energy by a compression caused by the forces of the adsorbent in the second layer. Such forces would act to pull additional molecules part way into the first layer. Actually the data on helium, neon, argon and krypton<sup>2</sup> can be shown to yield values of the differential lateral interaction energy in very close agreement with those calculated from the two-dimensional van der Waals equation up to values of  $\theta$  of almost 0.5. It is the object of this paper

(1) J. G. Aston and J. Greyson, *J. Phys. Chem.*, **61**, 613 (1957).

(2) (a) C. H. Amberg, W. B. Spencer and R. A. Beebe, *Can. J. Chem.*, **33**, 305 (1955); (b) R. A. Beebe and D. M. Young, *J. Phys. Chem.*, **58**, 93 (1954); (c) J. Greyson and J. G. Aston, *ibid.*, **61**, 620 (1957).

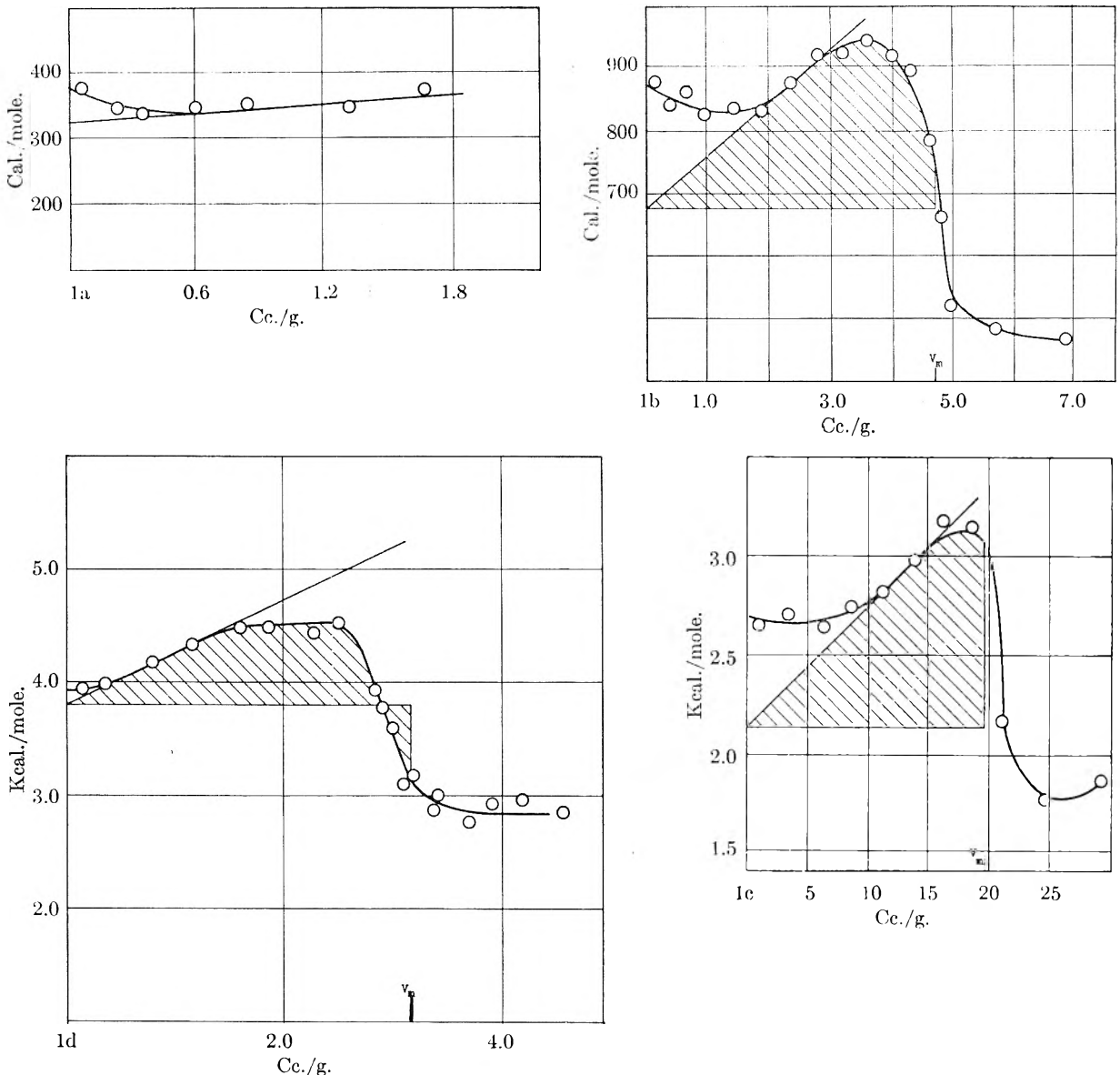


Fig. 1.—Curves of differential heats of adsorption,  $\bar{E}_1$ , vs. coverage, and the slopes: (a) helium, (b) neon, (c) argon, and (d) krypton.

to demonstrate this fact for apparently it has not yet been shown that lateral interaction on a uniform surface can be so simply described with respect to conventional van der Waals constants.

As far as we are aware the formula used in the previous paper has not been derived explicitly in terms of conventional van der Waals constants. For the sake of clarity this will be derived below and discussed along with the corresponding formula for the differential lateral interaction energy.

#### Discussion of Formulas

The expression for the lateral interaction energy in a mobile layer can be derived as follows: The equation relating  $(\partial E/\partial V)_T$  to the equation of state of the gas is

$$(\partial E/\partial V)_T - T(\partial P/\partial T)_V - P \quad (1)$$

The two-dimensional analog of (1) is

$$\left(\frac{\partial E_1}{\partial \Sigma}\right)_T = T \left(\frac{\partial \phi}{\partial T}\right)_\Sigma - \phi \quad (2)$$

where  $\phi$ ,  $\Sigma$  are surface pressure and area. The two-dimensional van der Waals equation is

$$\left(\phi + \frac{n^2 a'}{\Sigma^2}\right)(\Sigma - b') = nRT \quad (3)$$

where  $a'$ ,  $b'$  are the two-dimensional van der Waals constants. Upon inserting the expression for  $\phi$  from (3) into (2), we obtain

$$\left(\frac{\partial E_1}{\partial \Sigma}\right)_T = \frac{n^2 a'}{\Sigma^2}$$

on integrating

$$E_1 = n^2 a' \int_{\infty}^{\Sigma} \frac{1}{\Sigma^2} d\Sigma = -\frac{n^2 a'}{\Sigma}$$

If we put  $\Sigma/n =$  area per molecule  $= b'/\theta$ , then  $E_1 = na'/b'\theta$ . Since the ratio  $(a'/b')$  between the two-dimensional van der Waals constants and their three-dimensional analogs has been shown

(3) T. L. Hill, *J. Chem. Phys.*, **14**, 441 (1946).

(4) J. P. Oliver and S. Ross, "Proceedings of the Second International Congress of Surface Activity," Vol. 2, 1957, London, p. 46.

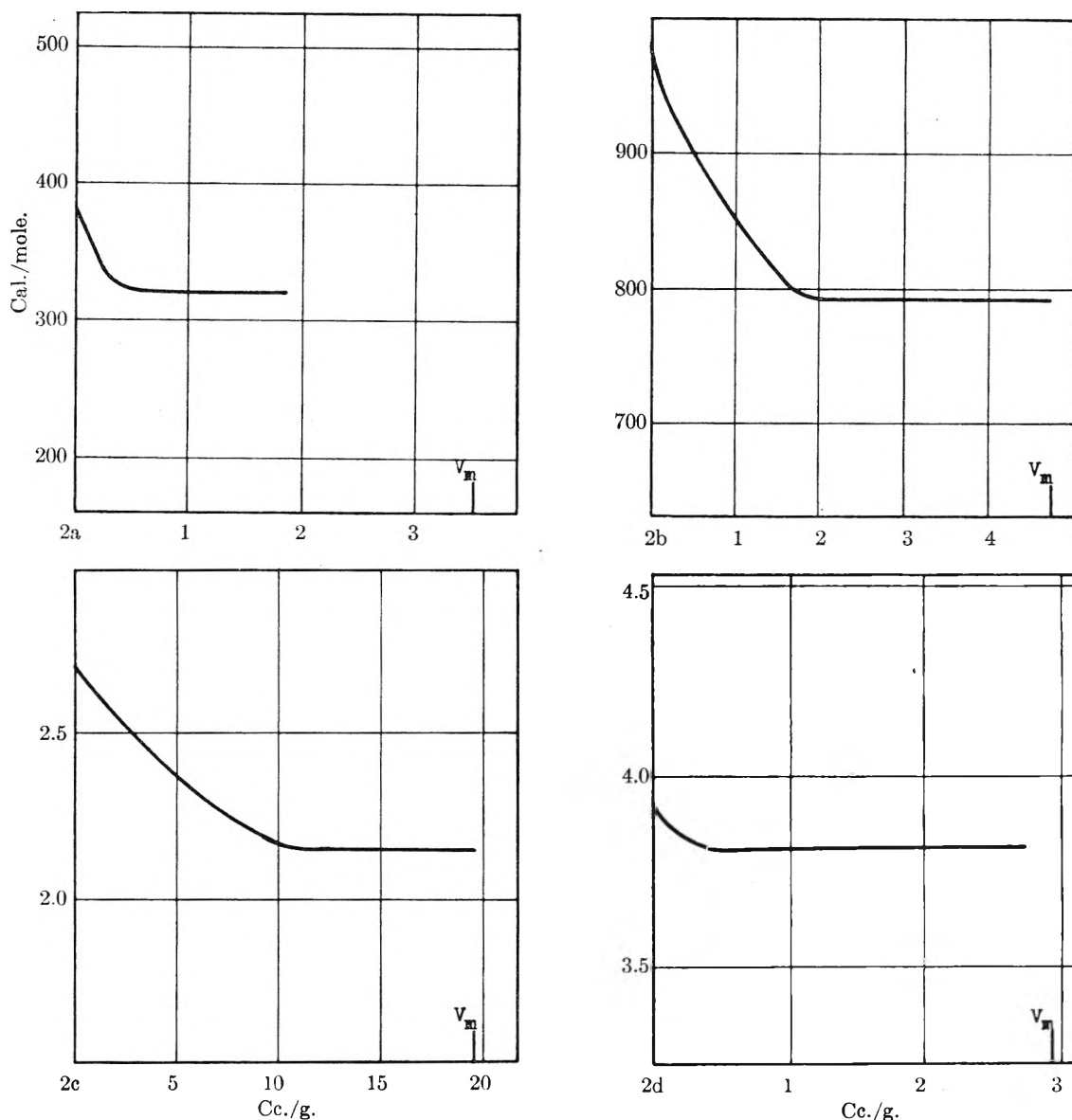


Fig. 2.—Corrected differential heats,  $\bar{E}_1$ , vs. coverage: (a) helium, (b) neon, (c) argon, and (d) krypton.

to be<sup>3</sup>  $(a/2b)$ , the expression for the integral lateral interaction energy then become

$$E_1 = na/2b\theta \quad (4a)$$

For a surface which contains one mole at a coverage,  $\theta$  (*i.e.*,  $n$  is unity)

$$\bar{E}_1 = a/2b\theta \quad (5)$$

The value of  $\bar{E}_1$  is then the lateral interaction energy per mole. Equation 5 is not in a form suitable for differentiation. The expression for the differential lateral interaction energy  $\bar{E}_1$  can be obtained by differentiating  $E_1$  from equation 4a with respect to the number of moles adsorbed  $n$ , only after substituting  $n/n_0$  for  $\theta$  with  $n_0$  equal to the number of moles in a monolayer. With this substitution

$$E_1 = n^2a/2bn_0 \quad (4b)$$

$$\bar{E}_1 = \frac{\partial}{\partial n} \left( \frac{n^2}{2b} - \frac{a}{n_0} \right) = \frac{a}{b} \theta \quad (6)$$

Oliver and Ross<sup>4</sup> obtained a mathematical description for the horizontal interaction energy of mobile

and immobile films. Their expression for the horizontal interaction energy of a mobile film is  $(\Delta H_b)_\theta = -2a\theta/\sigma_0$  where  $a$  is the two-dimensional van der Waals attractive constant and  $\sigma_0$  is the area per molecule. This expression becomes the same as our equation 6 if we set  $\sigma_0 = b'$  where  $b'$  is the constant in equation 3. Care should be taken not to confuse equation 5 with equation 4a. Equation 5 was used correctly in the previous paper. It is for this reason that we have given the derivation of equation 5.

### Discussion

The integral lateral interaction energy was obtained by Aston and Greyson<sup>1</sup> from the calorimetric heat curves by a graphical integration of the area enclosed between the bump in the heat curve and an extrapolation of the flat portion of the heat curve to the monolayer. As discussed by Aston and Greyson, the lateral interaction energies thus obtained do not fit equation 5 because of

compressive effect caused by molecules in the second layer. The value of the differential energy of lateral interaction as obtained from equation 4 by differentiation is given in equation 6. To find the coverage  $\theta$  at which the compressive effect becomes appreciable one notes equation 6 is linear in  $\theta$  with a slope  $a/b$ .<sup>5</sup> Thus  $E_1$  plotted against  $\theta$  yields a straight line passing through the origin.

Figures 1a, 1b, 1c and 1d show the heat of adsorption of helium,<sup>2c</sup> neon,<sup>2c</sup> argon<sup>2b</sup> and krypton<sup>2a</sup> on graphitized carbon black with the slopes of the graphs prior to the points of deviation due to the compressive effect. The deviation of the curves from straight line, with this slope on the side of higher coverage, starts at about  $\theta = 0.5$  for neon. For argon and krypton the point of deviation is at somewhat higher coverage. The slopes should intersect the ordinate at values equal to the differential heat of adsorption on the smooth surface with no lateral interaction energy since the lateral interaction is zero at  $\theta$  equal to zero. In column 2 of Table I are given the slopes of the graphs for the respective gases listed in column 1. In column 3 are given the value of  $a/b$ . The agreement is excellent for neon, argon and krypton. For helium the measured is three times the calculated value. This is certainly due to the fact that for helium the data are taken well above the critical temperature of helium (above 10°K.). While somewhat different slopes could have been drawn through the experimental points we have chosen the maximum slope that could reasonably be drawn by a conservative weighting of the experimental points.

In column 4, for comparison, are given the values of  $E_1$  per mole at the monolayer obtained according

(5) In reference 1 this was given incorrectly as  $a/2b$ .

to the method used by Aston and Greyson modified to be consistent with the present treatment. The experimental integral lateral interaction energy for comparison with the theory is correctly calculated from the curves in Fig. 1b, 1c and 1d if the area is taken between a horizontal line through a point where the slope intersects the ordinate and a curve. This curve is composed initially of the theoretical slope up to the point where the curve deviates from the experimental points and thereafter of the experimental curve. This area (col. 4) should, of course have the value  $a/2b$ , given in column 5, if the two-dimensional van der Waals equation applies.

TABLE I  
MEASURED AND THEORETICAL ENERGY OF LATERAL INTERACTION

	$\frac{\partial E_1}{\partial \theta}$ (max.) (cal./mole)	$a/b$ (cal./mole)	$E_1$ (Aston and Greyson modified) (cal./mole)	$a/2b$ (cal./mole)
Helium	105	35		
Neon	360	300	150	150
Argon	1160	1010	580	505
Krypton	1400	1410	480	705

From the increasing deviations from equation 6 proceeding from low to zero coverage one can make deductions about the heterogeneity. By subtracting the lateral interaction energy the curves in Fig. 2 are obtained. These graphs represent the differential heat of adsorption as a function of coverage when there is no lateral interaction. They indicate little heterogeneity as expected since it is for this reason that the lateral interaction is not impaired.

## THE PERMEABILITY OF COPPER TO HYDROGEN

BY D. W. RUDD, D. W. VOSE AND S. JOHNSON

*The Research and Development Laboratories of Metal Hydrides Incorporated, Beverly, Massachusetts*

*Received December 23, 1960*

The permeability of copper to hydrogen was investigated over a limited range of temperature and pressure (350 to 500°, 1.5 and 2.0 atmospheres). The resulting permeability,  $P$ , is found to obey the relationship:  $P = 21.2e^{-12,520 \pm 110/RT} \text{ cm.}^3$  (0°, 1 atm.)hr.<sup>-1</sup>/cm.<sup>2</sup> mm.<sup>-1</sup> (atm.)<sup>1/2</sup>.

### Introduction

The permeability of a metal to hydrogen or certain gases in general is thought to be a composite rate process involving processes of adsorption of the gas followed by solution in the metal with subsequent diffusion and desorption.<sup>1</sup> Published literature of the permeability of solids to gases is quite voluminous. From these efforts, several facts are observed. First, the permeability of metals to diatomic gases involves the passage through the metal of the individual atoms of the permeating gas. This is evidenced by the fact that the rate of permeation is directly proportional to the square root of the gas pressure. Second, the gas permeates

the lattice of the metal and not along grain boundaries. It was shown by Smithells and Ransley<sup>2</sup> that the rate of permeation through single crystal iron was the same after the iron had been recrystallized into several smaller crystals. Third, the permeation of gases to metals is specific in that only those gases which undergo activated adsorption by a metal can permeate it. Rare gases are not adsorbed by metals and attempts to measure permeabilities of these gases have proved unsuccessful. Ryder<sup>3</sup> found negative results on the permeability of iron to argon. Baukloh and Kayser<sup>4</sup> found nickel impervious to helium, neon, argon

(1) C. J. Smithells, "Gases and Metals," John Wiley and Sons, Inc., New York, N. Y., 1937, Chapter II.

(2) C. J. Smithells and C. E. Ransley, *Proc. Roy. Soc. (Lond.)*, **A150**, 172 (1935).

(3) H. M. Ryder, *Elec. F.*, **17**, 161 (1920).

or krypton. Nitrogen is adsorbed by iron and molybdenum but not by copper, and will permeate the former but not the latter. Fourth, it has been observed, at least for most common metals, that the rate of permeation is inversely proportional to the thickness of the metal membrane. Johnson and Larose<sup>5</sup> determined the rate of permeation of oxygen through silver to be linearly dependent on the reciprocal thicknesses of various silver foils. Similar results were noted by Lombard<sup>6</sup> for the system hydrogen-nickel and by Lewkonja and Baukloh<sup>7</sup> for hydrogen-iron. This would infer that, although adsorption is very important, at least in determining whether permeation will or will not ensue, it is not the rate-determining process. The opposite effect has been noticed in the case of Inconel-hydrogen<sup>8</sup> where, due to a film formation on the surface, the resulting reaction of hydrogen with this film is of such a nature that normal permeability behavior is not observed.

**Apparatus.**—The apparatus used in this study is shown in Fig. 1. The membrane is a thin disc (A), but is an integral part of an entire membrane assembly. The entire unit is one piece, being machined from a solid ingot of metal stock. When finished, the membrane assembly is about 5 inches long. Two membrane assemblies were made; the dimensions of the membrane are given in Table I.

TABLE I

Membrane no.	Diameter, in.	Thickness, in.
1	0.9993	0.0656
2	1.0000	0.1284

The wall thickness is large compared to the thickness of the membrane, being on the average in the ratio of 13 to 1. There exists in this design the possibility that some gas may diffuse around the corner section of the membrane where it joins the walls of the membrane assembly. If such an effect is present, it is of a small order of magnitude, as evidenced by the agreement of the values of specific rate (rate at unit area and thickness) between the two membranes under the same temperature and pressure. A thermocouple well (B) is drilled to the vicinity of the membrane. The entire membrane assembly is then encased in an Inconel jacket and mounted in a resistance furnace. The interior of the jacket is connected to an auxiliary vacuum pump and is always kept evacuated so that the membrane assembly will suffer no oxidation at the temperatures at which measurements are taken. The advantages of this configuration are: (1) There are no welds about the membrane itself, so that the chance of welding material diffusing into the membrane at elevated temperatures is remote. (2) It is possible to maintain the membrane at a constant temperature. Since the resulting permeation rate is very dependent upon temperature, it is advisable to be as free as possible from all temperature gradients. (3) It is possible to obtain reproducible results using different specimens. The only disadvantage to this configuration is the welds (at C) in the hot zone.

The gas leaving the downstream side of the membrane is pumped *via* a Toepler pump to a calibrated volume. Between the Toepler pump and the membrane assembly, there is a Dry Ice-acetone cold trap. Tank hydrogen is fed successively through a catalytic getter, a 3-foot tower of calcium hydride, and finally through a 12-inch column of titanium hydride maintained at about 1000°. From here, the hydrogen diffuses through a palladium coil housed in the top side of the membrane assembly. The pressure is allowed to build up to an excess of the desired amount and

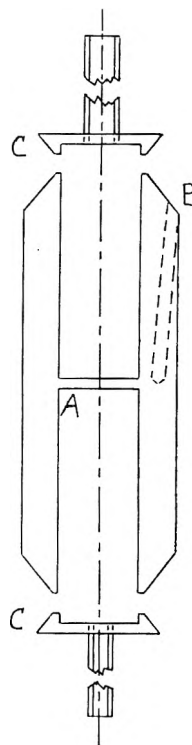


Fig. 1.—Cross section of membrane assembly for measuring the permeability of metals to hydrogen: A = membrane; B = thermocouple well; C = caps.

this excess bled off to a long column of mercury. By raising or lowering this column, the pressure can be maintained to a very precise degree. The temperature is controlled by Wheelco "capaciline" regulators and a recording potentiometer. This instrumentation is capable of maintaining the oven temperature to  $\pm 1^\circ$ . The temperature around the calibrated volume is read to  $\pm 0.5^\circ$ .

**Material.**—The copper used in this investigation was obtained from Vacuum Metals Corporation, Syracuse, New York.

The analysis of the material was as follows:

Al—<0.01	Te—<0.0006
W—<0.01	Sn—0.0002
Si—0.005	Bi—<0.0001
Fe—0.004	P—<0.001
Ni—<0.001	S—<0.002
Pb—<0.001	O—32 p.p.m.
As—<0.0008	Cu—balance
Sb—<0.0008	

**Experimental Accuracy.**—Utilizing the above equipment, the over-all accuracy of the measurements is in the range of  $\pm 1\%$ . The precision of the individual readings is often better than this. Before any measurements were made, both membranes were outgassed for 48 hours at 650°. The downstream section was evacuated by mercury diffusion pumps to a vacuum of  $10^{-6}$  mm. After the 48-hour period, a blank run was initiated at 600°. This run lasted 72 hours. At this time, no reading could be obtained at the calibrated volume. This means that the error in readings, due to leaks in the membrane assembly and the glass vacuum assembly, is less than  $0.000012 \text{ cm.}^3(0^\circ, 1 \text{ atm.})\text{hr.}^{-1}/\text{cm.}^2\text{mm.}^{-1}$ . Table II lists the experimental results.

### Discussion

The equation which is used to evaluate the quantity of gas permeating a metal barrier may be written in the form

$$\alpha = \frac{kDA}{L} (p_1^{1/2} - p_2^{1/2}) e^{-E_P/RT} t \quad (1)$$

where

(4) W. Baukloh and H. Kayser, *Z. Metallik.*, **26**, 156 (1934).

(5) F. M. G. Johnson and P. Larose, *J. Am. Chem. Soc.*, **46**, 1377 (1924).

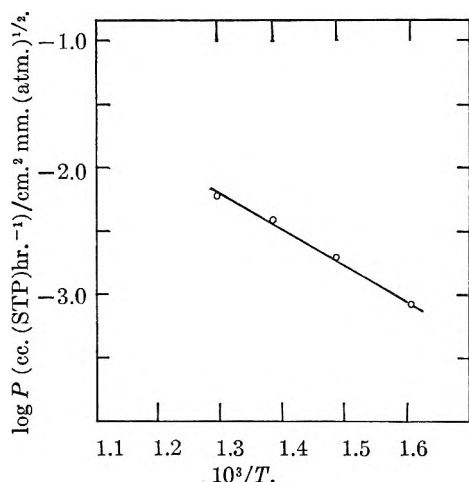
(6) V. Lombard, *Compt. rend.*, **177**, 116 (1923).

(7) G. Lewkonja and W. Baukloh, *Z. Metallik.*, **25**, 309 (1933).

(8) S. Johnson, "Permeability of Inconel to Hydrogen," private communication.

TABLE II  
 SUMMARY OF RESULTS OF THE PERMEABILITY OF COPPER TO HYDROGEN

T, °C.	P, atm.	Rate, cm. <sup>3</sup> hr. <sup>-1</sup>	Membrane I 0.0656" thick 0.9993" diameter		Rate, cm. <sup>3</sup> hr. <sup>-1</sup>	Membrane II 0.1284" thick 1.0000" diameter	
			Specific rate Cm. <sup>3</sup> (0°, 1 atm.) hr. <sup>-1</sup> Cm. <sup>2</sup> mm. <sup>-1</sup>	Permeability Cm. <sup>3</sup> (0°, 1 atm.) hr. <sup>-1</sup> Cm. <sup>2</sup> mm. <sup>-1</sup> (atm.) <sup>1/2</sup>		Specific rate Cm. <sup>3</sup> (0°, 1 atm.) hr. <sup>-1</sup> Cm. <sup>2</sup> mm. <sup>-1</sup>	Permeability Cm. <sup>3</sup> (0°, 1 atm.) hr. <sup>-1</sup> Cm. <sup>2</sup> mm. <sup>-1</sup> (atm.) <sup>1/2</sup>
350	1.5	0.00308	0.00101	0.00083	0.00159	0.00101	0.00083
350	2.0	.00365	.00116	.00082	.00183	.00118	.00082
400	1.5	.00715	.00234	.00191	.00366	.00235	.00192
400	2.0	.00826	.00270	.00191	.00420	.00269	.00191
450	1.5	.0138	.00452	.00368	.00705	.00452	.00368
450	2.0	.0160	.00522	.00368	.00812	.00519	.00367
500	1.5	.0217	.00707	.00577	.0110	.00705	.00575
500	2.0	.0251	.00817	.00577	.0127	.00811	.00573


 Fig. 2.—Temperature dependence of hydrogen permeating copper permeability vs. reciprocal temperature.  $P = 21.2e^{-12,600 \pm 110/RT}$ .

- $\alpha$  = quantity of gas permeating the barrier, cm.<sup>3</sup> (0°, 1 atm.)  
 $k$  = solubility constant of the gas-metal system  
 $D$  = diffusion constant  
 $A$  = area of the barrier, cm.<sup>2</sup>  
 $p_1$  = pressure on one face of the membrane, atm.  
 $p_2$  = pressure on the other face  
 $E_p$  = activation energy of permeation, cal./g.-atom  
 $L$  = thickness of the barrier, mm.  
 $t$  = time, hours

In this study, the downstream face was kept at vacuum so that  $p_2 = 0$ , essentially. The equation may be rearranged to give

$$\text{Specific rate} = Cp_1^{1/2}e^{-E_p/RT} \frac{\text{cm.}^3(0^\circ, 1 \text{ atm.})\text{hr.}^{-1}}{\text{cm.}^2 \text{ mm.}^{-1}} \quad (2)$$

where  $C = kD$ .

$$\text{Permeability} \equiv P = \frac{\text{Specific rate}}{p_1^{1/2}} = Ce^{-E_p/RT} \frac{\text{cm.}^3(0^\circ, 1 \text{ atm.})}{\text{cm.}^2 \text{ mm.}^{-1} (\text{atm.})^{1/2}} \quad (3)$$

Graphical representation of this equation is shown in Fig. 2. The pressure dependence is computed from the data of Table II at constant temperature. When the temperature is constant, equation 2 becomes

$$\text{Specific rate} = C_1 p_1^{1/2} \quad (4)$$

where  $C_1 = C \times e^{-E_p/RT}$

From equation 1, the rate of permeation should be inversely proportional to the thickness of the membrane. Equation 4 states that at constant temperature, the specific rate should be proportional to the square root of the pressure and that the permeability should be constant (equation 3). All these equations are confirmed by the data of Table II, indicating the valid assumption of a diffusion controlled permeation of hydrogen atoms through the metal barrier.

## POLAROGRAPHIC AND ACID PROPERTIES OF THORIUM PERCHLORATE IN ACETONITRILE

BY I. M. KOLTHOFF AND S. IKEDA

School of Chemistry, University of Minnesota, Minneapolis, Minnesota

Received December 23, 1960

Thorium perchlorate in acetonitrile (AN) behaves like a relatively strong dibasic acid with a first dissociation constant of about  $10^{-6}$  which is slightly less than that of sulfuric acid. The second dissociation constant is very much greater than that of sulfuric acid. Indication has been obtained that the  $\text{Th}(\text{ClO}_4)_2^{2+}$  ion is relatively stable in AN. The neutralization product formed upon titration with diphenylguanidine and the insoluble reaction product formed in electrolysis at  $-1.8$  volt (*vs.* s.c.e.) both contain about 2  $\text{ClO}_4^-$  per one thorium. The height of the polarographic wave of thorium perchlorate in AN is proportional to concentration. The reduction involves the evolution of hydrogen and not the formation of thorium amalgam. The value of the limiting current corresponds to the formation of a reaction product which contains about 2  $\text{ClO}_4^-$  per one thorium.

In the present paper the results are described of an extensive study of the polarography of thorium perchlorate in acetonitrile (AN). Well-defined

reduction waves have been observed. It was suspected that the cathodic current is not due to the formation of thorium amalgam, but to a reduction

of protons in perchloric acid formed by solvolysis or to a direct reduction of the proton in solvated thorium species to hydrogen. This was confirmed by electrolysis experiments at a stationary mercury cathode at potentials at which the polarographic limiting currents of thorium perchlorate were observed.

For a satisfactory interpretation of the polarographic behavior of thorium perchlorate in AN it was desirable to obtain information concerning its acid properties and solvolysis in AN and its degree of dissociation. Since such information is not available in the literature, an exploratory study has been made of the solvolysis and acid properties of solutions of the salt by determining the hydrogen ion concentration with a glass electrode and also spectrophotometrically with the aid of indicators. In addition the conductance of the salt has been determined over a wide range of concentrations. Titrations with diphenylguanidine as the base and the glass electrode as indicator electrode yielded information on the strength of the thorium salt as a mono- and dibasic acid.

### Experimental

**Materials Used. Acetonitrile.**—Technical grade methyl cyanide obtained from Eastman Kodak Co. was shaken with activated alumina followed by drying over anhydrous calcium chloride and magnesium sulfate and four distillations at  $81.0 \pm 0.5^\circ$  from phosphorus pentoxide in an all-glass still. The solvent was stored in a glass stoppered bottle in the dark and withdrawn—when needed—by means of an all-glass siphon provided with a drying tube containing anhydrous calcium chloride. The water content of the solvent was determined by the Karl Fischer method and found to be 0.0025%. The conductance was  $7 \times 10^{-7}$  ohm<sup>-1</sup> cm.<sup>-1</sup>.

Thorium perchlorate was prepared by a method used in this Laboratory by Willeboordse<sup>1</sup> from thorium nitrate by adding an excess of vacuum distilled 70% perchloric acid. The mixture was well stirred and the nitric acid and moisture removed in a dry nitrogen atmosphere. The salt was recrystallized from 0.2% aqueous perchloric acid and dried to constant weight in a vacuum oven at  $70^\circ$ . Decomposition occurred at higher temperatures. The thorium content of the salt was determined by precipitation as oxalate in 1 *N* hydrochloric acid solution and weighing as oxide<sup>2</sup> after ignition. Thorium was also determined by titration in aqueous medium with ethylenediamine tetraacetate using alizarine S as indicator.<sup>3</sup> Perchlorate was determined by the method recommended by Kurz, *et al.*,<sup>4</sup> by fusion of a mixture of the salt with sodium nitrite in a nickel crucible at  $550 \pm 50^\circ$  for 1.5 hours. The melt was dissolved in water, the excess nitrite removed by boiling with nitric acid and chloride titrated by the Volhard method. Perchlorate was also determined by an indirect alkalimetric method by adding in a volumetric flask to an aqueous solution of the salt an excess of standard 0.1 *N* sodium hydroxide. The mixture was shaken and diluted to the mark. The excess base was titrated in an aliquot of the filtrate with 0.1 *N* standard hydrochloric acid using methyl red as an indicator. The water content was determined by dissolving a weighed amount of the salt in anhydrous methanol and titrating with Karl Fischer reagent.<sup>5</sup> The average of 6 determinations yielded a water content of  $4.36 \pm 0.04\%$ . The results (average of 3 determinations for each method) of the thorium and perchlorate analyses were referred to the anhydrous salt Th(ClO<sub>4</sub>)<sub>4</sub>. Thorium content, calcd. 36.85%,

found 36.98% (gravimetric) and 37.27% (titrimetric). Perchlorate content, calcd. 63.15%, found 62.80% (Volhard) and 62.95% (alkalimetric). From the analysis it appears that the over-all composition of the salt is Th(ClO<sub>4</sub>)<sub>4</sub> · 1.7H<sub>2</sub>O. Solutions in AN up to a concentration of  $1 \times 10^{-2}$  *M* were clear and remained so on standing,  $2 \times 10^{-2}$  *M* solutions became turbid soon after the preparation as a result of solvolysis (*vide infra*).

**Anhydrous Perchloric Acid.**—Much of the work on the effect of perchloric acid on the polarography and on the hydrogen ion concentration of thorium perchlorate was carried out with a solution of the acid in anhydrous acetic acid<sup>6</sup> until it was discovered that acetic acid reacts with thorium perchlorate (*vide infra*) with the liberation of hydrogen ions. All the experiments were then repeated by synthesizing anhydrous perchloric acid solutions from barium perchlorate and 100% sulfuric acid prepared from oleum and 96% acid. The barium salt was recrystallized from water and dried to constant weight in a vacuum oven at  $100^\circ$ . In a 10-ml. volumetric flask of 0.42 g. of the barium salt was dissolved in AN, 0.0800 ml. of 100% sulfuric acid was added from an ultramicroburet, and the volume adjusted to 10 ml. After thorough mixing the mixture was centrifuged for 10 minutes at 3500 r.p.m. The clear supernatant liquid was 0.25 *M* in perchloric acid and 0.07% in water. The anhydrous solution of the acid was prepared on the day when it was used.

**Tetraethylammonium Perchlorate.**—This salt was prepared and purified as described in a previous paper.<sup>6</sup>

*o*-Nitroaniline and *p*-chloro-*o*-nitroaniline, used as indicator bases, were Eastman Kodak products and recrystallized from alcohol.

**Techniques. Polarographic cell.**—This cell was the same as that used by Knecht<sup>7</sup> for polarographic measurements in *N*-methylacetamide as a solvent. All polarograms were determined in the absence of oxygen by passing high-purity Linde nitrogen through and over the solution. Because of the relatively high vapor pressure of AN (80 mm. at  $25^\circ$ ) the gas was presaturated with AN by passing it through two wash-bottles containing the solvent. All experiments were carried out in a thermostat at  $25.00^\circ$ . A saturated calomel electrode (s.c.e.) in aqueous medium was used as reference electrode. Electrolytic contact with the solution in the cell was made in the way described by Coetzee.<sup>6</sup> The salt bridge was inserted into the polarographic cell only when the polarogram was run. The dropping mercury electrode had the following characteristics in 0.1 *M* tetraethylammonium perchlorate solution:  $m = 1.12$  mg./sec.;  $t = 5.6$  sec. at 0 volt *vs.* s.c.e., 4.6 sec. at  $-1.0$  volt and 3.5 sec. at  $-1.7$  volt. Potential values reported were corrected for the *iR* drop across the cell. The resistance of the cell containing 0.1 *M* tetraalkyl perchlorate was  $1505 \pm 50$  ohms as measured with an Industrial Instruments Inc. No. RC-IB conductance bridge. Reported values of limiting or diffusion currents have been corrected for the residual current.

The electrical conductivity of solutions of thorium perchlorate in AN at  $25 \pm 0.02^\circ$  was determined with the above conductance bridge. The constants of the two conductance cells used were 0.1957 and 0.03763, respectively.

The hydrogen ion concentration was determined spectrophotometrically with *o*-nitroaniline and *p*-chloro-*o*-nitroaniline as indicators by measuring the absorption of the alkaline forms in Pyrex cells with a path length of 1.8 cm. in a Beckman DU spectrophotometer at a wave length of 410  $\mu$  at  $25^\circ$ . The pH was also determined potentiometrically with a Beckman pH meter. The glass electrode was soaked in the solvent before use. A 0.1 *M* solution of sodium perchlorate in AN was used as a salt bridge to make contact with the saturated calomel electrode. Controlled potential electrolysis was carried out at a potential of  $-1.8$  to  $-1.85$  volt (*vs.* s.c.e.) in a nitrogen atmosphere in a cell containing 25 ml. of thorium perchlorate solution which was 0.1 *M* in tetraethylammonium perchlorate. A layer of mercury was used as the cathode. A glass rod with blades placed in the mercury served as a stirrer during electrolysis. The cell was provided with 2 glass tubes separated from the cell by sintered glass disks. One sidearm contained a platinum foil electrode as anode placed in the same solution as contained in the electrolysis cell. The other side tube also

(1) F. Willeboordse, Ph.D. Thesis, University of Amsterdam 1959, p. 157.

(2) W. F. Hillebrand and G. E. F. Lundell, "Applied Inorganic Analysis," 2nd ed., John Wiley and Sons, Inc., New York, N. Y., 1953.

(3) V. Suk and M. Malart, *Chemist Anal.*, **45**, 30 (1956).

(4) E. Kurz, G. Kober and M. Bier, *Anal. Chem.*, **30**, 1938 (1958).

(5) J. Mitchell, Jr., and D. M. Smith, "Aquometry," Interscience Publishers, Inc., New York, N. Y., 1948.

(6) See I. M. Kolthoff and J. F. Coetzee, *J. Am. Chem. Soc.*, **79**, 870, 1852, 6110 (1957).

(7) L. A. Knecht, Ph.D. Thesis, University of Minnesota, 1958.

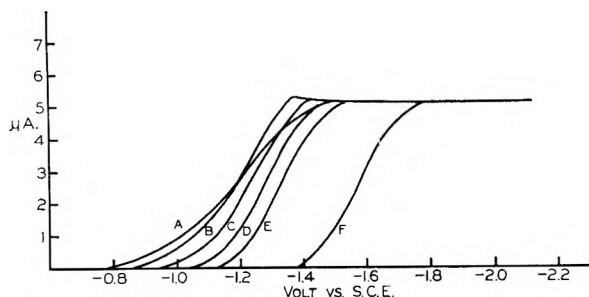


Fig. 1.—Effect of water on polarogram of  $0.5 \times 10^{-3} M$  thorium perchlorate in  $0.1 M$  tetraethylammonium perchlorate. Concentration of water: A, 0.005%; B, 1%; C, 5%; D, 10%; E, 20%; F, 50%.

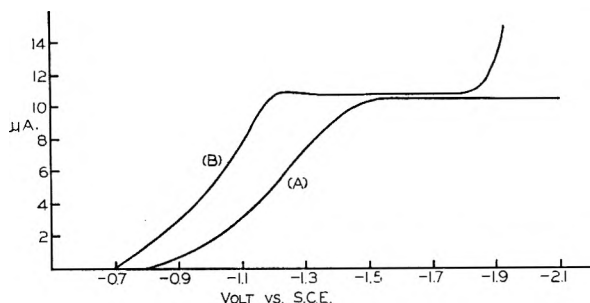


Fig. 2.—Effect of acetic acid on polarogram of  $1 \times 10^{-3} M$  thorium perchlorate. A, no acetic acid added; B, with  $1.0 \times 10^{-2} M$  acetic acid.

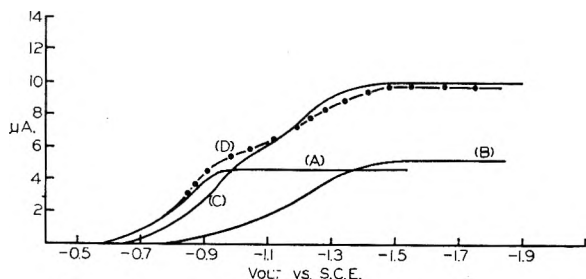


Fig. 3.—Polarograms of mixtures of perchloric acid and thorium perchlorate. A,  $0.001 M$   $HClO_4$ ; B,  $0.0005 M$   $Th(ClO_4)_4$ ; C, mixture of  $0.001 M$   $HClO_4$  and  $0.0005 M$   $Th(ClO_4)_4$ ; D, summation of curves A and B.

contained the same solution as contained in the cell; into it was placed a saturated potassium chloride salt bridge in agar gel to make contact with a saturated calomel electrode. The level of the solutions in the side tubes was lower than in the cell to prevent entering of solution from the side tubes into the cell during electrolysis. The salt bridge was placed in the side tube only when the potential of the mercury pool was checked during the electrolysis. The potential of the mercury could be kept constant during the electrolysis with the aid of a Fisher controlled potential electroanalyzer. Nitrogen was passed through during electrolysis. The bottom of the cell was provided with a three-way stopcock which allowed collection of the mercury in a nitrogen atmosphere after the electrolysis and also of the aqueous layer in the cell.

### Experimental Results

**Polarography of Thorium Perchlorate.**—Unless otherwise stated all figures refer to freshly prepared solutions,  $0.1 M$  tetraethylammonium perchlorate being the supporting electrolyte. The residual current  $i_r$  varied between  $-0.2 \mu a.$  at  $+0.4$  volt (*vs. s.c.e.*) to  $+0.5 \mu a.$  at  $-2.8$  volts, indicating high purity of solvent and supporting electrolyte. Reported diffusion currents have been corrected for

$i_r$ . Thorium perchlorate yields a reduction wave with a well-defined limiting current, which was found proportional to the thorium concentration (see Table I). At concentrations greater than  $1.5 \times 10^{-3} M$  thorium perchlorate irregular results were obtained and the polarogram had an appearance of three waves, the last one with a slight maximum at  $-1.85$  volt, the diffusion current becoming constant at  $-2.15$  volts. Apparently these irregularities are caused by the separation of a slightly soluble basic salt interfering with the evolution of hydrogen at the electrode<sup>6</sup> (*vide infra*). The waves are drawn out indicating irreversible reduction. The half wave potential at about  $-1.2$  volt was found to shift slightly to more negative

TABLE I  
POLAROGRAPHY OF THORIUM PERCHLORATE IN PURE AN

Concn. $Th(ClO_4)_4$ , $M \times 10^3$	$E_{1/2}$ ( <i>vs. s.c.e.</i> )	$i_d$ , $\mu a.$	$I_d$
0.2	-1.18	2.2	8.42
0.5	-1.18	5.3	8.16
1.0	-1.20	10.4	8.02
1.5	-1.22	15.6	7.96

TABLE II  
CONDUCTANCE OF THORIUM PERCHLORATE

Normality <sup>a</sup>	$\Lambda_f^b$	$\Lambda_a^c$
$4 \times 10^{-2}$	37.75	38.25
$2 \times 10^{-2}$	44.70	
$4 \times 10^{-3}$	61.50	63.50
$2 \times 10^{-3}$	71.50	
$4 \times 10^{-4}$	100.00	104.5

<sup>a</sup>  $1 M = 4 N$ . <sup>b</sup> Subscript f refers to fresh solutions. <sup>c</sup> Subscript a refers to solutions aged for a week.

potentials with increasing concentration of thorium salt which is probably caused by the water content of the salt. Addition of water made the waves less drawn out and displaced them to more negative potentials (Fig. 1). It is remarkable that even in the presence of 50 vol./vol. % of water the limiting current remained unchanged. Irregularities in the polarogram of  $2 \times 10^{-3} M$  thorium perchlorate disappeared in the presence of 1% water, and the limiting current was twice the value found in  $1 \times 10^{-3} M$  solution. Aging of the thorium perchlorate solution for two days hardly affected the shape of the polarograms and the limiting currents remained unchanged. In a study of the effect of perchloric acid on the polarograms a solution of the acid in acetic acid was used first. Only one wave was observed in the mixtures, the wave observed in thorium perchlorate solution alone being displaced to more positive potentials. This effect must be attributed to an interaction between thorium perchlorate and acetic acid with the formation of perchloric acid. As is evident from Fig. 2, addition of acetic acid alone to the thorium solution displaces the wave to more positive potentials, while the limiting current increases only a few per cent. In separate experiments it was shown that addition of acetic acid greatly increases the hydrogen concentration of thorium perchlorate solutions. In order to eliminate the acetic acid effect solutions of perchloric acid prepared by metathesis from barium perchlorate and sulfuric acid were used. At



the time when the acid was added to the thorium perchlorate the solution of the acid had aged for several hours, which may account for the fact that the half wave potential was  $-0.8$  volt, while Coetzee<sup>6</sup> observed a value of  $-0.7$  volt by addition of solutions of perchloric acid in acetic acid to acetonitrile and measuring without aging. A double wave was observed in mixtures of fresh perchloric acid and thorium perchlorate, the first one corresponding roughly to that of perchloric acid and the second to that of the thorium perchlorate. In Fig. 3 the wave of the mixture is compared with that obtained by summation of the individual waves. In mixtures of perchloric acid and thorium perchlorate of varying composition and ratio the total limiting current was always found equal to the sum of the individual currents within the experimental error.

**Controlled Potential Electrolysis.**—During the electrolysis of 25 ml. of  $1 \times 10^{-2} M$  thorium perchlorate at 0–1.8 volt (*vs.* s.c.e.) at an average current of about 3.8 milliamperes the solution became turbid, while tiny gas bubbles were observed to be evolved from the surface of the mercury when the gas stream of nitrogen was stopped. After about 5 hours of electrolysis the mercury was collected while current was passing, washed with AN in a nitrogen atmosphere and used in the dropping mercury electrode. The residual currents obtained in 0.1 *M* tetraalkylammonium perchlorate and in 0.1 *M* perchloric acid were the same as those observed with pure mercury. If thorium amalgam had been formed during the electrolysis an anodic wave would have been observed. The bulk of the mercury was evaporated *in vacuo*; a trace of a greyish residue remained which was dissolved in aqua regia. After removing the acid by evaporation the residue gave a positive test for thorium with alizarin S.<sup>8</sup> However, the amount was only of the order of 0.02 mg. If the current passed through during electrolysis would have been 100% efficient in the reduction of thorium(IV) to the amalgam, about 40 mg. of thorium should have been formed.

The turbid aqueous layer was collected and filtered. The precipitate was washed with acetonitrile, dried in a vacuum desiccator, weighed, and analyzed for thorium by titration with EDTA<sup>3</sup> and perchlorate.<sup>4</sup> The *pH* of the filtrate, in which chloride was found to be absent, was determined with the glass electrode and found to be 6.7 *pH* units greater than the *pH* of the solution before electrolysis. The thorium content of the filtrate was determined titrimetrically. Three electrolysis experiments were carried out at the end of which only 2 to 3% of the thorium was found in the filtrate. The molar ratio of perchlorate to thorium in the precipitates obtained in three electrolysis experiments was 1.92, 1.86 and 1.80, respectively.

**Conductance of Thorium Perchlorate.**—Results obtained at  $25.00 \pm 0.02^\circ$  are reported in Table II. It is seen that the equivalent conductance increases slightly after aging for one week.

#### Hydrogen Ion Concentration. Glass Electrode.

(8) D. V. N. Sarma and B. H. S. V. Raghana Rao, *Anal. Chim. Acta*, **13**, 142 (1955).

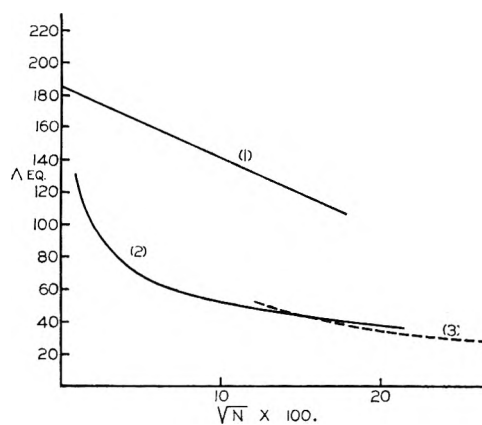


Fig. 4.—Equivalent conductance *vs.* square root of normality. 1, perchloric acid<sup>6</sup>; 2, thorium perchlorate; 3, aluminum perchlorate.<sup>12</sup>

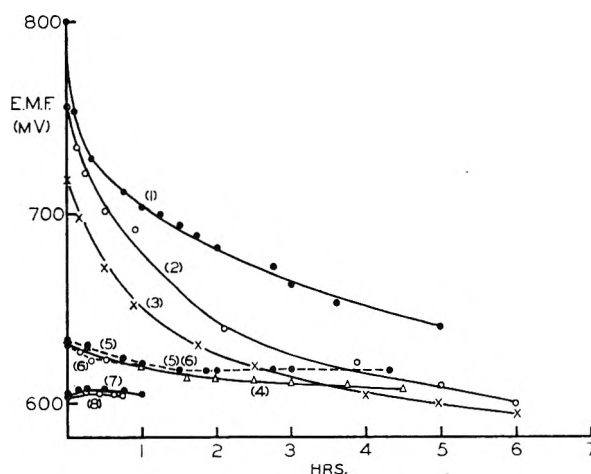


Fig. 5.—Potential-time curves at glass electrode in methyl cyanide 0.01 *M*  $HClO_4$  solution: 1, fresh; 2, aged 24 hr.; 3, aged 38 hr.; 4, aged 1 week. 0.01 *M*  $Th(ClO_4)_4$  solution: 5, fresh; 6, aged for a week; 0.001 *M*  $Th(ClO_4)_4$  solution: 7, fresh; 8, aged for a week.

—Potentiometric measurements gave only approximate results. It has been found in this Laboratory by Chantooni<sup>9</sup> that the *pH* of a fresh perchloric acid solution markedly increases on aging because of formation of a basic species derived from the solvent. This effect probably accounts for the fact that the initial value of the potential measured in fresh 0.01 *M* perchloric acid decreases with increasing age of the solution. Also, the potential in fresh perchloric acid solution rapidly decreases with time of contact with the glass electrode, the rate of decrease becoming less with increasing age of the perchloric acid solution, as illustrated in Fig. 5. Hardly any effect of aging was found in thorium perchlorate solutions (Fig. 4) and the potential soon attained a constant value. The rapid change of potential *versus* time in fresh perchloric acid solutions made such solutions poor standards for references purposes. Spectrophotometrically the *pH* of fresh perchloric acid solutions could be determined accurately. In order to see whether the *pH* values found potentiometrically and spectrophotometrically were of the same order of magnitude e.m.f. measurements were made in per-

(9) M. Chantooni, Jr., Ph.D. Thesis, University of Minnesota, 1960

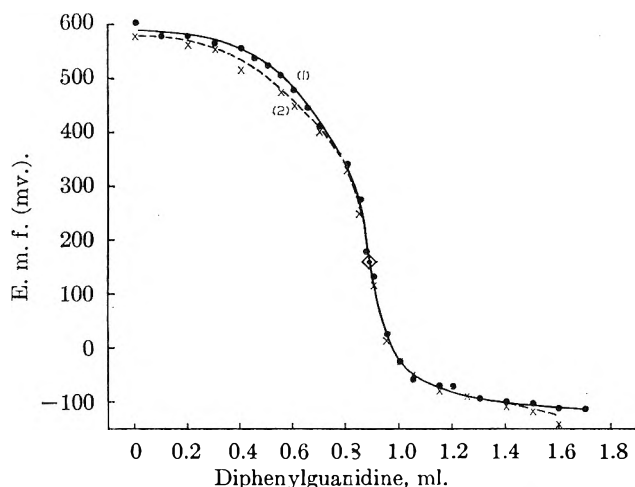


Fig. 6.—Potentiometric titration of 5 ml. of 0.001  $M$   $\text{Th}(\text{ClO}_4)_4$  with 0.01  $M$  diphenylguanidine. ( $\diamond$  denotes end-point) 1, no salt added; 2, in 0.1  $M$  tetraethylammonium perchlorate.

chloric acid solutions of concentrations between  $10^{-2}$  and  $5 \times 10^{-4} M$  and in 0.01 and 0.001  $M$  thorium perchlorate solutions. The readings were taken 5 minutes after placing the glass electrode in the solutions. In 0.01  $M$  perchloric acid the e.m.f. was in three independent measurements 0.787; 0.798, and 0.807 volt; average 0.796; in 0.001  $M$  acid 0.705, 0.726 and 0.714; average 0.718; and in 0.0005  $M$  acid 0.690, 0.702 and 0.694; average 0.695. In 0.01  $M$  thorium perchlorate the e.m.f. was 0.624, 0.628, 0.630 volt; average 0.628; in 0.001  $M$  thorium perchlorate 0.598, 0.602, 0.606; average 0.602, corresponding to hydrogen ion concentrations of  $7 \times 10^{-5}$  and  $3 \times 10^{-5}$ , respectively.

TABLE III

$K_{\text{HI}^+}$  AND  $K_{\text{H}_3\text{O}^+}$  IN 0.001  $M$   $\text{HClO}_4$ - $\text{H}_2\text{O}$  MIXTURES AT 25°  
 $p$ -chloro- $o$ -nitroaniline concn.  $8.2 \times 10^{-6}$ ;  $K_{\text{HI}^+} = 1.8 \times 10^{-4}$

$C_{\text{H}_2\text{O}}$ $\times 10^2$ , $M$	$R$	$[\text{HI}^+]$ $\times 10^5$ , $M$	$[\text{H}^+]$ $\times 10^5$ , $M$	$[\text{H}_3\text{O}^+]$ $\times 10^4$ , $M$	$K_{\text{H}_3\text{O}^+}$ $\times 10^3$
0.13 <sup>a</sup>	4.52	6.7	8.13	1.2	..
2.33	1.02	4.1	1.83	7.76	6.5
2.88	0.82	3.7	1.48	8.15	6.4
3.43	.62	3.1	1.12	8.57	5.5
4.53	.42	2.4	0.76	9.00	4.9
5.63	.32	2.0	.58	9.22	4.7
6.73	.24	1.5	.43	9.42	4.1
8.93	.17	1.2	.30	9.58	3.8
10.03	.13	0.9	.23	9.68	3.3

Av. value of  $K_{\text{H}_3\text{O}^+} = 5 \times 10^{-3}$

<sup>a</sup> This is water content of solvent.

**Spectrophotometric Method.**— $o$ -Nitroaniline was used as indicator for the determination of the  $p\text{H}$  of  $2 \times 10^{-4}$  and  $5 \times 10^{-4} M$  solutions of thorium perchlorate and  $p$ -chloro- $o$ -aniline for  $1 \times 10^{-3}$ ,  $2 \times 10^{-3}$  and  $1 \times 10^{-2} M$  solutions. The absorbance and molar absorption coefficients of the alkaline forms of the indicators were determined at 410  $m\mu$ . The absorbancy index of the  $o$ -nitroaniline was  $2.76 \times 10^4$  and that of the  $p$ -chloro- $o$ -nitroaniline indicator was  $2.71 \times 10^4$ . The conventional relation was used in the calculation

$$[\text{H}^+] = [\text{HI}^+]/[\text{I}] \times K_{\text{HI}^+} = RK_{\text{HI}^+} \quad (1)$$

of the solvated hydrogen ion concentration from the measured absorbancy, which gave the concentration of I. Since the total concentration  $[\text{I}] + [\text{HI}^+]$  of the indicator was known,  $[\text{HI}^+]$  and also the ratio  $R$  of  $[\text{HI}^+]/[\text{I}]$  became known. In order to calculate the hydrogen ion concentration in thorium perchlorate solutions from data obtained with indicators it was necessary to first determine  $K_{\text{HI}^+}$  and also the effect of water on the indicator equilibrium. It appeared that water acts as a fairly strong base in AN and the value of

$$K_{\text{H}_3\text{O}^+} = [\text{H}^+][\text{H}_2\text{O}]/[\text{H}_3\text{O}^+] \quad (2)$$

was determined in mixtures of fresh perchloric acid and water in AN with  $p$ -chloro- $o$ -nitroaniline as indicator. In these experiments the stock solution of perchloric acid in acetic acid was used. The water content of the solvent was only  $1.3 \times 10^{-3} \pm 0.1 \times 10^{-3} M$  but was taken into account in the calculation of  $K_{\text{HI}^+}$  and  $K_{\text{H}_3\text{O}^+}$ . Perchloric acid is completely dissociated in AN<sup>6</sup>; hence

$$C_{\text{HClO}_4} = [\text{H}^+] + [\text{H}_3\text{O}^+] + [\text{HI}^+] \quad (3)$$

and

$$C_{\text{H}_2\text{O}} = [\text{H}_3\text{O}^+] + [\text{H}_2\text{O}] \quad (4)$$

in which  $C_{\text{HClO}_4}$  and  $C_{\text{H}_2\text{O}}$  denote the analytical concentrations of perchloric acid and water, respectively. An approximate value of  $K_{\text{HI}^+}$  was calculated from  $R$  found in solutions to which no water had been added. Then approximate values of  $K_{\text{H}_3\text{O}^+}$  were calculated in the mixtures containing water. Using the average of the approximate values of  $K_{\text{H}_3\text{O}^+}$  the calculations were repeated for the solutions to which no water had been added. This was repeated until  $K_{\text{HI}^+}$  remained constant. Results are given in Tables III and IV. Concentrations instead of activities were used in the calculation of the constants. This seems justified as far as  $K_{\text{HI}^+}$  is concerned, since the activity coefficients of  $\text{H}^+$  and  $\text{HI}^+$  may be considered to be the same in dilute solutions. A definite decrease of  $K_{\text{H}_3\text{O}^+}$  with increasing water content was found which may be due to an increasing activity coefficient of water with an increase in its concentration. An average value of  $K_{\text{H}_3\text{O}^+}$  of  $4.5 \times 10^{-3}$  is obtained from Tables III and IV, giving  $K_{\text{HI}^+} = 1.8 \times 10^{-4}$ . The average value of  $K_{\text{H}_3\text{O}^+}$  was used in the calculation of  $K_{\text{HI}^+}$  of  $o$ -nitroaniline from spectrophotometric measurements in very dilute perchloric acid solutions. Based on the measurements by Chantooni<sup>9</sup> in very dilute perchloric acid solutions a value of  $1.4 \times 10^{-3}$  was found. The results of the determination of hydrogen ion concentration in freshly prepared thorium perchlorate solutions are reported in Table V.

**Potentiometric Titration of Thorium Perchlorate with Diphenylguanidine (DG).**—The titrations were carried out using the glass electrode as indicator electrode. Five ml. of 0.001  $M$  thorium perchlorate was titrated with 0.01  $M$  DG without added electrolyte and also in the presence of 0.1  $M$  tetraethylammonium perchlorate. The results are reproduced in Fig. 6. Both in the presence and

TABLE IV

 $K_{HI^+}$  AND  $K_{H_3O^+}$  IN 0.005 M  $HClO_4$ - $H_2O$  MIXTURES AT 25°
Indicator concn.  $8.2 \times 10^{-5}$  M;  $K_{HI^+} = 1.8 \times 10^{-4}$ 

$\frac{CH_2O}{M} \times 10^2$	R	$[HI^+] \times 10^5$	$[H^+] \times 10^5$	$[H_3O^+] \times 10^5$	$K_{H_3O^+} \times 10^5$
0.13	23.8	7.9	4.3	0.69	
0.68	14.2	7.7	2.5	2.42	4.6
1.23	10.0	7.5	1.8	3.12	5.5
1.78	66.2	6.9	1.1	3.83	4.2
2.33	4.3	6.7	0.77	4.16	3.9
2.88	3.2	6.3	.58	4.36	3.6
3.43	2.3	5.7	.41	4.53	3.1
3.98	1.8	5.3	.33	4.62	2.9
4.53	1.5	4.9	.27	4.68	2.8
5.63	1.1	4.2	.20	4.76	(2.6)

Av. value of  $K_{H_3O^+} = 4 \times 10^{-3}$ 

TABLE V

HYDROGEN ION CONCENTRATION IN THORIUM PERCHLORATE SOLUTIONS

Concn. of *o*-nitroaniline (*o*-NA)  $5.6 \times 10^{-5}$  M, of *p*-chloro-*o*-nitroaniline (*p*-Cl-*o*-NA)  $1.25 \times 10^{-4}$  M

Concn. thorium perchlorate, M	Indicator	R	$[H^+] \times 10^5$	$K_{Th(IV)} \times 10^5$
$2 \times 10^{-4}$	<i>o</i> -NA	0.42	0.6	1.0
$5 \times 10^{-4}$	<i>o</i> -NA	.86	1.2	1.2
$1 \times 10^{-3}$	<i>p</i> -Cl- <i>o</i> -NA	.16	2.8	1.9
$2 \times 10^{-3}$	<i>p</i> -Cl- <i>o</i> -NA	.25	4.4	2.7
$10 \times 10^{-3}$	<i>p</i> -Cl- <i>o</i> -NA	.49	8.8	4.2

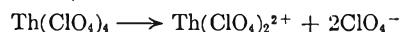
absence of supporting electrolyte the end-point where the second derivative of  $\Delta E/\Delta C$  was zero was obtained after addition of 0.88 ml. of 0.01 M DG, corresponding to a composition at the end-point of  $Th[(ClO_4)_{2.2}S_{1.8}]$ , in which S may be  $OH^-$  and (or)  $CH_2CN^-$ . In the absence of the tetraalkyl salt the solution remained clear, but in the presence of the salt precipitation occurred near the end-point.

### Discussion

The estimated potential in aqueous medium of the system  $Th^{4+} + 4e \rightleftharpoons Th$  is  $-1.90$  volt vs. NHE.<sup>10</sup> This very negative potential combined with the extensive hydrolysis of thorium salts is responsible for the fact that no reduction wave to thorium amalgam is observed at the d.m.e. In unbuffered aqueous solutions Masek<sup>11</sup> reported a drawn out wave related to various steps in the hydrolysis. Although the potential of the thorium system in AN is expected to be less negative,<sup>6</sup> and the solvolysis of the thorium salt is less pronounced than in water, the polarographic waves of thorium perchlorate must be attributed to hydrogen evolution. This conclusion is substantiated by electrolysis experiments at controlled potential in which less than 0.5% of the current passed through the thorium perchlorate solution produced thorium amalgam. No definite statement can be made which thorium species is(are) responsible for the occurrence of the hydrogen wave in AN.

In Fig. 4 are plotted equivalent conductances versus the square root of normalities of perchloric

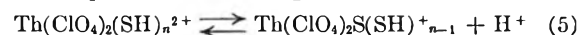
acid,<sup>6</sup> aluminum perchlorate,<sup>12</sup> and thorium perchlorate. Only perchloric acid behaves like a strong electrolyte and the two salts as reasonably strong electrolytes of about equal strength. The equivalent conductance of perchloric acid at infinite dilution is  $184.5^6$  at 25° in AN and we may expect a value of the order of 200 for thorium perchlorate. In 0.0001 M solution (Table II) the equivalent conductance is only 100 and it decreases continuously with increasing concentration. Thus, in not too dilute solutions incomplete dissociation may be postulated, as



in which  $Th(ClO_4)_2^{2+}$  represents a solvated ion. There are several experimental observations which indicate that the  $Th(ClO_4)_2^{2+}$  is a relatively stable ion in AN.

In the electrolysis experiments at controlled potential the precipitate formed contained 1.9 moles of perchlorate per mole of thorium, corresponding to  $Th(ClO_4)_{1.9}S_{2.1}$ , in which S is the lyate ion of AN and(or)  $OH^-$ . Also, in the titration of thorium perchlorate with diphenylguanidine the end-point was found to correspond to the formation of  $Th(ClO_4)_{2.2}S_{1.8}$ .

Although the glass electrode was not relied upon to give exact values of the pH, it was gratifying to find a close agreement between the hydrogen ion concentration in 0.01 and 0.001 M thorium perchlorate obtained with the glass electrode ( $7 \times 10^{-5}$  and  $3 \times 10^{-5}$ , resp.) and the indicator method ( $8.8 \times 10^{-5}$  and  $2.8 \times 10^{-5}$ , resp.). From this agreement it may be concluded that there is no Lewis acid-base reaction between the indicator and the thorium species and that the indicator method is reliable for the determination of the hydrogen ion concentration. An effort has been made to calculate the acid dissociation constant of the thorium species considering it as a monobasic acid



in which SH denotes solvent or(and) water and  $H^+$  the solvated proton. In spite of many efforts

$K_{Th(IV)} = [Th(ClO_4)_2S(SH)^{+_{n-1}}][H^+]/[Th(ClO_4)_2(SH)_n^{2+}]$  it has not been possible to prepare anhydrous thorium perchlorate. Decomposition occurred when the salt containing 1.7 moles of water was dried *in vacuo* at 70° for longer periods of time. In the calculation of  $K_{Th(IV)}$  from the data in Table V the water content of 1.7 moles per mole of thorium perchlorate had to be taken into account. The concentration of  $Th(ClO_4)_2S(SH)^{+_{n-1}}$  is equal to the sum of the concentrations of the hydrogen ion in its various forms, *i.e.*

$$[Th(ClO_4)_2S(SH)^{+_{n-1}}] = [H^+] + [H_3O^+] + [HI^+]$$

$[H^+]$  and  $[HI^+]$  were obtained directly from the measurement and  $[H_3O^+]$  was calculated from equation 2. Calculated values of  $K_{Th(IV)}$  are given in the last column of Table V. The constant was found to increase regularly from  $1.0 \times 10^{-6}$  in  $2 \times 10^{-4}$  M thorium perchlorate to  $4.2 \times 10^{-6}$  in 0.01 M solution. This increase may be due to the fact that concentrations instead of activities

(10) W. M. Latimer, "Oxidation Potentials," 2nd ed., Prentice-Hall, Inc., Englewood Cliffs, N. J., 1952, p. 297.

(11) J. Masek, *Coll. Czechoslovak Chem. Comms.*, **24**, 159 (1959).

(12) F. G. Hackenberg and H. Ulich, *Z. anorg. allgem. Chem.*, **243**, 99 (1939).

were used in the calculations and also to association of part of the water with the thorium. The dissociation constant is of the same order of magnitude as  $K_1$  of sulfuric acid for which Chantooni<sup>9</sup> found a value of  $5.5 \times 10^{-5}$ . From the titration data in Fig. 6 it can be inferred that the second dissociation constant of  $\text{Th}(\text{ClO}_4)_2\text{S}(\text{SH})_{n-1}$  is also relatively large. The potential at the mid-point in the titration of the first hydrogen corresponds to a  $K$  of the order of  $10^{-6}$  and of the second hydrogen of about  $10^{-7}$ .

It is of interest to note that the half wave potential of thorium perchlorate (in 0.1  $M$  tetraalkyl perchlorate) of  $-1.26$  volt is equal to that of sulfuric acid.<sup>6</sup> The effect of water on the half wave potential of the thorium solution was found to be similar to that in sulfuric acid. The height of the wave was found proportional to the thorium concentration in the range between  $2 \times 10^{-4}$  and  $2 \times 10^{-3} M$ . The diffusion current was 2-3 times greater than that of an equimolar solution of perchloric acid. Although the diffusion coefficient and even the kind of the reduced species is not known, it is reasonable to state that the approxi-

mate over-all composition of the reduction product corresponds to  $\text{Th}(\text{ClO}_4)_2\text{S}_2$ , which is similar to that of the insoluble reduction product formed in the electrolysis at controlled potential and to that at the end-point in the titration of thorium perchlorate with diphenylguanidine. Although the limiting current appears to be diffusion controlled it is possible that the current is kinetic in nature and attributable to a reduction of solvated hydrogen ions produced in the reaction in equation 3. However, a direct reduction of the proton in  $\text{Th}(\text{ClO}_4)_2(\text{SH})_{n-1}^{2+}$  or/and another thorium species is not excluded. A mixture of perchloric acid and thorium perchlorate yields a polarogram (Fig. 3) corresponding to that of a mixture of a strong and a weaker acid, like perchloric and sulfuric acid.

**Acknowledgment.**—This research was supported by the United States Air Force through the Air Force Office of Scientific Research of the Air Research and Development Command, under Contract No. AF49(638)519. Reproduction in whole or in part is permitted for any purpose of the United States Government.

## THE HEATS OF COMBUSTION AND FORMATION OF THIAADAMANTANE

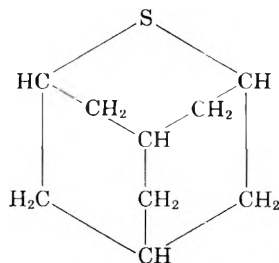
By J. L. LACINA, W. D. GOOD AND J. P. McCULLOUGH

Contribution No. 103 from the Thermodynamics Laboratory, Petroleum Research Center, Bureau of Mines, U. S. Department of the Interior, Bartlesville, Oklahoma

Received January 7, 1961

The heat of combustion of thiaadamantane, a saturated organic sulfur compound with four fused, six-membered rings forming a cage-like molecule, was measured by rotating-bomb calorimetry. An experimental technique was developed for confining samples of volatile solids in sealed polyester envelopes for precision combustion calorimetry. The heat of formation of thiaadamantane in the solid state at  $298.15^\circ\text{K}$ . is  $-34.29$  kcal. mole<sup>-1</sup>, referred to graphite, hydrogen gas and rhombic sulfur.

The heat of combustion of thiaadamantane was determined in this Laboratory as part of a continuing program of thermodynamic studies of organic sulfur compounds important in petroleum technology. The molecule of this unusual saturated organic compound consists of four six-membered rings fused into a cage-like structure.



The hydrocarbon analog is adamantane (diamantane, tricyclo[3.3.1.1.3,7]decane).

### Experimental

**Material.**—The sample of thiaadamantane was supplied by the British Petroleum Company, Limited, through the courtesy of Dr. R. A. Dean and was used as received. It had been purified by crystallization from benzene and cyclohexane followed by sublimation. The compound could not be purified by zone refining since decomposition occurs at the

melting point. Repeated crystallization caused no change in the infrared spectrum, and no impurity peaks could be detected by gas-liquid chromatography. In the combustion calorimetry reported here, recovery of sulfuric acid in the combustion products was  $99.94 \pm 0.04\%$  of that expected from the stoichiometry of the combustion reaction.

**Apparatus and Procedures.**—The rotating-bomb calorimeter, laboratory designation BMR-III, is similar to a calorimeter previously described.<sup>1</sup> The platinum-lined bomb Pt-3b, internal volume 0.350 l., has been described.<sup>2</sup> The material, too volatile to be weighed without confinement, was pressed into pellets, which were sealed in envelopes of polyester film.<sup>2</sup> Other experimental details for the precision combustion calorimetry of organic sulfur compounds have been described.<sup>3</sup>

**Units of Measurements and Auxiliary Quantities.**—All data reported are based on the 1951 International Atomic Weights<sup>4a</sup> and fundamental constants<sup>4b</sup> and the definitions:  $0^\circ\text{C} = 273.15^\circ\text{K}$ .; 1 cal. = 4.184 (exactly) joules. The laboratory standard weights had been calibrated at the National Bureau of Standards.

For use in reducing weights in air to *in vacuo*, in converting the energy of the actual bomb process to the isothermal

(1) W. D. Good, D. W. Scott and Guy Waddington, *J. Phys. Chem.*, **60**, 1080 (1956).

(2) W. D. Good, D. R. Douslin, D. W. Scott, Ann George, J. L. Lacina, J. P. Dawson and G. Waddington, *ibid.*, **63**, 1133 (1959).

(3) W. N. Hubbard, C. Katz and G. Waddington, *ibid.*, **58**, 142 (1954).

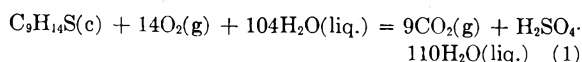
(4) (a) E. Wichers, *J. Am. Chem. Soc.*, **74**, 2447 (1952); (b) F. D. Rossini, F. T. Gucker, Jr., H. L. Johnston, L. Pauling and G. W. Vinal, *ibid.*, **74**, 2699 (1952).

process, and in reducing to standard states,<sup>5</sup> the following values, all for 25°, were used: density,  $\rho = 1.179 \text{ g. ml.}^{-1}$ ; specific heat,  $c_p = 0.33 \text{ cal. deg.}^{-1} \text{ g.}^{-1}$ ; and  $(\partial E/\partial P)_T = -0.0028 \text{ cal. atm.}^{-1} \text{ g.}^{-1}$ .

**Calibration.**—The energy equivalent of the calorimetric system,  $\varepsilon(\text{Calor.})$ , was determined by combustion of benzoic acid (National Bureau of Standards standard sample 39h which was certified to evolve  $26,434 \pm 3 \text{ j.g.}^{-1}$  when burned under specified conditions). Eight calibration experiments gave the value,  $\varepsilon(\text{Calor.}) = 4025.54 \pm 0.19 \text{ cal. deg.}^{-1}$  (mean and standard deviation).

### Results

**Calorimetric Results.**—Eight combustion experiments were performed with thiaadamantane. It is impractical to report all experiments in detail, but data for a single experiment selected as typical are summarized in Table I. All data reduction was done by high speed digital computer. The value of  $\Delta Ec^\circ/M$  for thiaadamantane in Table I refers to reaction 1.



The results of six combustion experiments follow.

$$\Delta Ec^\circ/M: \quad -9278.55, \quad -9276.43, \quad -9278.41, \quad -9277.52, \\ -9277.94, \quad -9278.40 \text{ cal. g.}^{-1}$$

$$\text{Mean:} \quad -9277.87 \text{ cal. g.}^{-1}$$

$$\text{Std. dev. of the mean:} \quad \pm 0.30 \text{ cal. g.}^{-1}$$

**Derived Results.**—The molal values of  $\Delta Ec^\circ$ , the standard change in internal energy, and  $\Delta Hc^\circ$ , the standard heat of combustion, (reaction 1) were computed to be  $-1431.28 \pm 0.23^6$  and  $-1434.24 \pm 0.23^6 \text{ kcal. mole}^{-1}$ , respectively. To calculate

(5) W. N. Hubbard, D. W. Scott and G. Waddington, "Experimental Thermochemistry," F. D. Rossini, Editor, Interscience Publishers, Inc., New York, N. Y., 1956, Chapter 5, pp. 75-128.

(6) Uncertainties are the "uncertainty interval" equal to twice the final over-all standard deviation of the mean (F. D. Rossini, ref. 5, p. 319).

TABLE I<sup>a</sup>

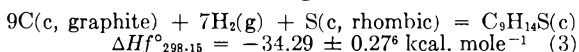
SUMMARY OF TYPICAL COMBUSTION EXPERIMENT

$m'$ (Thiaadamantane), g.	0.82357
$m''$ (polyester), g. (at % rel. hum.)	0.07029(59)
$\Delta t_c = t_f - t_i - \Delta t_{\text{corr.}}$ , deg.	1.99137
$\varepsilon(\text{Calor.})(-\Delta t_c)$ , cal.	-7616.34
$\varepsilon(\text{Cont.})(-\Delta t_c)^b$ , cal.	-27.37
$\Delta E_{\text{ign.}}$ , cal.	1.30
$\Delta E_{\text{dec.}}(\text{HNO}_3 + \text{HNO}_2)$ , cal.	7.00
$\Delta E$ , cor. to st. states, <sup>c</sup> cal.	5.28
$-m''' \Delta Ec^\circ/M$ (fuse), cal.	4.70
$-m'' \Delta Ec^f/M$ (polyester), cal.	383.87
$m' \Delta Ec^\circ/M$ (Thiaadamantane), cal.	-9278.55
$\Delta Ec^c/M$ (Thiaadamantane), cal. g. <sup>-1</sup>	-9278.55

<sup>a</sup> The symbols and abbreviations of this table are those of ref. 5, except as noted. <sup>b</sup>  $\varepsilon^f(\text{Cont.})(t_i - 25^\circ) + \varepsilon^f(\text{Cont.})(25^\circ - t_f + \Delta t_{\text{corr.}})$ . <sup>c</sup> Items 81-85, incl., 87-91, incl., 93 and 94 of the computation form of ref. 5.

the heat of formation of thiaadamantane, values of the heat of formation of carbon dioxide and water were taken from Circular 500,<sup>7</sup> and  $\Delta H^\circ_{298.15}$  for  $\text{S}(\text{s, rhombic}) + 3/2\text{O}_2(\text{g}) + 111\text{H}_2\text{O}(\text{liq.}) = \text{H}_2\text{SO}_4 \cdot 110\text{H}_2\text{O}(\text{liq.}) \quad (2)$

the reaction 2 was taken to be  $-143.84 \text{ kcal.}$  This datum was obtained by applying appropriate dilution corrections<sup>7</sup> to the value of the heat of formation of  $\text{H}_2\text{SO}_4 \cdot 115\text{H}_2\text{O}(\text{liq.})$  recently determined in this Laboratory.<sup>8</sup> Combination of these values allows calculation of the heat of formation of solid thiaadamantane according to reaction 3.



(7) F. D. Rossini, D. D. Wagman, W. H. Evans, S. Levine and I. Jaffe, "Selected Values of Chemical Thermodynamic Properties," National Bureau of Standards Circular 500, 1952.

(8) W. D. Good, J. L. Lacina and J. P. McCullough, *J. Am. Chem. Soc.*, **82**, 5589 (1960).

## THE REFLECTANCE SPECTRA OF CHLOROCOBALTOUS AND CHLOROFERRI COMPLEX IONS ON DOWEX-1 ANION-EXCHANGE RESIN

BY EMILE RUTNER

Lewis Research Center, National Aeronautics and Space Administration, Cleveland, Ohio

Received January 14, 1961

A study has been made of the reflectance spectra of the chlorocobaltous and chloroferri complex ions adsorbed onto Dowex-1  $\times 10$  resin from 7.25 and 9.5 *N* HCl solutions, respectively. The spectra of the chlorocobaltous complex on the resin had minima at 695, 665 and 635  $m\mu$  that are the same bands observed in absorption spectra in 7.25 *N* HCl which have previously been assigned to  $\text{CoCl}_4^-$ . From the reflectance spectra, the absorptivity of the adsorbed material for the observed bands was estimated by two methods, both of which gave somewhat larger values than those obtained for the species in solution, but were not at all comparable with the smaller absorptivities obtained from the reflectance spectra of anhydrous  $\text{CoCl}_2$ . The spectra of the chloroferri complex on the resin had one peak at 362  $m\mu$  that corresponded to a band previously assigned to  $\text{FeCl}_4^-$ . However, there was not the same degree of similarity between the resin and solution spectra as for the chlorocobaltous complex.

### Introduction

Several investigators have offered evidence<sup>1-4</sup> to indicate that  $\text{Co}^{++}$  in HCl solution exists as an anion  $[\text{Co}(\text{H}_2\text{O})_6-x\text{Cl}_x]^{(2-n)+}$  where  $x = 0, 4, 5, 6$ , and, correspondingly,  $n = 0, 2, 3, 4$ . Most of this

(1) O. R. Howell and A. Jackson, *Proc. Roy. Soc. (London)*, **A142**, 587 (1933).

(2) O. R. Howell and A. Jackson, *ibid.*, **A155**, 33 (1936).

(3) O. R. Howell and A. Jackson, *J. Chem. Soc.* 1268 (1936).

(4) L. I. Katzin and E. Gebert, *J. Am. Chem. Soc.*, **72**, 5464 (1950).

evidence has been obtained by measuring the variation of optical density as a function of  $\text{Cl}^-$  concentration in a variety of solutions. By this technique it has been postulated that in concentrated solutions the principal anion, especially in the case of dilute  $\text{Co}^{++}$ , is  $\text{CoCl}_4^-$  and that the spectral absorption bands due to this species have maxima at 615, 625, 665 and 695  $m\mu$  and are not affected by the presence of other cations.

By the use of methods similar to that used for the  $\text{CoCl}_2$  solutions, it has been concluded from the variation of the optical density of ferric chloride and HCl solutions as a function of wave length that the highest chloroferri complex is  $\text{FeCl}_4^-$ .<sup>5,6</sup> However,  $\text{FeCl}_4^-$  is not the predominant species unless the concentration of HCl is greater than 12 *N*; for example, the spectra in 9.5 *N* HCl are due to the combined absorption of  $\text{FeCl}_3$  and  $\text{FeCl}_4^-$ .<sup>6</sup> At lower concentrations of HCl, some contribution to the spectrum due to the species having the general formula  $[\text{FeCl}_n]^{(3-n)+}$  where  $n = 0, 1, 2, 3, 4$  is evident. An analysis of the spectra of this system has led to the conclusion<sup>6</sup> that the principal absorption peaks of  $\text{FeCl}_4^-$  are located at 360, 310, 240  $\mu$ , those of  $\text{FeCl}_3$  at 390, 340 and 250  $\mu$ , and those for the composite spectrum of  $\text{FeCl}_4^-$  and  $\text{FeCl}_3$  in 9.86 *N* HCl at 315 and 243  $\mu$ .

In order to obtain additional information concerning the nature of the chlorometallic complexes, species have been isolated from solution by adsorption on an anion-exchange resin from HCl solutions, where an attempt has been made to identify them by comparison of the resin reflectance spectra and solution absorption spectra as to band structure and absorptivities. The concentrations of HCl chosen for the study of the chlorocobaltous and chloroferri complexes were those for which the distribution coefficients for the ions between the resin and solutions were near the maxima.

### Experimental

**Materials.**—The  $\text{CoCl}_2$  used was C.P.  $\text{CoCl}_2 \cdot 6\text{H}_2\text{O}$  that was dehydrated at 110°. A stock solution containing 9.25 g./l. in 7.25 *N* HCl was prepared, and the desired concentrations were obtained by diluting various quantities of the stock solution with 7.25 *N* HCl.

Solutions of  $\text{FeCl}_3$  were made by dissolving pure Fe wire in aqua regia, eliminating the nitrogen oxides with excess HCl, gently evaporating almost to dryness, and dissolving the residue in 250 ml. of 9.5 *N* HCl. This original solution was then diluted to give the desired concentrations.

The ion-exchange resin used was a styrene quaternary ammonium type in chloride form, Dowex-1  $\times 10$  (200 to 400 mesh), which had been air-dried and had a moisture content of 9.6% as determined by heating at 104°. The measured average diameter of the resin beads was 0.144 mm. before adsorption and 0.155 mm. after adsorption.

Samples of  $\text{CoCl}_2$  on resin were prepared by adding 30 ml. of the desired solution concentration to 10 g. resin, allowing the resin to stand for 1 hour at room temperature, and filtering through a porous glass crucible. Longer contact times between resin and solution (24 hr.) had no effect on the spectrum. All samples were air-dried by suction for 1 hour before placing them in a container which was a 1.5 inch bakelite bottle cap fitted with a 1/4-inch-thick Lucite window. The window was pressed down tightly onto the powder to give a smooth surface. Samples of  $\text{FeCl}_3$  on the resin were prepared similarly except that 25 ml. of solution was used per 10 g. of resin.

Reflectance spectra were obtained by using a Beckman DU spectrophotometer equipped with a reflectance attachment, the bottle cap being cemented to the sample holder; and the transmittance spectra were obtained using 1-cm. cells to hold the solution in the spectrophotometer.

The reflectance is given by  $R = (I/I_s)$ , where  $I$  is the reflected intensity from the sample and  $I_s$  is that from a standard of comparison. The standard used for the Co samples was LiF, while that for the Fe samples was  $\text{MgCO}_3$ . It was later found that the LiF had a reflectance of 95% of that of  $\text{MgCO}_3$ . All data were corrected so that  $I_s$  and  $R$  refer to  $\text{MgCO}_3$ . Further corrections were made for the re-

flectance from the Lucite windows. The r.m.s. deviation from the mean value of  $R$  for two samples of LiF over the range of wave lengths that were of interest, i.e., 335 to 800  $\mu$ , was 0.75% while the r.m.s. deviation of two samples of resin over this range of wave lengths was 2.3%.

**Discussion and Treatment of the Data.**—It was found that the experimentally observed variations of the reflectivity of the resin with the concentration of the adsorbed species followed the relations given by Johnson<sup>7</sup> and Kortum and Haug<sup>8</sup> for the chlorocobaltous ion but not for the chloroferri ion.

Johnson's relation<sup>7</sup> was derived for a model

$$R = m \left[ 1 + \frac{2 \exp[y \ln(1-m) - 2kd]}{1 - \exp[y \ln(1-m) - 2kd]} \right] \quad (1)$$

wherein the reflecting material consists of layers of thickness  $d$  and of optical absorptivity  $k$  ( $\text{cm.}^{-1}$ ), and from which the fraction of light reflected at each interface is  $m$ , the Fresnel reflectivity. The quantity  $y$  is chosen to make  $R = 1$  when  $k = 0$ .

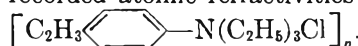
In applying relation 1 to determine the absorption coefficient of the adsorbed material on the resin, the following assumptions were made.

(1) The adsorbed material was distributed homogeneously through the resin with a concentration  $c$ , which was proportional to that in the solution and was determined by the distribution coefficient,  $D = 23$ , in 7.25 *N* HCl.<sup>9</sup> The linear absorption coefficient used in relation 1 is then given by

$$k = K \frac{\rho_r}{\rho_{Co}} c + k_r \quad (2)$$

where  $K$  is the absorptivity of the ion species on the resin,  $k_r$  is the absorptivity of the resin, and  $\rho_r/\rho_{Co}$  is the ratio of the densities of the resin and the adsorbed species. The density of the adsorbed species was taken to be that of  $\text{CoCl}_2$ ; i.e.,  $\rho_{Co} = 3.35$  g./ml.

(2) The index of refraction of the resin used,  $n = 1.62$ , was assumed to be unaffected by the adsorbed material. The value of  $n$  was obtained from the recorded atomic refractivities<sup>10</sup> for the structure



(3) The value  $m = 0.060$  is the average value of the Fresnel reflectance for incident angles from 0 to 45° on a surface whose topography can be represented by the surface assumed by packed spheres. Since the value of  $m$  only varies from 0.056 to 0.061 in going from 0 to 45°, it is rather insensitive to the shape of the particles.

Figure 1 shows the dependence of the reflectance at the minima 695, 665 and 635  $\mu$ , on the concentration. Figure 2 shows a spectrum of the resin with no adsorbed material, and it is noted that the reflectivity is constant in the region where the chlorocobaltous ion absorbs; using relation 1 corresponds to a value of  $k_r = 0.80$ .

The curves of Fig. 2 show the dependence of  $R$  on  $c$  as calculated from equation 1 for  $K = 4.9 \times 10^4$   $\text{cm.}^{-1}$  for the 695 and 665  $\mu$  bands, and  $K = 3.2 \times 10^4$   $\text{cm.}^{-1}$  for the 635  $\mu$  bands.

(7) P. D. Johnson, *J. Opt. Soc.* **42**, 978 (1952).

(8) G. Kortum and P. Haug, *Z. Naturforsch.*, **8A**, 372 (1953).

(9) G. E. Moore and K. A. Kraus, *J. Am. Chem. Soc.*, **74**, 843 (1952).

(10) N. A. Lange, ed., "Handbook of Chemistry and Physics," 6 Ed., Handbook Publishers, Inc., Sandusky, Ohio, 1946, p. 1025.

(5) R. Myers, D. E. Metzler and E. H. Swift, *J. Am. Chem. Soc.*, **72**, 3767 (1950).

(6) G. A. Gamlen and D. O. Jordan, *J. Chem. Soc.*, 1435 (1953).

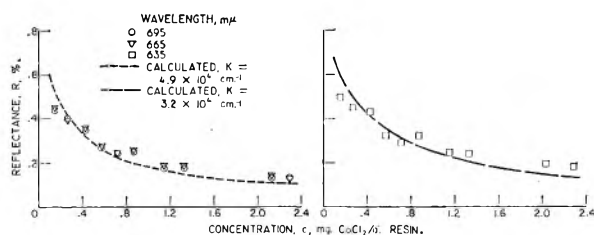


Fig. 1.—Reflectance vs. concentration of  $\text{CoCl}_2$  on Dowex-1  $\times$  10 anion-exchange resin for three adsorption peaks: (a) 695, (b) 665, and (c) 635  $m\mu$ . Reflectances calculated using relation 1 with  $m = 0.060$ ,  $k_r = 0.80 \text{ cm.}^{-1}$  for resin and  $K (\text{cm.}^{-1}) = 4.9 \times 10^4$  for (a) and (b) and  $K = 3.2 \times 10^4$  for (c).

Kortum and Haug<sup>3</sup> give the following relation between the reflectance and absorptivity

$$\frac{(1-R)^2}{2R} = \frac{k}{s} \quad (3)$$

where  $s(\text{cm.}^{-1})$  is a scattering coefficient. Substitution of equation 2 gives

$$\frac{(1-R)^2}{2R} = \frac{K}{s} \frac{\rho_r}{\rho_{\text{Co}}} c + \frac{k_r}{s} \quad (4)$$

or a linear plot of  $(1-R)^2/2R$  versus  $c$ . The experimental data have been treated in this manner and are plotted in Fig. 3. Kortum states that  $s$  is nearly the same for all materials and gives values for glass particles of 160 for  $10\mu$  particles and  $s = 70$  for  $100\mu$  particles. Using the smaller value of  $s$ , which may be in error by a factor of 2, and the observed slopes, the absorptivity of the adsorbed material is  $K = 2.7 \times 10^5 \text{ cm.}^{-1}$  for the 695 and 665  $m\mu$  bands, and  $K = 1.8 \times 10^5 \text{ cm.}^{-1}$  for the 635  $m\mu$  band.

In an attempt to understand the differences in the absorptivities as calculated from relations 1 or 4, it is noted that, in addition to the uncertainty in  $s$ , equation 1 is assumed to apply to a measured reflectivity where a first-surface term, *i.e.*, a term that is independent of  $k$ , has a value equal to  $m$  while the  $R$  in Kortum's formula is not the measured  $R$  but rather the measured  $R$  less an unspecified first-surface term. However, equation 1 overestimates this term, since reflectivities as low as  $m/2$  were observed for the highest chloroferri concentrations.

It is of interest to make expansions of 1 and 3 for the case of small  $R$ , that is, large  $kd$ . Relation 1 becomes

$$\frac{1}{R-m} = \frac{y}{2} \left(1 + \frac{m}{2}\right) + \frac{kd}{m} \quad (5)$$

while relation 3 becomes

$$\frac{1}{R} = 2 + \frac{2k}{s} \quad (6)$$

If top-surface reflectance is considered,  $1/(R-m)$  can be compared with  $1/R$ . Since  $y$  has approximately the value of 2, the constant terms differ. However, a relation is obtained for the scattering coefficient,  $s = 2m/d$ , which has the same dependence on  $d$  that has been observed.<sup>3</sup>

The reflectance spectrum of  $\text{CoCl}_2$  (anhyd.) for particles of mean diameter of 0.05 mm. showed bands at 590 and 535  $m\mu$ . The absorption coefficients calculated by the use of relation 1 were for  $n = 2.0$ , 200 and 78  $\text{cm.}^{-1}$ , respectively. The value of  $n$  was calculated from the ion refractivities

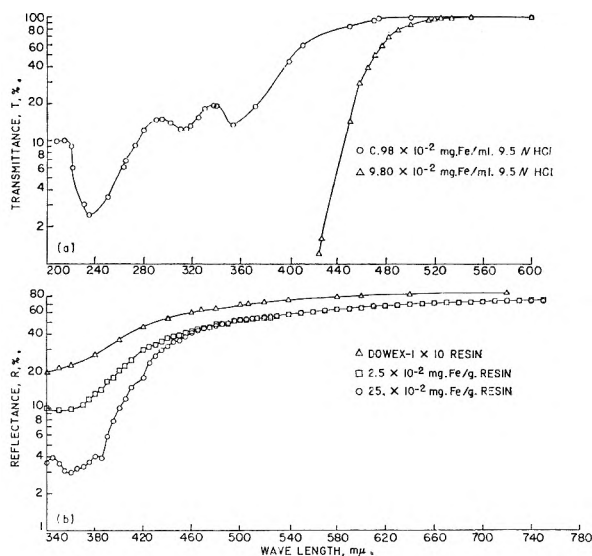


Fig. 2.—(a) absorption spectra of  $\text{FeCl}_3$  in 9.5  $N$   $\text{HCl}$ ; (b) reflectance spectra of Dowex-1  $\times$  10 resin and of chloroferri ion on resin.

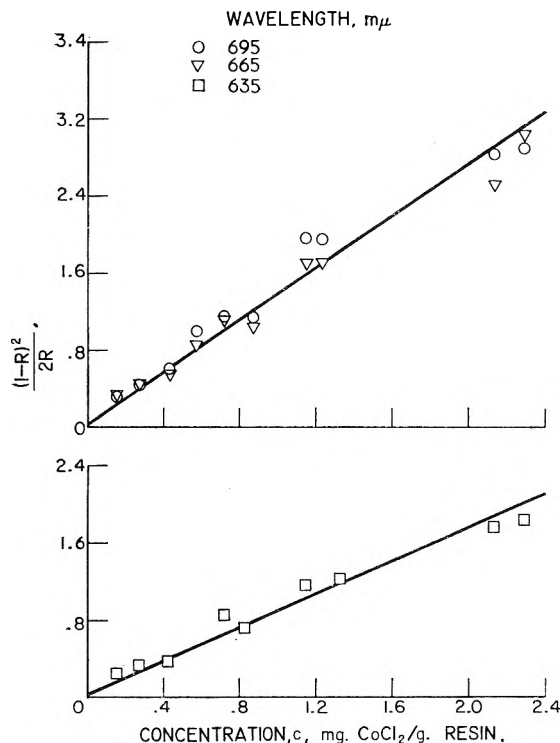


Fig. 3.— $(1-R)^2/2R$  vs.  $c$  (mg.  $\text{CoCl}_2/\text{g. resin}$ ) for  $\text{CoCl}_2$  on Dowex-1  $\times$  10 anion-exchange resin for three adsorption peaks: (a) 695, (b) 665, and (c) 635  $m\mu$ .

as given by Gladstone and Hubbert,<sup>11</sup> and a density of 3.35 g./ml. for the  $\text{CoCl}_2$  (anhyd.).

The absorption spectra of the solutions were treated in the usual manner with absorption maxima being observed at (a) 690, (b) 665, and (c) 625  $m\mu$  for  $\text{CoCl}_4^-$ . The corresponding molar absorption coefficients,  $\epsilon = [\text{cm.}^{-1} \times 1 \times \text{m.}^{-1}] (\ln)$ , obtained from Beer's law plots are: (a) and (b)  $2.3 \times 10^2$ , and (c)  $1.6 \times 10^2$ , respectively. Assuming that

(11) J. H. Gladstone and Walter Hubbert, *J. Chem. Soc.*, 67, 855 (1895).

the density of the  $\text{CoCl}_2$  in solution was 3.35 g./ml., that of anhydrous  $\text{CoCl}_2$ , the values of  $K$  ( $\text{cm.}^{-1}$ ) are: (a) and (b)  $5.8 \times 10^3$ , and (c)  $4.0 \times 10^3$ .

Examination of the chlorocobaltous spectra indicates that the solution and resin spectra are similar, which leads to the conclusion that the species on the resin is the same as in solution. The similarity in the spectra can be attributed to the fact that the electron energy levels are not significantly affected by adsorption or by the ion-exchange reaction, which is in agreement with the observation<sup>3</sup> that various cations do not affect the spectra of  $\text{CoCl}_2$  in HCl. The absorption coefficients for the adsorbed material, although obtained only to order-of-magnitude accuracy, are sufficiently in agreement with the species in solution to further support the idea that the two species are the same, and the work of others indicates the observed species to be  $\text{CoCl}_4^-$ .

The reflectance spectra of the chloroferri complex on the resin is somewhat obscured by the

significant absorption of the resin for wave lengths less than 460  $\mu$ . Only the resin sample prepared from the most concentrated solution ( $9.8 \times 10^{-2}$  mg. Fe/ml. 9.5 N HCl) had a spectrum that showed structure; and, contrarily, structure was observed only in the absorption spectra of the least concentrated solution (0.98 mg. Fe/ml.), which had bands at 236, 312 and 355  $\mu$ , as shown in Fig. 2. Gamelen and Jordan<sup>6</sup> attributed the first two to  $\text{FeCl}_3$  and the latter to  $\text{FeCl}_4^-$ .

The similarities between the solution absorption and resin reflectance spectra are not readily apparent. However, there is a common band at about 360  $\mu$  that is probably due to  $\text{FeCl}_4^-$ , and much of the solution spectra of this species is obscured by the absorption due to  $\text{FeCl}_3$ .

**Acknowledgment.**—The author wishes to express his thanks to Mr. Leonard Vavruska of the Harshaw Scientific Co. for the use of a reflectance attachment and to Dr. James Blue for constructive criticism.

## DISTRIBUTION EXPERIMENTS IN FUSED SALTS. I. THE DISTRIBUTION OF THALLIUM CHLORIDE BETWEEN $\text{KNO}_3$ AND $\text{AgCl}$ AND BETWEEN $\text{K}_2\text{S}_2\text{O}_7$ AND $\text{AgCl}$

BY JOHN H. KENNEDY

*Explosives Department, E. I. du Pont de Nemours & Co., Wilmington, Delaware*

*Received January 23, 1961*

Several pairs of immiscible fused salts have been found, and the distribution of solutes in these two phase systems is being studied. The distribution of thallium chloride in the systems  $\text{KNO}_3$ - $\text{AgCl}$  and  $\text{K}_2\text{S}_2\text{O}_7$ - $\text{AgCl}$  was found to depend on two equilibria which are the true distribution of thallium chloride molecules between the two phases and the association of thallium and chloride ions in the  $\text{KNO}_3$  (or  $\text{K}_2\text{S}_2\text{O}_7$ ) phase. The two equilibrium constants were determined graphically for both systems from a series of experiments in which potassium chloride was added, and the distribution of thallium between  $\text{AgCl}$  and  $\text{KNO}_3$  (or  $\text{K}_2\text{S}_2\text{O}_7$ ) was measured as a function of the chloride concentration in the  $\text{KNO}_3$  (or  $\text{K}_2\text{S}_2\text{O}_7$ ) phase. The distribution constant ( $K_{\text{TlCl}(\text{KNO}_3)/\text{TlCl}(\text{AgCl})}$ ) was found to be 0.02 while the association constant for  $\text{TlCl}$  in  $\text{KNO}_3$  was 0.14 kg./mole. The corresponding values in the case of  $\text{K}_2\text{S}_2\text{O}_7$  were 0.04 and 2.0 kg./mole, respectively.

Even though the distribution of solutes between two immiscible liquid phases is of scientific and practical importance, no work has been published on the distribution of solutes between two immiscible fused salts. The only literature reference to solvent extraction using fused salts is in a review article by Gruen, Fried, Grof and McBeth who mention that tri-butyl phosphate/low melting nitrate salts and  $\text{B}_2\text{O}_3/\text{KCl-LiCl}$  entectic form two phase systems.<sup>1</sup>

Potentially, this could have a large field of application since fused salts have widely varying properties, but unfortunately, most fused salt pairs are completely miscible. However, some immiscible pairs were discovered in our work including the systems  $\text{AgCl}/\text{KNO}_3$ ,  $\text{AgCl}/\text{K}_2\text{S}_2\text{O}_7$ ,  $\text{AgCl}/\text{KH-SO}_4$ ,  $\text{AgCl}/\text{KBF}_4\text{-NaBF}_4$ , and  $\text{PbCl}_2/\text{KBF}_4\text{-NaBF}_4$ . With these, we have begun a study of the distribution of various solutes between the two phases.

### Experimental

Figure 1 shows the apparatus which was used for the distribution experiments. The two solvents were melted in

the flask and maintained at 480° for all experiments in this report. The solute was added, and the mixture was stirred for 15 minutes. The two phases were allowed to separate. Then the plug of frozen salt in the capillary tube was melted by turning on the auxiliary heater, and the molten mixture flowed out the capillary tube into the sample collector. Several portions of each phase were collected by rotating the sample holder.

The light layers ( $\text{KNO}_3$  or  $\text{K}_2\text{S}_2\text{O}_7$ ) were analyzed for thallium polarographically. The samples were dissolved in sodium citrate. 1 *F* hydrochloric acid was added and the samples were boiled to coagulate silver chloride. After filtering, adjusting the pH to 7.4 (pH of pure sodium citrate) and diluting to volume such that the final citrate concentration was 1 *F*, the solutions were scanned polarographically. Thallium gives a reversible wave at  $-0.50$  v. vs. S.C.E.

The silver chloride layers were analyzed by first dissolving the sample in concentrated ammonium hydroxide and adding sodium citrate. The samples were then acidified and filtered. The pH was adjusted to 7.4, and the samples were handled as the light layers from this point.

Lead, copper, tungsten, cobalt and zinc were determined polarographically in the light layer, while barium, iodide and bromide were determined gravimetrically. Lead was determined polarographically in the silver chloride layer after dissolving in ammonium hydroxide and precipitating silver chloride by acidification. Tungsten, copper, cobalt, zinc and phosphorus were determined in the silver chloride phase by emission spectroscopy.

Mixtures of chloride and bromide ions were precipitated as  $\text{AgCl}$  and  $\text{AgBr}$  which were dried and weighed. The  $\text{AgBr}$

(1) D. M. Gruen, S. Fried, P. Graf and R. L. McBeth, Proceedings of the UN International Conference on the Peaceful Uses of Atomic Energy, 2nd Conference, Geneva, Sept. 1958, Vol. 28, 1958, p. 112.



was converted to AgCl by heating in a stream of chlorine gas and reweighed. The amounts of chloride and bromide ions present were calculated from these two weights.

### Results and Discussion

The fused salts which were studied had low viscosities, low vapor pressures, low mutual solubilities, and were stable for long periods of time. Table I shows the mutual solubilities of three of the systems. The mutual solubilities are comparable to many water-organic liquid-liquid systems which are used in solvent extraction processes.

TABLE I

MUTUAL SOLUBILITIES FOR THE SYSTEMS<sup>a</sup> KNO<sub>3</sub>-AgCl, KHSO<sub>4</sub>-AgCl, K<sub>2</sub>S<sub>2</sub>O<sub>7</sub>-AgCl

Solubility in AgCl	Wt. %	Solubility of AgCl in light phase	Wt. %
K <sub>2</sub> S <sub>2</sub> O <sub>7</sub>	0.8	K <sub>2</sub> S <sub>2</sub> O <sub>7</sub>	0.86
KHSO <sub>4</sub>	.8	KHSO <sub>4</sub>	0.66
KNO <sub>3</sub>	.6	KNO <sub>3</sub>	1.84

<sup>a</sup> The light phases were analyzed for Ag and Cl. The AgCl phase was analyzed for K.

The density differences were large (AgCl 4.8, KNO<sub>3</sub> 1.76, K<sub>2</sub>S<sub>2</sub>O<sub>7</sub> 2 g./ml.) so that phase separation was extremely fast. Since AgCl was so much more dense than the other salts they will be referred to as the light phase.

Table II lists a number of the solutes studied to date in three systems. Most of the solutes remained in the light phase, except bromide and iodide which were found in the silver chloride phase.

TABLE II

DISTRIBUTION COEFFICIENTS<sup>a</sup>

Compound	$K^b$		
	KNO <sub>3</sub>	K <sub>2</sub> S <sub>2</sub> O <sub>7</sub>	KHSO <sub>4</sub>
PbCl <sub>2</sub>	20	>300	200
Na <sub>2</sub> WO <sub>4</sub>	(100)		>200
CuCl <sub>2</sub>		100	80
CoCl <sub>2</sub>		>250	>300
Na <sub>3</sub> PO <sub>3</sub>	>100	>100	~1
KI	<0.01		(0.01)
KBr	0.01	(0.01)	
ZnCl <sub>2</sub>		(100)	
BaCl <sub>2</sub>	(100)		

<sup>a</sup> The underlined element was analyzed for. (100) signifies that the AgCl layer was not analyzed, but essentially all of the element was found in the light phase. <sup>b</sup> The distribution coefficient is  $\frac{(\text{mg./g. of solvent})_{\text{light}}}{(\text{mg./g. of solvent})_{\text{AgCl}}}$ .

There are a number of factors which may be important in determining the solubility of inorganic solutes in fused salts, but their relative importance is not known. The ionic character of the solute does not seem to be of prime importance since both zinc chloride (which is highly associated near the melting point) and barium chloride (which is completely ionic) remained in the light phase. In spite of the possibility of complexation with chloride ion, cobalt and copper do not elect to reside in the silver chloride phase.

Another possible factor is the structure of the solute and solvents. Silver chloride is cubic and probably retained some of its lattice structure at 480° which is only slightly above the melting

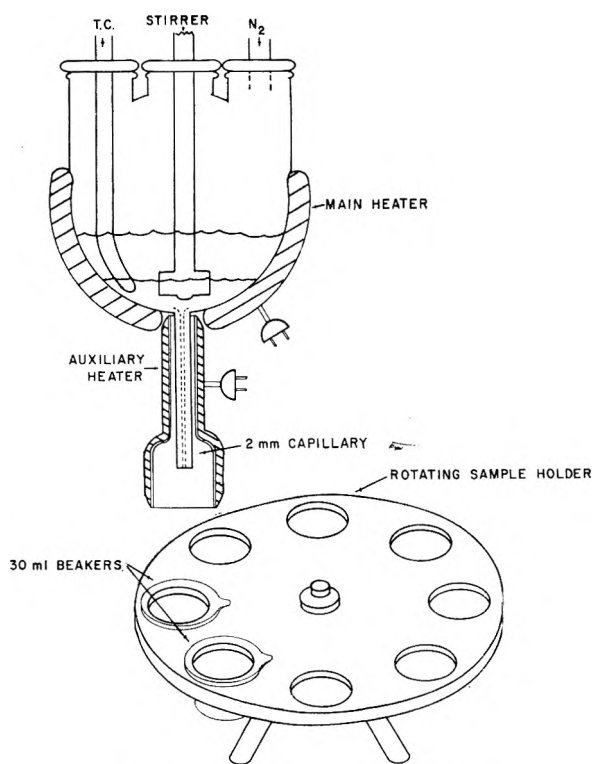


Fig. 1.—Solvent extraction apparatus.

point (454°). It was thought therefore that a cubic solute might prefer the AgCl phase. Thallium(I) chloride was found to distribute nearly equally between the two liquid phases. A thorough investigation of the thallium chloride distribution was made in order to observe the factors which control distribution in fused salt systems.

Three experiments were run to ensure that equilibrium was reached and Table III shows the results. In one, thallium chloride was added to the light phase, then silver chloride was added; in a second, thallium chloride was added to silver chloride and then the light phase was added; while in the third, thallium chloride was added to the mixture of solvents. The excellent agreement among distribution coefficients indicated that equilibrium was achieved. Several portions of each phase were analyzed for thallium and found to be identical; thus, each of the phases was homogeneous.

TABLE III

CHECK ON EQUILIBRIUM CONDITIONS FOR FUSED SALT DISTRIBUTIONS

Conditions	Distribution coefficient	
	KNO <sub>3</sub> /AgCl	K <sub>2</sub> S <sub>2</sub> O <sub>7</sub> /AgCl
TlCl added to light phase	1.51	0.62
TlCl added to AgCl	1.54	.64
TlCl added to mixture	1.50	.61

The distribution coefficient was studied as a function of thallium concentration and the results are shown in Table IV. The coefficient should be constant for a simple molecular distribution, but both systems showed a decrease with increasing concentration. The effect was more pronounced in the KNO<sub>3</sub>-AgCl system.

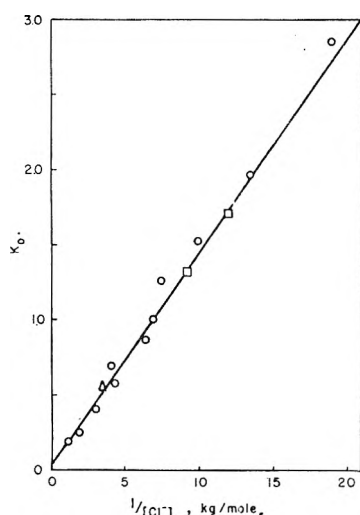


Fig. 2.—Determination of true distribution constant and association constant in  $\text{AgCl-KNO}_3$  system.

TABLE IV

DISTRIBUTION (AT  $480^\circ$ ) AS A FUNCTION OF THALLIUM CONCENTRATION

TlCl, mg.	Distribution coefficient $\text{KNO}_3/\text{AgCl}$	$\text{K}_2\text{S}_2\text{O}_7/\text{AgCl}$
50	1.97	0.97
100	1.91	.95
150	1.78	
200	1.81	.93
300	1.71	
400	1.72	.92
500	1.63	
600	1.63	
800	1.57	.92
1000	1.35	
2000	1.22	

One possible explanation for this change in distribution would be polymerization in one or both phases. However, if this were true, such species as  $\text{Tl}_{10}$  in  $\text{AgCl}$  and  $\text{Tl}_9$  in  $\text{KNO}_3$  would have to be postulated to account for the very small change observed. Another possible explanation for this change would be an activity effect, either a decrease in the thallium activity coefficient in the silver chloride phase or an increase in the light phase as the thallium concentration increased. The former would be reasonable since the activity coefficients of solutes in aqueous systems decrease with increasing concentration, but both the  $\text{KNO}_3\text{-AgCl}$  and  $\text{K}_2\text{S}_2\text{O}_7\text{-AgCl}$  systems should then show the same effect. Actually, the effect in the  $\text{K}_2\text{S}_2\text{O}_7\text{-AgCl}$  system was much smaller.

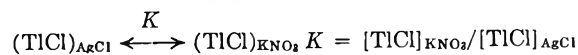
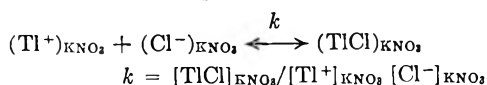
The other possibility, an increase in activity coefficient as the thallium concentration increased would not be expected unless a chemical effect was taking place. The only other substance besides thallium whose concentration was also changing in these experiments was chloride ion, and in another series of experiments this was avoided by using thallium nitrate as the solute. The results are shown in Table V.

The distribution coefficient was constant supporting the theory that the distribution coefficient decrease observed when thallium chloride was the

TABLE V  
DISTRIBUTION (AT  $480^\circ$ ) AS A FUNCTION OF THALLIUM CONCENTRATION

TlNO <sub>3</sub> , mg.	Distribution coefficient $\text{KNO}_3/\text{AgCl}$
50	2.33
100	2.32
200	2.25
700	2.17
1000	2.33

solute was due to  $\epsilon$  thallium-chloride interaction. This could be explained by the equilibria



where  $k$  is the association constant for  $\text{TlCl}$  in the potassium nitrate phase and  $K$  is the true distribution constant for  $\text{TlCl}$  between potassium nitrate and silver chloride. The observed distribution coefficient is

$$K_0 = ([\text{Tl}^+]_{\text{KNO}_3} + [\text{TlCl}]_{\text{KNO}_3}) / [\text{TlCl}]_{\text{AgCl}}$$

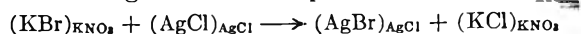
Substituting in the expressions for the equilibrium constants, one obtains the relationship

$$K_0 = K + K/k[\text{Cl}^-]_{\text{KNO}_3}$$

Thus, a plot of  $K_0$  vs.  $[\text{Cl}^-]_{\text{KNO}_3}^{-1}$  should be a straight line with an intercept of  $K$  and a slope of  $K/k$ . A series of experiments were run in which various amounts of potassium chloride were added to the mixture, and the observed distribution coefficient was measured as a function of the chloride concentration in the potassium nitrate phase. The results are plotted in Fig. 2. The constants were calculated to be  $K = 0.02$  and  $k = 0.14 \text{ kg./M}$ .

The equation predicts that the thallium concentration does not affect the observed distribution coefficient. This was shown by using various amounts of thallium nitrate (see Table V), but was also demonstrated by using two concentrations of thallium chloride (200 and 1000 mg.) and analyzing the potassium nitrate phase for chloride. The points are shown as squares on Fig. 2.

Potassium bromide was substituted for potassium chloride in the hopes of studying the ionization of thallium bromide; however, no bromide was found in the potassium nitrate phase. Evidently the following reaction took place



because an equivalent amount of potassium chloride (corrected for the distribution of potassium chloride between the two phases) was found in the potassium nitrate phase. The potassium nitrate phase was analyzed for chloride and the point is shown as a triangle in Fig. 2. The point fell on the line which supports the theory that the controlling factor was chloride in the potassium nitrate phase, since the silver bromide in the silver chloride phase did not change the observed distribution coefficient.

A similar plot was made for the  $\text{K}_2\text{S}_2\text{O}_7\text{-AgCl}$  system, and the constants were found to be  $K = 0.04$  and  $k = 2.0 \text{ kg./M}$ . Thus,  $\text{KNO}_3$  is much more of an ionizing solvent than  $\text{K}_2\text{S}_2\text{O}_7$  since the

TABLE VI  
TWO-STAGE EXTRACT ON WITH AgCl AND LEACH WITH KNO<sub>3</sub> OF THALLIUM CHLORIDE  
200 mg. of TlCl in 50 g. KNO<sub>3</sub>

Extraction 1			Extraction 2			Leach				
Phase	TlCl, mg.		Phase	TlCl, mg.		Phase	TlCl, mg.			
	Found	Calcd.		Found	Calcd.		Found	Calcd.		
KNO <sub>3</sub>	...	57	→	KNO <sub>3</sub>	16	17	KNO <sub>3</sub>	55	67	
AgCl	...	143	+	AgCl	..	40	→	AgCl	146	122

association constant for thallium chloride was so much smaller. Also, the cubic TlCl seemed to be highly soluble in the silver chloride phase since the distribution constants (light phase/AgCl) were so low.

Another cubic compound which was found to have a high solubility in silver chloride was potassium chloride. In the series of experiments when potassium chloride was added, it was found that the observed distribution coefficient was 1.2 in the KNO<sub>3</sub>-AgCl system and 0.4 in the K<sub>2</sub>S<sub>2</sub>O<sub>7</sub>-AgCl system.

It was also found that the high distribution coefficients observed for lead chloride (PbCl<sub>2</sub>) were decreased by the addition of large amounts of potassium chloride (the results of these studies will be published later).

The possibility of using this method for solvent extraction processes was shown by carrying out a two step extraction and leach of thallium chloride in the KNO<sub>3</sub>-AgCl system. The results are shown in Table VI. Two hundred mg. of TlCl was dissolved in 50 g. of KNO<sub>3</sub> and 2 g. of KCl, and the mixture was contacted with 50 g. of AgCl. The phases were separated, and the KNO<sub>3</sub> phase was contacted a second time with 50 g. of AgCl and 2 g. of KCl. Less than 10% of the thallium remained in the KNO<sub>3</sub> phase after these two ex-

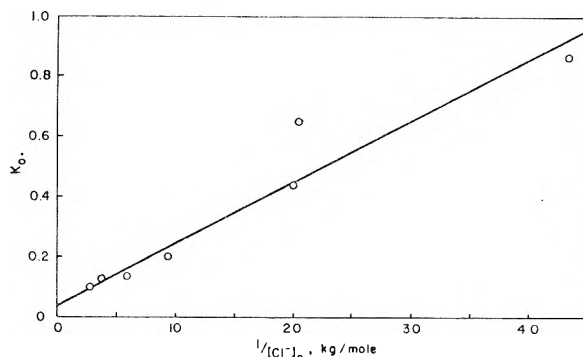


Fig. 3.—Determination of true distribution constant and association constant in AgCl-K<sub>2</sub>S<sub>2</sub>O<sub>7</sub> system.

tractions. The amount found checked well with the amount calculated from the equilibrium constants. The two AgCl phases were then leached with 100 g. of KNO<sub>3</sub>, and again the amount of thallium in each phase could be calculated from the constants.

Thus, distribution experiments in fused salt systems will shed light on the nature of fused salts and the factors which control solubility of solutes in them. These experiments may also point out new ways to solve separation problems.

## VAPOR-PHASE PHOTOLYSIS OF FORMIC ACID<sup>1</sup>

BY RALPH GORDEN, JR., AND P. AUSLOOS

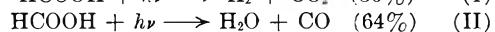
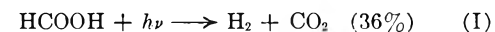
Division of Physical Chemistry, National Bureau of Standards, Washington, D. C.

Received February 3, 1961

The direct photolysis and the Hg(<sup>3</sup>P<sub>1</sub>) photosensitized decomposition of HCOOH and DCOOH have been investigated in the presence and absence of radical scavengers. The results indicate, in contrast to those of earlier investigations, that besides reactions I and II which involve intramolecular rearrangements  $\text{HCOOH} + h\nu \rightarrow \text{H}_2\text{O} + \text{CO}$  (I) and  $\text{HCOOH} + h\nu \rightarrow \text{H}_2 + \text{CO}_2$  (II) radical-producing primary processes must be considered as well. It will be shown that process  $\text{HCOOH} + h\nu \rightarrow \text{HCO} + \text{OH}$  is the most important source of free radicals in the direct photolysis of formic acid. The effect of temperature on the rate of formation of the products was investigated in some detail. Above 200° three different chain processes were found to occur: (a)  $\text{H} + \text{HCOOH} \rightarrow \text{H}_2\text{O} + \text{HCO}$ ,  $\text{HCO} \rightarrow \text{H} + \text{CO}$ ; (b)  $\text{H} + \text{HCOOH} \rightarrow \text{H}_2 + \text{COOH}$ ,  $\text{COOH} \rightarrow \text{CO}_2 + \text{H}$ ; (c)  $\text{H} + \text{HCOOH} \rightarrow \text{HCOO} + \text{H}_2$ ,  $\text{HCOO} \rightarrow \text{H} + \text{CO}_2$ .

### Introduction

Earlier investigations using both direct photolysis and mercury-photosensitization indicate that no free radicals are produced from HCOOH. Ramsperger and Porter<sup>2</sup> explained the formation of the products CO, CO<sub>2</sub>, H<sub>2</sub> and H<sub>2</sub>O at the wave lengths between 2260 and 2500 Å. by two intramolecular rearrangements



Gorin and Taylor<sup>3</sup> concluded that at wave lengths between 1900 and 2540 Å. the dimer decomposed to yield only CO<sub>2</sub> and H<sub>2</sub>. They found no significant evidence for H-atoms in experiments carried out in the presence of parahydrogen. Burton<sup>4</sup> drew the same conclusion from experiments based on the mirror techniques.

Bates and Taylor<sup>5</sup> investigated the mercury-

(1) This research was supported by a grant from the U. S. Public Health Service, Department of Health, Education and Welfare. Part of this work was presented by one of the authors (R.G., Jr.) in partial fulfillment of the M.S. requirements of the American University.

(2) H. C. Ramsperger and C. W. Porter, *J. Am. Chem. Soc.*, **48**, 1267 (1926).

(3) E. Gorin and H. S. Taylor, *ibid.*, **56**, 2042 (1934).

(4) M. Burton, *ibid.*, **58**, 1655 (1936).

(5) J. R. Bates and H. S. Taylor, *ibid.*, **49**, 2438 (1927).

TABLE I  
 PHOTOLYSIS OF HCOOH AT 30°

HCOOH	Mole/cc. × 10 <sup>6</sup>		Rate, cc./min. × 10 <sup>3</sup>					Type of irradiation
	Scav.		H <sub>2</sub>	CO	CO <sub>2</sub>	C <sub>2</sub> H <sub>4</sub>	C <sub>4</sub> H <sub>10</sub>	
0.97	None		0.098	0.17	0.19			Direct photolysis with Corning-filter 9-54
.97	[C <sub>2</sub> H <sub>4</sub> ]	0.030	.017	.14	.14	0.036	0.031	Direct photolysis with Corning-filter 9-54
.97	[O <sub>2</sub> <sup>18</sup> ]	.014	.016	.13				Direct photolysis with Corning-filter 9-54
.97	None		1.29	5.55	1.9			( <sup>3</sup> P <sub>1</sub> )Hg sensitized
.97	[O <sub>2</sub> <sup>16</sup> ]	.018	0.024	0.79	2.2			( <sup>3</sup> P <sub>1</sub> )Hg sensitized
.97	[O <sub>2</sub> <sup>18</sup> ]	.012	.020	.38	3.0			( <sup>3</sup> P <sub>1</sub> )Hg sensitized

 TABLE II  
 EFFECT OF SCAVENGERS

T, °C.	Mole/cc. × 10 <sup>6</sup>		Rate, cc./min. × 10 <sup>3</sup>								Type of irradiation		
	DCOOH	Scav.	H <sub>2</sub>	HD	D <sub>2</sub>	CO	CO <sub>2</sub>	Ethane	C <sub>4</sub> H <sub>8</sub> D <sub>2</sub>	C <sub>4</sub> H <sub>8</sub> D		C <sub>4</sub> H <sub>10</sub>	
2	0.38	None	0.0049	0.033	0.014	0.23	0.10						Direct photolysis with Corning 9-54 filter
2	0.38	[CO <sub>2</sub> ]	.0030	.032	.015	.23	...						
101	1.29	None	.017	.99	.085	1.5	1.4						
100	1.29	[O <sub>2</sub> <sup>18</sup> ]	.038	.10	.011	1.7	1.5						
203	1.24	None	.72	1.5	.41	1.8	2.4						
203	1.27	[O <sub>2</sub> <sup>16</sup> ]	.034	.042	0.19	.12	2.6	2.4					
36	1.0	[C <sub>2</sub> H <sub>4</sub> ]	.031	.0030	.0098	.0011	0.13	.098	0.017	0.012	0.010	0.0024	
35	1.0		.053	.0035	.0089	.0016	.11	.080	.017	.012	.009	.0021	
34	1.0	None	.031	.26	.107	2.9	.69						( <sup>3</sup> P <sub>1</sub> )Hg sensitized
35	1.0	[C <sub>2</sub> H <sub>4</sub> ]	.031	.099	.21	.021	3.1	.97	.20	.074	.12	.076	
70	3.81	None	.020	.066	.0031	0.055	.15						Radiolysis
70	3.81	[I <sub>2</sub> ]	0.47	.0019	.0016	.00066	.055	.075					

photosensitized decomposition of formic acid at 2537 Å. and found process II to be three times more important than process I. More recently, Kebarle and Lossing<sup>6</sup> reinvestigated the Hg(<sup>3</sup>P<sub>1</sub>) photosensitized decomposition of HCOOH at low pressures (10–25 μ) in a specially designed reactor connected to a mass spectrometer. In this study the products were explained exclusively by the intramolecular rearrangements I and II. The relative distribution of the products was similar to the one found by Bates and Taylor.

In the present study the direct photolysis and Hg(<sup>3</sup>P<sub>1</sub>) sensitized photolysis of HCOOH and DCOOH has been reinvestigated in an attempt to establish the importance of free radical production in the primary act. The fact that free radicals are produced in the photolysis of acetic acid<sup>7</sup> and methyl formate,<sup>6,8</sup> as well as in the liquid-phase photolysis of formic acid<sup>9</sup> seemed to justify a more extensive investigation.

### Experimental

**Apparatus.**—The gas phase was photolyzed in a quartz cell (10 cm. in length, 5 cm. in diameter) enclosed in a heavy aluminum furnace provided with double quartz windows. The temperature was automatically controlled within one-half of a degree.

A Hanovia S 100 lamp was used in the direct photolysis experiments. In the Hg(<sup>3</sup>P<sub>1</sub>) sensitized experiments the source was a flat-spiral, low-pressure mercury arc. Unless otherwise stated, a Corning-filter 9-54, transmitting radiation at wave lengths greater than 2200 Å. was used. Conversions were about 1% in all experiments. A few γ-ray radiolysis experiments were performed with an experimental arrangement identical to the one described before.<sup>10</sup>

**Analysis.**—The analytical section of the vacuum system consisted of a sequence of traps, a modified Ward still, and a

Toepler pump. In most experiments the non-condensable products and CO<sub>2</sub> were removed at -130° and subsequently analyzed on the mass spectrometer. In those done in the presence of ethylene, the C<sub>2</sub>, CO<sub>2</sub> and C<sub>4</sub> fractions were removed separately at -175, -155 and -110°, respectively.

**Materials.**—HCOOH (98%) was obtained from Eastman Kodak and was distilled in order to remove most of the water present. The fractions used in this investigation contained 0.5 to 1% water.

DCOOH was obtained from Merck and Company. One sample was used without any further purification. The major impurity was H<sub>2</sub>O (about 5%). Distillation of a second sample reduced the water content to 1%. The mass spectrum cracking pattern was very similar to the one reported by Ropp and Melton for DCOOH.<sup>11</sup>

The O<sub>2</sub><sup>16</sup> used was an assayed sample from Airco. The sample of O<sub>2</sub><sup>18</sup> was obtained from Isomet Corporation and had an isotopic purity of 98%.

### Results

**A. HCOOH.**—The products measured in experiments performed at 30° are presented in Table I. In the direct photolysis, oxygen and ethylene reduce the H<sub>2</sub> yields considerably, while the CO yields are only slightly affected. In the Hg(<sup>3</sup>P<sub>1</sub>) sensitized decomposition both the H<sub>2</sub> and the CO yields are strongly reduced by O<sub>2</sub>. The CO and CO<sub>2</sub> produced in the HCOOH-O<sub>2</sub><sup>18</sup> mixtures did not contain O<sup>18</sup>.

**B. DCOOH.**—The results given in Tables II and III indicate that in the direct photolysis at low temperatures HD, D<sub>2</sub>, CO and CO<sub>2</sub> are the major volatile products. At 25° a change in conversion from 0.2 to 0.85% had no effect on the rate of formation of these products. Most of the experiments listed were performed with the sample containing 5% H<sub>2</sub>O. Those performed with the sample containing less than 1% H<sub>2</sub>O gave very similar results, except for a slightly higher D<sub>2</sub> yield.

Colorimetric tests for formaldehyde in the direct

(6) P. Kebarle and F. P. Lossing, *Can. J. Chem.*, **37**, 389 (1959).

(7) P. Ausloos and E. W. R. Steacie, *ibid.*, **33**, 1530 (1955).

(8) P. Ausloos, *ibid.*, **36**, 383 (1958).

(9) D. Smithies and E. J. Hart, *J. Am. Chem. Soc.*, **82**, 4775 (1960).

(10) L. Stief and P. Ausloos, *J. Phys. Chem.*, **65**, in press (1961).

(11) G. A. Ropp and C. E. Melton, *J. Am. Chem. Soc.*, **80**, 3509 (1958).

TABLE III  
 EFFECT OF TEMPERATURE

T, °C.	Mole/cc. × 10 <sup>4</sup> (DCOOH)	Rate, cc./min. × 10 <sup>4</sup>				
		H <sub>2</sub>	HD	D <sub>2</sub>	CO	CO <sub>2</sub>
Corning filter 9-54						
156	0.108	0.011	0.086	0.052	0.19	0.17
203	.108	.03	.099	.048	.23	.25
257	.108	.09	.36	.14	.54	.64
156	.35	.038	.28	.12	.49	.48
203	.35	.096	.29	.19	.60	.76
257	.35	.41	1.1	.47	1.4	2.1
306	.35	1.5	5.2	1.6	3.4	7.6
101	1.29	0.017	0.99	0.085	1.5	1.4
160	1.23	.19	1.0	.47	1.6	1.8
203	1.24	.72	1.5	.42	1.8	2.5
257	1.14	1.9	4.3	1.7	4.1	7.3
Full arc						
42	0.35	0.053	1.1	0.98	3.2	2.0
76	.35	.066	1.2	1.1	3.3	2.3
110	.35	.072	1.1	1.1	2.8	2.3
153	.35	.099	1.2	.96	3.0	2.5
204	.35	.27	1.4	1.3	3.3	2.9
254	.35	.94	2.7	2.1	4.8	5.4
276	.35	1.6	4.7	2.7	5.5	8.5
306	.35	2.8	16	6.1	12	22

photolysis experiments were negative. At 306° the pyrolysis of formic acid accounted for at most 5%, and at all other temperatures less than 2%, of the over-all decomposition.

(a) **Effect of Scavengers.**—The products obtained in experiments with scavengers have been given in Table II and the results of comparison experiments without scavengers, obtained under otherwise identical conditions, are included.

The results given in Table II may be summarized as follows: 1. Addition of a large concentration of CO<sub>2</sub> in the direct photolysis at 2°, has no effect on the HD, D<sub>2</sub>, or CO yields. 2. Oxygen strongly inhibits the hydrogen yield at 100 and 203°, but only slightly affects the rates of formation of CO and CO<sub>2</sub>. 3. In the direct photolysis, ethylene reduced the yields of HD and D<sub>2</sub> without greatly affecting those of CO and CO<sub>2</sub>. CH<sub>2</sub>DCH<sub>2</sub>CH<sub>2</sub>CH<sub>2</sub>D was the major constituent of the butane fraction. The ethane fraction consisted of C<sub>2</sub>H<sub>6</sub>, C<sub>2</sub>H<sub>5</sub>D and C<sub>2</sub>H<sub>4</sub>D<sub>2</sub>. 4. In the Hg(<sup>3</sup>P<sub>1</sub>)-sensitized decomposition only the D<sub>2</sub> yield is appreciably reduced by C<sub>2</sub>H<sub>4</sub>. The large quenching cross section of ethylene may be responsible for the increase in the rate of formation of H<sub>2</sub>. 5. The rates of formation of H<sub>2</sub>, HD, D<sub>2</sub>, CO and CO<sub>2</sub> were determined in the vapor-phase radiolysis. I<sub>2</sub> inhibits strongly the yields of H<sub>2</sub>, HD and D<sub>2</sub>, but that of CO is unaffected.

(b) **Effect of Temperature.**—The effect of temperature on the direct photolysis of DCOOH at constant incident intensity has been investigated at different concentrations (Table III). The results of experiments performed with the full arc at one concentration have been included in the same table and are also presented in Fig. 1. The data of Table III may be summarized as follows: 1. At temperatures below 200° the yield of D<sub>2</sub> is considerably greater in the experiments at full arc

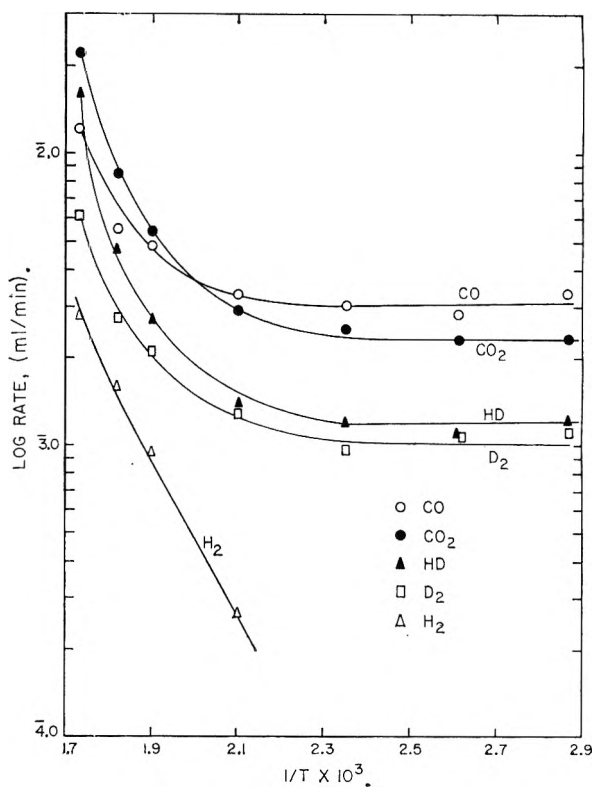


Fig. 1.

than in those performed with a Corning filter 9-54. 2. In the experiments at full arc there is only a very small variation of the rates of formation of HD, D<sub>2</sub>, CO and CO<sub>2</sub> in the temperature range 42 to 204°. 3. Above 200° the rates of formation of all products increase sharply with temperature.

C. **The Photolysis of CD<sub>3</sub>COCD<sub>3</sub> in Presence of HCOOH.**—A few experiments were performed in which CD<sub>3</sub>COCD<sub>3</sub> has been photolyzed in the presence of HCOOH at 3130 Å. (Corning 0-53) and at constant incident intensity. The data given in Table IV indicate that above 201° there is a pronounced increase in the yields of H<sub>2</sub>, HD, CO and CO<sub>2</sub>. At the low temperatures the rate of production of H<sub>2</sub> is considerably smaller than the rate of formation of CO<sub>2</sub>.

### Discussion

A. **HCOOH.**—The results given in Table I show that the ratios CO/CO<sub>2</sub> obtained in the direct photolysis and in the Hg(<sup>3</sup>P<sub>1</sub>) photosensitized decomposition are comparable to those reported previously. However, the fact that (a) the H<sub>2</sub> yield is in all cases smaller than the CO<sub>2</sub> yield, and (b) the production of H<sub>2</sub> is reduced markedly in the presence of efficient H-atom scavengers, such as C<sub>2</sub>H<sub>4</sub> or O<sub>2</sub>, clearly indicates that processes other than I and II have to be invoked to explain the product distribution.

B. **DCOOH.** (a) **The Primary Process.**—These primary processes have to be considered

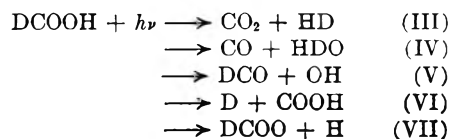


TABLE IV  
 PHOTOLYSIS OF  $CD_3COCD_3$  IN PRESENCE OF  $HCOOH$ 

$T$ °C.	Mole/cc. $\times 10^1$		Rate, cc./min. $\times 10^4$							
	$[CD_3COCD_3]$	$[HCOOH]$	$H_2$	HD	$D_2$	$CD_3H$	$CD_4$	Ethane	CO	$CO_2$
152	0.70	0.70	0.02	0.01	0.002	0.80	0.09	1.89	2.6	0.55
201	.67	.67	.13	.02	.004	1.5	.2	1.13	2.5	1.1
225	.64	.64	.61	.066	.006	2.2	.31	1.01	3.1	1.9
251	.61	.61	2.4	.18	.007	2.4	.50	0.95	3.8	4.7

1. **Intramolecular Rearrangements.**—In the direct photolysis the low yields of HD as compared to those of CO and  $CO_2$  in the presence of scavengers (ethylene and oxygen) indicate that process III cannot account for more than 5% of the over-all yield.

In the  $Hg(^3P_1)$  sensitized experiments it is somewhat more difficult to estimate the relative importance of III, in view of the large quenching cross section of ethylene. It can be seen, however, that even in the absence of ethylene the yield of HD is considerably less than that of  $CO_2$ . Moreover, the yield of  $H_2$  is greatly reduced in the sensitized photolysis of  $HCOOH$  in the presence of oxygen, although that of  $CO_2$  is not diminished. The latter argument is not as conclusive in view of a possible deactivation or reaction of a triplet excited state with oxygen.

The importance of process IV is difficult to estimate. The independence of the yield of CO over a wide temperature range and in the presence of oxygen, can either be explained by the occurrence of process IV<sup>12</sup> or by the decomposition of an excited formyl radical formed in process V. The large yields of  $D_2$  and CO in the full arc experiments as compared to the filtered light runs may be ascribed to the decomposition of excited DCO radicals formed in process V.

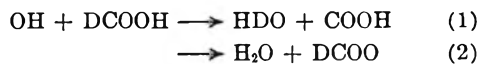
The reduction of the CO yield in the  $Hg(^3P_1)$  sensitized photolysis of  $HCOOH$  in the presence of  $O_2$  may be due to a quenching of process IV or V by oxygen.

It can be deduced from the radiolysis experiments performed in the presence and in the absence of  $I_2$ , that a process such as III is unimportant in the radiolytic decomposition of formic acid. The independence of the CO yield in the radiolysis can be explained in a way similar to that for the case of the direct photolysis.

2. **Dissociative Processes.**—In order to establish the relative importance of the dissociation processes V, VI and VII, a complete understanding of the secondary reaction mechanism is required. However, a few observations can be made. The very small yield of  $H_2$  in the experiments at low temperature can be considered as an indication of the unimportance of process VII. This conclusion is based, however, on the assumption that H atoms will abstract to some extent from the hydroxyl group.

A rough estimate of the number of atoms scavenged by ethylene can be made by taking into consideration the yields of ethane and butane in the direct photolysis of either  $HCOOH$  or  $DCOOH$

in the presence of ethylene. A maximum value for the hydrogen atom yield can be obtained by assuming that two hydrogen atoms are consumed for each butane or ethane molecule formed. It can thus be deduced from the results given in Tables I and II that the expression 2(ethane + butane) is closely comparable to the  $CO_2$  yield corrected for the intramolecular contribution from process III.<sup>13</sup> From this it may tentatively be concluded that only one H or D atom is produced for each  $CO_2$  molecule. These results can best be explained by taking into consideration process V followed by the secondary reactions



and the further decomposition of DCOO and COOH. From the butane yields obtained in the direct photolysis of  $DCOOH-C_2H_4$  mixtures it can be deduced that the steady state concentrations ratio (D/H) is equal to approximately 2.5.<sup>14</sup> This would imply that reaction 2 is faster than reaction 1, or that DCOO is less stable than COOH.

**Secondary Reactions.**—The sharp increase of all products above 202° indicates that a chain reaction takes place under these conditions.<sup>15</sup> The experiments in which acetone has been photolyzed in the presence of  $HCOOH$  lead to the same conclusion. The increase of the rate of formation of CO in the photolysis of  $DCOOH$  can be explained by



followed by a decomposition reaction



The increase of the yield of CO in the photolysis of  $CD_3COCD_3-HCOOH$  mixtures as well as the fact that  $H_2 < CO_2$  in the photolysis of  $HCOOH$  is consistent with this reaction mechanism. Reactions 3, 4 and 5 are comparable to reaction 6 which has been proposed<sup>9</sup> to explain the results obtained in the liquid-phase photolysis of  $HCOOH$



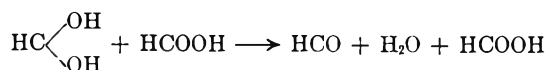
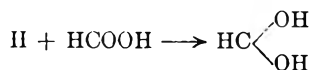
or for reaction sequence such as

(13) The HD yield in the scavenger experiments is here considered as a measure of process III.

(14) This value is based on the assumption that the only fate of the hydrogen atom is addition to ethylene. The fact that an increase in the ethylene concentration (Table II) does not greatly affect the butane or ethane yields indicates that all thermal H or D atoms have been scavenged.

(15) It has been shown in earlier studies<sup>1</sup> that at room temperature the quantum yield for decomposition in the direct photolysis is close to unity. Consequently, the increase in the CO and  $CO_2$  yields cannot be explained by a decomposition of DCO, COOH or DCOO formed in a primary process.

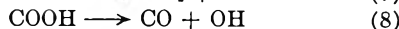
(12) Step IV is analogous to the intramolecular rearrangement of formates into CO and the corresponding alcohol. The latter process has been shown to occur in the liquid-phase direct photolysis<sup>1</sup> and in the  $Hg(^3P_1)$  sensitized decomposition in the vapor phase.<sup>1</sup>



which has been suggested to occur<sup>16</sup> in the radiolysis of aqueous formic acid solutions.

It is rather difficult to distinguish between reaction 6 and a reaction such as 3 or 4. The importance of reaction 6 will greatly depend on the thermal stability of, and the mode of decomposition, of the COOH radical.

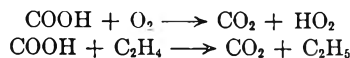
The  $\Delta H$  of the decomposition reactions 7 and 8



can be estimated to be 1 and 26 kcal., respectively.<sup>17</sup> It may thus be assumed that COOH is a thermally unstable species, which decomposes according to reaction 7. The negligible effect of CO<sub>2</sub> on the yields of CO, HD and D<sub>2</sub> in the photolyses of DCOOH at 2° (Table II), as well as the minor effect of scavengers on the yields of CO<sub>2</sub> in the photolysis of DCOOH are consistent with a low activation energy for reaction 7. It should be pointed out, however, that the occurrence of reactions such as

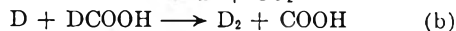
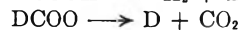
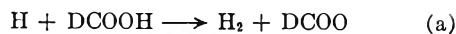
(16) W. J. Garrison, W. Bennett and M. Tayko, *J. Chem. Phys.*, **24**, 631 (1956).

(17) The following values were accepted:  $\Delta H_f^\circ(\text{H}) = 52$ ,  $\Delta H_f^\circ(\text{CO}_2) = -94.1$ ,  $\Delta H_f^\circ(\text{CO}) = -27.2$ ,  $\Delta H_f^\circ(\text{OH}) = 10.1$ ,  $\Delta H_f^\circ(\text{COOH}) = -43.1$ . The heat of formation of COOH was deduced from the bond strength  $D(\text{CH}_3\text{-COOH}) = 93.0$  (G. Glockler, *J. Phys. Chem.*, **62**, 1049 (1958)),  $\Delta H_f^\circ(\text{CH}_3) = 32.5$  and  $\Delta H_f^\circ(\text{CH}_3\text{COOH}) = 103.6$ . A value which is 1 kcal. lower can be obtained using  $D(\text{H-COOH}) = 99.9$  (G. Glockler, *ibid.*, **62**, 1049 (1958)),  $H_f^\circ(\text{HCOOH}) = -90$ . This would lead to a  $\Delta H^\circ$  of 0 and 25 kcal. for reaction 7 and 8, respectively. No matter which value is accepted for  $\Delta H_f^\circ(\text{COOH})$  reaction 8 will always be 25 kcal. more endothermic than reaction 7.

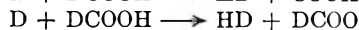
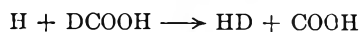


would also be in agreement with the latter observation.

The sharp rise of the rates of formation of H<sub>2</sub>, D<sub>2</sub> and CO<sub>2</sub> above 150° indicates the following two chain mechanisms occur.



It is obvious that HD may be produced by either of the reactions



The invariance of yields of most products at temperatures below 150°, especially at short wave lengths, is, however, more difficult to understand. A plausible explanation can be given, assuming that translationally excited D atoms are produced, which abstract H and D atoms from DCOOH. The hydrogen atoms produced from the subsequent thermal decomposition of COOH and DCOO may at low temperatures react exclusively by reactions 3 and 4, thus preventing a chain process from taking place. The very low H<sub>2</sub> and HD yields in the acetone-HCOOH experiments at temperatures below 200° clearly indicates, in view of the high CO<sub>2</sub> yields, that the thermal H atoms react by a reaction similar to 3, instead of taking part in an H atom abstraction process.

**Acknowledgment.**—The authors wish to express their appreciation to Prof. W. A. Noyes, Jr., for his critical examination of this manuscript prior to publication.

## THE THERMODYNAMIC PROPERTIES OF THE METHYL KETONE SERIES

By J. K. NICKERSON, K. A. KOBE<sup>1</sup> AND JOHN J. MCKETTA

*Department of Chemical Engineering at The University of Texas, Austin, Texas*

*Received March 13, 1961*

The vapor heat capacity and heat of vaporization of methyl ethyl ketone and methyl *n*-propyl ketone have been determined experimentally. Second virial coefficients have been calculated from the Clapeyron relation and these coefficients and heat capacity data have been correlated to determine the parameters for the Stockmayer potential function. Molecular structure, spectroscopic information and vapor heat capacity data were used to evaluate the barriers to internal rotation in the methyl ethyl ketone molecule and to compute tables of the thermodynamic functions for this compound. The thermodynamic functions for the methyl ketone series<sup>2</sup> have been calculated by a method of increments.

As part of a program for the study of the properties of selected industrially important oxygenated hydrocarbons, the vapor heat capacities of methyl ethyl ketone and methyl *n*-propyl ketone have been determined experimentally in a pressure range of one-fourth to seven-fourths atmospheres and a temperature range of 70 to 200°. The heats of vaporization have been measured in a pressure range from one-fourth to seven-fourths atmospheres. Second virial coefficients have been calcu-

lated from the Clapeyron relation and these coefficients and heat capacity data have been correlated to determine the parameters for the Stockmayer potential function. Molecular structure, spectroscopic information from the literature, and vapor heat capacity data herein reported were used to evaluate the barriers to internal rotation in the methyl ethyl ketone molecule and to compute tables of the thermodynamic functions for this compound at selected temperatures from 0 to 1500°K. The thermodynamic functions for methyl *n*-propyl ketone were calculated by a method of increments. This incremental method was then used to pro-

(1) Deceased.

(2) Methyl ketone series here refers to a series which may be represented by CH<sub>3</sub>-CO-R where R is a *n*-paraffin.

vide the thermodynamic functions for the *n*-alkyl methyl ketone series.

### Experimental

**Physical Constants and Definitions.**—The data reported here are based on the 1956 Atomic Weights,<sup>3</sup> the values of the fundamental physical constants reported by Rossini, *et al.*,<sup>4</sup> and the following definitions: 0°C. = 273.15°K. and 1 cal. = 4.1840 abs. joules. Temperatures are on the defined International Temperature Scale.

**Material.**—The sample of methyl ethyl ketone was supplied by Celanese Corporation of America from their reagent stock which was originally purchased from Eastman Kodak Company, listed as catalog number 383 by the latter. This material was about 99% pure with water and secondary butyl alcohol as the chief impurities. The sample of methyl *n*-propyl ketone was supplied by Carbide and Carbon Chemical Company from their reagent stock. Both of these ketones were further purified by storage over anhydrous calcium sulfate followed by distillation in a packed column. The distillates had a boiling range of less than 0.1°. The samples were then vacuum distilled (simple bulb-to-bulb) into receivers for introduction into the apparatus. A blanket of helium was used in the distillation column so the samples never contacted air or water vapor.

No evidence of cracking or polymerization was observed in the course of the experimental work although methyl ethyl ketone undergoes slow condensation between 100 and 200°. The heat capacity was measured at the beginning and end of operations at the same temperature and no change was noted in the values obtained for either compound. The temperature at the surface of the boiling liquid and the temperature in the condensing section of the apparatus were monitored and the results indicated no change in the composition of either compound.

**Apparatus.**—The apparatus used to measure the vapor heat capacities and heats of vaporization was the flow calorimeter used by Pennington and Kobe<sup>6</sup> and the same type described by Waddington, *et al.*<sup>7</sup> and includes the modifications discussed by McCullough, *et al.*<sup>8</sup> Temperature and energy measurements were made with a White Double Potentiometer. The unsaturated type standard cell used with the potentiometer was recently certified by the National Bureau of Standards. The standard resistors used were calibrated against a set of standards maintained by the Department of Physics at The University of Texas. The results of five calibrations in three years varied less than 0.01% from the mean. All the platinum resistance thermometers in the apparatus were calibrated against a platinum resistance thermometer which was certified at the National Bureau of Standards in 1955.

Each value of the vapor heat capacity herein reported was found by measuring the apparent heat capacity at four flow rates and extrapolating to the limiting case. The approximate rates which were used are 0.04, 0.07, 0.12 and 0.22 mole per minute.

**Heat of Vaporization.**—The heat of vaporization of methyl ethyl ketone was determined at five temperatures corresponding to vapor pressures between one-fourth and seven-fourths atmospheres. These values, shown in Table I, are the average of at least three determinations at each temperature and the intervals are maximum deviation from the mean. The accuracy uncertainty of the values reported is estimated at not greater than 0.1%. These data may be represented within the accuracy uncertainty by the relationship

$$\Delta H_v = 921.1(535.7 - T)^{0.402} \quad (1)$$

where  $\Delta H_v$  is in cal. mole<sup>-1</sup> and  $T$  is in degrees Kelvin.<sup>9</sup>

(3) E. Wichers, *J. Am. Chem. Soc.*, **78**, 3235 (1956).

(4) F. D. Rossini, F. T. Gucker, H. L. Johnston, L. Pauling and G. W. Vinal, *ibid.*, **74**, 2699 (1952).

(5) Shell Chemical Corporation, "Methyl Ethyl Ketone," 63-64, Shell Chemical Corporation, New York, 1950.

(6) Robert E. Pennington and Kenneth A. Kobe, *J. Am. Chem. Soc.*, **79**, 300 (1957).

(7) (a) G. Waddington, S. S. Todd and H. M. Huffman, *ibid.*, **69**, 22 (1947) and (b) G. Waddington and D. R. Douslin, *ibid.*, **69**, 2275 (1947).

(8) J. P. McCullough, D. W. Scott, R. E. Pennington, I. A. Hossenlopp and G. Waddington, *ibid.*, **76**, 4791 (1954).

TABLE I

### THE MOLAL HEAT OF VAPORIZATION OF METHYL ETHYL KETONE

Temp., °K.	Pressure, mm. <sup>2</sup>	$\Delta H_v$ , cal.
314.61	188.7	8069 ± 1
338.69	475.3	7005 ± 1
352.54	758.3	7476 ± 1
362.58	1029.7	7308 ± 5
370.57	1299.2	7180 ± 2

<sup>a</sup> Vapor pressures were calculated from the equation<sup>5</sup>  $\log P = 21.78963 - 2441.9/T - 4.70504 \log T$ .

Values for the heat of vaporization of methyl ethyl ketone at its normal boiling point have been reported by earlier investigators and are presented in Table II for easy comparison. It may be pointed out that values for the heat of vaporization determined with a flow calorimeter have been found to be lower than values measured by other means or derived from other methods. For example, Bennewitz and Rossner<sup>10</sup> reported a value for the heat of vaporization of acetone that was 3.0% higher than the value reported by Pennington and Kobe,<sup>6</sup> and Matthews<sup>11</sup> reported a value that was 2.0% higher.

TABLE II

### SELECTED VALUES OF THE HEAT OF VAPORIZATION OF METHYL ETHYL KETONE AT 79.50°, CAL. MOLE<sup>-1</sup>

$\Delta H_v$	% Deviation from 7476	Ref.	Method of determin.
7830	4.7	Bennewitz and Rossner <sup>10</sup>	Measd. directly
7619	1.9	Matthews <sup>11</sup>	Measd. directly, accuracy estimated as 1%
7600	1.7	Felsing, Shofner and Garlock <sup>14</sup>	Calcd. from vapor pressure data using Clapeyron relation
7476	0.0	This research	Measd. directly, accuracy estimated as 0.1%

The heat of vaporization of methyl *n*-propyl ketone was determined at five temperatures corresponding to vapor pressures between one-fourth and seven-fourths atmospheres. These values, shown in Table III, are the average of at least three determinations at each temperature and the intervals are the maximum deviation from the mean. The accuracy uncertainty of the values reported is estimated as not greater than 0.2%. These data may be represented within the accuracy uncertainty by the relationship

$$\Delta H_v = 1053.5(564.0 - T)^{0.357} \quad (2)$$

where  $\Delta H_v$  is in cal. mole<sup>-1</sup> and  $T$  is in °K.<sup>12</sup>

**Vapor Heat Capacity.**—The vapor heat capacity of methyl ethyl ketone was determined at five temperatures ranging from 347.2 to 467.2°K. selected pressures between one-fourth and seven-fourths atmospheres. The results are presented in Table IV. The accuracy uncertainty of these data is estimated as being not greater than 0.2%.

A value of the heat capacity has been reported by Bennewitz and Rossner<sup>10</sup> as being equal to 29.8 cal. mole<sup>-1</sup> at 410°K. This compares with a value of 31.0 cal. mole<sup>-1</sup> found by this research.

The vapor heat capacity of methyl *n*-propyl ketone was determined at five temperatures ranging from 369 to 454°K. at selected pressures between one-fourth and seven-fourths atmospheres. The results are presented in Table V. The accuracy uncertainty of these data is estimated as being not greater than 0.3%.

(9) The constant 535.7 in eq. 1 is the value of the critical temperature in °K. reported by K. A. Kobe, H. R. Crawford and R. W. Stephenson, *Ind. Eng. Chem.*, **47**, 1767 (1955).

(10) K. Bennewitz and W. Rossner, *Z. physik. Chem.*, **B39**, 126 (1938).

(11) J. H. Matthews, *J. Am. Chem. Soc.*, **56**, 2682 (1934).

(12) The constant 564.0 in eq. 2 is the value of the critical temperature in °K. reported in reference 9.



TABLE III

THE MOLAL HEAT OF VAPORIZATION OF METHYL *n*-PROPYL KETONE

Temp., °K.	Pressure, mm. <sup>a</sup>	$\Delta H_v$ , cal.
334.87	187.0	8636 ± 6
360.56	474.9	8229 ± 8
375.33	757.8	7979 ± 7
386.04	1035.7	7825 ± 2
394.57	1309.6	7685 ± 3

<sup>a</sup> Vapor pressures were calculated from the equation:  $\log P = 7.02825 - 1313.9/(214.52 + t)$  where  $P$  is in mm. and  $t$  is in °C.

TABLE IV

THE MOLAL HEAT CAPACITY OF METHYL ETHYL KETONE VAPOR IN CALORIES PER DEGREE

Temp., °K.	347.15	372.15	397.15	432.15	467.15
$C_p$ (1299.2 mm.)			31.32	32.17	33.54
$C_p$ (1029.7 mm.)		30.21	30.80		
$C_p$ (758.3 mm.)		29.71	30.52	31.84	33.55
$C_p$ (475.3 mm.)	28.46	29.19	30.21		
$C_p$ (188.7 mm.)	27.63	28.75	29.91	31.57	33.19
$C_p^0$	27.11	28.45	29.73	31.48	33.13
-TB'' (obsd.) <sup>a</sup>	2.04	1.19	0.74	0.36	0.22
-TB'' (calcd.) <sup>a</sup>	1.96	1.26	0.84	0.52	0.35

<sup>a</sup> -TB'' is equal to the limiting value of  $(\partial C_p/\partial P)_T$  at zero pressure. The units are cal. deg.<sup>-1</sup> mole<sup>-1</sup> atm.<sup>-1</sup>.

TABLE V

THE MOLAL HEAT CAPACITY OF METHYL *n*-PROPYL KETONE VAPOR IN CALORIES PER DEGREE

Temp., °K.	369.00	394.00	414.00	434.00	454.00
$C_p$ (1309.6 mm.)			39.31	40.05	41.03
$C_p$ (1035.7 mm.)			38.79		
$C_p$ (757.8 mm.)		37.25	38.37	39.44	40.61
$C_p$ (474.9 mm.)	35.44	36.79	38.03		
$C_p$ (187.0 mm.)	34.65	36.32	37.60	38.93	40.10
$C_p^0$	34.17	36.00	37.38	38.72	39.95
-TB'' (obsd.) <sup>a</sup>	2.01	1.26	1.00	0.77	0.63
-TB'' (calcd.) <sup>a</sup>	2.14	1.42	1.03	0.77	0.61

<sup>a</sup> -TB'' is equal to the limiting of  $(\partial C_p/\partial P)_T$  at zero pressure. The units are cal. deg.<sup>-1</sup> mole<sup>-1</sup> atm.<sup>-1</sup>.

### Correlation of the Effects of Gas Imperfection

**Second Virial Coefficient from Heats of Vaporization.**—The heats of vaporization may be used to calculate the second virial coefficient from the Clapeyron relation when suitable vapor pressure data are available. For methyl ethyl ketone the vapor pressure data of the Shell Corporation<sup>5</sup> were selected as the most reliable and have been summarized in the equation

$$\log P = 21.78963 - 2441.9/T - 4.70504 \log T \quad (3)$$

where  $P$  is in mm. and  $T$  is in degree Kelvin. This expression may be differentiated and used in the Clapeyron relation to calculate the virial coefficients at each temperature at which the heat of vaporization was measured.

The Shell vapor pressure data were chosen from those reported<sup>5,13,14</sup> because the values for the pressure calculated from equation 3 more closely approached the vapor pressures measured with the flow calorimeter apparatus in this research.

Precise vapor pressure data for methyl *n*-propyl ketone in the desired pressure range could not be found in the literature. In order to evaluate the

(13) R. R. Dreisbach and S. A. Shrader, *Ind. Eng. Chem.*, **41**, 2870 (1949).

(14) (a) W. A. Felsing, I. Shofner and N. B. Garlock, *J. Am. Chem. Soc.*, **56**, 2252 (1934); (b) M. G. Mayberry and J. G. Aston, *ibid.*, **56**, 2682 (1934).

virial coefficients, the vapor pressure data measured with the flow calorimeter were fit to the Antoine equation so that the sum of the squares of the deviations was a minimum. Although the accuracy uncertainty of the data is estimated as only 2 mm., the accuracy of the rate of change of pressure with temperature is sufficient to give good results when used in the Clapeyron relation. The values for the virial coefficient calculated by this means have a reasonable order of magnitude and the plot *versus* temperature has a typical shape. In view of the extreme sensitivity of  $B$  to  $dP/dT$ , these values of  $B$  indicate that the expression for  $dP/dT$  does not contain any great inaccuracies. The following Antoine equation was used

$$\log P = 7.02825 - 1313.9/(214.52 + t) \quad (4)$$

where  $P$  is in mm. and  $t$  is in °C.

**Heat Capacity in the Ideal Gas State.**—The expression for the heat capacity of a real gas may be derived from the thermodynamic relationship

$$[C_p - C_p^0 = - \int_0^P T(\partial^2 V/\partial T^2)_{PdP}]_T \quad (5)$$

and the following equation of state

$$PV/RT = 1 + B/V \quad (6)$$

The indicated substitution and simplification result in

$$C_p = C_p^0 - TB''P + R[T/V]^2[BB'' + V(B' - B/T)^2/(V + 2B)] \quad (7)$$

where the primes represent differentiation with respect to temperature. The right-hand term of equation 7 which is non-linear in  $P$  is very small compared to the other terms. In the treatment of the data the non-linear term is estimated and subtracted from  $C_p$ . The slope of the resulting straight line is  $-TB''$  which in turn may be used to calculate more accurately the non-linear term. Thus by iteration a final equation may be found which represents the data. The curves in Fig. 1 and 2 demonstrate the ability to represent gas imperfections using only the second virial in correlating the heat capacity data. The calculated values were obtained by adding the final calculated non-linear terms to the observed values of  $-TB''P$ .

**Intermolecular Potential Energy.**—The values of  $B$ , calculated from the Clapeyron relation and heats of vaporization, and the values of the observed  $-TB''$  given in Tables IV and V were used to select the parameters of Stockmayer potential functions.<sup>15</sup> This function makes use of three parameters:  $t^*$ ,  $E$  and  $b_0$ . However, only two parameters are independent since one is a function of the other and the dipole moment. The value selected for the dipole moment of methyl ethyl ketone was 3.18 debyes.<sup>16</sup> The only value reported for methyl *n*-propyl ketone is 2.75 debyes,<sup>17</sup> and this source gives 2.75 debyes as the value of the dipole moment for all ketones. In view of this, a value for the dipole moment of methyl *n*-propyl ketone was selected to give the best fit to the experimental values of  $B$  and  $-TB''$ .

(15) W. H. Stockmayer, *J. Chem. Phys.*, **9**, 398 (1941).

(16) C. J. F. Botcher, *Physica*, **6**, 59 (1939).

(17) Claude Cherrier, *Compt. rend.*, **225**, 997 (1947).

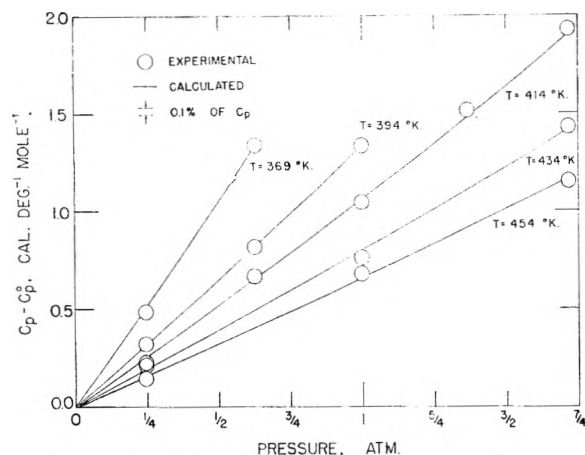


Fig. 1.—The vapor heat capacity of methyl ethyl ketone as a function of pressure.

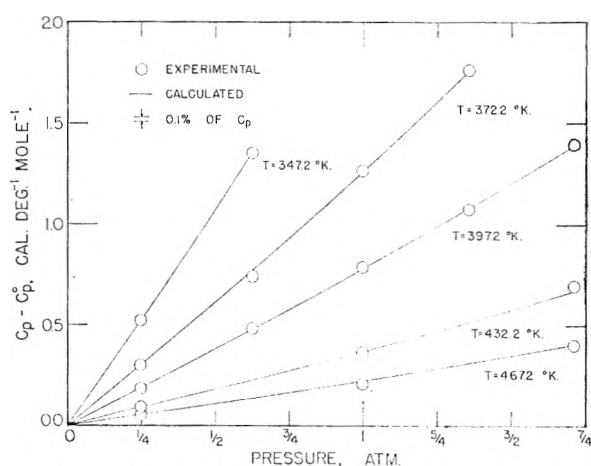


Fig. 2.—The vapor heat capacity of methyl *n*-propyl ketone as a function of pressure.

The values of the constants for methyl ethyl ketone were found to be

$$\begin{aligned} t^* &= 0.9 \\ E &= 852 \text{ cal. mole}^{-1} \\ b_0 &= 84.60 \text{ cc. mole}^{-1} \end{aligned}$$

The calculated values of  $-TB''$  are compared with the observed values in Table IV and the calculated values of  $B$  are compared with experimentally measured values in Table VI. The large percentage difference between the calculated and observed values of  $-TB''$  is due in part to the small absolute value of  $-TB''$  and to the extreme sensitivity of  $-TB''$  to heat capacity. For example, at 190° the observed value of  $-TB''$  may be changed from 0.22 to 0.32 cal. deg.<sup>-1</sup> mole<sup>-1</sup> atm.<sup>-1</sup> by raising the values of  $C_p$  at 1299.2 and 758.3 mm., 0.1 and 0.05%, respectively. In view of this sensitivity and the fact that only two parameters are used, representation by the Stockmayer function is good.

The values of the constants for methyl *n*-propyl ketone were found to be

$$\begin{aligned} t^* &= 0.4 \\ E &= 850 \text{ cal. mole}^{-1} \\ b_0 &= 59.53 \text{ cc. mole}^{-1} \end{aligned}$$

The value of the dipole moment that corresponds to this set of constants is 2.46 debyes. The calcu-

TABLE VI  
CALCULATED AND EXPERIMENTAL SECOND VIRIAL COEFFICIENTS, CUBIC CENTIMETERS PER MOLE

	Temp., °K.	$-B$ (exptl.)	$-B$ (calcd.)
Methyl ethyl ketone	314.61	1968	2040
	338.69	1589	1538
	352.54	1362	1350
	362.58	1228	1220
	370.57	1130	1124
Methyl <i>n</i> -propyl ketone	334.87	2635	2375
	360.56	1760	1796
	375.33	1540	1563
	386.04	1377	1388
	394.57	1280	1288

lated and observed values of  $-TB''$  and  $B$  are compared in Table V and Table VI, respectively.

TABLE VII

FUNDAMENTAL VIBRATIONAL FREQUENCIES FOR 2-THIABUTANE AND METHYL ETHYL KETONE

—CH <sub>2</sub> -S-CH <sub>2</sub> -CH <sub>3</sub> —		—CH <sub>2</sub> -CO-CH <sub>2</sub> -CH <sub>3</sub> —	
Designation	Frequency	Frequency	Designation
C-S-C bend	216	260	C-C-C bend
C-C-S bend	355	406	C-C-C bend
		515	C=C=O bend
		598	C=C=O bend
C-S stretch	679	760	C-C stretch
CH <sub>2</sub> rock	727	760	CH <sub>2</sub> rock
C-S stretch	757	1175	C-C stretch
CH <sub>3</sub> rock	956	1000	CH <sub>3</sub> rock
C-C stretch	973	947	C-C stretch
CH <sub>3</sub> rock	1042	1000	CH <sub>3</sub> rock
CH <sub>3</sub> rock	1062	1090	CH <sub>3</sub> rock
CH <sub>3</sub> rock	1098	1090	CH <sub>3</sub> rock
CH <sub>2</sub> wag	1264	1205	CH <sub>2</sub> wag
CH <sub>2</sub> twist	1311	1255	CH <sub>2</sub> twist
CH <sub>3</sub> bend	1323	1365	CH <sub>3</sub> bend
CH <sub>3</sub> bend	1378	1365	CH <sub>3</sub> bend
CH <sub>2</sub> def	1435	1355	CH <sub>2</sub> def
CH <sub>3</sub> def	1435 [2]	1420 [2]	CH <sub>3</sub> def
CH <sub>3</sub> def	1435 [2]	1460 [2]	CH <sub>3</sub> def
		1710	C=O stretch
C-H stretch	2950 [8]	2950 [8]	C-H stretch

#### Calculation of the Thermodynamic Properties of Methyl Ethyl Ketone

In order to compute the thermodynamic functions for methyl ethyl ketone the following preliminary steps were necessary: (1) molecular structure was used to calculate the over-all moments of inertia and the reduced moments of inertia for internal rotations; (2) fundamental vibrational assignments were made from observed infrared and Raman spectral data; and (3) functions for the potential barrier height to internal rotation were chosen so that the calculated values of the vapor heat capacity agreed with the experimental values.

**Rotational Constants.**—Skeletal bond lengths and angles in the methyl ethyl ketone molecule have been reported by Romers and Creutzberg<sup>18</sup> as follows: 1.24 Å. for the C=O bond length, 1.525 Å. for the C-C bond lengths, 1.09 Å. for the C-H bond lengths, 118.5° for the C-C=O angles, and

(18) C. Romers and J. E. G. Creutzberg, *Rec. trav. chim.*, 75, 331 (1956).

tetrahedral angles in the methyl groups. Two rotational isomers of methyl ethyl ketone are possible—the *trans* or extended configuration of  $C_s$  symmetry and the *skew* or *gauche* configuration of  $C_1$  symmetry. However, there is evidence that only one form, that of  $C_s$  symmetry, exists in any appreciable quantity at ordinary temperatures. This form of the molecule, in which the carbon and oxygen atoms are coplanar, was therefore used as a basis for all the calculations.

The evidence for this choice follows: (1) Only six bands appear in the spectra between 200 and 800  $\text{cm}^{-1}$ . If two forms of the molecule existed more bands should be found in this region. (2) Sirkar and Bishui<sup>19</sup> concluded that the molecule has a plane of symmetry because certain bands in Raman spectra were found to be totally depolarized. (3) Electron diffraction studies and approximate calculations led Romers and Creutzberg<sup>18</sup> to describe the structure of methyl ethyl ketone in the vapor state as a configuration in which the oxygen atom is coplanar with a zigzag chain of carbon atoms.

The set of structural parameters indicated above were used in the procedure described by Kilpatrick and Pitzer<sup>20</sup> to calculate the moments of inertia.

The product of the three principal moments of inertia for over-all rotation was calculated to be  $5961 \times 10^{-117} \text{ g.}^3 \text{ cm.}^6$ . The moments of inertia for internal rotation were found to be  $4.996 \times 10^{-40}$ ,  $5.037 \times 10^{-40}$  and  $25.161 \times 10^{-40} \text{ g. cm.}^2$  for  $\text{CH}_3\text{-CO}$ ,  $\text{CH}_3\text{-CH}_2$  and skeletal rotation, respectively.

**Vibrational Assignment and Barriers to Internal Rotation.**—Before the thermal data could be used to obtain information about the barriers hindering internal rotation an adequate vibrational assignment was necessary. Raman<sup>19,21-24</sup> and infrared<sup>25-27</sup> data were selected from the observed spectra presented in the literature and vibrational frequencies for this molecule were assigned as shown in Table VII. Each frequency has been designated as a particular mode of vibration in the molecule in order to make the presentation clear and orderly. However, since the assignment has been made to calculate the vibrational contribution to the thermodynamic functions, only the number and magnitude of the frequencies are important and inaccurate designations will not affect the results of the calculation.

Assuming a predominant concentration of one rotational isomer, there should appear in the 200–800  $\text{cm}^{-1}$  region of the spectra four skeletal bending, one C–C stretch and one  $\text{CH}_2$  rocking frequencies, or a total of six frequencies. Only five

strong lines have been observed and Kohlrausch<sup>21</sup> reports a zero intensity line at 812  $\text{cm}^{-1}$ . The latter has been interpreted as a combination of frequencies or the second harmonic of 406  $\text{cm}^{-1}$ .

Thompson and Torkington,<sup>27</sup> Titeica<sup>24</sup> and Lecompte, Gray and Taboury<sup>23</sup> all have assigned the lines at 406, 515, 598 and 760  $\text{cm}^{-1}$  as C–C bend, C–C=O bend, C–C=O bend and C–C stretch, respectively. The line at 260  $\text{cm}^{-1}$  reported by Sirkar and Bishui<sup>19</sup> and Kohlrausch and Koppl<sup>21</sup> has been assigned as a C–C–C bending frequency, and the  $\text{CH}_2$  rocking frequency which should appear around 700  $\text{cm}^{-1}$  was assumed to have an accidental degeneracy with the C–C stretch at 760  $\text{cm}^{-1}$ .

Thompson and Torkington<sup>27</sup> assign 947 and 1170  $\text{cm}^{-1}$  as C–C stretch frequencies and 1090  $\text{cm}^{-1}$  as a  $\text{CH}_3$  rocking frequency. The weak lines at 1030, 1110, 1220, 1292 and 1499  $\text{cm}^{-1}$  have been interpreted as combinations of fundamental frequencies or results caused by impurities in the samples. An average value of 2950  $\text{cm}^{-1}$  has been used for the thermodynamically unimportant C–H stretch frequencies.

In Table VII the vibrational assignment for 2-thiabutane ( $\text{CH}_3\text{-S-C}_2\text{H}_5$ ) presented by Scott, *et al.*,<sup>28</sup> is compared with the author's assignment for methyl ethyl ketone. The similarity between the two molecules indicates that the assigned fundamental frequencies should be of the same order of magnitude, which in fact is the case.

There are three internal rotations in the methyl ethyl ketone molecule—two methyl rotations and one ethyl rotation. The  $\text{CH}_3\text{-CO}$  rotation is similar to the methyl rotation in acetone<sup>29</sup> and the potential hindering this rotation was assumed to be the same, *i.e.*,  $V = 1000/2(1 + \cos 3\phi)$ . The  $\text{CH}_3\text{-CH}_2$  rotation would normally be hindered by a three-fold cosine barrier with a height of about 3000 cal. mole<sup>-1</sup>. However, in order to explain the high predominance of the *trans* form of the molecule an attractive force was assumed between the oxygen and the methyl group which is attached to the methylene group. This force may be represented by a value of 600 cal. mole<sup>-1</sup> which is then subtracted from the 3000 cal. mole<sup>-1</sup> to give a new barrier height of 2400 cal. mole<sup>-1</sup>. The model of an equilibrium between rotational isomers was used to evaluate the contribution for the rotation of the ethyl group. The barrier for rotation of the *trans* form was assumed to be 1000 cal. mole<sup>-1</sup> which is the same as in acetone. The energy of the *trans* to *skew* reaction was assumed to be 700 cal. mole<sup>-1</sup> (the value found in butane<sup>30</sup>) plus the value which is a measure of the attractive force between oxygen and the extended methyl group. This value, which was noted above as 600 cal. mole<sup>-1</sup>, was selected to give the best fit between calculated and experimental data. Therefore only one parameter was used to fit the data.

With the parameters which have been selected and in the experimental temperature range, the

- (19) S. C. Sirkar and B. M. Bishui, *Indian J. Phys.*, **20**, 35 (1946).  
 (20) J. E. Kilpatrick and K. S. Pitzer, *J. Chem. Phys.*, **17**, 1064 (1949).  
 (21) K. W. F. Kohlrausch and F. Koppl, *Z. physik. Chem.*, **B24**, 370 (1923).  
 (22) P. Koteswaram, *Indian J. Phys.*, **14**, Pt. 5, 341 (1941).  
 (23) J. Lecompte, E. Gray and F. J. Taboury, *Bull. soc. chim. France*, **774** (1947).  
 (24) R. Titeica, *Ann. Phys.*, [11] **1**, 533 (1934).  
 (25) C. Cherrier, *Compt. rend.*, **225**, 997 (1947).  
 (26) J. Lecompte, M. Josien and J. Lascombe, *Bull. soc. chim. France*, **163** (1956).  
 (27) H. W. Thompson and P. Torkington, *J. Chem. Soc.*, **640** (1945).

- (28) D. W. Scott, H. L. Finke, J. P. McCullough, M. E. Gross, K. D. Williamson, G. Waddington and H. M. Huffman, *J. Am. Chem. Soc.*, **73**, 261 (1951).  
 (29) R. E. Pennington and K. A. Kobe, *ibid.*, **79**, 300 (1957).  
 (30) N. Sheppard and G. J. Szasz, *J. Chem. Phys.*, **17**, 86 (1949).

calculated values represent the experimental values within the accuracy uncertainty of 0.2%, as shown in Table VIII. The molal entropy of liquid methyl ethyl ketone at 25° herein calculated is compared with the Third Law value reported by Parks, *et al.*<sup>31</sup> in Table IX. The agreement is an indication of the reliability of the calculations in the lower range of temperature.

TABLE VIII

CALCULATED AND OBSERVED VALUES OF THE MOLAL HEAT CAPACITY OF METHYL ETHYL KETONE IN CALORIES PER

Temp., °K.	$C_p^0$ (obsd.)	$C_p^0$ (calcd.)
347.15	27.11	27.10
372.15	28.45	28.41
397.15	29.73	29.69
432.15	31.48	31.46
467.15	33.13	33.17

<sup>a</sup> Maximum deviation between calculated and observed is 0.14%. Average deviation between calculated and observed is 0.10%.

TABLE IX

THE MOLAL ENTROPY OF LIQUID METHYL ETHYL KETONE AT 298.15°K. IN CALORIES PER DEGREE

$S^0$	82.51 <sup>a</sup>
Expansion to $P = 0.1192$ atm. <sup>b</sup>	4.23
Gas imperfection	- 0.15 <sup>c</sup>
$\Delta S_V$	-27.87 <sup>d</sup>
$S$ (liquid)	58.72
Third Law $S$ (liquid)	57.7 ± 0.6 <sup>e</sup>

<sup>a</sup> The calculated standard entropy of gaseous methyl ethyl ketone. <sup>b</sup> Calculated with equation 3. <sup>c</sup> Calculated with the parameters for the second virial coefficient evaluated here and the tables of D. R. Douslin and G. Waddington, *J. Chem. Phys.*, **23**, 2453 (1955) and J. O. Hirschfelder, C. F. Cuttriss and R. B. Bird, "Molecular Theory of Gases and Liquids," John Wiley and Sons, New York, N. Y., 1954, p. 1147-53. <sup>d</sup> Calculated with equation 1. <sup>e</sup> Reference 30.

**Thermodynamic Functions.** The vibration assignment, product of principal moments of inertia, reduced moments of inertia of internal rotating groups, barriers to internal rotation and the energy difference between rotational isomers discussed above were used to compute the values of the thermodynamic functions of methyl ethyl ketone in the ideal gas state at selected temperatures from 0 to 1500°K. and are presented in Table X.

The harmonic oscillator contributions were calculated on the IBM 650 computer at The University of Texas. Restricted rotations were calculated from the tables of Pitzer and Gwinn.<sup>32</sup>

The value for the heat of combustion of methyl ethyl ketone reported by Parks, Mosley and Peterson<sup>33</sup> and the values of the heats of formation of water and carbon dioxide<sup>34</sup> were used to compute the heat of formation of methyl ethyl ketone in the reaction at 298.15°K. The heat of formation

(31) G. S. Parks, W. D. Kennedy, R. E. Gates, J. R. Mosley, G. E. Moore and M. L. Renquist, *J. Am. Chem. Soc.*, **78**, 56 (1956).

(32) K. S. Pitzer and W. D. Gwinn, *J. Chem. Phys.*, **10**, 428 (1942).

(33) G. S. Parks, J. R. Mosley and P. V. Peterson, Jr., *ibid.*, **18**, 152 (1950).

(34) D. D. Wagman, J. E. Kilpatrick, W. J. Taylor, K. S. Pitzer and F. D. Rossini, *J. Research Natl. Bur. Standards*, **34**, 143 (1945).



at 298.15°K., the thermodynamic functions in Table X, and the thermodynamic functions of hydrogen, carbon and oxygen<sup>34</sup> were used to compute values of the heat of formation, free energy of formation, and logarithm of the equilibrium constant of formation of methyl ethyl ketone at selected temperature from 0 to 1500°K. These data are presented in Table X.

### Calculation of the Thermodynamic Properties of the Methyl Ketone Series

It has been the aim of this work to measure the vapor heat capacities of methyl ethyl ketone and methyl *n*-propyl ketone and to establish a systematic procedure that will extend the heat capacity data to higher members of the homologous series of methyl alkyl ketones. The other thermodynamic functions can likewise be extended. Because the statistical method of calculations is so complex when applied to a large molecule like methyl *n*-propyl ketone, the thermodynamic functions of the latter have been calculated by a method of increments.

**Method of Increments.**—When a *n*-alkyl group in a molecule is lengthened by  $-CH_2-$ , the change in a thermodynamic function is called the  $CH_2$  increment. These increments are independent of the length of the *n*-alkyl chain and of the type of groups which make up the rest of the molecule. Therefore when the thermodynamic properties are known for several lower members of a homologous series, the properties of the higher members may be estimated if suitable  $CH_2$  increments are chosen. As the length of the chain grows the  $CH_2$  increments tend to become constant and approach the values of the standard  $CH_2$  increments<sup>35</sup> in the *n*-paraffin series. Then at a given temperature the heat capacity of methyl *n*-propyl ketone may be expressed as the sum of the heat capacity of methyl ethyl ketone plus the standard  $CH_2$  increment for heat capacity plus a new increment  $I$ . It was found that  $I$  can be represented over the experimental temperature range by the function

$$I = -229.3e^{-0.01612T} \quad (8)$$

This form of equation was chosen not only because it represented the experimental data, as shown in Table XI, but also because the magnitude of  $I$  becomes small as temperature increases. In fact above 600°K. the contribution of  $I$  is negligible. It is reasonable that this "correction" for the  $CH_2$  increment should approach zero at the higher temperatures where more ideal behavior may be expected.

The values for the heat capacity were calculated at the five temperatures where experimental measurements were made and at 100° intervals between 500 and 1500°K. inclusive. These results were fitted to a fifth order polynomial which goes through the origin so that the sum of the squares of the deviations was a minimum. The vapor heat capacity of methyl *n*-propyl ketone may thus be expressed by

(35) W. B. Person and G. C. Pimentel, *J. Am. Chem. Soc.*, **75**, 532 (1953).

TABLE X

THE MOLAL THERMODYNAMIC FUNCTIONS OF METHYL ETHYL KETONE IN THE IDEAL GAS STATE<sup>a</sup>

$T$ , °K.	$C_p^0$ , cal. deg. <sup>-1</sup>	$S^0$ , cal. deg. <sup>-1</sup>	$(H^0 - H_0^0)/T$ , cal. deg. <sup>-1</sup>	$H^0 - H_0^0$ , kcal.	$-(F^0 - H_0^0)/T$ , cal. deg. <sup>-1</sup>	$-\Delta F_{f0}^0$ , <sup>b</sup> kcal.	$\Delta F_{f0}^0$ , <sup>b</sup> kcal.	$\log H^0$ <sup>b</sup>
0	0	0	0	0	0	53.21	-53.21	Infinite
273.15	23.29	80.48	16.02	4.377	64.45	57.81	-38.41	30.73
298.15	24.56	82.51	16.69	4.975	65.83	58.37	-36.82	27.00
300	24.65	82.66	16.74	5.021	65.92	58.40	-36.69	26.73
400	29.84	90.28	19.36	7.742	70.92	59.80	-29.16	15.93
500	34.71	97.37	21.96	10.98	75.21	60.99	-21.31	9.31
600	39.02	104.03	24.45	14.67	80.31	61.99	-13.24	4.82
700	42.75	110.29	26.80	18.76	83.49	62.79	-5.02	1.57
800	46.00	116.19	29.01	23.21	87.18	63.40	+3.30	-0.90
900	48.82	121.76	31.05	27.95	90.70	63.87	11.68	-2.84
1000	51.27	127.01	32.95	32.95	94.06	64.17	20.11	-4.40
1100	53.39	132.00	34.72	38.19	97.28	64.34	28.55	-5.67
1200	55.22	136.72	36.36	43.63	100.36	64.40	37.02	-6.74
1300	56.82	141.20	37.87	49.24	103.32	64.41	45.48	-7.65
1400	58.21	145.45	39.28	54.99	106.18	64.35	53.82	-8.42
1500	59.42	149.51	40.58	60.87	108.93	64.23	62.38	-9.09

<sup>a</sup> In order to maintain internal consistency and incremental accuracy, the values in this table are given to more significant figures than are justified by their absolute accuracy. <sup>b</sup> The standard heat, standard free energy and common logarithm of the equilibrium constant for the formation of methyl ethyl ketone by the reaction



TABLE XI

CALCULATED AND OBSERVED VALUES OF THE MOLAL HEAT CAPACITY OF METHYL *n*-PROPYL KETONE IN CALORIES PER

Temp., °K.	DEGREE <sup>a</sup>	
	$C_p^0$ (obsd.)	$C_p^0$ (calcd.)
369.0	34.17	34.25
394.0	36.00	36.01
414.0	37.38	37.37
434.0	38.72	38.69
454.0	39.95	39.98

<sup>a</sup> Maximum deviation between calculated and observed is 0.23%. Average deviation between calculated and observed is 0.09%.

$$C_p = 0.11649T - 7.1091 \times 10^{-5}T^2 + 1.8810 \times 10^{-8}T^3 - 5.9485 \times 10^{-12}T^5 \quad (9)$$

**Thermodynamic Functions.**—The thermodynamic functions for methyl *n*-propyl ketone are presented in Table XII. The values for the heat capacity in Table XI were calculated from equation 9.

The value for the entropy of methyl *n*-propyl ketone at 1500°K. was found by adding the standard CH<sub>2</sub> increment<sup>35</sup> for entropy to the value of the entropy of methyl ethyl ketone. The entropies at the other temperatures were derived from the value at 1500°K. and proper manipulation and integration of equation 9. Although this procedure is approximate for evaluating the absolute entropy, differences derived from entropy values in Table XII represent the best values which can be derived from the experimental data. The values for the

TABLE XII

THE THERMODYNAMIC FUNCTIONS OF METHYL *n*-PROPYL KETONE IN THE IDEAL GAS STATE

Temp., °K.	$C_p^0$	$S^0$	$(H^0 - H_0^0)/T$	$-(F^0 - H_0^0)/T$
0	0	0	0	0
273.15	26.90	89.16	15.23	73.93
298.15	28.91	91.61	16.37	75.24
300.00	29.06	91.79	16.46	75.33
400	36.42	101.18	20.80	80.38
500	42.80	110.01	24.77	85.24
600	48.32	118.31	28.41	89.90
700	53.06	126.13	31.75	94.38
800	57.13	133.48	34.80	98.68
900	60.62	140.42	37.59	102.83
1000	63.61	146.97	40.14	106.83
1100	66.20	153.15	42.49	110.66
1200	68.44	159.01	44.64	114.37
1300	70.41	164.57	46.62	117.95
1400	72.16	169.85	48.46	121.39
1500	73.75	174.89	50.16	124.73

thermodynamic properties of methyl *n*-butyl ketone may be estimated by adding the values of the standard CH<sub>2</sub> increments<sup>35</sup> to the values of methyl *n*-propyl ketone. The thermodynamic functions of the higher members of the methyl ketone series may be predicted by extension of the same method.

**Acknowledgment.**—Part of this work was carried out under an Esso Research and Engineering Company Grant. The authors are grateful for the interest and support of the donor company.

# NOTES

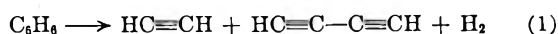
## SOME KINETICS OF THE CARBONIZATION OF BENZENE, ACETYLENE AND DIACETYLENE AT 1200°

By R. S. SLYSH AND C. R. KINNEY

Department of Fuel Technology, The Pennsylvania State University, University Park, Pa.

Received August 4, 1960

When benzene is heated to 1200° in a helium stream at a concentration of 0.1 mole % and at residence times of 4 milliseconds, the primary products of decomposition are mainly a molecule each of acetylene, diacetylene and hydrogen,<sup>1</sup> reaction 1.



The kinetics of this reaction are complicated by the fact that about 12% of biphenyl is also produced. No doubt dissociation of a hydrogen atom from benzene is a primary reaction and it is probable that the phenyl radical produced undergoes further decomposition which results in acetylene and diacetylene. Because no proof of the reaction mechanism was obtained, no mechanism will be suggested. However, the fact that no six-carbon, open-chain product was observed by gas chromatography may be of significance. Both acetylene and diacetylene decompose at 1200°; this is of interest in connection with the decomposition of benzene. Consequently, kinetic data for these hydrocarbons also are included.

### Experimental

The kinetics of the pyrolysis of benzene, acetylene and diacetylene were studied in apparatus described previously.<sup>1</sup> Essentially the procedure was to pass the hydrocarbon in a helium stream through a porcelain tube 20 cm. by 5 mm. inside diameter. The tube was heated by a platinum resistance furnace which was regulated by a recording temperature controller to within  $\pm 1^\circ$ . The temperature of the gas stream rose to the temperature of the furnace on travelling about 5 cm. through the tube. It then remained constant within about 5° for a distance of 5 cm., and then fell very rapidly owing to a water-cooled coil of copper tubing wound around the exit. The furnace temperature was regulated so that the calculated temperature of pure helium passing through the tube was between 1200 and 1205°, based on measured temperatures obtained from a calibrated platinum-platinum 10% rhodium thermocouple inserted in the gas stream. This thermocouple was withdrawn during runs with hydrocarbons.

The product gases were passed through a Dry Ice-acetone cooled trap and then through two traps cooled with liquid nitrogen. Uncondensed gases, mainly methane and hydrogen, were oxidized to carbon dioxide and water and the amounts of these gases calculated from these data. The gases condensed at liquid nitrogen temperatures included acetylene, ethylene, methylacetylene, allene, diacetylene and vinylacetylene. The amounts were determined by a Perkin-Elmer 154C Vapor Fractometer.

### Discussion

The rate of disappearance of benzene at 1200°, at a concentration of 0.1 mole % and at residence times of 4 to 112 milliseconds is exponential with time as shown in Fig. 1. Plotted semilogarith-

mically, a straight line can be drawn through the points implying disappearance by first-order kinetics and giving a rate constant of 20.6 sec.<sup>-1</sup>. This first-order behavior was tested further by increasing the initial contraction of benzene by five and ten times. In each case the percentage benzene decomposed remained constant to within an experimental error of about 5%, confirming first-order behavior. This conclusion agrees with previous work<sup>2</sup> and the work of Tesner and co-authors<sup>3</sup> who developed quite a different technique.

The percentage of benzene decomposed rises from about 10 to 90% with contact times of 4 to 112 milliseconds, respectively, Table I, and therefore covers a wide range of the decomposition of benzene at the temperature and concentration used. The decomposition products at 4 milliseconds are characterized by large amounts of acetylene and diacetylene, but considerable quantities of carbon, polymer or tar, and biphenyl also are produced, Table I. At longer contact times the proportion of these products decreases and carbon is produced instead. Smaller amounts of methane, ethylene, methylacetylene, allene and vinylacetylene which appear are undoubtedly secondary products.

TABLE I

YIELD OF PRODUCTS, WEIGHT % OF BENZENE DECOMPOSED  
Initial concn. of benzene, 0.1 mole %; 1200°

Contact time, millisecc.	4	8	56	112
% of feed decomposed	9.8	22.4	68.0	90.0
Carbon	12.8	16.7	62.0	76.4
Polymer or tar	16.4	10.2	4.9	2.3
Biphenyl	12.2	10.9	a	a
Acetylene	26.4	25.0	17.5	12.1
Diacetylene	28.0	22.1	4.6	2.7
Methane	3.3	3.7	2.0	2.5
Ethylene	2.0	1.4	0.1	a
Methylacetylene + allene	1.9 <sup>b</sup>	1.5	a	a
Vinylacetylene	0.8	0.5	c	c
Hydrogen	2.0	2.0	6.0	6.2
Total products, %	105.8	94.0	97.1	102.2

a Trace. b Methylacetylene 1.4%; allene 0.5%. c None detected.

Because acetylene and diacetylene appear to be primary products in the decomposition of benzene, the kinetic behavior of these hydrocarbons under similar conditions also has been studied. Their rates of disappearance with residence time are shown in Fig. 1. Acetylene, in contrast with both benzene and diacetylene, is more stable thermally and it was necessary to increase its concentration to

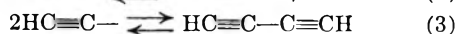
(2) D. B. Murphy, H. B. Palmer, C. R. Kinney, "Conference on Industrial Carbon and Graphite," Society of Chemical Industry, London, 1958, p. 77.

(3) P. A. Tesner and A. I. Yecheistova, *Dokl. Acad. Nauk., S.S.S.R.*, **87**, No. 6, 1029 (1952); P. A. Tesner and I. S. Rafalkes, *ibid.*, **87**, 821 (1952).

(1) C. R. Kinney and R. S. Slysh, "Proceedings of the Fourth Conference on Carbon," Pergamon Press, London, 1960, p. 199.

0.5 mole % to get sufficient decomposition to measure the products satisfactorily at contact times as low as 8 milliseconds. At this concentration, about 1% is decomposed at 8 milliseconds and 23% at 112. The shape of the disappearance curve in Fig. 1 shows that the rate of decomposition accelerates, at least to 112 milliseconds. Possibly this is due to the deposition of carbon which acts as a catalyst.

The yields of decomposition products from acetylene vary from those obtained from benzene in several respects. The percentage converted to carbon at a short residence time is larger and there is less tar or polymer, Table II. The most important product after carbon is diacetylene. Since such a large amount of diacetylene is produced in spite of its higher rate of decomposition, Fig. 1, and since diacetylene yields acetylene on pyrolysis, Table III, it seems likely that these reversible reactions occur



Acetylene also produces rather large quantities of methylacetylene, allene and methane, Table II. The mechanism by which these odd-numbered carbon derivatives is formed has not been proven, but their appearance in the decomposition products of benzene should be noted because they may be characteristic of acetylene decomposition rather than benzene.

The rate of disappearance of diacetylene when

TABLE II

YIELD OF PRODUCTS, WEIGHT % OF ACETYLENE DECOMPOSED

Initial concn. of benzene, 0.1 mole %; 1200°			
Contact time, millisecc.	8	56	112
% of feed decomposed	1.2	6.9	22.8
Carbon	36.4	48.3	50.6
Polymer or tar	4.5	7.0	7.5
Diacetylene	32.0	19.6	20.0
Methane	4.5	8.4	13.0
Ethylene	<sup>b</sup>	5.6	1.5
Methylacetylene	18.2	2.1	1.1
Hydrogen	4.5	3.5	2.9
Total products, %	100.1	94.5	96.6

<sup>a</sup> A trace of vinylacetylene was detected at 8 milliseconds but none at longer contacts. <sup>b</sup> Trace.

TABLE III

YIELD OF PRODUCTS, WEIGHT % OF DIACETYLENE DECOMPOSED

Initial concn. of acetylene 0.5 mole %; 1200°			
Contact time, millisecc.	8	56	112
% of feed decomposed	21.0	69.1	92.2
Carbon	44.5	63.6	70.6
Polymer or tar	12.0	2.9	<sup>b</sup>
Acetylene	37.2	21.8	19.2
Methane	1.6	4.4	4.2
Ethylene	0.8	0.3	0.2
Hydrogen	0.4	1.5	1.5
Total products, %	96.5	94.5	95.7

<sup>a</sup> Traces of methylacetylene, allene and vinylacetylene were detected at all contact times. <sup>b</sup> Trace.

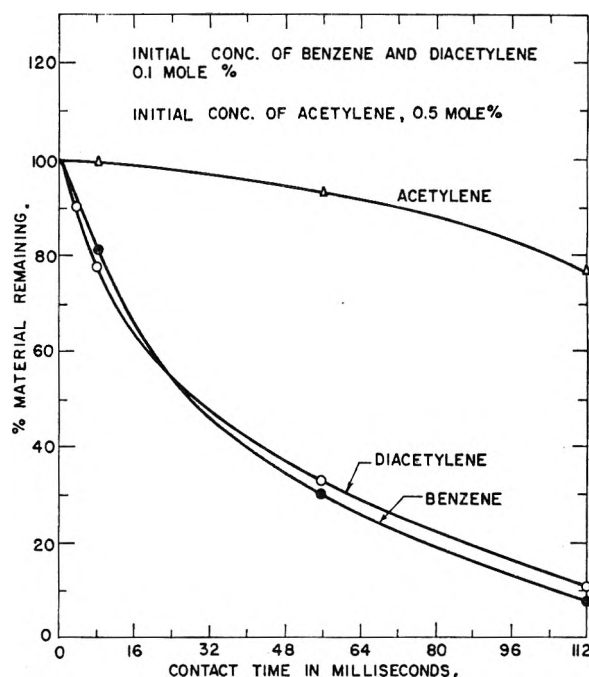


Fig. 1.—Effect of contact time on the rate of pyrolysis of benzene, diacetylene and acetylene.

heated to 1200° at a concentration of 0.1 mole % is shown in Fig. 1. The rate constant calculated from the data is 22.4 seconds<sup>-1</sup>. No doubt the mechanism of decomposition is complex because of the variety of products obtained, Table III. However, the diacetylene molecules that are decomposed are converted to carbon more completely than either benzene or acetylene. The next largest product is acetylene, which probably involves the dissociation of diacetylene to acetylenyl radicals which then capture hydrogen atoms by collision with diacetylene molecules, as indicated by the reverse of reactions 3 and 2. In this connection, the production of diacetylenyl radicals may account for the larger conversion of diacetylene to carbon than that of acetylene. The other decomposition products observed are similar to those obtained from benzene and acetylene.

The results of the investigation show that benzene decomposition is first order at 1200°. Of the products diacetylene also decomposes by first-order kinetics, but acetylene decomposes at an accelerating rate suggesting that a decomposition product, possibly carbon, affects the rate in a marked manner.

**Acknowledgment.**—This paper is based on research performed under a contract with the U. S. Atomic Energy Commission.

## STEPWISE ADSORPTION OF KRYPTON ON NICKEL

BY D. C. FOX AND M. J. KATZ

U. S. Army Signal Research and Development Laboratory, Fort Monmouth, New Jersey

Received September 20, 1960

The adsorption of krypton on nickel powders, sintered at temperatures between 200–600°, has

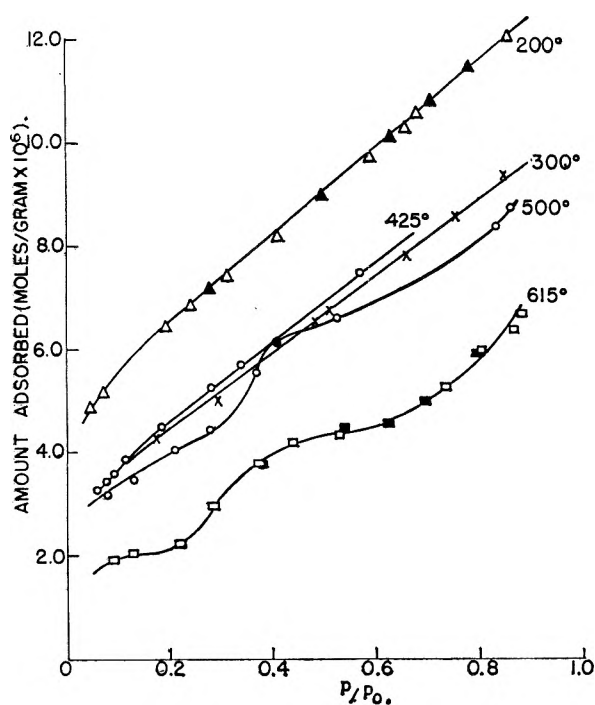
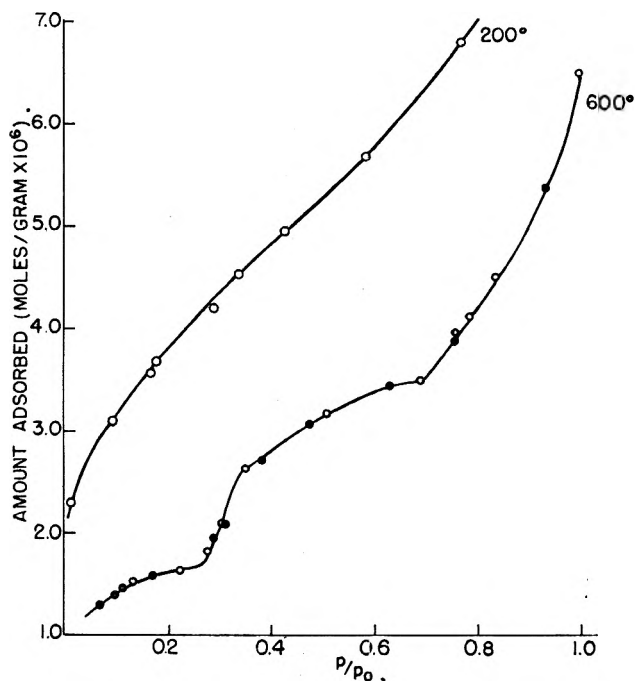


Fig. 1.—Adsorption of krypton on nickel at 78°K.: (1a) change in isotherm with sintering temperature.



(1b) Detailed isotherm on low area sample shows the reversibility in scanning isotherm steps.

been found to generate stepwise isotherms. Criticism of the multilayer theory of physical adsorption by Hill<sup>1</sup> and especially by Halsey,<sup>2</sup> has led to models with stepwise adsorption as a consequence. Except for isolated instances, however, such isotherms steps have not been generally ob-

served. The most notable examples are the isotherms obtained by Beebe and co-workers<sup>3</sup> for krypton on a heat treated carbon black and by Polley<sup>4</sup> *et al.*, on a series of graphitized carbon blacks. The present work notes the occurrence of the phenomenon in a new system in the hope of contributing to an explanation.

#### Experimental

The nickel samples were finely divided powders of high purity prepared by one of two methods: (1) thermal decomposition of nickel carbonyl; (2) hydrogen reduction of nickel ions from solution. Metallic impurities were in the spectrographic range; oxygen averaged about 0.5%, carbon about 0.05%. Assayed reagent grade krypton was obtained from Airco. The adsorption apparatus consisted of sample tube with thermocouple well, gas buret, McLeod gage for pressure calibrations and a thermistor as the pressure sensing element. The essential features of such an apparatus have been described by Rosenberg.<sup>5</sup> The thermistors were obtained from the Victory Engineering Co., Union, N. J. While they offer the advantage of continuous pressure monitoring, lack of stability limited precision to approximately  $\pm 1\%$  of the pressure reading over most of the region of interest. Insensitivity at high relative pressures limited the accuracy in the vicinity of  $p_0$ , while the electronic circuitry set the practical lower limit at about 0.02 relative pressure.

Sintering tendencies were studied as a function of outgassing temperature, following initial pump down at 200° for a minimum of 16 hours. After each outgassing, an adsorption isotherm was obtained with krypton at liquid nitrogen temperatures. This procedure was continued, heating the sample to successively higher temperatures 16 hours at each temperature, up to approximately 600°, without interim exposure to air. All relative pressures refer to the saturation vapor pressure of the solid krypton. Calculated corrections for thermal transpiration were less than experimental error.

#### Results and Discussion

Typical adsorption isotherm series which parallel the morphological transformations are shown in Figs. 1a and 1b. These reflect the progressive changes in the surface with increasing sintering temperatures. BET plots of the data using relative pressures up to 0.25 were used to calculate the specific surface areas. Representative values showing the changes with temperature are given in Table I.

Samples outgassed at 200° yielded smooth isotherms with reasonably linear BET plots. The chemically precipitated nickels give characteristic type II sigmoidal curves similar to the results reported by O. Beeck, *et al.*,<sup>6</sup> for krypton on evaporated nickel films. The carbonyl nickel isotherms, such as those of Fig. 1, exhibit long linear regions with no apparent tendency to rise sharply at high relative pressures. However, the existence of a limiting value, as suggested by Singleton and Halsey,<sup>7</sup> is not definite because thermistor readings were not sufficiently reliable in the vicinity of  $p_0$ . The samples undergo a continuous decrease in surface area with outgassing temperatures up to

(3) C. H. Amberg, W. B. Spencer and R. A. Beebe, *Canadian J. Chem.*, **33**, 305 (1955).

(4) M. H. Polley, W. D. Schaeffer and W. R. Smith, *J. Phys. Chem.*, **57**, 469 (1953).

(5) A. J. Rosenberg, *J. Am. Chem. Soc.*, **78**, 2929 (1956).

(1) A thorough review is given by T. L. Hill in "Advances in Catalysis," Vol. IV, Academic Press, Inc., Publishers, New York, N. Y., 1952, pp. 211-258.

(2) Ref. 1, G. D. Halsey, Jr., pp. 259-269.

(6) O. Beeck, A. W. Ritchie and A. Wheeler, *J. Colloid Sci.*, **3**, 505 (1948).

(7) J. H. Singleton and G. D. Halsey, *J. Phys. Chem.*, **58**, 1011 (1954).



TABLE I  
VARIATION OF SURFACE AREA WITH SINTERING TEMPERATURES

Sintering region, °C.	Surface area, m. <sup>2</sup> /g.	
	Carbonyl Ni	Ni (by reduction in soln.)
200	0.60	.6
300	.43	.5
400	.42	1.4
500	.36	0.79
600	.21	0.60

400° even though sintering is not usually thought to occur below this temperature.<sup>8</sup> Although there is usually an appreciable reduction in surface area there is as yet no definite transition in the shape of the isotherm. At 500° the first well defined steps are obtained and these are further accentuated at 600°. Desorption points fall on the adsorption curve and retrace the steps going down. The inflection points before and after plateaus are at approximately 0.3 and 0.8 relative pressure (referred to the saturation vapor pressure of solid krypton). The second plateau occurs at roughly twice the monolayer coverage. The 600° isotherm in Fig. 1a was repeated on a sample reduced in hydrogen at 350° at one atmosphere static pressure. Curves for the reduced and unreduced samples were coincident within experimental error.

The morphological changes which occur during sintering are very marked in the electron micrographs.<sup>9</sup> The original particle is composed of sharply defined crystallites with very characteristic dendritic projections. These projecting spikes have frequently recurring angles indicating that they are bounded by (331) or other high energy, non-equilibrium faces. It is the occurrence of such faces to which the special tendency of these powders to sinter has been attributed. After sintering at about 600° the spikes disappear and the particle profiles are smooth and rounded. In place of the complicated internal structure of intergrown crystallites, there are relatively smooth plateaus with distinct growth planes.

The Debye-Scherrer X-ray patterns for the sintered and unsintered material are also very revealing. The structure, cubic face-centered nickel, is unchanged. After sintering, however, the diffuse lines, especially for the high angle reflections, become very sharp. From this it may be concluded that the reduction in surface area is the result of crystallite growth. The absence of hysteresis in the adsorption isotherms as well as the low value of  $v/v_m$  at higher relative pressures argue against a sintering mechanism involving the filling in or collapse of capillaries.

Our results confirm the occurrence of stepwise isotherms as predicated by Halsey<sup>10</sup> on a model for a homogeneous surface with lateral adsorbate interactions. The sintering evidently proceeds by growth at the expense of the high energy surfaces, replaced in the transformed particle by surfaces which are more uniform geometrically and

energetically. These are inferences from crystallographical considerations, and it would be of interest to obtain supporting evidence by measurements of the heat of adsorption.

Since the monocrystalline projections of the unsintered particle indicate a considerable degree of ordering, the surface heterogeneity must be assumed to originate in the small crystallites or in intercrystallite effects. The case is similar to Rhodin's<sup>11</sup> results on polycrystalline copper. However, in the case of his studies on single crystal copper surfaces, one would expect surface homogeneity to be manifested by isotherm steps with sufficiently sensitive measurements extended to higher relative pressures.

Particle diameters taken from electron micrograms are from one to five times that calculated from the surface area. The sintering, which is accompanied by a two-to-threefold reduction in surface while the particle size is essentially unaltered, thus results in a much smoother surface. Aston<sup>12</sup> has pointed out for the case of krypton on graphitized carbon that the high energy edge sites would not be expected to affect the course of adsorption substantially, except at low coverages. It seems probable, therefore, that a change in energy distribution of the crystallite surfaces themselves is most important in accounting for the transformation in the isotherms. This is borne out by the fact that the greatest reduction in surface does not occur necessarily between 400 and 500° where the first steps are generated.

**Acknowledgment.**—The authors are indebted to Mr. W. F. Nye for assistance with electron microscopy, to Dr. J. A. Kohn for crystallographic data and to Dr. E. M. Weiss for providing the nickel samples.

(11) T. N. Rhodin, Jr., *J. Am. Chem. Soc.*, **72**, 4343, 5691 (1950).

(12) J. G. Aston and J. Greyson, "Second International Congress of Surface Activity," Vol. II, Academic Press, Inc., Publishers, New York, N. Y., 1957.

## A THERMODYNAMIC STUDY OF SOME COÖRDINATION COMPLEXES OF BIVALENT METAL IONS WITH HISTAMINE<sup>1</sup>

BY W. CHANNING NICHOLAS AND W. CONARD FERNELIUS

*Department of Chemistry of the Pennsylvania State University, University Park, Penna.*

Received October 21, 1960

Formation constant data were obtained recently for some 2-picolyamines and 2-(2-aminoethyl)pyridine with several bivalent metal ions.<sup>2</sup> These data were compared to those for the corresponding ethylenediamines and 1,3-propanediamine by dividing the free energy (or preferably enthalpy) of formation of the stepwise chelation reactions by the free energy of formation (or enthalpy) of the entirely protonated ligand. The denominator in such a ratio was regarded as proportional to the

(1) This investigation was carried out under contract AT(30-1)-907 between The Pennsylvania State University and the U. S. Atomic Energy Commission.

(2) D. E. Goldberg and W. C. Fernelius, *J. Phys. Chem.*, **63**, 1248 (1959).

(8) P. W. Selwood, *J. Am. Chem. Soc.*, **78**, 3893 (1956).

(9) C. F. Cook, Jr., W. F. Nye and F. W. Leonhard, paper presented at Ottawa, Canada, Electrochemical Society, Oct. 1958.

(10) G. D. Halsey, *J. Chem. Phys.*, **16**, 931 (1948).

TABLE I

VALUES FOR THE THERMODYNAMIC QUANTITIES  $\log K_n$ ,  $-\Delta F_n^0$ ,  $-\Delta H_n^0$  AND  $\Delta S_n^0$  INVOLVED IN THE REACTION AT 10, 20, 30 AND 40° AND IONIC STRENGTH  $\rightarrow 0$  OF SEVERAL BIVALENT METAL IONS WITH HISTAMINE

Ion	n	$\log K_n$				$-\Delta F_n^0$		$-\Delta H_n^0$		$\Delta S_n^0$	
		10°	20°	30°	40°	30°	40°	10-40°	30°	40°	30°
H <sup>+</sup>	1	10.35 ± 0.01	10.01 ± 0.01	9.70 ± 0.01	9.40 ± 0.03	13.4	13.4	13.4	13.5	13.4	0
	2	6.83 ± .02	6.05 ± .01	5.87 ± .02	5.60 ± .03	8.1	8.0	8.05	7.9	10.1	-7
Cu <sup>++</sup>	1	10.25 ± .01	9.82 ± .01	9.50 ± .01	9.12 ± .02	13.3	13.2	13.2	13.1	15.5	-1
	2	7.02 ± .04	6.69 ± .02	6.45 ± .02	6.20 ± .03	9.1	9.0	8.9	8.9	11.6	-9
Ni <sup>++</sup>	1	7.36 ± .05	7.03 ± .03	6.77 ± .05	6.06 ± .04	9.5	9.4	9.4	9.4	10.9	-5
	2	5.43 ± .05	5.22 ± .03	5.01 ± .02	4.85 ± .02	7.0	7.0	6.9	6.9	8.2	-4
	3	3.39 ± .06	3.20 ± .04	3.25 ± .09	3.20 ± .04	4.4	4.3	4.5	4.6	2.3	7
Co <sup>++</sup>	1	5.52 ± .02	5.16 ± .02	5.08 ± .02	5.01 ± .05	7.1 <sub>5</sub>	6.9	7.0	7.2	6.9	-1
	2	4.01 ± .01	3.77 ± .03	3.76 ± .03	3.63 ± .03	5.2	5.1	5.2	5.2	4.8	1 <sub>6</sub>
Cd <sup>++</sup>	1	5.12 ± .02	4.83 ± .02	4.80 ± .01	4.54 ± .05	6.6	6.5	6.6 <sub>5</sub>	6.5	7.4	-3
	2	3.60 ± .03	3.40 ± .05	3.39 ± .02	3.25 ± .08	4.7	4.6	4.7	4.7	4.4	1

strength of the sigma bond in the chelation process so that ratios higher than those for simple diamines should indicate stabilization other than by sigma bonding (presumably by  $\pi$ -bonding). Similar ratios computed from formation constant data for histamine, 4-(2-aminoethyl)-imidazole, are presented here. The stabilization is even greater than for 2-(2-aminoethyl)-pyridine. Previous work on histamine-metal ion systems was done in 0.1 M KCl at only two temperatures and did not include Cd<sup>++</sup>.<sup>3-6</sup>

### Experimental and Results

The preparation of solutions of metal ions, measurements and calculations were performed as described previously.<sup>1</sup> Solutions of histamine were prepared from the hydrochloride by means of anion-exchange resins.<sup>6</sup> The results are given in Table I.

### Discussion

**Acid Dissociation Constants.**—For histamine the values of  $pK_2$  (for BH<sup>+</sup>) and  $pK_1$  (for BH<sub>2</sub><sup>2+</sup>) are both greater than those for 2-(2-aminoethyl)-pyridine—the former is almost equal to that for 1,3-propanediamine.

**Formation Constants.**—The complexes of histamine are more stable than those of 2-(2-aminoethyl)-pyridine as would be expected of a stronger base.<sup>7</sup> The comparison in Table II shows that the stabilization of complexes of a 4-(2-aminoethyl)-imidazole due to the heterocyclic nitrogen is slightly greater than that of 2-(2-aminoethyl)-pyridine.

TABLE II  
STABILIZATION DUE TO DOUBLY-BONDED NITROGEN

i		$\Delta F_i$		$\Delta H_i$	
		$(\Delta F_{H_1})_{Cu}$	$(\Delta F_{H_2})_{Ni}$	$(\Delta H_1)_{Cu}$	$(\Delta H_2)_{Ni}$
Histamine	1	0.62	0.44	0.66	0.47
	2		.32		.35
2-(2-Aminoethyl)-pyridine	1	.56	.38	.57	.47
	2		.24		.27
1,3-Propanediamine	1	.51	.33	.51	.38
	2		.23		.30

(3) J. Z. Hearon, D. Burk and A. L. Schade, *J. Natl. Cancer Inst.*, **9**, 337 (1949).

(4) A. Albert, *Biochem. J.*, **50**, 693 (1952).

(5) B. L. Mickel and S. C. Andrews, *J. Am. Chem. Soc.*, **77**, 323, 5291 (1955).

(6) C. R. Bertsch, W. C. Fernelius and E. P. Block, *J. Phys. Chem.*, **62**, 444 (1958).

(7) R. J. Bruehlman and F. H. Verhoek, *J. Am. Chem. Soc.*, **70**, 1401 (1948).

## THE CALCULATION OF LIQUID MOLE FRACTIONS AND ACTIVITY COEFFICIENTS FROM ACTIVITY DATA

BY SHERRIL D. CHRISTIAN, EDWARD NEPARKO, HAROLD E. AFFSPRUNG AND FRANK GIBBARD

Department of Chemistry, The University of Oklahoma, Norman, Oklahoma

Received October 24, 1960

A previous paper<sup>1</sup> described a method for determining activity coefficients of components in binary liquid mixtures from measurements of vapor density and total vapor pressure. Liquid phase compositions were not measured, directly but were calculated from the expression

$$x_1 = d \ln a_2 / (d \ln a_2 - d \ln a_1) \quad (1)$$

where  $a_1$  and  $a_2$  are the activities of components 1 and 2, respectively, and  $x_1$  is the mole fraction of component 1 in the liquid phase. Equation 1 is derived from the constant temperature, constant pressure form of the Gibbs-Duhem equation.

The vapor density method referred to above yields activity values directly, but it is necessary to curve-fit  $a_2$  as a function of  $a_1$  in order to calculate liquid composition and activity coefficients. Therefore, it was decided to develop a computer program for calculating activity coefficients and liquid mole fractions from tables of values of  $a_2$  and  $a_1$  for binary systems at constant temperature.

In using the equilibrium still, and a number of other activity methods, values of  $a_2$  and  $a_1$  are obtained as a function of  $x_1$ , and it is often desirable to check these data for self-consistency with the Gibbs-Duhem equation. A computer program which makes possible the calculation of  $x_1$  from tables of  $a_2$  and  $a_1$  values should prove useful for this purpose.

It was proposed that such a program be developed and tested on several systems for which  $a_2$ ,  $a_1$  and  $x_1$  have all been measured directly. A comparison between calculated and experimental  $a_2$  vs.  $x_1$  and  $a_1$  vs.  $x_1$  curves would provide an indication of the applicability and accuracy of the computational method.

(1) S. Christian, E. Neparko and H. Affsprung, *J. Phys. Chem.*, **64**, 412 (1960).

### Method of Calculation

Equation 1 may be rearranged to give the expression

$$x_1 = 1/(1 - a_2 da_1/a_1 da_2) \quad (2)$$

Using this relation, if  $a_1$  is known as a function of  $a_2$ ,  $x_1$  may be calculated for any given value of  $a_1$ .

The function

$$f = (a_1 + a_2 - 1)/a_2 \quad (3)$$

proved very useful for curve-fitting purposes. For all of the systems studied,  $f$  varied slowly and uniformly as  $a_1$  changed from 0 to 1. For an ideal solution  $f = 0$  for all values of  $a_1$  and  $a_2$ . In the case of solutions deviating positively from ideality,  $0 < f < 1$ , and for negatively deviating solutions,  $f < 0$ .

Because of the convenient properties of the function  $f$ , curve-fitting was accomplished using the expression

$$f = Aa_1 + Ba_1^2 + Ca_1^3 \quad (4)$$

where  $A$ ,  $B$  and  $C$  are parameters chosen to give a least-squares fit of data. There is no constant term in equation 4, since  $f = 0$  when  $a_1 = 0$  for all binary solutions.

Equation 3 may be rearranged to yield the expression

$$a_2 = (a_1 - 1)/(f - 1)$$

from which the activity relations required in equation 2, and, hence,  $x_1$  may be calculated. The activity coefficients of components 1 and 2 ( $\gamma_1$  and  $\gamma_2$ ) are computed from the expressions

$$\gamma_1 = a_1/x_1 \text{ and } \gamma_2 = a_2/(1 - x_1)$$

### Results

Six binary systems for which liquid-vapor equilibrium studies have been reported were chosen for testing the validity of the method of calculation. One of the systems deviates negatively from Raoult's law, while the others show varying degrees of positive deviation.

Figure 1 depicts results of calculations based on the data of Sameshima<sup>2</sup> for the system acetone-diethyl ether. Experimental  $a_1$  vs.  $x_1$  and  $a_2$  vs.  $x_1$  points are plotted, along with activity curves calculated as described above.

The systems 1-propanol-benzene, reported by Brown and Smith<sup>3</sup> and chloroform-acetone, by Zawidzki<sup>4</sup> are similarly treated in Figs. 2 and 3. Computed values for the constants  $A$ ,  $B$  and  $C$  of equation 4 are given for these systems in Table I. The table also includes calculated values of  $A$ ,  $B$  and  $C$  for the systems acetone-benzene at 45°, reported by Brown and Smith<sup>5</sup>; acetone-carbon tetrachloride at 45°, by Brown and Smith<sup>3</sup> and 2-propanol-benzene at 25°, by Olsen and Washburn.<sup>6</sup> To illustrate the behavior of the function used in the curve-fitting technique, a plot of  $f$  vs.  $a_1$  for the system acetone-diethyl ether system is shown in Fig. 4.

(2) J. Sameshima, *J. Am. Chem. Soc.*, **40**, 1489 (1918).

(3) I. Brown and F. Smith, *Aust. J. Chem.*, **12**, 407 (1959).

(4) J. v. Zawidzki, *Z. physik. Chem.*, **35**, 129 (1908).

(5) I. Brown and F. Smith, *Aust. J. Chem.*, **10**, 423 (1957).

(6) A. Olsen and E. Washburn, *J. Phys. Chem.*, **41**, 457 (1937).

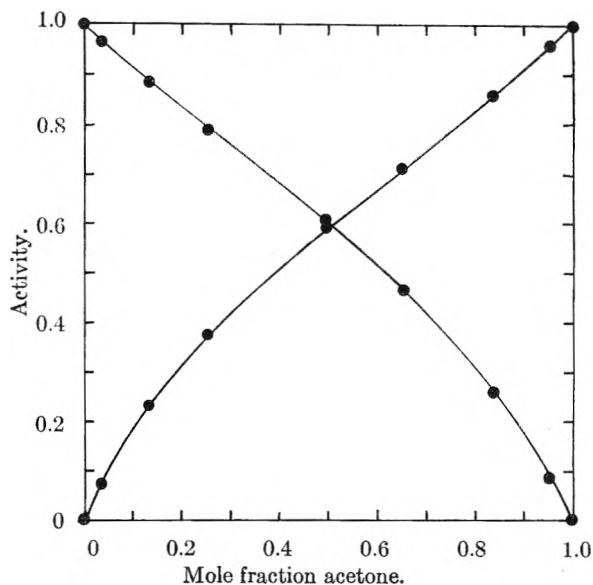


Fig. 1.—Activity vs. mole fraction for the system acetone-diethyl ether at 30°. Curves are calculated, points are experimental.

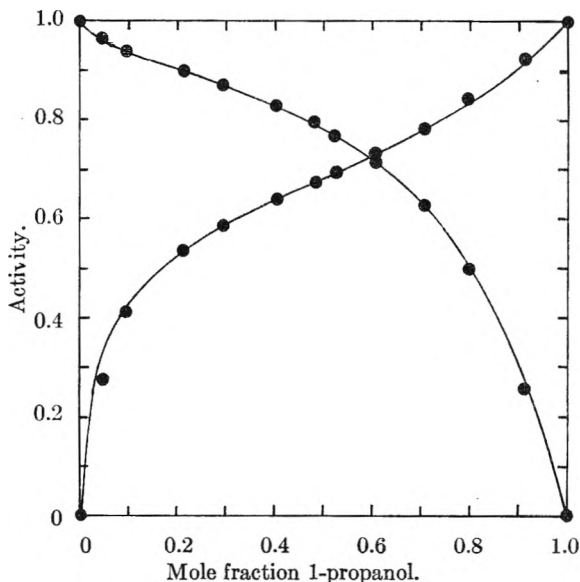


Fig. 2.—Activity vs. mole fraction for the system 1-propanol-benzene at 45°. Curves are calculated, points are experimental.

### Discussion

An examination of Figs. 1-3 reveals that agreement between experimental and computed activity vs. liquid mole fraction curves is satisfactory. Liquid mole fractions calculated from sets of  $a_1$ ,  $a_2$  values closely approximate the directly measured values.

TABLE I  
VALUES OF THE CONSTANTS  $A$ ,  $B$  AND  $C$

Component 1	System Component 2	$t$ , °C.	$A$	$B$	$C$
Acetone	Benzene	45	0.425	-0.128	0.025
Acetone	Diethyl ether	30	.587	-.077	.012
Acetone	Carbon tetra- chloride	45	.725	-.166	-.050
1-Propanol	Benzene	45	.806	.478	-.560
Isopropyl alc.	Benzene	25	.943	-.056	-.018
Chloroform	Acetone	35.17	-1.013	.831	.223

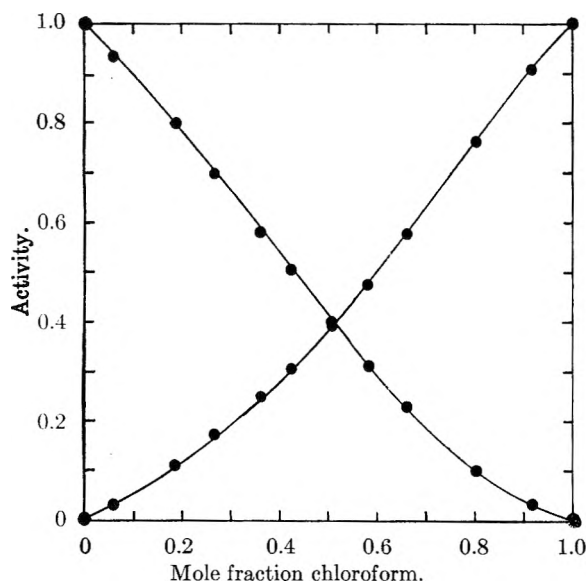


Fig. 3.—Activity vs. mole fraction for the system chloroform-acetone at 35.17°. Curves are calculated, points are experimental.

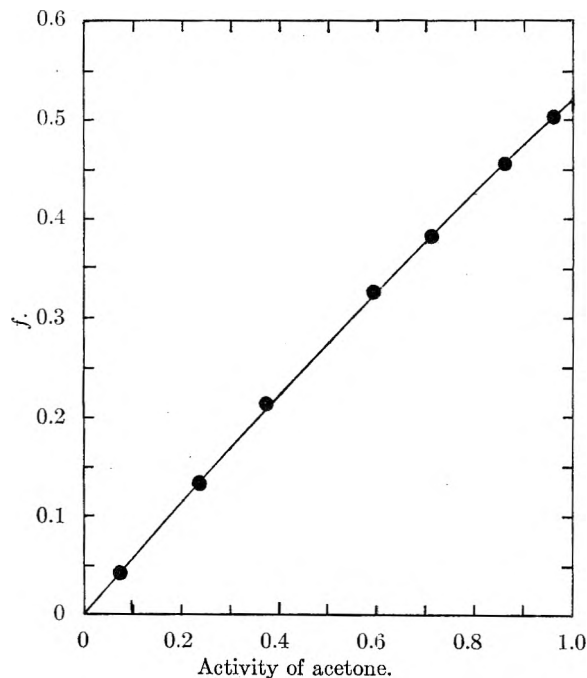


Fig. 4.—Dependence of  $f$  on  $a_1$  for the system acetone-diethyl ether at 30°.

The values of the constants  $A$ ,  $B$  and  $C$  may be used to calculate  $\gamma^0$ , the limiting value of the activity coefficient of a component as the mole fraction of that component approaches zero. From equations 3 and 4 it follows that

$$A = \lim_{a_1 \rightarrow 0} \left( \frac{f}{a_1} \right) = \lim_{a_1 \rightarrow 0} \left( 1/a_2 + \frac{a_2 - 1}{a_2 a_1} \right)$$

$$\text{or } A = 1 - x_1/(x_1 \gamma_1^0) = 1 - 1/\gamma_1^0,$$

$$\text{and } \gamma_1^0 = 1/(1 - A)$$

Similarly,  $\gamma_2^0 = 1/(1 - A - B - C)$ . The constant  $A$  is, of course, the initial slope of a plot of  $f$  vs.  $a_1$ , and  $A + B + C$  is the value of  $f$  at  $a_1 = 1$ . Therefore, even without computing  $A$ ,  $B$  and  $C$ , limiting

activity coefficients readily may be obtained graphically from plots similar to the one in Fig. 4.

Previous work in this Laboratory has been directed toward simplifying calculation and measurement of activity coefficients of binary non-electrolyte mixtures. The Gibbs-Duhem equation reduces by one the number of measurable quantities required in the calculation of activity coefficients. Thus, measurement over the entire concentration range of any two of the quantities  $x_1$ ,  $a_2$ ,  $a_1$  and  $P$  (total pressure) for volatile binary mixtures makes possible the calculation of the remaining two.<sup>7</sup>

The vapor density method referred to above<sup>1</sup> and the present technique rely on  $a_2$  vs.  $a_1$  data. A method for the computation of activity coefficients from  $P$  vs.  $x_1$  values has also been reported.<sup>8</sup> The same method may be used to calculate both  $\gamma_1$  and  $\gamma_2$  from  $a_1$  vs.  $x_1$  or  $a_2$  vs.  $x_1$  data. Further, if  $P$  vs.  $a_1$  data are available,  $a_2$  may be calculated directly from the equation of state of the vapor phase. Then the present program may be applied to calculate liquid mole fractions and activity coefficients.

One advantage of using  $a_2$  vs.  $a_1$  data, and avoiding measurement of  $x_1$ , is that it is frequently possible to use a vapor density, refractive index, spectrophotometric, or other continuous instrumental technique to analyze the vapor phase. Liquid concentrations may be varied arbitrarily in a closed system, preventing interaction of the solution with the air and making possible the rapid determination of activities.

The IBM 650 computer program developed here is available through the University of Oklahoma Computer Laboratory. Computing time was less than 1 minute per system for the binary mixtures studied.

**Acknowledgments.**—The authors are indebted to the National Science Foundation for financial support of this project. In addition, they wish to express their appreciation for the computer time donated by the University of Oklahoma Computer Laboratory.

(7) Knowledge of the equation of state of the vapor phase is also required; frequently it is assumed that at low pressures the vapors obey the ideal gas equation.

(8) S. Christian, *J. Phys. Chem.*, **64**, 764 (1960).

## A NEW RELATION FOR PHYSICAL PROPERTIES OF $n$ -ALKANES AND $n$ -ALKYL COMPOUNDS<sup>1</sup>

BY ALEKSANDER KREGLEWSKI AND BRUNO J. ZWOLINSKI

*Chemical and Petroleum Research Laboratory, Carnegie Institute of Technology, Pittsburgh 13, Pennsylvania*

Received October 31, 1960

Many efforts have been made to find accurate relationships for predicting physical properties of homologous series of compounds as a function of molecular structure to better than 0.1%. Some of the most accurate equations have been developed by Rossini and his co-workers.<sup>2</sup> The purpose of

(1) This work was performed as part of the Manufacturing Chemists' Association Research Project.

this note is to describe a new relation that has been found recently for correlating and predicting certain intensive physical properties of normal paraffins and their monosubstituted normal alkyl derivatives as a function of the number of carbon atoms ( $m$ ).

Kurata and Isida<sup>3</sup> using Flory's expression for the free energy of a polymeric chain developed a hole theory treatment for  $n$ -paraffin liquids and found that the effective length of a carbon skeleton chain should be proportional to the two-thirds power of the number of carbon atoms ( $m^{2/3}$ ) when  $m > 5$ . Using this result, we have found that some physical properties ( $y$ ) such as the normal boiling point ( $T_b$ ), the critical temperature ( $T_c$ ), the critical pressure ( $P_c$ ), the heat of vaporization ( $\Delta H_v$ ), and the Antoine vapor pressure constant  $B$ , follow the simple functional relation

$$y_\infty - y = a'e^{-b'x} \quad (1)$$

where  $x = m^{2/3}$  and  $a'$  and  $b'$  are adjustable parameters.

In logarithmic form, we have

$$\log(y_\infty - y) = a - bm^{2/3} \quad (2)$$

where

$$\begin{aligned} a &= \log a' \\ b &= 0.43429b' \\ y_\infty &= \text{reference point at infinity } (m^{2/3} = \infty) \end{aligned}$$

For  $m = 0$ , we have  $y = y_0 = y_\infty - a'$ .

This procedure was applied to the selected values of the physical properties of the normal alkanes found in the data tables of API Research Project 44.<sup>4</sup> By a trial and error procedure the values of  $y_\infty$  for three of the physical properties were determined for hydrocarbons with  $m = 5, 10, 15$  and are given in Table II. The two remaining adjustable parameters were calculated by the least squares procedure for  $m = 5$  to 18. The results for the normal boiling points of the  $n$ -alkanes are given in Table I and show a mean deviation of 0.03% from the observed values. The mean deviation for the heats of vaporization is approximately 0.1%. The observed values for  $\Delta H_v$  used in finding the constants given in Table II are those calculated from observed Antoine constants without corrections for vapor imperfections

$$\Delta H_v = 4.57568BT^2/(C' + T)^2 \text{ (cal./mole)} \quad (3)$$

The value of  $B_\infty$  was determined from smoothed points. For  $n$ -alkanes, equation 2 holds for  $m \geq 3$ .

To test for internal consistency, the Antoine constant,  $C'$  ( $C' = C - 273.160$ ), was calculated from equation 3 using the values at infinity for  $(\Delta H_v)_\infty$ ,  $B_\infty$  and  $(T_b)_\infty$  (at 760 mm.) yielding a value of  $C'_\infty = -572$ . The value of  $C'_\infty$  calculated directly from the Antoine equation by substitution of  $B_\infty$  and  $T_\infty$  at 50 and 760 mm. (see Table II), is  $-556$ . In view of the insensitivity of the  $C'$

(2) K. Li, R. L. Arnett, M. B. Epstein, R. B. Ries, L. P. Bitler, J. M. Lynch and F. D. Rossini, *J. Phys. Chem.*, **60**, 1400 (1956).

(3) M. Kurata and S. Isida, *J. Chem. Phys.*, **23**, 1126 (1955).

(4) American Petroleum Institute Research Project 44. "Selected Values of Properties of Hydrocarbons and Related Compounds." Chemical and Petroleum Research Laboratory, Carnegie Institute of Technology, Pittsburgh 13, Pennsylvania. (Loose-leaf data sheets, extant, 1960).

value, the internal agreement of the  $y_\infty$  values is satisfactory.

The new exponential relation also reproduces very well the observed values of critical temperatures of  $n$ -alkanes (up to  $m = 10$ ), but the deviations from values correlated by other investigators are very large for higher homologs. It is suspected that these correlated values are in error which is borne out by some recent studies by Ambrose, Cox and Townsend.<sup>5</sup> The logarithmic relation holds very well for the physical properties of  $n$ -alkyl compounds and other hydrocarbon derivatives (e.g.,  $n$ -olefins,  $n$ -alkyl benzenes, thio-alcohols). Furthermore, it was found that the same point at infinity holds for  $n$ -alkanes and their derivatives; that is

$$y_\infty(n\text{-alkanes}) = y_\infty(n\text{-alkyl compounds}) \quad (4)$$

Although such a relation is expected on physical grounds for homologous series, it was firmly established for the physical properties in this study.

Using relation 4, equation 2 for the boiling points ( $T_A$ ) of normal 1-olefins becomes

$$\log(1078 - T_A) = 3.03702 - 0.0505662m^{2/3} \quad (y_0 = -11)$$

which in the range of 5 to 16 carbon atoms holds to a deviation of 0.01%. In the case of the  $n$ -alkylbenzenes when  $m \geq 6$ , the adjustable constants for  $T_b$  are:  $a = 2.90547$ ,  $b = 0.043197$ ,  $y_0 = 274$ , and for  $\Delta H_v$  are:  $a = 4.75711$ ,  $b = 0.014442$ ,  $y_0 = 5338$ .

TABLE I  
THE NORMAL BOILING POINTS OF  $n$ -ALKANES

$m$	B.p. obsd. <sup>4</sup>	B.p. calcd. (eq. 2)	Dev., %
1	111.67	(118.8)	.....
2	184.53	(181.5)	.....
3	231.09	230.91	-0.08
4	272.66	272.73	+ .03
5	309.234	309.33	+ .03
6	341.900	342.06	+ .05
7	371.587	371.71	+ .03
8	398.825	398.87	+ .01
9	423.958	423.94	- .00
10	447.283	447.22	- .01
11	469.050	468.95	- .02
12	489.438	489.31	- .03
13	508.594	508.45	- .03
14	526.675	526.53	- .03
15	543.774	543.61	- .03
16	559.953	559.81	- .02
17	575.04	575.19	+ .02
$\infty$	.....	1078	.....

TABLE II  
CONSTANTS OF EQUATION 2 FOR CERTAIN PROPERTIES OF  $n$ -ALKANES

Property	$y_\infty$	$a$	$b$	$y_0$
B.p. (in °K.) at 760 mm.	1078	3.03191	0.0499901	1.7 <sup>a</sup>
B.p. (in °K.) at 50 mm.	989	2.99615	.0431882	-2.2 <sup>a</sup>
$\Delta H_v$ (cal./mole) at the normal b.p.	62500	4.79747	.016848	-230
Antoine constant $B$	$\approx 3010$ ( $\pm 100$ )	.....	.....	.....

<sup>a</sup> These values indicate that for  $n$ -alkanes  $y \approx y_\infty - a'$ .

(5) D. Ambrose, J. D. Cox and R. Townsend, *Trans. Faraday Soc.*, **56**, 1 (1960).

The constants  $y_{\infty}$  should be considered pure numbers without any physical significance; first, because  $dy/dm$  although it decreases with rising  $m$  cannot be expected to become equal to zero; second, because there is no proof that Kurata and Isida's exponent ( $2/3$ ) is constant for  $m > 20$ . For these reasons, extrapolations to  $m > 20$  involving formula 2 may be unreliable.

Additive properties which are primarily determined by molecular size and number such as molar volume (or density) and refractive index do not obey equation 2.

The logarithmic relation shows great promise in correlating, selecting and predicting the intensive properties such as  $T_b$ ,  $T_c$ ,  $P_c$ ,  $B$  and  $\Delta H_v$  for various homologous series.

## EVIDENCE OF THE INTRAMOLECULAR VIBRATIONAL EFFECT IN *p*-BENZOQUINONE

By JEHANBUX F. BAGLI<sup>1</sup>

Department of Chemistry, Laval University, Québec, P.Q. Canada  
Received November 7, 1960

Splitting of the carbonyl bands in infrared spectra, resulting from coupling between the two vibrations having the same energy is well-known, and aptly demonstrated for acyl and aroyl peroxides<sup>2</sup> and for anhydrides.<sup>3</sup> The observation of Cooke<sup>4</sup> that the lower frequency carbonyl band of the anhydrides can be further resolved, into a doublet, under suitable conditions is recently confirmed by Jones and his collaborators.<sup>5</sup> They have further demonstrated the solvent dependency and the concentration independency of the intensity of such split bands, and have suggested their origin in a Fermi resonance with the overtone of a low lying fundamental vibration.

Although certain substituted *p*-benzoquinones<sup>6</sup> show two bands in the carbonyl region, attempts to detect evidence of vibrational resonance between the stretching modes of the two carbonyl groups of benzoquinones have hitherto failed. There are, however, reports available in the literature of the presence of two<sup>6</sup> bands in the carbonyl region of the infrared spectra of *p*-benzoquinone. In the light of the recent findings on the Fermi resonance coupling<sup>7</sup> in the carbonyl compounds, and in view of some observations on the infrared spectra of some substituted *p*-benzoquinones in this Laboratory, it was deemed necessary to examine the infrared spectrum of *p*-benzoquinone in some detail.

(1) National Research Council of Canada postdoctoral fellow, 1959-1960.

(2) W. H. T. Davison, *J. Chem. Soc.*, 2456 (1951).

(3) L. J. Bellamy, "The Infrared Spectra of Complex Molecules," John Wiley and Sons, Inc., New York, N. Y., 1958, p. 127.

(4) R. G. Cooke, *Chemistry and Industry*, 142 (1955).

(5) R. N. Jones, C. L. Angell, T. Ito and R. J. D. Smith, *Can. J. Chem.*, **37**, 2007 (1959).

(6) (a) W. Flaig and J. C. Salfeld, *Ann.*, **626**, 215 (1959); (b) D. J. Cosgrove, D. G. H. Daniels, J. K. Whitehead and J. D. S. Goulden, *J. Chem. Soc.*, 4821 (1952); (c) M. L. Josien and J. Deschamps, *J. chim. phys.*, **52**, 213 (1955).

(7) (a) C. L. Angell, P. J. Krueger, R. Lauzon, L. C. Leitch, K. Noack, R. J. D. Smith and R. N. Jones, *Spectrochim. Acta*, **11**, 926 (1959); (b) P. Yates and L. L. Williams, *J. Am. Chem. Soc.*, **80**, 5396 (1958).

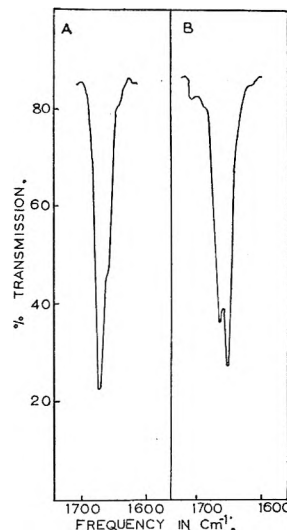


Fig. 1.—Infrared spectra in C=O stretching region of *p*-benzoquinone (0.1 M): A, in CS<sub>2</sub>; B, in CHCl<sub>3</sub>.

### Experimental

The freshly purified samples of *p*-benzoquinone and chloro-*p*-benzoquinone were used. The infrared spectra were recorded in solvents of varying polarity (Table I), at 0.1 M concentration, with a Beckman IR-4 spectrophotometer using a sodium chloride prism. The spectra of *p*-benzoquinone at varying concentrations (Table II) were also recorded under identical conditions.

### Results and Discussions

Whereas the carbonyl stretching region of the spectrum of *p*-benzoquinone in carbon disulfide exhibits a high frequency band at 1670 cm.<sup>-1</sup> and a low frequency band as an inflection at 1658 cm.<sup>-1</sup>; the one in chloroform has two distinct bands, one at 1674 cm.<sup>-1</sup> and the other at 1662 cm.<sup>-1</sup> (Fig. 1). The ratios of  $E_{\max}^{(a)}$  of the band at the higher frequency (band X), to that of the band at lower frequency (band Y) in the solvents of varying polarity are listed in Table I. Similar ratios at varying concentration are listed in Table II.

TABLE I  
CARBONYL ABSORPTION IN VARIOUS SOLVENTS

Solvent	C=O stretching frequency, cm. <sup>-1</sup>		Intensity ratio (a) Band X/ Band Y
	Band X	Band Y	
A. <i>p</i> -Benzoquinone			
CS <sub>2</sub>	1670	1658	2.09
CCl <sub>4</sub>	1675	1661	1.34
CHCl <sub>3</sub>	1674	1662	0.77
CH <sub>2</sub> Cl <sub>2</sub>	1672	1661	0.80
CS <sub>2</sub> /CHCl <sub>3</sub> (1:1) <sup>a</sup>	1674	1663	1.13
CCl <sub>4</sub> /CHCl <sub>3</sub> (1:1) <sup>a</sup>	1674	1662	0.88
B. Chloro- <i>p</i> -benzoquinone			
CS <sub>2</sub>	1682	1660	1.44
CCl <sub>4</sub>	1686	1665	1.04
CHCl <sub>3</sub>	1685	1663	1.21
CH <sub>2</sub> Cl <sub>2</sub>	1683	1663	1.18

<sup>a</sup> Percentage by weight.

The intensity ratio of band X/band Y obtained for *p*-benzoquinone shows typical variation, with the change in polarity of the solvents, as that demonstrated by carbonyl compounds, where Fermi resonance coupling is shown<sup>6,7</sup> to prevail. Further-

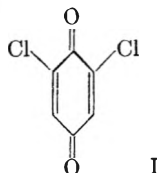
TABLE II  
INTENSITY RATIO FOR *p*-BENZOQUINONE IN CHCl<sub>3</sub> AT VARIOUS CONCENTRATIONS

Concn., moles/l.	Intensity ratio (ε <sub>max</sub> ) Band X/Band Y <sup>(a)</sup>
0.2	0.79
.15	.73
.1	.77
.05	.75

more, the intensity ratio of the carbonyl doublet peaks is independent of the concentration. This evidence coupled with the fact that no conformationally isomeric structures of this molecule are possible, suggests strongly an intramolecular vibrational effect as a cause of this splitting. It seems reasonable that the splitting could be caused by the coupling of the carbonyl frequency either with the overtone of an infrared inactive fundamental mode, or with a combination band. That such a coupling could occur with the pure harmonic overtone of the out-of-plane C-H bending mode (882–885 cm.<sup>-1</sup>), seems less likely, as it would become necessary to assume a large anharmonicity effect (ca. 100 cm.<sup>-1</sup>) to lower this vibration.

The case of chloro-*p*-benzoquinone is of special interest. It exhibits two bands in the carbonyl region, the relative intensity of which is independent of the nature of the solvent used (Table I), suggesting that Fermi resonance coupling is not the cause of this splitting. Also, the unperturbed frequencies of the stretching vibrations of the two carbonyl groups in this case should be sufficiently different so as to prevent<sup>8</sup> any vibrational resonance between them. There are available in the literature a few cases<sup>9</sup> where a carbonyl band in the infrared spectrum of an α,β-unsaturated ketone is shifted (Δν ca. 13–17 cm.<sup>-1</sup>) by the introduction of a halogen atom on the sp<sup>2</sup> carbon α to the carbonyl group. The Δν (>C=O) value between the two bands of the chloro-*p*-benzoquinone is in good agreement with those reported<sup>8,9</sup> for the saturated and the α,β-unsaturated ketones. It thus seems plausible to attribute the 1680–1685 cm.<sup>-1</sup> band to the >C=O with the halogen atom α to it, and the 1660–1664 cm.<sup>-1</sup> band to the >C=O flanked by two hydrogen atoms.

The above assignments are further substantiated by the fact that Δν (>C=O) value between the two carbonyl bands of 2,6-dichloro-*p*-benzoquinone (I) is exactly double<sup>10</sup> of that of the chloro-*p*-benzoquinone.



**Acknowledgment.**—The author wishes to thank Dr. P. L'Ecuyer for his encouragement during this work.

(8) Compare cyclohexanone and α-chloro(equatorial)-cyclohexanone, E. J. Corey and H. J. Burke, *J. Am. Chem. Soc.*, **77**, 5418 (1955).

(9) (a) G. R. Allen, Jr., and M. J. Weiss, *ibid.*, **82**, 2840 (1960);

(b) R. N. Jones, P. Humphries and K. Dohriner, *ibid.*, **72**, 956 (1950).

(10) J. F. Bagli, unpublished results.

## HYDRATION STUDIES FOR THE EXTRACTION OF INORGANIC NITRATES BY ALCOHOLS

By W. J. McMANAMEY

Chemical Engineering Department, University of Sydney, N.S.W., Australia

Received November 9, 1960

When electrolytes are extracted from aqueous solution as hydrated complexes by organic solvents which are partially miscible with water the water content of the solvent phase will consist both of hydrate water (bound to the electrolyte molecules) and free water (in equilibrium with the water in the aqueous phase). Yates, *et al.*,<sup>1</sup> determined the amount of free water by assuming that the ratio of the free water molality in the solvent phase to the water activity in the aqueous phase was constant at all electrolyte concentrations, and found the apparent hydration numbers of a number of chlorides and perchlorates in 2-octanol from the slope of the plot of the hydrate water molality (taken as the difference between the total water content of the solvent phase and its free water content) against the corresponding electrolyte molality in the solvent phase. These hydration numbers were constant over wide electrolyte molality ranges. This procedure is applied here to the investigation of the apparent hydration numbers of cobalt(II) and zinc nitrates in *n*-butyl alcohol, pentyl alcohol and *n*-hexyl alcohol, cupric nitrate in *n*-butyl alcohol and pentyl alcohol, and cobalt(II) and nickel(II) chlorides in *n*-butyl alcohol. The result with the solvents *n*-butyl alcohol and pentyl alcohol were obtained as part of this work and the data for *n*-hexyl alcohol were obtained from Templeton and Daly.<sup>2</sup>

### Experimental

All the electrolytes were Analytical Reagent quality except the zinc nitrate, which was commercial purity. The alcohols were purified by fractional distillation of commercial pure *n*-butyl alcohol and commercial pentanol. Analysis for the nitrates was carried out by ignition to the oxides, for the chlorides gravimetrically with silver nitrate, and for water in the alcohol phases by the Karl Fischer technique. When cupric nitrate was the solute the correction suggested by Mitchell and Smith<sup>3</sup> was applied to the water content to allow for the reaction between the Karl Fischer reagent and the cupric ion.

Mixtures with two liquid phases were equilibrated at 25° in the equilibrium flasks designed by Prince and Hunter,<sup>4</sup> using a procedure similar to theirs. When a solid phase was present ground glass stoppered cylinders were used.

**Hydration Studies.**—Since the alcohols (particularly *n*-butyl alcohol) are significantly soluble in water the water activity in the aqueous phases will not be the same as in solutions of the electrolytes in water alone. For electrolyte solutions in water the water activity is usually related to the electrolyte molality, and the relationships in the aqueous phases were assumed to be similar. However, in these phases, the electrolyte molality can be

(1) P. C. Yates, R. Laran, R. E. Williams and T. E. McCore, *J. Am. Chem. Soc.*, **75**, 2212 (1953).

(2) C. C. Templeton and L. K. Daly, *ibid.*, **73**, 3989 (1951).

(3) J. Mitchell and D. M. Smith, "Aquametry," Interscience Publishers, New York, N. Y., 1948, p. 260.

(4) R. G. H. Prince and T. G. Hunter, *Chem. Eng. Sci.*, **6**, 215 (1957).

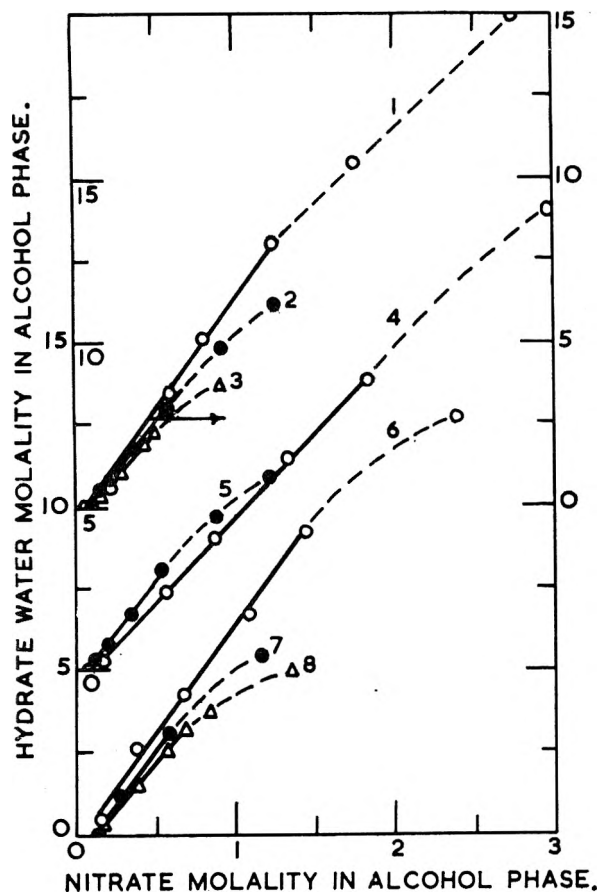


Fig. 1.—Hydration plot: 1,  $\text{Co}(\text{NO}_3)_2$ -*n*-butyl alcohol; 2,  $\text{Co}(\text{NO}_3)_2$ -pentyl alcohol; 3,  $\text{Co}(\text{NO}_3)_2$ -*n*-hexyl alcohol; 4,  $\text{Cu}(\text{NO}_3)_2$ -*n*-butyl alcohol; 5,  $\text{Cu}(\text{NO}_3)_2$ -pentyl alcohol; 6,  $\text{Zn}(\text{NO}_3)_2$ -*n*-butyl alcohol; 7,  $\text{Zn}(\text{NO}_3)_2$ -pentyl alcohol; 8,  $\text{Zn}(\text{NO}_3)_2$ -*n*-hexyl alcohol.

defined either as g. moles/1000 g. of water or as g. moles/(1000 g. of water and solvent). The greatest difference between these definitions occurs when *n*-butyl alcohol is the solvent and so the apparent hydration numbers for  $\text{Co}(\text{NO}_3)_2$ ,  $\text{Cu}(\text{NO}_3)_2$  and  $\text{Zn}(\text{NO}_3)_2$  in this solvent were calculated using both definitions, with water activities calculated from osmotic coefficients given by Robinson and Stokes.<sup>5</sup> The greatest difference between the hydration numbers for the same nitrate determined in both ways was only 0.2 and the first definition was arbitrarily adopted for the other alcohols.

As significant differences were found between the nitrates and chlorides, the former are discussed first. The Henry's law constant for each alcohol (the ratio of the free water molality in the alcohol phase to the water activity in the aqueous phase) was determined from the lowest experimental electrolyte molality for all alcohols except *n*-hexyl alcohol. The value for each of the other alcohols was almost the same for all the nitrates— $13.1 \pm 0.2$  for *n*-butyl alcohol and  $5.3 \pm 0.2$  for pentyl alcohol. The liquid-liquid equilibrium data available for the systems with *n*-hexyl alcohol as solvent were all for appreciable nitrate molalities

in the *n*-hexyl alcohol phase.<sup>2</sup> The Henry's law constant for *n*-hexyl alcohol was, therefore, obtained from the systems nickel(II) nitrate-*n*-hexyl alcohol<sup>6</sup> and aluminum nitrate-*n*-hexyl alcohol,<sup>7</sup> for which results were available with low nitrate molalities in the *n*-hexyl alcohol phase. In the absence of experimental determinations of the activities of water in either nickel or aluminum nitrate solutions water activities were obtained by assuming that, at low molalities in the water phase, nickel(II) and cobalt(II) nitrate solutions have the same water activity at the same molality and that aluminum and chromium nitrate solutions are also similar in this respect. A Henry's law constant of  $3.8 \pm 0.1$  was thus obtained for *n*-hexyl alcohol.

When the procedure of Yates, *et al.*, was applied to the  $\text{CoCl}_2$  and  $\text{NiCl}_2$  results the calculated free water molalities in the butyl alcohol phases were found to be higher than the total water molalities over most of the chloride molality range, so producing negative values of the hydrate water molality. Thus the actual water activity in the aqueous phase must be much lower than the value calculated from the chloride molality, suggesting that the dissolved *n*-butyl alcohol has more influence on the chloride than the nitrate solutions. This effect may be connected with the greater efficiency of chlorides than the nitrates as salting-out agents for *n*-butyl alcohol.

The apparent hydration numbers of the nitrates determined from the slopes of the straight line portions of the plots of hydrate water molality against nitrate molality in the alcohol phases (Fig. 1) are given in Table I together with the nitrate molality range in the aqueous phase for which the apparent hydration number is constant.

TABLE I

System	Apparent hydration number	Molality range in aqueous phase
$\text{Co}(\text{NO}_3)_2$ - <i>n</i> -butyl alcohol	7.0	0-3.8
$\text{Co}(\text{NO}_3)_2$ -pentyl alcohol	6.4	0-4.2
$\text{Co}(\text{NO}_3)_2$ - <i>n</i> -hexyl alcohol	5.8	0-4.4
$\text{Cu}(\text{NO}_3)_2$ - <i>n</i> -butyl alcohol	5.3	0-4.0
$\text{Cu}(\text{NO}_3)_2$ -pentyl alcohol	5.3	0-4.4
$\text{Zn}(\text{NO}_3)_2$ - <i>n</i> -butyl alcohol	6.2	0-4.2
$\text{Zn}(\text{NO}_3)_2$ -pentyl alcohol	6.2	0-4.4
$\text{Zn}(\text{NO}_3)_2$ - <i>n</i> -hexyl alcohol	5.2	0-4.9

The decrease in slope at high electrolyte molalities in the solvent phase was also found by Yates, *et al.*, and, as they suggested, could be caused by a replacement of water by the alcohols or by the adoption of some less highly solvated structure. The apparent hydration numbers are intermediate between those for the similar perchlorates (cobalt(II) perchlorate, 14.7) and chlorides (zinc chloride, 2.2) in 2-octanol.<sup>1</sup> Yates, *et al.*, explained the difference between the perchlorates and chlorides by the inability of the perchlorate ion to approach the cation closely, either as a coordinating anion or in the formation of an electrostatic ion pair, (as is shown by the very high activity coefficients

(5) R. A. Robinson and R. H. Stokes, "Electrolyte Solutions," Butterworths, London, 1955.

(6) C. C. Templeton and L. K. Daly, *J. Phys. Chem.*, **56**, 215 (1952).

(7) C. C. Templeton, *ibid.*, **54**, 1255 (1950).



found in concentrated aqueous solutions of perchlorates) and so the cation is left free to form a highly hydrated structure. Since the activity coefficients in aqueous solutions of the nitrates are intermediate between those in perchlorate and chloride solutions of similar concentrations the intermediate position of their apparent hydration numbers is in accord with this hypothesis.

**Acknowledgment.**—The author wishes to thank the referee for his helpful comments.

### THE REACTION OF ALKYL MERCURIC IODIDES WITH ACID IN THE PRESENCE OF OXYGEN<sup>1</sup>

BY MAURICE M. KREEVOY AND RICHARD L. HANSEN<sup>2</sup>

School of Chemistry, University of Minneapolis, Minneapolis, Minn.

Received November 10, 1960

In the course of another investigation<sup>3</sup> it was found that the reactions of isopropyl and *t*-butylmercuric iodides with aqueous, non-halogen acids are profoundly influenced by the presence of oxygen. The reaction involved has by no means been completely characterized but it was felt advisable to report on our preliminary results because of the unusual nature of some of them.

#### Results

The reactions were carried out in sealed ampoules of about 5-ml. capacity containing about 3 ml. of aqueous solution. In most experiments the substrate concentration was  $10^{-4} M$  and the space above the solution was filled with air so that more than a hundred-fold excess of oxygen was present. The progress of each reaction was followed by observing the build-up of optical density at 2700 Å. In each isopropylmercuric iodide experiment, one-half mole of mercuric iodide was produced per mole of starting material. Its identity was confirmed by adding excess sodium iodide and observing the characteristic ultraviolet spectrum of the  $HgI_4^-$  ion. Because of the smallness of the quantities involved, it has not yet been possible to identify the organic products. Good pseudo first-order kinetics were observed in all cases and rate constants were obtained graphically. The plots were comparable with those obtained previously.<sup>4</sup> Individual rate constants were reproducible within a few per cent. Because half a mole of mercuric iodide was produced per mole of substrate, it was assumed that half a mole of substrate was being inactivated as  $RHg^{\oplus}$  and rate constants were obtained from eq. 1.<sup>3</sup> If this assumption should ultimately prove false, these

$$k_1 = \frac{2.303}{2(t - t_0)} \log \frac{(D_{\infty} - D_0)}{(D_{\infty} - D_t)} \quad (1)$$

(1) (a) This work was supported in part by the Air Force Office of Scientific Research, through contract no. AF 49(638)711, in part by the National Science Foundation, through grant no. N.S.F.-G5434, and in part by the Graduate School of the University of Minnesota. Reproduction in whole or in part is permitted for any purpose of the United States Government.

(2) Sun Oil Co. fellow 1958-1959; Du Pont Co. fellow summer, 1959.

(3) M. M. Kreevoy and R. L. Hansen, *J. Am. Chem. Soc.*, **83**, 626 (1961).

(4) M. M. Kreevoy, *ibid.*, **79**, 5927 (1957).

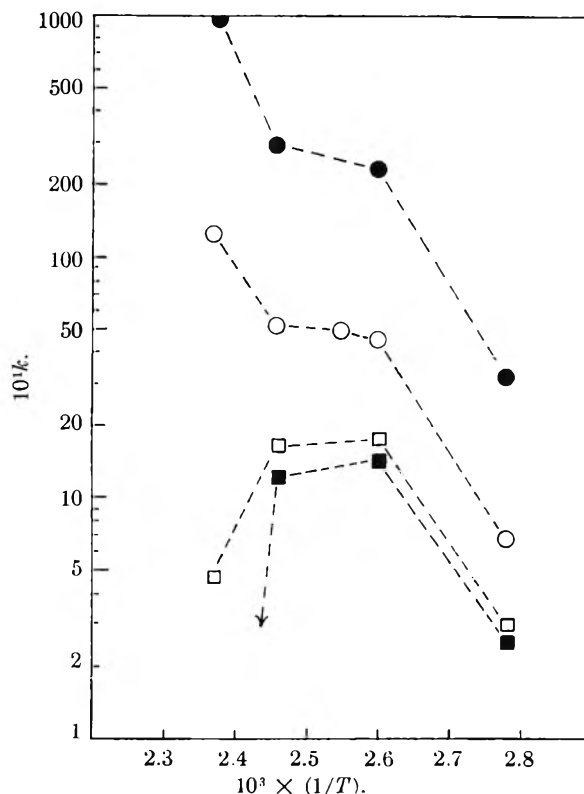


Fig. 1.—Dependence of rate on temperature: first-order rate constants at 0.136 *M* perchloric acid are ○; first-order rate constants at 0.0136 *M* perchloric acid are □;  $k_H$ 's are ● and  $k_O$ 's are ■. The ordinates are logs of rate constants and the numerical scale shows the rate constants themselves.

would all be in error by a factor of two.

With isopropylmercuric iodide, the rate was studied as a function of perchloric acid concentration at  $111.0 \pm 0.5^\circ$ . The acid concentrations studied ranged up to 0.2 *M*. The pseudo first-order rate constants showed a linear dependence on the acid concentration with a non-zero intercept. They are given by eq. 2 with an average deviation of 9%. The reality of the intercept was verified by observing that the reaction did proceed in the

$$k_1 = k(HClO_4) + k_0 \quad (2)$$

$$k_H = 2.7 \times 10^{-4} \text{ l. mole}^{-1} \text{ sec.}^{-1}$$

$$k_0 = 1.1 \times 10^{-5} \text{ sec.}^{-1}$$

absence of acid although no rate constants were obtained under these conditions. At  $111^\circ$  and 0.0136 *M* perchloric acid the inclusion of 0.167 *M* sodium perchlorate in the reacting solution caused a 60% increase in rate.

The rate with isopropylmercuric iodide was studied as a function of temperature at 0.136 and 0.0136 *M* perchloric acid. Figure 1 shows the logarithms of the first-order rate constants plotted against reciprocal temperature. The quantities  $k_H$  and  $k_O$  were obtained at each temperature from eq. 2, and their logarithms are also plotted against reciprocal temperature in Fig. 1. It is evident that neither of the two first-order rate constants obeys the Arrhenius rate law.<sup>5</sup> That portion of the reaction which is independent of acid concen-

(5) A. A. Frost and R. G. Pearson, "Kinetics and Mechanism," John Wiley and Sons, Inc., New York, N. Y., 1953, p. 23.

tration,  $k_0$ , fails to obey the Arrhenius rate law most spectacularly of all, apparently rising to a maximum around 120° and falling to zero at 147°. This strange behavior is not due to changes in the solubility of oxygen because the solubility of oxygen in water is nearly temperature independent in the pertinent range of temperatures.<sup>6</sup> More careful experimental work may show that  $k_H$  does obey the Arrhenius (and the Eyring) rate laws. The four points shown appear to represent scatter about a line. Considering that each  $k_H$  is the slope of a line determined from only two experiments, that scatter may not be in excess of the uncertainty in the points.

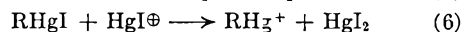
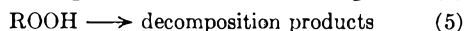
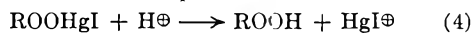
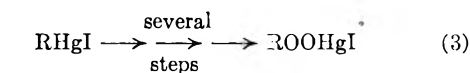
At all temperatures,  $k_H$  is considerably larger than the second-order rate constant for acid cleavage obtained in the absence of oxygen. At 111°, for example,  $k_H$  is  $2.69 \times 10^{-4}$  l. mole<sup>-1</sup> sec.<sup>-1</sup>, while the second-order rate constant for acid cleavage in the absence of oxygen is  $1.3 \times 10^{-6}$  l. mole<sup>-1</sup> sec.<sup>-1</sup>.

The reaction of *t*-butylmercuric iodide was not thoroughly investigated because of the solubility difficulties encountered, but there, also, oxygen had a very profound effect on the observed rates. For example, with 0.136 *M* perchloric acid and ampoules sealed in air, a first-order rate constant of  $3.32 \times 10^{-5}$  l. mole<sup>-1</sup> sec.<sup>-1</sup> was obtained at 100°. Under identical conditions but with each ampoule bubbled with oxygen-free nitrogen for one minute before sealing, the rate constant was  $1.39 \times 10^{-8}$  l. mole<sup>-1</sup> sec.<sup>-1</sup>. The latter may still be higher than the oxygen-free rate because more stringent precautions had to be taken to reach a minimum rate at higher temperatures.<sup>3</sup>

### Discussion

To our knowledge, there is no previous report of a reaction between organomercurials and oxygen, although it is well known that other organometallics react with oxygen and the reactions have been extensively studied.<sup>7</sup>

Equations 3-6 show an attractive path by which the present reaction might proceed.



The temperature dependence of the rate, particularly at the lower acid concentrations, strongly suggests that the key steps, represented in eq. 3, are decidedly unusual in character. More mechanistic speculation does not seem in order at this stage.

### Experimental

The general procedures used in preparing solvents and reagents have been described previously,<sup>4</sup> as has the preparation of the substrates.<sup>3</sup> All of the "aqueous" solutions referred to above actually contained 2% of methanol since the substrates were handled as stock solutions in that solvent.

(6) H. A. Pray, C. Schweickert and B. Minnich, *Ind. Eng. Chem.*, **44**, 1146 (1952).

(7) H. Hock, H. Kropf and F. Ernst, *Anzwe. Chem.*, **71**, 541 (1959).

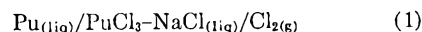
## SOME THERMODYNAMIC PROPERTIES OF THE SYSTEM PLUTONIUM CHLORIDE-SODIUM CHLORIDE FROM ELECTRO-MOTIVE FORCE DATA

By R. BENZ AND J. A. LEARY

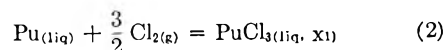
University of California, Los Alamos Scientific Laboratory, Los Alamos, New Mexico

Received November 12, 1960

Recently a study<sup>1</sup> of the free energy of formation of PuCl<sub>3</sub> in the binary system PuCl<sub>3</sub>-KCl was made using potentiometric methods. This paper is a report on e.m.f. data as a function of temperature and composition obtained from galvanic cells of the type



The cell reaction is



The thermodynamic formation quantities are derived and compared with those taken from the previous study.

### Experimental

**Materials.**—PuCl<sub>3</sub> was prepared as previously described.<sup>2</sup> The plutonium used for the metal electrodes was 99.8 ± 0.1% pure by chemical analysis. Sodium chloride (Baker and Adamson, A.C.S. grade) was dried, melted in a quartz container under an atmosphere of hydrogen chloride, cast into a stick form and stored in a vacuum desiccator. The melting point of the sodium chloride was determined to be 801 ± 2° in agreement with the reported value.<sup>3</sup> Hydrogen chloride (Matheson Co.) was dried with magnesium perchlorate. Argon (Linde Air Products) was dried with phosphorus pentoxide. Chlorine gas (Matheson Co., 99.3% pure) was used without further treatment. The pressure of the chlorine gas, which was measured with an accuracy of ± 1 mm. in the range 588 to 598 mm., was corrected to one atmosphere by assuming the gas to be ideal and adding  $(-RT \ln p)/2$  to the observed e.m.f. values.

The chemical composition of each solution (25 to 75 g. total weight) was based upon the composition by weight of the component salts.

**Apparatus and Procedure.**—The apparatus and procedure has been described.<sup>1</sup>

A single measurement usually extended over a period of 5 minutes. During this period the e.m.f. readings were verified to be reproducible after applying for two seconds an electrodepositing current of 15 ma. at 2.5 v. and, again, after applying for two seconds an electrodisolving current. After a measurement was completed, adjustments were made to establish a new temperature equilibrium, shifted by 10 to 30°, increasing and decreasing at alternate measurements such that alternate equilibrium temperatures were approached from above and below. Such a series of potentiometric measurements was carried out on each of the liquid solutions<sup>4</sup> in the temperature range 640 to 755° for the PuCl<sub>3</sub> mole fractions 0.750, 0.700, 0.600 and 0.500. The cells remained reversible for periods of from 2 to 11 hours.

### Results

**Calculations.**—The notation employed by Wagner<sup>5</sup> for the thermodynamic mixing properties is followed. The subscript 1 denotes liquid  $\frac{1}{2}$ PuCl<sub>3</sub> and 2 denotes liquid sodium chloride.  $X_1$  and  $X_2$

(1) R. Benz, *J. Phys. Chem.*, **65**, 81 (1961).

(2) R. Benz, Milton Kahn and J. A. Leary, *ibid.*, **63**, 1983 (1959).

(3) National Bureau of Standards Circular No. 500, 1952, p. 804.

(4) C. W. Bjorklund, J. G. Reavis, J. A. Leary and K. A. Walsh, *J. Phys. Chem.*, **63**, 1774 (1959).

(5) C. Wagner, "Thermodynamics of Alloys," Addison-Wesley Press, Inc., New York, N. Y., 1952, Chap. 1.

denote the mole fractions of  $\text{PuCl}_3$  and  $\text{NaCl}$ , respectively. The reference state for the relative partial quantities is that of the supercooled liquid  $\text{PuCl}_3$  at  $973^\circ\text{K}$ . and one atmosphere.

The e.m.f., denoted by  $\epsilon$ , was determined at various compositions of the electrolytic solutions as a function of temperature. After having been corrected to that of one atmosphere of chlorine gas (corrections ranged from 0.010 to 0.012 v.) and for thermoelectric effects in the external circuit (corrections ranged from 0.005 to 0.008 v.), these data were represented (least squares fit) by linear equations of the form

$$\epsilon x_1 = ax_1 + bx_1 T$$

where  $a_{X_1}$  and  $b_{X_1}$  are constants for the solution of  $\text{PuCl}_3$  having mole fraction  $X_1$  and  $T$  denotes the absolute temperature. The experimental points fit the linear equation with a standard deviation of 0.001 to 0.002 v. The results are given analytically in Table I.

TABLE I

POTENTIOMETRIC DATA AS A FUNCTION OF TEMPERATURE FOR THE FORMATION OF  $\text{PuCl}_3$  IN THE LIQUID BINARY SYSTEM  $\text{PuCl}_3\text{-NaCl}$  AT VARIOUS COMPOSITIONS

$x_1$	$\epsilon$ , v.	Max. dev., mv.	Temp. range, $^\circ\text{K}$ .	No. of e.m.f. determin.
0.750	$2.984 - 0.5280 \times 10^{-3} T$	$\pm 2$	974 to 1028	22
.700	$2.996 - .5242 \times 10^{-3} T$	$\pm 1$	945 to 978	5
.600	$3.002 - .5220 \times 10^{-3} T$	$\pm 4$	913 to 1020	16
.500	$3.004 - .5069 \times 10^{-3} T$	$\pm 3$	945 to 1017	9

The calculations involve, first, extrapolation of the data to the state of pure  $\text{PuCl}_3$  at  $973^\circ\text{K}$ . in order to obtain the thermodynamic quantities for the formation of the supercooled liquid salt. Using these results, the relative partial molar free energies of mixing liquid  $\text{PuCl}_3$  were computed. Finally, using these data and data taken from the literature, the standard formation quantities for solid  $\text{PuCl}_3$  were computed. Further details of these calculations are described below.

The free energy ( $\Delta F_1$ ), entropy ( $\Delta S_1$ ) and enthalpy ( $\Delta H_1$ ) of formation of  $\text{PuCl}_3$  in the liquid  $\text{PuCl}_3\text{-NaCl}$  solutions at  $973^\circ\text{K}$ . for the various compositions were computed using the formulas

$$\Delta F_1 = -3F\epsilon x_1 \quad (4)$$

$$\Delta S_1 = - \left( \frac{\partial}{\partial T} \Delta F_1 \right)_p \quad (5)$$

$$\Delta H_1 = \Delta F_1 + 973\Delta S_1 \quad (6)$$

The results are shown in Table II. The value of the free energy of formation of pure supercooled liquid  $\text{PuCl}_3$ , which will be denoted  $\Delta F_1^*$ , represents the arithmetic average of the values obtained upon extrapolating the function  $F_1^E/X_2^2$  for the various solutions to the state  $X_1 = 1.000$ .  $F_1^E$  denotes the excess partial free energy of mixing  $\text{PuCl}_3$ , i.e.,  $F_1^E = \Delta F_1 - \Delta F_1^* - RT \ln X_1$ . The entropy of formation of pure supercooled liquid  $\text{PuCl}_3$ ,  $\Delta S_1^*$ , was taken as the arithmetic average of the excess entropy of formation of  $\text{PuCl}_3$ ,  $\Delta S_1^E = \Delta S_1 + R \ln X_1$ , for the solutions. The enthalpy of formation of pure supercooled liquid  $\text{PuCl}_3$  was obtained using the relation  $\Delta H_1^* = \Delta F_1^* + 973 \cdot$

$\Delta S_1^*$ . The relative partial molar free energy of mixing for supercooled liquid  $\text{PuCl}_3$  at  $973^\circ\text{K}$ . is given in column 5 of the same table.

The standard molar quantities for the formation for solid  $\text{PuCl}_3$  at  $973^\circ\text{K}$ . are given in the last row of Table III. These quantities were obtained by combining the reactions (a) and (b) in Table III. The data for reaction (b), the freezing of liquid  $\text{PuCl}_3$  at  $973^\circ\text{K}$ ., were obtained from Table IV of reference 1.

TABLE II

THE MOLAR THERMODYNAMIC QUANTITIES OF FORMATION OF LIQUID  $\text{PuCl}_3$  AND THE PARTIAL MOLAR FREE ENERGY OF  $\text{PuCl}_3$  FOR THE SYSTEM  $\text{PuCl}_3\text{-NaCl}$  AT  $973^\circ\text{K}$ .

$X_1$	$\Delta F_1$ , kcal.	$\Delta S_1$ , e.u.	$\Delta H_1$ , kcal.	$F_1^M$ , kcal.
1.000	-169	-36.9	-205	0
0.750	-171	-36.5	-206	-2
.700	-172	-36.3	-207	-3
.600	-173	-36.1	-208	-4
.500	-174	-35.1	-208	-5

TABLE III

THE STANDARD MOLAR THERMODYNAMIC QUANTITIES FOR THE FORMATION OF PURE  $\text{PuCl}_3$  IN THE SUPERCOOLED LIQUID AND IN THE SOLID STATE

Reaction at $973^\circ\text{K}$ .	$\Delta F$ , kcal.	$\Delta S$ , e.u.	$\Delta H$ , kcal.	Ref.
(a) $\text{Pu}_{(liq)} + \frac{3}{2} \text{Cl}_{2(g)} = \text{PuCl}_{3(liq)^*}$	-169	-36.9	-205	This work
(b) $\text{PuCl}_{3(liq)^*} = \text{PuCl}_{3(s)}$	-1.0	-14.7	-15.3	6
(c) $\text{Pu}_{(liq)} + \frac{3}{2} \text{Cl}_{2(g)} = \text{PuCl}_{3(s)}$	-170	-51.6	-220	

**Reliability.**—The use of an inert-porous-thoria partition for the purpose of reducing the rate of mutual dissolution of the metallic plutonium electrode and the electrolyte has been discussed.<sup>1</sup> The necessary conditions for reversibility were satisfied by all the galvanic cells, i.e., the e.m.f. was independent of time, independent of the direction of approach to temperature equilibrium and reproducible after passing a small electro-dissolving and electrodepositing current through the cell.

Electrolytic solutions of mole fraction  $X_1 < 0.5$  showed a weight gain after having been saturated with chlorine gas at  $700^\circ$  and quenched to room temperature. No data are reported for this range of composition since some plutonium must exist in an oxidation state higher than three and cells containing such electrolytes involve a mixed cell reaction. The Cl:Pu ratio in solutions of mole fractions  $X_1 > 0.5$ , after saturation with chlorine gas, was found to be  $3.0 \pm 0.1$  by chemical analysis. It is concluded that the concentration of a higher oxidation state is negligible for the reported data.

### Discussion

The standard free energy and entropy of formation of pure solid  $\text{PuCl}_3$  have been determined to be, respectively,  $-170$  kcal./mole and  $-52$  e.u. which agree with previous results<sup>1</sup> within the precision of the measurements. The  $\text{PuCl}_3\text{-NaCl}$  system exhibits negative deviations from Rault's law.

(6) G. L. Brewer, L. Bromley, P. W. Gilles and N. L. Lofgren, "The Transuranic Elements," National Nuclear Energy Series, Div. IV, Vol. 14B, McGraw-Hill New York, N. Y., 1949, pp. 851-886.

**Acknowledgments.**—We would like to thank R. D. Baker and W. J. Maraman for their interests which have been an encouragement throughout the progress of the work. We are indebted to J. W. Anderson and A. N. Morgan for the machined plutonium metal, to C. F. Metz, C. T. Apel, D. C. Croley and G. R. Waterbury for the chemical analyses and to R. E. Cowan and S. D. Stoddard for the thoria crucibles.

## ENERGIES OF THE GASEOUS ALKALINE EARTH HALIDES<sup>1</sup>

BY DANIEL CUBICCIOTTI

Stanford Research Institute, Menlo Park, California

Received November 12, 1960

The binding energies of the gaseous alkali halides have been calculated successfully by Berkowitz<sup>2</sup> with the method of Rittner.<sup>3</sup> Since the internuclear distances in the gaseous alkaline earth halides have been measured,<sup>4</sup> it seemed useful to attempt to calculate their binding energies.

In the method of Rittner the expression for the energy consists of terms for coulombic attraction polarization and "overlap" repulsion. For the alkaline earth halide molecules, which are assumed to be linear, the coulombic term consists of the attractions of the positive ion for the two negative ions and the repulsion between the negative ions. The coulombic energy becomes  $(-3.5e^2/r)$ , where  $r$  is the cation-anion distance. In each anion a dipole is induced by the field of the positive ion and the other anion. The field at the anion center is  $(7e/4r^2)$ , and the dipole moment induced is  $\alpha$  (its polarizability) times the field. The total energy contributed by this polarization is  $\alpha(7e/4r^2)^2$  times 2 (because there are two anions) times  $1/2$  (because half of the energy is stored in the dipoles). In the present treatment the dipole-dipole energy and the van der Waals dispersion energy are neglected because they are small, amounting at most to one-half per cent. of the total energy.

The overlap repulsion energy term is of an empirical nature. The form used by Rittner and Berkowitz for the alkali halides was  $A \exp(-r/\rho)$ . The parameter  $\rho$  was evaluated from the vibration frequencies of several gaseous alkali halides. It was found to be approximately the same for all the salts and roughly equal to the corresponding parameter for the crystalline solids. The parameter  $A$  was evaluated for each salt by using the condition that the energy be at a minimum at the equilibrium internuclear distance.

For the alkaline earth halides there is not sufficient information on the vibration frequencies to evaluate the parameter  $\rho$ . Therefore, the values determined for the solid alkali halides were used,

namely, 0.313 for fluorides, 0.318 for chlorides, 0.325 for bromides, and 0.332 for iodides.<sup>5</sup> The equations for the energy of formation of the alkaline earth halides at their equilibrium internuclear distances from the infinitely separated ions are

$$w = -\frac{3.5e^2}{r} - \frac{49e^2\alpha}{16r^4} + A \exp\left(-\frac{r}{\rho}\right)$$

$$\left(\frac{dw}{dr}\right)_{r_0} = 0 = +\frac{3.5e^2}{r_0^2} + \frac{49e^2\alpha}{4r_0^5} - \frac{A}{\rho} \exp\left(-\frac{r_0}{\rho}\right)$$

Thus at the equilibrium internuclear distance  $r_0$

$$w_0 = -\frac{3.5e^2}{r_0} \left(1 - \frac{\rho}{r_0}\right) - \frac{49e^2\alpha}{16r_0^5} \left(1 - \frac{4\rho}{r_0}\right) \quad (1)$$

Using the ionic polarizabilities given by Tesson, Kahn and Shockley<sup>6</sup> the energies calculated are given in the first column of Table I.

TABLE I

ENERGIES (KCAL./MOLE) OF THE REACTION  $MX_2(g) = M^{++}(g) + 2X^-(g)$  FOR THE ALKALINE EARTH HALIDES

	Caled. by		Caled. by eq. 2
	eq. 1	Expt.	
BeF <sub>2</sub>	662	748	748
Cl <sub>2</sub>	623	677	707
Br <sub>2</sub>	606	662	675
I <sub>2</sub>	565	641	624
MgF <sub>2</sub>	560	589	591
Cl <sub>2</sub>	511	555	533
Br <sub>2</sub>	490	530	513
I <sub>2</sub>	473	519	500
CaF <sub>2</sub>	484	502	502
Cl <sub>2</sub>	442	475	455
Br <sub>2</sub>	426	458	438
I <sub>2</sub>	409	453	425
SrF <sub>2</sub>	465	482	482
Cl <sub>2</sub>	416	450	427
Br <sub>2</sub>	402	431	413
I <sub>2</sub>	386	420	400
BaF <sub>2</sub>	445	436	463
Cl <sub>2</sub>	393	428	404
Br <sub>2</sub>	377	407	389
I <sub>2</sub>	363	389	377

The experimental values for the energy of formation from the infinitely separated ions are also given in Table I. They were taken from information from the National Bureau of Standards<sup>7</sup> plus the estimated heats of sublimation of the alkaline earth halides of Brewer.<sup>8</sup> The agreement between the experimental and calculated values is poor and in general is well outside the 1% error of measurement of the internuclear distance and the  $\pm 10$  to 20 kcal./mole which is the probable range of accuracy of the experimental heats.

Because of this lack of agreement a different set of assumptions was tried for the overlap repulsion term. The term was assumed to have the alternate form  $Ar^{-n}$  in which the values of  $n$  given by Pauling<sup>9</sup> were used. This set of  $n$ 's was pre-

(5) D. Cubicciotti, *J. Chem. Phys.*, **31**, 1646 (1959); **33**, 1579 (1960).

(6) J. R. Tesson, A. H. Kahn and W. Shockley, *Phys. Rev.*, **92**, 890 (1953).

(7) (a) F. D. Rossini, D. D. Wagman, W. H. Evans, S. Levine and I. Jaffe, National Bureau of Standards, Circular 500, 1952; (b) National Bureau of Standards Report 6484, 1959.

(8) L. Brewer, "Chem. and Met. of Misc. Matls.," NNS 1V-19B McGraw-Hill Book Co., New York, N. Y., 1950.

(9) L. Pauling, "The Nature of the Chemical Bond," Cornell Press, Ithaca, N. Y., 1960, 3rd Ed., Table 13-2, p. 509.

(1) This research was supported by the United States Air Force through the Air Force Office of Scientific Research of the Air Research and Development Command under Contract No. AF 49(638)-89. Reproduction in whole or in part is permitted for any purpose of the United States Government.

(2) J. Berkowitz, *J. Chem. Phys.*, **29**, 1386 (1958).

(3) E. S. Rittner, *ibid.*, **19**, 1030 (1951).

(4) P. A. Akishin and V. P. Spiridonov, *Kristallografiya (USSR)*, **2**, 475 (1958).

sumably derived from the compressibilities of the alkali halide crystals. The energy equation then becomes

$$w_0 = -\frac{3.5e^2}{r_0} \left(1 - \frac{1}{n}\right) - \frac{49e^2\alpha}{16r_0^4} \left(1 - \frac{4}{n}\right) \quad (2)$$

The values calculated from this equation are given in the last column of Table I. The agreement of this set with the experimental values is remarkably good.

Similar calculations were made for the alkali halides for which accurate internuclear distances had been measured. The two different equations representing the energies are

$$w_0 = -\frac{e^2}{r_0} (1 - R) - \frac{e^2}{2r_0^4} (\alpha_1 + \alpha_2)(1 - 4R) - \frac{2e^2\alpha_1\alpha_2}{r_0^7} (1 - 7R) - \frac{c}{r_0^6} (1 - 6R) \quad (3)$$

$$R = \frac{\rho}{r_0} \text{ for exp} \left(-\frac{r}{\rho}\right) \text{ repulsion} \quad (3a)$$

$$R = \frac{1}{n} \text{ for } r^{-n} \text{ repulsion} \quad (3b)$$

In this case the last two terms representing dipole-dipole interaction and van der Waals dispersion were kept because of the greater precision of the available experimental data. Values for  $c$  were taken from Mayer.<sup>10</sup>

The results of the two calculations are given in Table II. These are compared with experimental values compiled by Brewer.<sup>11</sup> It can be seen that although the energies given by the  $r^{-n}$  calculation are consistently greater than the  $\exp(-r/\rho)$ , the agreement of either calculation with the experimental is quite satisfactory.

TABLE II

ENERGIES (KCAL./MOLE) OF THE REACTION  $\text{MX}(\text{g}) = \text{M}^+(\text{g}) + \text{X}^-(\text{g})$  FOR THE ALKALI HALIDES

	Calcd. by eq. 3a	Expt.	Calcd. by eq. 3b
LiBr	143	144	147
I	134	135	140
NaCl	130	130	132
Br	125	124	128
I	118	117.5	122
KCl	118	115	119
Br	112	110	114
I	106	104	109
RbF	134	131	140
Cl	114	110	116
Br	109	105.5	111
I	103	99.5	105
CsF	134	128	142
Cl	111	110	114
Br	107	106	109
I	102	99	103

The  $\exp(-r/\rho)$  form can, of course, be made to express the energies of the alkaline earth halides as well; however, the value of  $\rho$  would not be almost a constant from one salt to another as it is for the alkali halides. The point to be made, perhaps, is not which analytic form gives the better

representation, but that our present state of knowledge of overlap repulsions is inadequate.

## VAPOR PRESSURE AND SOLID-VAPOR EQUILIBRIUM OF CdSe (Cadmium Selenide)

By G. A. SOMORJAI

IBM Research Center, Yorktown Heights, New York

Received November 14, 1960

CdSe is one of the more interesting II-VI intermetallic compounds because of its potentially useful photoconductive properties. Although the material melts at around 1240° it exhibits a significant vapor pressure appreciably below its fusion temperature and it has been postulated<sup>2,3</sup> that the vapor phase does not contain the molecular species, a condition believed to exist in all of the II-VI compounds vapors. The vapor pressures of CdSe in the temperature range of 800–950°K. were determined by Goldfinger<sup>3</sup> from mass spectrometric data. However, the data are the result of quasi equilibrium conditions, and it was felt that a re-evaluation of the vapor phase species and extension of the temperature range might be useful.

In the present investigation, the vapor pressure of CdSe has been measured in the temperature interval 975 to 1210°K. by two methods. One involved the application of a quartz Bourdon gauge to measure absolute equilibrium pressures above the sample and the other involved the dew-point technique which yields derived equilibrium vapor pressures. In the latter method one has to make an assumption as to the degree of dissociation of the molecules in the vapor phase. The application of two vapor pressure measurements, one direct and the other indirect, permits us to calculate the degree of dissociation of the vapor in equilibrium with the solid. If a proper model has been chosen as to the degree of dissociation, derived dew-point measurement data should overlap those obtained by Bourdon gauge measurements. If, however, one chooses an incorrect model for the calculations, the data resulting from the two measurements will not overlap, and the degree of dissociation in the vapor phase will be given directly by the ratio of the vapor pressures determined from the two measurements at any given temperature.

Since the vapor pressures measured were in the range 0.1–25 mm., with the majority of measurements made in the 0.1–10 mm. range, ideal vapor phase behavior was assumed.

### Experimental Procedure

CdSe obtained from the General Electric Company was purified further *via* sublimation *in vacuo*. Wet chemical and spectrographic analysis indicated the material was stoichiometric and pure to better than 1 part/thousand.

The total pressures were determined by means of a Bourdon gauge constructed of quartz which extends the temperature range for this instrument appreciably beyond its normal usage. It measures vapor pressures<sup>4</sup> in the range

(1) A. Reisman (IBM Research Center, Yorktown Heights, N. Y.), private communication.

(2) C. L. McCabe, *J. Metals*, **7**, 969 (1954).

(3) P. Goldfinger, Final Report, U. S. Air Force, AF 61(052)-19.

(4) V. J. Lyons, *J. Phys. Chem.*, **64**, 266 (1960).

(10) J. E. Mayer, *J. Chem. Phys.*, **1**, 270 (1933).

(11) L. Brewer and E. Brackett, private communication. The author is grateful to Prof. Brewer for allowing him to use these results in advance of publication.

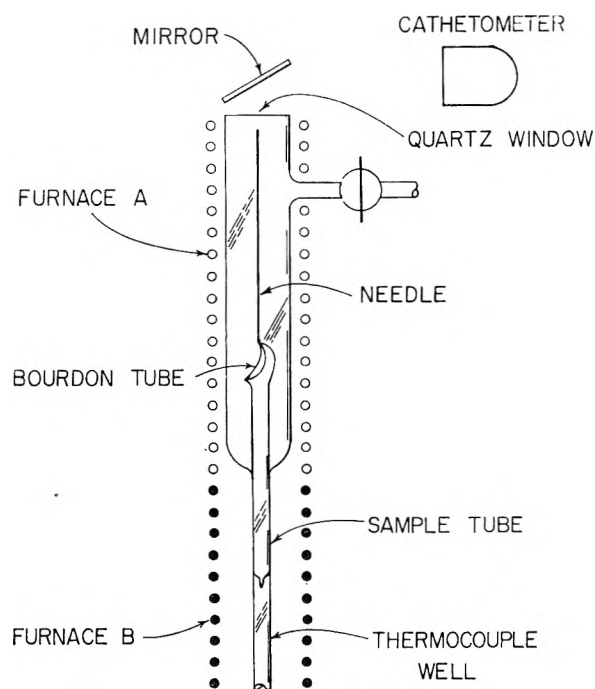


Fig. 1.—Quartz Bourdon gauge for total pressure measurements.

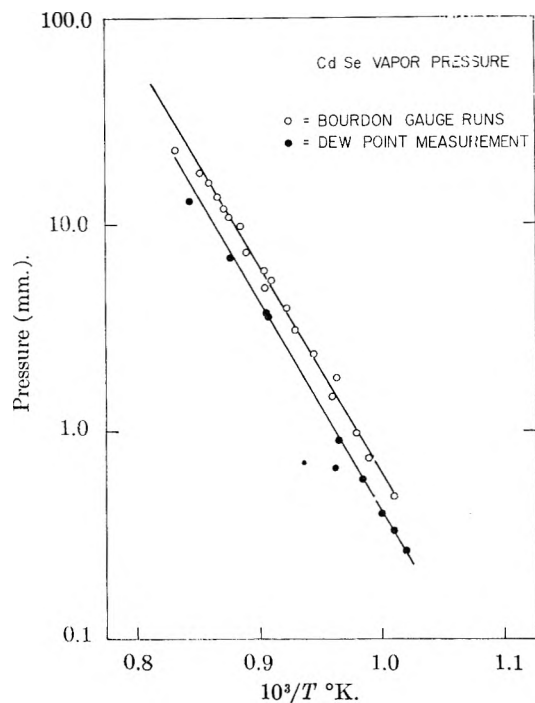


Fig. 2.—CdSe vapor pressure.

of 1 mm. to atmospheric pressures. Below 0.5 mm. the sensitivity of the gauge is too low to obtain accurate data. The temperature limit is 1250°, at which point permanent changes take place in the thin Bourdon spoon. As shown in Fig. 1, the Bourdon spoon is enclosed in a quartz tube with a side arm to which a stopcock is sealed. The sample tube is sealed to the lower end of the spoon. A 35 cm. long quartz fiber is attached to the top end of the Bourdon spoon to increase the accuracy of the measurement.

The gauge was baked out at 600° before loading under vacuum, in order to eliminate any possible contamination. After loading the sample tube with CdSe powder, both sides of the Bourdon gauge were evacuated simultaneously to a pressure of  $5 \times 10^{-5}$  mm. The sample tube then was sealed

by fusion and the upper part of the gauge was closed off by the stopcock.

Any pressure difference between the two volumes separated by the Bourdon spoon would make the attached quartz fiber deflect since the spoon is flexible. The sensitivity of the spoon and the length of the quartz needle determine the limit of the vapor pressure measurement on the low pressure side. The deflection of the quartz fiber due to pressure changes was observed with a Wild-Heerbrugg cathetometer and the probable reading error was of the order of 0.01 mm. The gauge was used as a null point instrument with the needle being brought back into null position after each sighting by equalizing the vapor pressure with nitrogen gas admitted through the stopcock at the upper part of the gauge. The nitrogen pressures were read with a mercury manometer.

The Bourdon gauge was placed in a Baker (E-3) high temperature furnace in such a manner that its spoon was in the middle of the hot zone. The furnace was controlled by a Wheelco 407 Temperature Controller. The sample tube was outside of the furnace and was surrounded by another furnace with a separate control.

The upper furnace temperature was raised to 1000° and allowed to equilibrate for 30 minutes, following which the quartz needle was brought into null position. The sample furnace was then turned on and the sample temperature was raised to 600°. Equilibrium was reached in one hour following which the sample temperature was raised in 30 degree steps. After each change in the sample temperature one hour was allowed for equilibrium to be attained. The sample temperature was measured with Pt-Pt, 10% Rh thermocouple.

There is a small deviation from the ideal equilibrium conditions because the Bourdon spoon has a somewhat higher temperature than the rest of the sample tube. This is necessary to prevent condensation of the vapor in the spoon. However, the spoon volume is very small compared to that of the sample tube, hence the error made by this temperature gradient is quite small. The sensitivity and reproducibility of the equipment was determined using CdCl<sub>2</sub> as a standard. Identical results were obtained with those reported in the literature.<sup>5</sup>

Dew-point measurements<sup>6</sup> were made in the range of 650–900°. For the determination of each experimental point a different quantity of CdSe, weighed to the nearest 0.01 mg., was placed in a quartz tube of known volume which subsequently was evacuated to  $5 \times 10^{-5}$  mm. at room temperature and sealed. The tube was placed in a long nichrome wound quartz tube furnace to provide gradient free temperatures, and it was visible from outside the furnace. A thermocouple well was located at one end of the tube. The temperature was measured by a Pt-Pt, 10% Rh thermocouple located in the well.

The furnace temperature was increased until all of the CdSe was in the vapor phase at which point nitrogen gas was blown into the thermocouple well until CdSe started to condense on the well wall. When the gas stream was stopped, the well returned to the original tube temperature. If this temperature was well above the dew-point the CdSe would disappear rapidly. The temperature then was lowered and the whole procedure was repeated. About 10° above the dew-point the evaporation rate is so slow that it took hours to complete the vaporization. Therefore, local heating was applied by an infrared lamp to speed up the evaporation. A small amount of CdSe was left on the well and was observed for an hour to note any change in the quantity of the condensate. This established the temperature to be above or below the dew-point. The procedure was repeated in a narrow temperature range until the dew point was located within  $\pm 1^\circ$ . If one assumes that CdSe exists as a monomer in the gas phase and that the vapor behaves as a perfect gas, then the vapor pressures can be calculated from the dew points by the ideal gas law.

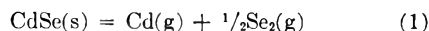
## Results and Discussion

Tables I and II give the vapor pressures obtained by the two measurements. The pressures are plotted as  $\log P$  vs.  $10^3/T$  in Fig. 2. The experimental points fell on two straight and parallel

(5) J. L. Barton and H. Bloom, *J. Phys. Chem.*, **60**, 1413 (1956).

(6) K. Weiser, *ibid.*, **61**, 531 (1957).

lines in the studied temperature range. The ratio of the two pressures at a given temperature is 1.51:1, indicating the degree of dissociation of CdSe in the vapor. Hence, within our experimental error, the data prove the existence of the equilibrium



Diatomic selenium is known to be the dominant species and generally used as a reference state<sup>7</sup> above the boiling point of selenium 958°K. On the other hand, there is no evidence<sup>8</sup> for diatomic cadmium in the vapor phase; therefore this possibility was ruled out as an alternate of equation 1.

The heat for the reaction can be calculated from the van't Hoff equation

$$\frac{d \ln K}{dT} = \frac{\Delta H^0}{RT^2} \quad (2)$$

One can express the equilibrium constant in terms of the total pressure, with the use of the law of partial pressures, as

$$K = \left(\frac{1.0}{1.5} P\right) \left(\frac{0.5}{1.5} P\right)^{1/2} = 0.385 P^{3/2} \quad (3)$$

If one assumes that  $\Delta H^0$  is constant over the studied temperature<sup>9</sup> range, direct integration yields

$$\log \frac{K_2}{K_1} = \frac{\Delta H^0}{R} \left( \frac{1}{T_1} - \frac{1}{T_2} \right) \quad (4)$$

$\Delta H^0 = 68.5$  kcal./mole at 1100°K. The vapor pressure of CdSe may be expressed from the data as a function of the temperature as

$$\log P_{\text{mm}} = -\frac{10020}{T^\circ\text{K.}} + 9.8 \quad (5)$$

From the heat of reaction and the heat of evaporation of liquid Cd metal,<sup>7</sup> the standard heat of formation of CdSe was calculated to be 44.6 kcal./mole at 1000°K. P. Goldfinger's<sup>3</sup> value of  $73.1 \pm 1.5$  kcal./mole for the heat of evaporation of CdSe at 900°K. according to eq. 1 is somewhat larger than the value reported in the present paper.

The author wishes to thank V. J. Lyons and T. G. Dunne for helpful discussions, J. Kucza for help with the experimental work and C. L. Fisher for constructing the quartz Bourdon gauge.

(7) D. R. Stull and G. C. Sinke, "Thermodynamic Properties of the Elements," A.C.S. Publication, 1956.

(8) K. K. Kelley, U. S. Bur. Mines, Bull. 383, 1935.

(9) S. Glasstone, "Thermodynamics for Chemists," D. Van Nostrand Co., New York, N. Y., 1947.

## 2,4-DIMETHYLENETETRABORANE: STRUCTURE FROM N.M.R. SPECTRA

BY I. SHAPIRO,<sup>1</sup> ROBERT E. WILLIAMS AND  
SIDNEY G. GIBBINS

Research Laboratory, Olin Mathieson Chemical Corporation, Pasadena,  
California

Received November 14, 1960

The compound formed by the reaction of ethylene and tetraborane had been tentatively identified as dimethylenetetaborane on the basis of its infrared spectrum and by chemical analysis.<sup>2</sup>

(1) Hughes Tool Company—Aircraft Division, Culver City, California.

The "cyclic" bridge structure of this compound now is confirmed by proton and B<sup>11</sup>-n.m.r. spectra obtained in this Laboratory. In addition the polyisotopic mass spectrum and vapor pressure data for this compound are reported.

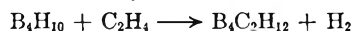
### Experimental

The reaction of ethylene with tetraborane to form dimethylenetetaborane has been carried out by both the low-temperature (70°) scaled tube method and the hot-cold reactor method.<sup>2</sup> The latter method is preferred for preparing larger samples of the compound. In either case, the compound is purified by fractionation<sup>2</sup> in standard high-vacuum apparatus.

The mass spectrum was obtained with a Consolidated Model 21-103 mass spectrometer operating at an ionizing potential of 70 v., and the n.m.r. spectra were obtained with a Varian V-4300 high resolution nuclear magnetic resonance spectrometer operating at 12.8 and 40 Mc. Vapor pressure values over the temperature range of -20 to 20° were obtained in an isoteniscope.

### Discussion

**Mass Spectrum.**—The polyisotopic mass spectrum of dimethylenetetaborane is given in Table I. There were no peaks observed above  $m/e$  80. The reduction of the data (calculated on the basis of 80% B<sup>11</sup> and 20% B<sup>10</sup>)<sup>3</sup> for the parent grouping ( $m/e$  67-80) to a monoisotopic spectrum leads to the conclusion that the molecule contains four boron atoms. The reduction of the spectrum on the basis of five boron atoms leads to significant negative values and, on the basis of three boron atoms, to appreciable residues. Consequently, the molecule must contain two carbon atoms with a balance of twelve hydrogen atoms, in agreement with the stoichiometry of the reaction<sup>2</sup>



From Table I the peak intensities at  $m/e$  79 and 80 are considerably less than those at  $m/e$  78 and immediately lower mass units; nevertheless, these peaks are real. Only 2% of  $m/e$  78 can be attributed to  $m/e$  79 for the C<sup>13</sup> contribution, *i.e.*, C<sup>12</sup>C<sup>13</sup> combination species. In this connection it is pointed out that in the case of tetraborane the mass spectral cut-off peak occurs at two mass units lower than the corresponding molecular weight.

**B<sup>11</sup>-N.M.R. Spectrum.**—The B<sup>11</sup>-n.m.r. spectrum of dimethylenetetaborane consists of a low-field doublet ( $J = 130$  c./s.) centered at  $\delta^4 = -4$ , and a high-field doublet ( $J = 145$  c./s.) centered at  $\delta = \sim 39$ . The peaks of the high-field doublet are about half the height but broader than the peaks of the low-field doublet.

From a comparison of the B<sup>11</sup>-n.m.r. spectra of dimethylenetetaborane and tetraborane<sup>5</sup> it is readily apparent that the low field triplet in tetraborane, representing BH<sub>2</sub> groups, has been transformed into a doublet (BH group) in the dimethylenetetaborane, thus indicating that substitution has occurred on the sites 2 and 4 boron nuclei. Alkyl substitution has shifted the low-field doublet ( $\delta = -4$ ) to lower field than the corresponding

(2) B. C. Harrison, I. J. Solomon, R. D. Hites and M. J. Klein, *J. Inorg. Nucl. Chem.*, **14**, 195 (1960).

(3) See ref. 10, I. Shapiro and J. Ditter, *J. Chem. Phys.*, **26**, 798 (1957).

(4) T. P. Onak, H. Landesman, R. E. Williams and I. Shapiro, *J. Phys. Chem.*, **63**, 1533 (1959).

(5) R. E. Williams, S. G. Gibbins and I. Shapiro, *J. Am. Chem. Soc.*, **81**, 6164 (1959).

TABLE I

POLYISOTOPIC MASS SPECTRUM OF DIMETHYLENETETRABORANE WITH PEAK INTENSITIES ADJUSTED TO MAXIMUM

VALUE OF 100 FOR  $m/e$  41

$m/e$	Intensity	$m/e$	Intensity	$m/e$	Intensity
80	0.7	57	6.6	35.5	0.8
79	1.9	56	2.6	35	17.2
78	28.6	55	1.2	34.5	0.3
77	33.4	54	0.5	34	7.6
76	57.9	53	4.0	33	2.4
75	50.0	52	14.6	32	0.6
74	34.0	51	33.4	31	.2
73	29.0	50	35.9	30	.1
72	19.8	49	45.4	29	.7
71	13.7	48	43.7	28	2.4
70	9.5	47	35.2	27	19.5
69	10.8	46	21.6	26	14.0
68	8.2	45	10.7	25	6.9
67	3.6	44	4.8	24	6.0
66	5.5	43	2.0	23	2.9
65	6.1	42	2.7	22	1.0
64	47.5	41	100	21	0.2
63	54.8	40	31.0	20	..
62	49.0	39	19.8	15	1.0
61	37.6	38	17.7	14	0.6
60	20.6	37	55.0	13	31.8
59	15.6	36.5	0.4	12	13.0
58	12.0	36	34.5	11	28.1

triplet of tetraborane ( $\delta = +6.5^4$ ). The high-field doublet (BH group) corresponding to sites 1 and 3 boron nuclei in the dimethylenetetraborane is shifted only slightly to lower field (less than 1  $\delta$ -unit) when compared to the corresponding doublet in tetraborane.

The spin-coupling ( $J_{H-B}$ ) in the high-field doublet (each member of the doublet actually is a septet due to spin-coupling with the 20%  $B^{10}$  isotope<sup>5</sup>) is less in the case of dimethylenetetraborane than in tetraborane, which probably accounts for an overlapping of the inner peaks of the septets to create a slight central peak between the members of the high-field doublet.

**$H^1$ -N.M.R. Spectrum.**—The proton spectrum (40 Mc.) was obtained at different power intensity levels in order to get proper resolution of the various peaks. The general contour of the spectrum is that of a very sharp, narrow and intense peak located off-center (toward low-field side) of a broad diffuse peak, with a number of small intensity peaks spaced throughout the spectrum but predominantly located on the low-field side of the broad diffuse peak.

The large single spike is attributed to the  $CH_2$  groups. The other peaks can be assigned to a pair of quartets representing the dissimilar B-H groups and to a bridge proton component (broad diffuse peak). The total width of this bridge component is fairly well defined ( $J = \sim 35$  c./s.) and is similar to that in other boron hydrides.<sup>5</sup> The peak position relationship of the bridge component to the quartet representing the hydrogens attached to the 1 and 3 boron nuclei is similar to that in tetraborane<sup>6</sup>; however, the quartet representing the 2- and 4-positions is shifted slightly more toward the low-field side than in the case of tetraborane.<sup>5</sup>

The proton spectrum is compatible with the  $B^{11}$  spectrum and with the interpretation of the cyclic bridge structure of 2,4-dimethylenetetraborane.

**Vapor Pressure.**—The vapor pressure data over the temperature range of  $-20$  to  $20^\circ$  is given in Table II. The calculated vapor pressures are obtained from the equation

$$\log P_{\text{mm}} = 10.22289 - \frac{3077.509}{T} + \frac{162748.8}{T^2}$$

This equation, obtained from the experimental data by the method of least squares, represents the data with an average deviation of 0.2 mm. The boiling point derived from this equation is approximately  $84^\circ$ . The heat of vaporization at  $298^\circ K$ . is found to be 9083 cal.

The single vapor pressure value at  $0^\circ$  reported previously<sup>2</sup> is in good agreement with the present data.

TABLE II

VAPOR PRESSURES OF DIMETHYLENETETRABORANE

$t, ^\circ C.$	V.p. obs., mm.	V.p. calcd., mm.	Dev., mm.
-23.1	3.30	3.30	0.0
-18.1	4.55	4.56	.0
-12.6	6.35	6.44	+ .1
-10.1	7.75	7.52	- .2
- 3.7	11.2	11.0	- .2
0	13.9	13.7	- .2
3.0	16.1	16.3	+ .2
6.9	20.0	20.4	+ .4
9.9	23.6	24.1	+ .5
14.3	30.9	30.7	- .2
18.3	38.5	38.0	- .5

Extrapolated boiling point  $\sim 84^\circ$

## A THERMODYNAMIC STUDY OF HOMOPIPERAZINE, PIPERAZINE AND N-(2-AMINOETHYL)-PIPERAZINE AND THEIR COMPLEXES WITH COPPER(II) ION

By JOSEPH M. PAGANO,<sup>1</sup> DAVID E. GOLDBERG AND W. CONARD FERNELIUS<sup>2</sup>

Department of Chemistry, The Pennsylvania State University, University Park, Pennsylvania

Received November 17, 1960

The effects of a number of factors on equilibria involving metal ion-amine complexes have been investigated.<sup>3</sup> However, none of these studies has included the coordination of a polyamine which, in order to coordinate, must shift from a more to a less stable conformation. Piperazine and some of its derivatives present an opportunity to study this situation. Although piperazine in its normal or "chair" conformation<sup>4</sup> would not be expected to act as a chelate group, a solid complex of N,N'-dimethylpiperazine in the "boat" conformation has been reported.<sup>5</sup>

(1) Holder of a National Science Foundation Research Participation award for the summer of 1960; State College at Bridgewater, Bridgewater, Massachusetts.

(2) Koppers Company, Inc., Pittsburgh 19, Pennsylvania.

(3) For references and discussion see C. R. Bertsch, W. C. Fernelius and B. P. Block, *J. Phys. Chem.*, **62**, 444 (1958).

(4) P. Andersen and O. Hassel, *Acta Chem. Scand.*, **3**, 1181 (1949), and later unpublished data as reported in ref. 5.



TABLE I  
VALUES FOR THE THERMODYNAMIC QUANTITIES  $\log K_n$ ,  $-\Delta F_n$ ,  $-\Delta H_n$  AND  $\Delta S_n$  FOR THE PROTONATION REACTIONS OF PIPERAZINE AND RELATED COMPOUNDS

$n$	$\log K_n$				$-\Delta F_n$ (kcal./mole)				$-\Delta H_n$ (kcal./mole)	$\Delta S_n$ (e.u.)
	10°	20°	30°	40°	10°	20°	30°	40°	10-40°	30°
Piperazine										
1	10.12 ± 0.07	9.89 ± 0.02	9.68 ± 0.00	9.48 ± 0.05	13.0	13.2	13.4	13.5	9.3	13
2	5.85 ± 0.05	5.63 ± 0.15	5.54 ± 0.05	5.37 ± 0.08	7.5	7.6	7.6	7.7	6.2	5
Homopiperazine <sup>a</sup>										
1	10.65 ± 0.04	10.41 ± 0.04	10.09 ± 0.12	9.86 ± 0.02	13.8	14.0	14.0	14.1	9.4	15
2	6.89 ± 0.08	6.70 ± 0.16	6.67 ± 0.17	6.28 ± 0.09	8.9	9.0	9.2	9.0	6.6	9
N-(2-Aminoethyl)-piperazine										
1	9.99 ± 0.05	9.63 ± 0.05	9.40 ± 0.06	9.13 ± 0.12	12.9	12.8	13.0	13.0	11.6	5
2	8.87 ± 0.02	8.51 ± 0.13	8.37 ± 0.02	8.06 ± 0.07	11.4	11.4	11.5	11.5	10.2	4
3	Too small to be measured									

<sup>a</sup> The actual temperatures of measurement with homopiperazine were 10.1, 20.2, 29.7 and 40.0°.

TABLE II  
VALUES FOR THE THERMODYNAMIC QUANTITIES  $\log K_n$ ,  $-\Delta F_n$ ,  $-\Delta H_n$  AND  $\Delta S_n$  FOR THE REACTION OF COPPER(II) ION WITH HOMOPIPERAZINE AND N-(2-AMINOETHYL)-PIPERAZINE

$n$	$\log K_n$				$-\Delta F_n$ (kcal./mole)				$-\Delta H_n$ (kcal./mole)	$\Delta S_n$ (e.u.)
	10°	20°	30°	40°	10°	20°	30°	40°	10-40°	30°
Homopiperazine <sup>a</sup>										
1	8.00 ± 0.11	7.92 ± 0.09	7.72 ± 0.12	7.55 ± 0.11	10.4	10.6	10.7	10.8	5.6	17
2	6.28 ± 0.17	6.19 ± 0.04	5.93 ± 0.14	5.84 ± 0.05	8.1	8.3	8.2	8.4	5.8	8
N-(2-Aminoethyl)-piperazine										
1	5.70 ± 0.19	5.51 ± 0.06	5.49	5.37 ± 0.23	7.3	7.4	7.6	7.6	4.6	10
2	3.84 ± 0.09	3.77 ± 0.18		3.69 ± 0.27	4.9	5.0		5.3	1.9	11

<sup>a</sup> The actual temperatures of measurement with homopiperazine were 10.1, 20.2, 29.7 and 40.0°.

The present investigation was undertaken to determine (1) whether or not piperazine and/or the closely related compounds, N-(2-aminoethyl)-piperazine and homopiperazine (1,4-diazacycloheptane) coordinate with copper(II) ion, (2) the energetics of the reactions where coordination takes place and (3) the energetics of protonation of the amines (see Tables I and II). It is thus possible to make the following comparisons: piperazine *vs.* a simple linear diamine, piperazine with a derivative having a third nitrogen atom in a position favorable to coordination, and piperazine *vs.* a homolog where the model indicates that the additional methylene group decreases the distance between the two nitrogen atoms in the "boat" conformation.

The base strengths of the three compounds are given in Table I. The values for piperazine at 20° are in excellent agreement with those of Schwarzenbach, *et al.*,<sup>6</sup>  $\log K_1 = 9.82$ ,  $\log K_2 = 5.68$  even though the latter determinations were for ionic strength 0.1 (NaNO<sub>3</sub>). Although homopiperazine is a somewhat stronger base than piperazine, the  $\Delta H$  values for the two amines are nearly identical. Further, the difference between the two protonation constants is greater for these secondary-amine nitrogens than is the difference between the two primary-amine nitrogens in ethylenediamine ( $\log K_n$  at 30° are 9.81 and 6.79).<sup>7</sup> In contrast to the

simple cyclic compounds, N-(2-aminoethyl)-piperazine has one primary-, one secondary- and one tertiary-amine nitrogen. The first protonation constant ( $\log K_1$ ) represents either the primary-amine or the secondary-amine nitrogen (probably the former) while the second protonation constant ( $\log K_2$ ) represents the other of these two nitrogen atoms. It will be noted that  $\log K_1$  is smaller than  $\log K_1$  for ethylenediamine or the simple piperazines whereas  $\log K_2$  is greater than  $\log K_2$  for any of these amines. Compare this situation to the values for N-(2-aminoethyl)-piperidine ( $\log K_1$  and  $\log K_2$  at 30° are 9.89 and 6.38).<sup>8</sup> However, the protonation constant for the tertiary-amine nitrogen ( $\log K_3$ ) is too small to be measured indicating that this nitrogen resembles the tertiary nitrogen atom in N(CH<sub>2</sub>CH<sub>2</sub>NH<sub>2</sub>)<sub>3</sub>.<sup>9</sup>

Piperazine formed complexes with copper(II) ion too weakly to prevent precipitation of the hydroxide. The association constants for the other amines are given in Table II. Titrations with up to approximately a 4:1 mole ratio of homopiperazine to copper(II) ion did not yield  $n$  values appreciably over 2. Thus this amine functions as a bidentate ligand. However, its complexes with Ni, Zn, Co(II), Mn(II) and Cd are too unstable to prevent precipitation of the hydroxides. The greater stability of the complex of homopiperazine with copper as compared to piperazine is confirmed by direct enthalpy titrations.<sup>10</sup> Whereas the  $\Delta H$

(5) O. Hassel and B. D. Pedersen, *Proc. Chem. Soc.*, 394 (1959).

(6) G. Schwarzenbach, B. Maissen and H. Ackermann, *Helv. Chim. Acta*, **36**, 2333 (1953).

(7) G. H. McIntyre, Jr., B. P. Block and W. C. Fernelius, *J. Am. Chem. Soc.*, **81**, 532 (1959).

(8) R. E. Reichard and W. C. Fernelius, *J. Phys. Chem.*, **65**, 380 (1961).

(9) T. Moeller, *ibid.*, **64**, 1083 (1960).

for the total protonation of the two cyclic amines are nearly identical, the  $\Delta H$  for the total association with Cu are 13.24 and 5.93 kcal./mole, respectively.

The experimental findings in the case of N-(2-aminoethyl)-piperazine with Cu necessitate care in interpretation. If one assumes that the ligand is terdentate, then the  $\bar{n}$  values exceed 2, corresponding to a coordination number greater than 6 for Cu, which is extremely unlikely because there is no reason to assume that the two nitrogens in the piperazine ring are more likely to coordinate in a simple derivative than in the parent compound. On the other hand, if the ligand is assumed to be bidentate, then  $\bar{n}$  values do not exceed 2, corresponding to a coordination number of 4 which is customary for Cu(II) in aqueous solution (neglecting possible hydration of the complex ion). The constants in Table II are calculated on the assumption that chelation is through the primary and tertiary nitrogen atoms and that the base strength of the secondary nitrogen is not altered by the coordination of the other nitrogens. The constants are about 1/100 of those for N-(2-aminoethyl)-piperidine ( $\log K_n$  at 30° are 7.77 and 5.83)<sup>8</sup> as is to be expected because of the much lower base strength of the tertiary nitrogen atom in the piperazine derivative.

#### Experimental

Piperazine (Union Carbide Chem. Co.) was recrystallized from alcohol: m.p. 103°, literature 104°. Homopiperazine<sup>12</sup> was distilled at 162–165° (723 mm.) (literature 168–170°<sup>13</sup> and 167° (764 mm.)<sup>14</sup>). Standard solutions prepared using freshly-boiled distilled water gave a neutral equivalent of 50.70 (calculated 50.10). N-(2-Aminoethyl)-piperazine (Dow Chemical Co.) distilled at 70° (ca. 1 mm.) as compared to a normal boiling point of 220.3–222.3° reported by the supplier and gave a neutral equivalent of 64.66 (calculated 64.56).

The preparation of solutions of metal ions, measurements and calculations were performed as described previously.<sup>15</sup>

(10) H. Kido, Ph.D. Dissertation, The Pennsylvania State University, Jan. 1961.

(11) A. Hoffman, *Ber.*, **23**, 3300 (1890).

(12) Kindly supplied by Dr. Richard C. Myerly, Union Carbide Chemicals Co.

(13) L. Bleier, *Ber.*, **32**, 1826 (1899).

(14) C. C. Howard and W. Marckwald, *ibid.*, **32**, 2042 (1899).

(15) D. E. Goldberg and W. C. Fernelius, *J. Phys. Chem.*, **63**, 1246 (1959).

## TOPOLOGIES OF B<sub>6</sub> AND B<sub>7</sub> HYDRIDES

BY WILLIAM N. LIPSCOMB

Department of Chemistry, Harvard University, Cambridge 38, Massachusetts

Received November 18, 1960

The formalization of the three-center bond descriptions into a set of valence rules for boron hydrides and their derivatives<sup>1,2</sup> has led to a very limited set of predictions of stable structures. Such ambiguities that remain for a given formula appear to be tautomers in transformations, and also seem to indicate, to some extent, reaction mechanisms and intermediates.<sup>2</sup> In spite of these successes the theory is quite incomplete, and hence we have been searching for compounds that require modification

(1) R. E. Dickerson and W. N. Lipscomb, *J. Chem. Phys.*, **27**, 212 (1957).

(2) W. N. Lipscomb, "Advances in Inorganic and Radiochemistry," Vol. 1, Academic Press, New York, N. Y., 1959, p. 117.

of these rules. This search has led to some further confirmation of the structures, tautomers and reaction mechanisms, particularly among the substituted amine derivatives of boron hydrides. The incompleteness of the theory itself has also led to an extension of these rules as described below.

Unlike the topology of hydrocarbons, the topology of boron hydrides has remained a somewhat complex formalism, which is somewhat difficult to apply with any sense of completeness, but which yields so far no simple rules that allow one to predict the number of possible valence and geometrical structures for a given empirical formula. Hence, a promising structure is easily overlooked, and therefore it is useful to have complete listings of satisfactory valence structures. Secondly, the present theory is incomplete in that no explicit assumptions have been made concerning the degree of compactness of the boron framework, but the most compact arrangement usually has been chosen, with the exception of the observed B<sub>9</sub> arrangement in B<sub>9</sub>H<sub>15</sub>. It was in this particular assumption that the rules of valence were so restrictive that we eliminated<sup>1,2</sup> all B<sub>7</sub> hydrides, based upon the most compact boron arrangement. This point of inconsistency between assumptions concerning B<sub>9</sub> and B<sub>7</sub> boron arrangements is removed in the present note, and hence the topology is extended to more open boron frameworks. When reliable thermochemical data become available it may be possible to show that these more open boron arrangements lead to less stable hydrides than the more compact frameworks.

Recent experimental studies also provide stimulus for an examination of B<sub>6</sub> and B<sub>7</sub> hydrides. Aside from B<sub>6</sub>H<sub>10</sub>, discovered by Stock,<sup>3</sup> other hydrides in the B<sub>6</sub> and B<sub>7</sub> range are not yet isolated and well characterized. Nevertheless, there are indications that such compounds exist, and careful techniques are likely to lead to their isolation. A B<sub>6</sub>H<sub>12</sub>(?), originally reported by Stock and Siecke,<sup>4</sup> later withdrawn,<sup>3</sup> and then tentatively suggested on newer evidence,<sup>3</sup> may have been present as a component of mixtures subjected to mass spectrographic studies.<sup>5,6</sup> Similarly, other mass spectrographic studies have been regarded<sup>7,8,5</sup> as suggestive of the occurrence of B<sub>7</sub> hydrides as components of mixtures. Also similarly, the earlier report of a B<sub>8</sub> hydride by Burg and Schlesinger<sup>9</sup> may be relevant to a mass spectrographic study,<sup>10</sup> and to vapor pressure evidence<sup>11</sup> concerning a B<sub>8</sub> hydride. These and related mass spectrographic studies,<sup>12–14</sup> from

(3) A. Stock, "Hydrides of Boron and Silicon," Cornell University Press, Ithaca, N. Y., 1933.

(4) A. Stock and W. Siecke, *Ber.*, **57**, 566 (1924).

(5) S. G. Gibbins and I. Shapiro, *J. Am. Chem. Soc.*, **82**, 2968 (1960).

(6) J. Kaufman, private communication, 1959.

(7) A. W. Schaefer, K. H. Ludlum and S. E. Wiberley, *J. Am. Chem. Soc.*, **81**, 3157 (1959).

(8) M. V. Kotlensky and R. Schaeffer, *ibid.*, **80**, 4517 (1958).

(9) A. B. Burg and H. I. Schlesinger, *ibid.*, **55**, 4009 (1933).

(10) I. Shapiro and B. Keilin, *ibid.*, **76**, 3864 (1954).

(11) R. Schaeffer, private communication, 1953.

(12) R. E. Dickerson, P. J. Wheatley, P. A. Howell and W. N. Lipscomb, *J. Chem. Phys.*, **27**, 200 (1957).

(13) R. E. Dickerson, P. J. Wheatley, P. A. Howell, W. N. Lipscomb and R. Schaeffer, *ibid.*, **25**, 606 (1956).

which no claims of new hydrides were made, are difficult to evaluate because of their brevity and the instabilities of the compounds, but they are at least suggestive enough to justify re-examination of the topological rules of valency in these hydrides.

**B<sub>6</sub> Hydrides.**—Consider the boron frameworks shown in a...d of Fig. 1. For a hydride B<sub>p</sub>H<sub>p+q</sub> containing *s* H bridges, *t* B-B-B three center bonds, *y* two center B-B bonds and *x* BH<sub>2</sub> groups, the hydrogen balance *s* + *x* = *q*, orbital balance *s* + *t* = *p* and electron balance *p* = *t* + *y* + *q*/2 yield the possibilities shown in Table I for B<sub>6</sub>H<sub>6+q</sub>.

TABLE I

VALUE OF <i>styz</i> FOR B <sub>6</sub> H <sub>6+q</sub>						
B <sub>6</sub> H <sub>6</sub>	B <sub>6</sub> H <sub>8</sub>	B <sub>6</sub> H <sub>10</sub>	B <sub>6</sub> H <sub>12</sub>	B <sub>6</sub> H <sub>14</sub>	B <sub>6</sub> H <sub>16</sub>	B <sub>6</sub> H <sub>8</sub>
6000	2410	4220	6030	6022	6014	6006
	1501	3311	5121	5113	5105	
		2402	4212	4204		
			3303			

For boron arrangement (b) no reasonable bond possibilities can be drawn; the obvious 6030 structure with C<sub>3v</sub> symmetry violates the connectivity rules. On the other hand, boron arrangement (a) yields three possible structures shown along with some of the bonds shown separately in Fig. 1. The arguments by which these structures were derived have not previously been given in detail, and hence we discuss the method here.

In arrangement (a) there are two boron atoms of excess connectivity -1, and therefore rather exposed, outer atoms. So far these have always been BH<sub>2</sub> groups, and hence we assign them as such to give these atoms then excess connectivity zero. Such extra B-H's may also be assigned to atoms of excess connectivity 0 or 1, in which case these atoms then become of excess connectivity 1 or 2. Then bonds are employed, each of which uses fewer orbitals from a given boron than the number of immediate neighbors to which it bonds. These bonds are placed so that the excess connectivities of all atoms are reduced to zero. Then the remaining bonds, single B-B bonds and bridge hydrogens which leave the excess connectivities unchanged are introduced so that one set of *styz* numbers is satisfied.

Now in arrangement (a) of Fig. 1, let us introduce 2 extra B-H's to obtain 2 BH<sub>2</sub> groups. This means that *x* ≥ 2. In addition let us retain<sup>2</sup> the twofold axis of the molecule. Hence *s* and *x* are even only. We are immediately reduced to the possibilities 2402, 4212, 6022, 4202 and 6014. Only one 6014 structure and only one 6022 structure can be sketched, and both are unsatisfactory in that they fail to connect B<sub>1</sub> with B<sub>1</sub> (Fig. 1a) for 6022, and B<sub>1</sub> with B<sub>0</sub> for 6014. The 2402 B<sub>6</sub>H<sub>10</sub> possibility is also unique, because each BH<sub>2</sub> group must be connected by at least one hydrogen bridge. Also, the one single bond of the 4212 B<sub>6</sub>H<sub>12</sub> structure must be at the molecular center, thus fixing the remaining bonds. Finally, the 4202 B<sub>6</sub>H<sub>14</sub> structure uniquely requires the two three center bonds connecting B<sub>1</sub> atoms, thus fixing its geometry. We leave open the question of their relative stabilities, but add that

(14) K. Eriks, W. N. Lipscomb and R. Schaeffer, *J. Chem. Phys.*, **22**, 754 (1954).

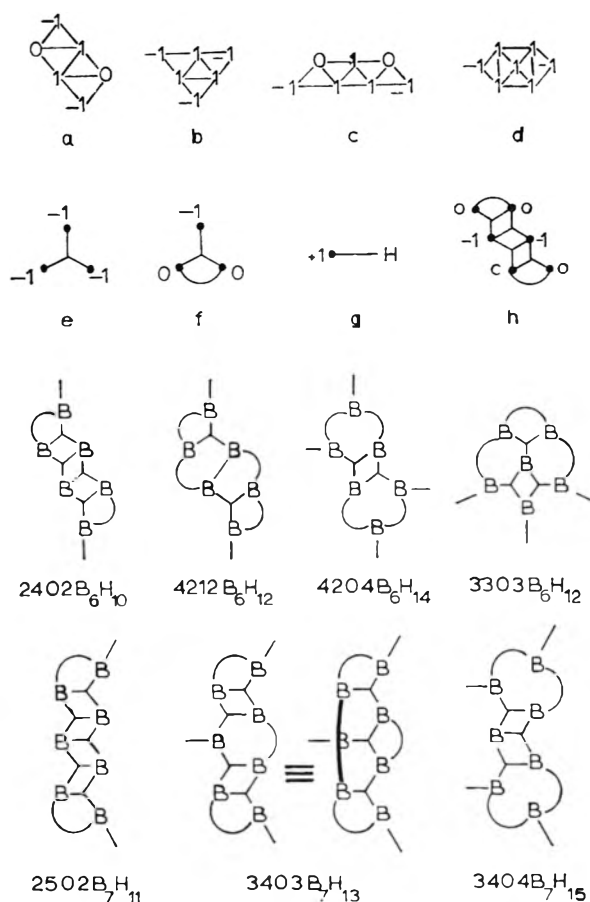


Fig. 1.—Summary of B<sub>6</sub> and B<sub>7</sub> hydride structures, based upon icosahedral fragments, in addition to 4220 B<sub>6</sub>H<sub>10</sub>, 3311 B<sub>6</sub>H<sub>10</sub> and 4212 B<sub>6</sub>H<sub>12</sub>.<sup>1</sup> Each symbol B in the diagrams is a BH, where the H is a terminal hydrogen atom. Boron frameworks and excess connectivities are shown as a...d, and bonds with excess negative connectivities are shown as e...h. The 4304 structure was independently proposed by Schaeffer, and the 3303 tautomer of 4212 B<sub>6</sub>H<sub>12</sub><sup>1</sup> and the 2502 structure were suggested by Kaczmarczyk. In summary, the more probable compounds, those with a symmetry plane, are B<sub>6</sub>H<sub>10</sub> (4220 ⇌ 3311), B<sub>6</sub>H<sub>12</sub> (4212 ⇌ 3303), B<sub>7</sub>H<sub>11</sub>, B<sub>7</sub>H<sub>13</sub> and B<sub>7</sub>H<sub>15</sub>. A slight distortion of these last three may be required to accommodate the two BH<sub>2</sub> groups furthest from the molecular centers.

there is an already predicted B<sub>6</sub>H<sub>12</sub> structure based upon the relatively compact pentagonal pyramidal arrangement of BH groups known<sup>12</sup> to exist in B<sub>6</sub>H<sub>10</sub>. A tautomer of B<sub>6</sub>H<sub>12</sub>, shown in Fig. 1, suggests hydrogen rearrangement in this molecule.

**B<sub>7</sub> Hydrides.**—The procedure is so nearly the same for a similar study of the possible B<sub>7</sub> hydrides that only the results are summarized in Fig. 1. No satisfactory structures were obtained from arrangement d. The general arguments leading to these structures also lead quite easily to the restrictions that *x* ≥ 2, *s* ≥ 2 and 1 ≤ *t* ≤ 4.

**Relations to Other Hydrides.**—A few general remarks are appropriate to suggest that these new results are part of a more general framework of valence and chemical behavior in boron compounds.

Possibilities for tautomerism appear here for B<sub>6</sub>H<sub>12</sub> in much the same form as was suggested<sup>15</sup> for stable B<sub>6</sub>H<sub>10</sub>, where a bridge H atom is adjacent

(15) W. N. Lipscomb, *J. Inorg. and Nuclear Chem.*, **11**, 1 (1959).

to an edge B-B bond. That these two forms of  $B_6H_{10}$  are readily interconvertible<sup>15</sup> is proposed<sup>16</sup> here as a hypothesis to account for the striking n.m.r. equivalence of the five outer B atoms. If so these n.m.r. data cannot support any given arrangement of the four extra hydrogens additional to those of the six BH units, and no conclusion<sup>17</sup> is therefore possible concerning the various causes of B<sup>13</sup> n.m.r. shifts, of which formal charges is only one, possibly less important, cause. In addition, it seems likely that the 3311 structure will never be isolated separately, for it is the more stable 4220 structure which occurs in the molecular crystals. Such tautomerisms are rather general properties of different geometrical structures having the same boron arrangement and number of hydrogen atoms.<sup>16</sup>

Such neutral molecules as the proposed<sup>19</sup> 2410  $B_6H_8$  may be unstable because of steric interactions of a BHB bridge in the same plane as the two adjacent H atoms of the BH groups, and possibly also because of the probable stability of octahedral  $B_6H_6^{-2}$ . An extension of the topological rules to exclude this feature may be useful in further limiting the possible structures of hydrides and ions.

Ions based upon these frameworks are easily derived from the rules already given.<sup>19</sup> A further suggestion concerning ions is that the proposed<sup>20</sup>  $B_6H_{11}^+$  ion could be stabilized by substituting Be for the apex B to yield a neutral  $BeB_5H_{11}$ , possibly further stabilized by substituting  $CH_3$  for H at the apex. The principle is, of course, a more general one.

Finally, it would be desirable if a general formula, not yet available, could be given for the number of possible structures of a given arrangement of first row atoms, because it is still quite easy to fail to exhaust all possibilities.<sup>21,22</sup>

Extension of the theory to include  $BH_3$  groups has already been proposed,<sup>15</sup> and an extension<sup>2</sup> to include B-B bonds between B atoms not having terminal B-H groups is consistent with the structures of the borides. The recent isolation here in cooperation with Mr. Russell Grimes of a centrosymmetric crystalline hydride slightly more volatile than decaborane and having only a low field doublet and a smaller high field singlet in the B<sup>11</sup> n.m.r. spectrum is suggestive to us of two  $B_5H_8$  residues, like those in  $B_5H_9$ , joined by an apical B-B bond. An X-ray diffraction study of a single crystal is in progress.

We wish to thank the Office of Naval Research and the Office of Ordnance Research for support.

(16) Dr. R. E. Williams has informed me that he has independently arrived at this conclusion.

(17) R. E. Williams, S. G. Gibbins and I. Shapiro, *J. Chem. Phys.*, **30**, 333 (1959).

(18) P. L. Hirshfeld, K. Eriks, R. E. Dickerson, E. L. Lippert, Jr., and W. N. Lipscomb, *ibid.*, **28**, 56 (1958).

(19) W. N. Lipscomb, *J. Phys. Chem.*, **62**, 381 (1958).

(20) W. N. Lipscomb, *J. Chem. Phys.*, **28**, 170 (1958).

(21) J. Reddy and W. N. Lipscomb, *J. Chem. Phys.*, **31**, 610 (1959).

(22) We therefore take this opportunity to call attention to a 2802  $B_{10}H_{14}$  tautomer, unlikely to exist because neutral molecules tend to isomerize  $BH_2$  groups toward bridge hydrogens when possible, and a 4450  $B_{10}H_{14}^{-2}$  of  $C_8$  symmetry related to the  $C_{1v}$  2632 possibility<sup>20</sup> by the process mentioned above for  $B_6H_8$ .

## THE N.M.R. SPECTRA OF DIMETHYLPROPIONAMIDE-IODINE SOLUTIONS

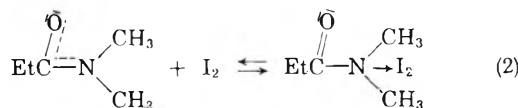
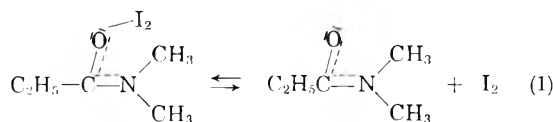
BY RUSSELL S. DRAGO AND DONALD BAFUS

Wm. A. Noyes Laboratory, University of Illinois, Urbana, Illinois

Received November 21, 1960

In a previous article<sup>1</sup> we have reported equilibrium constants and thermodynamic data determined by infrared spectroscopy for the system N,N-dimethylacetamide-iodine. The carbonyl frequency of the complexed amide occurs at lower frequency than that of the free amide, indicating that coordination occurs on the oxygen. It has recently been reported<sup>2</sup> that protonation of amides occurs principally on the oxygen but in aqueous acid solution proton exchange on the nitrogen has been detected by an n.m.r. study.

The n.m.r. spectra of solutions of dimethylpropionamide and iodine in carbon tetrachloride are similar to those obtained for dimethylacetamide and HCl in water. This has been interpreted to indicate that the Lewis acid iodine may interact with the nitrogen in a manner similar to the protonic acid in water. The system can be described by the equilibria



### Experimental

The purification procedures for the amide, carbon tetrachloride and iodine have been reported previously.<sup>1</sup> Nuclear magnetic resonance spectra were obtained using a Varian high resolution nuclear magnetic resonance spectrometer and associated magnet. A 60 m.c. probe was employed.

Samples were loaded into n.m.r. tubes that were dried *in vacuo* with  $P_2O_5$ . The tubes were sealed with Tygon tubing. It was found that sealing of the tubes with a torch produced decomposition products that lead to exchange broadening.

### Results and Discussion

Spectra typical of those obtained in  $CCl_4$  for the  $-N(CH_3)_2$  peak of the amide are illustrated in Fig. 1. A broadening of the peaks is observed as the iodine concentration is increased to 0.57 g. per 10 ml. of amide solution. A similar broadening is observed as the pH is increased in aqueous solution.<sup>2</sup> The broadening in water is ascribed to an interaction of the proton with the nitrogen of the amide in a fashion similar to that described in equation 2 for  $I_2$ .

The concentration of the species containing iodine coordinated to nitrogen is extremely low as evidenced by the infrared spectra. It is necessary to postulate that the rates of formation and dis-

(1) C. D. Schmulbach and R. S. Drago, *J. Am. Chem. Soc.*, **82**, 4484 (1960).

(2) G. Fraenkel and C. Franconi, *ibid.*, **82**, 4478 (1960), and references contained therein.

sociation of the nitrogen complex are very rapid. The methyl peaks then undergo exchange broadening and yet produce very little nitrogen complex at equilibrium in solution.<sup>3</sup>

At low temperatures the two methyl peaks sharpen and become well resolved. A similar effect is observed in aqueous acidic solution. This has been attributed to a decrease in the rate of the exchange protolysis in water<sup>2</sup> and can be attributed to a decrease in the rate of reaction 2 in the DMP-I<sub>2</sub> system.

An alternate explanation for the merging of the -N(CH<sub>3</sub>)<sub>2</sub> peaks as the iodine concentration is increased can be eliminated as a result of the low temperature study. This explanation would propose that in the addition compound, the iodine coordinated to oxygen would shield the N-methyl group pointing toward it, shifting the resonance to higher field and causing the two N-CH<sub>3</sub> peaks to coalesce. If this were the case, the equilibrium constant would be greater and the effect more noticeable at the lower temperature. Instead, the peaks were found to be sharper and more clearly resolved at the low temperature.

Data on the chemical shift of the -N(CH<sub>3</sub>)<sub>2</sub> group, as well as that of the methylene and methyl protons of the ethyl group are reported in Table I. Within experimental error of the measurement there is no change in the chemical shift. Even in the spectra obtained on solution III (see Fig. 1) where about half of the amide is present in the form of complex there is no appreciable change in the resonance of the N-(CH<sub>3</sub>)<sub>2</sub> or methylene protons. This indicates that the addition compound, whose heat of formation is about 5 kcal./mole, is held together mainly by dipole-induced dipole and London dispersion interactions and has a small amount of covalency in the bond.

TABLE I

LINE POSITIONS (c./s.) FOR DMP-I <sub>2</sub> SOLUTIONS IN CCl <sub>4</sub> <sup>3</sup>				
Molarity of soln.	Temp., °C.	-N(CH <sub>3</sub> ) <sub>2</sub>	-CH <sub>2</sub> -	-CH <sub>3</sub>
0.101 M DMP .0036 M I <sub>2</sub>	27	150	183, 191	257
		156	197, 206	264
				272
.101 M DMP .0373 M I <sub>2</sub>	27	148	182, 189	255
		154	197, 204	262
				270
.101 M DMP .0467 M I <sub>2</sub>	27	144	176, 183	250
		149	192, 199	258
				264
.101 M DMP .223 M I <sub>2</sub>	27	146	179, 187	253
		152	194, 200	261
				266
.101 M DMP .0481 M I <sub>2</sub>	2	145	179, 185	252
		151	143, 201	250
				266
.120 M DMP .479 M I <sub>2</sub>	-5	146	181, 188	255
		154	196, 203	262
				269

(3) The numerical values listed above were calculated from spectra obtained with a 60 m.c. probe. The data are reported in cycles per second measured from the external standard resonance for CH<sub>2</sub>Cl<sub>2</sub>.

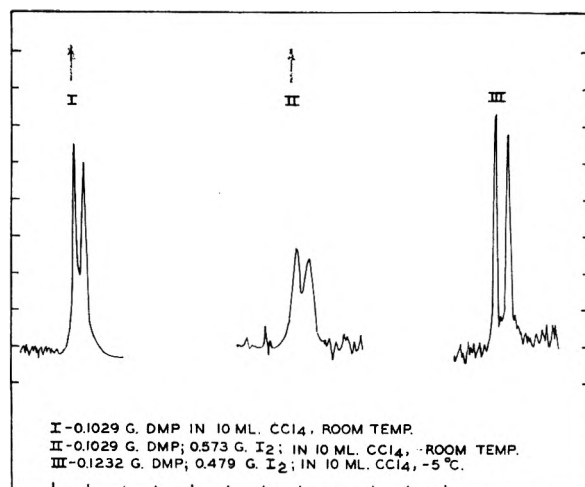


Fig. 1.—N.m.r. spectra of the -N(CH<sub>3</sub>)<sub>2</sub> doublet of DMP-I<sub>2</sub> solns.

**Acknowledgment.**—The authors wish to acknowledge the financial assistance of the Atomic Energy Commission through Contract No. AT 11-1-758.

## A SIMPLE ABSOLUTE METHOD FOR THE MEASUREMENT OF SURFACE TENSION

BY E. J. SLOWINSKI, JR., AND W. L. MASTERTON

*University of Connecticut, Storrs, Connecticut*

*Received November 21, 1960*

Many years ago Wilhelmy<sup>1</sup> suggested that one could determine the surface tension of a liquid by measuring the force exerted by its surface on a vertically-immersed plate. Harkins and Anderson<sup>2</sup> briefly investigated this approach in connection with their development of a film balance, and reported promising results. We have recently made some measurements of surface tension using a modified Wilhelmy method, with results that imply that the method warrants greater attention than it has received in the past.

Essentially our experiments involved determining the difference between the apparent weight of a thin metal cylinder as measured in air and as measured when the cylinder is wet by a liquid in which it is vertically-immersed to zero depth. This difference in apparent weight is related to the surface tension of the liquid by the very simple equation

$$2\pi(r_1 + r_2)\gamma = g\Delta W$$

where  $r_1$  and  $r_2$  are the outside and inside radii of the cylinder,  $g$  is the acceleration of gravity, and  $\Delta W$  is the apparent change in weight. The equation is exact and is essentially the one quoted by Harkins and Anderson.

Our experimental procedure was very straightforward. A platinum cylinder about 6 mm. high by 1.5 cm. in diameter was constructed from 0.15 mm. sheet, and was provided with a wire hanger. The cylinder diameter was measured to 0.1 mm. with a micrometer. The lower edge of the cylinder was made planar and the hanger adjusted so that the cylinder would hang with that edge in a horizontal

(1) L. Wilhelmy, *Ann. Physik*, **119**, 177 (1863).

(2) W. D. Harkins and T. F. Anderson, *J. Am. Chem. Soc.*, **59**, 2189 (1937).

plane. The cylinder was cleaned in a Bunsen flame and hung from the arm of a panless Chainomatic balance.

The liquid to be measured was poured into a 240-ml. beaker to a depth of about 3 cm. and the beaker placed on a small jack inside the balance under the cylinder. The system was given time to come to temperature equilibrium, and the cylinder weighed dry to 0.1 mg. With the balance arm held horizontal, the liquid level was raised slowly until the cylinder just touched its surface and was wet by it. At that point the liquid level dropped very slightly (about 0.1 mm.). By observing the liquid surface with a cathetometer during the raising operation we were able to return the surface to the height it had at the moment of wetting. The cylinder was then reweighed under these conditions of essentially zero immersion. Temperature was measured to 0.1° on a calibrated thermometer placed in the liquid after this weighing was made.

The results of surface tension measurements on five liquids of reagent grade are given in Table I. The values obtained show a mean deviation from interpolated values taken from the International Critical Tables of about 0.6%. If one uses the literature value for water for calibration of the rather poorly-known cylinder diameter, the mean deviation of the calculated values is about 0.45%, caused almost completely by a poor agreement in the results for carbon tetrachloride. The precision of this method as determined by measurements on these liquids on successive days averaged  $\pm 0.05\%$ .

TABLE I<sup>a</sup>

## RESULTS OF SURFACE TENSION MEASUREMENTS BY MODIFIED WILHELMY METHOD

Liquid	Temp., °C.	$\Delta W$ , g.	$\gamma$ calc., dynes/cm.	$\gamma$ ICT, dynes/cm.	$\gamma$ rel., dynes/cm.
Water	27.0	0.6869	72.00	71.72	...
Benzene	26.6	.2687	28.17	28.01	28.06
Toluene	27.4	.2645	27.72	27.59	27.61
Acetone	26.1	.2187	22.92	22.92	22.83
Carbon tetrachloride	26.9	.2513	26.34	25.91	26.24

$r_1 = 0.752$  cm.;  $r_2 = 0.737$  cm.;  $g = 980.3$  cm./sec.<sup>2</sup>;  
 $\gamma = g\Delta W/2\pi(r_1 + r_2)$ .

We believe the modified Wilhelmy method described has the distinct advantages of relatively high speed coupled with potentially very high absolute, or relative, accuracy. If one ignores the correction for fall of the liquid level at the moment of wetting, which affects the calculated value of surface tension by about 0.2%, one can easily and quickly make surface tension measurements with better than 1% accuracy on a du Nouy tensiometer modified by using the cylinder and method described.

The authors are grateful to the National Science Foundation for a grant in support of this work.

## HEXAGONAL IRON NITRIDES

BY AARON WOLD, RONALD J. ARNOTT AND NORMAN MENYUK  
 Lincoln Laboratory,<sup>1</sup> Massachusetts Institute of Technology, Lexington 78,  
 Massachusetts

Received November 26, 1960

It has been reported<sup>2,3</sup> previously that the iron

(1) Operated with support from the U. S. Army, Navy and Air Force.

(2) J. B. Goodenough, A. Wold and R. J. Arnett, *J. Appl. Phys.*, Supp., **30**, 343S (1960).

nitrides exhibit interesting magnetic properties. Three distinct types of iron nitrides are known. Fe<sub>3</sub>N, which is cubic, has a narrow compositional range and a moment of 2.25 Bohr magnetons per metal atom. The hexagonal Fe<sub>2</sub>N has a compositional range of  $2 \leq x \leq 3$ . Orthorhombic Fe<sub>2</sub>N has a small moment of  $\sim 0.19$  Bohr magneton per metal atom. However, hexagonal compounds, with compositions approximately Fe<sub>2</sub>N, possess moments up to ten times that of the orthorhombic samples.

It was decided to undertake a further study of the hexagonal compounds in order to determine whether the change in moment was gradual or showed a marked decrease when the crystal structure changed. Orthorhombic Fe<sub>2</sub>N was used as the starting material for the preparation of the hexagonal nitrides. It was prepared by first heating finely divided spectroscopic grade iron powder in a stream of hydrogen at 500° for one hour to remove traces of oxide and then heating in a purified ammonia atmosphere at 350° for four hours. The hexagonal nitrides were then prepared by the thermal decomposition of Fe<sub>2</sub>N at 450 to 500° under varying ammonia to hydrogen ratios. A range of composition of hexagonal Fe<sub>2</sub>N was obtained where  $2.8 \geq x \geq 2$ .

TABLE I

## PROPERTIES OF HEXAGONAL IRON NITRIDES

Compound	Cell volume	$\mu$ (Bohr magnetons/metal atom)
Fe <sub>2</sub> N (orth)	88.8	0.19
Fe <sub>2.04</sub> N	87.4	0.69
Fe <sub>2.10</sub> N	86.9	1.15
Fe <sub>2.28</sub> N	85.8	1.47
Fe <sub>2.31</sub> N	85.7	1.60
Fe <sub>2.36</sub> N	85.2	1.64
Fe <sub>2.38</sub> N	85.0	1.68
Fe <sub>2.44</sub> N	84.6	1.92
Fe <sub>2.67</sub> N	84.1	1.97
Fe <sub>2.69</sub> N	83.7	1.99
Fe <sub>2.80</sub> N	83.2	2.02

The per cent. nitrogen was determined by heating the nitrides in a stream of hydrogen at 800° and obtaining the weight loss. Iron was determined by standard analytical procedures. Saturation moments were obtained by extrapolating to infinite fields magnetic measurements made from 4100 to 10,800 oe. with a vibrating coil magnetometer. The results of chemical analysis and of crystallographic and magnetic measurements are summarized in Table I. The chemical compositions are plotted against the saturation moments in Fig. 1. It can be seen that between the compositions Fe<sub>2.05</sub>N and approximately Fe<sub>2.5</sub>N the moment varies linearly with the chemical composition. Below Fe<sub>2.05</sub>N there is a sharp drop off in the moment and above Fe<sub>2.5</sub>N saturation is reached. The cell volumes (not plotted) vary linearly with the moment above the composition Fe<sub>2.0</sub>N. Jack<sup>4</sup> has pointed out that the hexagonal-orthorhombic transition is sharp and takes place close to the composition Fe<sub>2</sub>N. The iron atoms retain

(3) R. J. Arnett and A. Wold, *J. Chem. Phys. Solids* **15**, No. 1/2, 152-156 (1960).

(4) K. H. Jack, *Acta Cryst.*, **5**, 404 (1952).

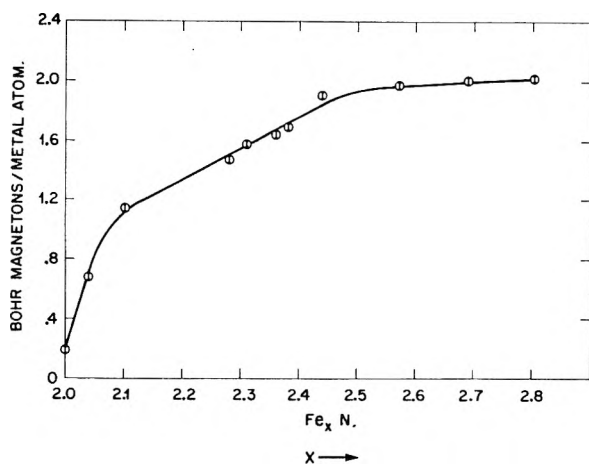


Fig. 1.

the same relative positions in both structures, but there is a shift in the nitrogen positions reducing the symmetry to orthorhombic. Our data, as shown in Fig. 1, indicate that there may be localized shifts of the nitrogen atoms to the orthorhombic positions before the orthorhombic symmetry is evident crystallographically. This would explain the sharp drop in moment below composition  $\text{Fe}_{2.1}\text{N}$ .

### SEDIMENTATION EQUILIBRIUM IN A DENSITY GRADIENT: AN EVALUATION OF THE ERRORS CAUSED BY REFRACTION OF LIGHT IN THE PHOTOMETRIC DETERMINATION OF MOLECULAR WEIGHT AND BUOYANT DENSITY

BY JOHN E. HEARST AND JEROME VINOGRAD

Contribution No. 2606 from the Gates and Crellin Laboratories of Chemistry, California Institute of Technology, Pasadena, Cal.

Received November 28, 1960

An experimental error exists in the use of absorption optics to evaluate concentration in a centrifuge cell in density gradient sedimentation studies.<sup>1</sup> This error is caused by the bending of the light in the refractive index gradient of the salt.<sup>2</sup> As the light passes through the cell it is bent toward the high density end of the cell, and as a result a single light sheet does not pass through a region of constant macromolecule concentration, Fig. 1.

In order to determine the magnitude of this effect and a method to minimize the resulting error, the photometric record of a Gaussian concentration distribution in the cell has been calculated. The equation for the actual concentration distribution is  $C = C_0 \exp(-x^2/2\sigma^2)$  where  $x = 0$  is defined as the point of maximum polymer concentration,  $C_0$  is the concentration at this point, and  $\sigma$  is the standard deviation of the Gaussian concentration distribution.

The following assumptions have been made for the calculation. (1) The Beer-Lambert laws apply

(1) M. Meselson, F. W. Stahl and J. Vinograd, *Proc. Natl. Acad. Sci.*, **43**, 581 (1957).

(2) T. Svedberg and K. O. Pedersen, "The Ultracentrifuge," Clarendon Press, Oxford, 1940, p. 259.

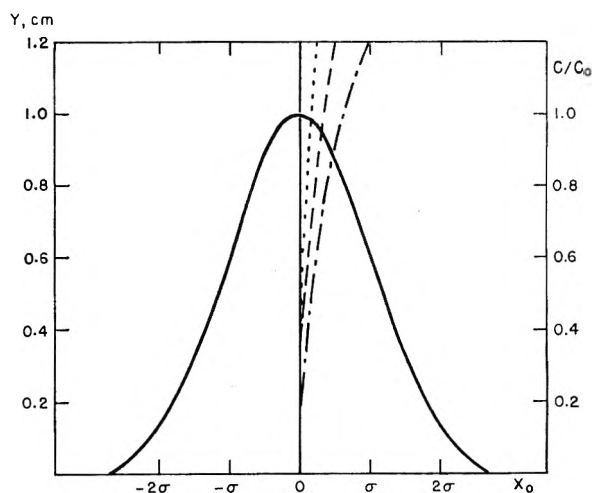


Fig. 1.—Plot of the light path through a Gaussian polymer concentration distribution for a liquid column of 1.2 cm. and varying values of  $N$ ; ———,  $N = 0$ ; ·····,  $N = 0.5$ ; - - - - ,  $N = 1.0$ ; - · - · - · ,  $N = 2.0$ . The centrifugal field is directed toward the right.

to the absorbing macromolecule in the centrifuge cell. (2) The deflection of the light caused by the salt concentration gradient is small. Experimentally the maximum deflection is between  $1$  and  $2^\circ$  through a 1.2 centimeter cell. (3)  $(1/n)(dn/dx)$  is constant over the width of the concentration band. This assumption is as good as the assumptions made in deriving the original expression for the Gaussian distribution in the cell.<sup>1</sup> (4) The light passing through the cell is collimated. (5) The refraction due to the polymer is negligible.

The equation for the path of light through a refractive index gradient for small deflections is<sup>2</sup>

$$x - x_0 = y\theta_0 + \frac{y^2}{2n} \frac{dn}{dx}$$

where  $y$  is the distance through which the light passes in the direction perpendicular to the direction of the gradient;  $\theta_0$  is the angle of incidence of the light (the angle being measured from the  $y$ -axis), which in the case of the centrifuge is equal to zero;  $x_0$  is the entrance position of the light into the gradient; and  $n$  is the refractive index of the solution.

If  $I$  is the light intensity,  $\epsilon$  the extinction coefficient of the absorbing polymer,  $c$  the concentration of the polymer, and  $s$  the distance along the optical path, the Beer-Lambert laws state that  $dI/I = -\epsilon c ds$ . Now  $ds = \sqrt{1 + (dy/dx)^2} dx$ , but since the deflection of the light is small,  $dy/dx \gg 1$  so that  $ds$  may be set equal to  $(dy/dx) dx$ . Evaluating  $(dy/dx)$  from the equation for the parabolic path of light given above, the intensity of any sheet of light entering the cell at  $x_0$  is determined by the equation

$$\ln \frac{I_0}{I} = \frac{\epsilon C_0}{\sqrt{2m}} \int_{x=x_0}^{x=\frac{ma^2}{2} + x_0} (x - x_0)^{-1/2} e^{-x^2/2\sigma^2} dx \quad (1)$$

$x$  is the distance from the center of the Gaussian concentration distribution,  $x_0$  is the distance from the center of the concentration distribution to the point at which a single light sheet enters the cell,

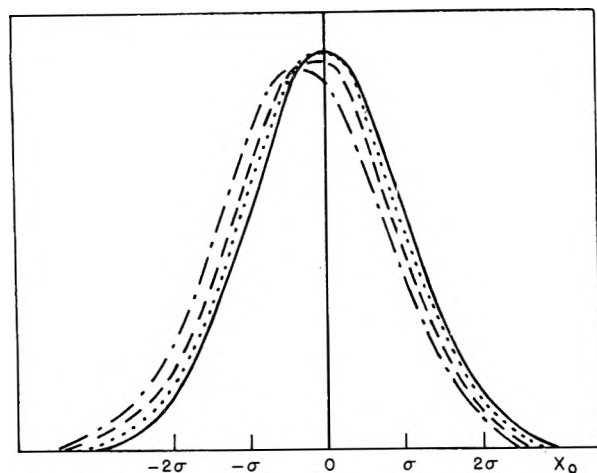


Fig. 2.—Plot of concentration distribution and resulting optical distributions: —,  $N = 0$ ; ·····,  $N = 0.5$ ; - - - - ,  $N = 1.0$ ; ·····,  $N = 2.0$ . The centrifugal field is directed toward the right.

$a$  is the height of the liquid column in the centrifuge cell, and  $m$  is  $(1/n)(dn/dx)$ . Expanding the exponential around  $x_0$ , and integrating, one obtains

$$\ln \frac{I_0}{I} = \epsilon C_0 a e^{-\frac{x_0^2}{2\sigma^2}} \left\{ \left[ 1 - \frac{1}{40} N^2 + \frac{1}{1152} N^4 \dots \right] - \left[ \frac{1}{6} N - \frac{1}{112} N^3 \dots \right] \frac{x_0}{\sigma} + \left[ \frac{1}{40} N^2 - \frac{1}{576} N^4 \dots \right] \times \left( \frac{x_0}{\sigma} \right)^2 - \left[ \frac{1}{336} N^3 \dots \right] \left( \frac{x_0}{\sigma} \right)^3 + \left[ \frac{1}{3456} N^4 \dots \right] \left( \frac{x_0}{\sigma} \right)^4 \dots \right\} \quad (2)$$

where  $N = ma^2/\sigma$ .

On first observation the correction to the concentration distribution is large. For example, at the value  $x_0 = \pm 2\sigma$  for  $N = 0.5$ , which is well within experimental conditions, the photometric record yields an apparent concentration from the sheet of light entering at  $x_0$ , which is in error by  $\pm 15\%$  from the actual concentration at  $x_0$ . This effect can be seen from Fig. 2 to be primarily a shift of the optical band center to lighter densities with little skewing of the band. Analytically this can be explained by observing that the  $-1/6 N x_0/\sigma$  term of the correction factor is by far the most significant  $x_0$  dependent term. Considering this fact, one can rewrite equation 2 in a Gaussian form with a different center and an added correction series of terms of smaller magnitude than those of equation 2.

$$\ln \frac{I_0}{I} = \epsilon C_0 a \left\{ e^{-\frac{\left(x_0 + \frac{ma^2}{6}\right)^2}{2\sigma^2}} + e^{-x_0^2/2\sigma^2} \left[ (-0.01110N^2 + 0.000772N^4 \dots) + (0.00662N^3 \dots) \frac{x_0}{\sigma} + (0.0110N^2 - 0.00155N^4 \dots) \left( \frac{x_0}{\sigma} \right)^2 - (0.00221N^3 \dots) \left( \frac{x_0}{\sigma} \right)^3 + (0.000257N^4 \dots) \left( \frac{x_0}{\sigma} \right)^4 \right] \right\} \quad (3)$$

If  $N < 0.50$  all the terms in the above expansion are  $< 0.011$  out to  $x_0 = \pm 2\sigma$ , and the optical error in concentration due to these terms is  $< 1\%$  out to

$\pm 2\sigma$ . The major effect under these conditions is to shift the optical band center a distance  $ma^2/6$  to the low density side of the concentration distribution center. This means that after superimposing the centers of the actual concentration distribution and the photometric record, the relative error of all points in the region  $-2\sigma \leq x_0 \leq 2\sigma$  on the photometric record will be less than  $1\%$ .

The band-center shift is a constant shift for all bands in the same gradient and cell. It is independent of the molecular weight of the polymer. The magnitude of the shift for a CsCl solution of density 1.700 and at a speed of 44,770 r.p.m. is 0.002 cm. This corresponds to a density shift of 0.0003 g./cc. For DNA of molecular weight  $12 \times 10^6$ , this shift amounts to about  $15\%$  of  $\sigma$ .  $N$  for these conditions is about 0.9.

Experimentally  $(1/n)(dn/dx)$  is most easily evaluated at  $589 \text{ m}\mu$  ( $N_{589}$ ), but for application in the above equations it must be evaluated at the wave length of light absorbed by the polymer, that is near  $257 \text{ m}\mu$  for DNA. A factor relating  $(1/n)(dn/dx)$  at the two wave lengths has been calculated from the partial molar refractions of CsCl<sup>3</sup> at infinite dilution and the molar refractions of pure water.<sup>4</sup> The factor

$$f = \frac{\left( \frac{1}{n} \frac{dn}{dx} \right)_{257}}{\left( \frac{1}{n} \frac{dn}{dx} \right)_{589}}$$

has a value between 1.21 and 1.22 for CsCl solutions of all concentrations. This correction has been applied in computing the numerical results in the previous paragraph.

The shift of band center does not affect the determination of molecular weight by this method. It is the expanded terms in equation 3 that will determine the magnitude of the optical error in molecular weight. This series must remain small or the Gaussian character of the distribution is lost. A practical maximum value of  $N$  is about 0.5 for a maximum error of  $1\%$  in the region  $-2\sigma \leq x_0 \leq 2\sigma$ . Below this value the Gaussian character of the optical distribution is not affected significantly. Since  $N$  is proportional to the square of the length of the liquid column, the higher order corrections become significant if a 30 mm. cell instead of a 12 mm. cell is used. In this case, the assumption of small angular deflections also becomes less justifiable.

The points beyond  $x_0 = \pm 2\sigma$  must be used with care, for the fractional change in concentration that a single light sheet experiences becomes large. This is demonstrated by the expanded part of equation 3. Although the magnitude of the correction diminishes at large  $x_0$ , the relative correction becomes large.

In conclusion, if experimental points are used only in the region  $-2\sigma \leq x_0 \leq 2\sigma$  and if experimental conditions are adjusted so that  $N < 0.5$ , the optical error in molecular weight will be negligible subject to the earlier assumptions.

(3) A. Heydweiller, *Physik. Zeitschr.*, **26**, 526 (1925).

(4) A. Heydweiller and Otto Grube, *Ann. Physik.* [4] **49**, 653 (1916).



**Acknowledgments.**—This investigation was supported in part by the National Science Foundation and by Grant H-3394 from the National Institutes of Health, United States Public Health Service.

## EFFECT OF HYDROPHOBIC BONDING ON PROTEIN REACTIONS<sup>1</sup>

BY HAROLD A. SCHERAGA

Department of Chemistry, Cornell University, Ithaca, New York

Received December 6, 1960

In a series of papers consideration has been given to the effects of side-chain hydrogen bonds on a variety of protein reactions such as ionization,<sup>2,3</sup> limited proteolysis,<sup>4,5</sup> association,<sup>6,7</sup> thermodynamics of reversible denaturation,<sup>8-11</sup> kinetics of denaturation,<sup>12</sup> ultraviolet difference spectra,<sup>13</sup> etc. In recent years, increasing attention has been given to interactions involving the *non-polar* side-chains of proteins, the so-called hydrophobic bond.<sup>14-16</sup> Calculations of the strength of a hydrophobic bond, based on a statistical mechanical treatment of aqueous hydrocarbon solutions, have been reported<sup>17</sup>; further refinements of this theory are being carried out to obtain more accurate values of  $\Delta F^0$ ,  $\Delta H^0$ ,  $\Delta S^0$  and  $\Delta V^0$ . Preliminary estimates<sup>17</sup> of the standard free energy of formation of a hydrophobic bond range from  $-0.5$  to  $-1.5$  kcal. per mole. These are comparable to the values  $0$  to  $-0.8$  kcal./mole for a heterologous single, side-chain hydrogen bond.<sup>2,3</sup> The purpose of the present note is to summarize *qualitatively* the effects of side-chain hydrophobic bonds on the same protein reactions listed above.

**Ionization.**—If an ionizable group is embedded among non-polar side-chains the effective dielectric constant of its environment is lower than that of water; also the surrounding water structure is more ordered than that in ordinary water. As a result, the  $pK$  of the ionizable group will be abnormally *high*.<sup>18,19</sup> Such an effect has been ob-

served for 3 of the 6 tyrosyl groups of ribonuclease by Shugar<sup>20</sup> and by Tanford, *et al.*<sup>21</sup> An abnormally *low*  $pK$  can be observed for an acid group HA (*i.e.*, even lower than that predicted in the previous hydrogen bonding theory<sup>2</sup>) if the conjugate base A can hydrogen bond to a donor DH and, *in addition*, the side-chain DH and A groups are so sterically confined by surrounding non-polar groups that, in effect, it is very difficult to rupture the hydrogen bond. This may account for the abnormally low  $pK$  of a COOH group in ribonuclease.<sup>11</sup>

**Limited Proteolysis.**—If hydrophobic interactions must be disrupted in order to liberate a peptide fragment in limited proteolysis, the observed free energy of hydrolysis will contain a contribution from the free energy required to break the hydrophobic bond, making it harder to liberate the peptide fragment. If, in addition, an ionizable group is embedded among non-polar side-chains in a native protein but is accessible to water after limited proteolysis, then the  $pK$ 's of the group in the native and hydrolyzed proteins will differ. This will give rise to a  $pH$ -dependence of the standard free energy of hydrolysis. The association of the S-peptide and S-protein after proteolysis of ribonuclease by subtilisin<sup>22</sup> could involve hydrophobic interactions. Such interactions are included in a postulated model of ribonuclease.<sup>23</sup>

**Association.**—There are numerous examples of protein association reactions, *e.g.*, the association of fibrin monomer which has been shown to involve intermolecular hydrogen bond formation between tyrosyl donors and histidyl acceptors.<sup>5,7</sup> If ionizable groups are accessible to water in the monomers but trapped in hydrophobic regions in the polymers, then the modified  $pK$ 's will give rise to changes in  $pH$  on association. In many cases, anomalous entropies of association have been encountered<sup>24-29</sup>; intermolecular hydrophobic bonding, with its attendant change in the water structure,<sup>17</sup> could account for these anomalies.

**Thermodynamics of Reversible Denaturation.**—Hydrophobic bonds will stabilize helical portions of a protein molecule and contribute to the standard free energy of denaturation. If, in addition, an ionizable group is embedded among non-polar side-chains in a native protein but is accessible to water in a reversibly denatured form, then the  $pK$ 's

(1) This investigation was supported by a research grant (E-1473) from the National Institute of Allergy and Infectious Diseases, of the National Institutes of Health, U. S. Public Health Service, and by a research grant (G-14792) from the National Science Foundation.

(2) M. Laskowski, Jr., and H. A. Scheraga, *J. Am. Chem. Soc.*, **76**, 6305 (1954).

(3) G. I. Loeb and H. A. Scheraga, *J. Phys. Chem.*, **60**, 1633 (1956).

(4) M. Laskowski, Jr., and H. A. Scheraga, *J. Am. Chem. Soc.*, **78**, 5793 (1956).

(5) M. Laskowski, Jr., S. Ehrenpreis, T. H. Donnelly and H. A. Scheraga, *ibid.*, **82**, 1340 (1960).

(6) J. M. Sturtevant, M. Laskowski, Jr., T. H. Donnelly and H. A. Scheraga, *ibid.*, **77**, 6168 (1955).

(7) S. Ehrenpreis, E. Sullivan and H. A. Scheraga, Abstracts of the 133rd A.C.S. meeting, p. 26-C, San Francisco, California, April, 1958.

(8) H. A. Scheraga, *J. Phys. Chem.*, **64**, 1917 (1960).

(9) H. A. Scheraga, R. A. Scott, G. I. Loeb, A. Nakajima and J. Hermans, Jr., *ibid.*, **65**, 699 (1961).

(10) A. Nakajima and H. A. Scheraga, *J. Am. Chem. Soc.*, **83**, 1575 (1961).

(11) J. Hermans, Jr., and H. A. Scheraga, *ibid.*, **83**, in press (1961).

(12) M. Laskowski, Jr., and H. A. Scheraga, *ibid.*, **83**, 266 (1961).

(13) M. Laskowski, Jr., S. J. Leach and H. A. Scheraga, *ibid.*, **82**, 571 (1960).

(14) I. M. Klotz, *Science*, **128**, 815 (1958).

(15) W. Kauzmann, *Advances in Protein Chem.*, **14**, 1 (1959).

(16) I. M. Klotz, *Brookhaven Symposia in Biology*, **13**, 25 (1960).

(17) G. Némethy and H. A. Scheraga, Abstracts of the 138th A.C.S. meeting, p. 4C, New York, N. Y., Sept. 1960; see also the discussion at the end of Klotz's paper.<sup>16</sup>

(18) C. Tanford and J. G. Kirkwood, *J. Am. Chem. Soc.*, **79**, 5333 (1957).

(19) C. Tanford, *ibid.*, **79**, 5340, 5348 (1957).

(20) D. Shugar, *Biochem. J.*, **52**, 142 (1952).

(21) C. Tanford, J. D. Hauenstein and D. G. Rands, *J. Am. Chem. Soc.*, **77**, 6409 (1955).

(22) F. M. Richards and P. J. Vithayathil, *J. Biol. Chem.*, **234**, 1459 (1959).

(23) H. A. Scheraga, *J. Am. Chem. Soc.*, **82**, 3847 (1960).

(24) M. Laskowski, Jr., and H. A. Scheraga, Abstracts of the 126th A.C.S. meeting, p. 60-C, New York, N. Y., Sept., 1954.

(25) P. Doty and G. E. Myers, *Disc. Faraday Soc.*, **13**, 51 (1953).

(26) R. F. Steiner, *Arch. Biochem. Biophys.*, **44**, 120 (1953); **49**, 71 (1954).

(27) H. Edelhoch, E. Katchalski, R. H. Maybury, W. L. Hughes, Jr., and J. T. Edsall, *J. Am. Chem. Soc.*, **75**, 5058 (1953).

(28) J. T. Edsall, R. H. Maybury, R. B. Simpson and R. Straessle, *ibid.*, **76**, 3131 (1954).

(29) F. Karush, in "Serological and Biochemical Comparisons of Proteins" (W. H. Cole, ed.), Rutgers Univ. Press, New Brunswick, N. J., 1958, p. 40.

of the group in the native and denatured forms will differ. This will give rise to a  $pH$ -dependence of the standard free energy of denaturation. While such a  $pH$ -dependence has heretofore been attributed to side-chain hydrogen bonding,<sup>8</sup> which has been shown to be involved in several protein denaturations,<sup>10,11</sup> it appears that a contribution from hydrophobic bonding is also involved in the case of ribonuclease.<sup>11</sup> In the latter case, a preliminary attempt already has been made to obtain a quantitative treatment.

**Kinetics of Protein Denaturation.**—If a native protein contains hydrophobic bonds which are ruptured in the formation of activated complexes, then these bonds will contribute to the standard free energy of activation. If, in addition, the production of activated complexes from native protein requires that ionizable groups emerge from a hydrophobic to an aqueous environment, then the rate will be  $pH$ -dependent. This  $pH$ -dependence can be deduced from the model previously used<sup>12</sup> to account for denaturation kinetics in terms of the involvement of side-chain hydrogen bonds.

**Ultraviolet Difference Spectra.**—If a chromophoric group is embedded among non-polar side-chains in a native protein and becomes accessible to water during a limited or extensive configurational change of the protein, there will be a perturbation of the spectrum of the chromophore.<sup>30-35</sup>

**Deuterium-Hydrogen Exchange.**—Linderström-Lang has interpreted the slow exchange of deuterium and hydrogen in terms of hydrogen bonding.<sup>36</sup> It is worthwhile devising experiments to determine whether the embedding of a group (having exchangeable hydrogens) among non-polar side-chains will lead to slow exchange.

The examples cited above illustrate the possible profound influence which hydrophobic bonds can have on protein reactions. An attempt is now being made to treat these effects *quantitatively*, as was done previously for side-chain hydrogen bonds.<sup>2-13</sup> Presumably both hydrophobic and hydrogen bonds exist between the side-chains of native proteins; if so, they may cooperate in providing stabilization of the native structure, as was suggested in the case of ribonuclease.<sup>11</sup>

ADDED IN PROOF.—Some of these problems also have been discussed by Tanford<sup>37</sup> in a recent paper.

**Acknowledgment.**—I should like to thank George Némethy for helpful discussions of these problems.

(30) D. B. Wetlaufer, J. T. Edsall and B. R. Hollingworth, *J. Biol. Chem.*, **233**, 1421 (1958).

(31) E. J. Williams and J. F. Foster, *J. Am. Chem. Soc.*, **81**, 865 (1959).

(32) C. C. Bigelow and I. I. Geschwind, *Compt. rend. trav. lab. Carlsberg*, **31**, 283 (1960).

(33) T. T. Herskovits and M. Laskowski, Jr., *J. Biol. Chem.*, **235**, PC56 (1960).

(34) S. Yanari and F. A. Bovey, *ibid.*, **235**, 2318 (1960).

(35) S. J. Leach and H. A. Scheraga, *ibid.*, **235**, 2827 (1960).

(36) K. Linderström-Lang, "Symposium on Peptide Chemistry," Chem. Soc. (London), Spec. Pub. No. 2, 1 (1955).

(37) C. Tanford, *J. Am. Chem. Soc.*, **83**, 1628 (1961).

## SELF-DIFFUSION IN LIQUIDS. III. TEMPERATURE DEPENDENCE IN PURE LIQUIDS<sup>1</sup>

BY R. E. RATHBUN AND A. L. BABB

Department of Chemical Engineering, University of Washington, Seattle, Washington

Received December 9, 1960

Self-diffusion coefficients were measured in benzene, carbon tetrachloride, methanol and ethanol over a wide range of temperatures using a capillary cell technique with carbon-14 labeled tracers. The apparatus and procedure have been fully described elsewhere.<sup>2,3</sup>

The ethanol-1-C<sup>14</sup> was purchased from the Volk Radiochemical Company. The uniformly labeled benzene was purchased from the Nuclear Chicago Corporation and the carbon tetrachloride-C<sup>14</sup> and methanol-C<sup>14</sup> were obtained from the Nuclear Instrument and Chemical Corporation. The chemicals used in diluting the tracers to the desired activity and in preparing the non-radioactive bulk solutions were of the highest grade commercially available. The benzene, carbon tetrachloride and methanol were reagent grade chemicals as obtained from Merck and Company, and the ethanol was pure anhydrous ethyl alcohol produced by the U.S. Industrial Chemical Company.

### Results and Discussion

In Tables I, II, III and IV, the measured self diffusion coefficients are tabulated and compared with data available in the literature (benzene,<sup>2,4,5</sup> carbon tetrachloride,<sup>7,9</sup> ethanol,<sup>2,4,6,9</sup> and methanol<sup>2,6,8,9</sup>). The new experimental values represent averages of three determinations (except where noted) and are reported with the maximum deviations from the average values.

The recommended average values reported in Tables I-IV were obtained from the reported diffusivities by weighting them in inverse proportion to their variances. The method of Davies and Pearson<sup>10</sup> was used to convert the ranges of the reported diffusivities shown into unbiased estimates of the population standard deviations from which the variances were determined. The recommended average values are reported together with the best values of their standard deviations.

The self-diffusion coefficient ( $D = \text{cm.}^2/\text{sec.}$ ) has been related to the viscosity ( $\eta = \text{g./}(\text{cm.})^2/\text{sec.}$ ), molar volume ( $V = \text{cm.}^3/\text{mole}$ ), and absolute temperature ( $T = ^\circ\text{K.}$ ) by the relation<sup>11,12</sup>

$$D\eta V^{1/3}/T = \beta \quad (1)$$

(1) This work was supported by the Office of Ordnance Research, U. S. Army.

(2) P. A. Johnson and A. L. Babb, *J. Phys. Chem.*, **60**, 14 (1956).

(3) A. P. Hardt, D. K. Anderson, R. Rathbun, B. W. Mar and A. L. Babb, *ibid.*, **63**, 2059 (1959).

(4) K. Graupner and E. R. S. Winter, *J. Chem. Soc.*, **1**, 1145 (1952).

(5) H. Hiraoka, J. Osugi and W. Jono, *Rev. Phys. Chem., Japan*, **28**, 52 (1958).

(6) J. R. Partington, R. F. Hudson and K. W. Baggeall, *J. chim. phys.*, **55**, 77 (1958).

(7) H. Watts, B. J. Alder and J. H. Hildebrand, *J. Chem. Phys.*, **23**, 659 (1955).

(8) H. Hiraoka, Y. Izui, J. Osugi and W. Jono, *Rev. Phys. Chem., Japan*, **28**, 61 (1958).

(9) A. P. Hardt, Ph.D. Thesis, University of Washington, 1957.

(10) O. L. Davies and E. S. Pearson, *Suppl. J. Roy. Statistical Soc.*, **1**, 76 (1934).

(11) E. N. da C. Andrade, *Phil. Mag.*, **17**, 496, 698 (1934).

(12) S. Glasstone, K. J. Laidler and H. Eyring, "The Theory of Rate Processes," McGraw-Hill Book Co., New York, N. Y., 1941.

TABLE I  
SELF-DIFFUSION COEFFICIENTS OF BENZENE,  $D \times 10^6$  CM.<sup>2</sup>/SEC.

Temp., °C.	This work	Ref. 4	Ref. 5	Ref. 2	Recommended av. values
6.8	1.42 ± 0.08				
15.0	1.70 ± .06	1.88 ± 0.01	1.83 ± 0.06		1.87 ± 0.006
25.0	2.21 ± .21	2.15 ± .05	2.13 ± .06	2.18 <sup>a</sup> ± 0.13	2.16 ± .02
35.0	2.51 ± .12	2.40 ± .03	2.44 ± .02		2.44 ± .01
45.0	2.81 <sup>a</sup> ± .16	2.67 ± .06	2.86 ± .03		2.84 ± .02
55.0	3.56 <sup>a</sup> ± .08				
65.0	4.07 ± .16				

<sup>a</sup> Based on six determinations.

TABLE II  
SELF-DIFFUSION COEFFICIENTS OF CARBON TETRACHLORIDE,  $D \times 10^6$  CM.<sup>2</sup>/SEC.

Temp., °C.	This work	Ref. 7	Ref. 9	Recommended av. values
25.0	1.30 ± 0.02	1.41	1.37 ± 0.06	1.32 ± 0.009
40.0	1.78 ± .04	1.87 <sup>b</sup>		1.82 ± 0.02
50.0	2.00 <sup>a</sup> ± .07			
60.0	2.44 ± .06			

<sup>a</sup> Based on six determinations. <sup>b</sup> Interpolated value.

TABLE III  
SELF-DIFFUSION COEFFICIENTS OF ETHANOL,  $D \times 10^6$  CM.<sup>2</sup>/SEC.

Temp., °C.	This work	Ref. 4	Ref. 6	Ref. 9	Ref. 2	Recommended av. values
6.8	0.618 ± 0.016					
15.0	0.810 ± .014	0.80 ± 0.01	0.768			0.770 ± 0.001
25.0	1.02 ± .03	1.05 ± .03	1.010	1.00 ± 0.05	1.02 ± 0.02	1.01 ± .001
35.0	1.28 ± .01	1.31 ± .07	1.300			1.30 ± .002
45.0	1.65 ± .04	1.70 ± .03				1.66 ± .02
55.0	2.06 ± .04					
65.0	2.61 ± .03					

TABLE IV  
SELF-DIFFUSION COEFFICIENTS OF METHANOL,  $D \times 10^6$  CM.<sup>2</sup>/SEC.

Temp., °C.	This work	Ref. 8	Ref. 6	Ref. 2	Ref. 9	Recommended av. values
-5.0	1.26 ± 0.05					
5.0	1.55 ± .04					
15.0	1.91 ± .01	1.84 ± 0.01	1.933			1.91 ± 0.003
25.0	2.34 ± .01	2.21 ± .02	2.32	2.37 ± 0.06		2.32 ± .006
35.0	2.74 ± .20		2.71			2.71 ± .03
40.0		3.01 ± .08			2.83 ± 0.08	2.89 ± .03
45.0	3.37 <sup>a</sup> ± .37					
55.0	3.88 ± .13					

<sup>a</sup> Based on six determinations.

TABLE V  
VALUES OF  $\beta$  FOR BENZENE AND ETHANOL,  $\beta \times 10^9$

Temp., °C.	Benzene	Ethanol
6.8	1.80	1.32
15.0	2.02	1.37
25.0	1.85	1.44
35.0	1.89	1.49
45.0	1.89	1.55
55.0	2.05	1.59
65.0	2.04	1.67

where  $\beta$  is a constant. Recently, Ottar,<sup>13</sup> using a random walk approach for molecules diffusing as monomers, obtained a value of  $2.06 \times 10^{-9}$  for  $\beta$ . In addition, Ree, Ree and Eyring<sup>14</sup> modified the

(13) B. Ottar, "Self-Diffusion and Fluidity in Liquids," Oslo University Press, Oslo, Norway, 1958.

(14) F. H. Ree, T. Ree and H. Eyring, *Ind. Eng. Chem.*, **50**, 1036 (1958).

original Eyring equation by including a parameter,  $\xi$ , which accounts for the average number of viscous shears of the neighboring molecules which causes one lattice position advancement by the diffusing molecule. If their proposed value of 5.6 for  $\xi$  is used, the constant  $\beta$  in equation 1 would have a value of  $2.08 \times 10^{-9}$ .

Values of  $D\eta V^{1/2}/T = \beta$  calculated from the recommended average diffusivities when available, or from the new experimental values, are presented

in Tables V and VI. Density and viscosity data were obtained from the literature.<sup>15-17</sup>

The  $\beta$  values were not constant with temperature as expected. The maximum deviations from the average values for benzene, carbon tetrachloride, ethanol and methanol were 6.7, 3.6, 12.1 and 6.2%, respectively. Moreover, the deviations were, in general, not random; and the values of  $\beta$  tended to increase with temperature. For ethanol and methanol, where association is known to occur, the molar volumes should not properly be based on the monomeric species. Consequently, the values

(15) American Petroleum Institute Research Project 44, "Selected Values of Physical and Thermodynamic Properties of Hydrocarbons and Related Compounds," Carnegie Press, Pittsburgh, 1953.

(16) "Handbook of Chemistry and Physics," 33rd Edition, Chemical Rubber Publishing Co., Cleveland, Ohio, 1951.

(17) J. Timmermans, "Physico-Chemical Constants of Pure Organic Compounds," Elsevier Publishing Co., Inc., New York, N. Y., 1960.

TABLE VI

VALUES OF  $\beta$  FOR CARBON TETRACHLORIDE AND METHANOL

Temp., °C.	$\beta \times 10^9$	
	Carbon tetrachloride	Methanol
-5.0		1.40
5.0		1.43
15.0		1.42
25.0	1.86	1.47
35.0		1.45
40.0	1.99	1.46
45.0		1.55
50.0	1.87	
55.0		1.53
60.0	2.00	

of  $\beta$  would tend to be low since no correction was applied to the molar volume to account for association effects. However, since association effects decrease as the temperature increases, the  $\beta$  values should increase with temperature as shown in Tables V and VI.

The data for benzene in Table V and carbon tetrachloride in Table VI indicate a slight temperature effect, but the average value of  $\beta$  for each liquid is within 10% of the theoretical value.

The data for carbon tetrachloride in Table VI were not reported for temperatures below 25°. At lower temperatures, dispersion of heavy tracer molecules leaving the capillary is not obtained; and as a result, the measured self-diffusivities are abnormally low. This effect could be corrected by stirring the bulk solution.

## DEUTERIUM ISOTOPE EFFECTS ON DISSOCIATION CONSTANTS AND FORMATION CONSTANTS<sup>1</sup>

BY NORMAN C. LI, PHILOMENA TANG AND RAJ MATHUR

Department of Chemistry, Duquesne University, Pittsburgh, Penna.  
Received December 3, 1960

A survey of the recent literature shows that kinetic deuterium isotope effects have been extensively studied; however, relatively little has been published on the effects in solution equilibria. This situation is not surprising because isotope effects on reaction velocities are much more pronounced than on equilibrium constants.

Several papers have appeared recently on the use of ordinary calomel-glass electrode couple for measurement of acidity in D<sub>2</sub>O solutions.<sup>2</sup> These authors have studied the relation between true and apparent pH of solutions in D<sub>2</sub>O and found the correction for DCl solutions and DClO<sub>4</sub> solutions in D<sub>2</sub>O to be +0.4 pH unit. In this paper we report the use of this method for the determination of acid dissociation constants of a number of organic acids containing different functional groups. The formation constants of metal complexes of

some of these organic acids have also been determined in D<sub>2</sub>O by a polarographic method. We have demonstrated experimentally for the first time that the deuterium isotope effect on acid dissociation constant can be attributed to the specific bond affected.

### Experimental

**Materials.**—Deuterium oxide, 99.8% D<sub>2</sub>O, was purchased from Bio-Rad Laboratories and used without further purification. Fully deuterated acetic acid was prepared from malonic acid and D<sub>2</sub>O according to the method of Halford and Anderson.<sup>3</sup> Histidylhistidine, obtained from Nutritional Biochemicals Corp., was found to be 80% pure,<sup>4</sup> the impurities being water of hydration and inert salt. All other chemicals were of C.P. grade.

**Procedure.**—pH measurements were made at 25° using a conventional calomel-glass electrode couple with a Beckman Model G pH meter, in both H<sub>2</sub>O and D<sub>2</sub>O systems. The pH meter was standardized in the usual way with buffers in water solution. In D<sub>2</sub>O systems, glass electrodes were conditioned by immersing for several days in D<sub>2</sub>O buffer solutions with no change in the observed pH readings on standing. The deuterium solutions were made by dissolving the anhydrous hydrogen compounds in deuterium oxide, except for hydrochloric acid, in which case the concentrated aqueous solutions were diluted with D<sub>2</sub>O. For the low concentrations investigated this did not alter the deuterium content by a significant amount. All the solutions used for pH measurements contained 0.02 M organic acid in 0.1 M sodium chloride and neutralized to different extents with acid or alkali. The total ionic strength of the solutions was kept at  $\mu = 0.11$ .

The pH of a 0.1 M NaCl, 0.01 M HCl solution in H<sub>2</sub>O is 2.10 and the apparent pH of a 0.1 M NaCl, 0.01 M DCl solution in D<sub>2</sub>O is 1.70. The apparent pH of a DCl solution in D<sub>2</sub>O is 0.40 unit less than a similar solution in H<sub>2</sub>O, and this has also been observed by previous workers.<sup>2b,5</sup> In solutions containing only dilute acid and sodium chloride, the concentration of H<sub>3</sub>O<sup>+</sup> in H<sub>2</sub>O solutions cannot differ appreciably from the concentration of D<sub>3</sub>O<sup>+</sup> in D<sub>2</sub>O, since in both cases there is essentially complete hydrogen ion transfer from the hydrochloric acid to the solvent. In order to calculate the acid dissociation constant in D<sub>2</sub>O, therefore, the pD of a solution in D<sub>2</sub>O can be determined by use of the equation

$$pD = "pH" + 0.40 \quad (1)$$

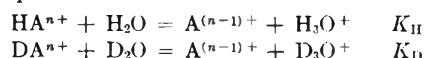
where "pH" is the apparent pH meter reading in D<sub>2</sub>O medium. Equation 1 has been obtained previously by Hyman, *et al.*,<sup>2b</sup> using perchloric acid, and by Glasoe and Long,<sup>2c</sup> using hydrochloric acid.

In aqueous systems, pH is defined as  $-\log C_{H_3O^+} - \log f_{\pm}$  where  $f_{\pm}$  is the activity coefficient. At a total ionic strength of 0.11 we have assumed  $-\log f_{\pm}$  to be 0.10,<sup>5</sup> and this value is used for all solutions studied in the present investigation.

Polarographic current-voltage curves were made with a Fisher Electropode. All potentials were measured at 25° against a saturated calomel electrode (S.C.E.) in the manner described by Li, *et al.*<sup>6,7</sup>

### Results and Discussion

(A) **pH Measurements.**—Table I lists the results obtained on the acid dissociation constants of organic acids containing two or more polar groups, and the deuterium isotope effect, measured by  $pK_D - pK_H$ . The equilibrium constants refer to the equilibria



(3) J. O. Halford and L. C. Anderson, *J. Am. Chem. Soc.*, **58**, 736 (1936).

(4) R. B. Martin and J. T. Edsall, *ibid.*, **82**, 1107 (1960).

(5) Symposium on pH Measurement, ASTM Special Technical Publication No. 190 (1956).

(6) N. C. Li and R. A. Manning, *J. Am. Chem. Soc.*, **77**, 5225 (1955).

(7) N. C. Li and M. C. Chen, *ibid.*, **80**, 5678 (1958).

(1) This investigation was supported by the U. S. Atomic Energy Commission through Contract No. AT(30-1)-1922 and by Research Grant NSF G7447 from the National Science Foundation.

(2) (a) K. Mikkelsen and S. O. Nielsen, *J. Phys. Chem.*, **64**, 632 (1960); (b) H. H. Hyman, A. Kaganove and J. J. Katz, Abstracts, Am. Chem. Soc., Atlantic City Meeting, Sept., 1959; (c) P. K. Glasoe and F. A. Long, Abstracts, Am. Chem. Soc., Atlantic City Meeting, Sept., 1959.

Examination of Table I shows that  $pK_D - pK_H$  is a linear function of  $pK_H$  for acid dissociation from specific groups. Linear plots of  $pK_D - pK_H$  vs.  $pK_H$  are obtained and the equations of the straight-lines are

$$\text{for } -\text{COO}: pK_D - pK_H = 0.086 + 0.124pK_H \quad (2)$$

$$\text{for } -\text{NH}_3^+ \text{ and } -\text{ImH}^+; pK_D - pK_H = 0.243 + 0.0417pK_H \quad (3)$$

The fifth and sixth columns of Table I give comparison between the observed values of  $pK_D - pK_H$  and the values calculated from equation 2 or 3. The agreement between the observed and calculated values is excellent.

TABLE I

ACID DISSOCIATION CONSTANTS OF ORGANIC ACIDS CONTAINING TWO OR MORE POLAR GROUPS,  $\mu = 0.11$ ,  $0, 25^\circ$

Organic acid	Acid group	$pK_H$	$pK_D - pK_H$	$pK_D - pK_H$ , calcd.
Glycolic acid	-COOH	3.74	0.53	0.55 <sup>a</sup>
Malonic acid	-COOH	2.86	.44	.44 <sup>a</sup>
Citric acid	-COOH	2.95 ( $pK_1$ )	.49	.45 <sup>a</sup>
	-COOH	4.38 ( $pK_2$ )	.64	.63
	-COOH	5.80 ( $pK_3$ )	.75	.80
Tricarballic acid	-COOH	3.50 ( $pK_1$ )	.53	.52 <sup>a</sup>
	-COOH	4.60 ( $pK_2$ )	.68	.66
	-COOH	5.75 ( $pK_3$ )	.80	.80
Glycine	-COOH	2.47	.39	.39 <sup>a</sup>
	-NH <sub>3</sub> <sup>+</sup>	9.65	.63	.64 <sup>b</sup>
Glycylglycine	-NH <sub>3</sub> <sup>+</sup>	8.18	.58	.58 <sup>b</sup>
Glycylglycylglycine	-COOH	3.28	.47	.49 <sup>a</sup>
	-NH <sub>3</sub> <sup>+</sup>	8.00	.58	.58 <sup>b</sup>
Imidazole	-ImH <sup>+</sup>	7.09	.56	.54 <sup>b</sup>
Histidine	-COOH	1.81	.33	.31 <sup>a</sup>
	-ImH <sup>+</sup>	6.11	.54	.50 <sup>b</sup>
	-NH <sub>3</sub> <sup>+</sup>	9.20	.63	.63 <sup>b</sup>
D-Leucyl-L-tyrosine	-COOH	2.87	.41	.44 <sup>a</sup>
	-NH <sub>3</sub> <sup>+</sup>	8.36	.60	.59 <sup>b</sup>
	-OH (tyrosine)	10.28	.79	
Histidyl-histidine	-ImH <sup>+</sup>	5.54	.51	.47 <sup>b</sup>
	-ImH <sup>+</sup>	6.80	.50	.53 <sup>b</sup>
	-NH <sub>3</sub> <sup>+</sup>	7.82	.57	.57 <sup>b</sup>

<sup>a</sup> Calcd. from equation 2. <sup>b</sup> Calcd. from equation 3.

Previous workers<sup>2,8,9</sup> have shown that the ratio of  $K_H/K_D$  should increase with decreasing acid strength. Högfeltd and Bigeleisen<sup>10</sup> conclude that the type of acid is more important than the acid strength in so far as the difference between  $pK_H$  and  $pK_D$  is concerned. We have demonstrated experimentally for the first time that the deuterium isotope effect does indeed depend on the specific bond affected (-COOH or -NH<sub>3</sub><sup>+</sup> and -ImH<sup>+</sup> bonds), but that within a series of similar bonds,  $pK_D - pK_H$  is a linear function of  $pK_H$ .

The  $pK_H$  for acetic acid is 4.64 at  $\mu = 0.11$ , and  $pK_D - pK_H = 0.49$ . The isotope effect for this acid is not given by equation 2, since acetic acid contains only one polar group, whereas equations 2 and 3 apply to organic acids which contain two or more polar groups. The  $pK$ 's for CD<sub>3</sub>COOD and CH<sub>3</sub>COOD in D<sub>2</sub>O at  $\mu = 0.11$ ,  $25^\circ$ , are 5.19

and 5.15, respectively. This difference, although small, may be ascribed to secondary isotope effect.<sup>11</sup>

(B) **Polarographic Measurement of Cadmium Complexes.**—For a reversible mercury dropping electrode reaction, the polarographic equation is

$$(E_{1/2})_c - (E_{1/2})_s = -0.0296 \log K_p - p \times 0.0296 \log (A) \quad (4)$$

where  $(E_{1/2})_c$  and  $(E_{1/2})_s$  are the half-wave potentials of Cd<sup>++</sup> in the presence and absence of a complexing agent A, respectively, and  $K$  is the formation constant of the cadmium complex

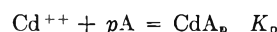


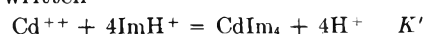
Table II summarizes the polarographic result obtained with D<sub>2</sub>O solutions containing  $5 \times 10^{-4} M$  Cd(NO<sub>3</sub>)<sub>2</sub>,  $0.15 M$  KNO<sub>3</sub> and varying concentrations of imidazole. A plot of  $E_{1/2}$  vs.  $-\log (\text{Im})$  yields a straight line with slope of 0.119, so that  $p = 4.0$ . The electrode reaction is reversible.

TABLE II

POLAROGRAPHIC MEASUREMENT OF CADMIUM COMPLEX OF IMIDAZOLE IN D<sub>2</sub>O,  $\mu = 0.15$ ,  $25^\circ$

(Im)	$-E_{1/2}$	$\log K_4$
0	0.576	
0.087	.672	7.49
.193	.713	7.49
.594	.768	7.39
.894	.792	7.49
1.005	.798	7.49
1.273	.810	7.49

The formation constant of the cadmium-imidazole complex in H<sub>2</sub>O,  $\mu = 0.15$ ,  $25^\circ$ , has previously been determined polarographically by Li, *et al.*<sup>12</sup>:  $\log K_4 = 7.48$ . Experimentally, there is no deuterium isotope effect on the formation constant of the cadmium-imidazole complex. This is as expected because the complexing agent is taken to be the uncharged imidazole. If the complexation reaction is written



then  $K' = K_4 K_H^4$ , where  $K_H$  is the acid dissociation constant of ImH<sup>+</sup>. The deuterium isotope effect on  $K'$  would then correspond to the fourth power of the isotope effect on the acid dissociation constant of imidazole,  $10^{-2.24}$  (see Table II).

The formation constants of the 1:2 cadmium complexes of histidine, glycylglycinate and glycylglycylglycinate in D<sub>2</sub>O,  $\mu = 0.15$ ,  $25^\circ$ , were determined polarographically in precisely the manner described by Li, *et al.*,<sup>6,7</sup> for the same complexes in H<sub>2</sub>O. The dropping mercury electrode reaction is reversible in every case. The  $pK_D$ 's of histidine, glycylglycine and glycylglycylglycine were taken from Table I. The formation constants in D<sub>2</sub>O,  $\log K_2$ , were calculated to be 11.3, 5.6 and 5.4, respectively. These values are about 0.2 log unit higher than the corresponding values in H<sub>2</sub>O.

The formation constant of the 1:2 cadmium complex of histidylhistidine has not hitherto been determined. We have studied this complex polarographically,  $\mu = 0.15$ ,  $25^\circ$ : in H<sub>2</sub>O,  $\log K_2 = 8.1$ ;

(8) G. N. Lewis and P. W. Schultz, *J. Am. Chem. Soc.*, **56**, 1913 (1934).

(9) C. K. Rule and V. K. LaMer, *ibid.*, **60**, 1974 (1938).

(10) E. Högfeltd and J. Bigeleisen, *ibid.*, **82**, 15 (1960).

(11) A. E. Halevi, *Tetrahedron*, **1**, 174 (1957); A. E. Halevi and M. Nussim, *Bull. Res. Council Israel*, **5A**, 263 (1956).

(12) N. C. Li, J. M. White and E. Doody, *J. Am. Chem. Soc.*, **76**, 6219 (1954).

in D<sub>2</sub>O,  $\log K_2 = 8.5$ . The acid dissociation constants of histidylhistidine in H<sub>2</sub>O and D<sub>2</sub>O were those of Table I.

In the complexation of histidine and the peptides to Cd<sup>++</sup>, the amino group probably is involved in binding. Since the amino hydrogens are easily exchanged in D<sub>2</sub>O medium, we would expect a slight deuterium isotope effect on the formation constants, as has been found to be the case.

**Acknowledgment.**—We wish to thank Mr. E. Tucci for preparing the fully deuterated acetic acid.

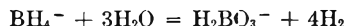
## KINETICS OF BOROHYDRIDE HYDROLYSIS

By W. H. STOCKMAYER, ROY R. MILLER AND ROBERT J. ZETO

Department of Chemistry, Massachusetts Institute of Technology, Cambridge 39, Massachusetts

Received December 9, 1960

Recently Davis and Swain<sup>1</sup> observed that the hydrolysis of borohydride ion



was subject to general acid catalysis, according to the expression

$$-d \ln (\text{BH}_4^-) / dt = k_1 = \sum_i k_i (\text{HA}_i)$$

From measurements of the rate over a wide range of pH with several buffer systems at 25°, they determined an accurate value of  $k_{\text{H}_3\text{O}^+}$  and reported approximate values for  $k_{\text{H}_3\text{BO}_3}$ ,  $k_{\text{HCO}_3^-}$  and  $k_{\text{H}_2\text{PO}_4^-}$ .

Our earlier studies<sup>2,3</sup> of the rate of this reaction supplement the results of Davis and Swain. Confining our experiments to the neighborhood of pH 9, but employing a range of buffer concentrations, we determined  $k_{\text{H}_3\text{O}^+}$  and  $k_{\text{H}_3\text{BO}_3}$  at 0.0 and 25.0° at an ionic strength of 0.16, and we also evaluated  $k_{\text{NH}_4^+}$  at 25°. Our value for  $k_{\text{H}_3\text{O}^+}$  at 25° is in good agreement with that of Davis and Swain, but our value for  $k_{\text{H}_3\text{BO}_3}$  is considerably higher than theirs.

### Experimental

Research grade potassium borohydride (Metal Hydrides, Inc., Beverly, Mass., over 96% KBH<sub>4</sub>) was used at an initial concentration of approximately 0.01 M in most runs. The iodate method<sup>4,5</sup> was used to determine borohydride concentrations. The buffers were prepared from H<sub>3</sub>BO<sub>3</sub>-NaOH or NH<sub>4</sub>Cl-NaOH, with addition of NaCl where necessary to bring the ionic strength to 0.16 M. All measurements of pH were made on a Beckman Model G meter at 25.0°. The values of pH in the borate solutions at 0° were evaluated from those measured at 25° from the known change in the ionization constant of boric acid<sup>6</sup> ( $5.79 \times 10^{-10}$  at 25° to  $3.09 \times 10^{-10}$  at 0°).

(1) R. E. Davis and C. G. Swain, *J. Am. Chem. Soc.*, **82**, 5949 (1960); earlier literature is quoted there.

(2) R. R. Miller, S.B. Thesis, M.I.T., May, 1958.

(3) R. J. Zeto, S.M. Thesis, M.I.T., January, 1959.

(4) D. A. Lyttle, E. H. Jensen and W. A. Struck, *Anal. Chem.*, **24**, 1843 (1952).

(5) E. H. Jensen, "A Study on Sodium Borohydride," Nyt Nordisk Forlag, Arnold Busch, Copenhagen, 1956.

(6) H. S. Harned and B. B. Owen, "The Physical Chemistry of Electrolytic Solutions," Reinhold Publ. Corp., New York, N. Y., Third Edition, 1958, p. 755.

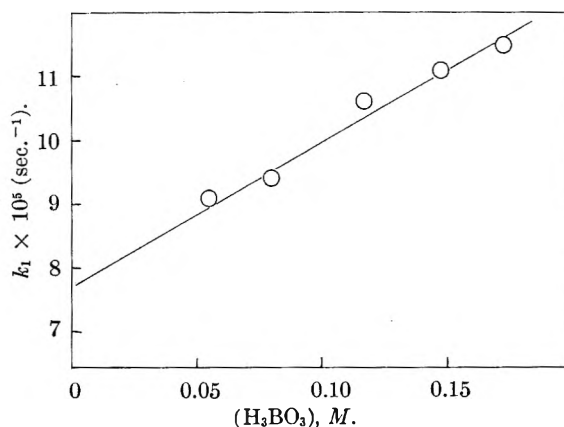


Fig. 1.—Pseudo-first-order rate constant  $k_1$ , for hydrolysis of borohydride at 0°, ionic strength 0.16 M and pH 9.27 ± 0.02, as a function of the molar concentration of undissociated boric acid.

### Results and Discussion

Results for the borate buffer system at 0.0° and pH 9.27 ± 0.02 are shown in Fig. 1, where the pseudo-first-order rate constant  $k_1$  is plotted against the molar concentration of un-ionized boric acid. The slope of the line gives directly the value of  $k_{\text{H}_3\text{BO}_3}$ , while that of  $k_{\text{H}_3\text{O}^+}$  is found from the intercept and the pH with an assumed value of 0.72 for the activity coefficient of any univalent ion in the solution. These constants and those found in similar fashion at 25° are collected in Table I. The energies of activation calculated from these results are  $9 \pm 1$  kcal. mole<sup>-1</sup> for the reaction with H<sub>3</sub>O<sup>+</sup> and  $14 \pm 2$  kcal. mole<sup>-1</sup> for that with H<sub>3</sub>BO<sub>3</sub>.

Our value for  $k_{\text{H}_3\text{O}^+}$  at 25° compares well with that of Davis and Swain,  $(10.0 \pm 0.4) \times 10^5$  M<sup>-1</sup> sec.<sup>-1</sup> at  $\mu = 0.10$  M; with a reasonable estimate of the difference in salt effect, their figure and ours agree to better than 10%. However, their estimate of  $k_{\text{H}_3\text{BO}_3}$  was  $(1 \pm 5) \times 10^{-4}$  M<sup>-1</sup> sec.<sup>-1</sup>, and even their upper limit is well below any figure that could accommodate our results (Table I).

TABLE I

REACTIONS OF BOROHYDRIDE ION WITH ACIDS	
Reaction	$k_i$ (M <sup>-1</sup> sec. <sup>-1</sup> ) <sup>a</sup>
BH <sub>4</sub> <sup>-</sup> + H <sub>3</sub> O <sup>+</sup> , 0°	$(2.0 \pm 0.2) \times 10^5$
H <sub>3</sub> O <sup>+</sup> , 25°	$(8 \pm 1) \times 10^5$
H <sub>3</sub> BO <sub>3</sub> , 0°	$(2.3 \pm 0.2) \times 10^{-4}$
H <sub>3</sub> BO <sub>3</sub> , 25°	$(2.0 \pm 0.3) \times 10^{-3}$
NH <sub>4</sub> <sup>+</sup> , 25°	$(1.5 \pm 0.4) \times 10^{-3}$

<sup>a</sup> All at ionic strength 0.16 M.

From the rates for H<sub>3</sub>O<sup>+</sup> and NH<sub>4</sub><sup>+</sup>, we estimate an exponent of well over 0.9 in the Brønsted catalysis law for acids of this charge type. Clearly the H-A bond of the attacking acid is very largely broken in the transition state. This conclusion is also supported by the magnitude of the observed difference in activation energy for the H<sub>3</sub>O<sup>+</sup> and H<sub>3</sub>BO<sub>3</sub> reactions, which within the experimental error equals the enthalpy of ionization of H<sub>3</sub>BO<sub>3</sub>. Since the enthalpy of ionization of NH<sub>4</sub><sup>+</sup> is about 12 kcal. mole<sup>-1</sup>, we might expect the activation energy for the NH<sub>4</sub><sup>+</sup> reaction with BH<sub>4</sub><sup>-</sup> to lie near 20 kcal. mole<sup>-1</sup>, as is in fact borne out by very rough results<sup>2</sup> for this reaction at 0°.

Finally, we record in Table II some observed values<sup>3</sup> of the rate constant for the second-order reaction between acetone and borohydride in water, at such high pH that the hydrolysis is completely negligible. These results were preliminary to an intended study of the competition between  $H_3O^+$  and acetone for borohydride at lower pH, in the hope of obtaining some information on the steps beyond the first hydride transfer. Competitive systems involving ferricyanide would also be specially interesting, since the rate-determining step of the reduction of ferricyanide by borohydride is known<sup>7,8</sup> to be the same as that of the hydrolysis. Since these projects have been abandoned, and since we are unaware of other observations of the temperature coefficient of the acetone reaction in water, we give the figures in Table II. Our rate at 24° is about 50% higher than that reported by Jensen.<sup>6</sup> The activation energy is found to be  $7.6 \pm 0.5$  kcal. mole<sup>-1</sup>.

TABLE II

REDUCTION OF ACETONE BY BOROHYDRIDE	
Temp., °C.	$k \times 10^2$ ( $M^{-1} \text{ sec.}^{-1}$ )
15	1.45
20	1.83
25	2.27, 2.33
30	2.73

(7) B. Lowry, S.B. Thesis, M.I.T., May, 1958.

(8) T. Freund, *J. Inorg. Nuclear Chem.*, **9**, 246 (1959).

## THE ELECTRONIC PROPERTIES OF ALKYL GROUPS. III. THE INTENSITY OF THE INFRARED NITRILE ABSORPTION IN *para*-ALKYLBENZONITRILES

BY THEODORE L. BROWN

*Noyes Chemical Laboratory, University of Illinois, Urbana, Illinois*

Received December 17, 1960

It was concluded from a study of the dipole moments of the *p*-alkylbenzonitriles in cyclohexane that the electron distribution in these molecules in the ground state does not reflect a preferential electron release from the alkyl groups *via* hyperconjugation.<sup>1</sup> There is some evidence, however, for a solvent effect in the dipole moment results. In dioxane, a basic solvent, the order of dipole moments, after correction for electrostatic effects, approaches the Baker-Nathan order: methyl > ethyl > isopropyl > *t*-butyl.

In this note the results of a study of the integrated intensity of the infrared  $C\equiv N$  band in the *p*-alkylbenzonitriles are reported. The intensity of this band in substituted benzonitriles is quite sensitive to the electronic properties of the *meta* or *para* substituent.<sup>2</sup> It was felt, therefore, that a determination of the band intensity in the *p*-alkyl compounds would provide data which would be of interest in evaluating the properties of the alkyl groups.

(1) T. L. Brown, *J. Am. Chem. Soc.*, **81**, 3232 (1959).

(2) P. J. Krueger and H. W. Thompson, *Proc. Roy. Soc. (London)*, **A250**, 22 (1958).

## Experimental

**Materials.**—The preparation and purification of the *p*-alkyl compounds have been described.<sup>1</sup> The solvents used were reagent grade materials, dried and distilled before use. The mixed pyridine-carbon tetrachloride solvent was made up to contain 16% pyridine *by volume*.

**Procedure.**—A Perkin-Elmer Model 21 spectrometer with sodium chloride optics was employed. The mechanical slit width was set at 0.022 mm., corresponding to a calculated spectral slit width of 7.0  $\text{cm.}^{-1}$ . A cell of 1.00 mm. thickness was employed; solution concentrations ranged from 0.01–0.08 *M*. At least four samples of varying concentration were examined for each compound. For each sample a value of apparent intensity was calculated; these were then graphed *vs.* the absorbance at band maximum. The best line was extrapolated to zero absorbance to obtain the limiting value of intensity. The curves were integrated over an interval of 65  $\text{cm.}^{-1}$  for the  $\text{CCl}_4$  and  $\text{CCl}_4$ -pyridine solutions, and over 78  $\text{cm.}^{-1}$  for the  $\text{CHCl}_3$  solutions. No wing corrections were employed.

**Results.**—The results of the intensity measurements are shown in Table I. The frequencies of band maxima were the same for all of the compounds in any one solvent. These were 2231, 2230 and 2232  $\text{cm.}^{-1}$  for carbon tetrachloride, chloroform and the mixed solvent, respectively. The half-intensity widths,  $\Delta\nu_{1/2}$ , in the three solvents were 11, 13.5 and 11.5  $\text{cm.}^{-1}$ , respectively, except that  $\Delta\nu_{1/2}$  for the butyl compound was about 1  $\text{cm.}^{-1}$  larger than those values in each case.

Every effort was made in this study to obtain a high degree of precision, since only small differences in the intensities were expected. The values listed in Table I are thought to be relatively accurate to within 0.01 intensity unit. Where comparison with other data is possible (only the methyl compound has been reported previously)<sup>2</sup> the agreement is good. The slightly higher value obtained in chloroform solution as compared with the previous one for *p*- $\text{CH}_3$  is the result of integrating over a larger interval.

TABLE I

Integrated Intensities of the  $C\equiv N$  Absorption in *p*-Alkyl-Benzonitriles in Various Solvents Intensities are in units of  $1 \times 10^4$  mole<sup>-1</sup> liter  $\text{cm.}^{-2}$ .

Solvent	<i>p</i> -Methyl	<i>p</i> -Ethyl	<i>p</i> -Isopropyl	<i>p</i> - <i>t</i> -Butyl
$\text{CCl}_4$	0.280	0.300	0.312	0.322
$\text{CHCl}_3$	.553	.560	.573	.589
$\text{C}_2\text{H}_5\text{N}-\text{CCl}_4$	.408	.402	.402	.413

## Discussion

The data in Table I show that in chloroform and carbon tetrachloride solvents the alkyl groups cause an increase in the  $C\equiv N$  band intensity in the inductive order. This order is essentially absent in the mixed solvent containing 16% pyridine. These results thus parallel the dipole moment data in showing a change in the relative order in basic solvents.

On the basis of a simple molecular orbital model for intensities in substituted aromatic compounds<sup>3</sup> it has been shown that the square root of the  $C\equiv N$  intensity in substituted benzonitriles should relate linearly to the electrophilic substituent constants,  $\sigma^+$ .<sup>4</sup> When the  $\sigma^+$  values for the *p*-alkyl groups are applied to this correlation it is found that the predicted intensities vary in the order: methyl > ethyl > isopropyl > *t*-butyl. This is the inverse of the order actually found in carbon tetrachloride, although in the more basic mixed solvent the changes in relative values are in the direction of the Baker-Nathan order. One can speculate that if the intensities were obtained in 90% aqueous

(3) T. L. Brown, *J. Phys. Chem.*, **64**, 1798 (1960).

(4) H. C. Brown and Y. Okamoto, *J. Am. Chem. Soc.*, **80**, 4979 (1958).

acetone, the solvent employed in the kinetic studies from which the  $\sigma^+$  values were obtained, the intensities would be in the order predicted from the  $\sigma^+$  values.

In the molecular orbital model for intensities mentioned above,<sup>3</sup> the ionization potential of the substituted benzene,  $C_6H_5X$ , from which the compound  $XC_6H_4CN$  is derived, is a quantity of major importance in determining the intensity of the vibrational transition. The transfer of electrons from the ring to the nitrile group which occurs in the vibrationally excited state is facilitated by an increase in the energy of the highest occupied level in the ring. This highest occupied level is taken to be the negative of the ionization potential of  $C_6H_5X$ . From the decrease in the ionization potential of the alkylbenzenes with increased branching of the alkyl group<sup>5</sup> it can be concluded that the intensity should increase with increased branching, as is observed. The variation in ionization potential in the alkylbenzenes is easily understood as resulting from electrostatic factors.<sup>6</sup> Calculations along these lines indicate that essentially all of the variation in intensity in carbon tetrachloride solvent can be understood as resulting from the variation in polarizability of the alkyl groups.

**Acknowledgment.**—This work was sponsored in part by the Office of Naval Research.

(5) W. C. Price, *Chem. Revs.*, **41**, 257 (1947).

(6) N. D. Coggeshall, *J. Chem. Phys.*, **32**, 1265 (1960).

## RATE OF FORMATION OF THE NICKEL COMPLEX OF PHEOPHYTIN *a*<sup>1</sup>

BY B. L. BAKER AND G. W. HODGSON

Contribution No. 136 from Research Council of Alberta, Edmonton, Canada

Received December 22, 1960

A knowledge of the kinetics of the formation of metal-porphyrin complexes in crude oil would throw considerable light on the nature of the conditions surrounding the formation of crude oil. Porphyrin-metal complexes found in crude oils apparently are derived from chlorophyll of the petroleum source material as indicated by the presence of an isocyclic ring in the petroleum porphyrin complexes corresponding to the isocyclic ring of chlorophyll.<sup>2</sup> Recent-sediment studies dealing with the origin of crude oil have confirmed the conclusions of kinetic studies<sup>3</sup> and simulated sedimentation work in which it was clear the chlorophyll *a* readily decomposes to pheophytin *a*.<sup>4</sup> Although metal-porphyrin complexes similar to, if not identical with, petroleum pigments have been reported in recent sediments, no clear-cut path of development of the pigments has been apparent from the results of examination of pigments in recent sediments.<sup>5</sup>

(1) Part of the work reported here was included in a dissertation in partial fulfillment of the requirements of the degree of master of science in the department of chemistry, University of Alberta, Edmonton, Canada.

(2) A. Trieb, *Angew. Chem.*, **49**, 682 (1936).

(3) M. A. Joslyn and G. Mackinney, *J. Am. Chem. Soc.*, **60**, 1132 (1938).

(4) G. W. Hodgson and B. Hitehon, *Bull. Amer. Assoc. Petrol. Geol.*, **43**, 2481 (1959).

Metal-pigment complexes are formed in displacement reactions in which the complexing cation displaces two protons from the nitrogens of the basic pigment structure.<sup>6</sup> Fleischer and Wang<sup>7</sup> have shown further that the combination of metal ions with porphyrins takes place with the metal ion first combining with the porphyrin to form a reaction intermediate which subsequently decomposes to the normal metalloporphyrin complex and two hydrogen ions. It is reasonable to suggest that the metal complexing of dihydroporphyrins such as pheophytin *a* and pheophorbide *a* takes place in a similar manner. Several major pigments—pheophytin *a*, pheophorbide *a*, pheoporphyrin, phylloerythrin, deoxophylloerythrin and deoxophylloerythroetioporphyrin—illustrate the chain of compounds extending from the chlorophyll *a* of the petroleum source material to the ultimate petroleum pigment. To gain a complete understanding of the reaction mechanisms involved it is obviously necessary to examine all the reactions in considerable detail. It was the object of the present study to examine the kinetics of one of the first reactions in the sequence—that of nickel complexing with pheophytin *a*.

### Experimental

The nickel-pheophytin *a* complexing reaction in methanol was carried out in sealed reaction tubes at four temperatures—74, 90, 103 and 115°. Three series of experiments were run at each temperature to define the order of reaction with respect to each reactant, the initial concentrations of the nickel acetate and pheophytin *a*, respectively, being  $1 \times 10^{-4}$  and  $4 \times 10^{-4}$  mole/l.,  $1 \times 10^{-4}$  and  $1 \times 10^{-4}$  mole/l., and  $4 \times 10^{-4}$  and  $1 \times 10^{-4}$  mole/l. with a precision of about  $\pm 0.5\%$ . At the end of the reaction period the tube was opened and the solution containing the nickel-pheophytin *a* complex transferred to ether from which the unreacted pheophytin *a* was removed by extraction with 12 *N* HCl. The concentration of the nickel complex of pheophytin *a* formed during the reaction was then determined by measurement of the 635  $m\mu$  peak height using the extinction coefficient established for the complex. Beer's law was found to apply in the concentration range involved.

### Results

The reaction between nickel and pheophytin *a* produced a substance with an absorption spectrum not unlike that shown for porphyrin salts by Aronoff.<sup>8</sup> Although Lamort<sup>9</sup> reported the formation of many metallic salts of pheophytin *a*, he specifically noted a failure to make the nickel complex of pheophytin *a*. In the present investigation, however, the nickel salt formed readily and its identity was confirmed by separating the complex and measuring its nickel content (6.23% theoretical, 6.25% found). The absorption spectrum of the nickel complex had absorption maxima at 410 and 635  $m\mu$  as the significant features. The molar extinction coefficient of the nickel complex in ether at 635  $m\mu$  was found to be  $7.0 \times 10^4$  l./mole/cm.

Experimental data for the rate of formation of the nickel complex of pheophytin *a* were obtained

(5) G. W. Hodgson, B. Hitehon, R. M. Eloffson, B. L. Baker and E. Peake, *Geochim. et Cosmochim. Acta*, **19**, 272 (1960).

(6) F. Basolo and R. G. Pearson, "Mechanism of Inorganic Reactions," John Wiley and Sons, Inc., New York, N. Y., 1958, p. 91.

(7) E. B. Fleischer and Jui H. Wang, *J. Am. Chem. Soc.*, **82**, 3498 (1960).

(8) S. Aronoff, *J. Phys. Chem.*, **62**, 428 (1958).

(9) C. Lamort, *Rev. Fermentations et Inds. Aliment.*, **11**, 34 (1956).



TABLE I  
RATE CONSTANTS FOR THE FORMATION OF THE NICKEL COMPLEX OF PHEOPHYTIN *a* CALCULATED FROM

$$\frac{\Delta x}{\Delta t} = k(a - x)^{0.7}(b - x)^{0.5} \quad \text{OVER THE TEMPERATURE RANGE 74 TO 115}^\circ$$

Concn. of reactants, moles/l.		Ratio constant			
Nickel acetate	Pheophytin <i>a</i>	74°	90°	103°	115°
1 × 10 <sup>-4</sup>	4 × 10 <sup>-4</sup>	3.24 ± 0.28 × 10 <sup>-6</sup>	1.93 ± 0.15 × 10 <sup>-5</sup>	5.92 ± 0.14 × 10 <sup>-5</sup>	1.72 ± 0.14 × 10 <sup>-4</sup>
1 × 10 <sup>-4</sup>	1 × 10 <sup>-4</sup>	3.25 ± .20 × 10 <sup>-6</sup>	1.78 ± .10 × 10 <sup>-5</sup>	6.06 ± .22 × 10 <sup>-5</sup>	1.30 ± .11 × 10 <sup>-4</sup>
4 × 10 <sup>-4</sup>	1 × 10 <sup>-4</sup>	3.70 ± .34 × 10 <sup>-6</sup>	1.80 ± .05 × 10 <sup>-5</sup>	5.77 ± .13 × 10 <sup>-5</sup>	1.19 ± .07 × 10 <sup>-4</sup>

for the four temperatures and the three initial concentrations of the two reactants. Extents of conversion were small, falling in the range of 2 to 25% for the reaction times involved, which ranged from only one to 32 hours so as to reduce the effects of side reactions which might have become important at higher conversions and to facilitate the summarization of the results by the use of initial-rate approximations.

To ascertain whether errors might arise through thermal instability of the complex, a series of measurements was made to evaluate the stability of the complex under the conditions of the rate measurements. In reaction periods twice or four times as large as the longest periods employed in the complexing experiments the recovery of complex in the degradation experiments was over 95%, except in the case of the 74° test, in which the recovery was about 90%. Clearly, no significant degradation of the nickel complex of pheophytin *a* took place in the course of the complexing reactions.

The coefficients in the general rate expression

$$\frac{dx}{dt} = k(a - x)^\alpha(b - x)^\beta$$

were estimated by solving the two sets of simultaneous equations arising from the experimental data in which *a* or *b* (for nickel acetate and pheophytin *a*, respectively) was held constant while the initial concentration of the other reactant was varied; in all cases  $dx/dt$  was replaced by the observed initial rate  $\Delta x/\Delta t$ . In this manner a series of evaluations for both  $\alpha$  and  $\beta$  was obtained, the value for  $\alpha$  ranging from 0.62 to 0.86 with standard deviations for each temperature ranging from 0.03 to 0.13, and the value for  $\beta$  from 0.46 to 0.66 with standard deviations from 0.04 to 0.12. The empirical rate constants for the complexing reactions at the four temperatures are given in Table I.

## THE TEMPERATURE DEPENDENCE OF THE $\Delta pD$ CORRECTION FOR THE USE OF THE GLASS ELECTRODE IN D<sub>2</sub>O

BY THOMAS H. FIFE AND THOMAS C. BRUCE<sup>1</sup>

Department of Chemistry, Cornell University, Ithaca, New York  
Received December 14, 1960

Lumry,<sup>2</sup> Hart<sup>3</sup> and co-workers have reported that the glass electrode yields an apparent *pD* that is lower than actually exists in solution by about

0.4 "pH" unit; *i.e.*,  $pD = \text{"meter pH reading"} + 0.4$ . More recent work by Glasoe and Long<sup>4</sup> (who employ the symbol  $\Delta pD$  for the numerical correction which must be added to the meter reading to obtain *pD*) and Mikkelsen and Nielsen<sup>5</sup> have established the following facts concerning the value of  $\Delta pD$ :

- (1) The potential difference is due solely to the glass electrode and not to diffusion phenomena at the liquid junction, etc.;
- (2) The value of  $\Delta pD$  is not dependent on whether the electrode is pre-soaked in H<sub>2</sub>O or D<sub>2</sub>O;
- (3)  $\Delta pD$  is not dependent on the acidities of the solutions investigated but remains essentially invariant from "pH 4-12"; and
- (4) The  $\Delta pD$  value appears to be independent of the type of glass electrode employed.

The present study to determine the temperature dependence (20 to 78°) of  $\Delta pD$  was predicated on the great utility of the glass electrode in determining acidities and (as used in the pH-stat<sup>6</sup>) rate constants in D<sub>2</sub>O. The determination of these values is of particular importance in the study of general and specific acid- and base-catalyzed reactions.

### Experimental

All measurements were made with a Radiometer TTT-la pH meter employing a Beckman Calomel electrode and a Metrohm type X microglass electrode. The solution whose acidity was being determined was contained in a Metrohm type EA-662 microtitration vessel which was thermostated by water circulated from a Precision Scientific water-bath ( $\pm 0.1^\circ$ ). The cell compartment possessed three  $\text{F}$  openings which accommodated the glass electrode, the salt bridge and an ordinary  $\text{F}$  cap (without grease). To prevent rapid flow of KCl from the salt bridge, at higher temperatures, there was fused to the end of the salt bridge the wick tip of a Beckman Calomel electrode. Before the determination of acidity values the glass electrode was pre-equilibrated for 12 hr. at the temperature to be employed.

Standard solutions of  $7.95 \times 10^{-4} N \pm 1.1\%$  of DCl in D<sub>2</sub>O (prepared from concentrated aqueous HCl and 99.5% + D<sub>2</sub>O) and HCl in H<sub>2</sub>O were prepared. The  $\Delta pD$  correction was then taken as the difference in the pH meter reading for the DCl and HCl solutions at each temperature. Determinations of  $\Delta pD$  carried out with solutions of 0.01 *M* DCl in D<sub>2</sub>O and HCl in H<sub>2</sub>O were found to agree within 0.02 pH unit with the values of  $\Delta pD$  determined at lower concentration.

### Results

In Fig. 1 are plotted the values of  $\Delta pD$  vs.  $1/T$ . The linear plot fits the experimental points with an average deviation of  $\pm 0.008$  pH unit and a maximum deviation of 0.02 pH unit. Included in the plot are the  $\Delta pD$  values of Glasoe and Long<sup>4</sup> determined at 25° with Beckman and modified Beckman electrodes and the value of Mikkelsen and Nielson<sup>5</sup> determined with a Radiometer glass

(1) To whom inquiries concerning the work should be addressed.  
(2) R. Lumry, E. L. Smith and R. R. Glantz, *J. Am. Chem. Soc.*, **73**, 4330 (1951).  
(3) R. G. Hart, Nat. Res. Council, Canada, CRE 423, June, 1949.

(4) P. K. Glasoe and F. A. Long, *J. Phys. Chem.*, **64**, 188 (1960).  
(5) K. Mikkelsen and S. O. Nielsen, *ibid.*, **64**, 632 (1960).  
(6) J. P. Phillips, "Automatic Titrators," Academic Press, New York, N. Y., 1959.

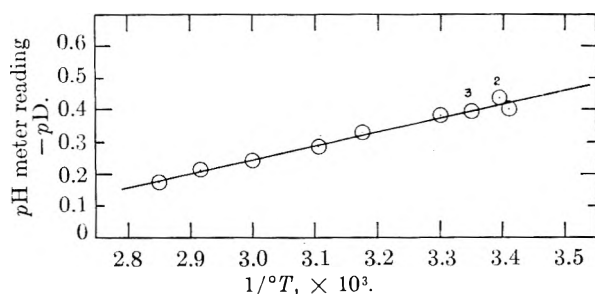


Fig. 1.—Plot of the experimentally determined glass electrode correction (pH meter reading -  $pD$ ) in  $D_2O$  vs.  $1/^\circ T$ . Point 2 is the correction value determined by Mikkelsen and Nielsen (22°; ref. 5) and point 3 is that of Glasco and Long (25°; ref. 4).

electrode at 22°.

The formula which provides the electrode correction ( $\pm 0.02$  pH units) is

$$pD = \text{pH meter reading} + \frac{4.29 \times 10^2}{^\circ T} - 1.04 \quad (1)$$

ADDED IN PROOF.—Extension of these studies has shown that equation (1) holds only for low resistance electrodes designed for measurements at ambient temperatures. Thus, in contrast to the Metrohm X (400 megohm at 20°) electrode used here the  $\Delta pD$  values for the Metrohm H (500 megohm at 30°) electrode is 0.33 at 78° and 0.29 at 100°. For the latter determinations a specially designed thermostated deep cell with a vapor lock was employed. This alteration in cell design did not alter the  $\Delta pD$  values for the type X electrode.

**Acknowledgment.**—This work was supported by grants from the National Institutes of Health and the National Science Foundation.

## POLAROGRAPHY IN WATER AND WATER-ETHANOL. I. URANIUM(VI) IN CHLORIDE AND PERCHLORATE MEDIA IN ONE MOLAR ACID

BY WILLIAM VES CHILDS AND EDWARD S. AMIS

Chemistry Department of the University of Arkansas, Fayetteville, Arkansas

Received December 23, 1960

The polarographic reduction of U(VI) has been studied in 1  $M$  acid solution in water, ethanol and water-ethanol media as a function of the chloride concentration, the ethanol concentration and the uranyl concentration. The polarograms were run using a Sargent Model XV recording polarograph, potentials and cell resistances were measured using a Leeds and Northrup Model K2 type potentiometer and an Industrial Instruments Model RC16B a.c. conductivity bridge respectively.

The cell was designed to prevent contamination of the solution about the d.m.e. with material from the salt bridge. No maximum suppressor was used.

Current measurements were made of the true current values, " $i_{\max}$ " at the termination of drop life by using the top of the recorder tracing.

The diffusion current,  $i_d$ , was measured at  $-0.4$  v. vs. the saturated calomel electrode using a saturated lithium acetate solution as a salt bridge.

The second reduction wave of U(VI) was noted but it was not suitable for study since it merged with the hydrogen discharge wave and had poor definition.

Using the Ilkovic equation, the diffusion current constant,  $I$ , was calculated. This " $I$ " was not a true diffusion current constant as shown by the non-linearity of the plot of  $i_d$  vs.  $C$ , but at a given concentration it is a convenient function to compare in different media because it is corrected for changes in  $m^{2/3}t^{1/6}$ .

Applied potentials, as corrected for  $iR$  losses, plotted vs.  $\log [(i_d - i)/i]$  gave lines, the linearity and slopes of which indicate the reversibility of the reduction.

Using Lingane's<sup>1</sup> equation, plots of  $E_{1/2}$  vs. log chloride concentration, gave straight lines parallel to the abscissa in 0.001  $M$  uranyl solutions in water and the reduction apparently is reversible.

In various alcohol concentrations, there is first a slight decrease in  $I$  with chloride out to about 0.02  $M$  chloride, then a steady increase with increasing chloride concentration. The viscosity of these solutions was found to increase slightly with increasing chloride concentration so that it is seen the change in  $I$  cannot be due to viscosity effects. This increase in  $I$  could be attributed either to the faster diffusion of the chlorouranium(VI) complex compared to the aquo complex, or the faster disproportionation of the chlorouranium(V) complex, probably the former. Marked minima were observed for  $I$  in low chloride concentrations which are hard to explain.

The data for 21.6, 43.0, 79.3 and 92.2 weight % ethanol in perchlorate media indicate the reduction to be reversible with one electron transferred. As the chloride concentration increases, especially in ethanol-rich solvents, the reduction appears to be irreversible and to approach a two-electron reduction. This conclusion is drawn from the slope of the  $E_{1/2}$  vs.  $\log [(i_d - i)/i]$  plots and the large increase of the diffusion currents.

The plot of  $\log [(i_d - i)/i]$  vs.  $-E$  in 0.040 and 0.050  $M$  chloride in 92.2 weight % ethanol gives a plot with two straight segments, with the slopes of 0.044 and 0.063. This type of plot may be interpreted as meaning two reduction processes with closely associated half-waves.

Plots of  $-E_{1/2}$  vs. logarithm of the chloride concentration, especially in ethanol-rich solvents, show that  $E_{1/2}$  is strongly dependent upon chloride concentration. The values of the  $(p - q)/a$  factor in the Lingane equation<sup>1</sup> are negative and, except perhaps for the limiting value in 92.2 weight % ethanol, are fractional.

The values of  $-E_{1/2}$  at selected chloride concentrations were found first to increase with increasing weight per cent. ethanol out to about 25 weight % ethanol, then to remain constant or decrease relatively slowly depending on the molarity of chloride, and finally decrease more precipitously depending on the molarity of the chloride (see Fig. 1).

Beginning at about 50 weight % ethanol,  $I$  decreases rapidly with weight per cent. ethanol in

(1) J. J. Lingane, *Chem. Revs.*, 291 (1941).

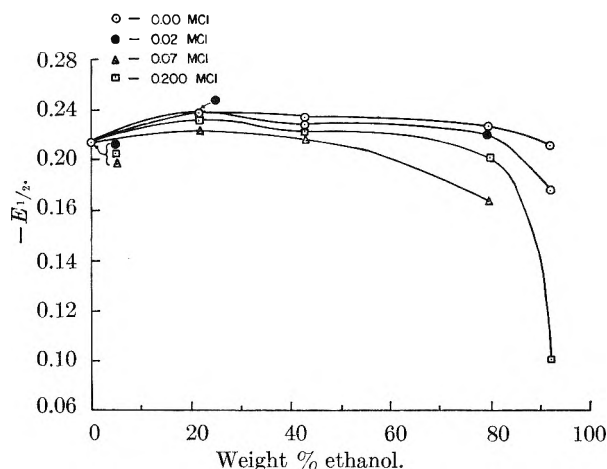


Fig. 1.— $-E_{1/2}$  as function of ethanol concentration at selected chloride concentrations.

perchlorate solutions; and in chloride solutions depending on the molarity of the chloride,  $I$  increases rapidly beginning at about 80 weight % ethanol. In 1.000  $M$  perchlorate solutions,  $I$  has the values of  $1.98 \times 10^{-3}$ ,  $1.97 \times 10^{-3}$ ,  $2.03 \times 10^{-3}$ ,  $1.72 \times 10^{-3}$  and  $1.49 \times 10^{-3}$  in water, 21.6, 43.0, 79.3 and 92.2 weight % ethanol in water, respectively. In 0.07  $M$  chloride ion solutions containing 0.930  $M$  perchlorate ion  $I$  has the values  $1.98 \times 10^{-3}$ ,  $2.00 \times 10^{-3}$ ,  $1.91 \times 10^{-3}$ ,  $2.05 \times 10^{-3}$  and  $3.36 \times 10^{-3}$  in water, 21.6, 43.0, 79.3 and 92.2 weight % ethanol in water, respectively. These were two opposite extremes, between which data for other chloride concentrations in similar solvent composition ranges fell. In chloride solution the values of  $I$  broke sharply upward at about 80 weight % ethanol. In perchlorate,  $I$  more gradually decreases beginning at about 43 weight % ethanol.

Depending upon the molarity of uranyl ion,  $i_d$  decreases up to about 40 weight % ethanol, where it passes through a minimum, and then increases to a maximum at about 80 weight % ethanol. This minimum probably is due to viscosity effects and the maximum could arise from selective solvation.

The authors wish to thank the United States Atomic Energy Commission for Contract AT-(40-1)-2069 which supported this research financially.

## IMPROVEMENTS IN THE DESIGN OF CONDUCTIVITY CELLS

BY KAROL J. MYSELS

Chemistry Department, University of Southern California, Los Angeles 7, California

Received January 6, 1961

Many different types of conductivity cells adapted to a variety of purposes have been described. The present note deals with improvements developed in this Laboratory over a period of years which have greatly facilitated conductivity measurements of electrolyte solutions without sacrificing accuracy or precision.

The use of a poorly designed conductivity cell can cause significant errors in the measurement of electrolyte conductivity if it introduces sub-

stantial capacitances involving parts of the solution at different potentials. This is the so-called "shunt effect" and is revealed, as shown by Jones and Bollinger,<sup>1</sup> by an apparent decrease in resistance as the frequency of the measuring current is increased, especially at higher frequencies. Polarization errors due to insufficient platinizing of the electrodes have the same effect which is especially marked at lower frequencies. Hence, a good criterion of cell accuracy is that resistance does not change with frequency. The cells described below showed no frequency effect exceeding 0.01% from 0.5 to 10 kilocycles.

As shown by Jones and Bollinger<sup>1</sup> the shunt effect can be avoided by keeping the contact tubes (connecting the electrodes to outside conductors) widely separated and also by keeping the filling tubes far apart. This is now the standard procedure and presents no difficulty when the cell constant is large so that the electrodes are well separated and there is no limitation on the volume of solution used. However, when the cell constant becomes small so that the electrodes must be close together and the volume of the solution is reduced, this design becomes quite unwieldy as exemplified by the cell shown in Fig. 14 *K* of Jones and Bollinger. The shunt effect, however, can also be eliminated by keeping both filling tubes at the same potential and at a sufficient distance from the contact tubes. This is illustrated by the cell of Fig. 1 where the inlet tubes are located in the middle of the cell and in a plane at right angles to that of the contact tubes. The cell requires only 8 cc. of solution and because of its shape can be rinsed easily.

The determination of conductivity and especially of differences of conductivity of solutions of varying concentrations is greatly facilitated if the solutions are prepared directly in the conductivity cell by successive dilutions or additions. The doughnut-type dilution cell shown in Fig. 2 was developed for such measurements.

The magnetic stirrer located in the base of the dilution cell permits thorough stirring of the contents without removing the cell from the thermostated bath. It forces the liquid into the doughnut-shaped measuring region, around the two electrodes, and thence into the bottle-shaped reservoir from which it is sucked out again through the middle. This mixing motion is extremely efficient and the speed of stirring has to be controlled to avoid formation of a vortex and dispersion of air through the whole cell.

The use of dilution cells is greatly facilitated if the cell constant varies little or preferably not at all as the volume of the solution is changed. For cells of the type shown in Fig. 2 the change amounts to less than 0.01% between a minimum volume covering the two inlets of the main reservoir and a three times larger one filling the reservoir. This result is attained by making the two orifices in the doughnut at mid-points between the electrodes so that the potential at these openings is equal and there is no tendency for the electric current to leave the doughnut. The hydrody-

(1) G. Jones and G. M. Bollinger, *J. Am. Chem. Soc.*, **53**, 411 (1931).

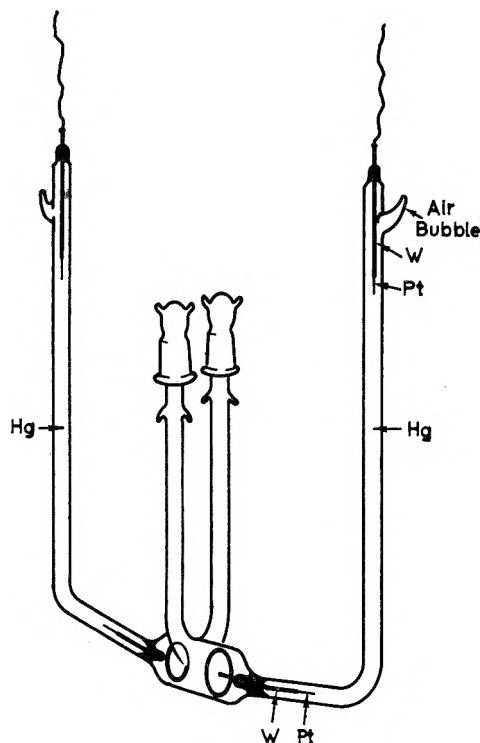


Fig. 1.—A low volume, low cell constant conductivity cell.

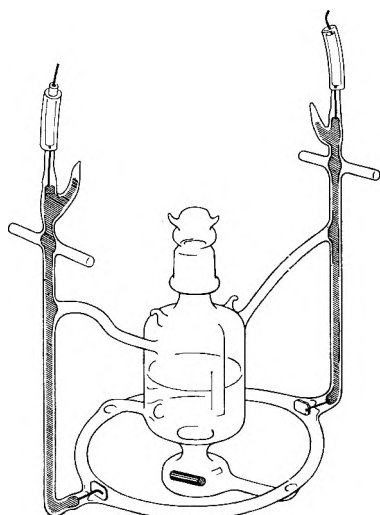


Fig. 2.—A doughnut-type dilution or titration conductivity cell whose cell constant is independent of volume of liquid.

namic flow and the flow of current are thus completely separated.

The size and internal diameter of the doughnut can be varied over a wide range to give different cell constants. The cell shown in the figure has a cell constant of 36. By reducing the size of the doughnut and increasing somewhat the internal diameter a cell constant of 3 has been obtained. This could be pushed somewhat further but for low cell constants where electrodes are close together, other designs<sup>2,3</sup> are quite satisfactory. The main purpose of the doughnut design is to provide

(2) H. M. Daggett, E. J. Bair and C. A. Kraus, *J. Am. Chem. Soc.*, **73**, 799 (1951).

(3) P. Mukerjee, K. J. Mysels and C. I. Dulin, *J. Phys. Chem.*, **62**, 1390 (1958).

a high and at the same time in varying cell constant.

Both types of cells shown are constructed of Pyrex glass with platinum electrodes and supporting wires. These supporting wires are welded to tungsten rods which are sealed to the Pyrex in the conventional way, but with a lip of the Pyrex covering the weld and a little of the platinum wire.<sup>4</sup> In this way a completely tight joint is obtained, yet the solution is kept out of contact with tungsten for all practical purposes.

Electric contact to the electrode is made as usual by mercury held in a glass tube. This assures good thermal contact with the thermostated bath and no possibility of uncontrolled heat input from the outside through the electrodes to the solution being measured. (This could be the case if a copper or silver wire inside a glass tube were used as a connection.) To avoid spillage and contamination, the glass tube is sealed and contact to the bridge is made through another sealed-in tungsten wire bearing a pigtail. To prevent breakage by frequent flexing at the attachment of the pigtail, a piece of macaroni or Tygon tubing is used as a protector. Entrapment of a little air with the mercury is advantageous in reducing the "hammer" effect when mercury flows in the tube. This sealed construction also ensures a constant dry weight of the cell.

A little bit of platinum wire is spot welded to each end of the tungsten wire in contact with the mercury. This assures a constant and negligibly small resistance of the contact arms which can be checked by filling the cell with mercury before platinization.

The connection between the base and the reservoir of the dilution cell should be made wide enough to permit the introduction and removal of the magnetic stirrer. Teflon-coated stirrers then can be used since they can be introduced after the cell is completed but cannot stand the annealing procedure. Otherwise, a glass-enclosed stirrer has to be inserted during the construction of the cell. Such non-removable stirrers permit a slight reduction in the minimum volume of the cell but seem to be the most breakable part of the whole construction.

**Acknowledgment.**—These improvements were evolved in collaboration with many co-workers, in particular Dr. D. Stigter, Dr. C. I. Dulin, Mrs. P. Kapauan, and Dr. R. J. Otter, and were realized by the glassblowing skill of Mr. Robert H. Greiner.

This work was supported in part by the Office of Naval Research. Reproduction for purposes of the U. S. Government is permitted.

(4) R. H. Greiner, *Fusion*, **7**, no. 4, 11 (1960).

## THE FREE ENERGY OF SILICON CARBIDE FROM ITS SOLUBILITY IN MOLTEN LEAD

BY DAVID H. KIRKWOOD AND JOHN CHIPMAN

Department of Metallurgy, Massachusetts Institute of Technology, Cambridge, Mass.

Received February 8, 1961

The free energy formation of silicon carbide was determined by Humphrey, Todd, Coughlin and

King<sup>1</sup> from measurements of the heat of combustion and the heat capacity at low and high temperatures. Their results received confirmation in the work of Chipman, Fulton, Gokcen and Caskey<sup>2</sup> who determined the activity coefficient of silicon in molten iron and the solubility of SiC in molten Fe-Si solution.

On the other hand, Baird and Taylor<sup>3</sup> measured the equilibrium pressure of CO in the reaction  $\text{SiO}_2 + 3\text{C} = \text{SiC} + 2\text{CO}$  and found a pressure very much lower than would be calculated from Humphrey's free energy data. Their experiments have been repeated with good agreement by Kay and Taylor.<sup>4</sup> This suggests that the free energy of either  $\text{SiO}_2$  or of SiC may be in error, and if the error can be ascribed to SiC, this compound is much less stable than indicated by Humphrey's work. Drowart, DeMaria and Inghram<sup>5</sup> have studied the dissociation of silicon carbide at higher temperatures with the aid of  $\epsilon$  mass spectrometer while Drowart and DeMaria<sup>6</sup> using the same method have measured the vapor pressure of silicon. From these results Smiltens<sup>7</sup> has shown that the compound is more stable than the thermochemical data indicate. These discrepancies require a decision based on an independent method.

Experiments on the solubility of silicon in lead were conducted in silica crucibles, held in the furnace at a temperature of  $1420 \pm 2^\circ$  at the bottom of a long silica tube 2 cm. i.d. which was filled with argon. Samples were obtained by sucking small portions of the solution into silica tubes of the types shown in Fig. 1. Experiments were also conducted in which liquid lead and hexagonal (alpha) silicon carbide were brought into equilibrium in a graphite crucible surrounded by the same silica sheath. Equilibrium was also approached from the high-silicon side and the identity of the precipitated SiC was verified by X-ray diffraction.

The solubility of silicon in lead at  $1420^\circ$  was found to be 0.45% by weight (average of six samples). The silicon layer contained 13.7 weight % lead. The solubility of silicon carbide at the same temperature in the presence of graphite was found to be 0.015 weight % (average of 5 best samples).

The compositions of the conjugate layers at  $1420^\circ$  are therefore  $N_{\text{Si}} = 0.032$  and  $N_{\text{Pb}} = 0.021$ . The activity coefficient of silicon in the lead-rich liquid is 31. That such solutions even though quite dilute may exhibit marked deviation from Henry's law has been shown recently by Wriedt<sup>3</sup> and by Worrell.<sup>8</sup> Their method employs the rea-

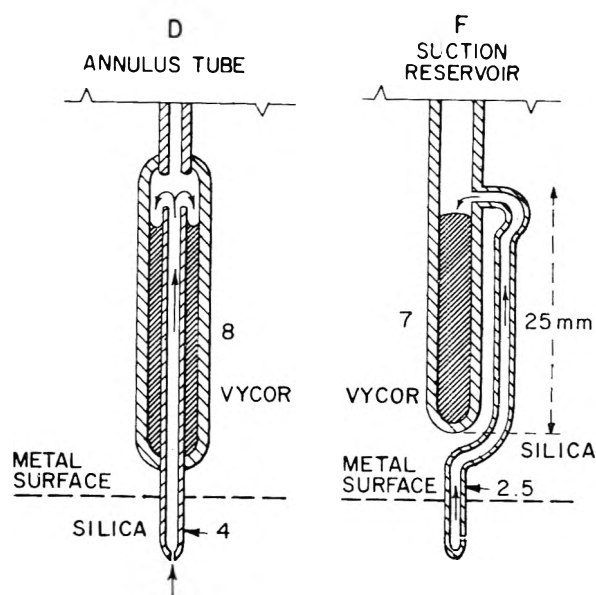


Fig. 1.—Samplers; numbers are outside diameters in mm.

sonable assumption that the function  $\alpha_{\text{Si}} = \ln \gamma_{\text{Si}} / (1 - N_{\text{Si}})^2$  is a linear function of  $N_{\text{Si}}$ . The calculation leads to a value of  $\gamma_{\text{Si}} = 36$ , for the solution in equilibrium with SiC and graphite, in which  $N_{\text{Si}} = 0.0011$ . Assumption of a constant value of  $\alpha_{\text{Si}}$  leads to  $\gamma_{\text{Si}} = 39$  which is not a significant difference. The free energy of formation of alpha SiC from liquid Si and graphite is  $\Delta F_{1693}^0 = RT \ln 0.040 = -10.8$  kcal. It is difficult to assess the probable accuracy of this value. The chief uncertainty lies in the hazards of sampling and analysis of such a dilute solution at high temperatures. The authors would not suggest an accuracy better than  $\pm 1$  kcal.

TABLE I

COMPARISON OF VALUES FOR THE FREE ENERGY OF FORMATION OF SiC AT 1693°K. (KCAL.)

Method	$\Delta F^0$ ( $\alpha$ -SiC) (hexagonal)	$\Delta F^0$ ( $\beta$ -SiC) (cubic)
Combustion calorimetry <sup>1</sup>	- 9.2	-10.3
Equilibrium		
$\text{SiO}_2 + 3\text{C} = \text{SiC} + 2\text{CO}$ <sup>4</sup>	....	- 5.8
Dissociation <sup>7</sup>	-15.0	....
Solubility in iron <sup>2</sup>	....	-10.7
Solubility in lead	-10.8	....

The present extent of disagreement is shown in Table I in which values of several observers are compared at  $1420^\circ$ . The agreement between solubility measurements and thermochemical results offers support for these intermediate values. Further work is in progress with other metallic solvents.

In view of the results of Taylor and co-workers on the  $\text{SiO}_2$ -C-SiC-CO equilibrium, the independent results for SiC suggest a re-examination of the free energy of SiO<sub>2</sub>.

**Acknowledgments.**—The authors wish to thank Dr. J. Smiltens of the Air Force Cambridge Research Center for providing the sample of hexagonal SiC used in these experiments. They would also wish to thank John d'Entremont for his con-

(1) G. L. Humphrey, S. S. Todd, J. P. Coughlin and E. G. King, Bureau of Mines Report of Investigations 4888, 1952.

(2) J. Chipman, J. C. Fulton, N. Gokcen and C. R. Caskey, *Acta Met.*, **2**, 439 (1954).

(3) J. D. Baird and J. Taylor, *Trans. Faraday Soc.*, **54**, 526 (1958).

(4) D. A. R. Kay and J. Taylor, *ibid.*, **56**, 1372 (1960).

(5) J. Drowart, G. DeMaria and M. G. Inghram, *J. Chem. Phys.*, **29**, 1015 (1958).

(6) J. Drowart and G. DeMaria, in "Silicon Carbide," J. R. O'Connor and J. Smiltens, Editors, Pergamon Press, New York, N. Y., 1960, p. 16.

(7) J. Smiltens, *J. Phys. Chem.*, **64**, 368 (1960).

(8) H. Wriedt and W. Worrell (independently) unpublished calculations.

tributions to the design and fabrication of the samplers and Donald L. Guernsey for his careful analytical work.

### SOME PHYSICAL PROPERTIES OF AQUEOUS PICOLINIC ACID SOLUTIONS

By R. A. ROBINSON<sup>1</sup> AND R. W. GREEN

University of New England, Armidale, N.S.W., Australia and University of Sydney, N.S.W., Australia

Received January 23, 1961

We have measured the density, refractive index and viscosity of some aqueous picolinic acid solutions at 25°. Picolinic acid was purified by sublimation at low pressure. Vacuum corrections were applied to the weights in making up the solutions. Densities were measured by the usual pycnometer method, refractive indices with an Abbe instrument and viscosities in an Ostwald viscometer. Kinetic energy corrections were made to the viscosity data. The results are given in Table I.

TABLE I

DENSITY, REFRACTIVE INDEX AND VISCOSITY OF AQUEOUS PICOLINIC ACID SOLUTIONS AT 25°<sup>a</sup>

%	<i>m</i>	<i>c</i>	<i>x</i>	<i>d</i> , g. ml. <sup>-1</sup>	<i>n</i>	<i>η/η</i> <sup>0</sup>
5.093	0.4359	0.4193	0.00779	1.0135 <sub>9</sub>	1.3431	1.103
8.711	.7751	.7258	.01377	1.0257 <sub>0</sub>	1.3520	1.193
9.730	.8755	.8135	.01553	1.0292 <sub>4</sub>	1.3538	1.214
10.77	.9804	.9035	.01736	1.0327 <sub>3</sub>	1.3561	1.248
15.34	1.472	1.306	.02583	1.0483 <sub>5</sub>	1.3669	1.394
20.41	2.083	1.768	.03617	1.0663 <sub>4</sub>	1.3788	1.604
25.01	2.709	2.201	.04653	1.0833 <sub>4</sub>	1.3889	1.829
28.96	3.311	2.582	.05629	1.0976 <sub>9</sub>	1.3997	2.109
35.69	4.508	3.256	.07511	1.1232 <sub>9</sub>	1.4165	2.744
40.69	5.573	3.777	.09124	1.1427 <sub>7</sub>	1.4297	3.459
47.71	7.411	4.538	.1178	1.1709 <sub>2</sub>	1.4491	5.127

<sup>a</sup> *x* = mole fraction of picolinic acid; *n* = refractive index.

The partial molal volume at infinite dilution is 83.8 ml. mole<sup>-1</sup>; that of pyridine is 77.5 ml. mole<sup>-1</sup> calculated from the density of its aqueous solutions<sup>2</sup> or 80.9 ml. mole<sup>-1</sup> from the density of the pure liquid. The Traube increment for the carboxylic group (15.8 ml. mole<sup>-1</sup>) added to the molal volume of pyridine therefore gives at least 93 ml. mole<sup>-1</sup> for picolinic acid.

The refractive index measurements probably were accurate within ±0.0002: the refractivity at infinite dilution therefore cannot be calculated with accuracy but it is approximately 31.9 ml. mole<sup>-1</sup>. That of pyridine is 23.97 ml. mole<sup>-1</sup> and the usual increment for the carboxyl group predicts 30.1 for picolinic acid. Thus the observed molal volume is low and the refractivity high. This may well be due to the fact that picolinic acid exists mainly in the zwitterion form<sup>3</sup> with increased resonance.

The high viscosities are notable: a 48% solution is about as viscous as a 38% sucrose solution at the same temperature. The relative viscosities can be represented with an average deviation of 0.005 by Vand's modification<sup>4</sup> of the Einstein equation<sup>5</sup>

$$\ln \eta/\eta^0 = \frac{2.5 \bar{V}c}{1 - Q\bar{V}c}$$

where  $\bar{V} = 0.0917$  l. mole<sup>-1</sup> is an "effective molal volume" and  $Q = 0.873$  is an interaction parameter.

(4) V. Vand, *J. Phys. Chem.*, **52**, 277 (1948).

(5) A. Einstein, *Ann. Phys.*, **19**, 289 (1906).

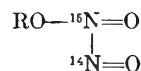
### THE ISOTOPE EXCHANGE REACTION BETWEEN LABELLED NITRIC OXIDE, <sup>15</sup>NO AND NITROSYL CHLORIDE, <sup>14</sup>NOCl<sup>1</sup>

By LESTER P. KUHN AND CHESTER BUTKIEWICZ

Ballistic Research Laboratories, Aberdeen Proving Ground, Md.

Received January 21, 1961

In a previous paper<sup>2</sup> it was shown that a bimolecular exchange reaction occurs between <sup>14</sup>NO and RO<sup>15</sup>NO which is first order in nitric oxide and first order in nitrite ester. The reaction between nitric oxide and nitrate esters to yield nitrogen dioxide and nitrite ester, on the other hand, was found to be first order in nitrate ester but independent of nitric oxide pressure. It was concluded that the isotope exchange reaction between nitric oxide and nitrite esters occurs through the formation of an unstable intermediate which



rearranges to give the exchanged products and does not occur by way of a displacement on alkyl oxygen. The object of the present work was to make a similar study of the reaction between labelled nitric oxide and nitrosyl chloride.

The reaction was run in an infrared cell having CaF<sub>2</sub> windows. The reaction mixture was analyzed for <sup>14</sup>NOCl and <sup>15</sup>NOCl by means of infrared spectroscopy. The respective bands in the region of 5.5 μ are nicely resolved by the CaF<sub>2</sub> prism as shown in Fig. 1. It was found that at 25° with initial pressures of <sup>14</sup>NOCl of 5 to 10 mm., and at pressures of <sup>15</sup>NO such that the ratio NO/NOCl varied from 0.3 to 3, equilibration was complete in three minutes, which was the time required to get an infrared spectrum after the gases were mixed in the cell. The half-life of this reaction under our experimental conditions must therefore be of the order of seconds or less. Because of the speed of the reaction it was not possible to obtain kinetic data or to determine the order of the reaction with the technique we employed.

The thermal decomposition of nitrosyl chloride has been studied thoroughly. At temperatures below 250° the reaction is second order in NOCl and the rate constant<sup>3</sup> is 10<sup>11.8</sup> exp(-22000/RT) mole<sup>-1</sup> cc. sec.<sup>-1</sup>. The half-life of the bimolecular decomposition under our experimental conditions according to this rate constant would be about 10<sup>10</sup> seconds. At 300° the decomposition proceeds by a two-step mechanism<sup>4</sup>

(1) This work was supported by the Office of Ordnance Research, Durham, N. C.

(2) L. Kuhn and H. Gunthard, *Helv. Chim. Acta*, **43**, 607 (1960).

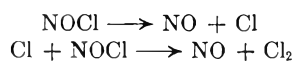
(3) I. Welinsky and H. A. Taylor, *J. Chem. Phys.*, **6**, 466 (1938).

(4) P. G. Ashmore and J. Chanmugan, *Trans. Faraday Soc.*, **49**, 270 (1953).

(1) Correspondence to R. A. Robinson, National Bureau of Standards, Washington 25, D. C.

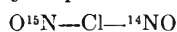
(2) "International Critical Tables," Vol. III, McGraw-Hill Book Co., Inc., New York, N. Y., 1928, p. 112.

(3) R. W. Green and H. K. Tong, *J. Am. Chem. Soc.*, **78**, 4896 (1956).

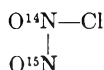


The rate constants for the two steps are  $10^{12} \exp(-38000/RT)$  sec.<sup>-1</sup> and  $10^{13} \exp(-1100/RT)$  mole<sup>-1</sup> cc. sec.<sup>-1</sup>, respectively. According to this mechanism the half-life for the decomposition of NOCl under our conditions would be about  $10^{16}$  seconds. It is clear that the rapid isotope exchange reaction which we have observed cannot take place by a rate-determining decomposition of <sup>14</sup>NOCl followed by a rapid reaction of <sup>15</sup>NO with Cl or Cl<sub>2</sub>, since the rate of decomposition of NOCl by either the bimolecular or unimolecular is much too slow. It seems highly likely that the isotope exchange reaction involves the attack of <sup>15</sup>NO upon <sup>14</sup>NOCl.

We can picture this reaction as taking place in either of two ways: The first possibility is a displacement reaction on chlorine in which the transition state may be pictured as



The second possibility is the formation of a short-lived intermediate which rearranges to give the



exchanged products. The new bond that is formed in the intermediate involves the unshared pair of electrons of the nitrogen of NOCl being donated to the NO. If the first possibility is correct then one should find a similar bimolecular reaction between NO and NO<sub>2</sub>Cl (first-order in NO and first-order in NO<sub>2</sub>Cl) to give NO<sub>2</sub> and NOCl. If, on the other hand, the second possibility is correct one would not expect to find a reaction between NO and NO<sub>2</sub>Cl whose rate was dependent upon the pressure of NO since NO<sub>2</sub>Cl does not have an unshared pair of electrons and hence is incapable of forming the postulated intermediate.

A rapid reaction<sup>5</sup> does in fact, occur between NO and NO<sub>2</sub>Cl to give NO<sub>2</sub> and NOCl which is first order in both NO and NO<sub>2</sub>Cl, whose rate constant is  $0.8 \times 10^{12} \exp(-6900/RT)$  mole<sup>-1</sup> cc. sec.<sup>-1</sup>. This reaction has a half-life of several seconds under our conditions of temperature and pressure. Thus we conclude that the isotope exchange reaction between <sup>15</sup>NO and <sup>14</sup>NOCl and the reaction between NO and NO<sub>2</sub>Cl proceed by a displacement on chlorine and not *via* the formation of the intermediate pictured above. It is interesting to note that whereas this reaction takes place *via* a displacement on chlorine, the analogous reaction involving nitrite esters does not take place *via* a displacement on oxygen. Thus we have another example of the frequently observed phenomenon that free radical reactions occur readily by displacement at a univalent atom (halogen or hydrogen) but not at a polyvalent atom.

#### Experimental

<sup>15</sup>NO was made in the manner previously described.<sup>2</sup> <sup>14</sup>NOCl was purchased from the Matheson Company and purified by distillation.<sup>6</sup> The infrared spectrum of the puri-

(5) E. Freiling, H. Johnston and R. Ogg, *J. Chem. Phys.*, **20**, 327 (1952).

(6) "Inorganic Syntheses," McGraw Hill Book Co., New York, N. Y., 1939, p. 55.

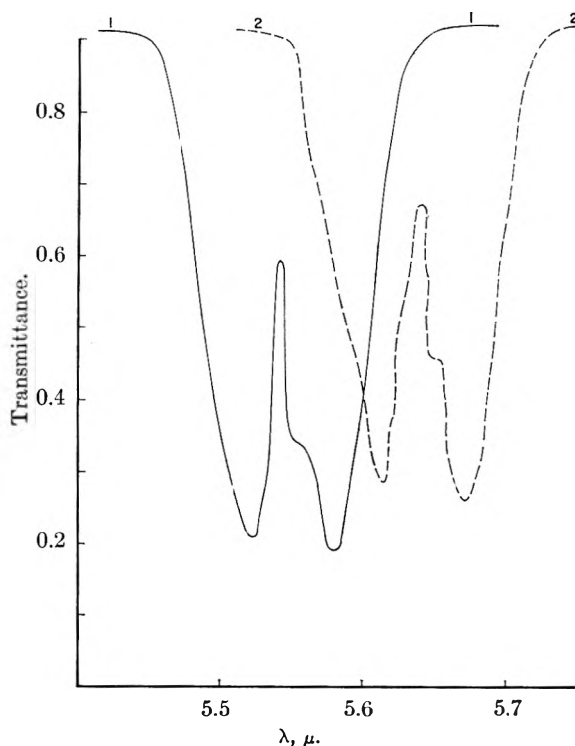


Fig. 1.—(1) <sup>14</sup>NOCl; (2) <sup>15</sup>NOCl, pressure 10 mm., cell length 20 mm.

fied material showed that it was essentially free of the two major impurities, HCl and NO<sub>2</sub>. The gases were introduced into a 5-cm. infrared cell with CaF<sub>2</sub> windows at the desired pressure using a conventional vacuum line. The mercury of the manometer was protected from the NOCl by a layer of perfluorokerosene. The spectra were obtained with a Perkin-Elmer Model 21 Spectrometer equipped with a CaF<sub>2</sub> prism.

## ACIDITY CONSTANT OF A PROTEIN CONJUGATE IN D<sub>2</sub>O

BY W.-Y. WEN AND I. M. KLOTZ

Department of Chemistry, Northwestern University, Evanston, Illinois  
Received October 28, 1960

The relative strengths in solution of hydrogen bonds involving protons and deuterium atoms, respectively, have been the subject of numerous investigations.<sup>1-6</sup> For isolated molecules in the gaseous state, heats of dimerization<sup>7</sup> show clearly that bonding by deuterium is stronger, but only slightly so. For solutes in solution, however, there are competing effects between substituents of the solute and the solvent, and the net effect on physico-chemical behavior of the solute is not easy to predict.

We have recently<sup>8,9</sup> interpreted the shifts in

(1) S. Korman and V. K. LaMer, *J. Am. Chem. Soc.*, **58**, 1396 (1936).

(2) F. C. Nachod, *Z. physik. Chem.*, **A182**, 193 (1938).

(3) A. H. Cockett and A. Ferguson, *Phil. Mag.*, **28**, 693 (1939).

(4) F. A. Long and D. Watson, *J. Chem. Soc.*, 2019 (1958).

(5) M. Calvin, J. Hermans, Jr., and H. A. Scheraga, *J. Am. Chem. Soc.*, **81**, 5048 (1959).

(6) G. Dahlgren, Jr., and F. A. Long, *ibid.*, **82**, 1303 (1960).

(7) A. E. Potter, Jr., P. Bender and H. L. Ritter, *J. Phys. Chem.*, **59**, 250 (1955).

(8) I. M. Klotz, *Science*, **128**, 815 (1958).

(9) I. M. Klotz and H. A. Fiess, *Biochim. et Biophys. Acta*, **38**, 57 (1960).

acidity constants of groups conjugated to proteins in terms of a crystallization of water around certain side chains of the macromolecule. It seemed of interest, therefore, to see whether any difference could be observed for hydration by deuterium oxide as compared to normal water. For this purpose we have measured the  $pK_a$  of dimethylaminonaphthalenesulfonyl chloride bound (separately) to protein and to a reference small molecule in  $D_2O$  and  $H_2O$ , respectively.

#### Experimental

**Materials.**—Crystalline bovine serum albumin was purchased from Armour and Co. The 1-dimethylaminonaphthalene-5-sulfonyl chloride was a purified product of the California Corporation for Biochemical Research. Heavy water was obtained from the Stuart Oxygen Co. and warranted to be 99.5%  $D_2O$ .

**Preparation of Conjugates.**—To a solution of  $6.7 \times 10^{-5} M$  serum albumin in  $0.1 M NaHCO_3$  was added, at  $0^\circ$ , a ten-fold molar excess of dimethylaminonaphthalenesulfonyl chloride, in acetone solution at a concentration of  $0.007 M$ . The mixture was stirred in the cold for 21 hours and then passed through an anion-exchange resin (IRA-400) to remove any hydrolyzed uncoupled dye. The effluent was dialyzed against water in the cold for two days to remove acetone and salt. The final outside solution showed no fluorescence, whereas the solution inside the cellophane casing showed strong fluorescence under an ultraviolet lamp with  $360 m\mu$  radiation. The conjugated protein was isolated by lyophilization. Absorbance measurements at  $341 m\mu$  with a sample of this material in aqueous solution at  $pH$  9 indicated 7.0 moles bound dye per mole protein, if we assume a molar absorptivity of  $3.36 \times 10^3 l. mole^{-1} cm^{-1}$  as found by Hartley and Massey<sup>10</sup> for the chymotrypsin-dye conjugate.

The glycine-dye conjugate was the same sample as that used previously.<sup>9</sup> Its molar absorptivity in  $D_2O$  was  $4.43 \times 10^3 l. mole^{-1} cm^{-1}$ , not significantly different from the value reported<sup>10</sup> in  $H_2O$ ,  $4.55 \times 10^3$ .

**Titration Procedure.**—The solid conjugate with protein or glycine was dissolved in  $H_2O$  and  $D_2O$ , respectively, to give a solution with an absorbance of 0.3–0.4 near  $340 m\mu$ . Dissolution of solute in  $D_2O$  was followed by a hydrogen-deuterium exchange reaction which lowers the purity of  $D_2O$ . However, since the protein concentration used was only about  $10^{-5} M$ , the decrease in  $D_2O$  content would not exceed 0.1% and is, therefore, completely negligible. Likewise no correction was applied for the exchange reaction caused by the addition of minute quantities of  $HCl$  or  $NaOH$  used to change the  $pD$  of the solution.

The  $pH$ 's (or  $pD$ 's) of the solutions were measured with a Beckman  $pH$  meter, model G. In a  $D_2O$  solution  $pD$  may be computed from the empirical equation of Glasoe and Long<sup>11</sup>

$$pD = pH\text{-meter reading} + 0.40 \quad (1)$$

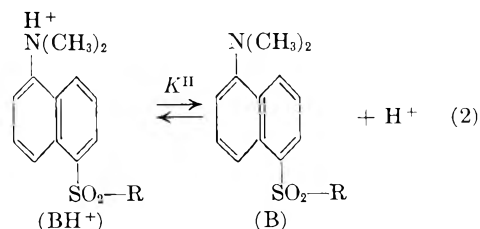
where the  $pH$ -meter reading is obtained with a glass electrode-calomel electrode combination standardized to read  $pH$  in  $H_2O$  solutions.

Absorption spectra were obtained with a Beckman DU spectrophotometer at about  $25^\circ$ .

For each solution of conjugate the spectrum was measured over a series of  $pH$ 's as described previously<sup>9</sup> until enough data had been accumulated to provide a smooth spectrophotometric titration curve.

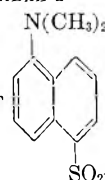
#### Results and Discussion

The acid-base equilibria being studied may be represented by the equation



and a corresponding equation in which  $D^+$  dissociates instead of  $H^+$ .

TABLE I

ACID-BASE EQUILIBRIA OF  IN WATER AT  $25^\circ$

Nature of R	$pK^H$ in $H_2O$	$pK^D$ in $D_2O$	$\Delta pK$
Glycine	3.95 <sup>a</sup>	4.47	0.48
Bovine serum albumin	1.47	1.84	0.38

<sup>a</sup> Taken from ref. 9.

When R represents a small molecule, in our case a glycine residue, the dissociation can be described by the equation

$$pH = pK^H + \log \frac{(B)}{(BH^+)} \quad (3)$$

or by

$$pD = pK^D + \log \frac{(B)}{(BD^+)} \quad (4)$$

$pK$ 's can be evaluated readily by simple graphical methods.<sup>9</sup> When R is a large protein molecule, for example bovine serum albumin, equations 3 and 4 no longer adequately correlate the ionization equilibria. Nevertheless, since we are interested in the present context merely in a comparison of behavior in  $H_2O$  and  $D_2O$ , we may define  $pK$  for the dye-protein conjugate as that  $pH$  at which  $(B) = (BH^+)$  or that  $pD$  at which  $(B) = (BD^+)$ .

Acidity constants so calculated are assembled in Table I.

The shift in  $pK$  of the dye as one goes from glycine to the macromolecular protein is large in either solvent,  $H_2O$  or  $D_2O$ , being 2.52 units in the former and 2.62 in the latter liquid. It is clear then that both solvents produce a marked masking of the titrated dimethylamino group. The difference in masking effect between the two solvents is only 0.10 unit, a quantity which is not larger than the combined uncertainties in the determination of the various  $pK$ 's involved. We conclude, therefore, that differences between hydrogen-bonding strengths in liquid water versus hydration water of proteins, are not appreciably different in  $D_2O$  as compared to  $H_2O$ .

**Acknowledgment.**—This investigation was carried out with the aid of a grant from the National Science Foundation.

(10) B. S. Hartley and V. Massey, *Biochim. et Biophys. Acta*, **21**, 58 (1956).

(11) P. K. Glasoe and F. A. Long, *J. Phys. Chem.*, **64**, 188 (1960).



# COMMUNICATIONS TO THE EDITOR

## SOME ASPECTS OF THE ROTATING SECTOR DETERMINATION OF THE ABSOLUTE RATE CONSTANTS IN RADICAL POLYMERIZATION REACTIONS: A CORRECTION

Sir:

In a recent paper Kwart has made valuable contributions to the rotating sector theory,<sup>1</sup> but has made an incorrect statement concerning the paper of Matheson, *et al.*:<sup>2</sup> "The treatment of these authors deals only with cases where the thermally induced and other dark reaction rates are accounted in the dark periods and are neglected in the light periods of a full cycle of sector alternation." The treatment of ref. 2 includes the "dark" initiation both during the light and the dark parts of the sector cycle. The basic assumption is clearly stated. "The magnitude of the "dark" rate of initiation is unaffected by light." In other words, the rate of initiation during the dark part of the cycle is, during the light part of the cycle, additive to the rate of initiation due to the light. No assumptions are made as to the source of the dark initiation, as to whether it is due to thermal, to impurity, or to stray light initiation, only that the "dark" rate of initiation adds to the additional initiation resulting when the sector permits the cell to be irradiated.

In ref. 2 the total rate of initiation in the light period is expressed as  $2qfI_a$ , purely as a formal convenience. However, it is clear that  $2qfI_a$  includes the dark rate of initiation (subject to additivity assumption above), because the rate of initiation in the dark is expressed as  $2qfnI_a$ , where " $n^{1/2}$  is the ratio of the steady dark rate to the steady light rate."

In application of the theory<sup>2</sup> the value of  $n^{1/2}$  was determined from the *experimentally measured* steady dark and steady light rates. Therefore, if the polymerization mechanism used by us or by Kwart is correct,  $n$  is the ratio of the steady dark rate of initiation to the steady light rate of initiation, for the case where all sources of initiation experimentally contributing to the steady light rate are included.

In Kwart's notation:

$$n = \rho / (fI + \rho) = \gamma^2$$

LABORATOIRE DE CHIMIE PHYSIQUE  
DE LA FACULTÉ DES SCIENCES  
11 RUE PIERRE CURIE  
PARIS 5<sup>e</sup>, FRANCE

MAX MATHESON<sup>3</sup>

RECEIVED FEBRUARY 9, 1961

## AMINE BORANES. II. PYRIDINE BORANE-PROPANOL REACTION KINETICS<sup>1</sup>

Sir:

A previously reported study of the reaction of pyridine-B-diarylboranes with water established a mechanism involving attack on a boron-hydrogen bond by a water proton and eventual removal of H<sup>-</sup> in the rate-determining step.<sup>2</sup> We would like to report evidence indicating that amine-boranes may react by loss of amine rather than H<sup>-</sup> in the slow step.

We investigated the reaction of pyridine-borane, Py·BH<sub>3</sub>, in 1-propanol with the following results. The rate is of first order in borane over several half-lives, as measured by reducing strength toward KIO<sub>3</sub> indicating no buildup of -BH<sub>2</sub> intermediates. The rate is practically unaffected and is not decreased by addition of pyridine. The rate in pure water is less than 5% of the rate in pure propanol at the same conditions. On dilution of propanol with water the rate decreases while addition of *p*-dioxane increased the rate. The pertinent data are summarized in Table I. The rate constants for alcohol-water mixtures given in Table II follow the Kirkwood relation.<sup>3</sup> A linear log  $k$  vs.  $(D - 1)/2(D + 1)$  plot ( $D$  = dielectric constant of the mixture) is obtained only from the first order constants which are independent of alcohol concentration. The plot has a negative slope.

TABLE I  
FIRST ORDER RATE CONSTANTS FOR PYRIDINE-BORANE

Solution	Temperature, °C.	$k \times 10^5$ (sec. <sup>-1</sup> )
1-Propanol	50.00	1.86
50% <i>p</i> -dioxane (by vol.)	50.00	5.72
50% H <sub>2</sub> O (by vol.)	50.00	0.445
1-Propanol 0.46 M py <sup>-</sup>	54.26	3.02
1-Propanol	54.26	3.13

TABLE II  
FIRST ORDER RATE CONSTANTS FOR PYRIDINE-BORANE IN 1-PROPANOL-WATER MIXTURES, 50.00°

%H <sub>2</sub> O by weight	$k \times 10^5$ (sec. <sup>-1</sup> )	%H <sub>2</sub> O by weight	$k \times 10^5$ (sec. <sup>-1</sup> )
0.0	1.89	40.0	0.557
10.0	0.998	50.0	0.461
20.0	0.760	55.4	0.445
30.0	0.583	60.0	0.403

We interpret these data in terms of rate determining dissociation of py·BH<sub>3</sub> into BH<sub>3</sub> and pyridine in the solvent. The reverse reaction is negligible as evidenced by the lack of retardation

(1) Paper I, G. E. Ryschkeiwitsch, *J. Am. Chem. Soc.* **82**, 3290 (1960).

(2) M. F. Hawthorne and E. S. Lewis, *ibid.*, **80**, 4296 (1958).

(3) A. A. Frost and R. G. Pearson, "Kinetics and Mechanism," John Wiley and Sons, Inc., New York, N. Y., 1953, p. 130.

(1) H. Kwart, *J. Phys. Chem.*, **64**, 1250 (1960).

(2) M. S. Matheson, E. E. Auer, E. B. Bevilacqua and E. J. Hart, *J. Am. Chem. Soc.*, **71**, 497 (1949).

(3) Guggenheim Fellow on leave from Argonne National Laboratory.

by added pyridine. The dielectric constant effect is one expected for a reduction of charge separation in the transition state consistent with amine dissociation but not with hydride transfer. The argument is reinforced by the independence of rate from alcohol concentration implied by the data. Finally, we observed that on methyl substitution of the pyridine ring the reaction rate is decreased, giving the rate order pyridine-BH<sub>3</sub> > 3-picoline BH<sub>3</sub> > 4-picoline BH<sub>3</sub>. This is the order expected for amine dissociation on the basis of the base strengths of the pyridines. The observed substitution effects for the hydride transfer reaction<sup>2</sup> would have predicted the opposite order of rates.

DEPARTMENT OF CHEMISTRY  
UNIVERSITY OF FLORIDA  
GAINESVILLE, FLORIDA

G. E. RYSCHKEWITSCH  
E. R. BIRNBAUM

RECEIVED MAY 15, 1961

ON THE PAPER "PYROLYSIS OF ALLYL  
CHLORIDE" BY L. J. HUGHES AND W. F.  
YATES

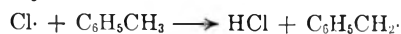
Sir:

In 1954 I published a paper<sup>1</sup> concerning the primary mechanism of thermal decomposition of allyl chloride. The major decomposition products in toluene as a carrier gas were found to be hydrogen chloride, fibenzyl and propylene, the amount of allene being less than 3% of HCl.

These products are evidence that the primary mechanism of decomposition is the cleavage of the C-Cl bond

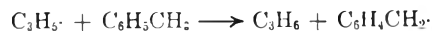


followed by the reaction



to a certain extent by

(1) A. E. Shilov, *Doklady Akad. Nauk SSSR*, **98**, 601 (1954); *C.A.*, **49**, 11605f (1955).



and by recombinations of allyl and benzyl radicals. In agreement with this mechanism the activation energy was found to be 59.3 kcal./mole, which is equal to the C-Cl bond energy in C<sub>3</sub>H<sub>5</sub>Cl.

The very small amount of allene indicates that the molecular splitting



does not play an important part in the decomposition.

The mechanism found<sup>1</sup> was given correctly in *Chemical Abstracts*<sup>2</sup> and was discussed by Semenov.<sup>3</sup> However, I have to repeat the data here, since in the paper "Pyrolysis of Allyl Chloride" by J. L. Hughes and W. F. Yates,<sup>4</sup> these authors did not correctly quote my work. They write: "Shilov indicates that allene and methylacetylene are the major products of the pyrolysis." As stated above, I found in fact only small amounts of allene. As to methylacetylene I did not find it and did not mention it in my paper. Moreover, Hughes and Yates write that I "indicate that the primary reaction is the loss of HCl to form allene."

Thus the conclusions ascribed to me by these authors seem to be opposite to those expressed in my paper.

INSTITUTE OF CHEMICAL PHYSICS  
OF THE USSR ACADEMY OF SCIENCES  
MOSCOW, U.S.S.R.

A. E. SHILOV

RECEIVED APRIL 18, 1961

(2) However, there is a slight inaccuracy in *C.A.* Instead of "Very small amounts of allene and formation of dibenzyl are evidence for a radical mechanism," as written in my paper, the *C.A.* wording is "The formation of (PhCH<sub>2</sub>)<sub>2</sub> and allene indicates radical type reaction." Thus the words "small amounts" were omitted. It was probably a misprint, since the mechanism given further in *C.A.* involves no allene at all.

(3) N. N. Semenov, "Some Problems of Chemical Kinetics and Reactivity" (see p. 255 of the Pergamon Edition).

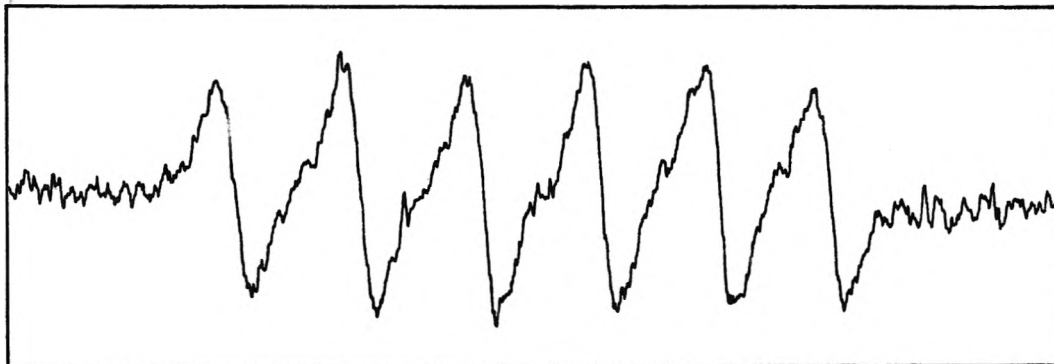
(4) L. J. Hughes and W. F. Yates, *J. Phys. Chem.*, **64**, 1789 (1960).

# EPR HIGH SENSITIVITY IN AQUEOUS SOLUTIONS

(ELECTRON PARAMAGNETIC RESONANCE)

The V-4501 100 kc EPR Spectrometer, when used with the V-4548 Aqueous Solution Sample Cell, offers to the scientist excellent sensitivity for investigating paramagnetic species in solvents of high dielectric loss. Manganese in aqueous solutions at  $10^{-6}$  molarity can be observed with approximately 10:1 signal-to-noise ratio.

## $10^{-6}$ Molar $Mn^{++}$



Modulation . . . . . 20 gauss peak-to-peak  
Response . . . . . 1 second  
Power at Cavity . . . 180 mW  
Sample at Room Temperature

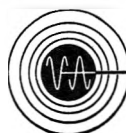
Electron paramagnetic resonance in aqueous solutions is complicated by the fact that water has a high dielectric loss at typical microwave frequencies. The V 4501 Spectrometer employs a rectangular  $TE_{102}$  resonant sample cavity. The difficulty of dielectric loss in this sample cavity can be overcome by using a flat sample cell which constrains the sample in the nodal plane of minimum r-f electric field (and maximum r-f magnetic field).

With the increasing use of EPR in various fields of biology, this development is of considerable significance. For example, there is a rising interest in the role of metals in biological systems. Many of these metals happen to be paramagnetic with concentrations which vary from  $10^{-4}$  to  $10^{-7}$  molar. Use of high sensitivity EPR equipment, often permits positive identification of the metal, a deter-

mination of its valence state, and a quantitative measurement of concentration.

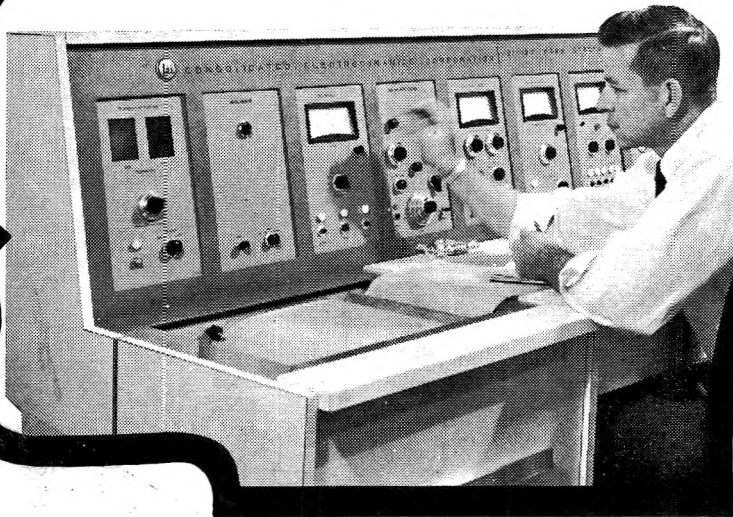
A particularly important metal is manganese, which, as  $Mn^{++}$ , has been detected in enzymes and living cells. A dilute aqueous solution of this ion is therefore a suitable material to investigate the sensitivity of EPR equipment for biological applications. The spectrum above is a trace of  $10^{-6}$  molar  $Mn^{++}$  obtained with the Varian EPR Spectrometer system. The well known six line hyperfine pattern arising from the  $5/2$  nuclear spin of  $Mn^{55}$  is evident. To check the reproducibility, quantitative  $10^{-6}$  M solutions of  $MnCl_2$ ,  $MnSO_4$ , and  $MnNO_3$  were prepared, and the observed signal heights of these three samples were found to be the same within  $\pm 5\%$ .

*For literature which fully explains the 100 kc EPR Spectrometer and its application to basic and applied research in physics, chemistry, biology and medicine, write the Instrument Division.*



**VARIAN associates**  
PALO ALTO 52, CALIFORNIA

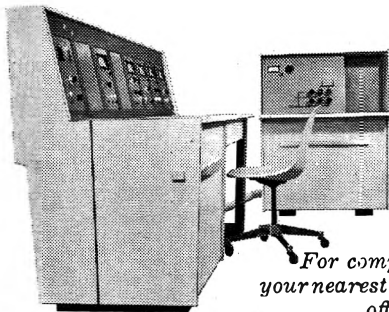
*CEC makes the  
only medium-priced  
MASS SPECTROMETER  
FOR ANALYTICAL LABORATORIES  
that features human engineered  
packaging. This is it...*



CEC's all-new 21-130 Mass Spectrometer offers the same accuracy, precision, sensitivity and scan speed you'll find only in the largest instruments of its kind.

All this plus a totally new "human" engineered packaging concept that means: Greater accessibility (modular electronics on pull-down chassis) . . . Convenience in the grouping of operating controls by function, with each operable and adjustable from the front . . . Lighter weight because it's built on a welded extruded aluminum frame with formica-over-honeycomb cabinet panels.

Look at its features: A built-in direct writing oscillograph recording system using five galvanometers . . . a stainless steel inlet system . . . a built-in micromanometer. And performance? Mass range from  $m/e$  2 to 230 continuous with unit resolution up to  $m/e$  200.



*For complete information call  
your nearest CEC sales and service  
office or write today for  
Bulletin CEC 21130-X3.*

Analytical & Control Division

**CEC**

**CONSOLIDATED ELECTRODYNAMICS / pasadena, calif.**

A SUBSIDIARY OF **Bell & Howell** • FINER PRODUCTS THROUGH IMAGINATION